frontiers | Research Topics

Women in plant science - redox biology of plant abiotic stress 2022

Edited by
Laura De Gara, María C. Romero-Puertas, Christine Helen Foyer, Sabine Lüthje and Ana Zabalza

Published in
Frontiers in Plant Science

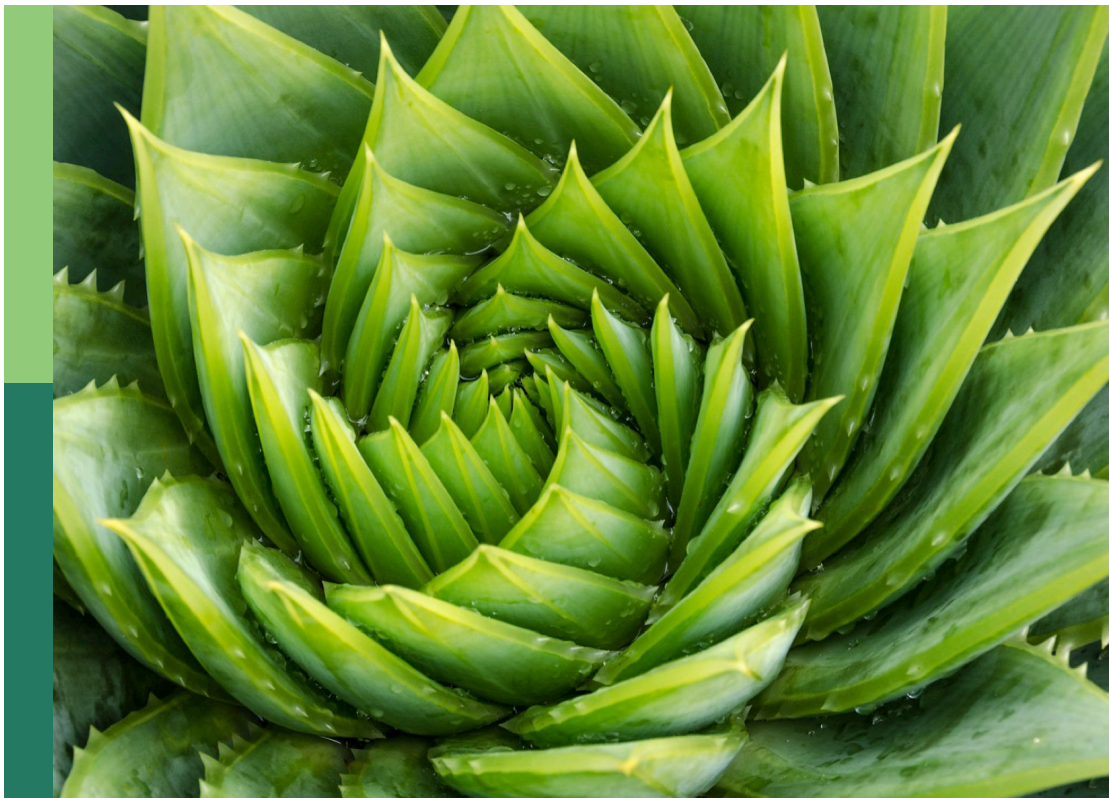

ISSN 1664-8714
ISBN 978-2-8325-3120-4
DOI 10.3389/978-2-8325-3120-4

About Frontiers

Frontiers is more than just an open access publisher of scholarly articles: it is a pioneering approach to the world of academia, radically improving the way scholarly research is managed. The grand vision of Frontiers is a world where all people have an equal opportunity to seek, share and generate knowledge. Frontiers provides immediate and permanent online open access to all its publications, but this alone is not enough to realize our grand goals.

Frontiers journal series

The Frontiers journal series is a multi-tier and interdisciplinary set of open-access, online journals, promising a paradigm shift from the current review, selection and dissemination processes in academic publishing. All Frontiers journals are driven by researchers for researchers; therefore, they constitute a service to the scholarly community. At the same time, the *Frontiers journal series* operates on a revolutionary invention, the tiered publishing system, initially addressing specific communities of scholars, and gradually climbing up to broader public understanding, thus serving the interests of the lay society, too.

Dedication to quality

Each Frontiers article is a landmark of the highest quality, thanks to genuinely collaborative interactions between authors and review editors, who include some of the world's best academicians. Research must be certified by peers before entering a stream of knowledge that may eventually reach the public - and shape society; therefore, Frontiers only applies the most rigorous and unbiased reviews. Frontiers revolutionizes research publishing by freely delivering the most outstanding research, evaluated with no bias from both the academic and social point of view. By applying the most advanced information technologies, Frontiers is catapulting scholarly publishing into a new generation.

What are Frontiers Research Topics?

Frontiers Research Topics are very popular trademarks of the *Frontiers journals series*: they are collections of at least ten articles, all centered on a particular subject. With their unique mix of varied contributions from Original Research to Review Articles, Frontiers Research Topics unify the most influential researchers, the latest key findings and historical advances in a hot research area.

Find out more on how to host your own Frontiers Research Topic or contribute to one as an author by contacting the Frontiers editorial office: frontiersin.org/about/contact

Women in plant science - redox biology of plant abiotic stress 2022

Topic editors

Laura De Gara — Campus Bio-Medico University, Italy

María C. Romero-Puertas — Department of Biochemistry, Cell and Molecular Biology of Plants, Experimental Station of Zaidín, Spanish National Research Council (CSIC), Spain

Christine Helen Foyer — University of Birmingham, United Kingdom

Sabine Lüthje — Universität Hamburg, Germany

Ana Zabalza — Public University of Navarre, Spain

Citation

De Gara, L., Romero-Puertas, M. C., Foyer, C. H., Lüthje, S., Zabalza, A., eds. (2023). *Women in plant science - redox biology of plant abiotic stress 2022*. Lausanne: Frontiers Media SA. doi: 10.3389/978-2-8325-3120-4

Table of contents

frontiers | Frontiers in Plant Science

TYPE Editorial
PUBLISHED 22 June 2023
DOI 10.3389/fpls.2023.1236150

OPEN ACCESS

EDITED AND REVIEWED BY
Dung Tien Le,
Bayer Crop Science, Vietnam

*CORRESPONDENCE
María C. Romero-Puertas
maria.romero@eez.csic.es
Christine H. Foyer
c.h.foyer@bham.ac.uk

RECEIVED 07 June 2023
ACCEPTED 12 June 2023
PUBLISHED 22 June 2023

CITATION
Romero-Puertas MC, Lüthje S, Zabalza A, de Gara L and Foyer CH (2023) Editorial: Women in plant science - redox biology of plant abiotic stress 2022. *Front. Plant Sci.* 14:1236150. doi: 10.3389/fpls.2023.1236150

Editorial: Women in plant science - redox biology of plant abiotic stress 2022

María C. Romero-Puertas[1]*, Sabine Lüthje[2], Ana Zabalza[3], Laura de Gara[4] and Christine H. Foyer[5]*

[1]Department of Biochemistry, Cell and Molecular Biology of Plants, Experimental Station of Zaidín, Spanish National Research Council (EEZ-CSIC), Granada, Spain, [2]Biodiversity of Crop Plants, Universität Hamburg, Institute of Plant Science and Microbiology, Oxidative Stress and Plant Proteomics Group, Hamburg, Germany, [3]Institute for Multidisciplinary Research in Applied Biology (IMAB), Universidad Pública de Navarra (UPNA), Pamplona, Spain, [4]Department of Science and Technology for Sustainable Development and Human Health, Università Campus Bio-Medico di Roma, Rome, Italy, [5]Department of Biosciences, University of Birmingham, Birmingham, United Kingdom

KEYWORDS

redox biology, plants, abiotic stress, hydrogen peroxide, nitric oxide

Editorial on the Research Topic
Women in plant science - redox biology of plant abiotic stress 2022

Introduction

Plants sustain all life on Earth. They are the basis for all the food that we eat, the oxygen that we breathe and our fossil fuels. They will also be essential in reducing atmospheric CO_2 levels to combat anthropogenic CO_2 release and sustaining the soil carbon sink. Plants are also extremely resilient, rapidly adjusting to continuous environmental changes. Rapid or acute changes in environmental conditions may however cause stress that results in complex responses and specific signalling local and long-distance pathways that underpin survival. These pathways include numerous signalling molecules, such as reactive oxygen, nitrogen and sulphur species (ROS/RNS/RSS). These function together with ions and phytohormones to adjust metabolism to prevailing environmental conditions. Some signalling molecules are able to generate protein post-translational modifications (PTMs) on target proteins, that affect their stability, localization, activity, binding to other proteins, etc. For example, redox PTMs involve reversible changes to cysteine thiol groups. These redox changes form the basis of hydrogen peroxide signalling and "Redox Biology". Understanding the mechanisms underlying plant responses to changing conditions, particularly environmental pollutants is one of the most challenging tasks in plant science. Understanding the regulation of these processes will allow better targeting of approaches to improve plant stress adaptation and sustainable yield increases.

The contributions and achievements of women are essential to the 2030 Agenda for Sustainable Development. The aim of this Research Topic was to bring together the latest advances and related information from researchers working in the field of redox biology, particularly in abiotic stress tolerance. We celebrate the success of female scientists and seek to empower and encourage their future work. Female scientists make significant contribution to all fields of plant science. Examples of their work is presented in this

Research Topic, in which all the articles have female corresponding authors. These papers not only highlight the importance of redox biology in plant responses to a diverse range of abiotic stresses, but they also present original advances in knowledge, approaches, and methods with potential applications in agriculture. Three reviews in this Research Topic summarise current concepts in redox biology, particularly PTMs and the role of oxidative metabolism in plant responses to abiotic stress.

Original research

Three of the original manuscripts presented in this Research Topic are related to the responses of plants to extremes of temperature. Unpredictable temperature extremes such as heatwaves that are linked to climate change, pose serious threat to plant development and yields. Jindal et al. identified the role of type-A arabidopsis response regulators (ARR), which are competitors of the main components of cytokinins (CKs) signalling, the transcription factors type-B ARRs, in plant response to heat stress (HSR). Type-A ARRs negatively mediate HSR in arabidopsis (*Arabidopsis thaliana* (L.) Heynh.) and mutants lacking functional ARRs experience a priming state increasing their thermotolerance to elevated temperatures, showing proteomic changes similar to that of a heat acclimation. Interestingly, type-A ARR mutants showed an enhancement of low molecular weight antioxidants such as ascorbate and glutathione. GENOMES UNCOUPLED 1 (GUN1) is a key protein for retrograde signalling from chloroplast to the nucleus and it has been shown to be essential in plant thermotolerance in arabidopsis in the manuscript by Lasorella et al. *gun1* mutants fail to induce a transient oxidative burst after heat shock treatment, which seems to be essential for the activation of stress responsive genes during the recovery period. The analysis of different redox and reactive oxygen species (ROS)-related parameters in wt and *gun1* mutants after heat shock treatment and recovery period suggests a key role for tylacoidal ascorbate peroxidise in GUN1-dependent thermotolerance. Furthermore, iodoacetyl tandem mass tags (iodo-TMT)-proteomic analysis in cold acclimated rape (*Brassica napus* L.) after freezing stress resulted in the identification of 171 differentially sulfenylated proteins involving this redox-dependent post-translational modifications (PTM) in plant response to cold (Liangqian et al.). Interestingly, enzymes from the Calvin-Benson-Bassham cycle were sulfenylated after freezing affecting to the metabolite levels resulted from this pathway, involving again the chloroplasts in plant acclimation to cold stress. In fact, carbon fixation is a critical issue to manage climate crises. Woody plants like Norway spruce (*Picea abies* L. Karst.) are important carbon sinks. Photosynthetically fixed carbon is stored in plant cell walls that are comprised primarily of polysaccharides (Verbančič et al., 2018). Plant respiratory burst oxidase homologs (Rboh) are involved in abiotic stress response and cell wall modification by the production of ROS. The focus of the contribution by Nickolov et al. was on the regulation of gymnosperm Rboh biochemistry. They demonstrated the regulation of PaRBOH1-mediated ROS production in Norway spruce by Ca^{2+} binding and phosphorylation with a combination of in silico analysis, biochemistry and phosphoproteomics. On the other hand, herbicides still are the most commonly used mechanisms for weed control, which is a big challenge for crop protection. Eceiza et al. linked oxidative metabolism with high concentration of the herbicide nicosulfuron sensitivity in pigweed (*Amaranthus palmeri* S.Watson) plants. Oxidative stress however is not the only causes of plant death. Interestingly, most of the oxidative parameters analysed under control conditions were similar in sensitive and resistant populations showing that sensitivity is not due to different initial oxidative status.

Technical advances

Allan et al. showed the development of a chip-based treatment technique paired with a reporter gene approach to measure cytosolic Ca^{2+} transients in arabidopsis in response to osmotic and salt stress. In contrast to published chip-based methods, the modification of the chip described here has the advantage to permit a more localized application of the treatment, a free choice of the direction of flow inside the chip and also a unilateral application of the test solution. This dual-flow RootChip (dfRC) could advance our understanding of how plants perceive and decode stress information in specific tissues at the cellular or subcellular levels. This is of relevance not only for stress research but also for other applications.

The results of the study were comparable to other studies using $Ca2^{+}$ reporters on NaCl and osmotic stress (also cited in the references). There are also a number of studies using $Ca2^{+}$ reporters on NaCl and osmotic stress (also cited in the references).

Reviews

Although the contamination of the environment with nanoplastic is an emerging issue worldwide, until recently the attention has not been drawn to the effects of nanoplastics in plants. Ekner-Grzyb et al. revises up-to-date information with special emphasis on the oxidative response. Exposure to nanoplastics leads to increase in reactive oxygen species, and the altered nutrient photosynthesis levels result in hampered plants growth. In addition, nanoplastics alert plants physiology through modulation of genes expression on the transcriptomic level. The knowledge generated in recent years on redox post-translational modifications and their interplay in the acclimatization processes of plants is gathered in the review by Martí-Guillen et al.. The overproduction of molecular reactive species, mainly reactive oxygen, nitrogen and sulphur species, has been recorded after abiotic stresses, and they can modify proteins by PTMs. This process is proposed to not occur randomly but that the enzymatic activity can be modulated by the modification of critical amino acid residues. The review focuses on the redox-based post transcriptional modifications of the enzymes that participate in the main stress-related pathways, such as oxidative metabolism, primary metabolism, cell signalling events, and photosynthetic metabolism. Especial attention to nitric oxide, which promotes the first step in the redox state of the thiol groups from cysteines, so-called S-nitrosylation, is paid in the review by Mata-Pérez et al. This review collects significant and recent advances in NO-dependent PTMs, in

particular, S-nitrosylation, in plant response to different abiotic stresses. Therefore, key results involving NO function in plant response to drought and salt stress, high and low temperature, mechanical wounding, heavy metals, hypoxia, UV radiation and ozone exposition are discussed.

Author contributions

MR-P prepared the draft with SL, LG and AZ contributions, CF worked on it and then all the authors contributed with their suggestions to the final version.

Funding

MR-P thanks Spanish Ministry of Science and Innovation for Financial support (PID2021-122280NB-I00). CF thanks BBSRC/GCRF (UK) for Financial support (BB/T008865/1). LG thanks Agritech National Research Center (European Union Next-Generation, EU), Piano Nazionale di Ripresa e Resilienza (PNRR)—Missione 4 Componente 2, Investimento 1.4—D.D. 1032 17/06/2022, CN00000022).

Conflict of interest

The authors declare that the research was conducted in the absence of any commercial or financial relationships that could be construed as a potential conflict of interest.

Publisher's note

Reference

Verbančič, J., Lunn, J. E., Stitt, M., and Persson, S. (2018). Carbon supply and the regulation of cell wall synthesis. *Mol. Plant* 11 (1), 75–94. doi: 10.1016/j.molp.2017.10.004

frontiers | Frontiers in Plant Science

TYPE Original Research
PUBLISHED 23 September 2022
DOI 10.3389/fpls.2022.968139

OPEN ACCESS

EDITED BY
Christine Helen Foyer,
University of Birmingham,
United Kingdom

REVIEWED BY
Vikas Srivastava,
Central University of Jammu, India
Shibin He,
Henan University, China

*CORRESPONDENCE
Břetislav Brzobohatý
brzoboha@ibp.cz
Ashverya Laxmi
ashverya_laxmi@nipgr.ac.in

†Lead contact

SPECIALTY SECTION
This article was submitted to
Plant Abiotic Stress,
a section of the journal
Frontiers in Plant Science

RECEIVED 13 June 2022
ACCEPTED 02 September 2022
PUBLISHED 23 September 2022

CITATION
Jindal S, Kerchev P, Berka M, Černý M, Botta HK, Laxmi A and Brzobohatý B (2022) Type-A response regulators negatively mediate heat stress response by altering redox homeostasis in Arabidopsis.
Front. Plant Sci. 13:968139.
doi: 10.3389/fpls.2022.968139

Type-A response regulators negatively mediate heat stress response by altering redox homeostasis in Arabidopsis

Sunita Jindal [1], Pavel Kerchev [1], Miroslav Berka [1], Martin Černý [1], Halidev Krishna Botta [2], Ashverya Laxmi [2]* and Břetislav Brzobohatý [1]*†

[1]Department of Molecular Biology and Radiobiology, Mendel University in Brno, Brno, Czechia, [2]National Institute of Plant Genome Research, New Delhi, India

Besides the long-standing role of cytokinins (CKs) as growth regulators, their current positioning at the interface of development and stress responses is coming into recognition. The current evidence suggests the notion that CKs are involved in heat stress response (HSR), however, the role of CK signaling components is still elusive. In this study, we have identified a role of the CK signaling components type-A Arabidopsis response regulators (ARRs) in HSR in Arabidopsis. The mutants of multiple type-A *ARR* genes exhibit improved basal and acquired thermotolerance and, altered response to oxidative stress in our physiological analyses. Through proteomics profiling, we show that the type-A *arr* mutants experience a 'stress-primed' state enabling them to respond more efficiently upon exposure to real stress stimuli. A substantial number of proteins that are involved in the heat-acclimatization process such as the proteins related to cellular redox status and heat shock, are already altered in the type-A *arr* mutants without a prior exposure to stress conditions. The metabolomics analyses further reveal that the mutants accumulate higher amounts of α-and γ-tocopherols, which are important antioxidants for protection against oxidative damage. Collectively, our results suggest that the type-A ARRs play an important role in heat stress response by affecting the redox homeostasis in Arabidopsis.

KEYWORDS

Arabidopsis response regulators, heat stress, cytokinins, oxidative stress, proteomics, metabolomics, heat-acclimatization

Introduction

Plants are continuously exposed to environmental temperature fluctuations. Unfavorably high temperature causes heat stress in all organisms and leads to disintegration of membrane lipids, protein misfolding and denaturation, oxidative burst, and increased membrane fluidity. The HS-induced ROS such as O_2^- and H_2O_2 damage organelles and inhibit cellular functions (Szymańska et al., 2017). For example, heat stress negatively influences chloroplast structure, thermal stability of the components of photosystem II and Rubisco activity ultimately resulting in reduced photosynthetic efficiency (Moore et al., 2021). The perception and signaling of heat stress is initiated by high temperature-induced changes in the plasma membrane. The enhanced fluidity of the membrane allows calcium channels to open and an inward flux of Ca^{2+} ions into the cytoplasm, in turn, initiates the heat stress response (HSR) (Abdelrahman et al., 2020).

Heat shock proteins (HSPs) and antioxidant enzymes are the two major classes of functional proteins that are induced during HSR. HSPs work as molecular chaperones and prevent irreversible protein aggregation (Wang et al., 2004). Further, the antioxidant system (AOS) maintains proper cellular levels of ROS through scavenging excessive free radicals. The AOS includes enzymatic components such as superoxide dismutase (SOD), catalase (CAT), ascorbate peroxidase (APX), guaiacol peroxidase (GPX), glutathione reductase (GR) etc., and the non-enzymatic components like ascorbic acid (AsA), reduced glutathione (GSH), α-and γ-tocopherols, carotenoids, flavonoids, and proline (Das and Roychoudhury, 2014) which cumulatively maintain the redox homeostasis.

During heat stress and drought, the phytohormone repertoire is changed markedly and interplays with ROS machinery in mediating stress responses (Xia et al., 2015; Devireddy et al., 2020). In recent years, cytokinins (CKs) have emerged as important phytohormones in mediating heat and water-deficit stress responses alongside their crucial role in growth and developmental plans (Černý et al., 2014; Nguyen et al., 2016; Bryksová et al., 2020; Prerostova et al., 2020). Changes in the endogenous CK levels during several abiotic stresses such as heat and drought prove to be straightforward evidence on the connection of CKs and stress responses (Hare et al., 1997; Todaka et al., 2017). A general trend is that the CK levels rise transiently in response to stress stimuli and decline over time if the stress condition is mild or moderate. In case of increased stress, the CK level remains high or does not return to the baseline level (Zwack and Rashotte, 2015). In addition to the changes in the CK levels, transcriptomic and proteomic studies also reveal a large overlap in the heat stress and CK response profiles in Arabidopsis (Černý et al., 2011; Černý et al., 2014). Further, external application of BAP as well as enhancement of endogenous CK levels by IPT overexpression improve antioxidant capacity in different plant species through activating antioxidant enzymes like CAT and APX (Xu et al., 2016; Hönig et al., 2018) which is crucial for overcoming HS-induced oxidative damage.

Although there is evidence on the involvement of CKs in HSR, the role of CK signaling is currently not understood. The CK signaling module consists of the receptor histidine kinases (AHKs), His-containing phosphotransfer proteins (AHPs) and the type-A and -B response regulators (ARRs). The central components of CK signaling, the type-B ARRs are the transcription factors which are competitively inhibited by the type-A ARRs in a negative feedback loop manner. The type-A ARRs compete with the type-B ARRs for phosphorylation, however, they lack the DNA binding domain for transcriptional activation hence working as the repressors of CK signaling (To et al., 2004). Mutation in the type-A *ARRs*, alleviates the competition for phosphorylation for the type-B ARRs and thus, the repression of the transcription factor type-B ARRs is lifted.

Such negative feedback loops are important for maintaining a delicate balance between the growth and stress response mechanisms and are particularly important under fluctuating environmental conditions (Jamsheer K et al., 2022). Being important growth regulators, it is obvious that the CK signaling is under such regulatory control. Knocking out the negative feedback loop in form of the mutations in type-A *ARRs* thus makes it reasonable to ask how CK signaling in the absence of functional type-A ARRs may influence plants' capacity to face environmental perturbation such as heat stress. In this study, using detailed physiological analysis we show the role of the type-A ARRs in HSR. In our proteomics studies, we identified that the multiple gene mutations in the type-A *ARRs* lead to an altered proteomic profile which account for the improved survival during the periods of heat stress. Through biochemical assays, together with metabolomic analyses, we also show that the type-A *arr* mutants have modified antioxidant capacity which could contribute to their enhanced ability to survive environmental situations causing oxidative stress.

Results

Cytokinin signaling components are differentially regulated by heat stress

Since there are several studies indicating the functional link between CKs and HSR, we analyzed the transcriptional regulation of 33 CK signaling component genes under heat stress using publicly available mRNA-Seq dataset "AT_mRNASeq_ARABI_GL-1" from Genevestigator (Hruz et al., 2008). We selected the datasets AT-00814 where heat stress was applied at 35°C for 4 hours to 4-weeks-old Arabidopsis

plants, AT-00751 in which 37°C was applied for 6 hours to 3-weeks-old Arabidopsis, and AT-00795 in which 42°C was applied up to 24 h to 3-weeks-old Arabidopsis plants. Out of the 33 analyzed genes, several of them were found to be differentially expressed under heat stress. The highest and most conserved effect was observed on the type-A *ARR* genes. Among these, the expression of 8 out of 10 genes was found to be strongly repressed under heat stress and exhibited a consensus among the different HS treatments (Figure 1). In one of the treatments, *AHP4* was upregulated whereas, *AHP1, 2, 5* and *6* were unchanged or slightly changed. In Our analysis, the highest and most conserved response of the type-A *ARR* genes to heat stress indicated their possible involvement in the HSR and therefore, we focused on the type-A *ARR* genes for our subsequent studies.

Loss of functional type-A *ARRs* improves basal and acquired thermotolerance

Down-regulation of the type-A *ARRs* upon an encounter to heat stress must have adaptive significance for the plants. Therefore, we tested that how type-A *arr* mutants respond to above-optimal high temperatures. Because of the functional redundancy among the type-A ARR family members, most of the single gene mutants are indistinguishable from the wild-type and the double and higher order mutants show increasing sensitivity to CKs (To et al., 2004). Therefore, we selected the higher order Arabidopsis mutants *arr3,4,5,6,8,9* and *arr5,6,8,9* lacking multiple type-A *ARR* genes for our studies. According to To et al., 2004, and in our observation, the quadruple mutant *arr5,6,8,9* was phenotypically indistinguishable from the wild-type under long-day conditions. The *arr3,4,5,6,8,9* mutant is smaller in the rosette area and root length, but we did not observe any differences in the growth progression relative to the wild-type. For basal and acquired thermotolerance assays, the seedlings were treated at a lethal temperature (45°C for 2.5 h) with and without heat acclimatization (37°C for 1 h followed by 2 h of recovery at 21°C) in an incubator. We observed that both the type-A *arr* mutants *arr5,6,8,9* and *arr3,4,5,6,8,9*, showed significantly enhanced thermotolerance in both the conditions (Figure 2A). The biomass accumulation after a recovery period of 6 days in the mutants was higher than the wild-type in both conditions, with more prominent effect on the heat-acclimatized plants (Figure 2B). Consistently, there was higher total chlorophyll accumulation in the *arr* mutants when normalized with the control growth (Figure 2B). Moreover, in the *arr* mutants, chlorophyll *a*/*b* ratio remained closer to control values (Figure S1). Also, carotenoid content (normalized with the control growth) stayed higher in the *arr* mutants (Figure S1). No statistically significant difference in the total chlorophyll/carotenoid ratio was observed between the wild-type and the *arr* mutants though a trend to decrease in the ratio was apparent in the *arr* mutants (Figure S1) as they accumulate carotenoids to higher levels. The heat stress response was further tested in different growth stages and experimental setups. Cultivation at sub-lethal temperature extended to 3 days was found to be lethal for the wild-type while *arr5,6,8,9* and *arr3,4,5,6,8,9* mutants recovered. However, a partial chlorosis was observed in the *arr5,6,8,9* mutant (Figure 2C). Various degrees of lethality were observed in all genotypes when soil-grown plants were exposed to a lethal temperature for 4 h. The highest survival rate was observed in *arr3,4,5,6,8,9* mutant followed by *arr5,6,8,9* mutant and the least in the wild-type (Figure 2D). Thus, the type-A *arr* mutants displayed significantly higher thermotolerance in all the tested experimental conditions. Collectively, these results identified that the type-A ARRs negatively mediate HSR in Arabidopsis and the lack of functional type-A ARRs leads to improved theromotolerance.

Differential accumulation of the proteins in the *arr* mutants

To investigate the effect of mutations in the type-A *ARR*s on the overall proteomic landscape and subsequently its effect on HSR, we conducted shotgun proteomics analyses from the wild-type and the type-A *arr* mutants *arr5,6,8,9* and *arr3,4,5,6,8,9*. Since the heat treatment at 45°C had severe negative effect on young seedling survival post-recovery, and the differences in the theromotolerance of the *arr* mutants compared to the wild-type were more prominent in heat-acclimatized groups (Figure 2A), we got interested to know what happens differently in the *arr* mutants after a short heat-acclimatization phase before they encounter a severe heat stress. For this, we treated 7 DAS (days-after-stratification) Arabidopsis seedlings at 37°C for 1 h and harvested them after 2 h of recovery at 21°C. For the untreated groups, 7 DAS seedlings were harvested at the same time point as the heat-treated group. From all the measured spectra, peptides matching 4657 *Arabidopsis thaliana* proteins were identified. Out of these, 3310 proteins with at least two unique peptides were selected for further analyses. First, we compared the proteome profiles of *arr5,6,8,9* and *arr3,4,5,6,8,9* mutants with respect to the wild-type under unstressed conditions to unravel the type-A ARR-regulated proteome and to see the difference on the impact of additional *arr* mutations. In the hextuple mutant, we identified a total number of 114 differentially accumulated proteins (DAPs) of which, 64 were up-regulated and 50 were down-regulated (Figure 3A). In the quadruple mutant, on the other hand, only 61 proteins were differentially accumulated where the number of up- and down-regulated DAPs was 38 and 23, respectively (Figure 3A), suggesting an additive effect of the *arr* mutations on the proteome. A complete list of the DAPs is given in Supplementary Table S1 and S2. To compare the accumulation patters of proteins in both the mutants, we

10.3389/fpls.2022.968139

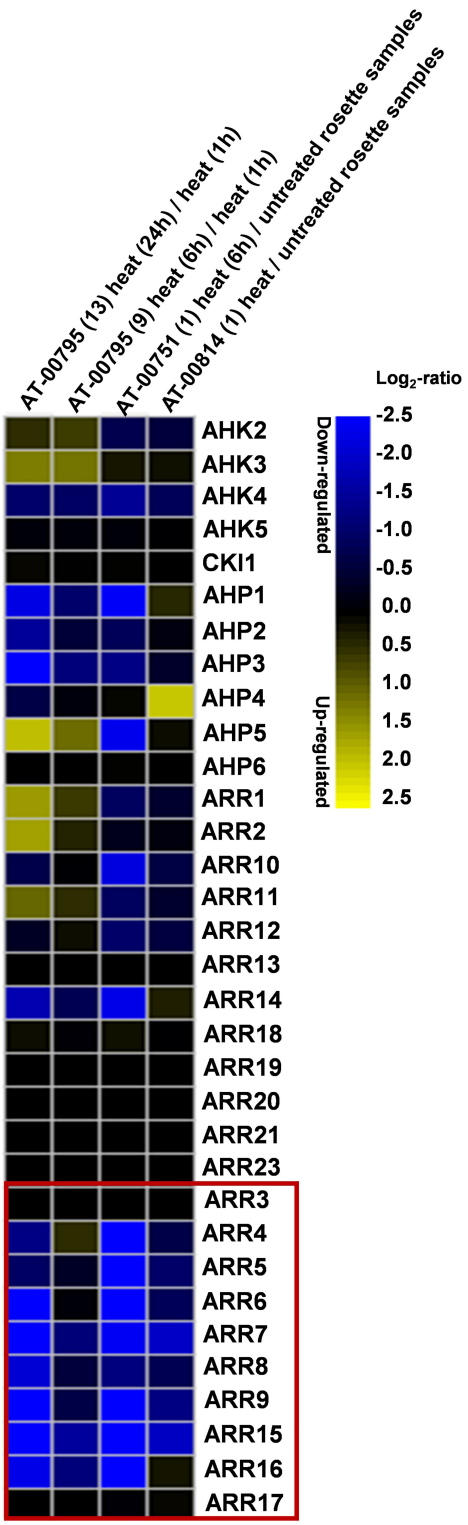

FIGURE 1
Cytokinin signaling genes are differentially regulated by heat stress. Analysis of the relative expression of *Arabidopsis thaliana* CK signaling genes using the publicly available mRNA-Seq dataset in which Arabidopsis plants were treated with heat stress conditions. The type-A *ARRs* are highlighted in the box. Heat map created using Genevestigator (https://genevestigator.com/).

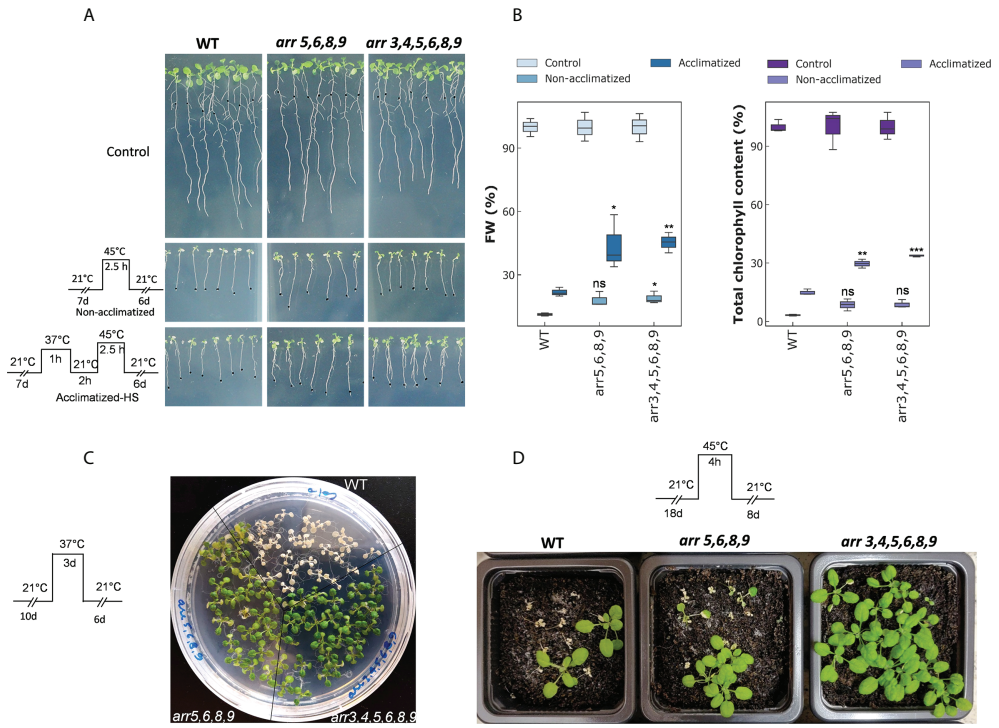

FIGURE 2
The effect of heat stress on the type-A *arr* mutants. **(A)** Phenotypic response of the 7 DAS (days-after-stratification) seedings subjected to heat stress conditions. Images are captured after 6 DOR (days-of-recovery). **(B)** Plots representing FW per seedling (left) and total chlorophyll content (right). FW and chlorophyll content are normalized with the control samples of each genotype to show the relative differences. The statistical significance is shown between the WT and *arr* mutants within the same treatment group. Error bars represent ± SE (two-way ANOVA, *P-value ≤ 0.05, Bonferroni *post-hoc* test, n=3, 13-15 plants were taken for each biological replicate). Asterisks represent the significant differences between the same treatment group of mutants in comparison to WT. **(C)** Effect of extended and moderate heat stress on 10 DAS seedlings. Images are captured after 6 DOR. **(D)** Effect of severe heat stress on 18 DAS plants. Images are captured after 8 DOR. Other photosynthetic pigments are shown in Supplementary Figure S1. ns, non-significant.

constructed a heat map. Hierarchical clustering of the top 200 proteins according to statistical significance highlighted clustering of these proteins into 6 groups (Figure 3B). In the clusters 1 and 5, the accumulation patters of the proteins were similar in the *arr5,6,8,9* and wild-type compared to the *arr3,4,5,6,8,9*. In clusters 2 and 3 the accumulation patters were similar in both the mutants compared to the wild-type. Clusters 4 and 6 had a smaller number of proteins for which accumulation levels were closer in the hextuple mutant and wild-type. This observation suggested that the proteome profile of the quadruple mutant was intermediate to that of the wild-type and *arr3,4,5,6,8,9* in terms of the number of DAPs as well as the level of accumulation as can be seen in the heat map. Due to the partially redundant functions of the gene family, the effect of the multiple gene mutations could be largely additive as appears from this result, however, the functional specificity of the particular gene family members cannot be ruled out. The additive effect of the lack of functional type-A *ARR* genes reflects in the physiological response of these mutants under HS conditions as the hextuple mutant exhibited higher thermotolerance than the quadruple mutant in our visual assessment (Figure 2).

Further, we carried out the gene ontology (GO) enrichment analysis of DAPs in both the mutants using Cytoscape v3.9.0 plugin Clugo (Bindea et al., 2009) (Figure 3C). In the hextuple mutant, the highest number of proteins (13 each) corresponded to the categories, 'response to abscisic acid' and 'lipid biosynthetic process', followed by 'sulfur compound metabolic process' (10). The other enriched GO terms were 'response to cytokinins', 'response to heat', 'alpha-amino acid biosynthetic process', 'response to light intensity', 'response to stimulus' and 'glycosyl compound metabolic process'. In quadruple mutant *arr5,68,9*, the only enriched GO term was 'response to toxic substance' (Figure 3C). The list of proteins in the enriched GO terms is given in Supplementary Table S1 and S2. The enrichment of the proteins involved in the response to cytokinins indicated an enhanced CK signaling in the *arr3,4,5,6,8,9* mutant. We observed that several proteins related to heat and/or oxidative stress response such as HOP3 (HSP70-HSP90 organizing protein 3), HSP17.4B/HSP17.6A,

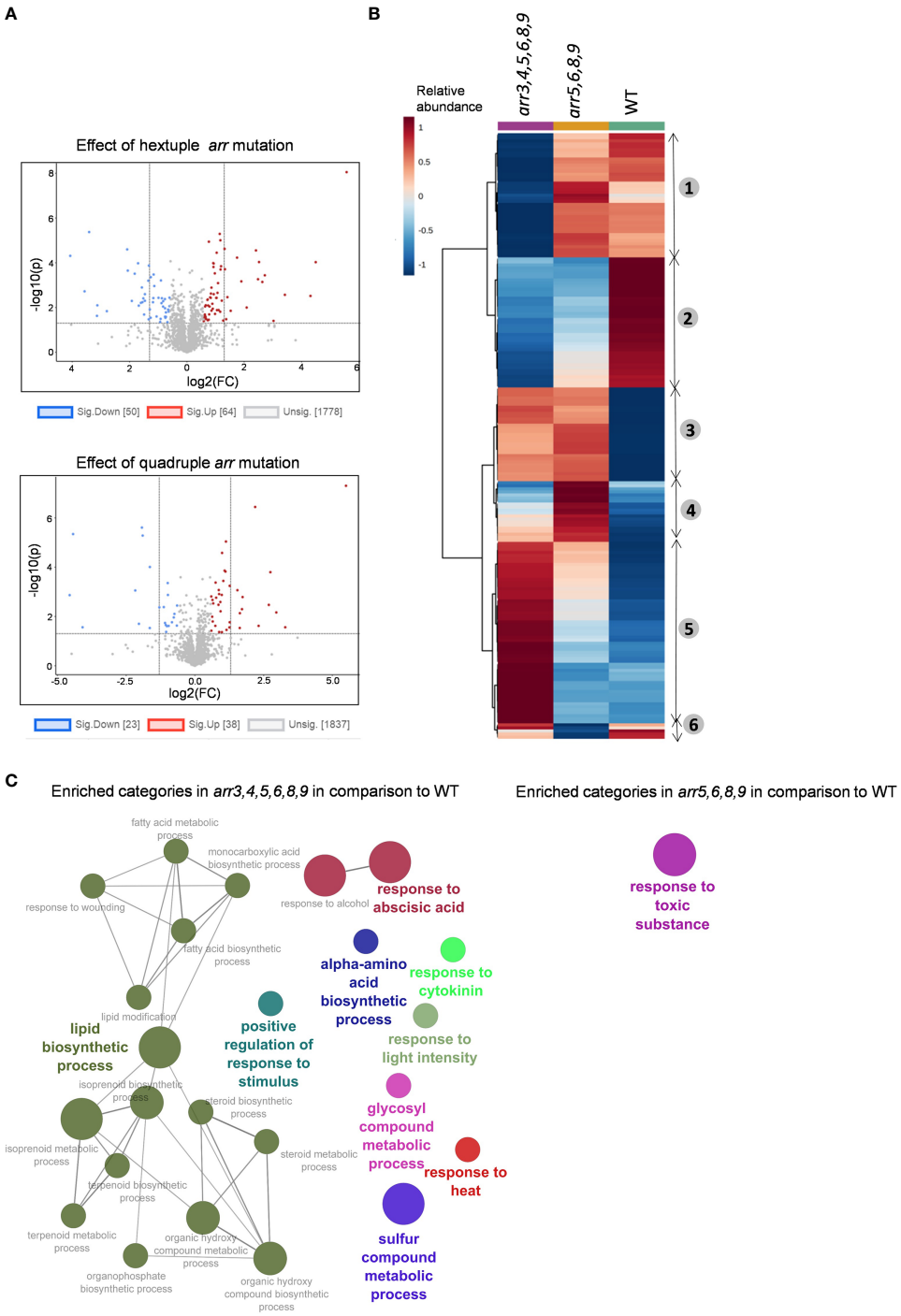

FIGURE 3
Comparison of the proteome profiles of the *arr* mutants under control conditions. **(A)** Volcano plot visualizations of the protein levels in *arr3,4,5,6,8,9* versus WT (upper) and *arr5,6,8,9* versus WT (lower). FC threshold is set to 1.5 and the P-value threshold is 0.05. **(B)** Hierarchical cluster analysis of the top 200 proteins according to statistical significance. The proteome profiles indicate the additive effect of the loss of type-A *ARR* genes. The quadruple mutant *arr5,6,8,9* shows an intermediate profile with respect to WT and hextuple mutant *arr3,4,5,6,8,9*. The heat map visualization and hierarchical clustering is carried out using MetaboAnalyst 5.0 and the numbers next to the heat map indicate six different clusters based on similarity in the accumulation pattern. **(C)** GO term functional grouping of the DAPs in the *arr* mutants as compared to WT. The network visualization is done in Cytoscape v3.9.0 plugin Clugo. The leading group name is based on the highest significance and only the pathways with a P-value ≤ 0.05 are shown. The nodes represent the GO terms and the size of the node represents term enrichment significance. At least 3 biological replicates are analyzed. **(A, C)**, The list of DAPs and proteins in enriched GO terms are given in Supplementary Table S1 and S2.

LIPOXYGENASE1 (LOX1), Peptidemethionine Sulfoxide Reductase 1 (PMSR1), Glutathione peroxides 2 (GPX2), Glutathione S-transferase theta 1 (GSTT1), Glutathione S-transferase U1 (GSTU1), ANNEXIN4 (ANN4), peroxidase 34 (PER34), a putative peroxidase AT4G26010.2, glutaredoxin and thioredoxin family proteins, and a respiratory chain NADH dehydrogenase were altered in one or both the mutants. A list of redox-related proteins that are differentially accumulated in the *arr* mutants in comparison to the wild-type are given in Supplementary Table S5. Many of the genes encoding these proteins are known oxidative stress marker genes. The higher accumulation of these proteins in the *arr* mutants indicated that the *arr* mutants experience a 'stress-primed' state which could be responsible for their increased thermotolerance upon a real encounter with elevated temperatures.

Acclimatory heat-regulated proteins are altered in the *arr* mutants prior to heat exposure

To further explore the basis of enhanced thermotolerance of the *arr* mutants, we analyzed how a heat-acclimatization phase triggers proteomic reprogramming differently in the *arr* mutants in comparison to the wild-type. We observed that the overall proteomic changes in the wild-type were higher than both the *arr* mutants as a total number of 137 proteins were significantly differentially accumulated in wild-type versus 111 and 104 in *arr3,4,5,6,8,9* and *arr5,6,8,9*, respectively (Figure 4A), indicating that heat treatment at 37°C induces more robust changes in the proteome in the wild-type than the *arr* mutants. The GO enrichment analysis of the heat-regulated DAPs in the wild-type seedlings retrieved the enriched functional categories such as 'heat acclimation', 'response to heat', 'response to hydrogen peroxide', 'sulfur compound metabolic process', 'organic acid metabolic process' and 'organophosphate biosynthetic process' (Figure S2A, Supplementary Table S3). The enrichment of the proteins related to heat and oxidative stress validated the heat treatment. Interestingly, some of the functional categories viz. 'response to heat', 'response to light intensity' and 'sulfur compound metabolic process' were also enriched in the *arr3,4,5,6,8,9* mutant as compared to the wild-type under control conditions indicating an overlap between the heat-induced proteome and the type-A ARRs-regulated proteome. Further, multiple factors/covariates data analysis was carried out to compare the proteomic response of wild-type and

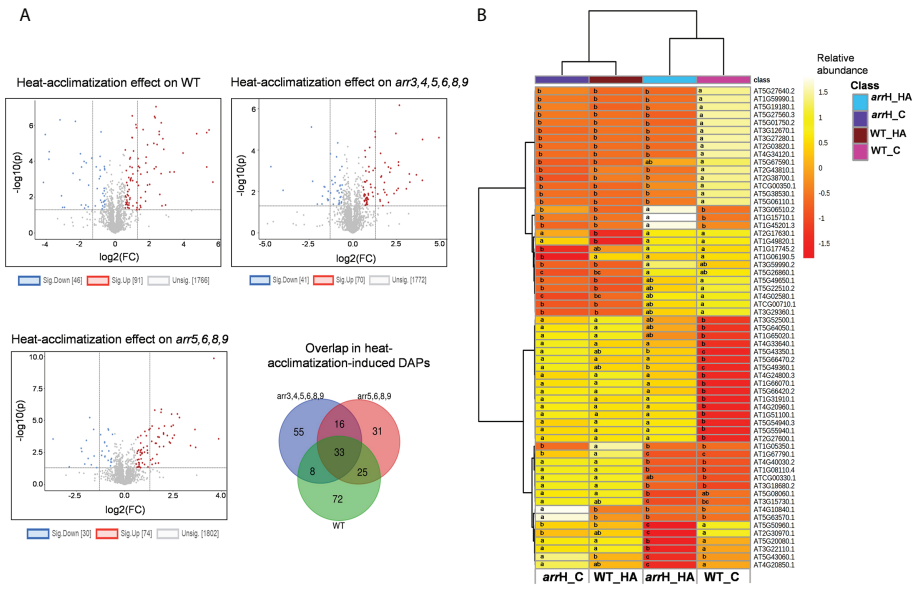

FIGURE 4
Proteomics changes triggered by heat-acclimatization in WT and *arr* mutants. **(A)** Comparison of the heat-acclimatization-induced proteomic changes in the WT and *arr* mutants. The 7 DAS seedlings were treated at 37°C for 1 h and the samples were harvested after a 2 h recovery phase at 21°C. FC threshold is set to 1.5 and the P-value threshold is 0.05. and **(B)** Heat map view of DAPs upon heat-acclimatization/mild heat treatment. Only the proteins that show statistical interaction in two-way ANOVA (genotype x treatment) at P-value ≤ 0.05 are shown in the heat map and the letters on the heat map indicate statistical significance in Turkey's test. The protein identities are listed on the right. The heat map scale indicates relative abundance. Treatments were performed in at least 3 biological replicates. The heat map visualization and hierarchical clustering are carried out using MetaboAnalyst 5.0. arrH_C: *arr3,4,5,6,8,9*_Control; arrH_HA: *arr3,4,5,6,8,9*_Heat-acclimatized; WT_C: WT_Control; WT_HA: WT_Heat-acclimatized. The list of DAPs upon heat-acclimatization in WT is given in Supplementary Table S3. The list of the proteins showing interaction effect in two-way ANOVA is given in Supplementary Table S4. The heat map view of the comparison of WT and *arr5,6,8,9* proteomes upon heat-acclimatization is given in Supplementary Figure S3.

arr3,4,5,6,8,9 upon heat-acclimatization. In two-way ANOVA analysis, a total number of 1687 proteins were found to be differentially accumulated, of which, 61 showed interactions (genotype x treatment). Intriguingly, the heat map visualization of these 61 proteins revealed that a high proportion of these proteins were already altered in the *arr3,4,5,6,8,9* mutant prior to heat-acclimatization and remained more stable after the short acclimatization phase (Figure 4B). Therefore, the proteome profile of the unstressed *arr3,4,5,6,8,9* significantly resembled the heat-acclimatized wild-type seedlings. The GO enrichment analysis of these 61 proteins showed the enrichment of biological function categories 'nucleobase-containing small molecule metabolic process', 'alpha-amino acid biosynthetic process' and 'response to metal ion' etc. (Figure S2B, Supplementary Table S4). A closer protein-by-protein look revealed that two cell-division and meristem development-related proteins Prohibitin4 (PHB4) and ZUOTIN-RELATED FACTOR1B (ZRF1B; AT5G06110.1) were repressed in the wild-type after heat-acclimatization phase. In the mutant, both these proteins were already maintained at a lower level and did not decline after treatment (Figure S2C). Similar accumulation pattern was observed for the CBS DOMAIN CONTAINING PROTEIN 2 (CBSX2). CBSX2 regulates thioredoxins which participate in the cellular redox system (Yoo et al., 2011). In contrast, several proteins directly or indirectly implicated in the oxidative and/or heat stress response such as the PYRIMIDINE DEAMINASE (PYRD), GPX2, GSTT1, PER57 and HOP3 were induced in the wild-type plants following an exposure to 37°C and short recovery period, whereas, in the *arr3,4,5,6,8,9* mutant, the levels of these proteins under control condition were already high and did not change as much as wild-type upon the heat treatment (Fig S2C). Proteins such as DJ1A (involved in oxidative stress), GLYOXALASE12 (ATGLYI2) and Arabidopsis Aldehyde Oxidase2 (AAO2), on the other hand, exhibited opposite induction pattern in the wild-type and the *arr3,4,5,6,8,9* mutant. ATGLYI2 is the first enzyme of the glyoxalase pathway through which methylglyoxal (MG), a toxic byproduct of glycolysis is detoxified. MG levels rise under abiotic stress, therefore the higher abundance of ATGLYI2 in the *arr3,4,5,6,8,9* mutant could possibly improve their capacity to detoxify stress-induced MG. We extended this analysis to the quadruple mutant *arr5,6,8,9* and found out that similar to the hextuple mutant *arr3,4,5,6,8,9*, some heat-regulated proteins are already altered in this mutant, however, the number of such proteins was relatively lower compared to the hextuple mutant which is in line with our other observations about the intermediate position of the *arr5,6,8,9* in the HSR and proteomic changes (Figure S3). Collectively, these results identified that the lack of functional type-A ARRs induces similar proteomic changes as that of a heat-acclimatization phase in wild-type for several proteins involved in heat and oxidative stress.

Metabolic responses due to elevated temperatures

Determination of the changes in metabolite dynamics provides a more conclusive picture of the physiological reprogramming in a system-wide manner. Therefore, we determined the changes in non-polar and polar metabolites accumulation in the Arabidopsis seedlings. We used the same samples which were used for proteomics analyses in which 7 DAS seedlings were subjected to a heat-acclimatization phase and mapped 60 polar and 36 non-polar metabolites. Our analysis revealed that a mild heat treatment/heat-acclimatization does not reflect at the level of metabolites in any genotype probably either because a brief exposure of 1 h at 37°C was too subtle to bring about a metabolomic response or due to the reason that we monitored only the rapidly induced metabolic changes as we harvested the samples after 2 h of recovery at 21°C. Nonetheless, we extended our analysis at higher temperature stress at 45°C with and without the acclimatization phase. Among the polar metabolites, we found out that, several sugars, sugar alcohols, amino acids and amines were promptly accumulated in response to severe heat stress irrespective of the acclimatization phase and genotype, however, this response was similar in the wild-type and the mutants (Figure S4A, B). As a biochemical response to HS, sugars are known to accumulate due to their osmoprotectant function (Melandri et al., 2021), and this observation validates our HS application. Among the non-polar metabolites that we mapped, an interesting observation was the higher accumulation of protective compounds α- and γ-tocopherols in both *arr5,6,8,9* and *arr3,4,5,6,8,9* mutants (Figure 5). To get a closer insight into the preferential accumulation of α- and γ-tocopherols in the *arr* mutants, we determined transcript levels of genes involved in tocopherol biosynthesis (Figure S5). The higher levels of α- and γ-tocopherols in the *arr* mutants correlated with the up-regulation of *VTE2, VTE3* and *VTE1* in the *arr3,4,5,6,8,9* mutant. *VTE2*, *VTE3* and *VTE1* encode the enzymes HGA phytyltransferase, a methyltransferase and a tocopherol cyclase, respectively, and due to their higher expression, the metabolic flux is probably directed more preferentially towards the biosynthesis of α- and γ-tocopherols. Similar to the proteomics data, *arr5,6,8,9* accumulated intermediate levels of α- and γ-tocopherols as compared to the wild-type and *arr3,4,5,6,8,9*. This trend was observed in all the temperature conditions and both the mutants accumulated higher amounts of α- and γ-tocopherols. α-tocopherol is known for its antioxidant activity and prevents lipid peroxidation by scavenging lipid peroxyl radicals in thylakoid membranes thus protecting the photosynthetic apparatus, while γ-tocopherol is predominantly found in the seeds and can be functionally replaced for α-tocopherols (Munné-Bosch, 2005; Munné-Bosch, 2019). A higher accumulation of tocopherols in the *arr* mutants is a strong indication of higher antioxidant capacity and supports our proteomics data. Taken together, our analyses revealed that heat

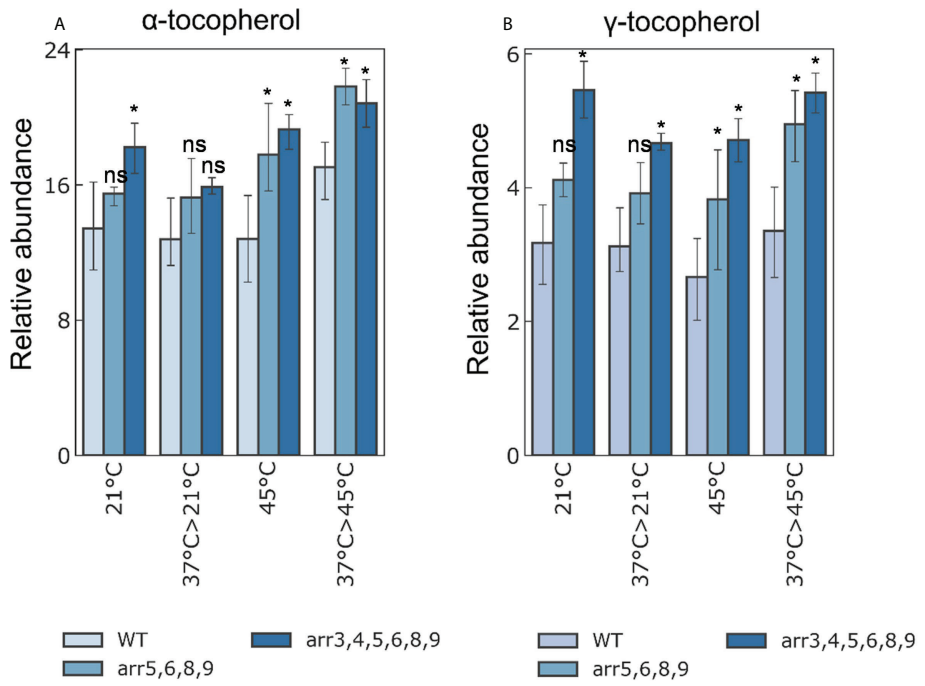

FIGURE 5
Relative accumulation of **(A)** α- and **(B)** γ-tocopherols under different temperature conditions. The 7 DAS seedlings were treated at different heat-stress conditions and samples were harvested for metabolomics analyses (21°C: Control; 37°C>21°C: 37°C for 1 h followed by 2 h recovery at 21°C; 45°C: 45°C for 2.5 h; 37°C>45°C: 37°C for 1 h followed by 2 h recovery at 21°C and 45°C for 2.5 h). The bars shown are the average of four biological replicates. Error bars represent ± SE (two-way ANOVA, *P-value ≤ 0.05, Bonferroni *post-hoc* test, n=3, 13-15 plants were taken for each biological replicate, ns not significant). The statistical differences shown in the graphs are the comparison of the *arr* mutants with respect to WT in the respective treatment group. A detailed overview of all the analyzed metabolites is given in Supplementary Figure S4. The tocopherol biosynthetic pathway and the relative expression levels of the pathway genes are shown in Supplementary Figure S5.

stress does not differentially induce the metabolomic changes in the *arr* mutants, however, we found out that the mutants accumulate higher amounts of protective antioxidant compound.

The type-A *arr* mutants show altered response to oxidative stress conditions

Our proteomics and metabolomics results strongly suggested links between the type-A ARRs and the redox-regulation machinery due to which the type-A *arr* mutants can better cope the heat stress-induced oxidative burst. We, therefore, tested the effect of direct oxidative stress on the plants by transferring the seedlings in the medium supplemented with various concentrations of hydrogen peroxide (1.0, 1.5, 4.5 mM H_2O_2) and methyl viologen (0.1, 0.5, 1.0 μM MV), an herbicide that induces ROS formation. We sealed the plates with parafilm and cling film to allow the accumulation of ROS. As the behavior of both the mutants were similar, we conducted this experiment on the higher order *arr3,4,5,6,8,9* mutant. As we anticipated, the *arr3,4,5,6,8,9* mutant exhibited an altered response to oxidative stress conditions after prolonged growth in the same sealed plates. We did not observe any difference in the physiological response of the mutant seedlings at the lower concentrations of MV. The highest tested concentration 1 μM MV was extremely inhibitory for all the seedlings, however, in our visual assessment, we observed that the *arr* mutant accumulated higher anthocyanins in the leaves and showed reduced chlorosis as compared to the wild-type. Further, under 1.5 μM H_2O_2, mutant plants exhibited a more robust root system and stress-induced flowering was delayed as compared to the wild-type (Figures 6A, S6).

In our GO enrichment analyses of the differentially accumulated proteins, we found an enrichment of the proteins functioning in 'sulfur compound metabolic processes' and 'oxidative stress' in the *arr* mutant. For example, GPX2, GSTT1, GSTU1, glutaredoxin and thioredoxin family proteins were differentially accumulated in the absence of functional type-A ARRs. Literature evidence also suggests that CKs can mediate the ascorbate-glutathione (ASC-GSH) pathway which are in the core of the redox hub (Foyer and Noctor, 2011; Porcher et al., 2021). This promoted us to ask if the type-A ARRs are also involved in the ascorbic acid-glutathione (AsA-GSH) pathway. We estimated the glutathione (GSH/GSSG) and ascorbate (ASC/

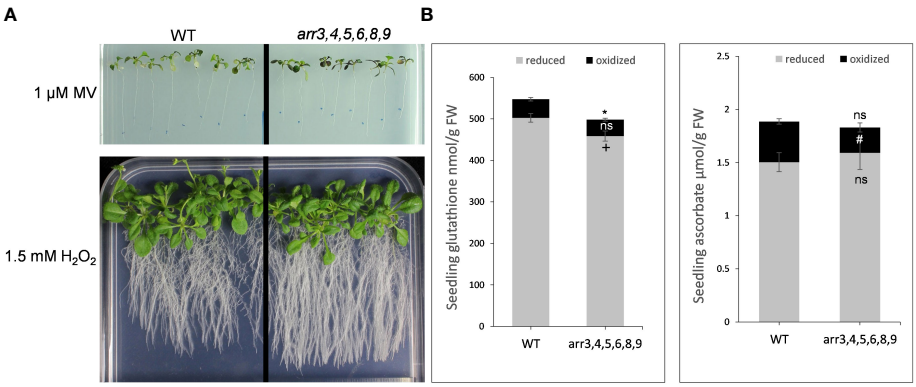

FIGURE 6
Oxidative stress response and cellular redox alterations in the absence of functional type-A ARRs. **(A)** Phenotypic response of Arabidopsis seedlings under oxidative stress conditions. 7 DAS seedlings grown on 0.5 X MS medium were transferred to the medium containing methyl viologen (MV) or H_2O_2. The images are captured after 2 weeks (for MV treatment) and 3 weeks (for H_2O_2 treatment) of transfer to the media containing MV or H_2O_2. The treatments were carried out in 4 biological replicates. **(B)** Glutathione and ascorbate content in WT and *arr3,4,5,6,8,9* mutant. Grey bars indicate the reduced forms of glutathione (GSH) or ascorbate (ASC) content, and black bars indicate the oxidized forms glutathione disulfide (GSSG) or dehydroascorbate (DHA). Average from four biological replicates are shown and the error bars indicate ± SE. Asterisk indicates a significant difference in total glutathione and ascorbate, + indicates a significant difference in reduced forms, and # indicates a significant difference in the oxidized forms between the wild-type and *arr* mutant P-value ≤ 0.05. ns, non-significant.

DHA) contents in 10 DAS wild-type and *arr3,4,5,6,8,9* seedlings. We found out that the level of total and reduced glutathione was lower in the *arr* mutant as compared to the wild-type (Figure 6B). While there was no significant difference in the level of total ascorbate, the oxidized form was significantly lower in the *arr* mutant compared to the wild-type (Figure 6B). These results, together with the metabolomic studies indicated that the type-A ARRs modulate the dynamics of the AsA-GSH-tocopherol triad.

Discussion

In this study, we identified the role of type-A ARRs in plant HSR. Several studies have previously indicated the involvement of CKs in abiotic stress responses. CK levels and stress conditions are shown to mutually affect each other. For example, high or low temperature stresses have been reported to modulate the endogenous CK levels (Hare et al., 1997; Todorova et al., 2005; Todaka et al., 2017; Prerostova et al., 2020) and, at the same time, exogenous or endogenous increase in the CK levels can improve antioxidant capacity in plant (Xu et al., 2016; Hönig et al., 2018; Berka et al., 2020). It is also reported that the molecular responses to heat and CK overlap (Černý et al., 2014). However, how various CK signaling components participate in the HSR is currently not known. Here, we show that the type-A ARRs negatively regulate HSR by altering the redox state of the plant.

While individual ARRs might have evolved to perform specialized functions, they are known to function in a partly redundant manner (To et al., 2004; Salomé et al., 2006). We observed that the physiological responses of the quadruple mutant were also subtle in comparison to the hextuple mutant. Notably, long-term exposure to sub-lethal temperature proved to be lethal for the wild-type, partial chlorosis was apparent in *arr5,6,8,9* mutant and *arr3,4,5,6,8,9* mutant recovered without any significant damage. Chlorosis is a part of leaf senescence. Heat-induced leaf senescence is stimulated by heat-induced levels of abscisic acid (ABA) and inhibited by type-B ARRs (Zhang et al., 2017). Activity of type-B ARRs is inhibited by a negative feedback regulation *via* type-A ARRs which is reflected in increasing sensitivity to CK in higher order type-A *arr* mutants (To et al., 2004). Thus, the absence of any significant heat-induced leaf senescence in *arr3,4,5,6,8,9* mutant might result from the highest activity of type-B ARRs fully counteracting ABA-induced senescence. Similarly, in our proteomics analyses, the number of DAPs and the extent of accumulation of certain DAPs was intermediate in the *arr5,6,8,9* mutant as compared to the wild-type and the *arr3,4,5,6,8,9* mutant. Such kind of additive effect is largely common for the members of a gene family. For example, the triple mutations in the type-B *ARR* genes cause a more prominent effect on drought tolerance as compared to double gene mutations (Nguyen et al., 2016).

Our proteomics analyses revealed that several proteins involved in the growth, metabolism, and stress responses were altered in the mutants lacking the type-A *ARR* genes and the hextuple *arr* mutant sported a strikingly similar proteomic landscape that the wild-type plants acquire upon heat-

acclimatization. This indicates the preparedness of these mutants to face the high temperature challenge. For example, higher accumulation of a riboflavin biosynthetic enzyme PYRD in the *arr3,4,5,6,8,9* mutant could positively affect the riboflavin content. Riboflavin acts as a stress-priming compound in plants and possesses antioxidant properties, and its moderately increased levels have been associated with the improved AOS and drought tolerance in Arabidopsis (Deng et al., 2014). Further, peroxidases/glutathione peroxidases (GPXs) and glutathione S-transferases (GSTs) are well-recognized for their positive role in abiotic stress tolerance due to their ROS-scavenging activity and thus they play important roles in determining cellular redox environment (Roxas et al., 1997; Liu et al., 2013; Zhang et al., 2019). Mostly higher accumulation of ferredoxin/thioredoxin family protein, peroxidase family protein, GPX2, GSTT1, GSTU1, NADH dehydrogenase-related protein and superoxide dismutase protein in one or both the *arr* mutants indicates and altered cellular redox environments in these mutants. Similarly, PMRSs that are present in all the sequenced organisms, repair oxidatively damaged proteins (Gustavsson et al., 2002; dos Santos et al., 2005). It is important to note that PMSR is referred as one of the minimal set of proteins sufficient for cell life (Mushegian and Koonin, 1996), highlighting its important position. The HOP family proteins work as cytosolic co-chaperones and play a major role in long-term acquired thermotolerance. The most heat-regulated of these is the HOP3 (Fernández-Bautista et al., 2018). The proteins discussed here are accumulated in higher amounts in one or both the type-A *arr* mutants even under control conditions. In addition, two cell-division and meristem development-related proteins PHB4 and ZRF1B are repressed upon heat-acclimatization in the wild-type plants. The already low level of these two proteins in the *arr3,4,5,6,8,9* mutant could be a contributing factor to the higher resistance of the mutant under heat stress as moderation of cell-division is an adaptive feature in fluctuating environments (Zhang et al., 2020). Taken together, our results indicated that the cellular environment of the *arr* mutants is more protective against the heat stress-induced oxidative damage, and it could be the major contributing factor for its improved theromotolerance in addition to the cell-cycle moderation. It will be interesting to further explore the molecular connections between the type-A ARRs and the proteins involved in heat-acclimatization process.

NADH dehydrogenases are important components of the electron transport chain in all the organisms. NADH dehydrogenase as well as NADH-dependent reductases are involved in the maintenance of the redox state (Schertl and Braun, 2014; Hyun and Lee, 2015). In our proteomics analyses, we found that 2 NADH dehydrogenases (FRO1 and AT4G02580.1) and a NADH-dependent reductase, CBR2 show differential accumulation upon heat-acclimatization in the *arr* mutant as compared to the wild-type. FRO1, also known as NDUFS4 is an NADH-ubiquinone oxidoreductase-like protein and mutation in the gene encoding this protein leads to constitutively reduced phosphorylation efficiency. The cellular metabolism adapts to this situation and provides moderate stress tolerance to plants (Meyer et al., 2009). In our analysis, heat-acclimatization leads to reduction in the level of FRO1 in the wild-type, whereas it is maintained at lower levels in the *arr* mutant indicating a preset adaptability in the mutant.

Tocopherols, commonly referred as vitamin E, are implicated in several abiotic stresses (Munné-Bosch, 2019). The Arabidopsis *vte1* and *vte4* mutants which are deficient in α-and γ-tocopherols show increased sensitivity to salt stress and accumulate higher levels of H_2O_2 and malondialdehyde (MDA) (Ellouzi et al., 2013). Increasing the levels of tocopherols through alteration in the biosynthetic pathway has been shown to improve the antioxidant capacity and abiotic stress tolerance in plants (Kanwischer et al., 2005; Abbasi et al., 2007; Yusuf et al., 2010; Ma et al., 2020). The higher accumulation of the tocopherols in the type-A *arr* mutants under unstressed as well as heat stress conditions is certainly an important feature by which the mutants resist or overcome the heat stress-induced damage. The quantitative effect on the *arr* quadruple and hextuple mutants on the accumulation of tocopherols indicate that the type-A ARRs regulate tocopherol biosynthesis in a functionally redundant manner. Our relative gene expression profiling of the tocopherol biosynthesis pathway genes reveals that *VTE2*, *VTE3* and *VTE1* are up-regulated in the *arr3,4,5,6,8,9* mutant and more studies in this direction will be interesting to dissect the type-A ARR control over the tocopherol biosynthesis.

Glutathione and ascorbate are widely known for their positive effect on various abiotic stress conditions and in maintaining redox homeostasis (Foyer and Noctor, 2011; Kerchev and van Breusegem, 2022). Glutathione is a major non-protein sulfur-containing compound. In our proteomics analysis, we found an enrichment of the proteins related to sulfur compound metabolic process in the type-A *arr* mutant. Our biochemical assays revealed that the total glutathione levels were lower in the *arr* mutant. While this observation seems counterintuitive because glutathione has a protective role in oxidative stress, we can assume that the type-A ARRs regulate the ASC-GSH-tocopherol axes in a selective manner. In line with our results, it has been shown previously that the overall antioxidant capacity is reduced in the plants with reduced CK-status due to mutation in CK receptor *AHK* genes and induction of CK degradation (Cortleven et al., 2014). In addition, in our independent study (in-communication), we found out that the activation of CK signaling differentially regulates the sulfur-starvation marker genes and is accompanied by a decrease in sulfate and GSH levels. In contrast, CK-deficient mutants were found to maintain higher GSH content and displayed enhanced tolerance to GSH-depleting agents in root growth assay strongly suggesting a CK-sulfur interplay in regulating plant

growth and stress responses. In the CK-deficient line *35S:CKX4*, which have increased CK degradation, accumulated higher amount of glutathione in control conditions and has almost no difference in the level of ascorbate. However, it had overall lower antioxidant capacity because of the different status of other antioxidant compounds (Cortleven et al., 2014). This indicates the negative impact of the CK-status on the glutathione accumulation. The precise functions of the CK signaling components in the antioxidant system and abiotic stress protection are yet to be defined, nonetheless, our study provides a starting point to unravel the molecular basis of the role of CK signaling in high temperature stress responses.

Photosynthetic pigment contents are known to drop in response to heat stress (García-Plazaola et al., 2017; Wang et al., 2018). Therefore, the pigment contents and their ratios can serve as indicators of stress tolerance. In our study, no statistically significant difference in chlorophyll and carotenoid contents was found between the wild-type and *arr* mutants under control conditions. However, the pigments were retained in the *arr* mutants at higher levels following heat stress treatments in accordance with the sensitized CK signaling in these mutants. The increase in pigment retention was further enhanced in acclimatized *arr* mutants. Previously, stimulation of CK biosynthesis was shown to result in increased contents of chlorophyll *a* and *b*, and carotenoids in transgenic tobacco (Cortleven and Valcke, 2012). Higher chlorophyll *a* retention in the *arr* mutants is in line with a finding in rice where CK treatment was shown to delay dark-induced senescence by accumulation of 7-hydroxymethyl chlorophyll, a precursor of chlorophyll *a*, and up-regulation of genes of the chlorophyll cycle which converts chlorophyll *a* to chlorophyll *b*, thereby maintaining chlorophyll *a*/*b* ratio (Talla et al., 2016). The higher retention of chlorophyll *a*/*b* ratio might indicate lower content of light-harvesting chlorophyll *a*/*b*-binding proteins (LHC) associated with PSII (LHCII) to transfer excitation energy to the PSII core complex (Xu et al., 1995). The decrease in LHCII resulting in reduction of light absorption cross-section of photosystems is an essential protection mechanism which allows plants to survive unfavorable conditions (Lichtenthaler, 1987; Špundová et al., 2003). Further, it is well established that carotenoid functions other than to light harvesting include photoprotection by either protecting photosynthetic systems against ROS or singlet energy dissipation by non-photochemical quenching (Young and Young, 1991; Loggini et al., 1999; Caffarri et al., 2001). Thus, the sensitized CK signaling in the type-A *arr* mutants contributes to both basal and acquired thermotolerance in Arabidopsis, at least partly, *via* suppression of heat-induced leaf senescence through stimulation of chloroplast protection or recovery and by enhancing the pool of low molecular weight antioxidants through increased carotenoid content.

Materials and methods

Plant material and growth conditions

The *Arabidopsis thaliana* Columbia-0 (Col-0) ecotype was used as wild-type control for all experiments. The quadruple mutant *arr5,6,8,9* and hextuple mutant *arr3,4,5,6,8,9* both are in the Col-0 background. The *arr5,6,8,9* (N25277) and *arr3,4,5,6,8,9* (N25279) mutant lines were obtained from NASC. The seeds were surface sterilized and stratified in dark for 3 days at 4°C and grown on 0.5X Murashige & Skoog medium (pH: 5.7) supplemented with 1% w/v sucrose and 0.8% w/v agar at 21°C and long day conditions (16 h light, 60 µmol m^{-2} s^{-1} PPFD provided by Philips TL-D fluorescent tubes) in a climate-controlled growth chamber (AR36LX, Percival, http://www.percival-scientific.com/) with 70% relative humidity. This media composition and growth conditions are used in all the experiments unless specified. The experiments on adult stages were performed in 5 cm tall pots filled with soil and perlite (1:1).

Stress treatments

For thermotolerance assay, the seedlings were initially grown at standard conditions as mentioned above for 7 days unless specified. To assess basal and acquired thermotolerance, we conducted experiments on two separate groups namely non-acclimatized and acclimatized. The seedlings of non-acclimatized group were treated with a lethal temperature 45°C for 2.5 h followed by recovery for 3-7 days at standard growth conditions. The acclimatized group was first exposed to a sub-lethal temperature 37°C for 1 h to initiate an acclimatory response, followed by 2 h of recovery at 21°C then transferred to 45°C for 2.5 h and subsequently allowed to recover along with the non-acclimatized group. The heat treatments were carried out in an incubator (BINDER GmBH, Germany) with the same light quantity as in the control conditions. A control group was grown in parallel at standard growth conditions. To access the effect of extended exposure at sub-lethal temperatures, wild-type and mutant seedlings were grown in the same plates for 10 days after stratification and then kept at 37°C for 3 days and returned to standard growth conditions. HS on the 18 DAS soil-grown plants was applied at 45°C for 4 h.

The oxidative stress treatment was carried out by transferring the 7 DAS seedlings to the media containing methyl viologen (0.1, 0.5 and 1 µM), and H_2O_2 (1.0, 1.5 and 4.5 µM). The plates were sealed with parafilm to maintain the oxidative environment and allowed to grow at standard growth conditions. The images were captured using Canon EOS 600D camera.

Measurement of stress-regulated biomass accumulation and content of photosynthetic pigments

The fresh weight of seedlings was measured on a microbalance. For chlorophyll and carotenoid estimation, the seedlings were placed in 80% (v/v) acetone at 4°C for overnight in the dark. Cell debris was pelleted by centrifugation at 7800 g for 10 min and the amount of chlorophyll *a* (12.21×A663-2.81×A646), chlorophyll *b* (20.13×A646-5.03×A663) and carotenoids [(1000×A470-1.82×Chl*a*-85.02×Chl*b*)/198] was measured at the wavelengths 663 and 646 and 470 nm using a spectrophotometer (Lichtenthaler and Wellburn, 1983; Lichtenthaler and Buschmann, 2001). The total amount of chlorophyll (Chl*a* + Chl*b*) and carotenoids was then quantified and normalized per seedling. For phenotypic analysis, the digital images were captured using Canon EOS 600D camera.

Metabolite extraction and GC-MS analysis

Arabidopsis seedlings were grown and treated as mentioned in the thermotolerance assay. An equal amount of plant tissue (50 mg) was harvested in four biological replicates. Samples were extracted in precooled MTBE : MeOH (3:1, v:v) mixture, spiked with 0.05 µg ml^{-1} of valine C13 and the extracts were vortexed followed by ice-cooled sonication for 15 min. The samples were centrifuged for 10 min at 17,000 g at 4°C and the supernatant was transferred to the new 2 ml microcentrifuge tubes and maintained on ice. An equal volume of H_2O:MeOH (3:1, v:v) was added and the samples were vortexed and finally centrifuged for 10 min at 17000 g at 4°C. Two aliquots from polar and nonpolar phase (100 µl) were taken to dryness in a speed vacuum concentrator and the dried residues were redissolved and derivatized for 90 min in 20 µL of 40 mg mL^{-1} O-methylhydroxyamine hydrochloride in pyridine at 30°C with continuous shaking. Next, 80 µL N-methyl-N-(trimethylsilyl) trifluoroacetamide was added and the mixture was incubated for additional 30 min at 37°C with continuous shaking. Gas chromatography-mass spectrometry was carried out on a Q Exactive GC Orbitrap GC-tandem mass spectrometer coupled to a Trace 1300 Gas chromatograph (Thermo Fisher Scientific, Waltham, MA, USA). The injector operated in a split mode (inlet temperature 250°C, split ratio 5, purge flow 5.0 mL/min, split flow 6.0 mL/min). Metabolites were separated on a TG-5SILMS GC Column (Thermo Fisher, 30 m × 0.25 mm × 0.25 µm) with helium as a carrier gas at a constant flow of 1.2 mL/min using a 28 min gradient (70°C for 5 min followed by 9°C per min gradient to 320°C and finally 10 min hold time) and ionized using electron ionization mode (electron energy 70 eV, emission current 50 µA, transfer line and ion source temperature 250°C). Mass spectra were recorded by scanning the range of 50 to 750 m/z. Chromatograms were analyzed using TraceFinder 4.1 with Deconvolution Plugin 1.4 (Thermo), Compound Discover (Thermo) and searched against the NIST2014, GC-Orbitrap Metabolomics library, and in-house library. Only metabolites fulfilling identification criteria (score ≥ 75 and ΔRI< 2%) were included in the final list. Quantitative differences were determined by manual peak assignment in Skyline 20.1, using extracted ion chromatograms (2 ppm tolerance).

Protein extraction and LC-MS analysis

The pellet from the MTBE: MeOH (3:1, v:v) extracted plant sample from metabolite extraction was further used for protein extraction. The pellet was washed with 0.5 ml of MeOH, lyophilized, and resuspended in 0.2-0.5 ml of protein extraction buffer consisting of 8M urea and 100mM ammonium bicarbonate at room temperature until dissolved. Next, aliquots corresponding to 100 µg of protein were reduced, alkylated with iodoacetamide, digested with trypsin (1:100, Promega) and desalted by C18 SPE. Finally, aliquots corresponding to 2.5 µg of peptide were analyzed by nanoflow C18 reverse-phase liquid chromatography using a 15 cm column (Zorbax, Agilent), a Dionex Ultimate 3000 RSLC nano-UPLC system (Thermo) and the Orbitrap Fusion Lumos Tribrid Mass Spectrometer, as described previously (Kameniarová et al., 2022; Saiz-Fernández et al., 2022). The measured spectra were recalibrated and searched against Araport 11 protein database by Proteome Discoverer 2.5, employing Sequest HT and MS Amanda 2.0 with the following parameters: Enzyme-trypsin, max two missed cleavage sites; MS1 tolerance-5 ppm; MS2 tolerance-15 ppm (MS Amanda), 0.1 Da (Sequest, Mascot); Modifications-carbamidomethyl (Cys) and up to three dynamic modifications including Met oxidation, Asn/Gln deamidation, N-terminal acetylation. Only proteins with at least two unique peptides were considered for the quantitative analysis. The resulting data were normalized and analyzed using MetaboAnalyst 5.0 online tool (Xia et al., 2009; Pang et al., 2021). The mass spectrometry proteomics data have been deposited to the ProteomeXchange Consortium *via* the PRIDE (Perez-Riverol et al., 2022) partner repository with the dataset identifier PXD034173

RNA isolation and qRT-PCR analysis

Total RNA was isolated by using RNeasy Plant Mini Kit (Qiagen). The RNA quality and quantity were assessed by NanoDrop 2000 spectrophotometer (Thermo Fisher Scientific, USA). cDNA was prepared using 1.0 µg of total RNA using RevertAid Reverse Transcriptase (Thermo Fisher Scientific, USA). qRT-PCR analysis was performed with 1:10 diluted cDNA samples using Luna® Universal qPCR Master Mix (New England Biolabs) on LightCycler 480 II (Roche, Germany) Real-Time PCR System. The primers used were designed using QuantPrime qPCR primer design tool (Arvidsson et al., 2008). The primers are listed in Supplementary Table S6. The relative quantification of mRNA level was calculated using the ΔΔCT method (Livak and Schmittgen, 2001).

Quantification of glutathione and ascorbate

The levels of glutathione and ascorbate were measured by the method described by (Queval and Noctor, 2007). Briefly, approximately 100 mg tissue derived from the whole seedlings grown under standard growth conditions was homogenized in 0.2 M HCl. After centrifugation, the pH of the resulting supernatant was adjusted to 5.0 by sodium phosphate buffer and 0.2 M NaOH. The total and oxidized glutathione and ascorbate were then quantified by the plate-reader assay.

Data availability statement

The datasets presented in this study are publicly available at the ProteomeXchange repository with the accession number: PXD034173, http://proteomecentral.proteomexchange.org/cgi/GetDataset?ID=PXD034173.

Author contributions

SJ, BB, and AL conceived the study. SJ, BB, and PK designed experiments. SJ and HKB performed thermotolerance assays. SJ, PK, and MČ performed proteomics studies and analysed data. SJ, PK, and MB performed metabolomics study. SJ performed all other experiments. SJ wrote the paper and BB and MČ reviewed the paper. BB and SJ revised the manuscript. BB acquired funding. All authors have read and agreed to the published version of the manuscript.

Funding

This work was supported by Ministry of Education, Youth and Sports of the Czech Republic (European Regional Development Fund-Project "Centre for Experimental Plant Biology" (Grant no. CZ.02.1.01/0.0/0.0/16_019/0000738) and the Internal Grant Schemes of Mendel University in Brno. Reg. no. CZ.02.2.69/0.0/0.0/19_073/0016670, funded by the ESF.

Conflict of interest

The authors declare that the research was conducted in the absence of any commercial or financial relationships that could be construed as a potential conflict of interest.

Publisher's note

All claims expressed in this article are solely those of the authors and do not necessarily represent those of their affiliated organizations, or those of the publisher, the editors and the reviewers. Any product that may be evaluated in this article, or claim that may be made by its manufacturer, is not guaranteed or endorsed by the publisher.

Supplementary material

The Supplementary Material for this article can be found online at: https://www.frontiersin.org/articles/10.3389/fpls.2022.968139/full#supplementary-material

References

Abbasi, A. R., Hajirezaei, M., Hofius, D., Sonnewald, U., and Voll, L. M. (2007). Specific roles of α- and γ-tocopherol in abiotic stress responses of transgenic tobacco. *Plant Physiol.* 143, 1720–1738. doi: 10.1104/PP.106.094771

Abdelrahman, M., Ishii, T., El-Sayed, M., and Tran, L.-S. P. (2020). Heat sensing and lipid reprograming as a signaling switch for heat stress responses in wheat. *Plant Cell Physiol.* 61, 1399–1407. doi: 10.1093/pcp/pcaa072

Arvidsson, S., Kwasniewski, M., Riaño-Pachón, D. M., and Mueller-Roeber, B. (2008). QuantPrime - a flexible tool for reliable high-throughput primer design for quantitative PCR. *BMC Bioinf.* 9, 1–15. doi: 10.1186/1471-2105-9-465

Berka, M., Luklová, M., Dufková, H., Berková, V., Novák, J., Saiz-Fernández, I., et al. (2020). Barley root proteome and metabolome in response to cytokinin and abiotic stimuli. *Front. Plant Sci.* 11. doi: 10.3389/FPLS.2020.590337

Bindea, G., Mlecnik, B., Hackl, H., Charoentong, P., Tosolini, M., Kirilovsky, A., et al. (2009). ClueGO: a cytoscape plug-in to decipher functionally grouped gene ontology and pathway annotation networks. *Bioinformatics* 25, 1091. doi: 10.1093/BIOINFORMATICS/BTP101

Bryksová, M., Hybenová, A., Hernándiz, A. E., Novák, O., Pěnčík, A., Spíchal, L., et al. (2020). Hormopriming to mitigate abiotic stress effects: A case study of N9-substituted cytokinin derivatives with a fluorinated carbohydrate moiety. *Front. Plant Sci.* 11. doi: 10.3389/fpls.2020.599228

Caffarri, S., Croce, R., Breton, J., and Bassi, R. (2001). The major antenna complex of photosystem II has a xanthophyll binding site not involved in light harvesting. *J. Biol. Chem.* 276, 35924–35933. doi: 10.1074/JBC.M105199200

Černý, M., Dyka, F., Bobál'Ová, J., and Brzobohatý, B. (2011). Early cytokinin response proteins and phosphoproteins of arabidopsis thaliana identified by proteome and phosphoproteome profiling. *J. Exp. Bot.* 62, 921–937. doi: 10.1093/jxb/erq322

Černý, M., Jedelský, P. L., Novák, J., Schlosser, A., and Brzobohatý, B. (2014). Cytokinin modulates proteomic, transcriptomic and growth responses to temperature shocks in arabidopsis. *Plant Cell Environ.* 37, 1641–1655. doi: 10.1111/pce.12270

Cortleven, A., Nitschke, S., Klaumünzer, M., AbdElgawad, H., Asard, H., Grimm, B., et al. (2014). A novel protective function for cytokinin in the light stress response is mediated by the ARABIDOPSIS HISTIDINE KINASE2 and ARABIDOPSIS HISTIDINE KINASE3 receptors. *Plant Physiol.* 164, 1470–1483. doi: 10.1104/PP.113.224667

Cortleven, A., and Valcke, R. (2012). Evaluation of the photosynthetic activity in transgenic tobacco plants with altered endogenous cytokinin content: lessons from cytokinin. *Physiol. Plant* 144, 394–408. doi: 10.1111/J.1399-3054.2011.01558.X

Das, K., and Roychoudhury, A. (2014). Reactive oxygen species (ROS) and response of antioxidants as ROS-scavengers during environmental stress in plants. *Front. Environ. Sci.* 2. doi: 10.3389/FENVS.2014.00053/BIBTEX

Deng, B., Jin, X., Yang, Y., Lin, Z., and Zhang, Y. (2014). The regulatory role of riboflavin in the drought tolerance of tobacco plants depends on ROS production. *Plant Growth Regul.* 72 (3), 269–277. doi: 10.1007/S10725-013-9858-8

Devireddy, A. R., Zandalinas, S. I., Fichman, Y., and Mittler, R. (2020). Integration of reactive oxygen species and hormone signaling during abiotic stress. *Plant J*, 105, 459–476. doi: 10.1111/tpj.15010

dos Santos, C. V., Cuiné, S., Rouhier, N., and Rey, P. (2005). The arabidopsis plastidic methionine sulfoxide reductase b proteins. sequence and activity characteristics, comparison of the expression with plastidic methionine sulfoxide reductase a, and induction by photooxidative stress. *Plant Physiol.* 138, 909. doi: 10.1104/PP.105.062430

Ellouzi, H., Hamed, K. B., Cela, J., Müller, M., Abdelly, C., and Munné-Bosch, S. (2013). Increased sensitivity to salt stress in tocopherol-deficient arabidopsis mutants growing in a hydroponic system. *Plant Signaling Behav.* 8, 2.e23136. doi: 10.4161/PSB.23136

Fernández-Bautista, N., Fernández-Calvino, L., Muñoz, A., Toribio, R., Mock, H. P., and Castellano, M. M. (2018). HOP family plays a major role in long-term acquired thermotolerance in arabidopsis. *Plant Cell Environ.* 41, 1852–1869. doi: 10.1111/PCE.13326

Foyer, C. H., and Noctor, G. (2011). Ascorbate and glutathione: The heart of the redox hub. *Plant Physiol.* 155, 2–18. doi: 10.1104/PP.110.167569

García-Plazaola, J. I., Portillo-Estrada, M., Fernández-Marín, B., Kännaste, A., and Niinemets, Ü. (2017). Emissions of carotenoid cleavage products upon heat shock and mechanical wounding from a foliose lichen. *Environ. Exp. Bot.* 133, 87. doi: 10.1016/J.ENVEXPBOT.2016.10.004

Gustavsson, N., Kokke, B. P. A., Härndahl, U., Silow, M., Bechtold, U., Poghosyan, Z., et al. (2002). A peptide methionine sulfoxide reductase highly expressed in photosynthetic tissue in arabidopsis thaliana can protect the chaperone-like activity of a chloroplast-localized small heat shock protein. *Plant J.* 29, 545–553. doi: 10.1046/J.1365-313X.2002.029005545.X

Hare, P. D., Cress, W. A., and van Staden, J. (1997). The involvement of cytokinins in plant responses to environmental stress. *Plant Growth Regul.* 23, 79–103. doi: 10.1023/a:1005954525087

Hönig, M., Plíhalová, L., Husičková, A., Nisler, J., and Doležal, K. (2018). Role of cytokinins in senescence, antioxidant defence and photosynthesis. *Int. J. Mol. Sci.* 19 (12), 4045. doi: 10.3390/IJMS19124045

Hruz, T., Laule, O., Szabo, G., Wessendorp, F., Bleuler, S., Oertle, L., et al. (2008). Genevestigator v3: a reference expression database for the meta-analysis of transcriptomes. *Adv. Bioinf.* 2008, 1–5. doi: 10.1155/2008/420747

Hyun, D. H., and Lee, G. H. (2015). Cytochrome b5 reductase, a plasma membrane redox enzyme, protects neuronal cells against metabolic and oxidative stress through maintaining redox state and bioenergetics. *Age (Omaha)* 37, 1–14. doi: 10.1007/S11357-015-9859-9

Jamsheer K, M., Jindal, S., Sharma, M., Awasthi, P., Sreejath, S., Sharma, M., et al. (2022). A negative feedback loop of TOR signaling balances growth and stress-response trade-offs in plants. *Cell Rep.* 39, 110631. doi: 10.1016/J.CELREP.2022.110631

Kameniarová, M., Černý, M., Novák, J., Ondrisková, V., Lenka, H., Berka, M., et al. (2022). Light quality modulates plant cold response and freezing tolerance. *Front. Plant Sci* 13, 887103. doi: 10.3389/FPLS.2022.887103

Kanwischer, M., Porfirova, S., Bergmüller, E., and Dörmann, P. (2005). Alterations in tocopherol cyclase activity in transgenic and mutant plants of arabidopsis affect tocopherol content, tocopherol composition, and oxidative stress. *Plant Physiol.* 137, 713. doi: 10.1104/PP.104.054908

Kerchev, P. I., and van Breusegem, F. (2022). Improving oxidative stress resilience in plants. *Plant J.* 109, 359–372. doi: 10.1111/TPJ.15493

Lichtenthaler, H. K. (1987). [34] chlorophylls and carotenoids: Pigments of photosynthetic biomembranes. *Methods Enzymology* 148, 350–382. doi: 10.1016/0076-6879(87)48036-1

Lichtenthaler, H. K., and Buschmann, C. (2001). Chlorophylls and carotenoids: Measurement and characterization by UV-VIS spectroscopy. *Curr. Protoc. Food Analytical Chem.* 1, F4.3.1–F4.3.8. doi: 10.1002/0471142913.FAF0403S01

Lichtenthaler, H. K., and Wellburn, A. R. (1983). Determinations of total carotenoids and chlorophylls a and b of leaf extracts in different solvents. *Biochem. Soc. Trans.* 11, 591–592. doi: 10.1042/BST0110591

Liu, D., Liu, Y., Rao, J., Wang, G., Li, H., Ge, F., et al. (2013). [Overexpression of the glutathione s-transferase gene from pyrus pyrifolia fruit improves tolerance to abiotic stress in transgenic tobacco plants]. *Molekuliarnaia biologiia* 47, 591–601. doi: 10.7868/S0026898413040101

Livak, K. J., and Schmittgen, T. D. (2001). Analysis of relative gene expression data using real-time quantitative PCR and the 2-ΔΔCT method. *Methods* 25, 402–408. doi: 10.1006/meth.2001.1262

Loggini, B., Scartazza, A., Brugnoli, E., and Navari-Izzo, F. (1999). Antioxidative defense system, pigment composition, and photosynthetic efficiency in two wheat cultivars subjected to drought. *Plant Physiol.* 119, 1091–1100. doi: 10.1104/PP.119.3.1091

Ma, J., Qiu, D., Gao, H., Wen, H., Wu, Y., Pang, Y., et al. (2020). Over-expression of a γ-tocopherol methyltransferase gene in vitamin e pathway confers PEG-simulated drought tolerance in alfalfa. *BMC Plant Biol.* 20, 1–16. doi: 10.1186/S12870-020-02424-1/FIGURES/9

Melandri, G., Thorp, K. R., Broeckling, C., Thompson, A. L., Hinze, L., and Pauli, D. (2021). Assessing drought and heat stress-induced changes in the cotton leaf metabolome and their relationship with hyperspectral reflectance. *Front. Plant Sci.* 12. doi: 10.3389/FPLS.2021.751868/BIBTEX

Meyer, E. H., Tomaz, T., Carroll, A. J., Estavillo, G., Delannoy, E., Tanz, S. K., et al. (2009). Remodeled respiration in ndufs4 with low phosphorylation efficiency suppresses arabidopsis germination and growth and alters control of metabolism at night. *Plant Physiol.* 151, 603–619. doi: 10.1104/PP.109.141770

Moore, C. E., Meacham-Hensold, K., Lemonnier, P., Slattery, R. A., Benjamin, C., Bernacchi, C. J., et al. (2021). The effect of increasing temperature on crop photosynthesis: from enzymes to ecosystems. *J. Exp. Bot.* 72, 2822. doi: 10.1093/JXB/ERAB090

Munné-Bosch, S. (2005). The role of alpha-tocopherol in plant stress tolerance. *J. Plant Physiol.* 162, 743–748. doi: 10.1016/J.JPLPH.2005.04.022

Munné-Bosch, S. (2019). Vitamin e function in stress sensing and signaling in plants. *Dev. Cell* 48, 290–292. doi: 10.1016/J.DEVCEL.2019.01.023

Mushegian, A. R., and Koonin, E. V. (1996). A minimal gene set for cellular life derived by comparison of complete bacterial genomes. *Proc. Natl. Acad. Sci. U.S.A.* 93, 10268. doi: 10.1073/PNAS.93.19.10268

Nguyen, K. H., Ha, C., Nishiyama, R., Watanabe, Y., Leyva-González, M. A., Fujita, Y., et al. (2016). Arabidopsis type b cytokinin response regulators ARR1, ARR10, and ARR12 negatively regulate plant responses to drought. *Proc. Natl. Acad. Sci. U.S.A.* 113, 3090–3095. doi: 10.1073/pnas.1600399113

Pang, Z., Chong, J., Zhou, G., de Lima Morais, D. A., Chang, L., Barrette, M., et al. (2021). MetaboAnalyst 5.0: narrowing the gap between raw spectra and functional insights. *Nucleic Acids Res.* 49, W388–W396. doi: 10.1093/NAR/GKAB382

Perez-Riverol, Y., Bai, J., Bandla, C., García-Seisdedos, D., Hewapathirana, S., Kamatchinathan, S., et al. (2022). The PRIDE database resources in 2022: a hub for mass spectrometry-based proteomics evidences. *Nucleic Acids Res.* 50, D543–D552. doi: 10.1093/NAR/GKAB1038

Porcher, A., Guérin, V., Leduc, N., Lebrec, A., Lothier, J., and Vian, A. (2021). Ascorbate–glutathione pathways mediated by cytokinin regulate H2O2 levels in light-controlled rose bud burst. *Plant Physiol.* 186, 910–928. doi: 10.1093/PLPHYS/KIAB123

Prerostova, S., Dobrev, P. I., Kramna, B., Gaudinova, A., Knirsch, V., Spichal, L., et al. (2020). Heat acclimation and inhibition of cytokinin degradation positively affect heat stress tolerance of arabidopsis. *Front. Plant Sci.* 11. doi: 10.3389/fpls.2020.00087

Queval, G., and Noctor, G. (2007). A plate reader method for the measurement of NAD, NADP, glutathione, and ascorbate in tissue extracts: Application to redox profiling during arabidopsis rosette development. *Anal. Biochem.* 363, 58–69. doi: 10.1016/J.AB.2007.01.005

Roxas, V. P., Smith, R. K., Smith, R. K., and Allen, R. D. (1997). Overexpression of glutathione s-transferase/glutathioneperoxidase enhances the growth of transgenic tobacco seedlings during stress. *Nat. Biotechnol.* 15:10, 988–991. doi: 10.1038/nbt1097-988

Saiz-Fernández, I., Đorđević, B., Kerchev, P., Černý, M., Horta Jung, M., and Brzobohatý, B. (2022). Differences in the proteomic and metabolomic response during the early stages of phytophthora cinnamomi infection of two quercus species with contrasting degrees of susceptibility. *Front. Microbiol* 13, 894533. doi: 10.3389/FMICB.2022.894533

Salomé, P. A., To, J. P. C., Kieber, J. J., and McClung, C. R. (2006). Arabidopsis response regulators ARR3 and ARR4 play cytokinin-independent roles in the control of circadian period. *Plant Cell* 18, 55. doi: 10.1105/TPC.105.037994

Schertl, P., and Braun, H. P. (2014). Respiratory electron transfer pathways in plant mitochondria. *Front. Plant Sci.* 5. doi: 10.3389/FPLS.2014.00163/BIBTEX

Špundová, M., Popelková, H., Ilík, P., Skotnica, J., Novotný, R., and Nauš, J. (2003). Ultra-structural and functional changes in the chloroplasts of detached barley leaves senescing under dark and light conditions. *J. Plant Physiol.* 160, 1051–1058. doi: 10.1078/0176-1617-00902

Szymańska, R., Ślesak, I., Orzechowska, A., and Kruk, J. (2017). Physiological and biochemical responses to high light and temperature stress in plants. *Environ. Exp. Bot.* 139, 165–177. doi: 10.1016/J.ENVEXPBOT.2017.05.002

Talla, S. K., Panigrahy, M., Kappara, S., Nirosha, P., Neelamraju, S., and Ramanan, R. (2016). Cytokinin delays dark-induced senescence in rice by maintaining the chlorophyll cycle and photosynthetic complexes. *J. Exp. Bot.* 67, 1839–1851. doi: 10.1093/JXB/ERV575

Todaka, D., Zhao, Y., Yoshida, T., Kudo, M., Kidokoro, S., Mizoi, J., et al. (2017). Temporal and spatial changes in gene expression, metabolite accumulation and phytohormone content in rice seedlings grown under drought stress conditions. *Plant J.* 90, 61–78. doi: 10.1111/tpj.13468

Todorova, D., Genkov, T., Vaseva-Gemisheva, I., Alexieva, V., Karanov, E., Smith, A., et al. (2005). Effect of temperature stress on the endogenous cytokinin content in arabidopsis thaliana (L.) heynh plants. *Acta Physiologiae Plantarum* 27, 13–18. doi: 10.1007/S11738-005-0031-5

To, J. P. C., Haberer, G., Ferreira, F. J., Deruère, J., Mason, M. G., Schaller, G. E., et al. (2004). Type-a arabidopsis response regulators are partially redundant negative regulators of cytokinin signaling. *Plant Cell* 16, 658. doi: 10.1105/TPC.018978

Wang, Q. L., Chen, J. H., He, N. Y., and Guo, F. Q. (2018). Metabolic reprogramming in chloroplasts under heat stress in plants. *Int. J. Mol. Sci.* 19 (3), 849. doi: 10.3390/IJMS19030849

Wang, W., Vinocur, B., Shoseyov, O., and Altman, A. (2004). Role of plant heat-shock proteins and molecular chaperones in the abiotic stress response. *Trends Plant Sci.* 9, 244–252. doi: 10.1016/J.TPLANTS.2004.03.006

Xia, J., Psychogios, N., Young, N., and Wishart, D. S. (2009). MetaboAnalyst: a web server for metabolomic data analysis and interpretation. *Nucleic Acids Res.* 37, W652–W660. doi: 10.1093/NAR/GKP356

Xia, X. J., Zhou, Y. H., Shi, K., Zhou, J., Foyer, C. H., and Yu, J. Q. (2015). Interplay between reactive oxygen species and hormones in the control of plant development and stress tolerance. *J. Exp. Bot.* 66, 2839–2856. doi: 10.1093/jxb/erv089

Xu, Y., Burgess, P., Zhang, X., and Huang, B. (2016). Enhancing cytokinin synthesis by overexpressing ipt alleviated drought inhibition of root growth through activating ROS-scavenging systems in agrostis stolonifera. *J. Exp. Bot.* 67, 1979. doi: 10.1093/JXB/ERW019

Xu, Q., Paulsen, A. Q., Guikema, J. A., and Paulsen, G. M. (1995). Functional and ultrastructural injury to photosynthesis in wheat by high temperature during maturation. *Environ. Exp. Bot.* 35, 43–54. doi: 10.1016/0098-8472(94)00030-9

Yoo, K. S., Ok, S. H., Jeong, B. C., Jung, K. W., Cui, M. H., Hyoung, S., et al. (2011). Single cystathionine β-synthase domain-containing proteins modulate development by regulating the thioredoxin system in Arabidopsis. *Plant Cell* 23 (10), 3577–3594. doi: 10.1105/TPC.111.089847

Young, A. J., and Young, A. J. (1991). The photoprotective role of carotenoids in higher plants. *Physiologia Plantarum* 83, 702–708. doi: 10.1111/J.1399-3054.1991.TB02490.X

Yusuf, M. A., Kumar, D., Rajwanshi, R., Strasser, R. J., Tsimilli-Michael, M., Govindjee,, et al. (2010). Overexpression of gamma-tocopherol methyl transferase gene in transgenic brassica juncea plants alleviates abiotic stress: physiological and chlorophyll a fluorescence measurements. *Biochim. Biophys. Acta* 1797, 1428–1438. doi: 10.1016/J.BBABIO.2010.02.002

Zhang, J., Shi, Y., Zhang, X., Du, H., Xu, B., and Huang, B. (2017). Melatonin suppresion of heat-induced leaf senescence involves changes in abscisic acid and cytokinin biosynthesis and signaling pathways in perennial ryegrass (*Lolium perenne* L.). *Environ. Exp. Bot.* 138, 36–45. doi: 10.1016/j.envexpbot.2017.02.012

Zhang, L., Wu, M., Teng, Y., Jia, S., Yu, D., Wei, T., et al. (2019). Overexpression of the glutathione peroxidase 5 (RcGPX5) gene from rhodiola crenulata increases drought tolerance in salvia miltiorrhiza. *Front. Plant Sci.* 9. doi: 10.3389/FPLS.2018.01950/BIBTEX

Zhang, H., Zhao, Y., and Zhu, J. K. (2020). Thriving under stress: How plants balance growth and the stress response. *Dev. Cell* 55, 529–543. doi: 10.1016/J.DEVCEL.2020.10.012

Zwack, P. J., and Rashotte, A. M. (2015). Interactions between cytokinin signalling and abiotic stress responses. *J. Exp. Bot.* 66, 4863–4871. doi: 10.1093/jxb/erv172

frontiers | Frontiers in Plant Science

TYPE Original Research
PUBLISHED 29 September 2022
DOI 10.3389/fpls.2022.1014295

OPEN ACCESS

EDITED BY
Christine Helen Foyer,
University of Birmingham,
United Kingdom

REVIEWED BY
Tiago Santana Balbuena,
São Paulo State University, Brazil
Aakanksha Wany,
PP Savani University, India

*CORRESPONDENCE
Xuan Yao
xuanyao@mail.hzau.edu.cn

SPECIALTY SECTION
This article was submitted to Plant Abiotic Stress, a section of the journal Frontiers in Plant Science

RECEIVED 08 August 2022
ACCEPTED 08 September 2022
PUBLISHED 29 September 2022

CITATION
Yu L, Dai Z, Zhang Y, Iqbal S, Lu S, Guo L and Yao X (2022) Proteome-wide identification of S-sulfenylated cysteines reveals metabolic response to freezing stress after cold acclimation in *Brassica napus*. *Front. Plant Sci.* 13:1014295. doi: 10.3389/fpls.2022.1014295

Proteome-wide identification of S-sulfenylated cysteines reveals metabolic response to freezing stress after cold acclimation in *Brassica napus*

Liangqian Yu[1], Zezhang Dai[1], Yuting Zhang[1], Sidra Iqbal[1,2], Shaoping Lu[1], Liang Guo[1,3] and Xuan Yao[1,3]*

[1]National Key Laboratory of Crop Genetic Improvement, Huazhong Agricultural University, Wuhan, China, [2]Department of Plant Breeding and Genetics, University of Agriculture, Faisalabad, Pakistan, [3]Hubei Hongshan Laboratory, Wuhan, China

Redox regulation plays a wide role in plant growth, development, and adaptation to stresses. Sulfenylation is one of the reversible oxidative post-transcriptional modifications. Here we performed an iodoTMT-based proteomic analysis to identify the redox sensitive proteins *in vivo* under freezing stress after cold acclimation in *Brassica napus*. Totally, we obtained 1,372 sulfenylated sites in 714 proteins. The overall sulfenylation level displayed an increased trend under freezing stress after cold acclimation. We identified 171 differentially sulfenylated proteins (DSPs) under freezing stress, which were predicted to be mainly localized in chloroplast and cytoplasm. The up-regulated DSPs were mainly enriched in photosynthesis and glycolytic processes and function of catalytic activity. Enzymes involved in various pathways such as glycolysis and Calvin-Benson-Bassham (CBB) cycle were generally sulfenylated and the metabolite levels in these pathways was significantly reduced under freezing stress after cold acclimation. Furthermore, enzyme activity assay confirmed that the activity of cytosolic pyruvate kinase and malate dehydrogenase 2 was significantly reduced under H_2O_2 treatment. Our study provides a landscape of redox sensitive proteins in *B. napus* in response to freezing stress after cold acclimation, which proposes a basis for understanding the redox regulation in plant metabolic response to freezing stress after cold acclimation.

KEYWORDS

redox regulation, redoxome, sulfenylation, freezing stress, proteomics, *Brassica napus*

Introduction

Post-translational modifications (PTMs) of proteins are necessary for formation of mature proteins that ultimately accumulate in plant cells (Smith and Kelleher, 2013). PTMs can occur spontaneously or enzymatically, which depend on the physico-chemical properties of reactive amino acids and their environments such as pH, redox status, and metabolites (Ryšlavá et al., 2013). It is also an effective way that cells can rapidly regulate the activity, intracellular localization, stability of proteins and protein-protein interactions during metabolism, development and stress responses, representing some of the quick plant responses to environmental changes (Huber and Hardin, 2004; Friso and van Wijk, 2015; Millar et al., 2019). There are seven known oxidative modifications of cysteine, five of which are reversible (Held and Gibson, 2012). Among these reversible oxidations of cysteine, S-nitrosylation (SNO) and S-sulfenylation (SOH) play a significant role in regulating cellular signaling in response to redox imbalance. SNO is a covalent addition of nitroso group (-NO) onto the reduced thiol of cysteines. The common endogenous sources of nitroso group include the nitric oxide synthase (NOS) family of enzymes (Foster et al., 2009). Sulfenylation on thiol (SH) of cysteine by H_2O_2 is a common spontaneous form of PTMs to produce sulfenic acid (SOH), which is transiently stable and can be further overoxidated to sulfinic (SO_2H) and sulfonic (SO_3H) acids (Antelmann and Helmann, 2011; Paulsen and Carroll, 2013). Cysteine sulfenate is also an important intermediate in the formation of disulfides within or between proteins (Hogg, 2003). This kind of reversible oxidation can protect cysteine residues against irreversible overoxidation to the sulfinic and sulfonic acids by formation of disulfides with proteins, glutathione, or other redox PTMs like S-sulfyhydration (R-SSH) (Hochgräfe et al., 2007; Zivanovic et al., 2019). A systematic and exhaustive approach for identification of oxidized cysteine residues is defined as a redox proteomic or redoxome analysis (Chiappetta et al., 2010). 2DE separation-based and MS-based methods have been applied and developed in plant research for over a decade, which would help establish the network of cysteine residue oxidation and provide clues to uncover its mechanism (Wang et al., 2012; Liu et al., 2014; Zhu et al., 2014; Huang et al., 2019).

ROS also play a role in the regulation of metabolic fluxes during stresses to prevent the oxidative damage on cell (Choudhury et al., 2017). Metabolic pathways in plant are sensitive to environmental changes which mainly manifest in inhibited photosynthesis, and metabolic imbalances can promote the generation and accumulation of reactive oxygen species (ROS) (Suzuki et al., 2012; Poonam et al., 2015). Moreover, it is a common strategy for plants to survive in adversity by slowing down the growth, and this so-called 'active' growth inhibition is supposed to be obtained through cell signal transduction (Zhang et al., 2020). H_2O_2 functions as a signaling molecule and its role in controlling plant growth and development has been given more consideration (Htet et al., 2019; Nazir et al., 2020). It has been revealed that H_2O_2 improves the tolerance of plants to both drought and salt stresses, which enables the plants to memorize and rapidly activate early signals during re-exposure to the stresses (Ellouzi et al., 2017). Modification of cysteine thiols by redox substances has been known as an important signaling mechanism for conveying cellular responses (Finkel, 2003; Tonks, 2005). Both biotic and abiotic stresses can cause ROS production, leading to modification of cysteine oxidation profiles (Suzuki et al., 2012; McConnell et al., 2019; Mhamdi, 2019). Different abiotic stresses and their combinations probably cause the formation of different ROS signatures *via* different ROS sensors, which can create a stress-specific signal for plant adaptation to stresses (Choudhury et al., 2017). Freezing stress is one of the major abiotic stress factors affecting the over-wintering rate and yield of rapeseed (Sun et al., 2010). Freezing injury is the most immediate injury for leaves which are directly exposed to air temperatures (Cavender-Bares, 2007). Understanding the physiological and molecular mechanism of winter rapeseed (*Brassica napus* L.) in response to freezing stress is essential for the improvement of cold and freezing tolerance of *B. napus*. However, little is known about the complex regulatory mechanism of *B. napus* response to freezing stress.

Oxidized metabolites and proteins have been revealed to function in signaling under oxidative conditions (Mueller and Berger, 2009; Noctor and Foyer, 2016). In addition to modified proteins and metabolic fluxes, ROS and RNS induced by stresses also interact with plant hormones (Freschi, 2013; Mur et al., 2013; Choudhury et al., 2017). H_2O_2 induces the reversible oxidation of the BRASSINAZOLE-RESISTANT1 (BZR1) transcription factor, which mediates BR signaling to regulate plant development (Tian et al., 2018). A newly identified H_2O_2 receptor, HPCA1, encoding an LRR receptor kinase, activates Ca^{2+} channels by its oxidized extracellular cysteine residues to further regulate stomatal closure (Wu et al., 2020). The transcription factor bZIP68 plays an important role in plant growth and the adaption to stresses. Its inactivation can improve the resistance to stresses by repressing plant growth, which is also controlled by the extent of its oxidation (Li et al., 2019). Multiple evidences suggest that the oxidative modification of cysteine by accumulated ROS is an important pattern of signal transduction for plants in adaptation to stresses. However, our knowledge of distribution and function of redox-sensitive proteins in plants remains limited. Therefore, it is necessary to carry out thorough and accurate identification of the endogenous oxidation modified proteins in plants.

Proteomic techniques have been widely used in the identification of PTMs, in which iodoTMT strategy, has been proved to be precise and sensitive enough to detect and quantify endogenous cysteine oxidation levels in a proteome-wide scale (Wojdyla et al., 2015). Applying this iodoTMT-based method we

identified the *in vivo* sulfenylated cysteine sites in *B. napus* under freezing stress after cold acclimation. Finally, we obtained 1,372 sulfenylated sites in 714 proteins, and 252 sites in 171 proteins were differentially sulfenylated under freezing stress after cold acclimation. The glycolysis and photosynthesis processes were potentially regulated by redox-mediated PTMs because multiple key enzymes in these pathways were differentially sulfenylated and the relevant primary metabolites were significantly reduced under freezing stress after cold acclimation. These findings provide a basis and inspiration for understanding the redox regulation in plant response to freezing stress. This is even more significant for winter rapeseed production, which is threatened by cold and freezing injury during the long winter.

Materials and methods

Plant growth and stress condition

B. napus cultivar zhongshuang11 seedlings were kept in a growth room under 22°C/(16 h light: am7:00-pm23:00)/18°C (8 h dark: pm23:00-am7:00) with 200 μmol s^{-1} m^{-2} light intensity for two weeks. After cold adaptation at 4°C under the same photoperiod condition and light intensity for one week, the plants were subjected to freezing stress at -4°C. Leaf samples for proteomic analysis were collected after a 4 h-freezing treatment and immediately quick-frozen with liquid nitrogen. The plants grown in room temperature were taken as control.

Experimental design and rationale

Three replicates were set for both control and treated samples. The intensity data obtained from mass spectrometer were normalized by 'mean normalization' method first. The iodoTMT-128 and iodoTMT-129 labelled peptides after arsenite reduction were considered as sulfenylated (R-SOH) peptides, while the TMT-126 and iodoTMT-127 labelled sites were considered as total cysteines after TCEP reduction in this study. The reductant TCEP can reduce blocked thiols and reversible modifications including sulfenylation. After that, we can label the total cysteines. While the sulfenylated cysteines (R-SOH) can be labeled after being specifically reduced by arsenite. The two reducing agents were added into fractions separated from the same sample for marking the reduction and oxidation states of thiols in the same sample. The ratio of normalized intensity of iodoTMT-128 to iodoTMT-126 (control) and iodoTMT-129 to iodoTMT-127 (stress) was calculated to characterize the sulfenylation level of sulfenylated cysteines, which was defined as %R-SOH (Cys-SOH/Cys-total), in a way that the interference of the sulfenylation level caused by changes in protein abundance can be eliminated. The protein abundance was characterized by normalized MS data of peptides labelled by iodoTMT-126 and iodoTMT-127 under control and salt stressconditions, respectively. The ratio of %R-SOH and protein abundance under stress condition to that under control were calculated. Both the differentially sulfenylated proteins and differentially expressed proteins were identified by a threshold of 1.2-fold change for for up-regulation and 0.83-fold change for for down-regulation. Three biological replicates were used for the calculation of protein abundance and sulfenylation level. A p-value ≤ 0.05 was considered statistically significant.

DAB staining

3,3′-Diaminobenzidine (DAB) staining was performed with some modifications to test the H_2O_2 level under freezing stress after cold acclimation, according to the procedure described previously (Daudi and O'Brien, 2012). Briefly, the fresh leaves were immersed in DAB solution (1 mg mL^{-1} DAB in 10 mM Na_2HPO_4 and 0.05% Tween 20). Samples were vacuum-infiltrated for 30 min and then incubated for 8 h at 25°C in the dark with gentle shaking at 50 rpm. For decoloring, samples were incubated in ethanol at 95°C for 10 min and subsequently kept in 75% ethanol at room temperature for visualization. The color intensity of stained leaves was quantified using ImageJ software. The experiment was repeated for three biological replicates.

Protein extraction

Proteins were extracted with a lysis buffer containing 8 M urea, 1% Triton-100, 1% protease inhibitor, and 50 mM S-Methyl methanethiosulfonate (MMTS) was added to the buffer for free thiols blocking (Wojdyla et al., 2015), followed by sonication for 5 min with pulse durations of 3s on/5s off at 300W for three times on ice using a high intensity ultrasonic processor (Scientz-5T, China). The remaining debris was removed by centrifugation at 20,000 g at 4°C for 10 min. The protein was then precipitated with cold 20% trichloroacetic acid (TCA) (Sigma, USA) for 2 h at -20°C. After centrifugation at 12,000 g at 4°C for 10 min, the supernatant was discarded. The pellet was washed with cold acetone for three times and finally dissolved in a buffer containing 50 mM ammonium bicarbonate and 8 M urea (pH 8.0). Protein concentration was determined with BCA kit (Beyotime biotechnology, China).

IodoTMT labeling and trypsin digestion

Control and freezing treated samples were reduced by 10 mM Tris (2-carboxyethyl) phosphine (TCEP) and arsenite for 1 h at 37°C in darkness, respectively. The peptides were then labeled according to the manufacturer's protocol for the

iodoTMT kit (Thermo, USA). Briefly, TMT reagent was thawed and reconstituted in methyl alcohol before incubated with protein. Reactions were quenched by adding 20 mM dithiothreitol (DTT) and incubation for 15 min. Samples were pooled together and precipitated with 4 volumes of cold acetone overnight at -20°C. Pellets were washed three times with cold acetone to remove excess iodoTMT™ reagents and desalted using Strata X C18 SPE column (Phenomenex, USA) and dried by vacuum centrifugation.

The protein was digested by trypsin according to the method previously described (Li et al., 2018). After redissolved in 8 M urea, the labeled proteins were reduced with 10 mM DTT (Sigma, USA) for 1 h at 37°C and alkylated with 20 mM iodoacetamide (IAM) (Sigma, USA) for 45 min at room temperature in darkness. Samples were diluted with 50 mM ammonium bicarbonate to reduce urea concentration below 2 M and then were digested with trypsin (Sigma, USA) by a first overnight digestion at 1:50 trypsin-to-protein mass ratio and a second 4 h-digestion at 1:100 mass ratio. Peptide solution after digestion was desalted and vacuum-dried.

HPLC fractionation and anti-TMT™ enrichment

Peptides were fractionated by high pH reverse-phase HPLC using Thermo Betasil C18 column (5 μm particles, 10 mm ID, 250 mm length). Briefly, peptides were first separated with a gradient of 8% to 32% acetonitrile (pH 9.0; Fisher Chemical, USA) over 60 min into 60 fractions and then were combined into 6 fractions. To enrich labeled peptides, tryptic peptides dissolved in IP buffer (150 mM NaCl, 250 mM Tris-HCl, pH 7.5) were incubated with pre-washed anti-TMT antibody beads (Thermo, USA) at 4°C overnight with gentle shaking. Peptides were enriched using anti-TMT antibody and four different labels were used for the labeling of R-SH (TMT-126 and TMT-127) and R-SOH (TMT-128 and TMT-129) in control and freezing treated samples, respectively. Then the beads were washed for four times with IP buffer and twice with ddH_2O. The bound peptides were eluted from the beads with 0.1% trifluoroacetic acid (TFA). Finally, the eluted fractions were desalted and vacuum-dried for LC-MS/MS Analysis.

LC-MS/MS analysis

The tryptic peptides dissolved in solvent A (0.1% formic acid and 2% acetonitrile in water) were directly loaded onto a reversed-phase analytical column (15 cm length, 75 μm i.d.). The gradient was comprised of an increase from 6% to 22% of solvent B (0.1% formic acid and 90% acetonitrile in water) for 60 min, 22% to 35% for 22 min and climbing to 80% in 4 min then holding at 80% for the last 4 min, all at a constant flow rate of 350 nL min^{-1} on an EASY-nLC 1000 UPLC system (Thermo, America).

The peptides were subjected to NSI source followed by tandem mass spectrometry (MS/MS) in Orbitrap Fusion™ Tribrid™ (Thermo, USA) coupled online to the UPLC. Intact peptides were detected in the Orbitrap at a resolution of 60,000. Peptides were selected for MS/MS using NCE setting as 35. Ion fragments were detected in the Orbitrap at a resolution of 15,000. MS/MS scans were acquired in a data-dependent procedure. For analysis on the Orbitrap, a full MS scan was followed by 20 MS/MS scans on the top 20 precursor ions above a threshold intensity greater than 5×10^3 in the MS survey scan with 15 s dynamic exclusion. The electrospray voltage was applied at 2.0 kV. An automatic gain control (AGC) target value of 5×10^4 was used to prevent overfilling of the orbitrap. For MS scans, the m/z scan range was 350 to 1,550. Fixed first mass was set as 100 m/z.

Western blot analysis of labeled proteins

Western blot was performed to detect the labeled proteins and 4 μg proteins of each sample were separated by discontinuous SDS-PAGE. The separated proteins were electrophoretically transferred onto a nitrocellulose membrane and then detected using a TMT monoclonal antibody (25D5) as the primary antibody (Thermo Fisher Scientific, catalog # 90075) and anti-mouse IgG2b produced in goat as the secondary antibody (Sigma, catalog #A3562). The membrane was developed by incubation in AP development solution (0.015% BCIP, 0.03% NBT in 0.5 M Tris-HCl, pH 9.5) for 2 min and then the picture was taken.

Database search

The MS/MS data were processed using Maxquant search engine (v.1.5.2.8). Tandem mass spectra were searched against *UniprotKB* and *B. napus* database (http://www.genoscope.cns.fr/brassicanapus/) concatenated with a reverse decoy database. A maximum of two missed cleavages were allowed for trypsin. Carbamidomethyl on cysteine was specified as fixed modification and sulfenylation on "Met" were specified as variable modifications. Following the procedures, we set "First search" as an initial andromeda search, after the recalibration, "Main search" was performed. The mass tolerance for precursor ions was set as 20 ppm in "First search" and 5 ppm in "Main search", and the mass tolerance for fragment ions was set as 0.02 Da. The identifications from the "First search" are not used in the actual results, and the false discovery rate (FDR) only been estimated after "Main search". FDR was adjusted to < 1% and minimum score for modified peptides was set > 40. For quantification method, iodoTMT-6plex was selected. All the

other parameters in MaxQuant were set to default values. The site localization probability was set as > 0.75.

Subcellular localization prediction and GO enrichment analysis

The subcellular localization of proteins was predicted by soft Wolfpsort (http://www.genscript.com/psort/wolf_psort.html), which is an updated version of PSORT/PSORT II for the prediction of eukaryotic sequences. For further understanding of redox network, GO enrichment analysis was performed to predict the functional characteristics of identified proteins. For GO enrichment analysis, proteins were classified by GO annotation into three categories: biological process, cellular compartment and molecular function. For each category, a two-tailed Fisher's exact test was employed to test the enrichment of the differentially expressed protein against all identified proteins. A p-value < 0.05 was considered statistically significant. Proteins in *B. napus* were aligned to all *Arabidopsis* proteins by BLASTP (Jacob et al., 2008), and the most significant proteins in *Arabidopsis* based on a probability threshold of 10^{-5} were selected for enrichment analysis.

Recombinant protein expression and purification

RNA was extracted from *B. napus* leaves using Transzol reagent (TransGen, ET101) according to manufacturer's instructions. cDNA was reverse-transcribed using TransScript One-Step gDNA Removal and cDNA Synthesis SuperMix (TransGen, AE311) according to the manufacturer's instructions. *BnA09.PK* (BnaA09G0493100ZS) and *BnA02.MDH2* (BnaA02G0032600ZS) were cloned into PET28a-c (+) expression vector using primers (PK-3100ZS-F: 5′GCGGAATTCATGCATTCGAGCCATCTCC3′, PK-3100ZS-R: 5′GCGCGGCCGCATCCTCAAGCTCGATGATCTTGA3′; MDH2-2600ZS -F: 5′ATGTCCGTGGAGATGCC3′, MDH2-2600ZS-R: 5′TTTCCTGATGAAGTCAACACCTTTCT3′). The constructs were expressed in *E. coli* cells (BL21DE3 pLySs). For expression induction, isopropyl ß-D-thiogalactoside (IPTG) was added to the culture to induce the expression of target proteins at a final concentration of 0.3 mM and bacteria were grown with agitation (200 rpm) for 8 h at 25° C. Proteins were extracted using a buffer containing 50 mM NaH_2PO_4, 300 mM NaCl, 10 mM imidazole and 1 mM phenyl-methyl-sulphonyl-fluoride (PMSF), adjusted to pH 8.0 with NaOH. To purify soluble (6xHis) recombinant proteins, the supernatants were incubated with Ni-NTA resin (Sangon Biotech). Elution of the bound proteins from the column was achieved with 50 mM NaH_2PO_4, 300 mM NaCl and 250 mM imidazole, adjusted to pH 8.0 with NaOH.

Enzyme activity assay

Pyruvate kinase (PK) catalyzes the production of pyruvate from phosphoenolpyruvate (PEP). Pyruvate kinase activity was detected by coupling the production of pyruvate to the conversion of NADH to NAD^+ by lactate dehydrogenase (Zhang and Liu, 2016). Reactions were started by the addition of purified BnA09.PK, and the linear region of the reaction lasts at least 5 min at 25°C. Standard reaction mixtures contained 100 mM HEPES-KOH, pH 7.0, 5% polyethylene glycol (PEG) 8000, 10 mM KCl, 12 mM $MgCl_2$, 2 mM PEP, 1 mM ADP, 0.2 mM NADH, and 1.5 units mL^{-1} desalted rabbit muscle lactate dehydrogenase. MDH catalyzes the conversion between oxaloacetic acid (OAA) and L-malate. The reaction mixtures contained 100 mM Tris-HCl (pH 7.4), 0.2 mM NADH and 2 mM OAA (Mekhalfi et al., 2014). After adding 1 µg BnA02.MDH2 protein, the reaction was started. For H_2O_2 treatment in the enzyme assay, the final H_2O_2 concentration in reaction buffer was 0.2 mM, 0.5 mM, 1 mM, 2 mM, 5 mM, 10 mM. The standard reaction system was taken as control. Enzyme activity was analyzed assayed by recording the changes in absorbance of NADH at the wavelength of 340 nm using an ultraviolet spectrophotometer.

Metabolite analyses by LC-MS/MS

Metabolite extraction and analyses was performed using a modified method described previously (Luo et al., 2007; Guo et al., 2014). The sampling time of plant materials for metabolite analysis was the same as that for proteomic analysis. About 100-200 mg of leaf was harvested and ground in liquid nitrogen. 1.8 mL of methanol/chloroform (7:3, v/v; -20°C) was added and mixed by vortex followed by the addition of 0.8 µg PIPES as the internal standard. The mixtures were maintained for 2 h at -20°C with occasional vortexing. Polar metabolites were extracted from the methanol/chloroform phase by the addition of 1.6 mL water to each sample and then centrifuged at 1000 rpm after vigorous vortexing. The methanol-water phase was then transferred to a new tube, and another 1.6 mL of water was added to each sample to extract polar metabolites one more time. The extracts were dried by N_2 aspiration at 50°C. The dried extract was dissolved with 200 µL water and filtered with 0.45 mM cellulose acetate centrifuge filters for metabolite analyses by LC-MS/MS. The metabolites were quantified by comparing with the peak area of internal standard.

Results

IodoTMT-based proteomic approach for identification of redox-sensitive proteins in *B. napus*

An iodoTMT-based proteomic approach was used in this study to investigate the change in protein abundance and

sulfenylation level under freezing stress after cold acclimation in *B. napus* (Figure 1). After cold acclimation, the leaves of *B. napus* displayed a low H_2O_2 content before freezing treatment (0 h), showing a similar level of H_2O_2 compared to that under normal condition (CK). However, an obvious accumulation of H_2O_2 was observed after freezing treatment, especially after 3-hour treatment (Figure S1). In order to obtain as many modified proteins as possible, we set the sampling time at 4 hours after treatment to perform the proteomic identification. Blocking the sulfhydryl group (-SH) on cysteine residues by MMTS to minimize the thiol (R-SH) from oxidation during protein extraction, which is necessary for maintaining the initial redox state of proteins (Figures 1A, B). After that, samples were split in two to perform the reduction process of TCEP and arsenite, respectively. Anti-TMT^{TM} antibody was used to enrich the peptides followed by the digestion of labeled proteins (Figures 1A, C). Then the enriched peptides were identified and quantified by LC-MS/MS (Figure 1C). Finally, the change in protein abundance and sulfenylation level can be analyzed. Western blot result showed a weak reduction ability of arsenite compared with TCEP (Figure 2A). The Pearson coefficient between replicates (Figure S2A) and quality control of MS (Figure S2B) proved a reliable quantitative proteomic data.

A total of 968 unique sulfenylated peptides were obtained from the MS data (Table S1) matched to 1,372 sulfenylated sites in 714 proteins (Table S2). Among these sulfenylated sites and proteins, 1,265 sites (92.2%) in 664 proteins existed in both control and freezing treated samples (Figure 2B). The majority of these sulfenylated proteins were predicted to localize in chloroplast, cytoplasm, nucleus, extracellular and mitochondria, and a few proteins were predicted to localize in plasma membrane, cytoskeleton, vacuolar membrane, endoplasmic reticulum, peroxisome and golgi apparatus (Figure 2C). These sulfenylated proteins were notably enriched in glycolysis, tricarboxylic acid cycle and photosynthesis processes and they were more likely to function in chlorophyll binding, transferase activity and GTPase activity (Figure 2D). Taken together, these findings demonstrate that the iodoTMT-based proteomic approach can effectively identify a large number of *in vivo* sulfenylated proteins.

Freezing stress caused a changed abundance of proteins *in vivo*

In order to analyze the change in protein abundance under freezing stress after cold acclimation in *B. napus*, 857 labeled R-SH sites in 458 proteins identified in at least two replicates were analyzed (Table S3). By labelling the total cysteines (R-SH) with TMT-126 (Control) and TMT-127 (Stress), we can evaluate the abundance change of sites and proteins by calculating the normalized intensity ratio of R-SH under stress condition to that under control condition. Among these 857 sites, there were 411 sites in 233 proteins showed significant changes in their abundance under freezing stress in *B. napus* (Figure 3A and Table S4). The abundance of 197 sites in 121 proteins were up-regulated and 214 sites in 113 proteins were down-regulated

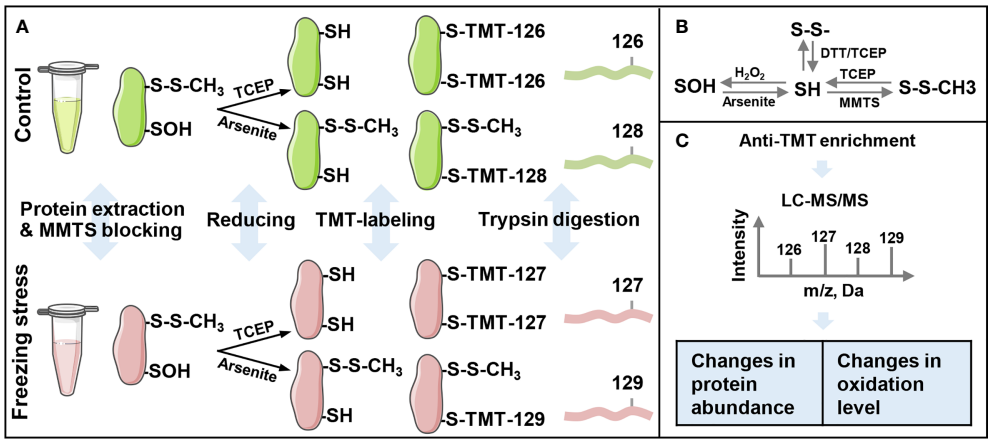

FIGURE 1
Workflow of the iodoacetyl tandem mass tags (iodoTMT)-based proteomic approach for the identification of sulfenylated cysteine sites. **(A)** The schematic of protein extraction, labeling and trypsin digestion processes. The iodo-TMT labels TMT-126 and TMT-127 were used to label free thiol (R-SH), and labels TMT-128 and TMT-129 were used to label sulfenylated thiol (R-SOH). **(B)** Thiol (SH) redox state change under different oxidants and reducing agents. SH, sulfhydryl group; S-S, disulfide bond; SOH, sulfenylation group; MMTS, S-Methyl Methanethiosulfonate; TCEP, Tris (2-carboxyethyl) phosphine; DTT, dithiothreitol. **(C)** Anti-TMT^{TM} antibody-based enrichment and LC-MS/MS analysis of peptides' intensity. Changes in expression levels are calculated by the ratio of TMT-127 (freezing stress) to TMT-126 (control) and changes in sulfenylation levels are calculated by the ratio of %R-SOH (TMT-129/TMT-127) under freezing stress to %R-SOH (TMT-128/TMT-126) under control condition.

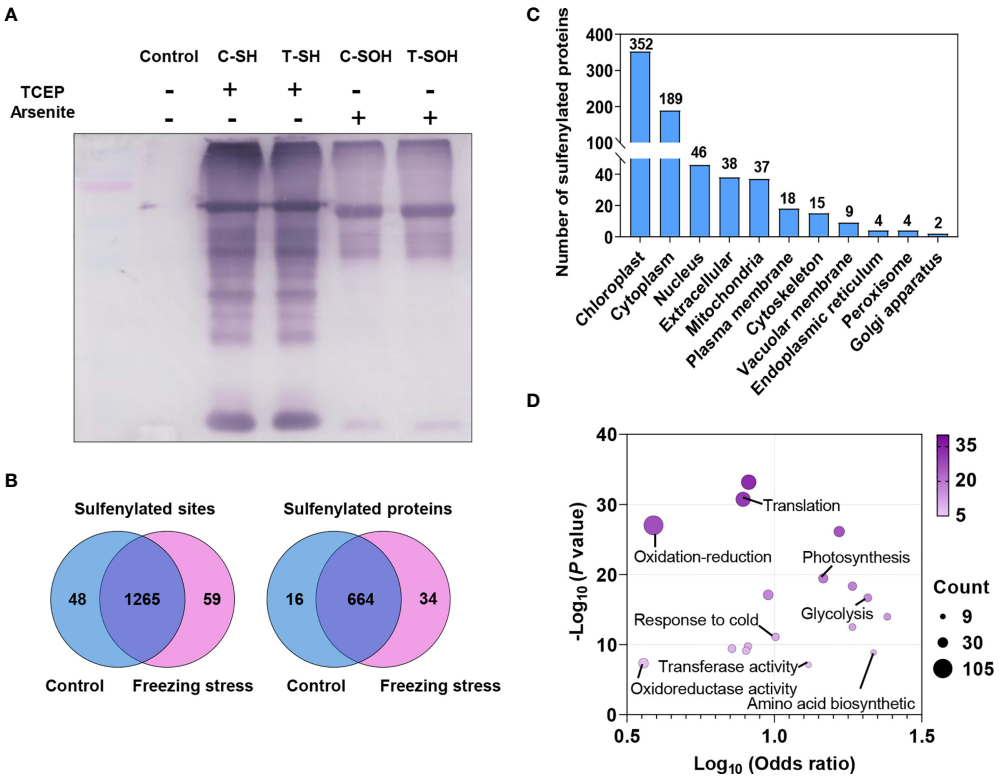

FIGURE 2
Sulfenylated sites and proteins identified by proteomic analysis in *B napus*. **(A)** The detection of total proteins reduced by TCEP and arsenite was performed by Western blotting using anti-TMT^{TM} antibody. Reduced (SH) and sulfenylated (SOH) proteins in control **(C)** and freezing treatment after cold acclimation (T) samples were labeled, respectively. Proteins without label were used as control. **(B)** Venn diagram showing the shared sulfenylated sites and proteins identified in control and stressed samples. The number of sites and proteins are listed in each diagram component, respectively. **(C)** The distribution of predicted subcellular localizations of sulfenylated proteins. **(D)** GO enrichment analysis of sulfenylated proteins. The Log_{10} (Odds ratio) is plotted on the x-axis. The size and color of dots indicate the number of sulfenylated proteins and the degree of enrichment (-Log_{10} (*P* value), $P < 0.05$), respectively.

under freezing stress after cold acclimation (Figure 3B and Table S4). GO enrichment analysis of these differentially expressed proteins (DEPs) showed that the up-regulated proteins were enriched in the processes of nucleotides synthesis and metabolism, translation and translation elongation and activities of nucleoside diphosphate kinase and translation elongation factor (Figure S3A). The down-regulated proteins were involved in carbon metabolism process and molecular functions such as ribulose-bisphosphate carboxylase activity, chlorophyll binding and lipid transport (Figure S3B).

Freezing stress caused fluctuations in the landscape of protein sulfenylation

In order to explore the effect of freezing stress after cold acclimation on the overall sulfenylation level of proteins in *B. napus*, we analyzed the %R-SOH of sulfenylated sites to reflect their sulfenylation level under control (%R-SOH = TMT-128/TMT-126) and stressed conditions (%R-SOH = TMT-129/TMT-127). There were 709 R-SOH sites in 402 proteins were identified in at last two replicates under both conditions (Table S5). By calculating the ratio of %R-SOH under stressed condition to that under control condition, we can estimate the sample-specific ratio of sulfenylated level to expression level of cysteines under stress (Table S5). In general, the treated sample displayed an increased %R-SOH when compared with the control samples (Figure 3C). This change was mainly due to the transformation from low sulfenylation level (0%-20%) to high sulfenylation level (20%-100%) of sites under freezing stress after cold acclimation (Figure 3D). In terms of the predicted subcellular distribution of sulfenylated proteins, the degree of % R-SOH increased in all compartments, especially in chloroplast and cytoplasm (Figures S4A, B). These results indicate that freezing stress after cold acclimation widely raise the sulfenylation level of sites and proteins *in vivo*.

Differentially sulfenylated sites and proteins under freezing stress after cold acclimation were identified by the threshold of

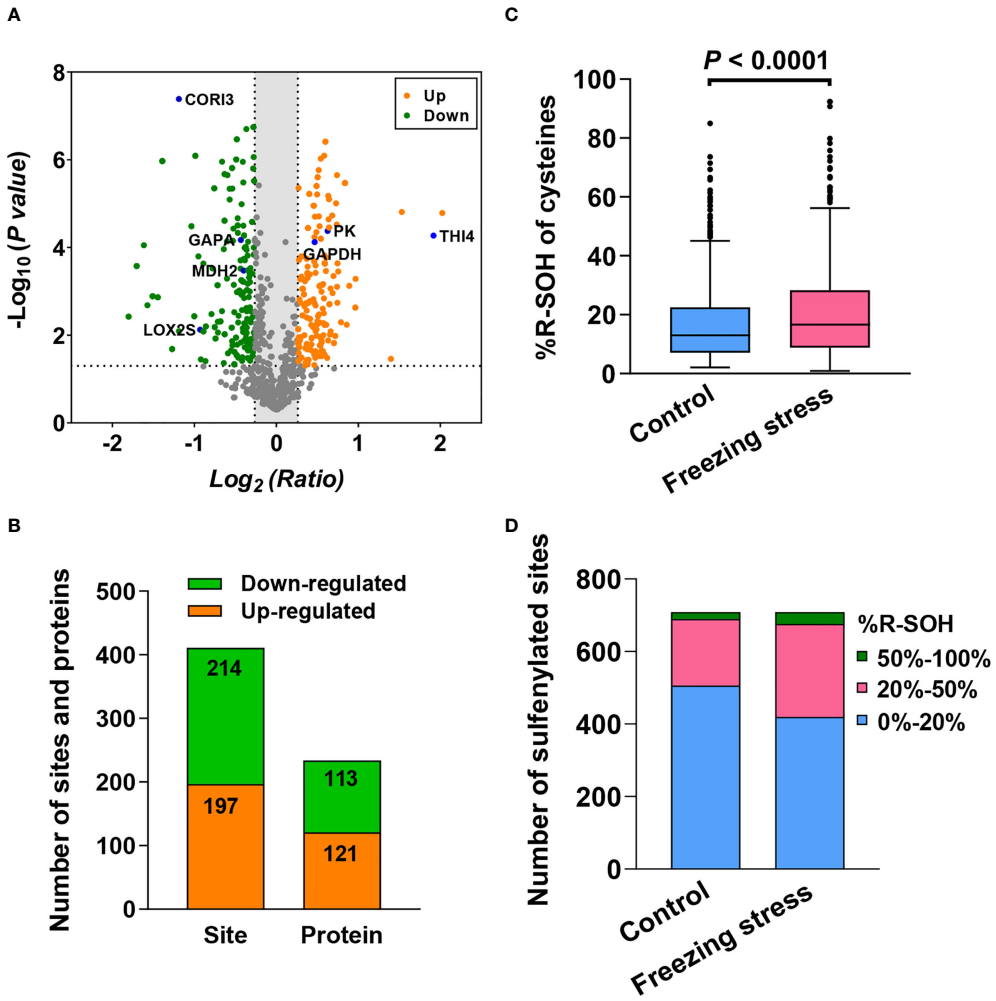

FIGURE 3
Freezing stress after cold acclimation caused the change in protein abundance and sulfenylation level (%R-SOH) of sites and proteins in *B napus*. **(A)** Volcano plot of the 857 sites quantified in at least 2 out of 3 replicates under both control and stressed conditions. The statistical significance -Log_{10} (*P* value) on the y-axis and the expression level change Log_2 (Ratio) on the x-axis. Ratio means the ratio of cysteine level under stress to that under control condition. Red dots represent the sites with up-regulated expression level (ratio > 1.2) and green dots represent the sites with down-regulated expression level (ratio < 0.83). The dotted line on the y-axis shows *P* value of 0.05, and the dotted lines on the x-axis show ratio of 1.2 and 0.83. Some known proteins in *A thaliana* are marked in blue in the volcano plot. **(B)** The number of sites and proteins with significant abundance changes under stress ($P < 0.05$). **(C)** Sulfenylation level of the 709 sites quantified in at least 2 out of 3 replicates under control and stressed conditions. %R-SOH means the proportion of modified state abundance to the total abundance of a single site, which was used to indicate the sulfenylation level. **(D)** %R-SOH distribution of the 709 sites under control and stressed conditions.

the %R-SOH ratio described above. The sites increased (ratio > 1.2) and decreased (ratio < 0.83) at their sulfenylation level were screened, respectively. A total of 714 sulfenylated proteins can be quantitatively evaluated, some of which have been reported as sulfenylated proteins in *A. thaliana* such as ribulose 1,5-bisphosphate carboxylase/oxygenase large subunit (RBCL) and glyceraldehyde-3-phosphate dehydrogenase (GAPDH) (Figure 4A; Table S2) (Alvarez et al., 2009; Wang et al., 2012; Liu et al., 2014; Liu et al., 2015). When comparing the %R-SOH of a single site under control and stressed conditions, besides a large number of sites with an increased sulfenylation level, a considerable proportion of sites displayed a decreased sulfenylation level, including some highly sulfenylated sites (Figure 4B). Among them, 252 sites in 171 proteins were differentially sulfenylated (Figure 4C; Table S6). 171 sites in 127 proteins were increased and 81 sites in 44 proteins were decreased in %R-SOH (Figure 4C; Table S6). There were 34 highly sulfenylated sites in 32 proteins with an increasing sulfenylation level (Table S7). Interestingly, 53 differentially sulfenylated sites in 49 proteins changed from low to high

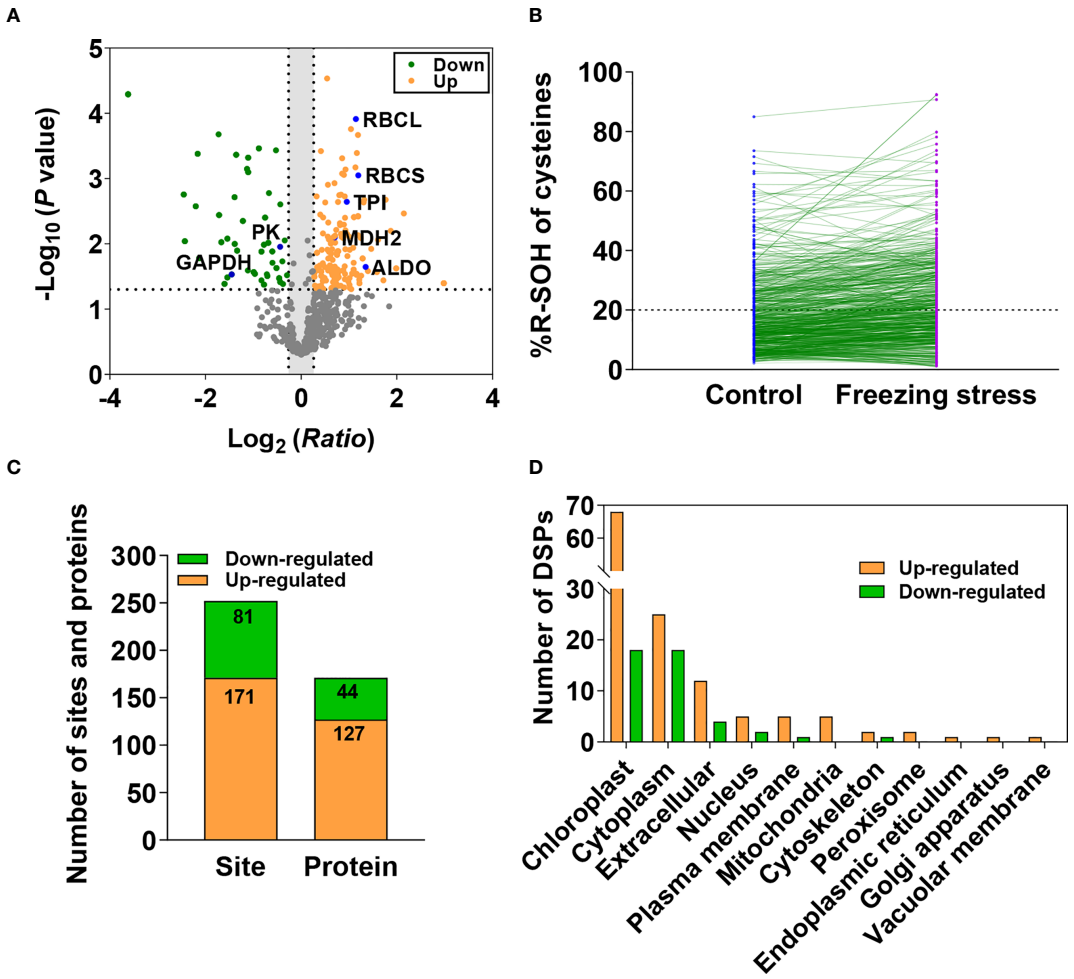

FIGURE 4
Differentially sulfenylated sites and proteins identified under freezing stress after cold acclimation in *B napus*. **(A)** Volcano plot of the 709 sites showing H_2O_2-dependent sulfenylation level change (ratio of %R-SOH) of cysteines, statistical significance -Log_{10} (*P* value) on the y-axis and sulfenylation level change Log_2 (*Ratio*) on the x-axis. Ratio means the ratio of %R-SOH under fstress condition to %R-SOH under control condition. Red dots represent the sites with increased sulfenylation level and green dots represent the sites with decreased sulfenylation level ($P < 0.05$). The dotted line on the y-axis shows *P* value of 0.05, and the dotted lines on the x-axis show ratio of 1.2 and 0.83. Sulfenylated proteins identified previously in *A thaliana* are marked in blue in the volcano plot. **(B)** The %R-SOH of the 709 sites under control (blue) and stressed (red) conditions. The %R-SOH is plotted on the y-axis and the split line represents %R-SOH equal to 20%. **(C)** The number of differentially sulfenylated sites and proteins ($P < 0.05$). **(D)** Subcellular localizations of the differentially sulfenylated proteins (DSPs).

sulfenylation level and some representative differentially sulfenylated sites and proteins were listed in Table 1. Moreover, 70 proteins displayed an increase sulfenylation level with a decreased expression level (Figure S5A). 12 proteins showed an increased trend both in expression level and sulfenylation level, while 11 proteins showed decreased trend both in expression level and sulfenylation level (Figure S5A). Most of the differentially sulfenylated proteins (DSPs) were predicted to localize in chloroplast and cytoplasm (Figure 4D). Based on GO enrichment analysis, proteins with an increased sulfenylation level were enriched in carbon utilization, photosynthesis and glycolysis, and molecular functions such as aldolase activity, catalase activity and chlorophyll binding (Figure S5B). These results suggest that the sulfenylation level of proteins are rearranged under freezing stress after cold acclimation, and stress-induced sulfenylation notably happen upon primary metabolism and enzymes in chloroplasts and cytoplasm.

In our previous studies, the change in protein abundance and sulfenylation level under salt-stressed condition was investigated in *B. napus* by the same approach (Yu et al., 2021). Comparison showed that 720 (74.4%) sulfenylated peptides were overlapped between the two studies (Figure S6A). Among the proteins with up-regulated expression level,

10.3389/fpls.2022.1014295

TABLE 1 Differentially sulfenylated sites and proteins changed from low to high sulfenylation level.

Position	Gene name	%R-SOH-CK	%R-SOH-T	Ratio	p-value	Protein description
350	BnaAnng23670D	0.186	0.286	1.538	0.010	ATPase 2, plasma membrane-type-like
116	BnaC08g32210D	0.189	0.296	1.567	0.012	Calvin cycle protein CP12-2, chloroplastic
215	BnaC06g28360D	0.177	0.277	1.568	0.008	Probable lactoylglutathione lyase, chloroplast
129	BnaA09g22540D	0.183	0.288	1.575	0.018	Chlorophyll a-b binding protein CP26, chloroplastic-like
284	BnaA02g00100D	0.132	0.216	1.629	0.008	Malate dehydrogenase 2, glyoxysomal
56	BnaC08g45680D	0.146	0.238	1.630	0.026	Coproporphyrinogen-III oxidase 1, chloroplastic
145	BnaA06g05150D	0.186	0.303	1.631	0.048	Superoxide dismutase 1
440	BnaCnng36310D	0.174	0.284	1.636	0.010	Fanconi anemia group I protein-like
223	BnaA03g53180D	0.149	0.248	1.663	0.006	Catalase-2
56	BnaA02g00470D	0.149	0.251	1.680	0.043	40S ribosomal protein S6-2-like
464	BnaA05g05840D	0.131	0.222	1.692	0.031	Ribulose bisphosphate carboxylase/oxygenase activase
227	BnaC08g36130D	0.178	0.302	1.697	0.025	Protein THYLAKOID FORMATION 1, chloroplastic-like
311	BnaCnng09500D	0.129	0.220	1.704	0.027	Haloacid dehalogenase-like hydrolase domain-containing protein
122	BnaA08g07940D	0.125	0.218	1.737	0.002	Photosystem I reaction center subunit III,
55	BnaA10g18270D	0.120	0.212	1.755	0.005	COX assembly mitochondrial protein 2-like
397	BnaC08g46180D	0.119	0.211	1.775	0.044	Glyceraldehyde-3-phosphate dehydrogenase GAPB
522	BnaA02g03770D	0.196	0.349	1.784	0.002	—
13	BnaC02g07040D	0.182	0.328	1.801	0.008	Nitrilase 2-like
573	BnaA05g00900D	0.146	0.264	1.813	0.001	Photosystem I P700 apoprotein A1 (chloroplast)
375	BnaC08g04910D	0.173	0.325	1.884	0.035	Triacylglycerol lipase-like 1
208	BnaC06g28580D	0.130	0.246	1.889	0.004	Cysteine/Histidine-rich C1 domain family protein
141	BnaA03g24350D	0.120	0.226	1.891	0.029	—
331	BnaA09g17390D	0.139	0.265	1.904	0.001	2-oxoglutarate dehydrogenase, mitochondrial-like
213	BnaA03g38340D	0.115	0.219	1.904	0.006	—
316	BnaC04g20620D	0.164	0.319	1.954	0.015	50S ribosomal protein L1, chloroplastic-like
77	BnaAnng27610D	0.116	0.235	2.019	0.012	Non-specific lipid-transfer protein D-like
149, 151	BnaC05g06200D	0.122	0.255	2.094	0.029	Violaxanthin de-epoxidase, chloroplastic-like
56	BnaA06g17780D	0.133	0.283	2.127	0.011	Tubulin beta-2 chain
127, 132	BnaC03g65520D	0.146	0.313	2.141	0.025	Aquaporin PIP2-7-like
227	BnaCnng05580D	0.096	0.212	2.198	0.001	Beta carbonic anhydrase 1, chloroplastic-like
140	BnaA03g25540D	0.105	0.236	2.236	0.029	ATP synthase gamma chain 1, chloroplastic
233	BnaA09g52790D	0.113	0.259	2.283	0.004	Myrosinase-like
230	BnaC05g42240D	0.095	0.222	2.323	0.035	Superoxide dismutase 1, mitochondrial-like
179	BnaC07g15490D	0.087	0.216	2.493	0.002	V-type proton ATPase subunit B1-like
117	BnaA06g30160D	0.099	0.302	3.052	0.009	Cysteine-rich repeat secretory protein 55-like
304	BnaA04g07450D	0.072	0.264	3.664	0.006	Glutamine synthetase, chloroplastic
468, 469, 473	BnaA01g18450D	0.040	0.317	7.894	0.040	Pyruvate, phosphate dikinase 1, chloroplastic

CK, the control samples; T, the treated samples.

11 proteins were up-regulated under both stressed conditions (Figure S6B). In addition, 16 proteins with increased sulfenylation level and 11 proteins with decreased sulfenylation level were identified under both freezing and salt stressed conditions (Figures S6C, D). These results indicate the stability of the iodoTMT-based approach for identification of sulfenylated proteins and freezing and salt stresses induce common and unique sulfenylation of proteins.

Freezing-induced alteration in primary metabolism pathway

Some DSPs identified by our proteomic data as well as a large number of the known redox-sensitive proteins participate in several pathways of primary metabolism, including glycolysis, the Calvin-Benson-Bassham (CBB) cycle, and the tricarboxylic acid (TCA) cycle (Figure S7). The results from metabolite profiling analysis also showed decreased level of metabolites in

glycolysis and CBB cycle pathways (Figure 5A). Based on the analysis of total cysteine level in proteins, we obtained the protein abundance of these enzymes. The glycolytic enzymes including triose phosphate isomerase (TPI), glyceraldehyde-3-phosphate dehydrogenase C (GAPC), enolase (ENO) and pyruvate kinase (PK) showed an increased abundance under freezing stress after cold acclimation (Figure 5B; Table S8), while enzymes like glyceraldehyde-3-phosphate dehydrogenase B (GAPB), TPI, fructose-1,6-bisphosphate aldolase (FBA) and ribose 5-phosphate isomerase (RPI) in CBB cycle were decreased in their abundance under stressed condition (Figure 5C; Table S8). However, the results from transcriptome analysis showed that key enzymes of glycolysis such as FBA, TPI, GAPC and PK did not decrease but significantly increase at the transcriptional level (Figure S8A'; Table S9). Similarly, the gene expression level of enzymes

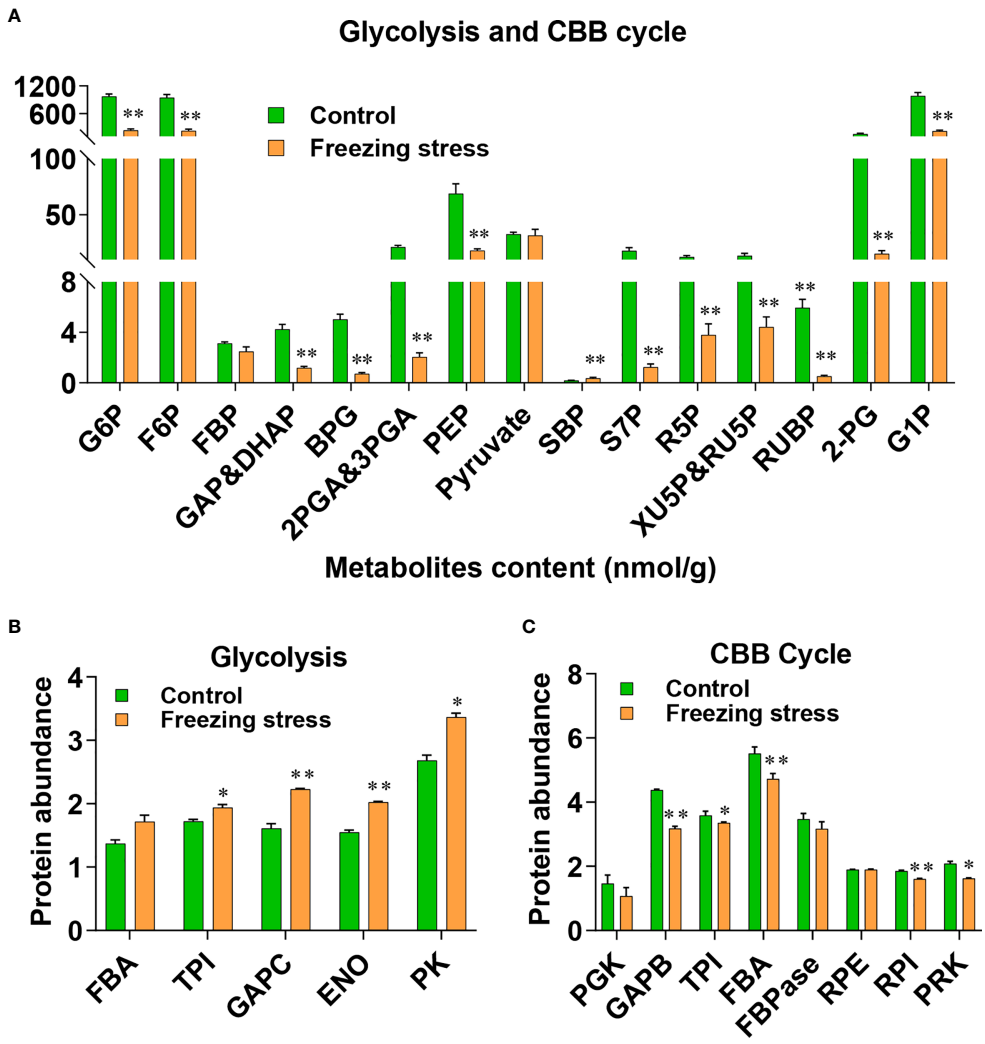

FIGURE 5
Metabolite level and protein abundance analysis of glycolysis pathway and Calvin-Benson (CBB) cycle. **(A)** Metabolite analysis of glycolysis pathway and CBB cycle. G6P, glucose-6-phosphate; F6P, fructose-6-phosphate; FBP, fructose-1,6-bisphosphate; GAP, glyceraldehydes-3-phosphate; DHAP, dihydroxyacetone-phosphate; BPG, 1,3-biophosphoglycerate; 2PGA, 2-phosphoglycerate; 3PGA, 3-phosphoglycerate; PEP, phosphoenol pyruvate; SBP, sedoheptulose-1,7-bisphosphate; S7P, sedoheptulose-7-phosphate; R5P, ribose-5-phosphate; RU5P, ribulose-5-phosphate; XU5P, xylulose 5-phosphate; RUBP, ribulose-1,5-bisphosphate; 2-PG, 2-phosphoglycolate; G1P, glucose-1-phosphate. Values are means ± SE (n = 6 biological replicates, $*P < 0.05$, $**P < 0.01$ compared with control using Student's t-test). **(B, C)** Protein abundance of enzymes involved in glycolysis pathway **(B)** and CBB cycle **(C)**. FBA, Fructose-1,6-bisphosphate aldolase; TPI, Triose phosphate isomerase; GAPC, glyceraldehyde-3-phosphate dehydrogenase; ENO, enolase; PK, pyruvate kinase; PGK, phosphoglycerate kinase; GAPB, glyceraldehyde-3-phosphate dehydrogenase B; FBPase, fructose-1,6-biphosphatase; RPE, ribulose-5-phosphate-3-epimerase; RPI, ribose 5-phosphate isomerase; Values are means ± SE (n = 3 biological replicates, $*P < 0.05$, $**P < 0.01$ compared with control using Student's t-test).

involved in the CBB cycle also showed no tendency to decrease, except for PGK and FBA (Figure S8B; Table S9). No significant difference in metabolite level was observed in TCA cycle (Figure S8C). In addition, the reductive power, the ratio of NADPH/$NADP^+$ in cells was significantly up regulated (Figure S8D). These results suggest that posttranslational modification, in addition to transcriptional and translational changes, plays an important role in metabolic response to freezing stress after cold acclimation.

Activity of pyruvate kinase and malate dehydrogenase was inhibited by H_2O_2

GO enrichment analysis revealed that a great number of enzymes were differentially sulfenylated (Figure S5B). Therefore, we explore the regulation of sulfenylation in enzyme activity. Cytosolic pyruvate kinase (PK) and cytosolic malate dehydrogenase (MDH2) were two key enzymes in glycolysis and TCA cycle, respectively. Both PK and MDH2 were differentially sulfenylated under freezing stress after cold acclimation in our data (Table S6). Only one peptide containing the sulfenylated site of cysteine 229 was identified in PK from the MS data (Figure 6A; Table S2), while three peptides containing the sulfenylated site of cysteine 147, 284 and 297, respectively, were identified in MDH2 (Figure 6B; Table S2). Both PK-Cys 229 and MDH2-Cys 284 showed significant changes in %R-SOH level (Table S6). The %R-SOH of PK-Cys 229 was decreased, whereas that of MDH2-Cys 284 was increased under stress (Figure 6C). We successfully purified these two proteins from *E. coli* (Figures S9A, B), and the enzyme activity assay under H_2O_2 treatment *in vitro* were performed. We observed a significant reduction in activity of PK and MDH2 after adding H_2O_2 in the reaction system and the degree of inhibition was enhanced with the increase of H_2O_2 concentration (Figure 6D). These results indicate that H_2O_2-induced inhibition of PK or MDH2 activity might be due to redox modification such as sulfenylation. A schematic model was drawn according to our results, showing the response and adaptation of *B. napus* plants under freezing stress (Figure 7).

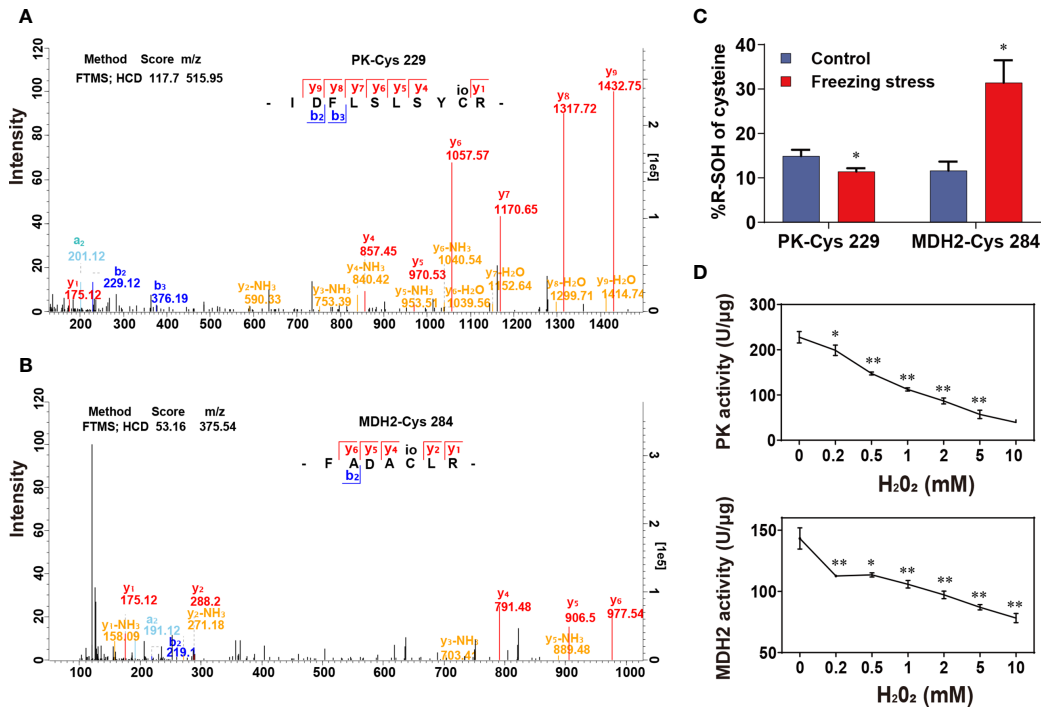

FIGURE 6
Effect of H_2O_2-induced sulfenylation on enzyme activity of pyruvate kinase (PK) and malate dehydrogenase 2 (MDH2). **(A, B)** Mass spectra of peptides containing PK-Cys 229 **(A)** and MDH2-Cys 284 **(B)**. The mass spectra scanning using fourier transform mass spectrometry (FTMS) and the fragmentation method is higher energy collision induced dissociation (HCD); Score, match degree between the fragment produced by the mass spectra and that recorded in the database; m/z, the ratio of mass to charge of the peptide; "IDFLSLSYCR" and "FADACLR" were the peptides sequence of PK and MDH2 identified in this study. **(C)** %R-SOH change of PK and MDH2. Values are means ± SD (n = 3 biological replicates, $*P < 0.05$ compared with control using Student's t-test). **(D)** Enzyme activity of PK and MDH2 under H_2O_2 treatment *in vitro*. Values are means ± SD (n = 3 technical replicates, $*P < 0.05$, $**P < 0.01$ compared with control using Student's t-test).

FIGURE 7
Schematic representation of the metabolic response induced by freezing stress. Under freezing stress, H2O2 accumulation induces sulfenylation of proteins, consequently affecting their functions, such as enzyme activity and binding ability. The modified proteins are involved in several metabolic processes, including CBB cycle and glycolysis, which further help the plants adapt to freezing stress.

Discussion

Various methods such as saturation differential in-gel electrophoresis (DIGE) and isotope-coded affinity tagging (ICAT) have been used to identify PTMs in plants (Leichert et al., 2008; Go et al., 2010; Zhu et al., 2014). But the number of proteins identified by previous methods is very limited and the reproducibility between different methods and repetitions is poor. IodoTMT-based strategy provides a robust and reproducible method for identification of the sulfenylated sites and quantification of the relative abundance of R-SH and R-SOH in proteins. Many 6-plex tandem mass tag (TMT) reagents have been used to quantify sulfenylation, and were assessed to reduce run-to-run variance (Murray et al., 2012; Pan et al., 2014). Due to the small amplitude change of modification, accurate determination of the endogenous levels of thiol modification have been proved to be difficult. Combined anti-TMT enrichment and LC-MS/MS analysis can largely improve the sensitivity of measurement (Wojdyla et al., 2015). We thus chose this method to screening differentially expressed and differentially sulfenylated proteins. In addition, little knowledge has been obtained on identification of endogenous sulfenylated proteins under abiotic stresses in plants. In our study, we focus on the DSPs induced by freezing stress after cold acclimation, which can cause severe damage to overwintering plants such as *B. napus*. Finally, we obtained 252 differentially sulfenylated sites in 171 proteins (Table S6), and the putative localization and function of these proteins were analyzed, which has an important reference significance for redox regulation of plant adaptability to stresses. Compared with the result on identification of sulfenylated cysteines under salt stress using the same method in our previous study (Yu et al., 2021), 74.4% peptides were found to be overlapped under both salt and freezing stress. However, only a few differentially expressed and differentially sulfenylated proteins were overlapped under the two stresses (Figures S6C, D). This indicated that the iodoTMT-based strategy has a good repeatability in comparing the modification levels between different samples. Besides, different stress treatments may induce the modification of different proteins.

Freezing stress after cold acclimation caused a decreased metabolic level of glycolysis and CBB cycle (Figure 5A). Redox regulation by S-nitrosylation (SNO) and S-glutathionylation (SSG) is required for plant adaptation to biotic and abiotic stresses, allowing fine-tuning of the CBB cycle (Michelet et al., 2013). In combination with metabolic, protein abundance and transcriptional analyses, we found strong inconsistencies in alteration of mRNA level, protein abundance and metabolic changes under stress (Figure 5 and Figure S8). For example, though the content of metabolites S7P, Xu5P, Ru5P and RuBP involved in the CBB cycle was significantly reduced (Figure 5A), there was no significant difference in mRNA level and protein abundance of TPI and FBPase under stress (Figure 5C and Figure S8B). Interestingly, TPI, FBA and FBPase, which catalyze the upstream reactions of these metabolites, was significantly increased at their sulfenylation level under stress, which may explain metabolic changes to some extent (Figure 5A, Table S6). PRK is an essential enzyme of the CBB cycle to produce RuBP in photosynthesis, and GAPDH/CP12/PRK complex plays a pivotal in the regulation of the CBB cycle (Marri et al., 2005). The ATP site and Ru5P site can be disrupted by the disulfide bond formed between Cys 17 and Cys 56 after oxidization, this redox-controlled switch further regulates the CBB cycle through the activation/deactivation of PRK and the reversible formation of the GAPDH/CP12/PRK ternary complex (Marri et al., 2009; Yu et al., 2020). We found that the sulfenylation level of PRK was significantly increased (Figure S7 and Table S6) and the content of its product RuBP was significantly decreased under stress (Figure 5A). The mRNA level of *PRK* was not significantly altered (Figure S8B), while the protein abundance of PRK showed a significant decrease under stressed condition (Figure 5C). These results suggest that post-transcriptional regulation and PTMs may work together in the regulation of PRK function in response to freezing stress after cold acclimation.

Many chloroplastic isoforms of glycolytic enzymes involved in the CBB cycle, such as FBA, TPI, PGK, PK and so on, were all identified as sulfenylated proteins in *B. napus* (Figure S7). Cytosolic glycolytic enzymes including GAPC, PGK, PGAM and ENO have been identified as potential

targets of redox modifications in various studies in *A. thaliana* (Dumont and Rivoal, 2019). The sulfenylated level of GAPC and PK were significantly decreased (Table S6 and Figure S7), and the mRNA level and protein abundance of TPI, GAPC, and PK were increased (Figure 5B). Moreover, the content of metabolites BPG, 2PGA, 3PGA and PEP in the glycolytic pathway was significantly reduced under stress (Figure 5A). H_2O_2 can repress the *in vitro* activity of cytosolic PK (Figure 6D), which was a freezing-induced differentially sulfenylated protein identified by our proteomic approach, consistent with the reduced metabolite contents in glycolysis under freezing stress after cold acclimation (Figure 5A). It was also found that the protein abundance of some glycolytic enzymes increased, while that of some Calvin-Benson cycle enzymes decreased under freezing stress after cold acclimation (Figure S8A). These results were consistent with a previous study, which revealed that the protein abundance of light-harvesting complex, cytochromes and rubisco in Calvin-Benson cycle was reduced under cold stress (Ermilova, 2020). Plant cells are able to hold a balance between growth and adaptation to stresses, and the reestablishment of the new homeostasis helps plants to have a recovery ability and exhibit a renewed growth by regulating the expression of growth-related genes and stress-related genes (Kazemi-Shahandashti and Maali-Amiri, 2018).

Cysteine is an active site that can be modified by a variety of posttranslational modifications, including oxidative modification such as SOH and SSG, other modification such as acylation, lipidation, acetylation, S-nitrosylation, methylation, palmitoylation and phosphorylation, as well as other active amino acids of the PTMs such as lysine, methionine, arginine and so on (Friso and van Wijk, 2015). It has been found that multiple PTMs such as phosphorylation, monoubiquitination, SSG, SNO control the activity, localization and turnover of these glycolytic enzymes (O'Leary and Plaxton, 2020), indicating that other types of PTMs also play considerable roles in the regulation of these enzymes. Different PTMs and crossover between them have also been extensively identified in eukaryotes (Meyer et al., 2012; Weinert et al., 2013; Zhang et al., 2013). These complex PTMs networks may work together to coordinate metabolic control. Proteomic screens have uncovered widespread SNO and SSG of plant glycolytic enzymes in plant cells, such as FBA, TPI, GAPC, PGK, ENO, PK (Dumont and Rivoal, 2019; O'Leary and Plaxton, 2020). Therefore, the inhibition of metabolic level in glycolysis under freezing stress after cold acclimation might also be regulated by other PTMs. Further study on the mechanism of posttranslational modification network was needed to help us understand the roles of PTMs in regulating plant metabolic adaptation to stresses.

H_2O_2 can be generated by electron transport chain during the light reaction in chloroplasts, especially when plants are suffered from environmental changes (Foyer and Noctor, 2016). Apoplast is also a main compartment of oxidative bursts. The accumulated H_2O_2 in apoplasts can enter the cytoplasm through water channel proteins called aquaporins in plasma membrane (Rodrigues et al., 2017). Previous studies have reported that the general modification of glycolytic enzymes results in not just slowing down of the metabolism for adaptation to an unfavorable environment, but also promotion of C-flux into the pentose phosphate pathway (PPP) to regenerate NADPH to detoxify ROS (Hildebrandt et al., 2015; Dumont and Rivoal, 2019). Our results also showed the increase in the ratio of NADPH/$NADP^+$ under freezing stress after cold acclimation (Figure S8D), consistent with the previous findings. Among the glycolytic enzymes, GAPC appears to be one of the most prominent targets of redox modifications, which function as a 'moonlighting' protein with redox-dependent changes in subcellular localization and biological function. Its re-localization to the nucleus occurred under sulfenylated conditions displays a moonlighting role as a transcription factor to induce gene expression of antioxidant enzymes (Hildebrandt et al., 2015; Schneider et al., 2018; Dumont and Rivoal, 2019). It remains to be explored whether there are other redox-sensitive proteins that function as moonlighting proteins participating in various actual jobs after oxidization. In future, in-depth functional research and structural analysis of posttranslational modified proteins will be of great significance for understanding of the regulatory function of redox PTMs.

Data availability statement

The original contributions presented in the study are publicly available in the database iProX (https://www.iprox.cn/) (Ma et al., 2019; Chen et al., 2022). This data can be found here: iProX, PXD034549.

Author contributions

XY and LG designed this study. LY, ZD and SI performed the experiments. YZ and LY did bioinformatics analysis. LY wrote the manuscript. XY, LG and SL revised the manuscript. All authors contributed to the article and approved the submitted version.

Funding

This research was funded by the Major Scientific and Technological Projects of Xinjiang Production and Construction Corps of China (2018AA005) and the 111 Project (B20051).

Acknowledgments

This research was funded by the Major Scientific and Technological Projects of Xinjiang Production and Construction Corps of China (2018AA005) and the 111 Project (B20051). This work is supported by the PTM Biolabs lnc. (Hangzhou, China) for technical assistance Additional supporting information may be found online in the Supporting Information section at the end of the article.

Conflict of interest

The authors declare that the research was conducted in the absence of any commercial or financial relationships that could be construed as a potential conflict of interest.

Publisher's note

Supplementary material

The Supplementary Material for this article can be found online at: https://www.frontiersin.org/articles/10.3389/fpls.2022.1014295/full#supplementary-material

References

Alvarez, S., Zhu, M., and Chen, S. (2009). Proteomics of arabidopsis redox proteins in response to methyl jasmonate. *J. Proteomics* 73, 30–40. doi: 10.1016/j.jprot.2009.07.005

Antelmann, H., and Helmann, J. D. (2011). Thiol-based redox switches and gene regulation. *Antioxid Redox Signal* 14, 1049–1063. doi: 10.1089/ars.2010.3400

Cavender-Bares, J. (2007). Chilling and freezing stress in live oaks (Quercus section virentes): intra- and inter-specific variation in PS II sensitivity corresponds to latitude of origin. *Photosynth. Res.* 94, 437–453. doi: 10.1007/s11120-007-9215-8

Chen, T., Ma, J., Liu, Y., Chen, Z., Xiao, N., Lu, Y., et al. (2022). iProX in 2021: connecting proteomics data sharing with big data. *Nucleic Acids Res.* 50, D1522–d1527. doi: 10.1093/nar/gkab1081

Chiappetta, G., Ndiaye, S., Igbaria, A., Kumar, C., Vinh, J., and Toledano, M. B. (2010). Proteome screens for cys residues oxidation: the redoxome. *Methods Enzymol.* 473, 199–216. doi: 10.1016/S0076-6879(10)73010-X

Choudhury, F. K., Rivero, R. M., Blumwald, E., and Mittler, R. (2017). Reactive oxygen species, abiotic stress and stress combination. *Plant J.* 90, 856–867. doi: 10.1111/tpj.13299

Daudi, A., and O'Brien, J. A. (2012). Detection of hydrogen peroxide by DAB staining in arabidopsis leaves. *Bio Protoc.* 2 (18), e263. doi: 10.21769/BioProtoc.263

Dumont, S., and Rivoal, J. (2019). Consequences of oxidative stress on plant glycolytic and respiratory metabolism. *Front. Plant Sci.* 10, 166. doi: 10.3389/fpls.2019.00166

Ellouzi, H., Sghayar, S., and Abdelly, C. (2017). H_2O_2 seed priming improves tolerance to salinity; drought and their combined effect more than mannitol in cakile maritima when compared to eutrema salsugineum. *J. Plant Physiol.* 210, 38–50. doi: 10.1016/j.jplph.2016.11.014

Ermilova, E. (2020). Cold stress response: An overview in chlamydomonas. *Front. Plant Sci.* 11, 569437. doi: 10.3389/fpls.2020.569437

Finkel, T. (2003). Oxidant signals and oxidative stress. *Curr. Opin. Cell Biol.* 15, 247–254. doi: 10.1016/S0955-0674(03)00002-4

Foster, M. W., Hess, D. T., and Stamler, J. S. (2009). Protein s-nitrosylation in health and disease: a current perspective. *Trends Mol. Med.* 15, 391–404. doi: 10.1016/j.molmed.2009.06.007

Foyer, C. H., and Noctor, G. (2016). Stress-triggered redox signalling: what's in pROSpect? *Curr. Opin. Cell Biol.* 39, 951–964. doi: 10.1111/pce.12621

Freschi, L. (2013). Nitric oxide and phytohormone interactions: current status and perspectives. *Front. Plant Sci.* 4, 398. doi: 10.3389/fpls.2013.00398

Friso, G., and van Wijk, K. J. (2015). Posttranslational protein modifications in plant metabolism. *Plant Physiol.* 169, 1469–1487. doi: 10.1104/pp.15.01378

Go, Y. M., Park, H., Koval, M., Orr, M., Reed, M., Liang, Y., et al. (2010). A key role for mitochondria in endothelial signaling by plasma cysteine/cystine redox potential. *Free Radic. Biol. Med.* 48, 275–283. doi: 10.1016/j.freeradbiomed.2009.10.050

Guo, L., Ma, F., Wei, F., Fanella, B., Allen, D. K., and Wang, X. (2014). Cytosolic phosphorylating glyceraldehyde-3-phosphate dehydrogenases affect arabidopsis cellular metabolism and promote seed oil accumulation. *Plant Cell* 26, 3023–3035. doi: 10.1105/tpc.114.126946

Held, J. M., and Gibson, B. W. (2012). Regulatory control or oxidative damage? proteomic approaches to interrogate the role of cysteine oxidation status in biological processes. *Mol. Cell Proteomics* 11, R111.013037. doi: 10.1074/mcp.R111.013037

Hildebrandt, T., Knuesting, J., Berndt, C., Morgan, B., and Scheibe, R. (2015). Cytosolic thiol switches regulating basic cellular functions: GAPDH as an information hub? *Biol. Chem.* 396, 523–537. doi: 10.1515/hsz-2014-0295

Hochgräfe, F., Mostertz, J., Pöther, D. C., Becher, D., Helmann, J. D., and Hecker, M. (2007). S-cysteinylation is a general mechanism for thiol protection of bacillus subtilis proteins after oxidative stress. *J. Biol. Chem.* 282, 25981–25985. doi: 10.1074/jbc.C700105200

Hogg, P. J. (2003). Disulfide bonds as switches for protein function. *A Debreceni Dèri Mózeum évkinyve* 28, 210–214. doi: 10.1016/S0968-0004(03)00057-4

Htet, Y., Lu, Z., Trauger, S. A., and Tennyson, A. G. (2019). Hydrogen peroxide as a hydride donor and reductant under biologically relevant conditions. *Chem. Sci.* 10, 2025–2033. doi: 10.1039/C8SC05418E

Huang, J., Willems, P., Wei, B., Tian, C., Ferreira, R. B., Bodra, N., et al. (2019). Mining for protein s-sulfenylation in arabidopsis uncovers redox-sensitive sites. *Proc. Natl. Acad. Sci. U.S.A.* 116, 21256–21261. doi: 10.1073/pnas.1906768116

Huber, S. C., and Hardin, S. C. (2004). Numerous posttranslational modifications provide opportunities for the intricate regulation of metabolic enzymes at multiple levels. *Curr. Opin. Plant Biol.* 7, 318–322. doi: 10.1016/j.pbi.2004.03.002

Jacob, A., Lancaster, J., Buhler, J., Harris, B., and Chamberlain, R. D. (2008). Mercury BLASTP: Accelerating protein sequence alignment. *ACM Trans. Reconfigurable Technol. Syst.* 1, 9. doi: 10.1145/1371579.1371581

Kazemi-Shahandashti, S. S., and Maali-Amiri, R. (2018). Global insights of protein responses to cold stress in plants: Signaling, defence, and degradation. *J. Plant Physiol.* 226, 123–135. doi: 10.1016/j.jplph.2018.03.022

Leichert, L. I., Gehrke, F., Gudiseva, H. V., Blackwell, T., Ilbert, M., Walker, A. K., et al. (2008). Quantifying changes in the thiol redox proteome upon oxidative stress *in vivo*. *Proc. Natl. Acad. Sci. U.S.A.* 105, 8197–8202. doi: 10.1073/pnas.0707723105

Li, Y., Liu, W., Zhong, H., Zhang, H. L., and Xia, Y. (2019). Redox-sensitive bZIP68 plays a role in balancing stress tolerance with growth in arabidopsis. *Plant J.* 100, 768–783. doi: 10.1111/tpj.14476

Liu, P., Zhang, H., Wang, H., and Xia, Y. (2014). Identification of redox-sensitive cysteines in the arabidopsis proteome using OxiTRAQ, a quantitative redox proteomics method. *Proteomics* 14, 750–762. doi: 10.1002/pmic.201300307

Liu, P., Zhang, H., Yu, B., Xiong, L., and Xia, Y. (2015). Proteomic identification of early salicylate- and flg22-responsive redox-sensitive proteins in arabidopsis. *Sci. Rep.* 5, 8625. doi: 10.1038/srep08625

Li, F., Wang, Y., Li, Y., Yang, H., and Wang, H. (2018). Quantitative analysis of the global proteome in peripheral blood mononuclear cells from patients with new-onset psoriasis. *Proteomics* 18, e1800003. doi: 10.1002/pmic.201800003

Luo, B., Groenke, K., Takors, R., Wandrey, C., and Oldiges, M. (2007). Simultaneous determination of multiple intracellular metabolites in glycolysis, pentose phosphate pathway and tricarboxylic acid cycle by liquid chromatography-mass spectrometry. *J. Chromatogr. A* 1147, 153–164. doi: 10.1016/j.chroma.2007.02.034

Ma, J., Chen, T., Wu, S., Yang, C., Bai, M., Shu, K., et al. (2019). iProX: an integrated proteome resource. *Nucleic Acids Res.* 47, D1211–d1217. doi: 10.1093/nar/gky869

Marri, L., Trost, P., Pupillo, P., and Sparla, F. (2005). Reconstitution and properties of the recombinant glyceraldehyde-3-phosphate dehydrogenase/CP12/phosphoribulokinase supramolecular complex of arabidopsis. *Plant Physiol.* 139, 1433–1443. doi: 10.1104/pp.105.068445

Marri, L., Zaffagnini, M., Collin, V., Issakidis-Bourguet, E., Lemaire, S. D., Pupillo, P., et al. (2009). Prompt and easy activation by specific thioredoxins of calvin cycle enzymes of arabidopsis thaliana associated in the GAPDH/CP12/PRK supramolecular complex. *Mol. Plant* 2, 259–269. doi: 10.1093/mp/ssn061

McConnell, E. W., Berg, P., Westlake, T. J., Wilson, K. M., Popescu, G. V., Hicks, L. M., et al. (2019). Proteome-wide analysis of cysteine reactivity during effector-triggered immunity. *Plant Physiol.* 179, 1248–1264. doi: 10.1104/pp.18.01194

Mekhalfi, M., Amara, S., Robert, S., Carrière, F., and Gontero, B. (2014). Effect of environmental conditions on various enzyme activities and triacylglycerol contents in cultures of the freshwater diatom, asterionella formosa (Bacillariophyceae). *Biochimie* 101, 21–30. doi: 10.1016/j.biochi.2013.12.004

Meyer, L. J., Gao, J., Xu, D., and Thelen, J. J. (2012). Phosphoproteomic analysis of seed maturation in arabidopsis, rapeseed, and soybean. *Plant Physiol.* 159, 517–528. doi: 10.1104/pp.111.191700

Mhamdi, A. (2019). The immune redoxome: Effector-triggered immunity switches cysteine oxidation profiles. *Plant Physiol.* 179, 1196–1197. doi: 10.1104/pp.19.00207

Michelet, L., Zaffagnini, M., Morisse, S., Sparla, F., Pérez-Pérez, M. E., Francia, F., et al. (2013). Redox regulation of the Calvin-Benson cycle: something old, something new. *Front. Plant Sci.* 4, 470. doi: 10.3389/fpls.2013.00470

Millar, A. H., Heazlewood, J. L., Giglione, C., Holdsworth, M. J., Bachmair, A., and Schulze, W. X. (2019). The scope, functions, and dynamics of posttranslational protein modifications. *Annu. Rev. Plant Biol.* 70, 119–151. doi: 10.1146/annurev-arplant-050718-100211

Mueller, M. J., and Berger, S. (2009). Reactive electrophilic oxylipins: pattern recognition and signalling. *Phytochemistry* 70, 1511–1521. doi: 10.1016/j.phytochem.2009.05.018

Mur, L. A., Prats, E., Pierre, S., Hall, M. A., and Hebelstrup, K. H. (2013). Integrating nitric oxide into salicylic acid and jasmonic acid/ ethylene plant defense pathways. *Front. Plant Sci.* 4, 215. doi: 10.3389/fpls.2013.00215

Murray, C. I., Uhrigshardt, H., O'Meally, R. N., Cole, R. N., and Van Eyk, J. E. (2012). Identification and quantification of s-nitrosylation by cysteine reactive tandem mass tag switch assay. *Mol. Cell Proteomics* 11, M111.013441. doi: 10.1074/mcp.M111.013441

Nazir, F., Fariduddin, Q., and Khan, T. A. (2020). Hydrogen peroxide as a signalling molecule in plants and its crosstalk with other plant growth regulators under heavy metal stress. *Chemosphere* 252, 126486. doi: 10.1016/j.chemosphere.2020.126486

Noctor, G., and Foyer, C. H. (2016). Intracellular redox compartmentation and ROS-related communication in regulation and signaling. *Plant Physiol.* 171, 1581–1592. doi: 10.1104/pp.16.00346

O'Leary, B., and Plaxton, W. C. (2020). Multifaceted functions of post-translational enzyme modifications in the control of plant glycolysis. *Curr. Opin. Plant Biol.* 55, 28–37. doi: 10.1016/j.pbi.2020.01.009

Pan, K. T., Chen, Y. Y., Pu, T. H., Chao, Y. S., Yang, C. Y., Bomgarden, R. D., et al. (2014). Mass spectrometry-based quantitative proteomics for dissecting multiplexed redox cysteine modifications in nitric oxide-protected cardiomyocyte under hypoxia. *Antioxid Redox Signal* 20, 1365–1381. doi: 10.1089/ars.2013.5326

Paulsen, C. E., and Carroll, K. S. (2013). Cysteine-mediated redox signaling: chemistry, biology, and tools for discovery. *Chem. Rev.* 113, 4633–4679. doi: 10.1021/cr300163e

Poonam, BhardwajR., Kaur, R., Bali, S., Kaur, P., Sirhindi, G., Thukral, A. K., et al. (2015). Role of various hormones in photosynthetic responses of green plants under environmental stresses. *Curr. Protein Pept. Sci.* 16, 435–449. doi: 10.2174/1389203716666150330125215

Rodrigues, O., Reshetnyak, G., Grondin, A., Saijo, Y., Leonhardt, N., Maurel, C., et al. (2017). Aquaporins facilitate hydrogen peroxide entry into guard cells to mediate ABA- and pathogen-triggered stomatal closure. *Proc. Natl. Acad. Sci. U.S.A.* 114, 9200–9205. doi: 10.1073/pnas.1704754114

Ryšlavá, H., Doubnerová, V., Kavan, D., and Vaněk, O. (2013). Effect of posttranslational modifications on enzyme function and assembly. *J. Proteomics* 92, 80–109. doi: 10.1016/j.jprot.2013.03.025

Schneider, M., Knuesting, J., Birkholz, O., Heinisch, J. J., and Scheibe, R. (2018). Cytosolic GAPDH as a redox-dependent regulator of energy metabolism. *BMC Plant Biol.* 18, 184. doi: 10.1186/s12870-018-1390-6

Smith, L. M., and Kelleher, N. L. (2013). Proteoform: a single term describing protein complexity. *Nat. Methods* 10, 186–187. doi: 10.1038/nmeth.2369

Sun, W. C., Jun-Yan, W. U., Fang, Y., Liu, Q., Yang, R. Y., Wei-Guo, M. A., et al. (2010). Growth and development characteristics of winter rapeseed northern-extended from the cold and arid regions in China. *Acta Agronomica Sin.* 36, 2124–2134. doi: 10.3724/SP.J.1006.2010.02124

Suzuki, N., Koussevitzky, S., Mittler, R., and Miller, G. (2012). ROS and redox signalling in the response of plants to abiotic stress. *Plant Cell Environ.* 35, 259–270. doi: 10.1111/j.1365-3040.2011.02336.x

Tian, Y., Fan, M., Qin, Z., Lv, H., Wang, M., Zhang, Z., et al. (2018). Hydrogen peroxide positively regulates brassinosteroid signaling through oxidation of the BRASSINAZOLE-RESISTANT1 transcription factor. *Nat. Commun.* 9, 1063. doi: 10.1038/s41467-018-03463-x

Tonks, N. K. (2005). Redox redux: revisiting PTPs and the control of cell signaling. *Cell* 121, 667–670. doi: 10.1016/j.cell.2005.05.016

Wang, H., Wang, S., Lu, Y., Alvarez, S., Hicks, L. M., Ge, X., et al. (2012). Proteomic analysis of early-responsive redox-sensitive proteins in arabidopsis. *J. Proteome Res.* 11, 412–424. doi: 10.1021/pr200918f

Weinert, B. T., Schölz, C., Wagner, S. A., Iesmantavicius, V., Su, D., Daniel, J. A., et al. (2013). Lysine succinylation is a frequently occurring modification in prokaryotes and eukaryotes and extensively overlaps with acetylation. *Cell Rep.* 4, 842–851. doi: 10.1016/j.celrep.2013.07.024

Wojdyla, K., Williamson, J., Roepstorff, P., and Rogowska-Wrzesinska, A. (2015). The SNO/SOH TMT strategy for combinatorial analysis of reversible cysteine oxidations. *J. Proteomics* 113, 415–434. doi: 10.1016/j.jprot.2014.10.015

Wu, F., Chi, Y., Jiang, Z., Xu, Y., Xie, L., Huang, F., et al. (2020). Hydrogen peroxide sensor HPCA1 is an LRR receptor kinase in arabidopsis. *Nature* 578, 577–581. doi: 10.1038/s41586-020-2032-3

Yu, L., Iqbal, S., Zhang, Y., Zhang, G., Ali, U., Lu, S., et al. (2021). Proteome-wide identification of s-sulphenylated cysteines in brassica napus. *Plant Cell Environ.* 44, 3571–3582. doi: 10.1111/pce.14160

Yu, A., Xie, Y., Pan, X., Zhang, H., Cao, P., Su, X., et al. (2020). Photosynthetic phosphoribulokinase structures: Enzymatic mechanisms and the redox regulation of the Calvin-Benson-Bassham cycle. *Plant Cell* 32, 1556–1573. doi: 10.1105/tpc.19.00642

Zhang, B., and Liu, J. Y. (2016). Cotton cytosolic pyruvate kinase GhPK6 participates in fast fiber elongation regulation in a ROS-mediated manner. *Planta* 244, 915–926. doi: 10.1007/s00425-016-2557-8

Zhang, H., Zhao, Y., and Zhu, J. K. (2020). Thriving under stress: How plants balance growth and the stress response. *Dev. Cell* 55, 529–543. doi: 10.1016/j.devcel.2020.10.012

Zhang, K., Zheng, S., Yang, J. S., Chen, Y., and Cheng, Z. (2013). Comprehensive profiling of protein lysine acetylation in escherichia coli. *J. Proteome Res.* 12, 844–851. doi: 10.1021/pr300912q

Zhu, M., Zhu, N., Song, W. Y., Harmon, A. C., Assmann, S. M., and Chen, S. (2014). Thiol-based redox proteins in abscisic acid and methyl jasmonate signaling in brassica napus guard cells. *Plant J.* 78, 491–515. doi: 10.1111/tpj.12490

Zivanovic, J., Kouroussis, E., Kohl, J. B., Adhikari, B., Bursac, B., Schott-Roux, S., et al. (2019). Selective persulfide detection reveals evolutionarily conserved antiaging effects of s-sulfhydration. *Cell Metab.* 30, 1152–1170.e13. doi: 10.1016/j.cmet.2019.10.007

frontiers | Frontiers in Plant Science

TYPE Original Research
PUBLISHED 13 October 2022
DOI 10.3389/fpls.2022.978586

OPEN ACCESS

EDITED BY
Sabine Lüthje,
University of Hamburg, Germany

REVIEWED BY
Martin Cerny,
Mendel University in Brno, Czechia
Joerg Durner,
Helmholtz Association of German Research Centres (HZ), Germany
Anja Liszkay,
UMR9198 Institut de Biologie Intégrative de la Cellule (I2BC), France

*CORRESPONDENCE
Anna Kärkönen
anna.happonen@luke.fi
Kazuyuki Kuchitsu
kuchitsu@rs.tus.ac.jp

†These authors have contributed equally to this work and share first authorship

‡PRESENT ADDRESS
Takamitsu Kurusu,
Department of Mechanical and Electrical Engineering, Suwa University of Science, Chino, Japan

SPECIALTY SECTION
This article was submitted to Plant Abiotic Stress, a section of the journal Frontiers in Plant Science

RECEIVED 26 June 2022
ACCEPTED 15 September 2022
PUBLISHED 13 October 2022

CITATION
Nickolov K, Gauthier A, Hashimoto K, Laitinen T, Väisänen E, Paasela T, Soliymani R, Kurusu T, Himanen K, Blokhina O, Fagerstedt KV, Jokipii-Lukkari S, Tuominen H, Häggman H, Wingsle G, Teeri TH, Kuchitsu K and Kärkönen A (2022) Regulation of PaRBOH1-mediated ROS production in Norway spruce by Ca^{2+} binding and phosphorylation. *Front. Plant Sci.* 13:978586. doi: 10.3389/fpls.2022.978586

Regulation of PaRBOH1-mediated ROS production in Norway spruce by Ca^{2+} binding and phosphorylation

Kaloian Nickolov [1,2†], Adrien Gauthier [1,3†], Kenji Hashimoto [4], Teresa Laitinen [1], Enni Väisänen [1,5], Tanja Paasela [1,6], Rabah Soliymani [7], Takamitsu Kurusu [4‡], Kristiina Himanen [1], Olga Blokhina [5], Kurt V. Fagerstedt [5], Soile Jokipii-Lukkari [2,8], Hannele Tuominen [9], Hely Häggman [2], Gunnar Wingsle [9], Teemu H. Teeri [1], Kazuyuki Kuchitsu [4*] and Anna Kärkönen [1,6*]

[1]Department of Agricultural Sciences, Viikki Plant Science Centre, University of Helsinki, Helsinki, Finland, [2]Department of Ecology and Genetics, University of Oulu, Oulu, Finland, [3]UniLaSalle, Agro-Ecology, Hydrogeochemistry, Environments & Resources, UP 2018.C101 of the Ministry in Charge of Agriculture (AGHYLE) Research Unit CS UP 2018.C101, Mont-Saint-Aignan, France, [4]Department of Applied Biological Science, Tokyo University of Science, Noda, Japan, [5]Organismal and Evolutionary Biology Research Programme, Faculty of Biological and Environmental Sciences, Viikki Plant Science Centre, University of Helsinki, Helsinki, Finland, [6]Natural Resources Institute Finland (Luke), Production Systems, Helsinki, Finland, [7]Meilahti Clinical Proteomics Core Facility, Biochemistry & Dev. Biology, University of Helsinki, Biomedicum-Helsinki, Helsinki, Finland, [8]Department of Plant Physiology, Umeå Plant Science Centre, Umeå University, Umeå, Sweden, [9]Department of Forest Genetics and Plant Physiology, Umeå Plant Science Centre, Swedish University of Agricultural Sciences, Umeå, Sweden

Plant respiratory burst oxidase homologs (RBOHs) are plasma membrane-localized NADPH oxidases that generate superoxide anion radicals, which then dismutate to H_2O_2, into the apoplast using cytoplasmic NADPH as an electron donor. *PaRBOH1* is the most highly expressed *RBOH* gene in developing xylem as well as in a lignin-forming cell culture of Norway spruce (*Picea abies* L. Karst.). Since no previous information about regulation of gymnosperm RBOHs exist, our aim was to resolve how PaRBOH1 is regulated with a focus on phosphorylation. The N-terminal part of PaRBOH1 was found to contain several putative phosphorylation sites and a four-times repeated motif with similarities to the Botrytis-induced kinase 1 target site in Arabidopsis AtRBOHD. Phosphorylation was indicated for six of the sites in *in vitro* kinase assays using 15 amino-acid-long peptides for each of the predicted phosphotarget site in the presence of protein extracts of developing xylem. Serine and threonine residues showing positive response in the peptide assays were individually mutated to alanine (kinase-inactive) or to aspartate (phosphomimic), and the wild type *PaRBOH1* and the mutated constructs transfected to human kidney embryogenic (HEK293T) cells with a low endogenous level of extracellular ROS production. ROS-producing assays with HEK cells showed that Ca^{2+} and phosphorylation synergistically activate the enzyme and identified several serine and threonine residues that are likely to be phosphorylated including a

novel phosphorylation site not characterized in other plant species. These were further investigated with a phosphoproteomic study. Results of Norway spruce, the first gymnosperm species studied in relation to RBOH regulation, show that regulation of RBOH activity is conserved among seed plants.

KEYWORDS

Norway spruce, respiratory burst oxidase homolog (RBOH), lignin formation, hydrogen peroxide, calcium ion, phosphorylation

Introduction

Conifers are woody land plants that dominate vast areas in terrestrial ecosystems especially in the Northern Hemisphere. They contribute to a large fraction of biomass and act as an important carbon sink, the carbon being mainly allocated to cell walls of wood tissues. Norway spruce (*Picea abies* L. Karst.) is one of the most economically important coniferous species with primary significance for the wood-processing industry and as a carbon storage. It is also a model gymnosperm species whose whole genome sequence has been revealed (Nystedt et al., 2013). In its secondary xylem (wood), cell walls contain ca. 27% of a phenolic polymer, lignin (Jaakkola et al., 2007). Lignin provides rigidity and structural support to cell wall polysaccharides.

The final polymerization steps in lignin biosynthesis take place *via* H_2O_2-utilizing peroxidase- or O_2-utilizing laccase-catalyzed oxidation of monolignols to phenolic radicals that then couple non-enzymatically as shown in Arabidopsis (*Arabidopsis thaliana*; Berthet et al., 2011; Novo-Uzal et al., 2013; Zhao et al., 2013; Shigeto and Tsutsumi, 2016; Dixon and Barros, 2019; Hoffmann et al., 2020; Rojas-Murcia et al., 2020; Blaschek and Pesquet, 2021; Blaschek et al., 2022), and various *Populus* species (Li et al., 2003; Lu et al., 2013; Lin et al., 2016; Qin et al., 2020). The relative contribution of these enzymes in lignification in the vasculature of plants *in vivo* and the specific isoenzymes that oxidize monolignols are not clearly known (Tobimatsu and Schuetz, 2019; Hoffmann et al., 2020; Hoffmann et al., 2022). In Arabidopsis, laccase and peroxidase isoenzymes localize differently in cell wall domains, with certain isoenzymes in the secondary cell walls of fibers and vessel elements, and the other ones in cell corners and middle lamella (Chou et al., 2018; Hoffmann et al., 2020). Recently, quadruple and quintuple loss of function laccase mutants of Arabidopsis were used to show that combinations of laccase isoenzymes are responsible for lignification in specific cell types and in different cell wall layers of primary xylem (Blaschek et al., 2022).

Localized apoplastic H_2O_2 production, required for the peroxidase-mediated lignification, is likely the regulatory factor that restricts the activity of peroxidases to certain locations in the lignifying cell wall (Hoffmann et al., 2020; Hoffmann et al., 2022). In the Casparian strip of the root endodermis of Arabidopsis, peroxidases have the main role in lignin formation (Lee et al., 2013). Mutation of five endodermal peroxidases leads to a total absence of lignification in the Casparian strip, whereas simultaneous abolishment of nine endodermis-expressed laccases has no effect on lignin formation (Rojas-Murcia et al., 2020). Hence, it seems that distinct enzymes are responsible for monolignol oxidation in various physiological phenomena and during different developmental stages.

During xylem development in Norway spruce, co-expression studies with monolignol biosynthesis genes raise both peroxidases and laccases as candidates for monolignol oxidation (Jokipii-Lukkari et al., 2017; Jokipii-Lukkari et al., 2018; Blokhina et al., 2019). In a Norway spruce cell culture that makes extracellular lignin (e.g. Simola et al., 1992; Kärkönen et al., 2002; Kärkönen and Koutaniemi, 2010), peroxidases seem to have the major role in monolignol activation since H_2O_2 scavenging from the medium efficiently inhibits lignin polymerization (Laitinen et al., 2017). Peroxidases need a source of apoplastic H_2O_2 used as an oxidant in monolignol activation, pointing out the role of enzymes able to generate apoplastic H_2O_2 in lignin polymerization.

Several plant cell wall- and plasma membrane-located sources can generate reactive oxygen species (ROS) such as superoxide anion radical, H_2O_2 and hydroxyl radical into the apoplast (Kärkönen and Kuchitsu, 2015; Smirnoff and Arnaud, 2019). These include respiratory burst oxidase homologues (RBOHs, also called NADPH oxidases) as well as various oxidases and peroxidases. RBOHs contain *heme* and flavin to utilize cytosolic NADPH as an electron donor and reduce O_2 in the apoplastic side of the plasma membrane to superoxide (Torres and Dangl, 2005; Suzuki et al., 2011). As an enzyme to produce potentially toxic substances, both the enzymatic activity and expression of RBOHs are strictly regulated (Kurusu et al.,

2015; Jiménez-Quesada et al., 2016). Superoxide dismutates to H_2O_2 and O_2 in a reaction catalyzed by superoxide dismutase (Ogawa et al., 1997; Karlsson et al., 2005) or non-enzymatically in the acidic pH of cell walls. Arabidopsis has ten *RBOH* genes (*AtRBOH*s), and the different isoenzymes perform various functions and participate in distinct signaling pathways (Miller et al., 2009; Suzuki et al., 2011; Waszczak et al., 2018; Kaya et al., 2019; Castro et al., 2021). Intensive studies in a model species Arabidopsis have shown various regulatory mechanisms of RBOHs, that are mentioned in the following paragraphs.

Proteomic studies have revealed *in vivo* phosphorylation of AtRBOHD in pathogen-induced defense and abiotic stress responses (Nühse et al., 2007; Kadota et al., 2014; Wang et al., 2020). Various types of protein kinases such as SNF1-related kinase 2 protein kinases such as open stomata 1 kinase (Ost1; Sirichandra et al., 2009), Ca^{2+}-dependent protein kinases (CPKs; Dubiella et al., 2013), Ca^{2+}-activated calcineurin B-like interacting protein kinases (CIPKs; Kimura et al., 2013; Drerup et al., 2013; Han et al., 2019), receptor-like cytoplasmic kinases such as Botrytis-induced kinase 1 (BIK1; Li et al., 2014; Kadota et al., 2014; Kadota et al., 2015) and RPM1-induced protein kinases (RIPK, Li et al., 2021), mitogen-activated protein kinase kinase kinase kinases (MAP4K) such as SIK1 (Zhang et al., 2018), L-type lectin receptor-like kinases such as DORN1 (Chen et al., 2017), and a cysteine-rich receptor-like protein kinase 2 (CRK2, Kimura et al., 2020) have been shown to contribute to activation of RBOHs by phosphorylating distinct amino acids. Fine-tuning ROS production in various physiological situations is facilitated by protein kinase-specific target sites in addition to some common target sites (Kadota et al., 2015; Chen et al., 2017; Han et al., 2019). Since various protein kinases are activated by different factors (e.g., stress-induced Ca^{2+}-signaling, pathogen- or damage-associated molecular patterns, i.e., PAMPs/DAMPs), target sites specific for certain kinases allow fine-tuning of ROS production by the same RBOH enzyme. Recently, a specific phosphatase contributing to the regulation of the RBOH activity was characterized (Han et al., 2019).

RBOHs have conserved Ca^{2+}-binding EF-hand motifs at the N-terminus (Oda et al., 2010). Elevating the cytosolic Ca^{2+} concentration induced by pathogens or damage is essential for RBOH-mediated ROS production i*n planta* (Ranf et al., 2011; Kadota et al., 2014). Heterologous expression of RBOHs in HEK293T cells confirmed activation by Ca^{2+}-binding to the EF-hand motifs (Ogasawara et al., 2008). Furthermore, Ca^{2+} binding and phosphorylation synergistically enhance the activity of RBOHs (Ogasawara et al., 2008; Takeda et al., 2008; Kimura et al., 2012; Han et al., 2019; Kaya et al., 2019). In addition to Arabidopsis, RBOH activity is regulated by Ca^{2+} and phosphorylation in monocotyledonous species such as rice (*Oryza sativa*; Takahashi et al., 2012).

Recent studies have shown that nitrosylation and persulfidation of cysteine residues at the C-terminus of AtRBOHD regulate the activity negatively and positively, respectively (Yun et al., 2011; Shen et al., 2020). Stability of AtRBOHD protein is controlled by ubiquitination at the C-terminus (Lee et al., 2020). Interaction with other regulatory proteins have also been shown (Kawarazaki et al., 2013; Kadota et al., 2015). Several studies suggest an important role of nitric oxide (NO) in regulating ROS production and scavenging (Gupta et al., 2020).

Involvement of RBOHs in the production of H_2O_2 necessary for the peroxidase-mediated lignin formation has been suggested in some herbaceous plants. During vascular xylem lignification and in *in vitro* tracheary element formation in zinnia (*Zinnia elegans*), RBOHs have been suggested to contribute to ROS production (Ros Barceló, 1998; Karlsson et al., 2005; Pesquet et al., 2013). In Arabidopsis, ROS produced by AtRBOHD/AtRBOHF are involved in cell wall damage-induced ectopic lignin formation (Denness et al., 2011) as well as lignin brace formation of the abscission layer in floral organs (Lee et al., 2018). In the Casparian strip of the root endodermis, AtRBOHF is the responsible enzyme involved in ROS production needed for lignification (Lee et al., 2013; Barbosa et al., 2019; Fujita et al., 2020). However, for peroxidase-mediated lignin formation in the vascular tissues of woody plants, no specific enzymes responsible for H_2O_2 production have so far been characterized.

Both the lignin-forming cultured cells and developing xylem of Norway spruce contain several plasma-membrane-located enzymes with the ability to generate superoxide anion radicals (and hence H_2O_2) (Kärkönen et al., 2014). In the cell culture, micromolar levels of H_2O_2 exist in the culture medium during lignin formation (Kärkönen and Fry, 2006; Kärkönen et al., 2009). Pharmacological experiments suggest that at least two enzymatic systems are involved in H_2O_2 generation: the one containing a *heme*, such as a peroxidase, and the other one a flavin, like in RBOH (Kärkönen et al., 2009). These observations raised an interest to investigate how RBOH activity is regulated in Norway spruce.

Thirteen putative *RBOH* genes (*PaRBOHs*) are expressed in developing xylem of Norway spruce (Jokipii-Lukkari et al., 2017; Jokipii-Lukkari et al., 2018; http://congenie.org/; Figure 1). Among them, *PaRBOH1* is the most highly expressed *RBOH* gene in the tissue-cultured Norway spruce cells during extracellular lignin formation (Laitinen et al., 2017). We retrieved data from Jokipii-Lukkari et al. (2017); Jokipii-Lukkari et al. (2018) to demonstrate that this gene has high expression also in developing xylem of mature trees (Figure 1A). Furthermore, it has high expression in developing xylem cells during cell wall lignification (Figure 1B).

In the present study, we focused on PaRBOH1 to characterize its ROS-producing activity and regulatory mechanisms for the first time in gymnosperms including coniferous species. We showed that the developing xylem of

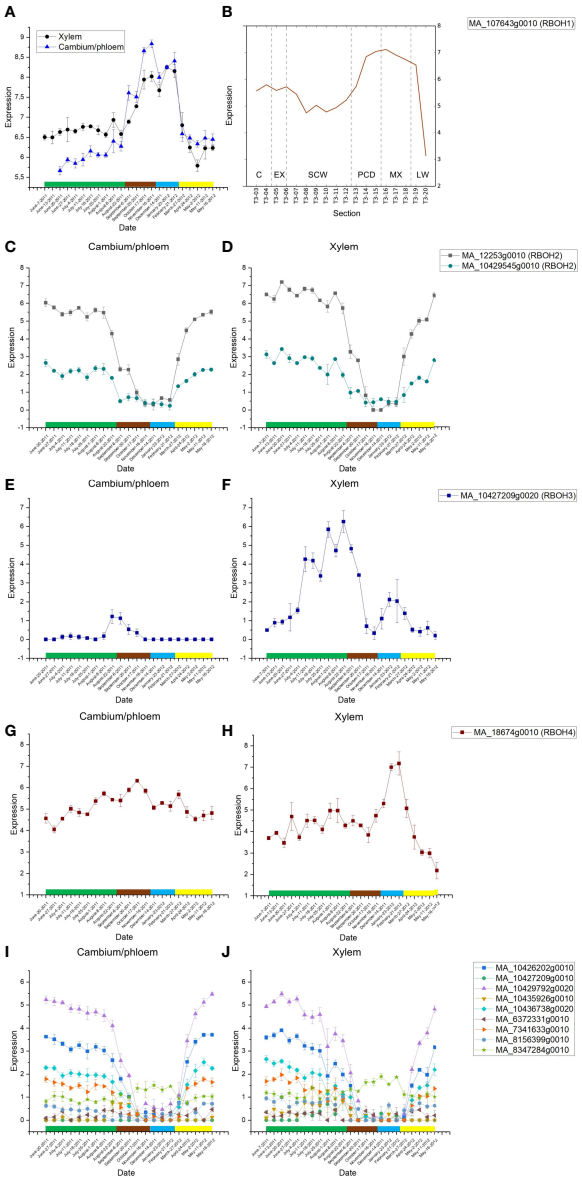

FIGURE 1
(A) Seasonal variation in the *PaRBOH1* expression in xylem and in combined cambium and phloem samples (data from Jokipii-Lukkari et al., 2018). *PaRBOH1* shows expression peak in late autumn and winter, and in mature xylem. Green rectangle, summer months June, July, and August; brown rectangle, autumn months September, October, and November; blue rectangle, winter months December, January, and February; and yellow rectangle, spring months March, April, and May. Values are means ± S.E. **(B)** Spatial expression pattern of *PaRBOH1* in the tangential section series across cambial region and current year wood. The data are retrieved from the NorWood web resource (http://NorWood.ConGenIE.org; Jokipii-Lukkari et al., 2017). The values correspond to variance stabilized gene expression. C, cambium; EX, xylem expansion; SCW, secondary cell wall formation; PCD, programmed cell death; MX, mature xylem; LW, previous year's latewood. **(C–J)** Seasonal gene expression patterns of other Norway spruce *PaRBOH* genes in combined cambium and phloem samples **(C, E, G, I)** and in xylem **(D, F, H, J);** data from Jokipii-Lukkari et al. (2018).

Norway spruce has a protein kinase activity to phosphorylate some specific sites of PaRBOH1. PaRBOH1 was shown to be activated by the phosphorylation and binding of Ca^{2+} to the EF-hand motifs synergistically. Comparison with angiosperm RBOHs as well as possible significance in lignification in xylem development will be discussed.

Material and methods

Cloning full-length cDNA of *PaRBOH1*

Degenerate primers were designed based on an alignment of several plant *RBOH* genes available in the NCBI database. Total RNA was isolated according to Chang et al. (1993) from the tissue-cultured spruce cells and from the developing xylem of a mature tree of Norway spruce (*Picea abies* L. Karst.). RNA was reverse transcribed to cDNA with SuperScript III reverse transcriptase according to manufacturer's instructions (Life Technologies Europe BV). Partial *RBOH* cDNA sequences were amplified with a polymerase chain reaction using the degenerate primers and Advantage 2 polymerase mix (Takara Bio). Rapid amplification of cDNA ends (3' and 5'RACE) was done using SMARTer RACE 5'/3' Kit (Takara Bio). PCR products were ligated to a pGEM-T easy vector (Promega) or to a pCR Blunt vector (Thermo Fisher Scientific) and transformed to DH5α competent *Escherichia coli* cells. With the full-length construct, it was necessary to cultivate the transformed cells at 28°C over two nights, since at 37°C the open reading frame was always disrupted with point mutations. The *PaRBOH1* coding sequence was submitted to a NCBI GenBank with an accession number HQ592777.2. Primers used for cloning are shown in Supplementary Table S1.

Online software predictions for possible post-translational modifications in the PaRBOH1 N-terminus

In order to identify possible post-translational modification (PTM) sites and other motifs in the N-terminal 400 amino acid residues' stretch of PaRBOH1 that exist before the transmembrane domains, several online databases and software tools for predicting protein PTMs were used -ScanProsite (de Castro et al., 2006; http://prosite.expasy.org/scanprosite); MotifScan (Pagni et al., 2007; http://myhits.isb-sib.ch/cgi-bin/motif_scan); P3DB (Yao et al., 2012a; Yao et al., 2014; http://www.p3db.org) together with Musite (Gao et al., 2010; Yao et al., 2012b; http://musite.net); PlantPhos (Lee et al., 2011; http://csb.cse.yzu.edu.tw/PlantPhos); DeepNitro (Xie et al., 2018; http://deepnitro.renlab.org/webserver.html). Where available, plant reference databases were used for the predictions. The outcomes from different tools were then compared, combined with the experimental evidence for PTMs of RBOH family members from other plant species.

Cloning, expression and purification of the N-terminal part of PaRBOH1

In order to be used as a kinase substrate in *in vitro* kinase reactions, the 400 amino acid N-terminal part of PaRBOH1 was recombinantly expressed in *E. coli*. A T7*lac*-controlled expression system was used. Briefly, the N-terminal region was amplified by PCR with forward 5'–AGTAGCATATGGGTTTTGGTAC–3' (incorporated NdeI site underlined) and reverse 5'–TTTCTCGAGGTTGTCTTCCACA–3' (incorporated XhoI site underlined) primers, using cDNA of *PaRBOH1* as a template. The PCR product was purified by precipitation with 0.3 M (final concentration) sodium acetate and washing the pellet with EtOH, after which it was dissolved in water. The PCR product was digested with NdeI and XhoI, and ligated into a similarly-digested pET32a (+) plasmid (Novagen). The insertion removed a Trx-tag, an N-terminal 6xHis-tag and a S-tag as well as proteases' cleavage sites and a multiple cloning site, and placed the open reading frame of the N-terminal sequence in frame with the codons of the C-terminal 6xHis-tag of the vector. After confirming the construct by sequencing, it was transformed into Rosetta™ 2 (DE3) competent cells (Novagen), chosen as a suitable bacterial expression system due to multiple rare codons in the coding sequence of the spruce gene. Large-scale expression of the PaRBOH1 N-terminus was performed at 25°C using the T7 auto-induction medium according to Studier (2005). The produced N-terminus was extracted from the bacterial cells with 8 M urea, captured on Ni-NTA agarose beads (QIAGEN), purified and eluted following QIAGEN's protocol for 6xHis-tagged protein batch purification under denaturing conditions. The protein was buffer-exchanged in PD-10 gel-filtration columns (GE Healthcare) into 25 mM MOPS-KOH, pH 7.2.

In vitro kinase assays: Preparation of crude protein extracts from developing xylem

Developing xylem of Norway spruce was collected from ca. 40 y-old trees grown in Ruotsinkylä, southern Finland in mid-/late June during active secondary growth as described in Väisänen et al. (2018), snap-frozen in liquid nitrogen, transported to a laboratory in dry ice, and stored at -80°C. The frozen samples were ground to a fine powder using an analytical mill (IKA A 11 basic, cooled with liquid nitrogen, 3 x 20 sec bursts), and stored at -80°C until use. To extract cytoplasmic proteins, the frozen xylem powder was added step-wise into a homogenization buffer (50 mM MOPS-KOH, pH 7.5, supplemented with 60 mM NaCl, 1 mM $CaCl_2$, 0.1%

(w/v) Triton X-100, 1.5% (w/v) polyvinylpolypyrrolidone (Polyclar AT), freshly added 5 mM dithiothreitol (DTT) and protease (Complete Mini EDTA-Free, Roche) and phosphatase (PhosSTOP, Roche) inhibitor cocktail tablets; 3 ml buffer/1 g cells). The mixture was incubated for 30 min on ice with occasional mixing, after which the large particles were pelleted by centrifugation (17 000 g, 10 min at 4°C). The supernatant was used immediately, or aliquoted and snap-frozen in liquid nitrogen and stored at -80°C until further assays.

In vitro kinase assays with PaRBOH1 N-terminus and short synthetic peptides

In vitro kinase assays were conducted similarly for the 400 amino acid long N-terminus of PaRBOH1 and for the 15 amino acid peptides with each predicted phosphorylation site (see below). In order to resolve the amino acids being phosphorylation target sites, short synthetic peptides were designed based on the summary of *in silico* predicted phosphorylation sites. Peptides of 15 (in one case 14) amino acid residues with N-terminal biotinylation and C-terminal amidation were custom-produced (ProteoGenix, Schiltigheim, France; ca. 70% purity). To avoid possible steric hindrance with biotin and the spruce kinase(s), putative phosphorylation target sites were designed to always be the tenth (one time ninth) residue in the peptides (Curran et al., 2011). Lyophilized peptide aliquots were suspended in 50% acetonitrile (to 5 mM stocks), from which 0.1 mM working dilutions were prepared in 25 mM MOPS-KOH, pH 7.2. The kinase reactions (50 µl total volume) contained MOPS-KOH, pH 7.2 (30 mM final concentration), 2 µg recombinant N-terminus or 20 µM synthetic peptide (or 25 mM MOPS-KOH pH 7.2 in blank controls), 10 µl crude cytoplasmic protein extract from developing xylem as a kinase source, 1 mM DTT (added fresh), 25 mM β-glycerophosphate, additives (5 mM $CaCl_2$, 5 mM $MgCl_2$, 5 mM $MnCl_2$, 2 mM EDTA and 5 mM EGTA in intended combinations) and 50 µM ATP (providing 10 kBq ^{33}P [γ-ATP] per reaction when radioactivity was used in detection). The reaction was started by addition of ATP, and incubated at 25°C for 30 min. The reactions with the N-terminus were stopped by addition of the Laemmli buffer followed by SDS-PAGE electrophoresis and staining with ProQ Diamond phosphoprotein gel stain (Molecular Probes/Invitrogen) or autoradiography. *In vitro* kinase peptide assays were stopped by dilution with 250 µl of ice-cold 25 mM MOPS-KOH, pH 7.2, and 5 µl of streptavidin agarose ultra-performance beads (SoluLink, USA) were added. After incubation at 4°C for one hour with occasional mixing, the beads were pelleted by centrifugation for 10 min at 17 000 g, and the supernatant was removed. After two washes with 500 µl ice-cold 25 mM MOPS-KOH, the beads were resuspended in 300 µl 25 mM MOPS-KOH, pH 7.2, and the whole reactions were transferred into scintillation vials containing 2.7 ml Optiphase Hisafe 3 scintillation fluid (PerkinElmer). Radioactivity was detected on a Wallac 1414 WinSpectral liquid scintillation counter (PerkinElmer) using the ^{45}Ca internal reference library. The signal in the blank controls was considered as a background, whose average value was subtracted from the sample values before calculations.

HEK cell assays to study regulation of PaRBOH1 activity

To study whether PaRBOH1 produces superoxide *in cellula*, and how its activity is regulated, the protein was heterologously expressed in human embryonic kidney (HEK) cells (line HEK293T) according to Kaya et al. (2019) and Kimura et al. (2022). HEK293T cells have low endogenous ROS production since they lack NADPH oxidases 2 and 5 (Ogasawara et al., 2008). HEK cells were maintained at 37°C in 5% CO_2 in Dulbecco's Modified Eagle's Medium nutrient mixture Ham's F12 (Wako) supplemented with 10% fetal bovine serum (HyClone). A coding sequence of *PaRBOH1* was inserted in a pcDNA3.1-Kozak-3xFLAG vector and transfected by using GeneJuice transfection reagent (Novagen) into HEK293T cells cultivated on 96-well plates (100 ng construct/well) according to manufacturer's instructions. Production of PaRBOH1 protein in HEK cells was verified by Western blotting using an antibody against the FLAG tag. ROS-producing activity assays were conducted as described in Ogasawara et al. (2008). Briefly, the culture medium was removed, and the cells were washed with Hanks' Balanced Salt Solution without any Ca^{2+} or magnesium (HBSS (-/-) buffer, Gibgo) after which the ROS assay solution containing horseradish peroxidase (Wako, 4 or 60 µg/ml) and L-012 sodium salt (Wako, 250 µM) in HBSS (-/-) buffer was added. After a stabilization period of 10 min, $CaCl_2$ (1 mM final concentration) and ionomycin, a Ca^{2+} ionophore (Calbiochem, 1 µM final), were simultaneously injected into the assay medium. ROS production was monitored by a luminol-based chemiluminescence technique using L-012 as a substrate for peroxidase as described in Kaya et al. (2019). Similarly, the effects of a protein serine/threonine phosphatase inhibitor calyculin A (Wako; 0.1 µM final) were tested. Additionally, diphenylene iodonium (DPI; 0.1, 0.5 and 5 µM), an inhibitor of flavin-containing enzymes, and a protein kinase inhibitor K252a (0.1 and 1 µM) were individually added to treatment wells prior to the assays to evaluate their effects on ROS production. To study the effect of Ca^{2+}, various concentrations of Ca^{2+} (0, 0.25, 0.5 and 1 mM) were added to assay wells immediately prior to the start of the experiment, and ionomycin (no Ca^{2+} supplementation with ionomycin in this case) injected at 20 min. Since ionomycin, calyculin A and DPI were originally

dissolved in DMSO, the effects of the corresponding volume of DMSO were tested to see that the effects were not due to DMSO.

In order to identify the amino acids being phosphorylated, candidate amino acids showing positive response in the short peptide activity assays were individually mutated to alanine (A; kinase-inactive) and aspartate (D; phosphomimic) (Dean et al., 1989). The mutants were generated by point-mutation primers using the SPRINP mutagenesis protocol (Edelheit et al., 2009). The primer sequences used in this study are shown in Supplementary Table S2. The full-length mutated constructs were tested in the HEK cell assays, and the ROS-producing activity compared to that of the non-mutated PaRBOH1 assayed in the same experiment. All experiments were conducted independently for at least three times with a similar trend in results.

Phosphoproteomic analysis of PaRBOH1

To determine the phosphorylated amino acids in the native PaRBOH1 during lignin formation *in planta*, microsomal membrane fraction (MF) of developing xylem was isolated (Kärkönen et al., 2014; Väisänen et al., 2018), proteins solubilized with 4% SDS and separated in an SDS-PAGE gel (with loading in every well). Proteins were transferred to a nitrocellulose membrane, and a Western blot conducted to membrane slices that located in both edges of the gel by using a custom-made antibody against PaRBOH1 (GenScript). By knowing the location of the PaRBOH1, the corresponding bands were cut out from the membrane, and the protein sent for proteomic analysis (see below).

In vitro kinase reactions using soluble and membrane-bound kinases from developing xylem

To determine phosphotarget sites for spruce endogenous kinases, an *in vitro* kinase reaction was conducted in a reaction that contained 25 mM MOPS-KOH, pH 7.2, 1 mM DTT, 25 mM β-glycerophosphate, 2 mM $CaCl_2$, 15 mM $MgCl_2$, 2 mM $MnCl_2$, phosSTOP (Roche), a protease inhibitor (EDTA-free, Roche), 10 mM NaATP (fresh, pH adjusted to neutral), 91.7 µg PaRBOH1 N-terminus and 500 µl of freshly prepared xylem cell extract in a final reaction volume of 2.5 ml. The reaction mixture was gently mixed and incubated at 25°C in the dark for 2 h with occasional mixing. After the reaction, the N-terminus was buffer-exchanged in an PD-10 column to phosphate buffer (12.8 mM Na-phosphate, pH 7.4, supplemented with 6 M urea and 320 mM NaCl). The eluate (3.1 ml) was mixed with an equal volume of Ni-NTA resin containing imidazole (1.25 mM final concentration) and incubated overnight at 10°C with slow (50 rpm) shaking, pipetted into two Qiagen columns (3.1 ml/column) at room temperature, and the flow-through collected. The resin was first washed with 6.2 ml of 2.5 mM imidazole in phosphate buffer; then with 6.2 ml of 5 mM imidazole in phosphate buffer. The bound proteins were eluted with 500 mM imidazole in phosphate buffer. Comparable eluates from two columns were combined and concentrated with an Amicon Ultra-4 10K centrifugal filter device (2800 g, 4°C, 30 min). Subsequently, the concentrated N-terminus was re-purified with the Ni-NTA resin. The proteins were separated in an SDS-PAGE gel, and pieces of the gel corresponding to the location of the N-terminus cut out for proteomic analysis. As a control, the PaRBOH1 N-terminus that did not go through any kinase reaction was separated in an SDS-PAGE gel, cut out and analyzed.

For the *in vitro* membrane-bound kinase reactions, a fresh MF containing all cellular membranes was prepared from Norway spruce developing xylem as described in Kärkönen et al. (2014) and Väisänen et al. (2018) with additional 50 mM β-glycerophosphate in the homogenization buffer. The MF obtained was washed by resuspending the pellets in 10 mM MOPS-KOH, pH 7.5, and the membranes were collected by ultracentrifugation (Beckman, 50.2Ti rotor, 200 000 g, 35 min at 4°C). The pellets were resuspended to 10 mM MOPS-KOH, pH 7.5, in a final volume of ca. 1 ml. An *in vitro* kinase reaction was conducted as described above for the soluble kinases except that 500 µl of freshly prepared xylem MF was used as a source of kinases in a final reaction volume of 2.5 ml. After 2 h, the membranes were pelleted (17 000 *g*, 30 min at 4°C). Surprisingly, the PaRBOH1 N-terminus was observed not to be soluble in the supernatant but pelleted with the MF membranes. Addition of increasing concentration of NaCl (up to 3 M in 10 mM MOPS-KOH, pH 7.5) was not able to release the N-terminus from the membranes, and thus, the membranes were incubated 10 min in 4% SDS at room temperature, centrifugated 10 min (1700 g at room temperature), and the supernatant collected. SDS was shown to liberate the N-terminus from the membranes (data not shown). To purify the N-terminus for phosphoproteomic analysis, the SDS-liberated proteins were buffer-exchanged in MidiTrap columns to 12.8 mM Na-phosphate buffer, pH 7.4, supplemented with 6 M urea and 320 mM NaCl, purified in Ni-NTA resin, and separated in an SDS-PAGE gel like described above. There was a fainter band migrating slightly slower (band 2) than the N-terminus (band 1; Supplementary Figure S1). Since phosphorylation increases the molecular weight, both bands were cut out for proteomic analysis.

Phosphoproteomic analysis

Excised protein gel band pieces were reduced and alkylated with 20 mM DTT and 50 mM iodoacetamide successively. The

proteins were digested by adding 0.5 µg trypsin (Promega) in 50 mM ammonium hydrogen carbonate, and the mixture was incubated overnight at room temperature (Vaarala et al., 2014). The peptides were cleaned using C18-reverse phase ZipTip™ (Millipore), resuspended in 1% trifluoroacetic acid (TFA) and sonicated in a water bath for 1 min.

Phosphopeptides in the digest were either directly detected by LC-MS^E or were TiO_2-enriched. Phosphopeptide enrichment was done using TiO_2 cartridges (Agilent Technologies) following the manufacturer's protocol. In brief, TiO_2 cartridges were primed and equilibrated with 50% acetonitrile (ACN)/45% water/5% NH_3 and 50% ACN/48% water/2% TFA successively. Peptides were bound, washed with equilibration solution and ultimately eluted with 80% H_2O/15% ACN/ 5% NH_3.

Digested proteins were injected for LC-MS^E analysis. The peptides were separated by Nano Acquity UPLC system (Waters) equipped with a Symmetry C18 reverse phase trapping column (180 µm × 20 mm, 5 µm particles; Waters), followed by an analytical BEH-130 C18 reversed-phase column (75 µm × 250 mm, 1.7 µm particles; Waters), in a single pump trapping mode. The injected sample analytes were trapped at a flow rate of 15 µl min^{-1} in 99.5% of solution A (0.1% formic acid, FA). After trapping, the peptides were separated with a linear gradient of 3 to 35% of solution B (0.1% FA/ACN), for 30 min at a flow rate 0.3 µl min^{-1} and a stable column temperature of 35°C. The samples were run in a data-independent analysis mode (MS^E) in a Synapt G2-S mass spectrometer (Waters), by alternating between low collision energy (6 V) and high collision energy ramp in the transfer compartment (20 to 45 V) and using a 1-sec cycle time. The separated peptides were detected online with a mass spectrometer, operated in a positive resolution mode in the range of *m/z* 50-2000 amu. Human [Glu^1]-fibrinopeptide B (Sigma, 150 fmol $µl^{-1}$) in 50% ACN/0.1% FA solution at a flow rate of 0.3 µl min^{-1} was used for lock mass correction, applied every 30 sec (Scifo et al., 2015).

Waters' ProteinLynx Global Server (PLGS V3.0) software was used to search for protein identifications. MS^E parameters were set as follows: low energy threshold of 135 counts, elevated energy threshold of 30 counts, and intensity threshold of precursor/ fragment ion cluster 750 counts. Database searches were carried out against *Picea abies, NCBInr* (release of May 2019; 28233 entries) with Ion Accounting algorithm and using the following parameters: peptide and fragment tolerance: automatic; maximum protein mass: 1000 kDa; minimum fragment ions matches per protein ≥ 7; minimum fragment ions matches per peptide ≥ 3; minimum peptide matches per protein ≥ 2; primary digest reagent: trypsin; missed cleavages allowed: 1; fixed modification: carbamidomethylation (C); variable modifications: phosphorylation (STY), and false discovery rate (FDR) < 4%. The method workflow was tested and validated beforehand by using β-casein for in-gel digestion and LC-MS^E analysis. The raw data of HDME LCMS runs, the PLGS 3.0 analysis result files, and the protein database used in the searches in ProteomeXchange (identifier PXD035518) are provided via Massive Spectrometry Interactive Virtual Environment (MassIVE Dataset): http://massive.ucsd.edu/ProteoSAFe/status.jsp?task=a3bd84481aa74996be9278bf1084c858

Construction of a PaRBOH1 hairpin for gene silencing

A ca. 300 bp DNA fragment (including the coding area for the repetitive motif) of the *PaRBOH1* cDNA (GenBank HQ592777.2) was amplified by PCR, using Phusion high-fidelity DNA polymerase (New England BioLabs) and forward 5'-TGTGGATAGAGTTGCCTTCAG-3' and reverse 5'-TCCACATATCCTTCATCTCCA-3' PCR primers, with attB sites for Gateway (Life Technologies) cloning added at their 5' ends. The gel-purified PCR product was inserted *via* Gateway BP recombination into pDONR™221 (Life Technologies) to create a pENTRY-*PaRBOH1*-i plasmid. After confirmation by sequencing, the *PaRBOH1* fragments were transferred *via* Gateway LR recombination to a custom-made plasmid with two attR cassettes in the opposite orientation (a generous gift from Ove Nilsson, Umeå Plant Science Centre, UPSC, Sweden), resulting in a "*PaRBOH1*-i-hairpin" construct, i.e., two inverted PaRBOH1 insertions separated by the maize ubiquitin intron. This construct was verified by BplI digestion.

Transformation of spruce embryogenic cultures

PaRBOH1-i-hairpin construct was used for stable transformation of an embryogenic 11:12:04 Norway spruce cell line. Embryogenic spruce cells were co-cultivated with *Agrobacterium tumefaciens* strain LBA4404 following established protocols at the spruce transformation facility at UPSC (Sofie Johansson and Ove Nilsson, *pers. comm;* von Arnold and Clapham, 2008). Following co-cultivation, the filter paper disks with pro-embryogenic masses were transferred onto fresh solid ½ LP medium (0.35% gelrite) supplemented with 300 mg l^{-1} cefotaxime for the recovery, followed by cultivation in the dark for 7-10 days.

Selection for transformants was conducted on solid ½ LP medium supplemented with 300 mg l^{-1} cefotaxime with initially 1 mM (for two weeks) and subsequently with 3 mM D-serine (for two weeks) in the dark at 20-21°C. Transgenic callus with vigorous growth was tested by genomic PCR for the presence

of *D-serine ammonia lyase* (*dsdA)* gene from *E. coli* (Erikson et al., 2005). For somatic embryo regeneration, transformed embryogenic cultures were cultivated first on solid pre-maturation (DKM) medium (Krogstrup, 1986) without plant growth regulators but supplemented with 3 mM D-serine. After cultivation in the dark for a week, the calli were transferred for maturation on DKM medium supplemented with 29 µM ABA, 3% sucrose and 3 mM D-serine for a total of 6 weeks. Fully developed embryos were dried for 3 weeks under high humidity in the dark, and subsequently germinated on solid medium containing minerals, vitamins, 3% sucrose and 0.5 g l^{-1} casein hydrolysate, pH 5.8.

For germination, plates were placed under constant red light at 20°C, and after 2-3 weeks, the plates were moved to constant white fluorescent light (Kvaalen and Appelgren, 1999) until roots and shoots were fully developed (Dobrowolska et al., 2017). Plantlets were acclimatized under 24 h light (150 µmol m^{-2} s^{-1}) at 20°C, and cultivated in a greenhouse under constant light for two years (with a short-day- and decreasing-temperature-induced dormancy in winter).

Real-time quantitative RT-PCR

In total 19 2-y-old plants were sampled for RT-qPCR: five independent transformant lines each having three biological replicates and four control plants, one being a full control and three half controls. Bark was peeled off from the stems, and the xylem was ground into powder with a mortar and pestle in liquid nitrogen. Total RNA was extracted from the powder according to Chang et al. (1993), and RNA was dissolved in 20 µl of nuclease-free water. Residual genomic DNA was digested with DNase I, and RNA was cleaned using Nucleospin RNA Clean-up Mini kit (Macherey-Nagel) according to the manufacturer's protocol. First-strand cDNA was synthesized using 1 µg of total RNA with SuperScript III reverse transcriptase (Invitrogen) according to manufacturer's instructions.

Amplification efficiencies of primers were determined using dilution series of cDNA prepared by combining equal amounts of first-strand cDNA from control plants. Primers were accepted if the efficiency was at least 1.8 with the standard error of less than 5%. *Glyceraldehyde 3-phosphate dehydrogenase*, *adenosine kinase* and *actin* genes were used as internal controls. PCR mixture was prepared in a 15 µl reaction volume using LightCycler 480 SYBR Green I Master mix (Roche), 0.5 µM of primers and 5 µl of diluted first-strand cDNA. The RT-qPCR was done in a LightCycler 480 instrument (Roche) with following program: 95°C for 10 min, 45 cycles of 95°C for 10 s, 57°C for 10 s, and 72°C for 10 s followed by a melting curve analysis. The data were analyzed using two different methods described in Lim et al. (2016) and Pfaffl (2001).

Results

Protein kinase activity of the developing xylem of Norway spruce to phosphorylate peptides from PaRBOH1

Sequence analysis showed that the N-terminal part of PaRBOH1 contains a four-times repeated motif whose sequence includes a SGPL-motif similar to that in the Botrytis-induced kinase 1 (BIK1) target site S39 in AtRBOHD (Kadota et al., 2014; Figure 2; Supplementary Table S3). In addition, the use of various *in silico* prediction programs resulted in identification of several candidate phosphorylation target sites in the N-terminus of PaRBOH1. A couple of putative nitrosylation sites were found in the transmembrane (C456) and in the C-terminal (C933) domains as well (Supplementary Table S4). *In vitro* protein kinase assays using the 400 amino acid N-terminus, non-labelled ATP or ^{33}P[γ-ATP], and an extract of developing xylem as a source of soluble kinases indicated that phosphorylation(s) indeed occurred. To test which of the predicted sites were phosphorylated by spruce kinases, biotin-labelled, 15 amino acid long peptides were synthesized with each predicted phosphorylation target site in the 10th (or 9th) position. *In vitro* kinase reactions were conducted with the peptides as kinase substrates and a crude extract of developing Norway spruce xylem as a kinase source. Out of 16 tested peptides, six showed a positive response in the *in vitro* kinase peptide assays (Table 1). In two of the positive peptides, two possible phosphorylation target sites located next to each other (T149 and S150; T174 and S175; Table 1), making the phosphosite assignment challenging.

ROS-producing activity of PaRBOH1 *in cellula*

To evaluate the regulation of PaRBOH1 activity *in cellula*, the wild type *PaRBOH1* gene was transiently expressed in HEK293T cells having a low level of endogenous extracellular ROS production. Even though the codon usage in conifers is partially different to that in humans, a protein of a correct size was shown to be produced in HEK cells (Figure 3A). Simultaneous injection of ionomycin, a Ca^{2+} ionophore (1 µM), and $CaCl_2$ (1 mM) induced a transient peak of ROS production in the PaRBOH1-transfected cells, but not in the empty-vector-transfected control cells (Figure 3B). Moreover, addition of diphenylene iodonium (DPI; 0.1-5 µM), an inhibitor of flavin-containing enzymes, inhibited ROS production (Figure 3B, D, F), indicating the ROS-producing activity of PaRBOH1. Decreasing Ca^{2+} concentration diminished the height of the ROS peak (Figure 3C), suggesting that Ca^{2+} influx and the following binding of Ca^{2+} to the EF-hand

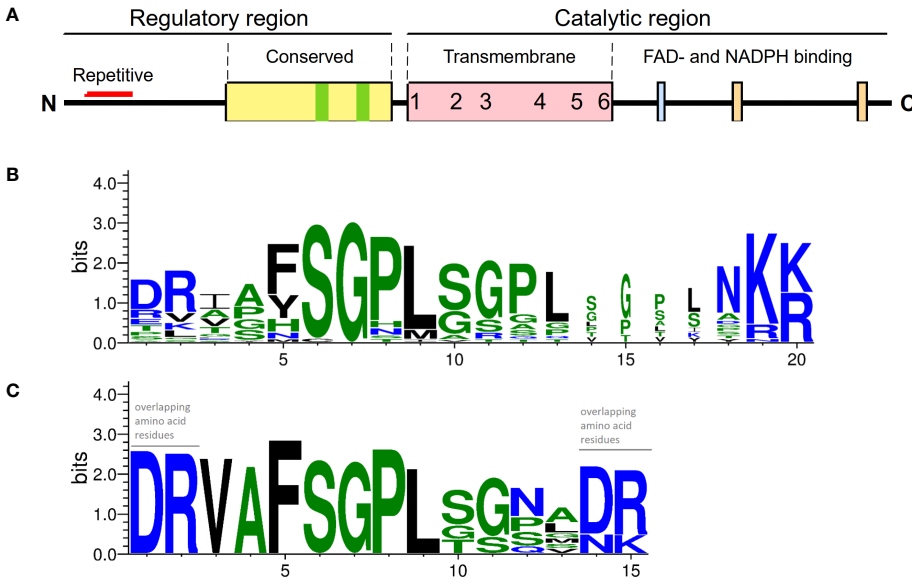

FIGURE 2
A primary structure of PaRBOH1. **(A)** A schematic model of the PaRBOH1 structure. **(B)** A sequence logo image of the conservation of the BIK1 target site corresponding to S39 in AtRBOHD in members of the plant *RBOH* gene family with up to three SGPL-like adjacent motifs (Supplementary Table S3A). **(C)** A sequence logo image of the BIK1 target site in the N-terminal repetitive motif generated using the four-times repeated motif from PaRBOH1 and the five-times repeated motif from its closest *P. taeda* homologue (Supplementary Table S3B). Sequence logos were generated by WebLogo (Crooks et al., 2004), hydrophilic charged (blue) and neutral (green) amino acid residues are indicated.

motifs of PaRBOH1 triggered ROS production. Hence, 1 mM $CaCl_2$ was used in the subsequent experiments.

Calyculin A, an inhibitor of protein phosphatases, increased the extracellular ROS levels from those in the DMSO-only treated cells (Figure 3D); this increase was stable for the 20-min experimental time after calyculin A addition. Vice versa, K252a, an inhibitor of a protein kinase, decreased the ionomycin-induced ROS peak in a concentration-dependent manner (Figure 3E). These observations suggest that protein phosphorylation is crucial in the regulation of the PaRBOH1 activity. Addition of calyculin A followed by an ionomycin-$CaCl_2$ treatment led to the strongest ROS burst, indicating that similar to several other RBOHs (Ogasawara et al., 2008; Kimura et al., 2012; Kaya et al., 2019), phosphorylation enhances the induction of PaRBOH1 activity by Ca^{2+} (Figure 3F).

Phosphorylation target sites in the PaRBOH1 N-terminus

To determine the phosphorylation target sites in the N-terminus responsible for regulation of the PaRBOH1 activity, the serine/threonine residues showing positive response in the *in vitro* kinase peptide assays and those in the repetitive sequence motif (Table 1) were individually mutated to alanine (A; kinase-inactive) and aspartate (D; phosphomimic), and the effects on ROS production were tested in HEK cells. Mutations of serine residues in the repetitive sequence motif (S32, S45, S58, S71; Figure 2C; Supplementary Table S3B) did not show any consistent differences in ROS production as compared to non-mutated, wild-type PaRBOH1 (Table 1; Figure 4). However, phosphoproteomic analysis of the PaRBOH1 N-terminus after *in vitro* kinase assays using spruce endogenous kinases from the developing xylem, on the other hand, showed that these serine residues, S32, S45/58 and S71, were phosphorylated by both soluble and membrane-bound protein kinases (Tables 1 and 2; Supplementary Data S1; Supplementary Figures S2-S8). In addition, several other serine and threonine residues were shown to be phosphorylated, with T149, S150 and T174 residues with the highest intensity (Table 2).

Mutations of the putative target sites (serine or threonine residues) did not affect the protein amounts of PaRBOH1 (Supplementary Figure S9). In the HEK cell assays, however, mutation of the following putative target sites (serine or threonine residues) to either alanine or aspartate residues showed clear responses in ROS production (either decreased/unaffected in case of alanine substitution or enhanced in case of aspartate substitution): S150, S160, T174, T190, T300, S374 (Figure 4). Mutations of S86 or S175 did not affect the ROS-producing response in HEK cells, whereas that of T149 did not give consistent responses. Phoshoproteomic results after *in vitro* kinase assays using spruce kinases were consistent with few

TABLE 1 Phosphorylation of the PaRBOH1 N-terminal serine (S) and threonine (T) residues in *in vitro* kinase assays with short peptides and the full N-terminus, and the effect of phosphorylation of these residues on the enzymatic activity in HEK cell assays.

(A)			(B)	(C)		
Position in PaRBOH1	**15-mer sequence**	**Response in *in vitro* kinase peptide assays**	**HEK cell assays**	**Phosphoproteomic analysis after *in vitro* kinase reactions**		
				Soluble kinases	**Membrane-bound kinases band 1**	**Membrane-bound kinases band 2**
S32		n.d.	A: ±, D: ±	+	+	+
S45		n.d.	A: ±, D: ±	+[¶, #]	+[¶, #]	+[¶, #]
S58		n.d.	A: ±, D: ±	+[¶, #]	+[¶, #]	+[¶, #]
S71		n.d.	A: ±, D: ±	+[#]	+[#]	+[#]
S86	PLNKR PGRR**S** ARFNI	+	A: ±, D: ±			
T149	LAKDL EKK**T**S FGSSI	+[†]	A: ±, D: ±	+	+	+
S150	LAKDL EKKT**S** FGSSI	+[†]	A: +, D: ++	+	+	+
S160	FGSSI IRNA**S** ARIKH	+	A: -, D: ++			
T174	VSQEL KRL**T**S FTKRS	+[‡]	A: 0, D: ++ +	+		
S175	VSQEL KRLT**S** FTKRS	+[‡]	A: 0, D: 0		+	
T190	HPGRL DRSK**T** GAHHA	–	A: 0, D: ++			
T300§	VDKNA DGRI**T** EEEVK	+	A: -, D: ++ +			
S374	TSLNL SQMI**S** QKLVP	+	A: -, D: ++ +			

(A) Sequences of peptides with N-terminal biotinylation were designed with the predicted phosphorylation site at the position 9 or 10 in the 15-mer (underlined bold character). The peptides showing enhanced phosphorylation (+) as compared to no-peptide controls in at least two independent *in vitro* kinase experiments are shown; -, no difference as compared to no-peptide control; [†,‡] the phosphotarget site cannot be distinguished based on *in vitro* kinase peptide assays; n.d., not determined. (B) For HEK cell assays, each putative phosphotarget site was mutated to alanine (A)/aspartate (D), and the effects on apoplastic ROS production evaluated according to Kaya et al. (2019). 0, similar ROS production as in the wild-type construct; -, decreased ROS production as compared to the wild-type construct; ±, no consistent response as compared to the wild-type construct; +, ++ or +++, enhanced ROS production as compared to the wild-type construct. [§] putative phosphosite overlaps the first EF hand. (C) Phosphorylated residues detected in the phosphoproteomic analysis of the PaRBOH1 N-terminus after *in vitro* kinase reactions using soluble cytoplasmic extract or microsomal membrane fraction of developing xylem of Norway spruce as sources for kinases. Band 1 and band 2 (Supplementary Figure S1): two bands cut out from the SDS-PAGE gel after membrane-bound kinases were used in *in vitro* kinase reaction followed by SDS-PAGE to separate the PaRBOH1 N-terminus. See Table 2 for details. [¶]S45 and S58 cannot be distinguished in the phosphoproteomic analysis. [#] Some phosphorylation also in the control PaRBOH1 N-terminus that did not go through the *in vitro* kinase assay.

detected phosphosites in the HEK cell assays (S150, T174; Tables 1 and 2; Supplementary Data S1). S150 corresponds to the T123 site in AtRBOHD, which is also a target site for BIK1. To our knowledge, T174 is a novel regulatory site not yet described in other species. Interestingly, T174D construct was able to induce the highest ROS production (ca. 3.5 times higher than in the wild type PaRBOH1; Figure 4).

Generation of *PaRBOH1*-silenced plants

To verify the function of PaRBOH1 *in planta*, a hairpin construct of *PaRBOH1* driven by a maize ubiquitin promoter was transformed to Norway spruce embryogenic cultures with the aim to silence the gene. After antibiotic selection, embryos were induced and plantlets regenerated from several putatively silenced lines originating from independent transformation events. Unfortunately, all but one of the non-transformed, genetically identical control plantlets (full-control) were lost. Hence, non-transformed plantlets from a genetically half-identical line were used as controls (half-controls). Due to differences in *PaRBOH1* expression in the full-control and half-control plants, the effects of gene silencing were difficult to conclude (data not shown). Thus, the role of PaRBOH1 in wood development still remains to be evaluated.

Discussion

Oxidation of monolignols, one of the final steps of lignification, involves either peroxidases or laccases in angiosperm species. In spite of the critical importance of lignin biosynthesis in coniferous tree species, however, its molecular mechanisms remain partially unknown. Our earlier studies suggested that peroxidases and the ROS-producing RBOHs play a major role in lignification (Kärkönen et al., 2009; Kärkönen et al., 2014; Laitinen et al., 2017). We therefore characterized the ROS-producing activity and its regulatory mechanisms of the most highly expressed RBOH,

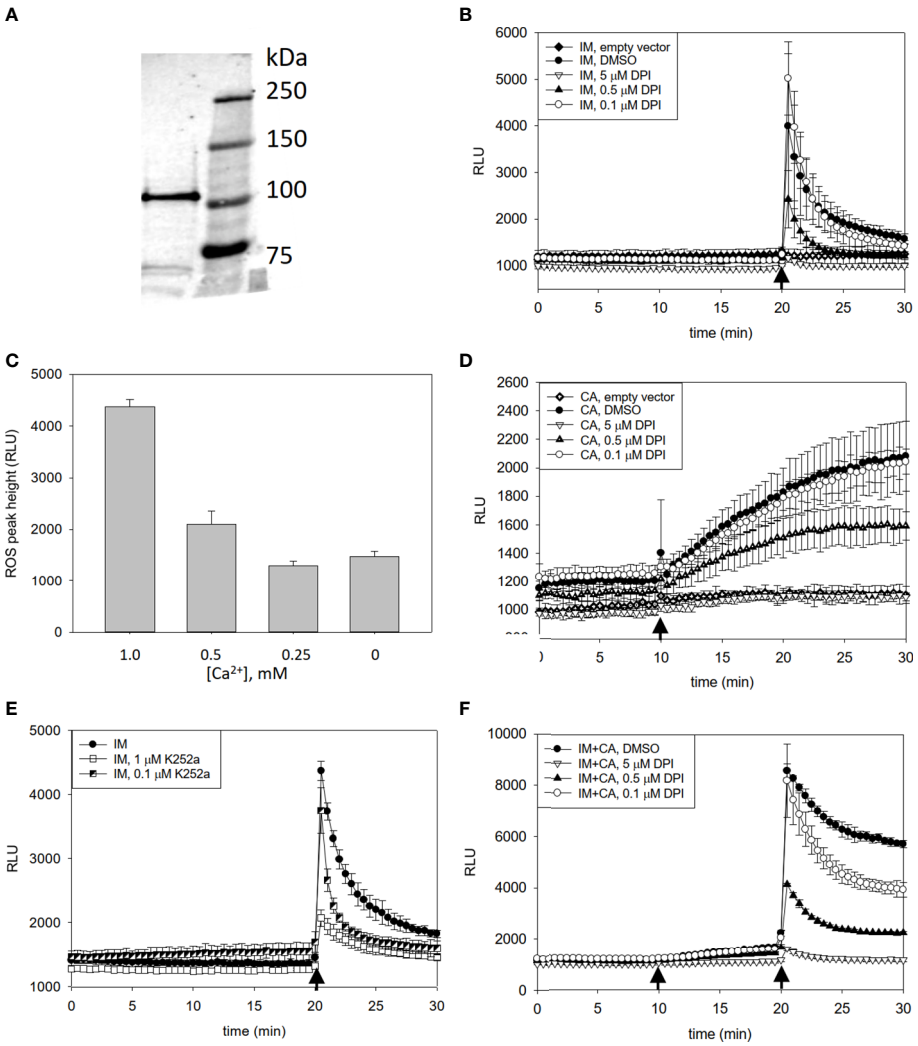

FIGURE 3
Detection of heterologously produced PaRBOH1 in HEK cells and effects of pharmacological inhibitors and Ca^{2+} on ROS production. **(A)** A protein of a correct size (107 kDa) is produced in HEK cells transfected with a *PaRBOH1* construct as revealed by a Western blot using an antibody against the FLAG-tag. **(B–F)** Effects of pharmacological inhibitors and Ca^{2+} on ROS production in human embryogenic kidney (HEK293T) cells transfected with *PaRBOH1*. **(B)** After measuring the baseline ROS production for 20 min, a Ca^{2+} ionophore ionomycin (IM; 1 µM) and 1 mM Ca^{2+} were simultaneously injected into the assay mixture. **(C)** Various concentrations of Ca^{2+} were externally added to assay wells just prior to the start of the experiment. IM was injected at 20 min. Maximum ROS peaks are shown. **(D)** After measuring the baseline ROS production for 10 min, a phosphatase inhibitor calyculin A (CA; 0.1 µM) was injected into the assay mixture. **(E)** Effect of a kinase inhibitor K252a on ROS production. K252a (0.1 or 1 µM) was supplemented to the assay mixture just prior to the start of an experiment. IM was injected at 20 min. **(F)** A combined effect of calyculin A and IM on ROS production. Calyculin A (0.1 µM) was injected at 10 min, and IM (1 µM) supplemented with 1 mM Ca^{2+} at 20 min. In Figure 3 **(B, D, F)**, an inhibitor of flavin-containing enzymes, diphenylene iodonium (DPI, 0.1, 0.5 or 5 µM), was supplemented to the assay mixture just prior to the start of an experiment. Control wells obtained a corresponding volume of DMSO. Data are expressed as relative luminescence units (RLU). Each data point represents the average of three wells analyzed in parallel (mean ± S.D.). The experiment was repeated for at least three times in separate experiments with similar trend in results. Arrows, time of injection.

PaRBOH1, in both the developing xylem (Figure 1) and the lignin-forming cell culture (Laitinen et al., 2017).

We have shown for the first time in gymnosperms and tree species that PaRBOH1 has the ROS-producing activity activated by both Ca^{2+} and phosphorylation (Figure 3). Indeed, the cell extract of the developing xylem showed protein kinase activity phosphorylating specific serine and threonine residues of PaRBOH1 (Table 1). Alike in other plant species' RBOHs, PaRBOH1 contains two EF-hand motifs in the cytosolic N-terminal region with a high sequence conservation to those present in AtRBOHs (Figure 5). Ca^{2+} binding to the EF-hand motifs has been shown to induce a conformational change that activates ROS production (Ogasawara et al., 2008; Oda et al., 2010). The results obtained with the Norway spruce PaRBOH1

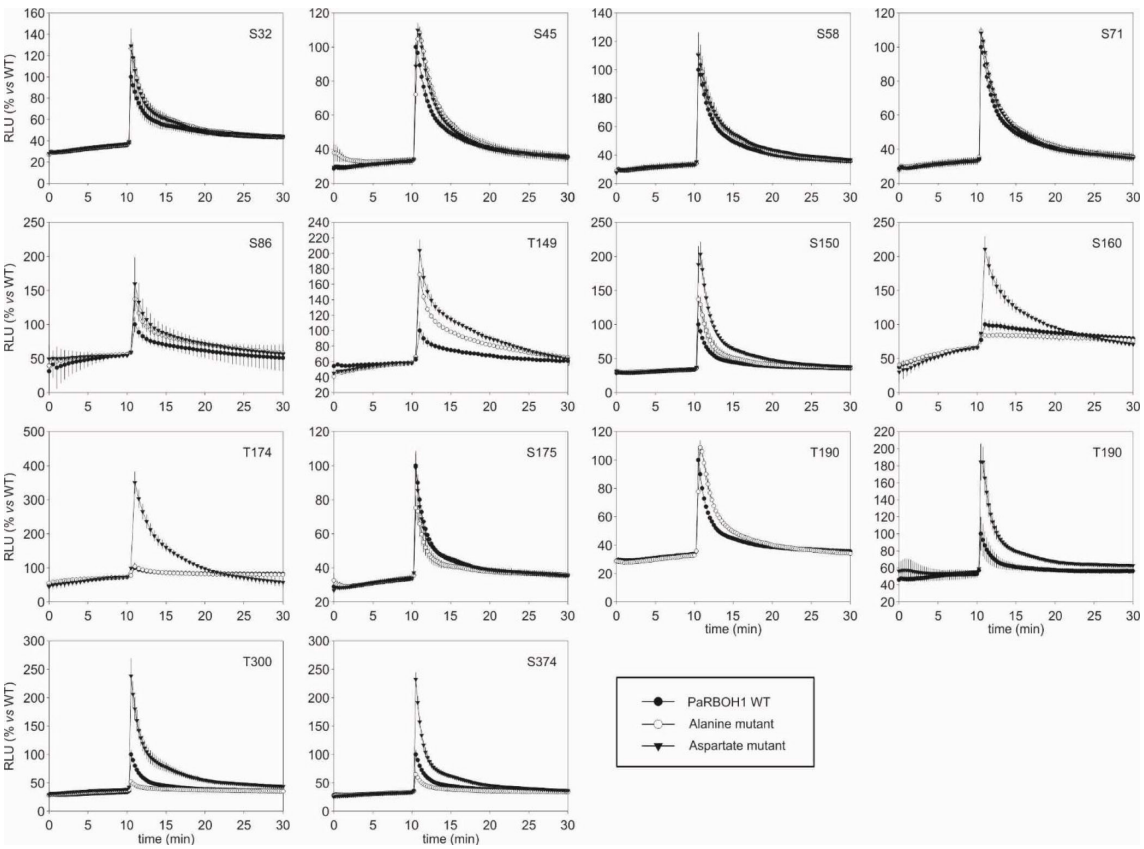

FIGURE 4
Impact of alanine (A) and aspartate (D) phosphosite substitution mutants of PaRBOH1 on ionomycin-induced ROS production in transfected HEK293T cells. ROS production was detected by luminol-amplified chemiluminescence. HEK cells were transiently transfected with *PaRBOH1* WT (wild type), *PaRBOH1* with serine/threonine-alanine mutation (A, kinase-inactive) or *PaRBOH1* with serine/threonine-aspartate mutation (D, phosphomimic) at the indicated PaRBOH1 phosphotarget site. ROS production activity of PaRBOH1 and its A and D mutants was measured in response to adding 1 μM ionomycin and 1 mM Ca^{2+} at 10 min and expressed as relative luminescence units (RLU; PaRBOH1 WT response was set to 100%). Results are means of three wells ± S.E. (n = 3). Similar results were obtained at least in three independent experiments.

in the present work support the idea that the synergistic activation by Ca^{2+} binding to the EF hand motifs and phosphorylation of several serine and threonine residues by protein kinases is a common regulatory mechanism conserved in seed plants (Ogasawara et al., 2008; Oda et al., 2010; Kaya et al., 2019).

In silico analysis followed by *in vitro* kinase assays were utilized to find out putative phosphorylation sites in the N-terminus of PaRBOH1 (Table 1). Next, a full-length *PaRBOH1* was transfected to HEK cells with each putative phosphotarget site individually mutated to alanine or aspartate, and the quantitative measurement of the ROS-producing activity conducted (Figure 4). These analyses combining the phosphoproteomic studies, *in vitro* phosphorylation, the quantitative assay of the ROS-producing activity and the site-directed mutagenesis showed that several serine and threonine residues seemed to be regulatory sites for the PaRBOH1 activity.

The phosphoproteomic analysis of the PaRBOH1 N-terminus after *in vitro* kinase assays using spruce soluble and membrane-bound kinases showed that S32, corresponding to S39 in AtRBOHD, and the following corresponding serine residues in the repetitive motif, *i.e.*, S45/58 and S71 were phosphorylated by both types of spruce endogenous kinases (Tables 1 and 2; Supplementary Data S1). In AtRBOHD, the site S39 is phosphorylated by BIK1 in the pathogen response in a Ca^{2+}-independent way (Li et al., 2014; Kadota et al., 2014). Since non-elicited spruce trees were used as origins of developing xylem, phosphorylation of these serine residues may have a regulatory role during normal development. None of these serine residues in the repetitive motif of PaRBOH1 (Figure 2C, Supplementary Table S3B), however, gave consistent responses in the HEK cell assays (Table 1; Figure 4). The lack of a reproducible and consistent response for the repetitive sequence serine residues in the HEK cell assays suggests that these serine residues may be

10.3389/fpls.2022.978586

TABLE 2 Phosphoproteomic analysis of the N-terminus of PaRBOH1.

	Control		Cytoplasmic soluble kinases		Membrane-bound kinases			
					band 1		band 2	
Residue		**TiO_2**		**TiO_2**		**TiO_2**		**TiO_2**
T5		2735						
T16	5450		10915		944			
	7.00%		**22.60%**		**5.67%**			
T22		1270						
S32			18191	21437	40310	52839	23208	11650
			0.18%		**0.65%**		**1.73%**	
S36			10915	13627	9217	4516		
			0.10%		**0.15%**			
S37						11362		
S45/S58	1097		32518	58464	107010	180890	43497	31290
	0.00%		**0.14%**		**0.84%**		**1.52%**	
T49				2870				
S71	2169		25280	5296	41740	26641	11852	
	0.02%		**0.28%**		**1.00%**		**1.43%**	
T75					5959			
					0.14%			
S119	1641							
	12.40%							
T149			3703	175051	167858	306829	4416	34697
			0.09%		**29.78%**		**1.61%**	
S150			113920		14393		38805	
			2.76%		**1.04%**		**30.91%**	
S154						822		
T174			217769	452372				
			23.90%					
S175						52547		
T177				89328		39460		
S188							19713	
							90.30%	
Y342	1245							
	3.24%							
S366					4167			
					1.30%			

Phosphorylated residues detected in the phosphoproteomic analysis of the PaRBOH1 N-terminus after *in vitro* kinase reactions using soluble cytoplasmic extract or microsomal membrane fraction of developing xylem of Norway spruce as sources for kinases. Control: in *Escherichia coli* produced PaRBOH1 N-terminus without any *in vitro* kinase reaction; Band 1 and band 2: two bands cut out from the SDS-PAGE gel after membrane-bound kinases were used in *in vitro* kinase reaction followed by SDS-PAGE to separate the PaRBOH1 N-terminus (Supplementary Figure S1). In the table, the upper numbers represent the intensity in the LC-MS^E analysis, and the numbers below (in bold) represent the percentage of phosphorylated *versus* non-phosphorylated peptide. TiO_2: titanium oxide enrichment.

phosphorylated by some specific protein kinases in spruce but cannot be phosphorylated by endogenous protein kinases in the HEK293T cells.

The phosphoproteomic analysis indicated that T174, which gave a positive response in the HEK cell assays (Figure 4), is a novel site not yet recognized in other species (Figure 5). In some putative phosphorylation sites, the phosphoproteomic analysis showed no phosphorylation in a few positive sites of the *in vitro* kinase peptide assays and/or of the HEK cell assays (S160, T190, T300, S374), or showed phosphorylation when HEK cell assays did not give a consistent response (S32, T149, S175; Table 1). Out of these, T300 locates in the first EF-hand motif (Figure 5). The assays showed that the phosphomimic mutant of T300 has elevated ROS production after ionomycin-Ca^{2+} injection (Table 1), which suggests a beneficial effect of a prior T300 phosphorylation for the Ca^{2+} binding to the EF-hand and the resulting increase in PaRBOH1 activity. T190 was chosen for the HEK cell assays even if it did not give a positive response in *in vitro* kinase peptide assays, since it corresponds to the

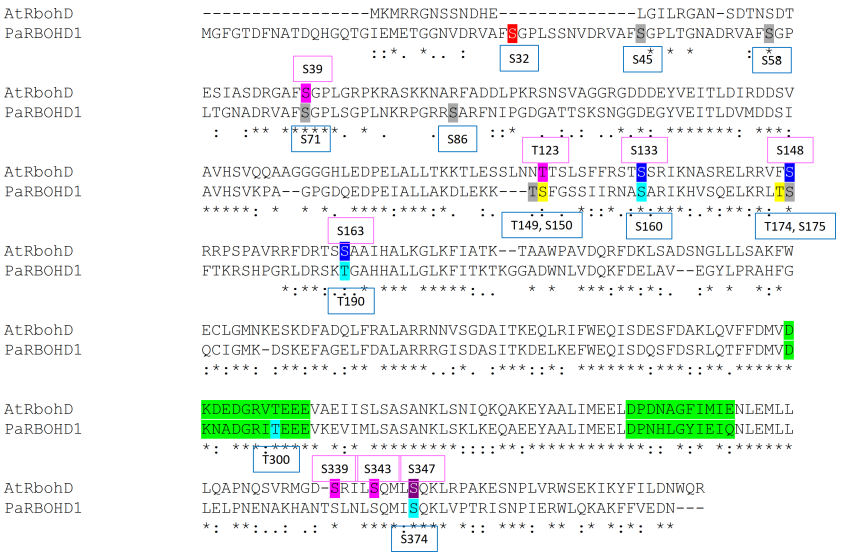

FIGURE 5
Phosphotarget sites in the N-terminus important for the PaRBOH1 activity, and comparison for those reported in AtRBOHD. The putative EF hands have been marked with a green colour. Colour codes in the AtRBOHD sequence: pink, a target site phosphorylated by BIK1; blue, a target site phosphorylated by CDKs; purple, a target site for both BIK1 and CDKs. Colour codes in the PaRBOH1 sequence: light blue, a phosphotarget site showing positive response in HEK cells; grey, a site showing no response in HEK cells; yellow, an amino acid having phosphorylation in the phosphoproteomic analysis and giving a positive response in HEK cell assays; red, an amino acid having phosphorylation in the phosphoproteomic analysis, but not giving a positive response in HEK cells. For references, see discussion.

S163 site in AtRBOHD that has been shown to be a regulatory site (Benschop et al., 2007). S374 corresponds to S347 in AtRBOHD that is a phosphotarget site for both CDKs and BIK1 (Dubiella et al., 2013; Li et al., 2014; Kadota et al., 2014). It should be noted that the peptide TSLNL SQMIS QKLVP used in the *in vitro* kinase peptide assays with S374 as its 10th amino acid also contains another serine at its 6th position. This serine is S370 in the PaRBOH1 sequence, and corresponds to S343 in AtRBOHD, which is a verified phosphotarget site for the BIK1 (Kadota et al., 2014). Although S370 was not mutated for the HEK cell assays, it is possible that it serves as a phosphotarget site also in HEK cells, and in developing xylem of Norway spruce.

In AtRBOHD, S8, S9, S39, T123, S148, S152, S163, S343 and S347 are phosphorylated in response to pathogen-associated molecular patterns (PAMPs; Benschop et al., 2007; Nühse et al., 2007; Dubiella et al., 2013; Kadota et al., 2014; Zhang et al., 2018; Li et al., 2021). BIK1, for example, phosphorylates S39, T123, S339 and S343 and S347 of AtRBOHD (Li et al., 2014; Kadota et al., 2014), and CPKs phosphorylate AtRBOHD at S133, S148, S163 and S347 (Dubiella et al., 2013; Kadota et al., 2014). A receptor-kinase for extracellular ATP, DORN1, in turn, phosphorylates S22 and T24 in AtRBOHD in *in vitro* and *in vivo*, however, phosphorylation of S22, and not of T24, is essential for the ATP-triggered ROS burst (Chen et al., 2017). It is possible that in spruce, similar to Arabidopsis, a pathogen attack activates novel type(s) of kinases (e.g. an ortholog of a BIK1), that are not active during developmental lignification, leading to phosphorylation of sites not detected now in the proteomic analysis.

The presence of the four-times repeated motif in PaRBOH1 containing sites recognized by the BIK1 suggests that the serine residues in these motifs have an important function at certain physiological conditions. In several RBOHs (e.g. in AtRBOHD), the motif is present only once (Figure 5; Supplementary Table S3A). Interestingly, however, loblolly pine (*Pinus taeda*) contains a RBOH (PITA 000006695-RA) that shares a high homology to PaRBOH1 (91.5% identity) and has a very similar repetitive motif repeated for five times in its N-terminus (Figure 2C; Supplementary Table S3B). In addition, grape (*Vitis vinifera*) RBOHB (VV14G08690) has the core SPGL motif repeated for four times in row with slight variations in the sequence (data not shown). Significance of these repetitive sequences of the putative phosphorylation sites observed in several plant species is an interesting topic to be studied in future studies.

In the HEK cell assays, the ROS levels produced by PaRBOH1 were relatively low (Figure 3). Different AtRBOHs are known to vary in the ROS-producing activity by 100-times in the HEK cell system (Kaya et al., 2019). In general, the PaRBOH1-formed ROS levels were comparable to those of AtRBOHA, -D and -E.

Some studies suggest an important role of nitric oxide (NO) in regulating ROS production and scavenging (Gupta et al., 2020). Indeed, S-nitrosylation of C890, consisting of a nitrosothiol (SNO) formation through the addition of a NO moiety to a thiol group of a cysteine residue, down-regulates the RBOHD activity by comprising the oxidative burst induced by pathogen and the hypersensitive response associated cell death (Yun et al., 2011). Additionally,

persulfidation of RBOHD cysteine residues by covalent addition of thiol groups at C825 and C890 enhanced ROS production in Arabidopsis (Shen et al., 2020). On the other side, NO-based post-translational modifications have been shown to modulate proteins involved in ROS scavenging, such as superoxide dismutase and ascorbate peroxidase, by S-nitrosylation and tyrosine nitration (Yang et al., 2015; Kolbert and Feigl, 2017). Out of the two predicted nitrosylation sites in PaRBOH1 sequence (Supplementary Table S4), first one is in the transmembrane area (Cys456) and the latter one close to the C-terminus (C933), approximately in the same area as the reported inhibitory nitrosylation event on C890 of RBOHD and therefore it deserves further investigation as a potential negative switch of RBOH activity in conifers.

This is the first study related to regulation of RBOH activity in gymnosperms including coniferous species. The data obtained indicate that regulation of RBOH activity by Ca^{2+} and phosphorylation is conserved in both gymnosperms and angiosperms including conifers, monocot and eudicot species. We have identified many putative phosphorylation sites by both soluble and membrane-bound protein kinases in the developing xylem. Identification of the responsible protein kinases expressed in the developing xylem would be an important and challenging future project. Transcriptomic data now available enable searches for candidate kinases among the similarly expressed genes. Once putative protein kinases are identified, co-expression of the putative kinases with PaRBOH1 in the heterologous expression system described in the present study would be useful to characterize the molecular regulatory mechanisms of PaRBOH1 by various protein kinases as well as phosphatases. In order to resolve the physiological significance of the PaRBOH1-mediated ROS production in Norway spruce, transgenic approaches are needed.

Data availability statement

The PaRBOH1 coding sequence has been submitted to a NCBI GenBank with an accession number HQ592777.2. The proteomic dataset generated for this study are included in the article / Supplementary Material. The raw data of HDME LCMS runs, the PLGS 3.0 analysis result files, and the protein database used in the searches in ProteomeXchange (identifier PXD035518) are provided via Massive Spectrometry Interactive Virtual Environment (MassIVE Dataset): http://massive.ucsd.edu/ProteoSAFe/status.jsp?task=a3bd84481aa74996be9278bf1084c858".

Author contributions

KN, AG, KHa, TL, HH, THT, KK and AK conceived the research and designed the experiments; KN, AG, KHa, TL, EV, TP, RS, TK, KHi, OB, SJ-L and AK performed the experiments; KN, AG, KHa, TL, EV, TP, RS, KHi, SJ-L and AK analyzed the data; KVF, HT and GW contributed materials/data/analysis tools; KN, AG, KHa, EV, TP, KK and AK wrote the manuscript with contributions of all authors. All authors contributed to the article and approved the submitted version.

Funding

This work was supported by Academy of Finland (AK; decisions 251390, 256174, 283245 and 334184, SJ-L; decisions 331172 and 335972), Viikki Doctoral Programme in Molecular Biosciences (TL, EV), Integrative Life Science Doctoral Program (TL, EV), Jenny and Antti Wihuri Foundation (EV), MEXT, Japan (KK; KAKENHI grant numbers 50211884 and 25114515), JSPS, Japan (KK; KAKENHI grant number 15H01239), and Tokyo University of Science International Exchange Program (KK). Proteomic analyses were performed at the Meilahti Clinical Proteomics Core Facility, HiLIFE, supported by Biocenter Finland.

Acknowledgments

We thank T. Warinowski and M. Huovila for cloning *PaRBOH1* cDNA.

Conflict of interest

The authors declare that the research was conducted in the absence of any commercial or financial relationships that could be construed as a potential conflict of interest.

Publisher's note

Supplementary material

The Supplementary Material for this article can be found online at: https://www.frontiersin.org/articles/10.3389/fpls.2022.978586/full#supplementary-material

References

Barbosa, I. C. R., Rojas-Murcia, N., and Geldner, N. (2019). The Casparian strip-one ring to bring cell biology to lignification? *Curr. Opin. Biotechnol.* 56, 121–129. doi: 10.1016/j.copbio.2018.10.004

Benschop, J. J., Mohammed, S., O'Flaherty, M., Heck, A. J. R., Slijper, M., and Menke, F. L. H. (2007). Quantitative phosphoproteomics of early elicitor signaling in *Arabidopsis*. *Mol. Cell. Proteomics* 6, 1198–1214. doi: 10.1074/mcp.M600429-MCP200

Berthet, S., Demont-Caulet, N., Pollet, B., Bidzinski, P., Cézard, L., Le Bris, P., et al. (2011). Disruption of *LACCASE4* and *17* results in tissue-specific alterations to lignification of *Arabidopsis thaliana* stems. *Plant Cell* 23, 1124–1137. doi: 10.1105/tpc.110.082792

Blaschek, L., Murozuka, E., Ménard, D., and Pesquet, E. (2022). Different combinations of laccase paralogs non-redundantly control the lignin amount and composition of specific cell types and cell wall layers in *Arabidopsis*. *bioRxiv preprint*. doi: 10.1101/2022.05.04.490011

Blaschek, L., and Pesquet, E. (2021). Phenoloxidases in plants – how structural diversity enables functional specificity. *Front. Plant Sci.* 12. doi: 10.3389/fpls.2021.754601

Blokhina, O., Laitinen, T., Hatakeyama, Y., Delhomme, N., Paasela, T., Zhao, L., et al. (2019). Ray parenchymal cells contribute to lignification of tracheids in developing xylem of Norway spruce. *Plant Physiol.* 181, 1552–1572. doi: 10.1104/pp.19.00743

Castro, B., Citterico, M., Kimura, S., Stevens, D. M., Wrzaczek, M., and Coaker, G. (2021). Stress-induced reactive oxygen species compartmentalization, perception and signalling. *Nat. Plants* 7, 403–412. doi: 10.1038/s41477-021-00887-0

Chang, S., Puryear, J., and Cairney, J. (1993). A simple and efficient method for isolating RNA from pine trees. *Plant Mol. Biol. Rep.* 11, 113–116. doi: 10.1007/BF02670468

Chen, D., Cao, Y., Li, H., Kim, D., Ahsan, N., Thelen, J., et al. (2017). Extracellular ATP elicits DORN1-mediated RBOHD phosphorylation to regulate stomatal aperture. *Nat. Commun.* 8, 2265. doi: 10.1038/s41467-017-02340-3

Chou, Y. E., Schuetz, M., Hoffmann, N., Watanabe, Y., Sibout, R., and Samuels, A. L. (2018). Distribution, mobility, and anchoring of lignin-related oxidative enzymes in Arabidopsis secondary cell walls. *J. Exp. Bot.* 69, 1849–1859. doi: 10.1093/jxb/ery067

Crooks, G. E., Hon, G., Chandonia, J.-M., and Brenner, S. E. (2004). WebLogo: a sequence logo generator. *Genome Res.* 14, 1188–1190. doi: 10.1101/gr.849004

Curran, A., Chang, I.-F., Chang, C.-L., Garg, S., Miguel, R. M., Barron, Y. D., et al. (2011). Calcium-dependent protein kinases from *Arabidopsis* show substrate specificity differences in an analysis of 103 substrates. *Front. Plant Sci.* 2. doi: 10.3389/fpls.2011.00036

Dean, A. M., Lee, M. H., and Koshland, D. E. (1989). Phosphorylation inactivates *Escherichia coli* isocitrate dehydrogenase by preventing isocitrate binding. *J. Biol. Chem.* 264, 20482–20486. doi: 10.1016/S0021-9258(19)47087-7

de Castro, E., Sigrist, C. J. A., Gattiker, A., Bulliard, V., Langendijk-Genevaux, P. S., Gasteiger, E., et al. (2006). ScanProsite: detection of PROSITE signature matches and ProRule-associated functional and structural residues in proteins. *Nucleic Acids Res.* 34, W362–W365. doi: 10.1093/nar/gkl124

Denness, L., McKenna, J. F., Segonzac, C., Wormit, A., Madhou, P., Bennett, M., et al. (2011). Cell wall damage-induced lignin biosynthesis is regulated by a reactive oxygen species- and jasmonic acid-dependent process in Arabidopsis. *Plant Physiol.* 156, 1364–1374. doi: 10.1104/pp.111.175737

Dixon, R. A., and Barros, J. (2019). Lignin biosynthesis: old roads revisited and new roads explored. *Open Biol.* 9, 190215. doi: 10.1098/rsob.190215

Dobrowolska, I., Businge, E., Abreu, I. N., Moritz, T., and Egertsdotter, U. (2017). Metabolome and transcriptome profiling reveal new insights into somatic embryo germination in Norway spruce (*Picea abies*). *Tree Physiol.* 37, 1752–1766. doi: 10.1093/treephys/tpx078

Drerup, M. M., Schlücking, K., Hashimoto, K., Manishankar, P., Steinhorst, L., Kuchitsu, K., et al. (2013). The calcineurin b-like calcium sensors CBL1 and CBL9 together with their interacting protein kinase CIPK26 regulate the *Arabidopsis* NADPH oxidase RBOHF. *Mol. Plant* 6, 559–569. doi: 10.1093/mp/sst009

Dubiella, U., Seybold, H., Durian, G., Komander, E., Lassig, R., Witte, C.-P., et al. (2013). Calcium-dependent protein kinase/NADPH oxidase activation circuit is required for rapid defense signal propagation. *Proc. Natl. Acad. Sci. U S A.* 110, 8744–8749. doi: 10.1073/pnas.1221294110

Edelheit, O., Hanukoglu, A., and Hanukoglu, I. (2009). Simple and efficient site-directed mutagenesis using two single-primer reactions in parallel to generate mutants for protein structure-function studies. *BMC Biotechnol.* 9, 61. doi: 10.1186/1472-6750-9-61

Erikson, O., Hertzberg, M., and Näsholm, T. (2005). The *dsdA* gene from *Escherichia coli* provides a novel selectable marker for plant transformation. *Plant Mol. Biol.* 57, 425–433. doi: 10.1007/s11103-004-7902-9

Fujita, S., De Bellis, D., Edel, K. H., Köster, P., Andersen, T. G., Schmid-Siegert, E., et al. (2020). SCHENGEN receptor module drives localized ROS production and lignification in plant roots. *EMBO J.* 39, e103894. doi: 10.15252/embj.2019103894

Gao, J., Thelen, J. J., Dunker, A. K., and Xu, D. (2010). Musite, a tool for global prediction of general and kinase-specific phosphorylation sites. *Mol. Cell. Proteomics* 9, 2586–2600. doi: 10.1074/mcp.M110.001388

Gupta, K. J., Kolbert, Z., Durner, J., Lindermayr, C., Corpas, F. J., Brouquisse, R., et al. (2020). Regulating the regulator: nitric oxide control of post-translational modifications. *New Phytol.* 227, 1319–1325. doi: 10.1111/nph.16622

Han, J.-P., Köster, P., Drerup, M. M., Scholz, M., Li, S., Edel, K. H., et al. (2019). Fine-tuning of RBOHF activity is achieved by differential phosphorylation and Ca^{2+} binding. *New Phytol.* 221, 1935–1949. doi: 10.1111/nph.15543

Hoffmann, N., Benske, A., Betz, H., Schuetz, M., and Samuels, A. L. (2020). Laccases and peroxidases co-localize in lignified secondary cell walls throughout stem development. *Plant Physiol.* 184, 806–822. doi: 10.1104/pp.20.00473

Hoffmann, N., Gonzales-Vigila, E., Mansfield, S. D., and Samuels, A. L. (2022). Oxidative enzymes in lignification. *Adv. Botanical Res.* pp, 1–35. doi: 10.1016/bs.abr.2022.02.004

Jaakkola, T., Mäkinen, H., and Saranpää, P. (2007). Effects of thinning and fertilisation on tracheid dimensions and lignin content of Norway spruce. *Holzforschung* 61, 301–310. doi: 10.1515/HF.2007.059

Jiménez-Quesada, M. J., Traverso, J. A., and de Dios Alché, J. (2016). NADPH oxidase-dependent superoxide production in plant reproductive tissues. *Front. Plant Sci.* 7. doi: 10.3389/fpls.2016.00359

Jokipii-Lukkari, S., Delhomme, N., Schiffthaler, B., Mannapperuma, C., Prestele, J., Nilsson, O., et al. (2018). Transcriptional roadmap to seasonal variation in wood formation of Norway spruce. *Plant Physiol.* 176, 2851–2870. doi: 10.1104/pp.17.01590

Jokipii-Lukkari, S., Sundell, D., Nilsson, O., Hvidsten, T. R., Street, N. R., and Tuominen, H. (2017). NorWood: a gene expression resource for evo-devo studies of conifer wood development. *New Phytol.* 216, 482–494. doi: 10.1111/nph.14458

Kadota, Y., Shirasu, K., and Zipfel, C. (2015). Regulation of the NADPH oxidase RBOHD during plant immunity. *Plant Cell Physiol.* 56, 1472–1480. doi: 10.1093/pcp/pcv063

Kadota, Y., Sklenar, J., Derbyshire, P., Stransfeld, L., Asai, S., Ntoukakis, V., et al. (2014). Direct regulation of the NADPH oxidase RBOHD by the PRR-associated kinase BIK1 during plant immunity. *Mol. Cell.* 54, 43–55. doi: 10.1016/j.molcel.2014.02.021

Kärkönen, A., and Fry, S. C. (2006). Effect of ascorbate and its oxidation products on H_2O_2 production in cell-suspension cultures of *Picea abies* and in the absence of cells. *J. Exp. Bot.* 57, 1633–1644. doi: 10.1093/jxb/erj197

Kärkönen, A., and Koutaniemi, S. (2010). Lignin biosynthesis studies in plant tissue cultures. *J. Integr. Plant Biol.* 52, 176–185. doi: 10.1111/j.1744-7909.2010.00913.x

Kärkönen, A., Koutaniemi, S., Mustonen, M., Syrjänen, K., Brunow, G., Kilpeläinen, I., et al. (2002). Lignification related enzymes in *Picea abies* suspension cultures. *Physiol. Plant* 114, 343–353. doi: 10.1034/j.1399-3054.2002.1140303.x

Kärkönen, A., and Kuchitsu, K. (2015). Reactive oxygen species in cell wall metabolism and development in plants. *Phytochemistry* 112, 22–32. doi: 10.1016/j.phytochem.2014.09.016

Kärkönen, A., Meisrimler, C.-N., Takahashi, J., Väisänen, E., Laitinen, T., Jiménez Barboza, L. A., et al. (2014). Isolation of cellular membranes from lignin-producing tissues of Norway spruce and analysis of redox enzymes. *Physiol. Plant* 152, 599–616. doi: 10.1111/ppl.12209

Kärkönen, A., Warinowski, T., Teeri, T. H., Simola, L. K., and Fry, S. C. (2009). On the mechanism of apoplastic H_2O_2 production during lignin formation and elicitation in cultured spruce cells - peroxidases after elicitation. *Planta* 230, 553–567. doi: 10.1007/s00425-009-0968-5

Karlsson, M., Melzer, M., Prokhorenko, I., Johansson, T., and Wingsle, G. (2005). Hydrogen peroxide and expression of hipI-superoxide dismutase are associated with the development of secondary cell walls in *Zinnia elegans*. *J. Exp. Bot.* 56, 2085–2093. doi: 10.1093/jxb/eri207

Kawarazaki, T., Kimura, S., Iizuka, A., Hanamata, S., Nibori, H., Michikawa, M., et al. (2013). A low temperature-inducible protein AtSRC2 enhances the ROS-

producing activity of NADPH oxidase AtRbohF. *Biochim. Biophys. Acta* 1833, 2775–2780. doi: 10.1016/j.bbamcr.2013.06.024

Kaya, H., Takeda, S., Kobayashi, M. J., Kimura, S., Iizuka, A., Imai, A., et al. (2019). Comparative analysis of the reactive oxygen species-producing enzymatic activity of Arabidopsis NADPH oxidases. *Plant J.* 98, 291–300. doi: 10.1111/tpj.14212

Kimura, S., Hunter, K., Vaahtera, L., Tran, H. C., Citterico, M., Vaattovaara, A., et al. (2020). CRK2 and c-terminal phosphorylation of NADPH oxidase RBOHD regulate reactive oxygen species production in Arabidopsis. *Plant Cell* 32, 1063–1080. doi: 10.1105/tpc.19.00525

Kimura, S., Kawarazaki, T., Nibori, H., Michikawa, M., Imai, A., Kaya, H., et al. (2013). The CBL-interacting protein kinase CIPK26 is a novel interactor of *Arabidopsis* NADPH oxidase AtRbohF that negatively modulates its ROS-producing activity in a heterologous expression system. *J. Biochem.* 153, 191–195. doi: 10.1093/jb/mvs132

Kimura, S., Kaya, H., Hashimoto, K., Wrzaczek, M., and Kuchitsu, K. (2022). "Quantitative analysis for ROS-producing activity and regulation of plant NADPH oxidases in HEK293T cells", in *Methods Molecular Biology, Vol. 2526, Reactive Oxygen Species in Plants*. Ed. A. Mhamdi (Totowa, US: Springer Protocols, Humana Press). doi: 10.1007/978-1-0716-2469-2_8

Kimura, S., Kaya, H., Kawarazaki, T., Hiraoka, G., Senzaki, E., Michikawa, M., et al. (2012). Protein phosphorylation is a prerequisite for the Ca^{2+}-dependent activation of *Arabidopsis* NADPH oxidases and may function as a trigger for the positive feedback regulation of Ca^{2+} and reactive oxygen species. *Biochim. Biophys. Acta* 1823, 398–405. doi: 10.1016/j.bbamcr.2011.09.011

Kolbert, Z., and Feigl, G. (2017). "Cross-talk of reactive oxygen species and nitric oxide in various processes of plant development," in *Reactive oxygen species in plants*. Eds. V. P. Singh, S. Singh, D. K. Tripathi, S. M. Prasad and D. Chauhan (New Jersey, USA: John Wiley & Sons), 261–289.

Krogstrup, P. (1986). Embryolike structures from cotyledons and ripe embryos of Norway spruce (*Picea abies*). *Can. J. For. Res.* 16, 664–668. doi: 10.1139/x86-116

Kurusu, T., Kuchitsu, K., and Tada, Y. (2015). Plant signaling networks involving Ca^{2+} and Rboh/Nox-mediated ROS production under salinity stress. *Front. Plant Sci.* 6. doi: 10.3389/fpls.2015.00427

Kvaalen, H., and Appelgren, M. (1999). Light quality influences germination, root growth and hypocotyl elongation in somatic embryos but not in seedlings of Norway spruce. *In Vitro Cell. Dev. Biol. Plant* 35, 437–441. doi: 10.1007/s11627-999-0064-3

Laitinen, T., Morreel, K., Delhomme, N., Gauthier, A., Schiffthaler, B., Nickolov, K., et al. (2017). A key role for apoplastic H_2O_2 in Norway spruce phenolic metabolism. *Plant Physiol.* 174, 1449–1475. doi: 10.1104/pp.17.00085

Lee, D., Lal, N. K., Lin, Z. J. D., Ma, S., Liu, J., Toruño, T., et al. (2020). Regulation of reactive oxygen species during plant immunity through phosphorylation and ubiquitination of RBOHD. *Nat. Commun.* 11, 1838. doi: 10.1038/s41467-020-15601-5

Lee, T.-Y., Bretaña, N. A., and Lu, C.-T. (2011). PlantPhos: using maximal dependence decomposition to identify plant phosphorylation sites with substrate site specificity. *BMC Bioinf.* 12, 261. doi: 10.1186/1471-2105-12-261

Lee, Y., Rubio, M. C., Alassimone, J., and Geldner, N. (2013). A mechanism for localized lignin deposition in the endodermis. *Cell* 153, 402–412. doi: 10.1016/j.cell.2013.02.045

Lee, Y., Yoon, T. H., Lee, J., Jeon, S. Y., Lee, J. H., Lee, M. K., et al. (2018). A lignin molecular brace controls precision processing of cell walls critical for surface integrity in *Arabidopsis*. *Cell* 173, 1468–1480. doi: 10.1016/j.cell.2018.03.060

Li, L., Li, M., Yu, L., Zhou, Z., Liang, X., Liu, Z., et al. (2014). The FLS2-associated kinase BIK1 directly phosphorylates the NADPH oxidase RbohD to control plant immunity. *Cell Host Microbe* 15, 329–338. doi: 10.1016/j.chom.2014.02.009

Li, P., Zhao, L., Qi, F., Htwe, N. M. P. S., Li, Q., Zhang, D., et al. (2021). The receptor-like cytoplasmic kinase RIPK regulates broad-spectrum ROS signaling in multiple layers of plant immune system. *Mol. Plant* 14, 1652–1667. doi: 10.1016/j.molp.2021.06.010

Li, Y., Kajita, S., Kawai, S., Katayama, Y., and Morohoshi, N. (2003). Down-regulation of an anionic peroxidase in transgenic aspen and its effect on lignin characteristics. *J. Plant Res.* 116, 175–182. doi: 10.1007/s10265-003-0087-5

Lim, K.-J., Paasela, T., Harju, A., Venäläinen, M., Paulin, L., Auvinen, P., et al. (2016). Developmental changes in Scots pine transcriptome during heartwood formation. *Plant Physiol.* 172, 1403–1417. doi: 10.1104/pp.16.01082

Lin, C. Y., Li, Q., Tunlaya-Anukit, S., Shi, R., Sun, Y.-H., Wang, J. P., et al. (2016). A cell wall-bound anionic peroxidase, PtrPO21, is involved in lignin polymerization in *Populus trichocarpa*. *Tree Genet. Genomes* 12, 22. doi: 10.1007/s11295-016-0978-y

Lu, S., Li, Q., Wei, H., Chang, M. J., Tunlaya-Anukit, S., Kim, H., et al. (2013). Ptr-miR397a is a negative regulator of laccase genes affecting lignin content in *Populus trichocarpa*. *PNAS* 110, 10848–10853. doi: 10.1073/pnas.130893611

Miller, G., Schlauch, K., Tam, R., Cortes, D., Torres, M. A., Shulaev, V., et al. (2009). The plant NADPH oxidase RBOHD mediates rapid systemic signaling in response to diverse stimuli. *Sci. Signal.* 2, ra45. doi: 10.1126/scisignal.2000448

Novo-Uzal, E., Fernández-Pérez, F., Herrero, J., Gutiérrez, J., Gómez-Ros, L. V., Bernal, M. Á., et al. (2013). From *Zinnia* to *Arabidopsis*: approaching the involvement of peroxidases in lignification. *J. Exp. Bot.* 64, 3499–3518. doi: 10.1093/jxb/ert221

Nühse, T. S., Bottrill, A. R., Jones, A. M. E., and Peck, S. C. (2007). Quantitative phosphoproteomic analysis of plasma membrane proteins reveals regulatory mechanisms of plant innate immune responses. *Plant J.* 51, 931–940. doi: 10.1111/j.1365-313X.2007.03192.x

Nystedt, B., Street, N. R., Wetterbom, A., Zuccolo, A., Lin, Y. C., Scofield, D. G., et al. (2013). The Norway spruce genome sequence and conifer genome evolution. *Nature* 497, 579–584. doi: 10.1038/nature12211

Oda, T., Hashimoto, H., Kuwabara, N., Akashi, S., Hayashi, K., Kojima, C., et al. (2010). Structure of the N-terminal regulatory domain of a plant NADPH oxidase and its functional implications. *J. Biol. Chem.* 285, 1435–1445. doi: 10.1074/jbc.M109.058909

Ogasawara, Y., Kaya, H., Hiraoka, G., Yumoto, F., Kimura, S., Kadota, Y., et al. (2008). Synergistic activation of the Arabidopsis NADPH oxidase AtrbohD by Ca^{2+} and phosphorylation. *J. Biol. Chem.* 283, 8885–8892. doi: 10.1074/jbc.M708106200

Ogawa, K., Kanematsu, S., and Asada, K. (1997). Generation of superoxide anion and localization of CuZn-superoxide dismutase in the vascular tissue of spinach hypocotyls: their association with lignification. *Plant Cell Physiol.* 38, 1118–1126. doi: 10.1093/oxfordjournals.pcp.a029096

Pagni, M., Ioannidis, V., Cerutti, L., Zahn-Zabal, M., Jongeneel, C. V., Hau, J., et al. (2007). MyHits: improvements to an interactive resource for analyzing protein sequences. *Nucleic Acids Res.* 35, W433–W437. doi: 10.1093/nar/gkm352

Pesquet, E., Zhang, B., Gorzsás, A., Puhakainen, T., Serk, H., Escamez, S., et al. (2013). Non-cell-autonomous postmortem lignification of tracheary elements in *Zinnia elegans*. *Plant Cell* 25, 1314–1328. doi: 10.1105/tpc.113.110593

Pfaffl, M. W. (2001). A new mathematical model for relative quantification in real-time RT–PCR. *Nucleic Acids Res.* 29, e45. doi: 10.1093/nar/29.9.e45

Qin, S., Fan, C., Li, X., Li, Y., Hu, J., Li, C., et al. (2020). LACCASE14 is required for the deposition of guaiacyl lignin and affects cell wall digestibility in poplar. *Biotechnol. Biofuels* 13, 197. doi: 10.1186/s13068-020-01843-4

Ranf, S., Eschen-Lippold, L., Pecher, P., Lee, J., and Scheel, D. (2011). Interplay between calcium signaling and early signaling elements during defence responses to microbe-or damage-associated molecular patterns. *Plant J.* 68, 100–113. doi: 10.1111/j.1365-313X.2011.04671.x

Rojas-Murcia, N., Hématy, K., Lee, Y., Emonet, A., Ursache, R., Fujita, S., et al. (2020). High-order mutants reveal an essential requirement for peroxidases but not laccases in Casparian strip lignification. *Proc. Natl. Acad. Sci. U.S.A.* 117, 29166–29177. doi: 10.1073/pnas.2012728117

Ros Barceló, A. (1998). The generation of H_2O_2 in the xylem of *Zinnia elegans* is mediated by an NADPH-oxidase-like enzyme. *Planta* 207, 207–216. doi: 10.1007/s004250050474

Scifo, E., Szwajda, A., Soliymani, R., Pezzini, F., Bianchi, M., Dapkunas, A., et al. (2015). Proteomic analysis of the palmitoyl protein thioesterase 1 interactome in SH-SY5Y human neuroblastoma cells. *J. Proteomics* 123, 42–53. doi: 10.1016/j.jprot.2015.03.038

Shigeto, J., and Tsutsumi, Y. (2016). Diverse functions and reactions of class III peroxidases. *New Phytol.* 209, 1395–1402. doi: 10.1111/nph.13738

Simola, L. K., Lemmetyinen, J., and Santanen, A. (1992). Lignin release and photomixotrophism in suspension cultures of *Picea abies*. *Physiol. Plant* 84, 374–379. doi: 10.1111/j.1399-3054.1992.tb04678.x

Sirichandra, C., Gu, D., Hu, H.-C., Davanture, M., Lee, S., Djaoui, M., et al. (2009). Phosphorylation of the Arabidopsis AtrbohF NADPH oxidase by OST1 protein kinase. *FEBS Lett.* 583, 2982–2986. doi: 10.1016/j.febslet.2009.08.033

Shen, J., Zhang, J., Zhou, M., Zhou, H., Cui, B., Gotor, C., et al. (2020). Persulfidation-based modification of cysteine desulfhydrase and the NADPH oxidase RBOHD controls guard cell abscisic acid signaling. *Plant Cell* 32, 1000–1017. doi: 10.1105/tpc.19.00826

Smirnoff, N., and Arnaud, D. (2019). Hydrogen peroxide metabolism and functions in plants. *New Phytol.* 221, 1197–1214. doi: 10.1111/nph.15488

Studier, F. W. (2005). Protein production by auto-induction in high density shaking cultures. *Protein Expr. Purif.* 41, 207–234. doi: 10.1016/j.pep.2005.01.016

Suzuki, N., Miller, G., Morales, J., Shulaev, V., Torres, M. A., and Mittler, R. (2011). Respiratory burst oxidases: the engines of ROS signaling. *Curr. Opin. Plant Biol.* 14, 691–699. doi: 10.1016/j.pbi.2011.07.014

Takahashi, S., Kimura, S., Kaya, H., Iizuka, A., Wong, H. L., Shimamoto, K., et al. (2012). Reactive oxygen species production and activation mechanism of the rice NADPH oxidase OsRbohB. *J. Biochem.* 152, 37–43. doi: 10.1093/jb/mvs044

Takeda, S., Gapper, C., Kaya, H., Bell, E., Kuchitsu, K., and Dolan, L. (2008). Local positive feedback regulation determines cell shape in root hair cells. *Science* 319, 1241–1244. doi: 10.1126/science.1152505

Tobimatsu, Y., and Schuetz, M. (2019). Lignin polymerization: how do plants manage the chemistry so well? *Curr. Opin. Biotechnol.* 56, 75–81. doi: 10.1016/j.copbio.2018.10.001

Torres, M. A., and Dangl, J. L. (2005). Functions of the respiratory burst oxidase in biotic interactions, abiotic stress and development. *Curr. Opin. Plant Biol.* 8, 397–403. doi: 10.1016/j.pbi.2005.05.014

Vaarala, O., Vuorela, A., Partinen, M., Baumann, M., Freitag, T. L., Meri, S., et al. (2014). Antigenic differences between AS03 adjuvanted influenza a (H1N1) pandemic vaccines: implications for pandemrix-associated narcolepsy risk. *PloS One* 9, e114361. doi: 10.1371/journal.pone.0114361

Väisänen, E., Takahashi, J., Jiménez Barboza, L. A., Deng, X., Teeri, T. H., Fagerstedt, K. V., et al. (2018). Isolation and purity assessment of membranes from Norway spruce. *Methods Mol. Biol.* 1696, 13–39. doi: 10.1007/978-1-4939-7411-5_2

von Arnold, S., and Clapham, D. (2008). Spruce embryogenesis. *Methods Mol. Biol.* 427, 31–47. doi: 10.1007/978-1-59745-273-1_3

Wang, P., Hsu, C. C., Du, Y., Zhu, P., Zhao, C., Fu, X., et al. (2020). Mapping proteome-wide targets of protein kinases in plant stress responses. *Proc. Natl. Acad. Sci. U S A.* 117, 3270–3280. doi: 10.1073/pnas.1919901117

Waszczak, C., Carmody, M., and Kangasjärvi, J. (2018). Reactive oxygen species in plant signaling. *Annu. Rev. Plant Biol.* 69, 209–236. doi: 10.1146/annurev-arplant-042817-040322

Xie, Y., Luo, X., Li, Y., Chen, L., Ma, W., Huang, J., et al. (2018). DeepNitro: Prediction of protein nitration and nitrosylation sites by deep learning. *Genom. Proteom. Bioinf.* 16, 294–306. doi: 10.1016/j.gpb.2018.04.007

Yang, H., Mu, J., Chen, L., Feng, J., Hu, J., Li, L., et al. (2015). *S*-nitrosylation positively regulates ascorbate peroxidase activity during plant stress responses. *Plant Physiol.* 167, 1604–1615. doi: 10.1104/pp.114.255216

Yao, Q., Bollinger, C., Gao, J., Xu, D., and Thelen, J. J. (2012a). P(^{3})DB: An integrated database for plant protein phosphorylation. *Front. Plant Sci.* 3. doi: 10.3389/fpls.2012.00206

Yao, Q., Gao, J., Bollinger, C., Thelen, J. J., and Xu, D. (2012b). Predicting and analyzing protein phosphorylation sites in plants using Musite. *Front. Plant Sci.* 3, 186. doi: 10.3389/fpls.2012.00186

Yao, Q., Ge, H., Wu, S., Zhang, N., Chen, W., Xu, C., et al. (2014). P^{3}DB 3.0: From plant phosphorylation sites to protein networks. *Nucleic Acids Res.* 42, D1206–D1213. doi: 10.1093/nar/gkt1135

Yun, B.-W., Feechan, A., Yin, M., Saidi, N. B. B., Le Bihan, T., Yu, M., et al. (2011). *S*-nitrosylation of NADPH oxidase regulates cell death in plant immunity. *Nature* 478, 264–268. doi: 10.1038/nature10427

Zhang, M., Chiang, Y.-H., Toruño, T. Y., Lee, D., Ma, M., Liang, X., et al. (2018). The MAP4 kinase SIK1 ensures robust extracellular ROS burst and antibacterial immunity in plants. *Cell Host Microbe* 24, 379–391. doi: 10.1016/j.chom.2018.08.007

Zhao, Q., Nakashima, J., Chen, F., Yin, Y., Fu, C., Yun, J., et al. (2013). *LACCASE* is necessary and nonredundant with *PEROXIDASE* for lignin polymerization during vascular development in *Arabidopsis*. *Plant Cell* 25, 3976–3987. doi: 10.1105/tpc.113.117770

frontiers | Frontiers in Plant Science

TYPE Review
PUBLISHED 20 October 2022
DOI 10.3389/fpls.2022.1027608

OPEN ACCESS

EDITED BY
Ana Zabalza,
Public University of Navarre, Spain

REVIEWED BY
María Carmen Martí,
Center for Edaphology and Applied Biology of Segura (CSIC), Spain
Keni Cota-Ruiz,
Michigan State University, United States

*CORRESPONDENCE
Jagna Chmielowska-Bąk
jagna.chmielowska@amu.edu.pl

SPECIALTY SECTION
This article was submitted to Plant Abiotic Stress, a section of the journal Frontiers in Plant Science

RECEIVED 25 August 2022
ACCEPTED 30 September 2022
PUBLISHED 20 October 2022

CITATION
Ekner-Grzyb A, Duka A, Grzyb T, Lopes I and Chmielowska-Bąk J (2022) Plants oxidative response to nanoplastic.
Front. Plant Sci. 13:1027608.
doi: 10.3389/fpls.2022.1027608

Plants oxidative response to nanoplastic

Anna Ekner-Grzyb[1], Anna Duka[2,3], Tomasz Grzyb[4], Isabel Lopes[5] and Jagna Chmielowska-Bąk[2*]

[1]Department of Cell Biology, Institute of Experimental Biology, Faculty of Biology, School of Natural Sciences, Adam Mickiewicz University, Poznań, Poland, [2]Department of Plant Ecophysiology, Institute of Experimental Biology, Faculty of Biology, School of Natural Sciences, Adam Mickiewicz University, Poznań, Poland, [3]Department of Mycology and Plant Resistance, Vasily Nazarovich Karazin (VN) Karazin Kharkiv National University, Kharkiv, Ukraine, [4]Department of Rare Earths, Faculty of Chemistry, Adam Mickiewicz University, Poznań, Poland, [5]Department of Biology & Centre for Environmental and Marine Studies (CESAM), University of Aveiro, Aveiro, Portugal

Pollution of the environment with plastic is an important concern of the modern world. It is estimated that annually over 350 million tonnes of this material are produced, wherein, despite the recycling methods, a significant part is deposited in the environment. The plastic has been detected in the industrial areas, as well as farmlands and gardens in many world regions. Larger plastic pieces degraded in time into smaller pieces including microplastic (MP) and nanoplastic particles (NP). Nanoplastic is suggested to pose the most serious danger as due to the small size, it is effectively taken up from the environment by the biota and transported within the organisms. An increasing number of reports show that NP exert toxic effects also on plants. One of the most common plant response to abiotic stress factors is the accumulation of reactive oxygen species (ROS). On the one hand, these molecules are engaged in cellular signalling and regulation of genes expression. On the other hand, ROS in excess lead to oxidation and damage of various cellular compounds. This article reviews the impact of NP on plants, with special emphasis on the oxidative response.

KEYWORDS

polystyrene (PS), oxidative stress, reactive oxygen species, lipid peroxidation, antioxidant enzymes

Abbreviations: NP, nanoplastic particles; MP, microplastic particles; PS, polystyrene; PMMA, polymethyl methacrylate; ROS, reactive oxygen species.

10.3389/fpls.2022.1027608

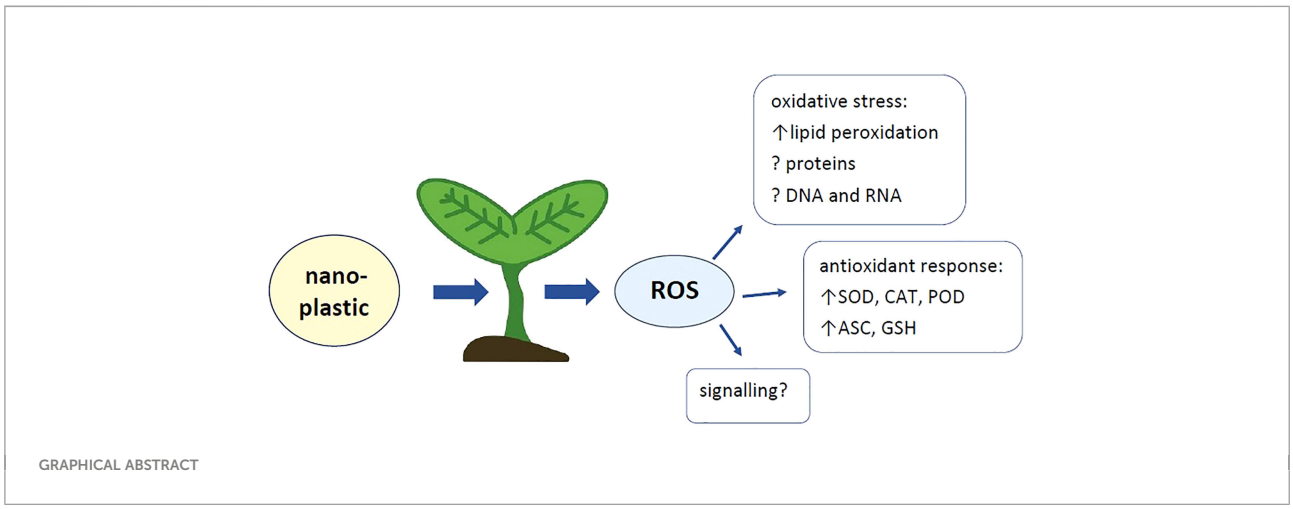

GRAPHICAL ABSTRACT

Introduction

Plastics in each form are composed of polymeric material in most cases industrially artificially synthesized, whether in the bulk form or as micro- and nanoparticles (MP and NP, respectively). Microplastic (MP) is considered plastic particles with sizes greater than 1 μm to 1 mm, but this definition is still not standardized, and other size ranges can be found in many reports or publications (Horton et al., 2017) Plastic fragments smaller than 1 μm are considered nanoplastic (NP) (Hartmann et al., 2019). Usually, plastics are synthetic organic compounds manufactured from fossil fuel-based chemicals like petroleum and natural gas. Natural polymers such as silk or rubber are also sources of plastics, but only synthetic plastics are non-biodegradable. The history of plastics starts with the beginning of the 20th century and the invention of Bakelite (Crespy et al., 2008). Since then, plastics have become one of the primary synthetic materials used. The evolution of production methods and many advantages of plastics over other materials such as glass, paper, wood, metals, or ceramics caused that in 2022, approximately 450-500 million tons of plastic will be produced (Geyer et al., 2017; Law and Narayan, 2022; Zhao et al., 2022).

The most frequently used plastics are composed of polyethylene (PE), polypropylene (PP), polystyrene (PS), polyvinyl chloride (PVC), and polyethylene terephthalate (PET) (Geyer et al., 2017; Schwarz et al., 2019; Zhao et al., 2022; Figure 1). Other types of plastic materials are polyurethanes (PUR) and polyester, polyamide, and acrylic (PP&A) fibres (Geyer et al., 2017). Polyethylene is produced in two forms: low-density PE (LDPE) and high-density PE (HDPE). Around 60% of solid plastic waste contains LDPE, HDPE and PP (Butler et al., 2011). However, plastic waste composition strongly depends on the place and varies between landfills, rivers, oceans or soil (Gwada et al., 2019; Schwarz et al., 2019; Antonopoulos et al., 2021). For example, in freshwaters and oceans, PE is the main component of plastics, followed by PP and PS - these three polymers together make up from 92.2 to 95.8% of waste (Schwarz et al., 2019).

The degradation of plastics is a long and complex process (Lucas et al., 2008). Estimates show that plastic materials require 250-1000 years to completely degrade, depending on chemical composition and structure (Chamas et al., 2020). It was one of the advantages of plastics responsible for their wide use. However, since plastics are considered a challenging environmental hazard after decomposition to MP and NP, their chemical stability and resistance become a problem because they decompose after a long period of time in the environment. Plastics in the environment undergo biodegradation or non-biodegradation processes (Lucas et al., 2008). Thermal degradation, photo- and oxidative degradation or hydrolysis are all examples of non-biodegradation (Lucas et al., 2008; Yee et al., 2021). Plastics, in the presence of sunlight and water, are naturally decomposed into simpler structures - oligomers and monomers (Lucas et al., 2008; Lambert and Wagner, 2016; Yee et al., 2021). Additionally, the chemical structure of polymers and their fragments also changes in the presence of water, oxygen and light, forming esters, ketones, alcohols, or even acids when the environment is acidic, which makes plastics more hydrophilic (Lucas et al., 2008; Chamas et al., 2020). The processes mentioned above occur only on the MP and NP surface, whereas the higher surface-to-volume ratio of NP makes them especially reactive. Some species of bacteria and other microorganisms such as *Aspergillus tubingensis*, *Pestalotiopsis microspore* or *Zalerion maritimum* can decompose plastics through enzyme-supported reactions (Lucas et al., 2008; Yuan et al., 2020). In the natural environment, both processes occur parallelly, i.e. plastic decomposition products, such as simple organic compounds, are assimilated by microbial cells, which may also affect the health of these organisms (Ng et al., 2018). Microorganisms are also responsible for accelerating plastic degradation, e.g. by covering the surface of plastics or infiltrating the porous plastic structures (Lucas et al., 2008; Gaur et al., 2020).

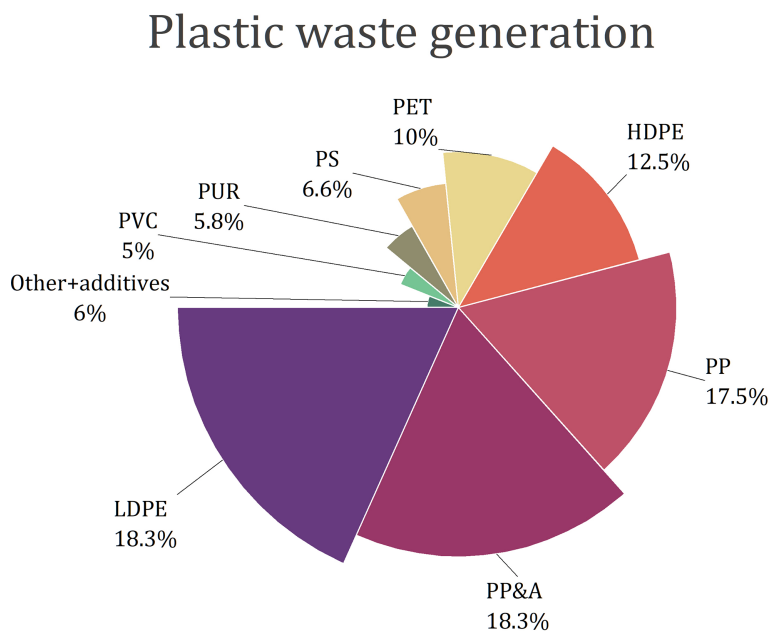

FIGURE 1
Composition of plastic waste generated globally in 2015 (Geyer et al., 2017).

Plastics contain chemical additives such as remaining solvents, catalysts, dyes, plasticizers and many others (Kiran et al., 2022). During the production of plastics, different chemical compounds are added to colorize or improve the resistance of polymers to the degradation (Kiran et al., 2022). Toxic or potentially toxic substances, such as Bisphenol A, are used to manufacture various plastics (Narevski et al., 2021; Kiran et al., 2022). Many plasticizers, such as 1,2-benzenedicarboxylic acid, chlorinated paraffins or formaldehyde are neurotoxic or carcinogenic (Kiran et al., 2022). Plastics can also be a vector of various chemicals, such as persistent organic pollutants (POPs), e.g. 1,1,1-Trichloro-2,2-bis[p-chlorophenyl]-ethane (DDT), polycyclic aromatic hydrocarbons, hexachlorobenzene, polychlorinated dibenzofurans and many other chemicals produced by the industry (Nizzetto et al., 2012; Antunes et al., 2013; Kodavanti et al., 2014; Hüffer and Hofmann, 2016; Bour et al., 2020; Gigault et al., 2021). Chemical similarity causes MP and NP to work as scavengers of toxic substances (Hüffer and Hofmann, 2016). Plastic micro- and nanoparticles can accumulate chemicals and serve as a carrier for long-range transport (Li et al., 2018; Kiran et al., 2022). Besides the POPs mentioned above, such substances as antibiotics or metals, e.g. Cr, Co, Ni, Cu, Zn, Cd and Pb can be accumulated and transported by micro- and nanoplastics (Holmes et al., 2012; Turner and Holmes, 2015; Li et al., 2018; Campanale et al., 2020).

Plastics are used in virtually all commercial and industrial sectors (Figure 2).

Detection of MP and NP in plants or environmental samples is complex and challenging to perform. The analytical procedures allowing for the identification of the size, type, size (Caputo et al., 2021), and quantity of plastic pollutants depend strongly on the type of plant and chemical composition of plastic particles. Usually, the biological material before analysis must be pre-treated to eliminate organic matter, salts, or minerals that affect the detection of MP and NP (Zhang et al., 2022). Plastic particles can also be extracted from the sample (Li et al., 2021a). The most popular techniques are based on fluorescence microscopy (Maes et al., 2017). Also, techniques based on light scattering, such as dynamic light scattering (DLS) (Caputo et al., 2021) and multiangle light scattering (MALS), are popular (Correia and Loeschner, 2018). Plastics can also be detected based on their chemical composition. The best results of such way of analysis give infrared (Hernandez et al., 2019) and Raman spectroscopy (Fang et al., 2020), NMR, double shot pyrolysis - gas chromatography/mass spectrometry GC-MS (py-GC/MS) (Li et al., 2021a), thermal desorption proton-transfer-reaction mass spectrometry (TD-PTR-MS) (Materić et al., 2022) and energy-dispersive X-ray spectroscopy (EDX). Besides, single particle inductively coupled plasma mass spectrometry (spICP-MS) can be helpful in the detection of MP and NP (Jiménez-Lamana et al., 2020). Most importantly, no universal method for detecting plastics in biological and environmental materials exists. Each procedure requires testing and validation before it is used for plastic determination. However, it is worth emphasizing that research on this topic is still ongoing.

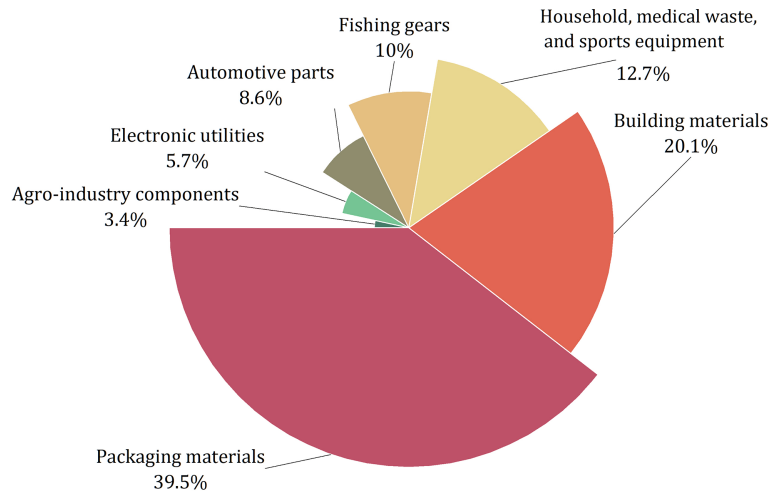

FIGURE 2
Plastic pollution sources (Horton et al., 2017; Pinto Da Costa et al., 2020; Kiran et al., 2022; Law and Narayan, 2022).

We often deal with two ways of introducing this pollutant into the environment - the primary or secondary MP and NP. The former is obtained in this form and used as, e.g. a carrier or abrasive material in cosmetics, toothpaste, detergents, personal care products, abrasive cleaning agents, plastic powder for moulding, and synthetic clothing, paints, electronics, etc. (Birch et al., 2020; Wang et al., 2020; Kihara et al., 2021; Kiran et al., 2022). The second type of NP and MP is the one that is created from larger fragments by their disintegration and degradation, e.g. under the influence of sunlight, temperature, humidity and wind, which account for 70-80% of all plastic released into the environment (Lambert and Wagner, 2016; Kiran et al., 2022). Most plastic pollution comes from anthropogenic activities, such as tire wear run off from roads, packaging, building materials, fishing gears, automotive parts, electronic utilities and agro-industry components (Geyer et al., 2017; Horton et al., 2017; Pinto Da Costa et al., 2020; Kiran et al., 2022; Law and Narayan, 2022; Castan et al., 2021; Huang et al., 2022), as well as from atmospheric transport (e.g. wind drift) (Figure 3). Agricultural activities perform a major role in introducing plastics into the soil through many ways, such as plastic mulching (which usually are not retrieved from the fields after its usage), use of plastic contaminated biosolids/sewage sludge for soil conditioning and use of plastic-containing wastewaters for irrigation (Liu et al., 2021; Castan et al., 2021; Huang et al., 2022). Once in the soil, plastics may be further transformed (through biodegradation and non-biodegradation processes, as explained previously) and transported and distributed in this compartment both horizontally and vertically. Many processes may contribute to such distribution in the soil (Figure 3). At the surface, activities of animals (e.g. digging, movement of animals on the surface) and agricultural tilling and harvesting may promote their horizontal distribution (Liu et al., 2021; Huang et al., 2021; Huang et al., 2022). Also, resuspension/remobilization (caused for example by wind or agricultural activities) may further contribute for their transport across soil surface. Vertically, the plastic particles may migrate into deeper soil layers through water's infiltration processes, movement across soil cracks or spaces/holes in the soil that were created by plant roots elongation or edaphic organisms or through being transported by edaphic organisms (either bioaccumulated in the body or adsorbed into the skin), among others (Figure 3; Rillig et al., 2017; Heinze et al., 2021; Huang et al., 2021; Huang et al., 2022). Adding to these environmental factors, intrinsic properties of NP and of the soil matrices also influences their mobility in the soil (Wu et al., 2020; Brewer et al., 2021). Namely, plastics size, polymer type and shape, may determine their transport across the soil. As an example, O'Connor and collaborators reported that at similar sizes, polyethylene plastic particles tended to be transported more easily than those made of polypropylene (O'Connor et al., 2019). Soil physical and chemical properties, such as pH, ionic strength, ionic composition, also influence the transport of NP. Corroborating this, Wu and collaborators, revealed that the retention of polystyrene nanoplastic particles (PS NP) in the soil was negatively correlated with pH and ionic strength, while the presence of iron and aluminium oxides was positively correlated with the retention of those NP in the soil (Wu et al., 2020).

Plastic particles were detected both in marine, freshwater and soil environments (Allen et al., 2022; Lehner et al., 2019; Rai et al., 2021; Huang et al., 2021). They were found in the soils in

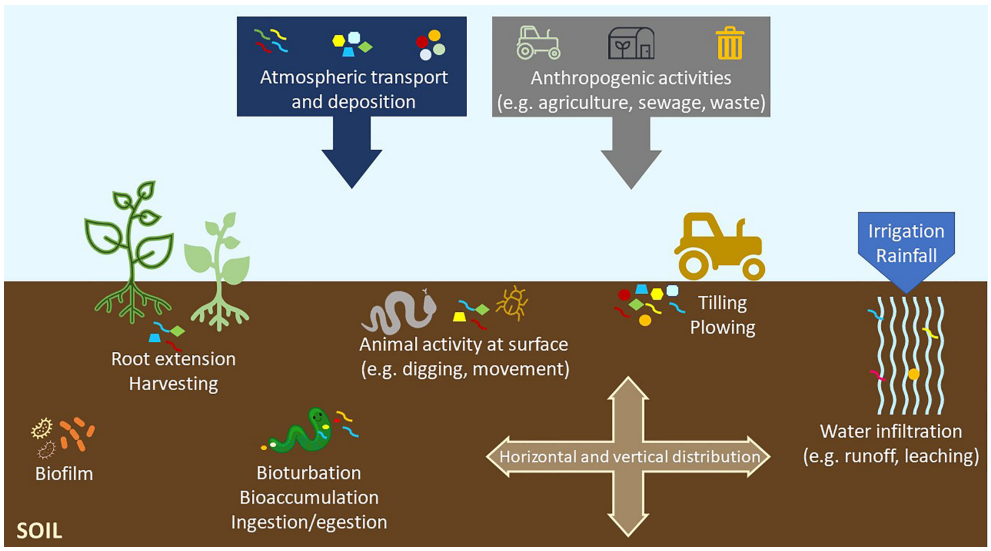

FIGURE 3
Sources of plastics in the terrestrial environment and factors that influence their vertical and horizontal distribution in the soil.

various regions of the world e.g. in Australia, China, Chile, Germany, Switzerland (He et al., 2018; Schmid et al., 2021; Prata et al., 2021; Lehner et al., 2019). Moreover, NP and MP were noted not only in industrious regions but also in home gardens, farmlands and agricultural lands. Notably, MP and NP entering the environment can be harmful to living organisms (Prata et al., 2021). It was presented that NP may cause changes in plant organisms, e.g. disturbing growth, germination, genetics, physiology, morphology, photosynthesis and uptake of nutrients (described in more detail in section 2) (Xiao et al., 2022; Gong et al., 2022; Wang et al., 2022; Lian et al., 2020; Lian et al., 2022). Studies on animals showed that NP and MP might influence such trait as survival, morphology, behaviour, histopathology, development and reproduction, and in consequences population dynamic (An et al., 2021; Venâncio et al., 2022; Liu et al., 2022a; Huang et al., 2021). In addition, plastic particles by themselves and chemicals released into the environment from plastic waste may threaten plants and animals. For example, styrene or bisphenol-A released from plastic waste strongly affects marine organisms' reproduction and the hormonal balance of animals, including terrestrial animals (Campanale et al., 2020). Moreover, the plastic particles may enter human bodies *via* three pathways: ingestion, inhalation and absorption by the skin (Prata et al., 2020). Among others, NP and MP may be transferred through food chains, e.g. from edible plants to humans. It was suggested that various types of NP constitute the most serious food and drinking water safety concerns (Pironti et al., 2021; Yee et al., 2021; UNEP, 2016). It was revealed that plastic particles may eventually enter the human bloodstream (Leslie et al., 2022) and may possibly affect human health (Lehner et al., 2019). Research conducted on human cell lines showed that MP and NP can induce apoptosis, oxidative stress, inflammation processes and gut microbiota dysbiosis of the cells (Yee et al., 2021).

There is increasing concern on the sufficient supply of safe food products that would meet the demands of growing human population. That is one of the reasons for rising interest in NP effect in plants within the scientific community, with four articles published in 2018 and already over eighty articles published in 2022 (Scopus database search with terms "nanoplastic*" AND "plant*", date of access: 19.09.2022). The aim of present work is comprehensive revision of the accessible literature on the topic of plants response to NP. Special emphasis is put on plants oxidative response, which on the one hand is recognized as the marker of stress intensity and on the other hand, as an important element of stress signalling network.

The impact of nanoplastic on plants

Uptake and accumulation

Despite the increasing awareness of the risks associated with NP contamination of the environment, the number of studies on their impact on plants is still limited. The results of laboratory studies show that NP can be effectively taken up by the plants both *via* roots (Zhou et al., 2021; Sun et al., 2020; Zhou et al., 2021; Bosker et al., 2019) and leaves (Lian et al., 2021; Sun et al., 2021) (Figure 4). Afterwards, NP can be accumulated in inner tissues and migrated to other parts of the organisms. First of all, plastic particles adhere to the plants' surface (Nolte et al., 2017; Xiao et al., 2022; Taylor et al., 2020). This process depends

mainly on the surface chemistry of the structures (Nolte et al., 2017; Xiao et al., 2022). Research revealed that positively charged NP adhered significantly more to the plant surfaces than the negatively charged ones (Xiao et al., 2022; Sun et al., 2021). The cause is electrostatic attraction to the negatively charged cell wall. However, the situation looks differently when internalisation is taken into consideration. Contrary to the adhesion, positively charged NP entered the plant tissues at a lower level than negatively charged nanoplastics (Sun et al., 2020).

There are suggested several mechanisms of interaction between plants and plastic particles (Azeem et al., 2021; Mateos-Cárdenas et al., 2021). The NP and MP may adhere externally onto plant tissues. It concern mostly particles bigger than 200 nm (Mateos-Cárdenas et al., 2021). The cell wall is the first physical barrier against entering of foreign substances, including NP and MP, into plant organisms (Milewska-Hendel et al, 2019). It prevents penetration of particles larger than cell wall pores. However, some studies revealed that NP bigger than cell wall pores might internalise through cracks in the wall (Li et al., 2020). When NP adhere to the surface they may be just adsorbed on it and may be entrapped on surface structures.

On the other hand, the NP may be internal taken up by plants, what depends mostly on their size and charge (what was mentioned above). The potential pathways for nanoparticles to enter plant cells can be plasmodesmata channels, endocytosis, ion transporters and aquaporins (Khan et al., 2019; Zhou et al., 2021). As mentioned above, there are two pathways of exposure: roots or foliar foliage (Figure 4). NP taken up by roots' hair or tip are transported to other organs, such as stems and leaves (Giorgetti et al., 2020; Sun et al., 2020; Xiao et al., 2022). One of the primary influences on this movement is the pull of transpiration (Li et al., 2020). In the case of foliar application, it was revealed that NP which adhere to leaves might be taken up through the stomatal opening (Sun et al., 2021; Lian et al., 2021). Afterwards, they are transported by phloem (Lian et al., 2021). NP enter vasculature and are then translocated downward to the roots in the vascular bundle. It was shown that plastic particles might be effectively accumulated in plant organisms. They were detected in epidermal cells, apoplast and xylem, as well as along the cell walls (Sun et al., 2020; Liu et al., 2022b; Zhou et al., 2021). The plastic nanoparticles (50 nm PS NP) were observed also inside the root cells, in cytoplasm and vacuoles (Spanò et al., 2022).

An uptake, translocation and accumulation depend on several factors. One of the most important is the size (Liu et al., 2022b). Smaller NP are better transported than larger ones. Similarly, aggregation may change their movement speed, mainly because of altering their size (Sun et al., 2021). The root NP uptake might be modulated by root exudates – low- and high molecular organic compounds, which were shown e.g. to interact with arbuscular mycorrhizal fungi (AMF) and plant growth promoting bacteria (PGPB), mitigate draught and metal stress and facilitate phosphorus (P) and iron (Fe) uptake (Chai and Schachtman, 2022). The compounds secreted to the soil by plants and microorganisms are referred also as extracellular polymeric substances (EPS). It has been shown that interaction of PS NP with EPS results in NP aggregation and significant increase in their mean hydrodynamic diameter (MHD), possibly affecting also their uptake (Giri and Mukherjee, 2022).

In the case of foliar application, after some time, aquaporin channels begin to shut down in response to NP stresses, which may cause a reduction in the uptake of NP (Zhou et al., 2021). In addition, root-to-shoot NP translocation can be altered by changes in transpiration pull in plants (Li et al., 2020). Moreover, upwards transport depends on exposure time (Li

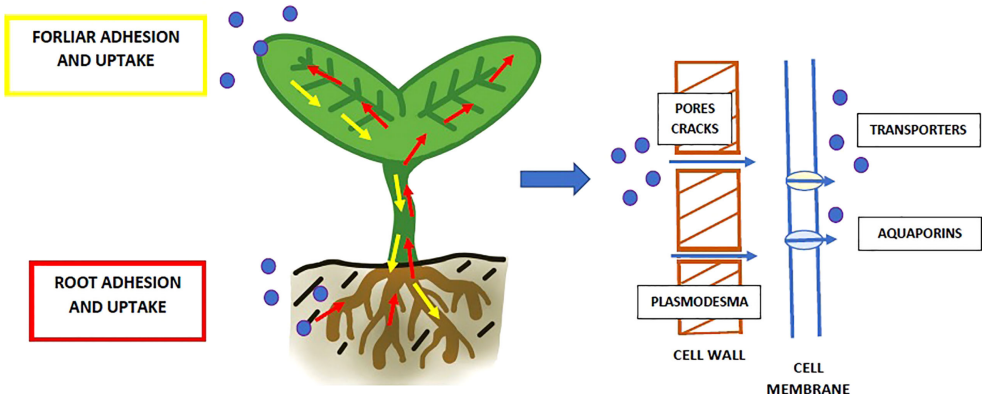

FIGURE 4
Uptake NP (blue dots) from the surrounded environment and transport through the plant organisms. Plastic particles may enter by roots (marked with red arrows) and leaves (marked with yellow arrows). The NP may enter the cell through pores and cracks in the cell wall and further through plasmodesma or transporters/aquaporins in the cell membrane.

et al., 2021a). Furthermore, both up and down movement may also be changed by such factors as NP surface charge and shape, presence of other substances, kind of media for plant growth and plant species (Sun et al., 2020; Zhou et al., 2021; Taylor et al., 2020).

Phytotoxicity

Nanoplastic has varying effects on plants growth. For instance, in wheat low PS NP concentration (0.01-10 mg/l; size between 151 and 870 nm) boosted the growth as reflected by increase in the roots and shoots biomass and relative root elongation (Lian et al., 2020). Simultaneously, a decrease in the shoot/root ratio has been observed (Lian et al., 2020). However, most of the reports indicate that NP at low concentration do not affect plants growth, while higher concentrations lead to growth reduction, as observed in *Arabidopsis* in response to 300 and 1000 mg/l of 70 nm PS-NH_2 (cultivation in soil) or 100, 500 and 1000 mg/l of 70 nm PS-NH_2 and 55 nm PS-SO_3H (cultivation in MS medium), broad bean seedlings in response to 100 mg/l of 100 nm PS NP, onion seedlings in response to 100 and 1000 mg/l of 50 nm PS PNs or rice seedlings in response to 50 and 100 mg/l of 20 nm PS NPs (Giorgetti et al., 2020; Jiang et al., 2019; Sun et al., 2020; Zhou et al., 2021). In the cited reports the NP were applied in the growing medium. In the case of foliar application, even lower concentrations negatively affected plants growth. Treatment of lettuce plants for 21 days with 100 nm PS NP at the concentrations of 0.1 and 1 mg/l resulted in decrease in plants height, leaf area and dry weight (Lian et al., 2021). The effects depend also on the diameter of the particles. In cucumber plants only 100 nm PS NP reduced roots length and thickness, while 300, 500 and 700 nm PS NP did not affect these parameters in a significant way (Li et al., 2021c). In the majority of the studies NP are applied in the form of polystyrene particles. However, the individual study using polymethyl methacrylate (PMMA) nanoparticles confirmed the negative impact of NPs on plants growth. In this study a concentration dependent decrease in the growth in response to 130 nm PMMA NP has been observed in lettuce (Yildiztugay et al., 2022).

The NPs-driven growth inhibition might be at least partially dependent on alterations in mineral homeostasis. In lettuce, foliar exposure to 90 nm PS NP resulted in lower Fe and Zn levels in the leaves and lower Fe, Zn, Cu and Mn levels in the roots (Lian et al., 2021). In turn treatment with 130 nm PMMA NP resulted in reduced content of Fe, Zn, Cu, Mn, Ca, Mo, K, P and B (Yildiztugay et al., 2022). Similarly, in cucumber,14-days long treatment with PS NP (100, 300, 500, and 700 nm) led to decrease in the content of Fe, Ca and Mg (Li et al., 2021c). The described studies provide evidence for the NP interaction with nutrients uptake. Due to the limited literature on the topic, it would be difficult to propose a possible mechanism standing behind the hampered uptake of specific elements. It is possible that, similarly to e.g. metals, NP compete for the sites in specific transporters or negatively affect transporters expression/activity.

Hampered growth might also results from disturbances in photosynthesis and respiration leading to reduced energy supply. Indeed, exposure of rice plants to neutrally charged nanoparticles (PS) as well as negatively (PS-COOH) and positively (PS-NH_2) charged NPs (size about 50 nm) resulted in decrease in net photosynthesis values, wherein the strongest effects were observed in response to PS-NH_2. Additionally, the positively charge PS NP caused decrease in the level of chlorophyll a and b (Wang et al., 2022). In lettuce 130 nm PMMA NP negatively affected maximum quantum yield of photosystem II (PSII) and potential photochemical efficiency (Yildiztugay et al., 2022).

The NP taken up by plants adversely affect their genetic material reflected e.g. by increase in micronuclei, C-metaphases and sticky chromosomes formation and impeded cell division (Giorgetti et al., 2020; Jiang et al., 2019; Spanò et al., 2022). For example, in meristems of onion, an inhibitory effect of 50 nm PS NP on the mitotic index (MI) at 100 and 1000 mg/l was observed. The MI in meristems decreased by 34.4% at 100 mg/l and by 41.9% at 10, 00 mg/l. It was found that the frequency of abnormal metaphases was 18.5%, while abnormal anaphases and telophases - 12.7%, when the NP at concentration 10 mg/l were applied. It is worth noting that the number of cytological anomalies did not increase with increasing NP concentrations (Giorgetti et al., 2020). The MI of rice root meristems under exposure to 50 nm PS NP decreased by 34.85% relative to control at the highest concentration (1000 mg/l) (Spanò et al., 2022). Similarly, reduction of MI in response to 100 nm PS NP were observed in castor bean (Jiang et al., 2019). Therefore, it can be assumed that NP exhibit cytotoxic effects and that the level of MI decrease depends on the concentration of nanoplastic and the plant species studied.

Nanoplastic is also known to lead to the formation of mitosis abnormalities. For instance, previous studies of onion have found an increase in micronuclei formation under exposure to 50 nm PS NP at the highest applied concentration of 1000 mg/l (Giorgetti et al., 2020). Exposure of castor bean to 100 nm PS NP also showed increased formation of micronuclei at the highest applied concentrations (100 mg/l) (Jiang et al., 2019). In addition, exposure to NP results in formation of C-metaphases, delayed metaphases, and sticky chromosomes detected during mitosis metaphase. Increased C-metaphases were observed at 100 and 1000 mg/l of 20-200 (mainly 100) nm PS NP and constituted the most common abnormality of mitosis in rice plants exposed to nanoplastic (Spanò et al., 2022). Treatment with NP also led to the formation of lagging chromosomes observed in anaphase and telophase. In total, cytological abnormalities of mitosis under NP exposure at the highest applied concentrations have been shown to reach about 30% in onion and 40% in rice, which is a large deviation in relation to the control plants (Giorgetti et al., 2020; Spanò et al., 2022).

Exposure to NP modulates genes expression on the transcriptomic level. Study carried out on *Arabidopsis thaliana* showed that seven weeks long exposure to 70 nm PS-NH_2 PS NP leads to up-regulation of genes associated with the secondary metabolism and attenuated levels of transcripts associated with ROS metabolism and stress response (Sun et al., 2020). In wheat 100 nm PS NP affected expression of genes associated with carbon and amino acid metabolism. In addition, alteration in the expression of genes related to cellular signalling were reported (Lian et al., 2022). In turn in rice, the genes related to antioxidant system, stress response, regulation of cell cycle and RNA and polysaccharides metabolism were differentially regulated under 50 nm PS NP treatment (Wang et al., 2022). The studies on duckweed revealed that even low 126 nm PS NP concentrations (0.015 μg/l) induced changes in the expression of genes e.g. associated with organelle envelope and inner membrane, oxidation-reduction processes, calcium signalling and tetrapyrrole binding. Exposure to higher concentrations (5 μg/l) resulted in up-regulation of genes associated with the response to stimuli and down-regulation of genes related to amino acid and carbohydrates transport and acetylo-CoA and thioester metabolism (Xiao et al., 2022).

The cited above studies show that NP may be effectively absorbed by plants and that their accumulation leads to the development of typical stress symptoms: reduced growth, alerted mineral homeostasis, decreased photosynthesis efficiency, genotoxic effects and modulation of genes expression, including down-regulation of basic metabolism associated genes and up-regulation of genes involved in defence mechanisms. Thus, it is evidenced that NP constitute an abiotic stress factor, which has been relatively recently introduced in the environment.

Plants oxidative response

Reactive oxygen species effects in plant cells

Plants oxidative status is dependent, on the one hand, on the production of reactive oxygen species (ROS) and, on the other hand, on the efficiency of their scavenging by the antioxidant system. The major species of reactive oxygen include superoxide anion ($O_2^{\cdot-}$), hydrogen peroxide (H_2O_2), hydroxyl radical (·OH) and singlet oxygen ($^1O_2$). These species differ in their origin, lifetime, reactivity and biological impact. Superoxide anion is recognized as the primary ROS, produced mainly in electron transport chains in chloroplasts and mitochondria and by a membrane bound enzyme, NADPH oxidase (NOX), also referred to as RBOH (respiratory burst oxidase homologs). This ROS is highly reactive but is readily converted to moderately reactive hydrogen peroxide (Fichman and Mittler, 2020; Farnese et al., 2016; Demidchik, 2015). Due to its relatively long lifetime (>1 ms) and ability to pass through specific aquaporins (Bienert et al., 2007; Rodrigues et al., 2017), H_2O_2 can travel a considerable distance and react, mainly with proteins, in various cellular compartments. In turn, hydroxyl radical is the least stable ROS with half lifetime measured in ns. It is the most reactive species and can cause considerable damage near the site of its formation. Singlet oxygen is produced mainly by chloroplasts through the transfer of energy from the triplet state of chlorophyll to oxygen. This ROS is characterized by relatively high reactivity and is the main source of oxidative damage of the photosystems in chloroplasts (Das and Roychoudhury, 2014; Dumanović et al., 2021). Reactive oxygen species are quenched by enzymatic and non-enzymatic antioxidants. The main antioxidant enzymes include superoxide dismutase (SOD), catalase (CAT) and peroxidases (POX). The groups of non-enzymatic antioxidants include e.g. ascorbic acid (ASC), glutathione (GSH), tocopherol, carotenoids and phenolic compounds (Dumanović et al., 2021).

Initially ROS were perceived solely as damaging agents, which cause oxidation and impairment of biomolecules including lipids, proteins and nucleic acids. Nowadays it is commonly acknowledged that certain ROS level is indispensable for proper cell functioning as they constitute important signalling elements and are engaged in regulation of gene expression, developmental processes and stress response. An important mode of their action is dependent on the oxidation of cysteine residues leading to the formation of disulphide bridges affecting protein structure and functioning. Oxidation of cysteine regulates the activity of various proteins including glyceraldehyde-3-phosphate dehydrogenase (GAPDH), mitogen-activated protein kinases (MAPK) and H_2O_2 sensing HPCA1 protein (Mittler, 2017; Castro et al., 2021). It is worth highlighting that some proteins, such as thioredoxins (TRX) and glutaredoxins (GRX), are especially prone to oxidation of cysteine residues and can act as redox signal transmitters. These molecules can mediate the oxidation and reduction state of cysteines in other proteins and thus work as redox switches (Martí et al., 2020).

In addition to the direct impact on proteins, ROS can modulate signalling network through interaction with other signalling elements such as calcium ions (Ca^{2+}), reactive nitrogen species (RNS), reactive sulphur species (RSS) plant hormones, mitogen activated protein kinases, transcription factors and other signalling associated proteins (Castro et al., 2021; Farnese et al., 2016). It is postulated that various signalling pathway are integrated in signalling hubs and that NADPH oxidase (RBOH) may constitute such signalling integration and coordination site. This membrane-bond enzyme can be regulated by calcium fluctuations, direct phosphorylation and binding of phosphatidic acid. In addition, an increasing amount of evidence shows that NADPH oxidase activity can be affected by S-nitrosation and presulfidation, connecting it with the RNS and RSS signalling pathways. Its activation leads to increased

production of $O_2^{\cdot}$, which is thereafter converted to the main ROS signalling molecule - H_2O_2. RBOH proteins are key elements in propagation of ROS waves, referred to as rapid, long-distance and autopropagating signals. The sequence of ROS wave generation includes accumulation of H_2O_2 in apoplast and its sensing by HPCA1 protein resulting in increased influx of Ca^{2+} into the cytosol. This in turn leads to activation of NADPH oxidases and amplification of ROS signal (Castro et al., 2021; Fichman and Mittler, 2020).

It is postulated that also the products of ROS-dependent oxidation can constitute signalling or gene regulatory elements. For instance, oxylipins, which can be formed as a result of lipid peroxidation, affect expression of numerous genes in *Arabidopsis* plants. The most frequent oxidative modification of ribonucleic acids, 8-hydroxyguanosine (8-OHG), is formed in a selective manner in specific transcripts, leading to their hampered translation and attenuate levels of certain proteins. This process is likely engaged in pathogenesis of neurodegenerative diseases in animals and in alleviation of seed dormancy in plants. In turn, small peptides derived from protein oxidation could, in addition to general information on the occurrence of oxidative stress, also transmit the information on its intensity, the type of over-produced species and stress localization (Chmielowska-Bąk et al., 2015).

As described above, ROS can modulate signalling through direct interaction with proteins (formation of disulphide bonds) including redox transmitters (e.g. TRX, GRX), interaction with other signalling elements (e.g. RNS, RSS, Ca^{2+}, MAPK) or possible generation of further signalling or gene regulatory elements (oxidized peptides, oxylipins, 8-OHG enriched transcripts). On the other hand, ROS excess might lead to oxidative damage of molecules and thus exhibits deleterious effects. Enhancement of ROS production is a common plant response to various stress conditions (Fichman and Mittler, 2020; Farnese et al., 2016; Demidchik, 2015). However, it is quite difficult to elucidate if stress-dependent ROS accumulation is a symptom of oxidative stress or signalling and/or regulatory response.

Oxidative response of plants to nanoplastic

An increasing number of reports show that, similarly to other stress factors, also NP induce an oxidative response in plants (summarized in Table 1). The studies show that even short-term exposure to NP can result in the accumulation of ROS. In onion seedling, treatment for 72 h with PS NP at the concentration of 1000 mg/l resulted in a significant increase in the H_2O_2 level. On the other hand, exposure to lower concentrations, 10 and 50 mg/l, had no significant effect. The results were confirmed by microscopic detection using Amplex Ultra Red probe showing concentration-dependent accumulation of H_2O_2 in the root tissues of the treated seedlings (Giorgetti et al., 2020). The NP effects might depend on their surface charge. In *Arabidopsis*, an increase in H_2O_2 and $O_2^{\cdot}$ level in response to PS NP was noted, wherein the positively charged NP (PS-NH_2) induced stronger H_2O_2 accumulation than the negatively charged ones (PS-SO_3H) (Sun et al., 2020). Similar results were obtained in dandelion and duckweed - in the studies, both positively as well as negatively charged NP caused an increase in the ROS level. However, the response was more pronounced in the case of PS-NH_2 (Gao et al., 2022; Xiao et al., 2022).

Accumulation of ROS leads to the oxidation and damage of cellular elements, wherein lipid peroxidation is probably the most frequently assessed oxidative stress marker. The commonly measured products of lipid peroxidation include malondialdehyde (MDA) and thiobarbituric acid reactive substances (TBARS). Independent studies on onion and broad bean seedlings treated for a short time with PS NP, revealed concentration-dependent changes in lipid peroxidation. The lower concentrations (10 mg/l) resulted in a decrease in TBARS/MDA levels, while the highest applied concentrations (100 mg/l in the case of broad bean and 1000 mg/l in the case of onion) led to intensified lipid peroxidation (Giorgetti et al., 2020; Jiang et al., 2019). Interestingly, in the case of broad bean, the same study showed that treatment with microplastic (MP) of 5 μm diameter did not affect MDA levels (Jiang et al., 2019). Size-dependent effects of NP on lipid peroxidation were also shown in cucumber. In response to a 14-day exposure, an increase in MDA level has been noted only in the case of 300 and 500 nm PS NP, while no effect has been observed in the case of 100 and 700 nm PS NP (Li et al., 2021c). In turn, study on rice indicated that the intensity of lipid peroxidation is dependent on the NP charge. In the roots, neutrally, negatively and positively charged NP augmented lipid peroxidation. However, the most significant effect was observed in the case of neutral PS NP. In turn, in the shoots, neutrally charged NP had no influence on lipid peroxidation, positively charged led to a significant TBARS accumulation, while treatment with negatively charged NP resulted in alleviated TBARS levels in relation to the control (Wang et al., 2022). Similarly, in duckweed the effect of PS- NH_2 on lipid peroxidation was stronger and induced by lower concentrations than the effect of PS-SO_3H (Xiao et al., 2022). The symptoms of oxidative stress were observed not solely by the application of PS NP but also in response to PMMA. In this case, application of PMMA particles to hydroponically grown lettuce resulted in accumulation of H_2O_2 and TBARS. However, it should be noted that in this case the particles were slightly bigger than in the other cited studies, with average diameter of 131 nm (Yildiztugay et al., 2022).

The majority of the described studies show NP-dependent increase in ROS level and intensified lipid peroxidation. However, there are also individual reports presenting opposite findings. In the roots of young rice seedlings, reduced H_2O_2 levels in response to lower PS NP concentration (100 mg/l) were reported, while higher concentrations did not affect ROS accumulation. In addition, PS NP-dependent decrease in the

TABLE 1 Summery of plant oxidative response to NP (≤100 nm); PS, polystyrene; PMMA, polymethyl methyacrylate; MD, malondialdehyde (marker of lipid peroxidation); TBARS, thiobarbituric acid reactive substances (marker of lipid peroxidation); APX, ascorbic peroxidase; CAT, catalase; POX, peroxidases; SOD, superoxide dismutase.

Plant species	NPs type, size and concentration	Treatment duration	NPs effect	References
castor bean (*Vicia faba*)	PS; 100 nm; 10, 50 and 100 mg/l	48 h	concentration dependent changes in lipid peroxidation and the activity of antioxidant enzymes	(Jiang et al., 2019)
wheat (*Triticum aestivum*)	PS; on average 87 nm; 10 mg/L	21 days	↑ lipid peroxidation	(Lian et al., 2020)
onion (*Allium cepa*)	PS; 50 nm; 10, 100 and 1000 mg/L	72 h	↑ lipid peroxidation and hydrogen peroxide accumulation	(Giorgetti et al., 2020)
arabidopsis (*Arabidopsis thaliana*)	PS; PS-SO_3H: 55 nm, PS-NH_2: 71 nm 300 and 1000 mg/L	7 days, 10 days, 7 weeks	↑ hydrogen peroxide and superoxide anion level modified genes expression	(Sun et al., 2020)
rice (*Oryza sativa*)	PS; 19 nm; 10, 50 and 100 mg/l;	16 days	↑ activity of antioxidant enzymes	(Zhou et al., 2021)
rice (*Oryza sativa*)	PS; 50 nm; 100 and 1000 mg/l	4 days	roots: ↓ hydrogen peroxide and TBARS levels ↑ APX and SOD activity Shoots: ↓ TBARS levels ↑ APX, POX and CAT activity	(Spanò et al., 2022)
rice (*Oryza sativa*)	PS, PS-COOH, PS-NH_2 50 nm 50 mg/l	7 days	Alerted activity of POD, SOD and CAT ↑ TBARS in response to PS-NH_2 ↓TBRAS in response to PS-COOH	(Wang et al., 2022)
cucumber (*Cucumis sativus*)	PS; 100, 300, 500, 700 nm; 50 mg/l	14 and 65 days	particle size dependent changes in lipid peroxidation and vitamin C level	(Li et al., 2021c)
lettuce (*Lactuca sativa*)	PS (foliar application); 0.1 and 1 mg/l; 100 nm	30 days	↓ decreased antioxidant activity	(Lian et al., 2021)
lettuce (*Lactuca sativa*)	PS; 100 nm 50 mg/l	21 days	↑ MDA level ↑ SOD activity	(Gong et al., 2022)
dandelion (*Taraxacum asiaticum*)	PS: PS-COOH, PS-NH_2 80 nm 1, 5, 10 mg/l	7 days	↑ hydrogen peroxide and superoxide anion level ↑ SOD and CAT activity ↑ ASC and GSH ↓ polyphenols, flavonoids	(Gao et al., 2022)
duckweed (*Lemna minor*)	PS: PS-SO_3H, PS-NH_2 Approx. 100 nm 2-50 μg/l	3 days	↑ hydrogen peroxide, superoxide anion and TBARS level	(Xiao et al., 2022)

TBARS levels was observed in seedlings roots and shoots. The authors propose that this effect could result from enhanced activity of the antioxidant system. Indeed, PS NP stimulated the activity of guaiacol peroxidase (POX), ascorbate peroxidase (APX) and superoxide dismutase (SOD) in the roots, while the activity of POX, APX and catalase (CAT) was induced in the shoots (Spanò et al., 2022). These results were confirmed by other studies on rice showing stimulation of peroxidases (POX), SOD and CAT in the roots in response to PS NP (Wang et al., 2022; Zhou et al., 2021). Similarly, in castor bean, treatment with PS NP resulted in enhanced activity of SOD and CAT, while POX showed increased activity by lower concentrations but a decrease in response to the higher concentration (Jiang et al., 2019). In dandelion, PS NP-dependent stimulation of SOD and CAT has been reported, wherein the response was the most prominent in the case of positively charged particles in relation to the neutrally and negatively charged ones (Gao et al., 2022). Exposure to PS NP can also modulate the level of non-enzymatic antioxidants. In cucumber, size-dependent effects on the accumulation of ascorbic acid (ASC) have been described -

100 nm PS NP causes an increase in the ASC level, whereas application of 500 nm PS NP resulted in the decrease in its level (Li et al., 2021c). PS NP-dependent increase in the level of ASC and glutathione (GSH) has been noted also in dandelion plants. On the other hand, exposure to PS NP led to a reduced content of polyphenols including flavonoids, which constitute a group of bioactive compounds with antioxidant activity (Gao et al., 2022).

In the environment, plants are frequently exposed to combined stress factors, which can further aggravate their negative impact. Recent study on lettuce focused on the combined action of FeNP and PS NP. The results showed that the nanoparticles form hetero-aggregates. Simultaneous application of Fe NP and PS NP also resulted in augmented Fe release and accumulation in plant tissues. In addition, an increase in the level of lipid peroxidation and augmented cell damage were noted in the treated plants (Gong et al., 2022).

The NP-dependent accumulation of ROS is convincingly evidenced. The extent of the reaction is dependent on various factors including NP concentration, size and charge. The ROS over-production is associated with intensified lipid peroxidation, which is a typical symptom of oxidative stress. In general, ROS accumulation might also lead to protein carbonylation and oxidation of nucleic acids (Das and Roychoudhury, 2014; Dumanović et al., 2021). To the best of our knowledge so far there is no information on NP driven modifications of proteins. However, there are reports showing the adverse impact of these particles on the genetic material reflected by an increase in the amount of micronuclei formation and/or cytological abnormalities and decreased mitotic index (Jiang et al., 2019; Giorgetti et al., 2020; Spanò et al., 2022). In addition, ROS might exert signalling and gene regulator role. Indeed, changes in gene expression in response to NP have been observed in *Arabidopsis*, rice, wheat and duckweed (Lian et al., 2022; Sun et al., 2020; Wang et al., 2022; Xiao et al., 2022). However, it is not known if the observed changes are dependent on ROS action.

Thus, it can be concluded that although the information on NP oxidative effects in plant is gradually increasing, there is still much to be examined. So far the reports are limited to few plant species: Arabidopsis, rice, wheat, onion, cucumber, lettuce and duckweed. In addition, the effects were studied mainly in response to long-term exposure and to one type of plastic - polystyrene. It is evidenced that NP induce ROS formation and peroxidation of lipids. However, there is no information on the oxidation of other cellular compounds including proteins and nucleic acids. In addition, NP-dependent ROS accumulation is examined in relation to their cytotoxicity, while little attention is given to the possible signalling and gene regulatory roles.

Conclusions

An increasing amount of evidence shows a progressive contamination of the environment with plastic, including nanoplastic particles (NP). It can be predicted that the problem will aggravate with time due to high plastic production and simultaneous long degradation time. Recent studies on plants show that exposure to NP leads to the development of toxicity symptoms including growth inhibition, alterations in mineral homeostasis and photosynthesis efficiency, decreased cell division and genotoxic effects (summarized in Figure 5). A common plant

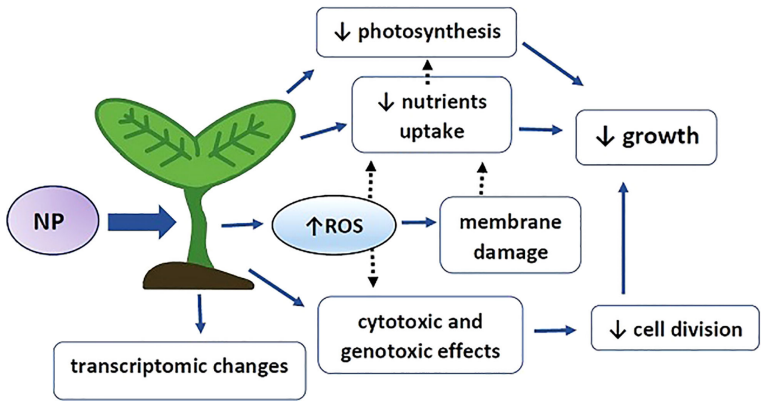

FIGURE 5
Graphical summary of NP impact on plants. NP – nanoplastic particles, ROS – reactive oxygen species, blue arrows – experimentally evidenced effects, black dotted arrow – possible interactions. Exposure to NP leads to increase in reactive oxygen species, hampered uptake of specific nutrients, decrease in photosynthesis efficiency and cyto- and genotoxic effects. ROS might mediate cyto- and genotoxic effect through direct interaction with genetic material and alert nutrient uptake through mediation of membrane damage. Decrease in the level of certain elements e.g. Fe and Mg might results in impaired chlorophyll synthesis and contribute to lower photosynthesis efficiency. Cyto- and genotoxic effects lead to decreased cell division. Alerted cell division, nutrient level and photosynthesis results in hampered plants growth. In addition, NP alert plants physiology through modulation of genes expression on the transcriptomic level.

response to abiotic stress factors, including environmental contaminants, is over-production of reactive oxygen species (ROS). Indeed, in most of the studies, exposure to NP also resulted in accumulation of superoxide anion and/or hydrogen peroxide, accompanied by intensified lipid peroxidation and stimulation of the antioxidant system. The published data indicated that the oxidative response is in general stronger in the case of positively charged and smaller plastic particles (when comparing MP to NP). However, the exact effects of NP-driven ROS, including their impact on the oxidation of proteins and nucleic acids and possible gene regulatory/signalling functions, still remain unexamined.

Author contributions

AE-G and JC-B elaborated manuscript concept, all authors participated in manuscript writing and editing. All authors contributed to the article and approved the submitted version.

Funding

The research on nanoplastic impact on plants carried out in the Department of Plant Ecophysiology is financed by statutory funding (JC-B) and by the National Science Centre, Poland, grant number UMO-2016/23/D/NZ8/01112 (AE-G). This work was supported in the scope of the project CESAM- UIDB/50017/2020 + UIDP/50017/2020 + LA/P/0094/2020, financed by national funds through the FCT/MEC (IL).

Acknowledgments

We would like to thank the members of COST action CA20101 "Plastics monitoRIng detectiOn RemedIaTion recoverY" for fruitful discussion on the topic of nanoplastic contamination and impact on plants.

Conflict of interest

The authors declare that the research was conducted in the absence of any commercial or financial relationships that could be construed as a potential conflict of interest.

Publisher's note

References

Allen, S., Allen, D., Karbalaei, S., Maselli, V., and Walker, T. R. (2022). Micro (nano)plastics sources, fate, and effects: What we know after ten years of research. *J. Hazard. Mater. Adv.* 6, 100057. doi: 10.1016/j.hazadv.2022.100057

An, D., Na, J., Song, J., and Jung, J. (2021). Size-dependent chronic toxicity of fragmented polyethylene microplastics to daphnia magna. *Chemosphere* 271, 129591. doi: 10.1016/j.chemosphere.2021.129591

Antonopoulos, I., Faraca, G., and Tonini, D. (2021). Recycling of post-consumer plastic packaging waste in EU: Process efficiencies, material flows, and barriers. *Waste Manage.* 126, 694–705. doi: 10.1016/j.wasman.2021.04.002

Antunes, J. C., Frias, J. G. L., Micaelo, A. C., and Sobral, P. (2013). Resin pellets from beaches of the Portuguese coast and adsorbed persistent organic pollutants. *Estuar. Coast. Shelf Sci.* 130, 62–69. doi: 10.1016/j.ecss.2013.06.016

Azeem, I., Adeel, M., Ahmad, M. A., Shakoor, N., Jiangcuo, G. D., Azeem, K., et al. (2021). Uptake and accumulation of Nano/Microplastics in plants: A critical review. *Nanomaterials* 11, 2935–2956. doi: 10.3390/nano11112935

Bienert, G. P., Møller, A. L. B., Kristiansen, K. A., Schulz, A., Møller, I. M., Schjoerring, J. K., et al. (2007). Specific aquaporins facilitate the diffusion of hydrogen peroxide across membranes. *J. Biol. Chem.* 282, 1183–1192. doi: 10.1074/jbc.M603761200

Birch, Q. T., Potter, P. M., Pinto, P. X., Dionysiou, D. D., and Al-Abed, S. R. (2020). Sources, transport, measurement and impact of nano and microplastics in urban watersheds. *Rev. Environ. Sci. Bio/Technol.* 19, 275–336. doi: 10.1007/s11157-020-09529-x

Bosker, T., Bouwman, L. J., Brun, N. R., Behrens, P., and Vijver, M. G. (2019). Microplastics accumulate on pores in seed capsule and delay germination and root growth of the terrestrial vascular plant lepidium sativum. *Chemosphere* 226, 774–781. doi: 10.1016/j.chemosphere.2019.03.163

Bour, A., Sturve, J., Höjesjö, J., and Carney Almroth, B. (2020). Microplastic vector effects: Are fish at risk when exposed *via* the trophic chain? *Front. Environ. Sci.* 8. doi: 10.3389/fenvs.2020.00090

Brewer, A., Dror, I., and Berkowitz, B. (2021). The mobility of plastic nanoparticles in aqueous and soil environments: A critical review. *ACS ES&T Water* 1, 48–57. doi: 10.1021/acsestwater.0c00130

Butler, E., Devlin, G., and McDonnell, K. (2011). Waste polyolefins to liquid fuels *via* pyrolysis: Review of commercial state-of-the-art and recent laboratory research. *Waste Biomass Valorization* 2, 227–255. doi: 10.1007/s12649-011-9067-5

Campanale, C., Massarelli, C., Savino, I., Locaputo, V., and Uricchio, V. F. (2020). A detailed review study on potential effects of microplastics and additives of concern on human health. *Int. J. Environ. Res. Public Health* 17, 1212–1237. doi: 10.3390/ijerph17041212

Caputo, F., Vogel, R., Savage, J., Vella, G., Law, A., Della Camera, G., et al. (2021). Measuring particle size distribution and mass concentration of nanoplastics and microplastics: addressing some analytical challenges in the sub-micron size range. *J. Colloid Interface Sci.* 588, 401–417. doi: 10.1016/j.jcis.2020.12.039

Castan, S., Henkel, C., Hüffer, T., and Hofmann, T. (2021). Microplastics and nanoplastics barely enhance contaminant mobility in agricultural soils. *Commun. Earth Environ.* 2, 193. doi: 10.1038/s43247-021-00267-8

Castro, B., Citterico, M., Kimura, S., Stevens, D. M., Wrzaczek, M., and Coaker, G. (2021). Stress-induced reactive oxygen species compartmentalization, perception and signalling. *Nat. Plants* 7, 403–412. doi: 10.1038/s41477-021-00887-0

Chai, Y. N., and Schachtman, D. P. (2022). Root exudates impact plant performance under abiotic stress. *Trends Plant Sci.* 27, 80–91. doi: 10.1016/j.tplants.2021.08.003

Chamas, A., Moon, H., Zheng, J., Qiu, Y., Tabassum, T., Jang, J. H., et al. (2020). Degradation rates of plastics in the environment. *ACS Sustain. Chem. Eng.* 8, 3494–3511. doi: 10.1021/acssuschemeng.9b06635

Chmielowska-Bąk, J., Izbiańska, K., and Deckert, J. (2015). Products of lipid, protein and RNA oxidation as signals and regulators of gene expression in plants. *Front. Plant Sci.* 6. doi: 10.3389/fpls.2015.00405

Correia, M., and Loeschner, K. (2018). Detection of nanoplastics in food by asymmetric flow field-flow fractionation coupled to multi-angle light scattering: possibilities, challenges and analytical limitations. *Anal. Bioanal. Chem.* 410, 5603–5615. doi: 10.1007/s00216-018-0919-8

Crespy, D., Bozonnet, M., and Meier, M. (2008). 100 years of Bakelite, the material of a 1000 uses. *Angew. Chemie Int. Ed.* 47, 3322–3328. doi: 10.1002/anie.200704281

Das, K., and Roychoudhury, A. (2014). Reactive oxygen species (ROS) and response of antioxidants as ROS-scavengers during environmental stress in plants. *Front. Environ. Sci.* 2. doi: 10.3389/fenvs.2014.00053

Demidchik, V. (2015). Mechanisms of oxidative stress in plants: From classical chemistry to cell biology. *Environ. Exp. Bot.* 109, 212–228. doi: 10.1016/j.envexpbot.2014.06.021

Dumanović, J., Nepovimova, E., Natić, M., Kuča, K., and Jaćević, V. (2021). The significance of reactive oxygen species and antioxidant defense system in plants: A concise overview. *Front. Plant Sci.* 11. doi: 10.3389/fpls.2020.552969

Fang, C., Sobhani, Z., Zhang, X., Gibson, C. T., Tang, Y., and Naidu, R. (2020). Identification and visualisation of microplastics/ nanoplastics by raman imaging (ii): Smaller than the diffraction limit of laser? *Water Res.* 183, 116046. doi: 10.1016/j.watres.2020.116046

Farnese, F. S., Menezes-Silva, P. E., Gusman, G. S., and Oliveira, J. A. (2016). When bad guys become good ones: The key role of reactive oxygen species and nitric oxide in the plant responses to abiotic stress. *Front. Plant Sci.* 7. doi: 10.3389/fpls.2016.00471

Fichman, Y., and Mittler, R. (2020). Rapid systemic signaling during abiotic and biotic stresses: is the ROS wave master of all trades? *Plant J.* 102, 887–896. doi: 10.1111/tpj.14685

Gao, M., Bai, L., Li, X., Wang, S., and Song, Z. (2022). Effects of polystyrene nanoplastics on lead toxicity in dandelion seedlings. *Environ. pollut.* 306, 119349. doi: 10.1016/j.envpol.2022.119349

Gaur, N., Chowdhary, R., Brunwal, D., and Singh, R. (2020). *Degradation of Plastic in Environment and Its Implications with Special Reference to Aromatic Polyesters*, in Handbook of environmental materials management. ed. C.M. Hussain (Springer, Cham.), 1–26. doi: 10.1007/978-3-319-58538-3_176-1

Geyer, R., Jambeck, J. R., and Law, K. L. (2017). Production, use, and fate of all plastics ever made - supplementary information. *Sci. Adv.* 3, 19–24. doi: 10.1126/sciadv.1700782

Gigault, J., El Hadri, H., Nguyen, B., Grassl, B., Rowenczyk, L., Tufenkji, N., et al. (2021). Nanoplastics are neither microplastics nor engineered nanoparticles. *Nat. Nanotechnol.* 16, 501–507. doi: 10.1038/s41565-021-00886-4

Giorgetti, L., Spanò, C., Muccifora, S., Bottega, S., Barbieri, F., Bellani, L., et al. (2020). Exploring the interaction between polystyrene nanoplastics and allium cepa during germination: Internalization in root cells, induction of toxicity and oxidative stress. *Plant Physiol. Biochem.* 149, 170–177. doi: 10.1016/j.plaphy.2020.02.014

Giri, S., and Mukherjee, A. (2022). Eco-corona reduces the phytotoxic effects of polystyrene nanoplastics in allium cepa: Emphasizing the role of ROS. *Environ. Exp. Bot.* 198, 104850. doi: 10.1016/j.envexpbot.2022.104850

Gong, D., Bai, X., Weng, Y., Kang, M., Huang, Y., Li, F., et al. (2022). Phytotoxicity of binary nanoparticles and humic acid on lactuca sativa l. *Environ. Sci. Process. Impacts* 24, 586–597. doi: 10.1039/d2em00014h

Gwada, B., Ogendi, G., Makindi, S. M., and Trott, S. (2019). Composition of plastic waste discarded by households and its management approaches. *Glob. J. Environ. Sci. Manage.* 5, 83–94. doi: 10.22034/gjesm.2019.01.07

Hartmann, N. B., Hüffer, T., Thompson, R. C., Hassellöv, M., Verschoor, A., Daugaard, A. E., et al. (2019). Are we speaking the same language? recommendations for a definition and categorization framework for plastic debris. *Environ. Sci. Technol.* 53, 1039–1047. doi: 10.1021/acs.est.8b05297

Heinze, W. M., Mitrano, D. M., Lahive, E., Koestel, J., and Cornelis, G. (2021). Nanoplastic transport in soil *via* bioturbation by lumbricus terrestris. *Environ. Sci. Technol.* 55, 16423–16433. doi: 10.1021/acs.est.1c05614

He, D., Luo, Y., Lu, S., Liu, M., Song, Y., and Lei, L. (2018). Microplastics in soils: Analytical methods, pollution characteristics and ecological risks. *TrAC Trends Anal. Chem.* 109, 163–172. doi: 10.1016/j.trac.2018.10.006

Hernandez, L. M., Xu, E. G., Larsson, H. C. E., Tahara, R., Maisuria, V. B., and Tufenkji, N. (2019). Plastic teabags release billions of microparticles and nanoparticles into tea. *Environ. Sci. Technol.* 53, 12300–12310. doi: 10.1021/acs.est.9b02540

Holmes, L. A., Turner, A., and Thompson, R. C. (2012). Adsorption of trace metals to plastic resin pellets in the marine environment. *Environ. pollut.* 160, 42–48. doi: 10.1016/j.envpol.2011.08.052

Horton, A. A., Walton, A., Spurgeon, D. J., Lahive, E., and Svendsen, C. (2017). Microplastics in freshwater and terrestrial environments: Evaluating the current understanding to identify the knowledge gaps and future research priorities. *Sci. Total Environ.* 586, 127–141. doi: 10.1016/j.scitotenv.2017.01.190

Huang, D., Chen, H., Shen, M., Tao, J., Chen, S., Yin, L., et al. (2022). Recent advances on the transport of microplastics/nanoplastics in abiotic and biotic compartments. *J. Hazard. Mater.* 438, 129515. doi: 10.1016/j.jhazmat.2022.129515

Huang, D., Tao, J., Cheng, M., Deng, R., Chen, S., Yin, L., et al. (2021). Microplastics and nanoplastics in the environment: Macroscopic transport and effects on creatures. *J. Hazard. Mater.* 407, 124399. doi: 10.1016/j.jhazmat.2020.124399

Hüffer, T., and Hofmann, T. (2016). Sorption of non-polar organic compounds by micro-sized plastic particles in aqueous solution. *Environ. pollut.* 214, 194–201. doi: 10.1016/j.envpol.2016.04.018

Jiang, X., Chen, H., Liao, Y., Ye, Z., Li, M., and Klobučar, G. (2019). Ecotoxicity and genotoxicity of polystyrene microplastics on higher plant vicia faba. *Environ. pollut.* 250, 831–838. doi: 10.1016/j.envpol.2019.04.055

Jiménez-Lamana, J., Marigliano, L., Allouche, J., Grassl, B., Szpunar, J., and Reynaud, S. (2020). A novel strategy for the detection and quantification of nanoplastics by single particle inductively coupled plasma mass spectrometry (ICP-MS). *Anal. Chem.* 92, 11664–11672. doi: 10.1021/acs.analchem.0c01536

Khan, M. R., Adam, V., Rizvi, T. F., and Zhang, B. (2019). Nanoparticle – plant Interactions : Two-way traffic. *Small* 1901794, 1–20. doi: 10.1002/smll.201901794

Kihara, S., Köper, I., Mata, J. P., and McGillivray, D. J. (2021). Reviewing nanoplastic toxicology: It's an interface problem. *Adv. Colloid Interface Sci.* 288, 102337. doi: 10.1016/j.cis.2020.102337

Kiran, B. R., Kopperi, H., and Venkata Mohan, S. (2022). Micro/nano-plastics occurrence, identification, risk analysis and mitigation: challenges and perspectives. *Springer Netherlands* 21, 169–203. doi: 10.1007/s11157-021-09609-6

Kodavanti, P. R. S., Royland, J. E., and Sambasiva Rao, K. R. S. (2014). *Toxicology of persistent organic pollutants. 3rd ed.* (Elsevier, Amsterdam, The Netherlands). doi: 10.1016/b978-0-12-801238-3.00211-7

Lambert, S., and Wagner, M. (2016). Characterisation of nanoplastics during the degradation of polystyrene. *Chemosphere* 145, 265–268. doi: 10.1016/j.chemosphere.2015.11.078

Law, K. L., and Narayan, R. (2022). Reducing environmental plastic pollution by designing polymer materials for managed end-of-life. *Nat. Rev. Mater.* 7, 104–116. doi: 10.1038/s41578-021-00382-0

Lehner, R., Weder, C., Petri-Fink, A., and Rothen-Rutishauser, B. (2019). Emergence of nanoplastic in the environment and possible impact on human health. *Environ. Sci. Technol.* 53, 1748–1765. doi: 10.1021/acs.est.8b05512

Leslie, H. A., van Velzen, M. J. M., Brandsma, S. H., Vethaak, A. D., Garcia-Vallejo, J. J., and Lamoree, M. H. (2022). Discovery and quantification of plastic particle pollution in human blood. *Environ. Int.* 163, 107199. doi: 10.1016/j.envint.2022.107199

Lian, J., Liu, W., Meng, L., Wu, J., Chao, L., Zeb, A., et al. (2021). Foliar-applied polystyrene nanoplastics (PSNPs) reduce the growth and nutritional quality of lettuce (Lactuca sativa l.). *Environ. Pollut.* 280, 116978. doi: 10.1016/j.envpol.2021.116978

Lian, J., Liu, W., Sun, Y., Men, S., Wu, J., Zeb, A., et al. (2022). Nanotoxicological effects and transcriptome mechanisms of wheat (Triticum aestivum l.) under stress of polystyrene nanoplastics. *J. Hazard. Mater.* 423, 127241. doi: 10.1016/j.jhazmat.2021.127241

Lian, J., Wu, J., Xiong, H., Zeb, A., Yang, T., Su, X., et al. (2020). Impact of polystyrene nanoplastics (PSNPs) on seed germination and seedling growth of wheat (Triticum aestivum l.). *J. Hazard. Mater.* 385, 121620. doi: 10.1016/j.jhazmat.2019.121620

Li, C., Gao, Y., He, S., Chi, H.-Y., Li, Z.-C., Zhou, X.-X., et al. (2021a). Quantification of nanoplastic uptake in cucumber plants by pyrolysis gas

Chromatography/Mass spectrometry. *Environ. Sci. Technol. Lett.* 8, 633–638. doi: 10.1021/acs.estlett.1c00369

Li, Z., Li, Q., Li, R., Zhou, J., and Wang, G. (2021c). The distribution and impact of polystyrene nanoplastics on cucumber plants. *Environ. Sci. pollut. Res.* 28, 16042–16053. doi: 10.1007/s11356-020-11702-2

Li, L., Luo, Y., Li, R., Zhou, Q., Peijnenburg, W. J. G. M., Yin, N., et al. (2020). Effective uptake of submicrometre plastics by crop plants *via* a crack-entry mode. *Nat. Sustain.* 3, 929–937. doi: 10.1038/s41893-020-0567-9

Liu, Y., Guo, R., Zhang, S., Sun, Y., and Wang, F. (2022b). Uptake and translocation of nano/microplastics by rice seedlings: Evidence from a hydroponic experiment. *J. Hazard. Mater.* 421, 126700. doi: 10.1016/j.jhazmat.2021.126700

Liu, Y., Shao, H., Liu, J., Cao, R., Shang, E., Liu, S., et al. (2021). Transport and transformation of microplastics and nanoplastics in the soil environment: A critical review. *Soil Use Manage.* 37, 224–242. doi: 10.1111/sum.12709

Liu, X., Zhao, Y., Dou, J., Hou, Q., Cheng, J., and Jiang, X. (2022a). Bioeffects of inhaled nanoplastics on neurons and alteration of animal behaviors through deposition in the brain. *Nano Lett.* 22, 1091–1099. doi: 10.1021/acs.nanolett.1c04184

Li, J., Zhang, K., and Zhang, H. (2018). Adsorption of antibiotics on microplastics. *Environ. pollut.* 237, 460–467. doi: 10.1016/j.envpol.2018.02.050

Lucas, N., Bienaime, C., Belloy, C., Queneudec, M., Silvestre, F., and Nava-Saucedo, J. E. (2008). Polymer biodegradation: Mechanisms and estimation techniques - A review. *Chemosphere* 73, 429–442. doi: 10.1016/j.chemosphere.2008.06.064

Maes, T., Jessop, R., Wellner, N., Haupt, K., and Mayes, A. G. (2017). A rapid-screening approach to detect and quantify microplastics based on fluorescent tagging with Nile red. *Sci. Rep.* 7, 44501. doi: 10.1038/srep44501

Martí, M. C., Jiménez, A., and Sevilla, F. (2020). Thioredoxin network in plant mitochondria: Cysteine s-posttranslational modifications and stress conditions. *Front. Plant Sci.* 11. doi: 10.3389/fpls.2020.571288

Mateos-Cárdenas, A., van Pelt, F. N. A. M., O'Halloran, J., and Jansen, M. A. K. (2021). Adsorption, uptake and toxicity of micro- and nanoplastics: Effects on terrestrial plants and aquatic macrophytes. *Environ. pollut.* 284, 117183. doi: 10.1016/j.envpol.2021.117183

Materić, D., Peacock, M., Dean, J., Futter, M., Maximov, T., Moldan, F., et al. (2022). Presence of nanoplastics in rural and remote surface waters. *Environ. Res. Lett.* 17, 054036. doi: 10.1088/1748-9326/ac68f7

Milewska-Hendel, A., Zubko, M., Stróż, D., and Kurczyńska, E. (2019). Effect of Nanoparticles Surface Charge on the Arabidopsis thaliana (L.) Roots Development and Their Movement into the Root Cells and Protoplasts. *Int. J. Mol. Sci.* 20, 1650–1671. doi: 10.3390/ijms20071650

Mittler, R. (2017). ROS are good. *Trends Plant Sci.* 22, 11–19. doi: 10.1016/j.tplants.2016.08.002

Narevski, A. C., Novaković, M. I., Petrović, M. Z., Mihajlović, I. J., Maoduš, N. B., and Vujić, G. V. (2021). Occurrence of bisphenol a and microplastics in landfill leachate: lessons from south East Europe. *Environ. Sci. pollut. Res.* 28, 42196–42203. doi: 10.1007/s11356-021-13705-z

Ng, E. L., Huerta Lwanga, E., Eldridge, S. M., Johnston, P., Hu, H. W., Geissen, V., et al. (2018). An overview of microplastic and nanoplastic pollution in agroecosystems. *Sci. Total Environ.* 627, 1377–1388. doi: 10.1016/j.scitotenv.2018.01.341

Nizzetto, L., Gioia, R., Li, J., Borgå, K., Pomati, F., Bettinetti, R., et al. (2012). Biological pump control of the fate and distribution of hydrophobic organic pollutants in water and plankton. *Environ. Sci. Technol.* 46, 3204–3211. doi: 10.1021/es204176q

Nolte, T. M., Hartmann, N. B., Kleijn, J. M., Garnæs, J., van de Meent, D., Jan Hendriks, A., et al. (2017). The toxicity of plastic nanoparticles to green algae as influenced by surface modification, medium hardness and cellular adsorption. *Aquat. Toxicol.* 183, 11–20. doi: 10.1016/j.aquatox.2016.12.005

O'Connor, D., Pan, S., Shen, Z., Song, Y., Jin, Y., Wu, W.-M., et al. (2019). Microplastics undergo accelerated vertical migration in sand soil due to small size and wet-dry cycles. *Environ. Pollut.* 249, 527–534. doi: 10.1016/j.envpol.2019.03.092

Pinto Da Costa, J., Rocha Santos, T., and Duarte, A. (2020). *The environmental impacts of plastics and micro-plastics use, waste and pollution: EU and national measures*. European Parliament, Directorate-General for Internal Policies of the Union, Brussels, doi: 10.2861/85472

Pironti, C., Ricciardi, M., Motta, O., Miele, Y., Proto, A., and Montano, L. (2021). Microplastics in the environment: Intake through the food web, human exposure and toxicological effects. *Toxics* 9, 224. doi: 10.3390/toxics9090224

Prata, J. C., da Costa, J. P., Lopes, I., Andrady, A. L., Duarte, A. C., and Rocha-Santos, T. (2021). A one health perspective of the impacts of microplastics on animal, human and environmental health. *Sci. Total Environ.* 777, 146094. doi: 10.1016/j.scitotenv.2021.146094

Prata, J. C., da Costa, J. P., Lopes, I., Duarte, A. C., and Rocha-Santos, T. (2020). Environmental exposure to microplastics: An overview on possible human health effects. *Sci. Total Environ.* 702, 134455. doi: 10.1016/j.scitotenv.2019.134455

Rai, P. K., Lee, J., Brown, R. J. C., and Kim, K.-H. (2021). Environmental fate, ecotoxicity biomarkers, and potential health effects of micro- and nano-scale plastic contamination. *J. Hazard. Mater.* 403, 123910. doi: 10.1016/j.jhazmat.2020.123910

Rillig, M. C., Ziersch, L., and Hempel, S. (2017). Microplastic transport in soil by earthworms. *Sci. Rep.* 7, 1336–1341. doi: 10.1038/s41598-017-01594-7

Rodrigues, O., Reshetnyak, G., Grondin, A., Saijo, Y., Leonhardt, N., Maurel, C., et al. (2017). Aquaporins facilitate hydrogen peroxide entry into guard cells to mediate ABA- and pathogen-triggered stomatal closure. *Proc. Natl. Acad. Sci.* 114, 9200–9205. doi: 10.1073/pnas.1704754114

Schmid, C., Cozzarini, L., and Zambello, E. (2021). Microplastic's story. *Mar. pollut. Bull.* 162, 111820. doi: 10.1016/j.marpolbul.2020.111820

Schwarz, A. E., Ligthart, T. N., Boukris, E., and van Harmelen, T. (2019). Sources, transport, and accumulation of different types of plastic litter in aquatic environments: A review study. *Mar. Pollut. Bull.* 143, 92–100. doi: 10.1016/j.marpolbul.2019.04.029

Spanò, C., Muccifora, S., Ruffini Castiglione, M., Bellani, L., Bottega, S., and Giorgetti, L. (2022). Polystyrene nanoplastics affect seed germination, cell biology and physiology of rice seedlings in-short term treatments: Evidence of their internalization and translocation. *Plant Physiol. Biochem.* 172, 158–166. doi: 10.1016/j.plaphy.2022.01.012

Sun, H., Lei, C., Xu, J., and Li, R. (2021). Foliar uptake and leaf-to-root translocation of nanoplastics with different coating charge in maize plants. *J. Hazard. Mater.* 416, 125854. doi: 10.1016/j.jhazmat.2021.125854

Sun, X.-D., Yuan, X.-Z., Jia, Y., Feng, L.-J., Zhu, F.-P., Dong, S.-S., et al. (2020). Differentially charged nanoplastics demonstrate distinct accumulation in arabidopsis thaliana. *Nat. Nanotechnol.* 15, 755–760. doi: 10.1038/s41565-020-0707-4

Taylor, S. E., Pearce, C. I., Sanguinet, K. A., Hu, D., Chrisler, W. B., Kim, Y.-M., et al. (2020). Polystyrene nano- and microplastic accumulation at arabidopsis and wheat root cap cells, but no evidence for uptake into roots. *Environ. Sci. Nano* 7, 1942–1953. doi: 10.1039/D0EN00309C

Turner, A., and Holmes, L. A. (2015). Adsorption of trace metals by microplastic pellets in fresh water. *Environ. Chem.* 12, 600–610. doi: 10.1071/EN14143

UNEP (2016). *Marine plastic debris and microplastics – Global lessons and research to inspire action and guide policy change*. United Nations Environment Programme, Nairobi (Unep), 1–192. Available at: https://ec.europa.eu/environment/marine/good-environmental-status/descriptor-10/pdf/Marine_plastic_debris_and_microplastic_technical_report_advance_copy.pdf.

Venâncio, C., Melnic, I., Tamayo-Belda, M., Oliveira, M., Martins, M. A., and Lopes, I. (2022). Polymethylmethacrylate nanoplastics can cause developmental malformations in early life stages of xenopus laevis. *Sci. Total Environ.* 806, 150491. doi: 10.1016/j.scitotenv.2021.150491

Wang, W., Ge, J., and Yu, X. (2020). Bioavailability and toxicity of microplastics to fish species: A review. *Ecotoxicol. Environ. Saf.* 189, 109913. doi: 10.1016/j.ecoenv.2019.109913

Wang, J., Lu, S., Guo, L., Wang, P., He, C., Liu, D., et al. (2022). Effects of polystyrene nanoplastics with different functional groups on rice (Oryza sativa l.) seedlings: Combined transcriptome, enzymology, and physiology. *Sci. Total Environ.* 834, 155092. doi: 10.1016/j.scitotenv.2022.155092

Wu, X., Lyu, X., Li, Z., Gao, B., Zeng, X., Wu, J., et al. (2020). Transport of polystyrene nanoplastics in natural soils: Effect of soil properties, ionic strength and cation type. *Sci. Total Environ.* 707, 136065. doi: 10.1016/j.scitotenv.2019.136065

Xiao, F., Feng, L.-J., Sun, X.-D., Wang, Y., Wang, Z.-W., Zhu, F.-P., et al. (2022). Do polystyrene nanoplastics have similar effects on duckweed (lemna minor l.) at environmentally relevant and observed-effect concentrations? *Environ. Sci. Technol.* 56, 4071–4079. doi: 10.1021/acs.est.1c06595

Yee, M. S.-L., Hii, L.-W., Looi, C. K., Lim, W.-M., Wong, S.-F., Kok, Y.-Y., et al. (2021). Impact of microplastics and nanoplastics on human health. *Nanomaterials* 11, 496. doi: 10.3390/nano11020496

Yildiztugay, E., Ozfidan-Konakci, C., Arikan, B., Alp, F. N., Elbasan, F., Zengin, G., et al. (2022). The hormetic dose-risks of polymethyl methacrylate nanoplastics on chlorophyll a fluorescence transient, lipid composition and antioxidant system in lactuca sativa. *Environ. Pollut.* 308, 119651. doi: 10.1016/j.envpol.2022.119651

Yuan, J., Ma, J., Sun, Y., Zhou, T., Zhao, Y., and Yu, F. (2020). Microbial degradation and other environmental aspects of microplastics/plastics. *Sci. Total Environ.* 715, 136968. doi: 10.1016/j.scitotenv.2020.136968

Zhang, W., Wang, Q., and Chen, H. (2022). Challenges in characterization of nanoplastics in the environment. *Front. Environ. Sci. Eng.* 16, 11. doi: 10.1007/s11783-021-1445-z

Zhao, X., Korey, M., Li, K., Copenhaver, K., Tekinalp, H., Celik, S., et al. (2022). Plastic waste upcycling toward a circular economy. *Chem. Eng. J.* 428, 131928. doi: 10.1016/j.cej.2021.131928

Zhou, C. Q., Lu, C. H., Mai, L., Bao, L. J., Liu, L. Y., and Zeng, E. Y. (2021). Response of rice (Oryza sativa l.) roots to nanoplastic treatment at seedling stage. *J. Hazard. Mater.* 401, 123412–123421. doi: 10.1016/j.jhazmat.2020.123412

frontiers | Frontiers in Plant Science

TYPE Review
PUBLISHED 26 October 2022
DOI 10.3389/fpls.2022.1027730

OPEN ACCESS

EDITED BY
Ana Zabalza,
Public University of Navarre, Spain

REVIEWED BY
Natalia Correa-Aragunde,
National University of Mar del Plata, Argentina
Joerg Durner,
Helmholtz Association of German Research Centres (HZ), Germany

*CORRESPONDENCE
Rosa M. Rivero
rmrivero@cebas.csic.es

SPECIALTY SECTION
This article was submitted to Plant Abiotic Stress, a section of the journal Frontiers in Plant Science

RECEIVED 25 August 2022
ACCEPTED 10 October 2022
PUBLISHED 26 October 2022

CITATION
Martí-Guillén JM, Pardo-Hernández M, Martínez-Lorente SE, Almagro L and Rivero RM (2022) Redox post-translational modifications and their interplay in plant abiotic stress tolerance.
Front. Plant Sci. 13:1027730.
doi: 10.3389/fpls.2022.1027730

Redox post-translational modifications and their interplay in plant abiotic stress tolerance

José M. Martí-Guillén[1,2], Miriam Pardo-Hernández[1], Sara E. Martínez-Lorente[1], Lorena Almagro[2] and Rosa M. Rivero[1]*

[1]Department of Plant Nutrition, Centro de Edafología y Biología Aplicada del Segura, Consejo Superior de Investigaciones Científicas, Murcia, Spain, [2]Department of Plant Biology, Faculty of Biology, University of Murcia, Murcia, Spain

The impact of climate change entails a progressive and inexorable modification of the Earth's climate and events such as salinity, drought, extreme temperatures, high luminous intensity and ultraviolet radiation tend to be more numerous and prolonged in time. Plants face their exposure to these abiotic stresses or their combination through multiple physiological, metabolic and molecular mechanisms, to achieve the long-awaited acclimatization to these extreme conditions, and to thereby increase their survival rate. In recent decades, the increase in the intensity and duration of these climatological events have intensified research into the mechanisms behind plant tolerance to them, with great advances in this field. Among these mechanisms, the overproduction of molecular reactive species stands out, mainly reactive oxygen, nitrogen and sulfur species. These molecules have a dual activity, as they participate in signaling processes under physiological conditions, but, under stress conditions, their production increases, interacting with each other and modifying and-or damaging the main cellular components: lipids, carbohydrates, nucleic acids and proteins. The latter have amino acids in their sequence that are susceptible to post-translational modifications, both reversible and irreversible, through the different reactive species generated by abiotic stresses (redox-based PTMs). Some research suggests that this process does not occur randomly, but that the modification of critical residues in enzymes modulates their biological activity, being able to enhance or inhibit complete metabolic pathways in the process of acclimatization and tolerance to the exposure to the different abiotic stresses. Given the importance of these PTMs-based regulation mechanisms in the acclimatization processes of plants, the present review gathers the knowledge generated in recent years on this subject, delving into the PTMs of the redox-regulated enzymes of plant metabolism, and those that participate in the main stress-related pathways,

such as oxidative metabolism, primary metabolism, cell signaling events, and photosynthetic metabolism. The aim is to unify the existing information thus far obtained to shed light on possible fields of future research in the search for the resilience of plants to climate change.

KEYWORDS

climate change, abiotic stress, plant tolerance, ROS, RNS, RSS, post-translational modifications, redox regulation

1 Introduction

Climate change is a global and current phenomenon that is changing the Earth's climate. The main impact of this phenomenon is the increase in the planet global temperature and the modification of rainfall patterns, among other negative effects. The main consequences are manifested in agricultural production, where annual, millionaire economic losses are estimated to progressively increase (Ali et al., 2017; Martinez et al., 2018).

Plants are exposed to abiotic stresses throughout their life cycle, such as salinity, drought, extreme temperatures and heavy metal toxicity, and biotic stresses, induced by organisms such as yeasts, fungi or viruses. We must also add that the different stresses act in nature in a combined way, giving rise to even greater damage. As plants are sessile organisms, their acclimatization and consequent tolerance to simple or combined stress exposure imply physiological, metabolic and molecular restructurings that allow their survival in this type of environment (Ahuja et al., 2010; Rivero et al., 2014; Ahanger et al., 2017; Ma et al., 2020).

These types of modifications allow plants to adapt to the unfavorable environments where they grow, and increase their survival rate. One of the first and fastest plants responses to harsh environments involves an overproduction of reactive chemical species, such as reactive oxygen (ROS), nitrogen (RNS) and sulfur (RSS) species. These molecules have a dual activity; under normal physiological conditions, their production is linked to cell signaling processes, however, under stress conditions, these are massively produced and accumulated (Zhou et al., 2022). The increase in the amounts of these molecules disturbs redox homeostasis, inducing damage to biomolecules and cellular components, such as membranous structures, proteins, nucleic acids, photosynthetic pigments, carbohydrates, hormones, and may even lead to cell destruction due to the oxidative, nitrosative or nitroxidative stress generated, which may trigger cellular apoptosis (Mittler, 2002; Møller et al., 2007; Bose et al., 2014; Martinez et al., 2018; Zhou et al., 2022). In its attempt to survive, the cell tries to buffer this oxidative stress by synthesizing and activating antioxidant enzymes, such as superoxide dismutases, ascorbate peroxidases, catalases, glutathione peroxidases and peroxyredoxins, and antioxidant molecules such as ascorbic acid, glutathione (GSH), melatonin, phenolic compounds, flavonoids, alkaloids and non-protein amino acids. RNS can be detoxified by enzymes such as phytoglobins, peroxyredoxins, tocopherols, flavonoids, ascorbic acid, molecular oxygen, and GSH. In contrast, RSS has a dual behavior with respect to ROS and RNS. These species are overproduced under stress conditions and, although they can modify biomolecules such as protein residues, they actively participate in the detoxification of ROS and RNS, acting as an extra molecular antioxidant system, decreasing the amounts of these two types of reactive species (Wilson et al., 2008; Suzuki et al., 2011; Vaahtera et al., 2014; Gupta and Igamberdiev, 2016; Arnao and Hernández-Ruiz, 2019; Hasanuzzaman et al., 2020; Pardo-Hernández et al., 2020; Paul and Roychoudhury, 2020; Pardo-Hernández et al., 2021; Matamoros and Becana, 2021; Martínez-Lorente et al., 2022).

The balance between the increase in amount reactive species and their detoxification is vital for plant survival. However, cell signaling events are complemented by other types of plant molecular responses. In the process of acclimatization and tolerance to stress conditions, an overproduction of reactive species modulates the expression of stress responses-related genes, and can also lead to the modification of key protein residues to restructure cellular metabolism (Martinez et al., 2018; Nadarajah, 2020; Matamoros and Becana, 2021). ROS, RNS and RSS have the capacity to generate post-translational modifications (PTMs) in the target proteins, some of which are reversible, while others are irreversible. These redox-based PTMs alter the physiological properties of the affected proteins, modifying their structure, function, stability and affinity with other related proteins, biomolecules or metabolites. The vast majority of PMTs are highly regulated and specific to each protein, and are able to enhance its activity, inhibit its function, protect critical residues against catalytic activity or promote its degradation by proteolytic mechanisms (Waszczak et al., 2015; Matamoros and Becana, 2021; Zhou et al., 2022).

Due to the importance of the different ROS, RNS and RSS on cellular metabolism and the functions they play in the acquisition of plant stress tolerance, this review aims to collect the abundant but very dispersed knowledge generated in this

scientific field in the last decades, to try to tackle what is currently known, starting from its biogenesis in plant cells, to its main functions and consequences, with special emphasis on the interplay between ROS, RNS, RSS, modification of main cellular components, redox-based PTMs of proteins, and their relationship with the induction of the plants' tolerance mechanisms to abiotic stress.

2 Reactive species: Biogenesis, interplay and antioxidant defense

2.1 Biogenesis

Reactive species of a chemical element are molecules that, as a result of their redox state, have a high capacity to react with cellular biomolecules. The most studied types are reactive oxygen (ROS), nitrogen (RNS) and sulfur (RSS) species (Gruhlke and Slusarenko, 2012; Del Río, 2015; Choudhury et al., 2017). Their biosynthesis takes place under any physiological condition (with or without stress), although under stress conditions, their production increases, and therefore their ability to initiate different cell signaling events and redox reactions with cellular components also increases (Brannan, 2010).

ROS are intermediates originating from atmospheric oxygen (O_2) with a different redox state. There are several types, with different reactivity and oxidizing capacities, among which we find hydrogen peroxide (H_2O_2), superoxide anion ($O_2^{\cdot-}$), singlet oxygen ($^1O_2$), and hydroxyl radical (·OH) (Mittler et al., 2011; Choudhury et al., 2017; Huang et al., 2019a). In plants, they are produced in varying proportions depending on the plant tissue and stage of development, in cellular organelles such as chloroplasts, mitochondria and peroxisomes (Figure 1), as well as cellular spaces such as the apoplast, through metabolic pathways where oxidase and peroxidase enzymes participate (Suzuki et al., 2011; Vaahtera et al., 2014; Janků et al., 2019). $^1O_2$ is produced in photosynthetic metabolism, as a result of the different excitation states of chlorophylls and the activity of reaction centers of photosystem II (Triantaphylidès and Havaux, 2009; Roach and Krieger-Liszkay, 2014; Foyer, 2018; Janků et al., 2019). $O_2^{\cdot-}$ is generated as a result of electronic transport in mitochondrial and photosynthetic chains, as well as by NADPH membrane oxidases (RBOHs) (Choudhury et al., 2017; Huang et al., 2019a; Matamoros and Becana, 2021). H_2O_2 is the most stable ROS, and has an intracellular diffusion capacity (Kim et al., 2018; Arnao and Hernández-Ruiz, 2019). It is generated by the activity of superoxide dismutase (SOD) as a consequence of the extinction of $O_2^{\cdot-}$ (Foyer, 2018; Janků et al., 2019).OH is the most reactive and unstable ROS, produced as a result of the cleavage of the double bond of H_2O_2 by means of the Fenton reaction (Arnao and Hernández-Ruiz, 2019; Huang et al., 2019a). It has the ability to react with many types of biomolecules that are very close to the microenvironment where it is generated (Hiramoto et al., 1996; Kärkönen and Kuchitsu, 2015; Huang et al., 2019a).

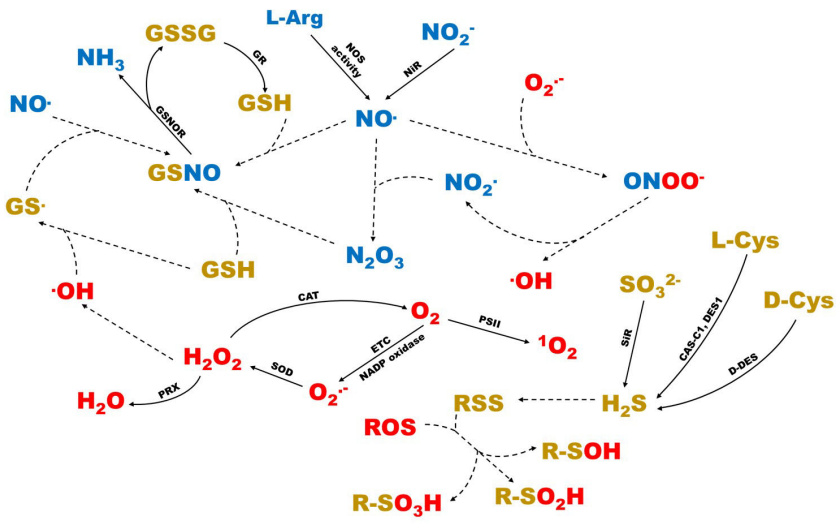

FIGURE 1
Schematic representation of the interactions between the different ROS, RNS and RSS in the plant cell. In red, the different types of ROS are shown. In blue, the different types of RNS are shown. In gold color, the different types of RSS are shown. Dashed arrows represent reactions that take place non-enzymatically. CAS-C1, cyanoalanine synthase c1; CAT, catalase; D-DES, D-cysteine desulfhydrase; DES1, L-cysteine desulfhydrase 1; ETC, electronic transport chains; GR, glutathione reductase; GSNOR, S-nitrosoglutathione reductase; NiR, nitrite reductase; PRX, peroxidase; PSII, photosystem II; SiR, sulfite reductase; SOD, superoxide dismutase.

RNS are highly reactive nitrogenous derivatives originating from nitric oxide (NO·), as a consequence of oxidative metabolism. The most common and studied species are NO·, nitrogen dioxide (NO_2.) and nitrogen oxide (III) (N_2O_3) (Vandelle and Delledonne, 2011; Arnao and Hernández-Ruiz, 2019). They can generate in the cytosol, as well as in organelles such as mitochondria, chloroplasts and peroxisomes (Figure 1), or through enzymatic and non-enzymatic mechanisms (Zhao, 2007; Gupta and Igamberdiev, 2016; Astier et al., 2018; Pardo-Hernández et al., 2020; Matamoros and Becana, 2021). NO·OH can be created from NO_2^- by nitrite reductase (NiR) enzyme, in the apoplast, chloroplasts, mitochondria, and cytoplasm, as well as from L-arginine, by L-arginine-dependent NO synthase (NOS) activity, in mitochondria, peroxisomes, chloroplasts, and cytoplasm (Wilson et al., 2008).

RSS are H_2S-derived molecules, among which we find the bisulfide anion (HS^-), radical thiyl (HS.), persulfides (RSSH) and polysulfides ($RS(S)_nH$), among others (Gruhlke and Slusarenko, 2012; Corpas et al., 2020; Fukudome et al., 2020). The biosynthesis of H_2S takes place in all cell organelles and the cytosol, by means of enzymes such as sulfite reductase (SiR), cyanoalanine synthase c1 (CAS-C1), L-cysteine desulfhydrase 1 (DES1), D-cysteine desulfhydrase and Nifs-like proteins (ABA3) (Aroca et al., 2018). Its oxidation results in the formation of thiyl radicals, which are able to establish disulfide bridges with other sulfur atoms, with the consequent formation of the different RSS (Corpas and Barroso, 2015).

2.2 Redox-based modifications of main cellular components

2.2.1 Lipids

Lipids, and especially polyunsaturated fatty acids (PUFAs), are susceptible to ROS-mediated oxidative modifications and RNS-mediated nitrosative modifications. ROS-induced modifications, such as ·OH and $^1O_2$, are generated mainly in galactolipids and phospholipids, resulting in the formation of lipid hydroperoxides that disturb the fluidity of membranes, increasing their permeability and damaging the proteins present within them (Mueller, 2004; Møller et al., 2007). RNS-induced modifications, such as NO· and $ONOO^-$, generate nitro-fatty acids, molecules that have been recently described as a result of the interaction between PUFA and RNS. In plants, nitro-oleic acid and nitro-linolenic acid have been mainly characterized, with the latter having the ability to modulate the expression of salinity abiotic stress-related, Cd^{2+} toxicity and wounding genes in *Arabidopsis*. In addition, other properties described for these nitro-fatty acids include their role as NO· donors, with the possibility of inducing RNS-based PTMs on specific proteins (Begara-Morales et al., 2019; Mata-Pérez et al., 2020; Begara-Morales et al., 2021), which will be described in more detail later.

2.2.2 DNA and RNA

ROS and RNS have the ability to modify nucleic acids by attacking the nitrogenous bases that compose them, especially guanine (G) (Møller et al., 2007; Chmielowska-Bąk et al., 2019). ROS, specifically.OH and $^1O_2$, modify the G bases to 8-hydroxydeoguanosine (8-OH-dG) in DNA and 8-hydroxyguanosine (8-OH-G) in RNA. The presence of these modifications in DNA induces mutations by base pairing error, as well as erroneous copies during the replication process (Møller et al., 2007; Poetsch, 2020; Huang et al., 2021). In addition, the presence of these oxidations can affect the methylation pattern of cytosines, involved in the regulation of gene expression (Halliwell, 2006). In RNA and mRNA, the appearance of oxidized nitrogenous bases is linked to their instability and premature degradation, as well as ribosomal blocking of translation (Simms et al., 2014; Chmielowska-Bąk et al., 2019; Katsuya-Gaviria et al., 2020; Sano et al., 2020). RNS, especially $ONOO^-$, modify G bases in DNA and RNA to 8-nitrodeoguanosine (8-NO_2-dG) and 8-nitroguanosine (8-NO_2-G), respectively, and GTP nucleotides to 8-NO_2-GTP molecules (Liu et al., 2012a; Chmielowska-Bąk et al., 2019; Petřivalský and Luhová, 2020). These modifications, specifically in the coding mRNAs, obstruct the correct reading by the ribosome, generating incomplete translations and truncated proteins, with the consequent lack of function, as is the case with oxidation by ROS (Chmielowska-Bąk et al., 2019).

2.2.3 Carbohydrates

It is known that some ROS, especially.OH, have the ability to react with free carbohydrates, such as sugars and polyols, and with structural cell wall polysaccharides. Studies suggest that its reaction with free sugars, such as mannitol, results in an antioxidant protection mechanism, preventing the ·OH reaction with more important cellular biomolecules, thus avoiding superior oxidative damage (Shen et al., 1997; Fry, 1998; Møller et al., 2007). However, indirectly, high oxidative stress conditions induce autoxidation of monosaccharides, with the consequent formation of dicarbonyls, especially glyoxal, methylglyoxal, and 3-deoxyglucosone. These reactive molecules can modify protein residues of Arg and Lys, generating glycation, a PTM linked to enzymatic inactivation (Chaplin et al., 2019; Rabbani et al., 2020; Matamoros and Becana, 2021).

2.2.4 Proteins

The 20 proteinogenic amino acids differ in their chemical reactivity and susceptibility to modifications and hosting any type of PTM. However, most are susceptible to modifications, either spontaneous or enzymatic (Friso and van Wijk, 2015). Redox-based PTMs occur spontaneously, depending on the chemical reactivity of the amino acids susceptible to this type of modification, as well as the concentration of ROS, RNS and

RSS, cellular antioxidant capacity, among other factors (Ryšlavá et al., 2013; Friso and van Wijk, 2015). Among these amino acids, those that contain sulfur stand out, especially those with reactive thiol groups: cysteine and methionine. Sulfur presents a wide range of oxidation states that allows different PTMs on the residues that contain it (Rinalducci et al., 2008; Akter et al., 2015; Waszczak et al., 2015). However, not all residues are equally susceptible to modification. This will depend on their dissociation constant (pKa), which in turn will be determined by the microenvironment of the residues: exposure and accessibility, amino acid sequence that flanks them, and local pH, among others (Go et al., 2015; Paul and Roychoudhury, 2020; Matamoros and Becana, 2021). Along with cysteine and methionine, other amino acids are susceptible to modification, such as tyrosine, tryptophan, threonine, lysine, arginine, and proline. However, the susceptibility of these with respect to sulfur-containing amino acids is much lower, so their modification will depend on their interaction with more unstable and aggressive reactive species (Rinalducci et al., 2008; Bizzozero, 2009; Ehrenshaft et al., 2015; Matamoros and Becana, 2021).

2.3 Interplay between the different reactive species

In addition to the independent cellular functions described above for ROS, RNS and RSS have the ability to react with each other, generating mixed reactive species. From the interaction between ROS and RNS, reactive species such as peroxynitrite ($ONOO^-$) arise, originated by the reaction between NO· and $O_2^{\cdot-}$, in any cellular space where the generation and coexistence of $O_2^{\cdot-}$ and NO· occurs, respectively. It is a highly oxidizing molecule, whose decomposition generates NO_2. as a product (Vandelle and Delledonne, 2011). The interaction between RNS and RSS can produce reactive species such as S-nitrosoglutathione (GSNO), which originates from the reaction between NO· and GSH. It is a mixed reactive species, considered a cellular reservoir of NO·, which is broken down by the NADH-dependent activity of the GSNO reductase (GSNOR) enzyme, into GSSG and NH_3 (Airaki et al., 2011; Zechmann, 2020). Lastly, the interaction between ROS and RSS can lead to the creation of reactive species such as sulfenic acids (R-SOH), from the reaction between the thiol groups and H_2O_2. These molecules are able to react with RSS, generating disulfide bridges, or react with ROS to generate sulfinic acids ($R\text{-}SO_2H$) and sulfonic acids ($R\text{-}SO_3H$) (Hasanuzzaman et al., 2020; Matamoros and Becana, 2021). Similarly, some ROS, such as the ·OH radical, can react with GSH, with the consequent formation of the radical thyil, which can react again with NO· for GSNO training (Begara-Morales et al., 2019). All these interactions and the consequent signaling processes take place in the different cellular organelles, with the cytosol being the cellular space where all the signaling triggered by reactive species is integrated (Noctor and Foyer, 2016). These interactions are shown, schematically, in Figure 1, which includes all the knowledge available on reactive species.

3 ROS, RNS and RSS dependent PTMs

3.1 PTMs induced by ROS

3.1.1 Cysteine oxidation

The oxidation of cysteine residues (Cys) is mediated by H_2O_2, and is linked to the protein structure folding stabilization and its catalytic activity modification (Bigelow and Squier, 2011). H_2O_2 reacts with the amino acid thiol group to generate sulfenic acid, in a sulfenylation process (Figure 2). Sulfenic acid can react, again, with H_2O_2 or with other thiols. The reaction of sulfenic acid with H_2O_2 leads to the formation of sulphinic acid, which can, in turn, react again with H_2O_2, with the consequent formation of sulfonic acid, in sulfinylation and sulfonylation processes, respectively (Matamoros and Becana, 2021). In contrast, the reaction between sulfenic acid and other thiols can generate intramolecular disulfide bridges and intermolecular disulfide bridges, and the latter may occur with different proteins or with the GSH reactive thiol (S-glutathionylation) (Friso and van Wijk, 2015; Matamoros and Becana, 2021). This type of oxidation and its different modifications affect the functionality of the enzyme that has them, especially if the Cys residues participate in structural stability by means of intramolecular disulfide bridges, or in the enzyme catalytic center (Huang et al., 2019b). The reactions described are schematically depicted in Figure 2. All of these PTMs are reversible by enzymes such as glutaredoxins, sulfiredoxins and thioredoxins, except for sulfonic acid formation, which is classified as irreversible and which entails the loss of function of the protein that has it and its consequent degradation (Rey et al., 2007; Meyer et al., 2009; Sevilla et al., 2015; Zhou et al., 2020; Matamoros and Becana, 2021).

3.1.2 Methionine oxidation

Similar to Cys, methionine (Met) residues are susceptible to oxidation especially by H_2O_2 (Vogt, 1995). This modification generates Met sulfoxides, resulting in the generation of sulfones if exposure to ROS is relatively high and prolonged (Figure 2) (Rinalducci et al., 2008). Met sulfoxides production is a type of PTM that is reversible by a family of Met sulfoxide reductases-mediated mechanisms. However, sulfones are listed as an apparently irreversible PTM (Rouhier et al., 2006; Tarrago et al., 2009; Friso and van Wijk, 2015), although more research is needed on this subject.

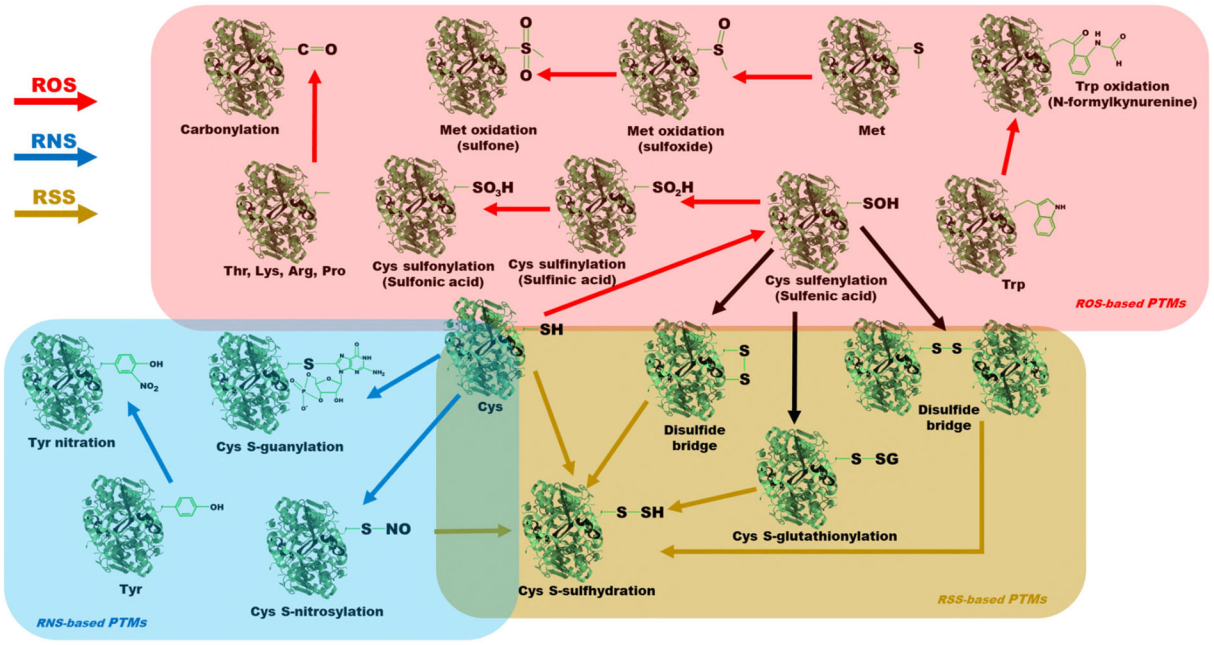

FIGURE 2
Schematic representation of the different redox-based PTMs of the different protein residues. In red, we find the different ROS-based PTMs: cysteine oxidation, methionine oxidation, tryptophan oxidation and carbonylation. In blue, the different RNS-based PTMs are shown: cysteine S-nitrosylation, cysteine S-guanylation and tyrosine nitration. In gold, the different RSS-based PTMs are indicated: cysteine S-sulfhydration.

The oxidation of Met, which is exposed on three sides in the outer part of the protein and therefore more susceptible to oxidative attack, has a mild effect on the proteins' structure and function in which it is produced. In fact, some studies suggest that these oxidized residues act as an antioxidant defense mechanism against ROS, protecting catalytic centers and structural domains whose alteration could affect protein function (Levine et al., 1996; Rinalducci et al., 2008). However, a protein with a high percentage of its Met residues oxidized can have its hydrophobicity modified, making it polar and hydrophilic, with its function irreversibly compromised (Rinalducci et al., 2008; Hardin et al., 2009).

3.1.3 Tryptophan oxidation

Tryptophan residues (Trp) are susceptible to ROS modification, especially by ·OH and $^1O_2$ (Rinalducci et al., 2008; Ehrenshaft et al., 2015). The oxidative attack breaks the ring of its chemical structure and generates N-formylkynurenine, a PTM classified as irreversible, which leads to the proteolysis of the enzyme that presents it (Shacter, 2000; Møller and Kristensen, 2006; Rinalducci et al., 2008). As with Met residues, some research suggests that exposure of Trp residues on the protein surface and its consequent oxidation could act as an antioxidant pathway for the protection of other critical residues needed for the proper functioning of the protein (Levine et al., 1996; Rinalducci et al., 2008).

3.1.4 Carbonylation

Carbonylation is a PTM generated by the reaction between ·OH and certain protein amino acids, such as threonine, lysine, arginine, or proline (Figure 2) (Møller et al., 2011; Friso and van Wijk, 2015). It is classified as an irreversible PTM that causes the loss of function of the protein in which it is found (Nyström, 2005; Lounifi et al., 2013). The fate of these proteins is generally degradation by cellular proteolytic complexes (Polge et al., 2009). However, it has recently been described that an excess of carbonylation can generate cytotoxic protein aggregates that, in animals, are linked to aging and some important diseases (Nyström, 2005; Bizzozero, 2009). In plants, carbonylation occurs in response to abiotic stress in proteins found in multiple cellular compartments, including mitochondria, chloroplasts and cytosol, as well as in different metabolic pathways, especially in photosynthetic metabolism and its complementary pathways (Calvin-Benson cycle and photorespiration), whose carbonylated enzymes are inactivated (Tanou et al., 2009; Mano et al., 2014; Smakowska et al., 2014; Friso and van Wijk, 2015; Matamoros and Becana, 2021). Examples of this type of modification are detailed in later sections.

3.2 PTMs induced by RNS

3.2.1 Cysteine S-nitrosylation

In the literature, it is common to find the terms "nitrosation" or "nitrosylation" described as a chemical or biochemical

reactions involving NO· and, occasionally, both terms are used to describe the same reaction with no distinction between "nitrosation"and/or "nitrosylation". To this respect, Heinrich et al. (2013) published an excellent review distinguishing between both terms. In this sense, Heinrich et al. (2013) described "nitrosation" as a reaction between a nucleophilic group and an electrophilic nitrosonium ion (NO^+) whereas "nitrosylation" is described as the direct addition of NO· to a molecule, which, in biological systems, usually refers to the different cellular macromolecules (Heinrich et al., 2013). In this review, the term "nitrosylation", as proposed by Heinrich et al. (2013), will be used to describe the processes by which the different protein residues undergo the addition of a NO· group to their structures.

S-nitrosylation is a PTM consisting of the covalent bonding of NO· groups with the reactive thiol groups in Cys residues (Figure 2), with the consequent formation of S-nitrosothiols (Puyaubert et al., 2014; Feng et al., 2019). The formation of this PTM is directly mediated by NO·, or by donors of NO· groups, such as GSNO and $ONOO^-$, and is catalogued as a reversible PTM through thioredoxins or GSH, in a process known as denitrosylation (Wang et al., 2006; Benhar et al., 2009; Zaffagnini et al., 2013; Feng et al., 2019). This PTM affects protein function, being able to enhance or inhibit its activity, depending on the protein and the residue modified (Feng et al., 2019). Due to its reversibility and its potential to modulate enzymatic activity, this type of PTM has garnered a lot of attention in various studies related to possible mechanisms of plant stress tolerance, so it will be discussed in detail later.

3.2.2 Cysteine S-guanylation

8-NO_2-GTP, an RNS generated by the reaction between ONOO- and GTP, can undergo a cycling process and become 8-NO_2-cGMP, which reacts with Cys residues, generating an irreversible PTM called S-guanylation (Figure 2) (Sawa et al., 2013; Petřivalský and Luhová, 2020). Under abiotic stress conditions due to excess light, it has been described in *Arabidopsis* that 8-NO_2-cGMP can react with Cys residues, as well as with H_2S and persulfides, in a global process involving stomatal closure, and thus, this PTM has been related with a putative plant acclimation response (Friso and van Wijk, 2015; Petřivalský and Luhová, 2020).

3.2.3 Tyrosine nitration

Tyrosine residues (Tyr) are susceptible to covalent modification by RNS in the aromatic ring of their chemical structure. This PTM consists of the addition of a NO_2. group from the reaction between $ONOO^-$ or NO_2. and the Tyr amino acid, with the consequent formation of 3-nitrotyrosine (Figure 2) (Rinalducci et al., 2008; Matamoros and Becana, 2021). This PTM is generally linked to a loss of function of the affected protein and its consequent degradation by proteolytic complexes. 3-nitrotyrosine residues increase the hydrophobicity of the protein that contains them and cause steric impediments that can affect the phosphorylation pattern of the residue, modifying the corresponding transduction pathways (Matamoros and Becana, 2021). The formation of this derivative is classified as irreversible, although it has been reported the existence of some mechanisms drived by denitrase activity that, exceptionally, could reverse it, both in animals and plants (Corpas et al., 2008; Kolbert et al., 2017).

3.3 PTMs induced by RSS

3.3.1 Cysteine S-sulfhydration

The reactive thiol groups of Cys residues can be modified to a persulfide group by the nucleophilic attack of HS^- (Figure 2), in a process called S-sulfhydration or persulfidation (Aroca et al., 2015; Aroca et al., 2017). In addition, as indicated above, thiol groups susceptible to this modification may previously be in different oxidation states, including sulfenic acids, disulfide bridges and Cys S-glutathionylated or S-nitrosylated residues (Filipovic and Jovanovic, 2017; Zhou et al., 2020; Matamoros and Becana, 2021). It is a reversible PTM by means of thioredoxins, which act by increasing or decreasing the catalytic activity of the enzyme that has it, although, characteristically, it can also act as a protection against irreversible oxidation states that lead to the loss of function of the protein or its destruction, such as the formation of sulfonic acids (Filipovic et al., 2018). This PTM, in turn, induces structural and functional modifications of proteins, as well as changes in their subcellular location, which may be important for signaling and acclimatization processes to stress (Mustafa et al., 2009; Paul and Snyder, 2012; Aroca et al., 2017).

4 Redox-based PTMs of oxidative metabolism-related proteins

The increase in intracellular reactive species as a result of stress exposure induces an increase in their antioxidant enzymes, in order to avoid irreversible damage to cellular components that compromise plant vitality. These enzymes, in addition, are subject to strict redox regulations, carried out by different PTMs in the residues of their structure, with some presenting multiple residues with redox-based PTMs, even multiple PTMs in the same residue, with similar or completely different functionalities.

In *Arabidopsis*, it has been described that the Cys32 residue of the ascorbate peroxidase (APX) enzyme can host two types of redox-based PTMs, S-nitrosylation and S-sulfhydration. Both PTMs increase the enzyme catalytic activity to detoxify H_2O_2, affording the plant a greater tolerance to ROS-induced oxidative stress (Aroca et al., 2015; Yang et al., 2015).

In pea, it has been characterized that its homologous enzyme houses several types of redox-based PTMs in its amino acid sequence, with different consequences on its catalytic activity. The Cys32 residue, included in the APX binding site, can be S-nitrosylated, with the consequent increase in the scavenger catalytic activity of H_2O_2. On the other hand, the Tyr235 residue, included in the pocket that encloses the heme group, can be irreversibly nitrated by $ONOO^-$, with the consequent enzymatic inactivation (Begara-Morales et al., 2014).

In addition, in *Arabidopsis*, the dehydroascorbate reductase 2 (DHAR2) enzyme can undergo two PTMs on its Cys20: Cys oxidation and Cys S-glutathionylation. H_2O_2 can cause an overoxidation of this Cys towards sulfenic and sulfonic acids, with the consequent decrease in enzyme activity. However, Cys20 may be S-glutathionylated, a mechanism by which covalent GSH binding protects the residue from irreversible overoxidation, suggesting a crucial role of Cys20 in the DHAR2 catalytic activity (Waszczak et al., 2014).

In pea, the monodehydro-ascorbate reductase (MDHAR) enzyme can be nitrated by $ONOO^-$ in its Tyr345 residue, three-dimensionally close to the His313 residue, included in the NADP binding site. This Tyr345 nitration is associated with a decrease in the enzyme catalytic activity (Begara-Morales et al., 2015; Kolbert et al., 2017).

In the *Antiaris toxicaria* tree, the ascorbate-glutathione relatedenzymes, involved in H_2O_2 detoxification, are also subject to redox regulation. These enzymes, such asAPX, MDHAR, DHAR and GR, undergo a carbonylation reaction with their consequent inactivation when the cellular H_2O_2 concentrations are high, as occurs under desiccation conditions (Bai et al., 2011). However, when plants were treated with NO·, these enzymes undergo S-nitrosylation with the concomitant increase in their catalytic activity. Therefore, both mechanisms can be described as antagonistics by which the cellular balance between H_2O_2 and NO· will control the activation/deactivaton of these enzymes (Bai et al., 2011).

In *Arabidopsis*, the GSNO reductase (GSNOR) enzyme, involved in thermotolerance, redox homeostasis, and NO· metabolism, can be S-nitrosylated in three different Cys residues preserved in plants: Cys10, Cys271 and Cys370. This redox-based PTM reduces the enzyme catalytic activity, with Cys370 being the preferred residue for S-nitrosylation (Guerra et al., 2016). S-nitrosylation has also been described in cucumber´s GSNOR with similar consequences (Niu et al., 2019).

The catalase (CAT) enzyme is subject to redox regulation by means of a multitude of different PTMs, even in different types of plant species. In both pea and *Arabidopsis*, Cys S-nitrosylation decreases the enzyme's catalytic activity, with this enzyme also inactivated by Cys S-sulfhydration in the latter plant (Ortega-Galisteo et al., 2012; Corpas et al., 2019; Palma et al., 2020). This PTM has also been described for the sweet pepper´s CAT, which is also susceptible to Tyr nitration, with the consequent decrease in its catalytic activity (Chaki et al., 2015; Corpas et al., 2019).

In contrast to other plant species, in tobacco, it has been shown that their exposure to NO· donors reduced the catalytic activity of APX and CAT enzymes Clark et al. (2000) suggested that this could be due to the formation of an iron-nitrosyl intermediate between NO· and the iron atom of the haem prosthetic group of these enzymes, compromising H_2O_2 scavenging (Clark et al., 2000).

Among these enzymes, those that use GSH as a substrate are also subject to redox regulation. In *Arabidopsis*, two glutathione-S-transferase enzymes, GSTF9 and GSTT23, are regulated by Met oxidation, with Met35 and Met47, respectively, being the residues where these PTMs have been described, in both cases reducing their catalytic activity (Jacques et al., 2015). In cucumber, it has been described that glutathione reductase (GR) may decrease its activity as a result of Cys S-nitrosylation (Niu et al., 2019).

Superoxide dismutase family (SODs) enzymes are also susceptible to this type of redox regulations. The *Arabidopsis* mitochondrial Mn-SOD (MSD1) enzyme can be nitrated in its Tyr63 residue, located near the active center of the enzyme, which may impede the accessibility of the substrate and, as a consequence, decrease its activity (Holzmeister et al., 2015; Kolbert et al., 2017). Similarly, the Mn-SOD (MSD2) enzyme from *Arabidopsis* can be nitrated in its Tyr68 residue, with similar consequences (Chen et al., 2022).

Yun et al. (2011) described in Arabodopsis a mechanism by which S-nitrosylation at its Cys890 abolished its capacity for ROS synthesis and, therefore, the initiation of the cell death process, governed by ROS, was compromised. This Cys890 and its S-nitrosylation was found to be conserved in the NADPH oxidase RBOHD human and fly homologous enzymes, suggesting that this process could be conserved for the regulation of the cell death (Yun et al., 2011). On the other hand, Romero-Puertas et al. (2007) described that the PrxII E enzyme had peroxynitrite reductase activity, which it was inhibited, along with its peroxidase activity, by NO·-mediated S-nitrosylation of its Cys121. The consequences of this S-nitrosylation were the increase in the cellular concentration of $ONOO^-$ with the concomitant increase in proteins that suffered nitration in their Tyr residues, suggesting a signaling mechanism mediated by $ONOO^-$ (Romero-Puertas et al., 2007).

In summary, the regulation of metabolism by means of a redox-based PTM can enhance the catalytic activity of an enzyme or decrease it. In turn, it is common to find specific enzymes that contain a multitude of residues susceptible to different redox regulations, as is the case of GSNOR, CAT or APX. This last enzyme, in addition, has a critical residue for its catalytic activity, Cys32, characterized in several plant species, which can present different types of redox-based PTMs, and which have been cataloged as having a special importance in the induction of tolerance to environmental stresses.

The information described on oxidative metabolism-related proteins is shown in Table 1.

TABLE 1 PTMs and their effect on the different oxidative metabolism-related proteins subjected to redox regulation.

Plant	Protein (Uniprot accession number)	PTM	Effect	Reference
Arabidopsis	**APX** (Q05431)	Cys-32 S-sulfhydration	Increased activity	(Aroca et al., 2015)
	APX (Q05431)	Cys-32 S-nitrosylation	Increased activity	(Yang et al., 2015)
Pea	**APX** (P48534)	Tyr-235 nitration	Decreased activity	(Begara-Morales et al., 2014)
	APX (P48534)	Cys-32 S-nitrosylation	Increased activity	(Begara-Morales et al., 2014)
Antiaris	**APX** (-)	Cys-S-nitrosylation	Increased activity	(Bai et al., 2011)
	APX (-)	Carbonylation	Decreased activity/Inactivation	(Bai et al., 2011)
Tobacco	**APX** (Q42941)	Cys-S-nitrosylation	Decreased activity/Inactivation	(Clark et al., 2000)
Arabidopsis	**DHAR2** (Q9FRL8)	Cys-20 oxidation	Decreased activity	(Waszczak et al., 2014)
	DHAR2 (Q9FRL8)	Cys-20 S-glutathionylation	Cys overoxidation protection	(Waszczak et al., 2014)
Antiaris	**DHAR** (-)	Cys-S-nitrosylation	Increased activity	(Bai et al., 2011)
	DHAR (-)	Carbonylation	Decreased activity/Inactivation	(Bai et al., 2011)
Pea	**MDHAR** (Q40977)	Tyr-345 nitration	Decreased activity	(Begara-Morales et al., 2015; Kolbert et al., 2017)
Antiaris	**MDHAR** (-)	Cys-S-nitrosylation	Increased activity	(Bai et al., 2011)
	MDHAR (-)	Carbonylation	Decreased activity/Inactivation	(Bai et al., 2011)
Arabidopsis	**GSNOR** (Q96533)	Cys-10, Cys-271, Cys-370 S-nitrosylation	Decreased activity	(Guerra et al., 2016)
Cucumber	**GSNOR** (A0A0A0KBZ1)	Cys-S-nitrosylation	Decreased activity	(Niu et al., 2019)
Pea	**CAT** (P25890)	Cys-S-nitrosylation	Decreased activity	(Ortega-Galisteo et al., 2012)
Arabidopsis	**CAT** (Q96528/P25819/Q42547)	Cys-S-sulfhydration	Inactivation	(Corpas et al., 2019)
	CAT (Q96528/P25819/Q42547)	Cys-S-nitrosylation	Decreased activity	(Palma et al., 2020)
Sweet pepper	**CAT** (Q9M5L6)	Cys-S-sulfhydration	Inactivation	(Corpas et al., 2019)
	CAT (Q9M5L6)	Tyr-nitration	Decreased activity	(Chaki et al., 2015)
Tobacco	**CAT** (P49319)	Cys-S-nitrosylation	Decreased activity/Inactivation	(Clark et al., 2000)
Arabidopsis	**GSTF9** (O80852)	Met-35 oxidation	Decreased activity	(Jacques et al., 2015)
Arabidopsis	**GSTT23** (Q9M9F1)	Met-47 oxidation	Decreased activity	(Jacques et al., 2015)
Antiaris	**GR** (-)	Cys-S-nitrosylation	Increased activity	(Bai et al., 2011)
	GR (-)	Carbonylation	Decreased activity/Inactivation	(Bai et al., 2011)
Cucumber	**GR** (A0A0A0K8Q7)	Cys-S-nitrosylation	Decreased activity	(Niu et al., 2019)
Arabidopsis	**MSD1** (O81235)	Tyr-63 nitration	Decreased activity	(Holzmeister et al., 2015)
Arabidopsis	**MSD2** (Q9LYK8)	Tyr-68 nitration	Inactivation	(Chen et al., 2022)
Arabidopsis	**RBOHD** (Q9FIJ0)	Cys-890 S-nitrosylation	Abolishes ROS production	(Yun et al., 2011)
Arabidopsis	**PrxII E** (Q949U7)	Cys-121 S-nitrosylation	Decreased peroxidase and peroxynitrite reductase activities	(Romero-Puertas et al., 2007)

5 Redox-based PTMs on primary metabolism-related proteins

Primary metabolism plant enzymes, including energy production and amino acid biosynthetic pathways, have also been described as subject to redox regulation.

In *Arabidopsis*, the nitrate reductase (NR) enzyme, involved in nitrate (NO_3^-) assimilation, has Met538 a residue, included in a phosphorylation motif, whose Ser534 is subject to phosphorylation/dephosphorylation events. H_2O_2-induced oxidation generates Met sulfoxide, a PTM that prevents the Ser538 residue from being phosphorylated (Hardin et al., 2009; Matamoros and Becana, 2021). The cellular persistence of NR depends on the phosphorylation state of Ser534 which, if phosphorylated, generates a canonical motif of a 14-3-3-binding site, allowing the binding of 14-3-3 proteins and their consequent degradation (MacKintosh and Meek, 2001). The binding of 14-3-3 proteins induces a conformational change in NR that prevents electron transfer from the enzyme's heme group to the molybdenum cofactor (Lambeck et al., 2012). Directed mutagenesis studies of the rice NR enzyme demonstrated how the absence of phosphorylation in the motif increased NO_3^- assimilation efficiencies (Han et al., 2022). This evidence suggests that ensuring the change of NO_3^- to NH_4^+ is necessary under stress conditions. However, it does not seem that the generation of NH_4^+ is diverted towards

the production of amino acids such as glutamine, since it has been observed that the glutamine synthetase (GS) enzyme of *Medicago* is inhibited by Tyr nitration in its Tyr167 residue, just as the homologous GS from *Arabidopsis* decreases its catalytic activity by Cys S-sulfhydration (Melo et al., 2011; Aroca et al., 2015). This persistence in NH_4^+ production could be necessary for the biosynthesis of other nitrogenous compounds, such as polyamines, molecules that have been described as participating in the processes of plant abiotic stress tolerance (Pathak et al., 2014; Chen et al., 2019; Marino and Moran, 2019).

The O-acetylserine(thiol)lyase A1 (OASA1) enzyme participates in the sulfur assimilation and biosynthesis of Cys metabolic pathways, and in *Arabidopsis*, the nitration of the Tyr302 residue causes its inactivation, as this residue is close to another key residue, Asn77, found in the O-acetylserine binding site (Álvarez et al., 2011; Vandelle and Delledonne, 2011). Álvarez et al. (2011) propose that the inactivation of OASA1 could represent a rapid regulatory mechanism by which the production of Cys and GSH is limited, localized, and under stress conditions, decreasing its antioxidant capacity and its ability to detoxify other reactive species, thus allowing the transduction of stress signals to the rest of the plant (Álvarez et al., 2011).

Tyr nitration has also been described in the S-adenosyl homocysteine hydrolase (SAHH) from sunflower, with its Tyr448 residue as preferably modifiable, based on *in silico* studies, and whose modification decreases its catalytic activity. This enzyme participates in the genomic DNA methylation cycle, so its inactivation could be a mechanism by which an epigenetic regulation of DNA takes place, with the consequent modification of gene expression in the stress tolerance process (Chaki et al., 2009; Akhter et al., 2021).

In pea, the NADP-isocitrate dehydrogenase (NADP-ICDH) enzyme decreases its activity by Tyr392 nitration, as does the malate dehydrogenase (MDH) enzyme, although in this case, it is through Cys S-nitrosylation (Ortega-Galisteo et al., 2012; Begara-Morales et al., 2013). Both enzymes are involved in energy metabolism and amino acid biosynthesis. The inactivation of NADP-ICDH is attributed to the process of root senescence (Begara-Morales et al., 2013); while in the case of MDH, recent studies have shown that rice plants deficient in plastidial MDH1 activity acquire saline stress tolerance by enhancing the biosynthetic pathway of vitamin B6 (Nan et al., 2020).

The consequences from the different types of redox regulations to which the described enzymes are subject, generally lead to a loss or decrease in their metabolic activity, or may even result in the partial deactivation of complete metabolic pathways, through the total inactivation of key enzymes. This is of vital importance for both the regulation of a specific metabolic pathway and for choosing these molecular targets in the selection and genetic editing of plants resilient to abiotic stress.

The information described on primary metabolism-related proteins can be found in Table 2.

6 Redox-based PTMs on cellular signaling-related proteins

Many important enzymes in cell signaling processes are also susceptible to redox regulation in different plant species. This regulation implies the fine tuning of certain important enzymes, which makes them prone to be included within the target molecules involved in the plants' tolerance to abiotic stresses. Although the information available in the literature on this subject is limited, it is important to mention some of the most important aspects described by some authors.

In *Arabidopsis*, it has been described that the protein arginine methyltransferase 5 (PRMT5) enzyme, involved in the transfer of methyl groups in arginine residues, can undergo S-nitrosylation in its Cys125 residue during stress responses. Hu et al. (2017) have described a stress tolerance mechanism linked to this PTM. The S-nitrosylation of Cys125 enhances its catalytic activity, inducing an increase in spliceosome methylation levels,

TABLE 2 PTMs and their effect on the different primary metabolism-related proteins subject to redox regulation.

Plant	Protein (Uniprot accession number)	PTM	Effect	Reference
Arabidopsis	**NR** (P11035)	Met-538 oxidation	Inhibition of phosphorylation at Ser-534	(Hardin et al., 2009; Matamoros and Becana, 2021)
Medicago	**GS** (O04999)	Tyr-167 nitration	Inactivation	(Melo et al., 2011)
Arabidopsis	**GS** (Q43127)	Cys-S-sulfhydration	Decreased activity	(Aroca et al., 2015)
Arabidopsis	**OASA1** (P47998)	Tyr-302 nitration	Inactivation	(Álvarez et al., 2011)
Sunflower	**SAHH** (A0A251SAA5)	Tyr-448 nitration	Decreased activity	(Chaki et al., 2009)
Pea	**NADP-ICDH** (Q6R6M7)	Tyr-392 nitration	Decreased activity	(Begara-Morales et al., 2013)
Pea	**MDH** (Q5JC56)	Cys-S-nitrosylation	Decreased activity	(Ortega-Galisteo et al., 2012)

causing the alternative processing of pre-mRNAs of genes related to stress tolerance (Hu et al., 2017).

In *Arabidopsis*, the small heat shock protein 21 (sHSP21) chaperone is regulated by oxidation of its Met residues. Met49, Met52, Met55 and Met59 could be oxidized, decreasing their catalytic activity progressively depending on the degree of oxidation, thereby achieving enzymatic inactivation in case of a certain degree of overoxidation (Gustavsson et al., 2002; Jacques et al., 2013).

In beans, the nitration of Tyr30, a residue located in the distal heme pocket of a leghemoglobin (Lb), an enzyme involved in O_2 transport and present in abundance in legume nodules, inactivates its catalytic activity. The PTM of this enzyme suggests a mechanism by which Lb acts as an $ONOO^-$ scavenger for the protection of the symbiotic complex in legumes (Sainz et al., 2015).

As described, it is important to deepen our knowledge on specific PTMs that are induced in important proteins that are part of cell signaling processes, to find targets susceptible to being genetically edited in the generation of plants that are more resilient to climate change.

6.1 Phosphorylation/dephosphorylation events

Cell signaling can take place by means of protein phosphorylation/dephosphorylation events, carried out by protein kinases and protein phosphatases. These types of enzymes are susceptible to PTMs, altering their ability to induce the corresponding signaling events, as well as certain phosphorylation/dephosphorylation motifs whose modification may be compromised by another type of redox-based PTM, such as that described for the Met538 residue of the NR enzyme.

In *Arabidopsis*, leucine-rich repeat receptor protein kinase (HPCA1) is a transmembrane receptor that undergoes redox regulation. Oxidation of the Cys421/Cys424 and Cys434/Cys436 residue pairs of HPCA1 by H_2O_2, in the extracellular domain of the protein, activates the intracellular kinase domain and induces its autophosphorylation, mediating the activation of Ca^{2+} channels in the process of stomatal closure in guard cells (Wu et al., 2020).

Another characterized example is the protein tyrosine phosphatase 1 (PTP1) enzyme. It is the only Tyr-specific PTP described in *Arabidopsis*, whose activity consists of repressing the production of H_2O_2 and regulating the activity of the Mitogen-Activated Protein Kinases (MAPKs) MPK3/MPK6. PTP1 presents a Cys catalytic residue, Cys265, whose irreversible overoxidation induced by H_2O_2 inhibits its activity. However, Cys265 may suffer S-nitrosylation, induced by NO·, in a mechanism by which it protects the catalytic residue from overoxidation and consequent enzymatic inactivation (Nicolas-Francès et al., 2022).

Another enzyme, *Arabidopsis* protein kinase SnRK2.6, may be S-nitrosylated in its Cys137 by NO· This residue is found next to the kinase catalytic site, and by housing the PTM, it inhibits its function. This is associated with disturbances in the proper functioning of the ABA-induced stomatal closure (Wang et al., 2015).

S-nitrosylation also takes place in the phosphoinositide-dependent kinase 1 (PDK1) enzyme of tomato. Its Cys128 residue can have this PTM, and the consequences of this modification are the inhibition of its kinase activity, and therefore of the phosphorylation events (Liu et al., 2017).

In maize, the cyclin-dependent kinase A (CDKA;1) enzyme can undergo Tyr nitration in its Tyr15 and Tyr19 residues. Both Tyr are on the ATP-binding site, and their nitration causes a decrease in affinity with ATP (Méndez et al., 2020). Similar events occur in its brassinosteroid insensitive 2 kinase (BIN2) enzyme by NO·-mediated modifications. It is a protein kinase that participates in the brassinosteroid-mediated response, and the S-nitrosylation of Cys162 compromises its assembly, and consequently, its kinase activity (Mao and Li, 2020). However, the BIN2 homologous enzyme from *Arabidopsis* is inactive until, as a consequence of an increase in ROS, its residues Cys59, Cys95, Cys99 and Cys162 undergo oxidation, with the subsequent formation of intramolecular disulfide bridges (Song et al., 2019).

Thus, the above describes some examples of plant enzymes linked to phosphorylation/dephosphorylation cell signaling events. Most redox-based PTMs on protein kinases and phosphatases inhibit their ability to introduce or remove phosphate groups into and from target proteins, modifying the corresponding cell signaling events.

6.2 Phytohormone-related signaling events

A part of the overall coordination of plant metabolism corresponds to cell signaling events carried out by phytohormones. These occur under physiological conditions for proper plant development, apical growth, root development and senescence, signaling under biotic stress conditions and pathogenesis, and abiotic stress, including salinity, drought, and extreme temperatures. In recent years, different experimental approaches have described how multiple proteins from the biosynthetic metabolism of these phytohormones and their signaling, are subject to a fine redox regulation.

Abscisic acid (ABA) metabolism and the signaling events in which this phytohormone is involved, require biosynthetic enzymes, receptors from the PYR/PYL/RCAR family, transcription factors, PP2C phosphatases and SnRK2 kinases (Skubacz et al., 2016). Multiple ABA receptors from the PYR/PYL/RCAR family have been described as being under redox

regulation by Tyr nitration. Under abiotic stress conditions, the increase in the ABA concentration is associated with the increase in ROS and RNS, with the consequent $ONOO^-$ formation. The ABA receptor Pyrabactin resistance 1 (PYR1) shows three Tyr residues with increased susceptibility to $ONOO^-$induced nitration. These residues, Tyr58, Tyr120 and Tyr143, are oriented and near the ABA-binding site, interfering in its appropriate binding and representing a mechanism by which nitrosative stress conditions locally limit the effects of ABA signaling (Castillo et al., 2015). In *Arabidopsis*, the transcription factors AtMYB2 and AtMYB30 are induced by abiotic stress. AtMYB2 participates in ABA-induced signaling, and AtMYB30 in the heat and oxidative stress hypersensitive response (Mabuchi et al., 2018; Jia et al., 2020; Pande et al., 2022). Both transcription factors are subject to redox regulation by S-nitrosylation, with Cys53 in AtMYB2, and Cys49 and Cys53 in AtMYB30 being the residues susceptible to modification, consequently decreasing their DNA binding activity (Serpa et al., 2007; Tavares et al., 2014; Pande et al., 2022). Another antagonistic behavior of NO· on ABA involves the transcription factor ABI5, which represses seed germination and growth. ABI5 is susceptible to S-nitrosylation in its residue Cys153, facilitating its degradation through E3 ligases and proteolytic complexes, consequently promoting germination (Albertos et al., 2015). Examples of SnRK2 kinases have been described in previous sections, with the example of SnRK2.6, involved in ABA-induced stomatal closure. These proteolytic complexes, especially the SCF-E3 ligase complex, have also been described as susceptible to S-nitrosylation in the subunits that compose it, enhancing the assembly and stability of the complex with itself and interactions with other proteins (Pande et al., 2022). The ASK1 subunit undergoes S-nitrosylation in its Cys37 and Cys118 residues, a modification that enhances the assembly with the rest of the subunits (Iglesias et al., 2018). The S-nitrosylation of the TIR1 subunit, in its Cys140 residue, enhances the assembly of the complex and is critical for its interaction and ubiquitination with the AUX/IAA repressor, involved in the induction of NO·-modulated auxin responses (Terrile et al., 2012).

The NO· balance has also been described as modulating the cytokinin response, negatively regulating its signaling. Cytokinin promotes increased kinase and phosphotransferase activity of proteins such as histidine phosphotransfer protein 1 (AHP1), an activity that is inhibited by NO·, through the S-nitrosylation of its Cys115 residue, attenuating the induction of the phytohormone response. Therefore, redox balance and the amount of NO· coordinate cytokinin-induced responses, mainly plant growth and development (Feng et al., 2013; Pande et al., 2022).

Different redox-based PTMs regulate the Yang cycle and ethylene biosynthesis. NO· regulates this cycle through modifications in enzymes such as S-adenosylmethionine synthase (SAMS). In *Arabidopsis*, the SAMS enzyme is inactivated by S-nitrosylation of its Cys114 residue (Lindermayr et al., 2006). The 1-aminocyclopropane-1-carboxylate oxidase 1 (ACO1) enzyme of tomato, involved in the initial steps of the ethylene biosynthesis pathway from SAM, undergoes S-sulfhydration in its Cys60 residue, decreasing the enzyme catalytic activity. Tomato's ACO2 enzyme is also inhibited by S-sulfhydration (Jia et al., 2018). Other types of proteins described under redox regulation are the master regulator transcription factors. In tomato, the master regulator transcription factor NOR, involved in fruit ripening, and acting upstream of ethylene biosynthesis, undergoes oxidation in the Met138 residue, decreasing its affinity for DNA. The decrease in affinity between a transcription factor and its DNA target sequence modifies the gene expression patterns that are under its regulation, and in the case of NOR, ripening-related genes (Jiang et al., 2020). These enzymatic inhibitions or decreased DNA binding activity in the case of transcription factors, decrease ethylene production. It is speculated that other enzymes from the Yang cycle and ethylene biosynthesis are subject to redox regulation, but more studies are needed to elucidate it.

Cell signaling events induced by the main hormones involved in biotic stress by pathogenesis processes, such as salicylic acid (SA) and jasmonic acid (JA), have been described as able to be modulated by NO· in nitrosative stress scenarios. NO· mainly has a negative and attenuating effect of the signaling induced by both phytohormones. This is shown with examples such as the S-nitrosylation of the Cys229 residue of the JAZ1 repressor from *Arabidopsis*, a modification that improves the union between the repressor and its co-repressors, inhibiting JA signaling (Pande et al., 2022). Likewise, in *Arabidopsis*, the increase in NO· induces S-nitrosylation of salicylic acid-binding protein 3 (AtSABP3) in its Cys280 residue, inhibiting its binding to SA and its carbonic anhydrase activity (Wang et al., 2009). NPR1, a pathogenesis master regulator, interacts with the basic leucine zipper TGA transcription factor to induce gene expression linked to the pathogen infection response. Both proteins have been described in *Arabidopsis*, as susceptible to redox-based PTMs. The activity of NPR1 occurs when the protein is in a monomeric state, but its residue Cys156 is susceptible to S-nitrosylation, a modification that enhances the assembly of an oligomeric state in the cytosol, and prevents the development of its function (Tada et al., 2008). Complementarily, other studies have shown that TGA1 is susceptible to S-nitrosylation and S-glutathionylation in its Cys260 and Cys266 residues, both redox-based PTMs protect TGA1 from an overoxidation state, and enhances its DNA binding activity in the presence of NPR1 (Lindermayr et al., 2010).

The information described on cellular signaling-related proteins is summarized in Table 3.

TABLE 3 PTMs and their effect on the different cellular signaling-related proteins subject to redox regulation.

Plant	Protein (Uniprot accession number)	PTM	Effect	Reference
Arabidopsis	**PRMT5** (Q8GWT4)	Cys-125 S-nitrosylation	Increased activity	(Hu et al., 2017)
Arabidopsis	**sHSP21** (P31170)	Met-49, Met-52, Met-55, Met-59 oxidation	Decreased activity/Inactivation	(Gustavsson et al., 2002; Jacques et al., 2013)
Bean	**LB** (P02234)	Tyr-30 nitration	Inactivation	(Sainz et al., 2015)
Arabidopsis	**HPCA1** (Q8GZ99)	Cys-421/Cys-424 and Cys-434/Cys-436 oxidation	Activation of intracellular kinase activity	(Wu et al., 2020)
Arabidopsis	**PTP1** (O82656)	Cys-265 S-nitrosylation	Cys overoxidation protection	(Nicolas-Francès et al., 2022)
	PTP1 (O82656)	Cys-265 oxidation	Inactivation	(Nicolas-Francès et al., 2022)
Arabidopsis	**SnRK2.6** (Q940H6)	Cys-137 S-nitrosylation	Inactivation	(Wang et al., 2015)
Tomato	**PDK1** (Q5I6E8)	Cys-128 S-nitrosylation	Inactivation	(Liu et al., 2017)
Maize	**CDKA;1** (P23111)	Tyr-15, Tyr-19 nitration	Lower affinity to ATP binding	(Méndez et al., 2020)
Maize	**BIN2** (-)	Cys-162 S-nitrosylation	Decreased activity	(Mao and Li, 2020)
Arabidopsis	**BIN2** (Q39011)	Cys-59, Cys95, Cys-99, Cys-162 oxidation	Activation/Increased activity	(Song et al., 2019)
Arabidopsis	**PYR1** (O49686)	Tyr-58, Tyr-120, Tyr-143 nitration	Inactivation	(Castillo et al., 2015)
Arabidopsis	**MYB2 TF** (Q9SPN3)	Cys-53 S-nitrosylation	Decreased the DNA binding activity	(Jia et al., 2020)
Arabidopsis	**MYB30 TF** (Q9SCU7)	Cys-49, Cys-53 S-nitrosylation	Decreased the DNA binding activity	(Mabuchi et al., 2018)
Arabidopsis	**ABI5 TF** (Q9SJN0)	Cys-153 S-nitrosylation	Triggers ABI5 degradation	(Albertos et al., 2015)
Arabidopsis	**ASK1** (Q39255)	Cys-37, Cys-118 S-nitrosylation	Enhances interactions	(Iglesias et al., 2018)
Arabidopsis	**TIR1** (Q570C0)	Cys-40 S-nitrosylation	Enhances interactions	(Terrile et al., 2012)
Arabidopsis	**AHP1** (Q9ZNV9)	Cys-115 S-nitrosylation	Decreased activity	(Feng et al., 2013)
Arabidopsis	**SAMS** (P23686)	Cys-114 S-nitrosylation	Inactivation	(Lindermayr et al., 2006)
Tomato	**ACO1** (P05116)	Cys-60 S-sulfhydration	Decreased activity	(Jia et al., 2018)
Tomato	**ACO2** (P07920)	Cys-S-sulfhydration	Decreased activity	(Jia et al., 2018)
Tomato	**NOR TF** (Q56UP6)	Met-138 oxidation	Decreased the DNA binding activity	(Jiang et al., 2020)
Arabidopsis	**JAZ1** (Q9LMA8)	Cys-229 S-nitrosylation	Enhances interactions	(Pande et al., 2022)
Arabidopsis	**SABP3** (P27140)	Cys-280 S-nitrosylation	Lower affinity to SA binding and inhibition of carbonic anhydrase activity	(Wang et al., 2009)
Arabidopsis	**NPR1** (P93002)	Cys-156 S-nitrosylation	Enhances oligomeric state	(Tada et al., 2008)
Arabidopsis	**TGA1 TF** (Q39237)	Cys-260, Cys-266 S-nitrosylation	Cys overoxidation protection and increased the DNA binding activity	(Lindermayr et al., 2010)
Arabidopsis	**TGA1 TF** (Q39237)	Cys-260, Cys-266 S-glutathionylation	Cys overoxidation protection and increased the DNA binding activity	(Lindermayr et al., 2010)

7 Role of redox-based PTMs on photosynthetic metabolism, photorespiration and Calvin-Benson cycle

The overall photosynthesis process, including the biosynthetic pathways of elements from the photosynthetic apparatus, as well as complementary metabolic pathways, such as photorespiration and the Calvin-Benson cycle, have been described under redox regulation by multiple studies.

In *shorgum*, the photosynthetic enzyme C4 phosphoenolpyruvate carboxylase (PEPCase) is inactivated *in vivo*, under salinity stress, and *in vitro*, by carbonylation of multiple residues, due to oxidative stress induced by high concentrations of ROS. However, both *in vivo* and *in vitro*, PEPCase can be S-nitrosylated, a PTM that has no significant impact on its catalytic activity, although it does attribute to the enzyme resistance to carbonylation, preserving its activity under stress conditions. This finding suggests that PEPCase S-nitrosylation is a mechanism of salinity stress tolerance (Baena et al., 2017). In spinach, the carbonylation of its phosphoribulokinase (PRK) enzyme also induces the inactivation of its catalytic activity (Mano et al., 2009; Mano et al., 2014). Similarly, in *Arabidopsis*, its sedoheptulose-1,7-bisphosphatase (SBPase) and ribulose-1,5-bisphosphate carboxylase (RuBisCO) enzymes have been described as carbonylation targets, a PTM that induces their catalytic inactivation (Liu et al., 2012b; Lounifi et al., 2013). In *Brassica*, the RuBisCO enzyme also suffers redox regulation by means of

Cys S-nitrosylation, causing an inhibition of its carboxylase activity (Abat and Deswal, 2009).

The oxidation of Trp to N-formylkynurenine by means of ROS has been described in two spinach proteins, linked to photosynthetic metabolism: the Trp352 residue of the CP43 subunit of PSII protein, and the Trp132 residue of the Lchb1 protein. These modifications have been associated to a mechanism of protein turnover to preserve the functionality of the photosynthetic apparatus under environmental stress conditions (Anderson et al., 2002; Rinalducci et al., 2005; Rinalducci et al., 2008). In *Arabidopsis*, Mg-protoporphyrin IX methyltransferase (CHLM), an enzyme linked to the biosynthesis of chlorophylls, is subject to redox regulation by means of the oxidation of its Cys111 and Cys115 residues. Both oxidations decrease this enzyme's methyltransferase activity (Richter et al., 2016).

In *Arabidopsis*, the catalytic activity of the glyceraldehyde 3-phosphate dehydrogenase (GAPDH) enzyme increases by 60% due to the sulfhydration of its Cys residues (Aroca et al., 2015; Palma et al., 2020), and it is reversibly inhibited by S-nitrosylation of its catalytic Cys149, which is mediated by NO· donors (Zaffagnini et al., 2013). However, in cucumber, its homologous GAPDH enzyme decreases its catalytic activity when it undergoes Cys S-nitrosylation (Niu et al., 2019). Similar consequences cause Cys S-nitrosylation of the glycolate oxidase (GO) enzyme in peas (Ortega-Galisteo et al., 2012). In this same plant, other proteins have been described as susceptible to redox-based PTMs. Hydroxypyruvate reductase (HPR) can undergo nitration in its Tyr198 residue, with the consequent decrease in its catalytic activity (Corpas et al., 2013). Similarly, Tyr205 nitration of the sunflower carbonic anhydrase (β-CA) enzyme under high temperature abiotic stress conditions, also decreases its catalytic activity by 43% (Chaki et al., 2013).

The consequences that have been described in photosynthetic metabolism and enzymes linked to photorespiration and Calvin-Benson cycle, are related to the decrease/inhibition of their metabolic activity, or may even force the proteolysis of elements of the photosynthetic apparatus and their turnover, as a result of an excessive amount of redox-based PTMs on their residues. These discoveries demonstrate that photosynthetic metabolism and complementary pathways are subject to strict redox regulation, whose main consequences lead to a decrease in photosynthetic functionality, as well as a decrease in the catalytic activity of the enzymes that compose it. The exposure to abiotic stresses is known to disrupt the proper functioning of photosynthesis, but redox inactivation suggests that, under these conditions, cellular metabolism needs to be restructured, and energy sources need to be redirected to other metabolic pathways that allow the plant to survive.

The information described on the PTMs of photosynthetic metabolism, photorespiration and Calvin-Benson cycle-related proteins is shown in Table 4.

8 Conclusions and future perspectives

Different plant abiotic stresses, including salinity, extreme temperatures, drought, and heavy metal toxicity, among others, are the main adverse factors that limit plant development and decrease crop yields globally. For this reason, from all areas of study in the plant world, many approaches intended to decipher the physiological, biochemical and molecular mechanisms by

TABLE 4 PTMs and their effect on proteins involved in photosynthetic metabolism, photorespiration and Calvin-Benson cycle.

Plant	Protein (Uniprot accession number)	PTM	Effect	Reference
Sorghum	**PEPCase** (P15804)	Carbonylation	Inactivation	(Baena et al., 2017)
	PEPCase (P15804)	Cys-S-nitrosylation	Protection against carbonylation	(Baena et al., 2017)
Spinach	**PRK** (P09559)	Carbonylation	Inactivation	(Mano et al., 2009; Mano et al., 2014)
Arabidopsis	**SBPase** (P46283)	Carbonylation	Inactivation	(Liu et al., 2012b)
Arabidopsis	**RuBisCO** (O03042)	Carbonylation	Inactivation	(Lounifi et al., 2013)
Brassica	**RuBisCO** (P48686)	Cys-S-nitrosylation	Inhibition of carboxylase activity	(Abat and Deswal, 2009)
Spinach	**CP43** (P06003)	Trp-352 oxidation	Inactivation/Turnover	(Anderson et al., 2002)
Spinach	**Lchb1** (P12333)	Trp-132 oxidation	Inactivation/Turnover	(Rinalducci et al., 2005)
Arabidopsis	**CHLM** (Q9SW18)	Cys-111 oxidation	Decreased activity	(Richter et al., 2016)
	CHLM (Q9SW18)	Cys-115 oxidation	Decreased activity	(Richter et al., 2016)
Arabidopsis	**GAPDH** (P25858)	Cys-S-sulfhydration	Increased activity	(Aroca et al., 2015)
	GAPDH (P25858)	Cys-149 S-nitrosylation	Inactivation	(Palma et al., 2020)
Cucumber	**GAPDH** (A0A0A0K8C1)	Cys-S-nitrosylation	Decreased activity	(Niu et al., 2019)
Pea	**GO** (-)	Cys-S-nitrosylation	Decreased activity	(Ortega-Galisteo et al., 2012)
Pea	**HPR** (-)	Tyr-198 nitration	Decreased activity	(Corpas et al., 2013)
Sunflower	**β-CA** (A0A251ULA9)	Tyr-205 nitration	Decreased activity	(Chaki et al., 2013)

which plants acclimatize to unfavorable conditions and tolerate abiotic stress exposure, or the simultaneity of different types of abiotic and biotic stresses.

The plants' perception of abiotic stresses induces different molecular response mechanisms, among which we highlight the overproduction of reactive chemical species, mainly ROS, RNS and RSS. These molecules are present in all plant subcellular compartments, either by *in situ* production or through diffusion, and induce both damages to cellular components and biomolecules, and redox modulation/regulation of metabolism by means of PTMs in specific proteins. These redox-based PTMs mainly include Cys oxidation and S-nitrosylation, Tyr nitration, carbonylation, Met oxidation, Trp oxidation and Cys S-sulfhydration. PTMs can be produced in susceptible residues of specific proteins, exclusively or in combination with other modifications, within the same protein and, even, the same residue, multiplying the redox-based proteoforms of the plant proteome and increasing the complexity of cell signaling processes.

Recent research has elucidated how specific proteins, belonging to specific metabolic pathways, such as those involved in energy production, amino acid biosynthesis, cell signaling events or the global photosynthetic process, modify their catalytic activity by hosting some type of redox-based PTMs. However, most of this knowledge has been obtained by *in vitro* tests, following speculations obtained from other experimental results.

In addition, and as mentioned above, when two or more abiotic stresses act together, the plants' response is very specific and cannot be deduced from their response against a single stress. In this sense, there is a very limited information in the literature on how redox-based PTMs affect plant metabolism under some type of simple abiotic stress, mainly salinity or high temperatures. However, there is absolutely no information on how these redox-based PTMs affect the plant's response to abiotic stress combination. Therefore, it is necessary to increase the research and characterization of new target proteins that are susceptible to modulation by redox-based PTMs, and to elucidate their function in the response of plants to abiotic stress. In addition, new lines of research are needed to delve into the identification of PTMs that give rise to new proteoforms with new functionalities induced by the combination of abiotic stresses, which would open new fields of knowledge in the identification of the mechanisms of plant tolerance to abiotic stress, in order to increase the resilience of crops to climate change.

Author contributions

JMM-G wrote the manuscript and designed the figures and tables. MP-H, SEM-L an LA contributed to the writing, editing and literature updating. RMR supervised, corrected and contributed with the writing and editing of the manuscript. All authors contributed to the article and approved the submitted version.

Funding

This research was supported by the Ministry of Economy and Competitiveness from Spain (Grant No. PGC2018-09573-B-100) to RMR; by the Spanish National Research Council (CSIC) (JAEINT_21_01293) to SEM-L; by University of Murcia Ph.D. contracts (Registry number 109144/2022) to JMM-G; and by the Ministry of Science and Innovation of Spain (Grant No. FPU20/03051) to MP-H (Murcia, Spain).

Acknowledgments

We sincerely acknowledge Mario G. Fon for proofreading the manuscript. We also apologize to all authors of papers not mentioned in this manuscript due to space limitations.

Conflict of interest

The authors declare that the research was conducted in the absence of any commercial or financial relationships that could be construed as a potential conflict of interest.

Publisher's note

References

Abat, J. K., and Deswal, R. (2009). Differential modulation of *S* -nitrosoproteome of *Brassica juncea* by low temperature: Change in *S* -nitrosylation of rubisco is responsible for the inactivation of its carboxylase activity. *Proteomics* 9, 4368–4380. doi: 10.1002/pmic.200800985

Ahanger, M. A., Tomar, N. S., Tittal, M., Argal, S., and Agarwal, R. M. (2017). Plant growth under water/salt stress: ROS production; antioxidants and significance of added potassium under such conditions. *Physiol. Mol. Biol. Plants* 23, 731–744. doi: 10.1007/s12298-017-0462-7

Ahuja, I., de Vos, R. C. H., Bones, A. M., and Hall, R. D. (2010). Plant molecular stress responses face climate change. *Trends Plant Sci.* 15, 664–674. doi: 10.1016/j.tplants.2010.08.002

Airaki, M., Sánchez-Moreno, L., Leterrier, M., Barroso, J. B., Palma, J. M., and Corpas, F. J. (2011). Detection and quantification of s-nitrosoglutathione (GSNO) in pepper (Capsicum annuum l.) plant organs by LC-ES/MS. *Plant Cell Physiol.* 52, 2006–2015. doi: 10.1093/pcp/pcr133

Akhter, Z., Bi, Z., Ali, K., Sun, C., Fiaz, S., Haider, F. U., et al. (2021). In response to abiotic stress, DNA methylation confers EpiGenetic changes in plants. *Plants* 10, 1096. doi: 10.3390/plants10061096

Akter, S., Huang, J., Waszczak, C., Jacques, S., Gevaert, K., Van Breusegem, F., et al. (2015). Cysteines under ROS attack in plants: a proteomics view. *J. Exp. Bot.* 66, 2935–2944. doi: 10.1093/jxb/erv044

Albertos, P., Romero-Puertas, M. C., Tatematsu, K., Mateos, I., Sánchez-Vicente, I., Nambara, E., et al. (2015). S-nitrosylation triggers ABI5 degradation to promote seed germination and seedling growth. *Nat. Commun.* 6, 8669. doi: 10.1038/ncomms9669

Ali, S., Liu, Y., Ishaq, M., Shah, T., Abdullah,, Ilyas, A., et al. (2017). Climate change and its impact on the yield of major food crops: Evidence from Pakistan. *Foods* 6, 39. doi: 10.3390/foods6060039

Álvarez, C., Lozano-Juste, J., Romero, L. C., García, I., Gotor, C., and León, J. (2011). Inhibition of arabidopsis O-acetylserine(thiol)lyase A1 by tyrosine nitration. *J. Biol. Chem.* 286, 578–586. doi: 10.1074/jbc.M110.147678

Anderson, L. B., Maderia, M., Ouellette, A. J. A., Putnam-Evans, C., Higgins, L., Krick, T., et al. (2002). Posttranslational modifications in the CP43 subunit of photosystem II. *Proc. Natl. Acad. Sci.* 99, 14676–14681. doi: 10.1073/pnas.232591599

Arnao, M. B., and Hernández-Ruiz, J. (2019). Melatonin and reactive oxygen and nitrogen species: a model for the plant redox network. *Melatonin Res.* 2, 152–168. doi: 10.32794/11250036

Aroca, A., Gotor, C., and Romero, L. C. (2018). Hydrogen sulfide signaling in plants: Emerging roles of protein persulfidation. *Front. Plant Sci.* 9. doi: 10.3389/fpls.2018.01369

Aroca, A., Schneider, M., Scheibe, R., Gotor, C., and Romero, L. C. (2017). Hydrogen sulfide regulates the Cytosolic/Nuclear partitioning of glyceraldehyde-3-Phosphate dehydrogenase by enhancing its nuclear localization. *Plant Cell Physiol.* 58, 983–992. doi: 10.1093/pcp/pcx056

Aroca, Á., Serna, A., Gotor, C., and Romero, L. C. (2015). S-sulfhydration: a cysteine posttranslational modification in plant systems. *Plant Physiol.* 168, 334–342. doi: 10.1104/pp.15.00009

Astier, J., Gross, I., and Durner, J. (2018). Nitric oxide production in plants: an update. *J. Exp. Bot.* 69, 3401–3411. doi: 10.1093/jxb/erx420

Baena, G., Feria, A. B., Echevarria, C., Monreal, J. A., and Garcia-Maurino, S. (2017). Salinity promotes opposite patterns of carbonylation and nitrosylation of c-4 phosphoenolpyruvate carboxylase in sorghum leaves. *Planta* 246, 1203–1214. doi: 10.1007/s00425-017-2764-y

Bai, X., Yang, L., Tian, M., Chen, J., Shi, J., Yang, Y., et al. (2011). Nitric oxide enhances desiccation tolerance of recalcitrant antiaris toxicaria seeds *via* protein s-nitrosylation and carbonylation. *PLos One* 6, e20714. doi: 10.1371/journal.pone.0020714

Begara-Morales, J. C., Chaki, M., Sánchez-Calvo, B., Mata-Pérez, C., Leterrier, M., Palma, J. M., et al. (2013). Protein tyrosine nitration in pea roots during development and senescence. *J. Exp. Bot.* 64, 1121–1134. doi: 10.1093/jxb/ert006

Begara-Morales, J. C., Chaki, M., Valderrama, R., Mata-Pérez, C., Padilla, M. N., and Barroso, J. B. (2019). The function of s-nitrosothiols during abiotic stress in plants. *J. Exp. Bot.* 70, 4429–4439. doi: 10.1093/jxb/erz197

Begara-Morales, J. C., Mata-Pérez, C., Padilla, M. N., Chaki, M., Valderrama, R., Aranda-Caño, L., et al. (2021). Role of electrophilic nitrated fatty acids during development and response to abiotic stress processes in plants. *J. Exp. Bot.* 72, 917–927. doi: 10.1093/jxb/eraa517

Begara-Morales, J. C., Sánchez-Calvo, B., Chaki, M., Mata-Pérez, C., Valderrama, R., Padilla, M. N., et al. (2015). Differential molecular response of monodehydroascorbate reductase and glutathione reductase by nitration and s-nitrosylation. *J. Exp. Bot.* 66, 5983–5996. doi: 10.1093/jxb/erv306

Begara-Morales, J. C., Sánchez-Calvo, B., Chaki, M., Valderrama, R., Mata-Pérez, C., López-Jaramillo, J., et al. (2014). Dual regulation of cytosolic ascorbate peroxidase (APX) by tyrosine nitration and s-nitrosylation. *J. Exp. Bot.* 65, 527–538. doi: 10.1093/jxb/ert396

Benhar, M., Forrester, M. T., and Stamler, J. S. (2009). Protein denitrosylation: enzymatic mechanisms and cellular functions. *Nat. Rev. Mol. Cell Biol.* 10, 721–732. doi: 10.1038/nrm2764

Bigelow, D. J., and Squier, T. C. (2011). Thioredoxin-dependent redox regulation of cellular signaling and stress response through reversible oxidation of methionines. *Mol. Biosyst.* 7, 2101. doi: 10.1039/c1mb05081h

Bizzozero, O. A. (2009). "Protein carbonylation in neurodegenerative and demyelinating CNS diseases," in *Handbook of neurochemistry and molecular neurobiology*. Eds. A. Lajtha, N. Banik and S. K. Ray (Boston, MA: Springer US), 543–562. doi: 10.1007/978-0-387-30375-8_23

Bose, J., Rodrigo-Moreno, A., and Shabala, S. (2014). ROS homeostasis in halophytes in the context of salinity stress tolerance. *J. Exp. Bot.* 65, 1241–1257. doi: 10.1093/jxb/ert430

Brannan, R. G. (2010). Reactive sulfur species act as prooxidants in liposomal and skeletal muscle model systems. *J. Agric. Food Chem.* 58, 3767–3771. doi: 10.1021/jf903587n

Castillo, M.-C., Lozano-Juste, J., González-Guzmán, M., Rodriguez, L., Rodriguez, P. L., and León, J. (2015). Inactivation of PYR/PYL/RCAR ABA receptors by tyrosine nitration may enable rapid inhibition of ABA signaling by nitric oxide in plants. *Sci. Signal* 8, ra89. doi: 10.1126/scisignal.aaa7981

Chaki, M., Álvarez de Morales, P., Ruiz, C., Begara-Morales, J. C., Barroso, J. B., Corpas, F. J., et al. (2015). Ripening of pepper (Capsicum annuum) fruit is characterized by an enhancement of protein tyrosine nitration. *Ann. Bot.* 116, 637–647. doi: 10.1093/aob/mcv016

Chaki, M., Carreras, A., López-Jaramillo, J., Begara-Morales, J. C., Sánchez-Calvo, B., Valderrama, R., et al. (2013). Tyrosine nitration provokes inhibition of sunflower carbonic anhydrase (β-CA) activity under high temperature stress. *Nitric. Oxide* 29, 30–33. doi: 10.1016/j.niox.2012.12.003

Chaki, M., Valderrama, R., Fernández-Ocaña, A. M., Carreras, A., López-Jaramillo, J., Luque, F., et al. (2009). Protein targets of tyrosine nitration in sunflower (Helianthus annuus l.) hypocotyls. *J. Exp. Bot.* 60, 4221–4234. doi: 10.1093/jxb/erp263

Chaplin, A. K., Chernukhin, I., and Bechtold, U. (2019). Profiling of advanced glycation end products uncovers abiotic stress-specific target proteins in arabidopsis. *J. Exp. Bot.* 70, 653–670. doi: 10.1093/jxb/ery389

Chen, H., Lee, J., Lee, J.-M., Han, M., Emonet, A., Lee, J., et al. (2022). MSD2, an apoplastic Mn-SOD, contributes to root skotomorphogenic growth by modulating ROS distribution in arabidopsis. *Plant Sci.* 317, 111192. doi: 10.1016/j.plantsci.2022.111192

Chen, D., Shao, Q., Yin, L., Younis, A., and Zheng, B. (2019). Polyamine function in plants: Metabolism, regulation on development, and roles in abiotic stress responses. *Front. Plant Sci.* 9. doi: 10.3389/fpls.2018.01945

Chmielowska-Bąk, J., Arasimowicz-Jelonek, M., and Deckert, J. (2019). In search of the mRNA modification landscape in plants. *BMC Plant Biol.* 19, 421. doi: 10.1186/s12870-019-2033-2

Choudhury, F. K., Rivero, R. M., Blumwald, E., and Mittler, R. (2017). Reactive oxygen species, abiotic stress and stress combination. *Plant J.* 90, 856–867. doi: 10.1111/tpj.13299

Clark, D., Durner, J., Navarre, D. A., and Klessig, D. F. (2000). Nitric oxide inhibition of tobacco catalase and ascorbate peroxidase. *MPMI* 13, 1380–1384. doi: 10.1094/MPMI.2000.13.12.1380

Corpas, F., and Barroso, J. (2015). Reactive sulphur species (RSS): possible new players in the oxidative metabolism of plant peroxisomes. *Front. Plant Sci.* 6. doi: 10.3389/fpls.2015.00116

Corpas, F. J., Barroso, J. B., González-Gordo, S., Muñoz-Vargas, M. A., and Palma, J. M. (2019). Hydrogen sulfide: A novel component in *Arabidopsis* peroxisomes which triggers catalase inhibition. *J. Integr. Plant Biol.* 61 (7), jipb.12779. doi: 10.1111/jipb.12779

Corpas, F. J., del Río, L. A., and Barroso, J. B. (2008). Post-translational modifications mediated by reactive nitrogen species. *Plant Signal Behav.* 3, 301–303. doi: 10.4161/psb.3.5.5277

Corpas, F. J., González-Gordo, S., and Palma, J. M. (2020). Plant peroxisomes: A factory of reactive species. *Front. Plant Sci.* 11. doi: 10.3389/fpls.2020.00853

Corpas, F. J., Leterrier, M., Begara-Morales, J. C., Valderrama, R., Chaki, M., López-Jaramillo, J., et al. (2013). Inhibition of peroxisomal hydroxypyruvate reductase (HPR1) by tyrosine nitration. *Biochim. Biophys. Acta* 1830, 4981–4989. doi: 10.1016/j.bbagen.2013.07.002

Del Río, L. A. (2015). ROS and RNS in plant physiology: an overview. *J. Exp. Bot.* 66, 2827–2837. doi: 10.1093/jxb/erv099

Ehrenshaft, M., Deterding, L. J., and Mason, R. P. (2015). Tripping up trp: Modification of protein tryptophan residues by reactive oxygen species, modes of detection, and biological consequences. *Free Radic. Biol. Med.* 89, 220–228. doi: 10.1016/j.freeradbiomed.2015.08.003

Feng, J., Chen, L., and Zuo, J. (2019). Protein s-nitrosylation in plants: Current progresses and challenges. *J. Integr. Plant Biol.* 61, 1206–1223. doi: 10.1111/jipb.12780

Feng, J., Wang, C., Chen, Q., Chen, H., Ren, B., Li, X., et al. (2013). S-nitrosylation of phosphotransfer proteins represses cytokinin signaling. *Nat. Commun.* 4, 1529. doi: 10.1038/ncomms2541

Filipovic, M. R., and Jovanovic, V. M. (2017). More than just an intermediate: hydrogen sulfide signalling in plants. *J. Exp. Bot.* 68, 4733–4736. doi: 10.1093/jxb/erx352

Filipovic, M. R., Zivanovic, J., Alvarez, B., and Banerjee, R. (2018). Chemical biology of H2S signaling through persulfidation. *Chem. Rev.* 118, 1253–1337. doi: 10.1021/acs.chemrev.7b00205

Foyer, C. H. (2018). Reactive oxygen species, oxidative signaling and the regulation of photosynthesis. *Environ. Exp. Bot.* 154, 134–142. doi: 10.1016/j.envexpbot.2018.05.003

Friso, G., and van Wijk, K. J. (2015). Posttranslational protein modifications in plant Metabolism1. *Plant Physiol.* 169, 1469–1487. doi: 10.1104/pp.15.01378

Fry, S. C. (1998). Oxidative scission of plant cell wall polysaccharides by ascorbate-induced hydroxyl radicals. *Biochem. J.* 332, 507–515. doi: 10.1042/bj3320507

Fukudome, M., Shimada, H., Uchi, N., Osuki, K., Ishizaki, H., Murakami, E., et al. (2020). Reactive sulfur species interact with other signal molecules in root nodule symbiosis in lotus japonicus. *Antioxidants* 9, 145. doi: 10.3390/antiox9020145

Go, Y.-M., Chandler, J. D., and Jones, D. P. (2015). The cysteine proteome. *Free Radical Biol. Med.* 84, 227–245. doi: 10.1016/j.freeradbiomed.2015.03.022

Gruhlke, M. C. H., and Slusarenko, A. J. (2012). The biology of reactive sulfur species (RSS). *Plant Physiol. Biochem.* 59, 98–107. doi: 10.1016/j.plaphy.2012.03.016

Guerra, D., Ballard, K., Truebridge, I., and Vierling, E. (2016). S-nitrosation of conserved cysteines modulates activity and stability of *S* -nitrosoglutathione reductase (GSNOR). *Biochemistry* 55, 2452–2464. doi: 10.1021/acs.biochem.5b01373

Gupta, K. J., and Igamberdiev, A. U. (2016). Reactive nitrogen species in mitochondria and their implications in plant energy status and hypoxic stress tolerance. *Front. Plant Sci.* 7. doi: 10.3389/fpls.2016.00369

Gustavsson, N., Kokke, B. P. A., Härndahl, U., Silow, M., Bechtold, U., Poghosyan, Z., et al. (2002). A peptide methionine sulfoxide reductase highly expressed in photosynthetic tissue in arabidopsis thaliana can protect the chaperone-like activity of a chloroplast-localized small heat shock protein. *Plant J.* 29, 545–553. doi: 10.1046/j.1365-313x.2002.029005545.x

Halliwell, B. (2006). Reactive species and antioxidants. redox biology is a fundamental theme of aerobic life. *Plant Physiol.* 141, 312–322. doi: 10.1104/pp.106.077073

Han, R., Li, C., Rasheed, A., Pan, X., Shi, Q., and Wu, Z. (2022). Reducing phosphorylation of nitrate reductase improves nitrate assimilation in rice. *J. Integr. Agric.* 21, 15–25. doi: 10.1016/S2095-3119(20)63386-X

Hardin, S., Larue, C., Oh, M.-H., Jain, V., and Huber, S. (2009). Coupling oxidative signals to protein phosphorylation *via* methionine oxidation in arabidopsis. *Biochem. J.* 422, 305–312. doi: 10.1042/BJ20090764

Hasanuzzaman, M., Bhuyan, M. H. M. B., Zulfiqar, F., Raza, A., Mohsin, S. M., Mahmud, J. A., et al. (2020). Reactive oxygen species and antioxidant defense in plants under abiotic stress: Revisiting the crucial role of a universal defense regulator. *Antioxidants (Basel)* 9, 681. doi: 10.3390/antiox9080681

Heinrich, T. A., Silva, R. S., Miranda, K. M., Switzer, C. H., Wink, D. A., and Fukuto, J. M. (2013). Biological nitric oxide signalling: chemistry and terminology. *Br. J. Pharmacol.* 169, 1417. doi: 10.1111/bph.12217

Hiramoto, K., Ojima, N., Sako, K., and Kikugawa, K. (1996). Effect of plant phenolics on the formation of the spin-adduct of hydroxyl radical and the DNA strand breaking by hydroxyl radical. *Biol. Pharm. Bull.* 19, 558–563. doi: 10.1248/bpb.19.558

Holzmeister, C., Gaupels, F., Geerlof, A., Sarioglu, H., Sattler, M., Durner, J., et al. (2015). Differential inhibition of arabidopsis superoxide dismutases by peroxynitrite-mediated tyrosine nitration. *J. Exp. Bot.* 66, 989–999. doi: 10.1093/jxb/eru458

Huang, D., Jing, G., Zhang, L., Chen, C., and Zhu, S. (2021). Interplay among hydrogen sulfide, nitric oxide, reactive oxygen species, and mitochondrial DNA oxidative damage. *Front. Plant Sci.* 12. doi: 10.3389/fpls.2021.701681

Huang, H., Ullah, F., Zhou, D.-X., Yi, M., and Zhao, Y. (2019a). Mechanisms of ROS regulation of plant development and stress responses. *Front. Plant Sci.* 10. doi: 10.3389/fpls.2019.00800

Huang, J., Willems, P., Wei, B., Tian, C., Ferreira, R. B., Bodra, N., et al. (2019b). Mining for protein s-sulfenylation in *Arabidopsis* uncovers redox-sensitive sites. *Proc. Natl. Acad. Sci. U.S.A.* 116, 21256–21261. doi: 10.1073/pnas.1906768116

Hu, J., Yang, H., Mu, J., Lu, T., Peng, J., Deng, X., et al. (2017). Nitric oxide regulates protein methylation during stress responses in plants. *Mol. Cell* 67, 702–710.e4. doi: 10.1016/j.molcel.2017.06.031

Iglesias, M. J., Terrile, M. C., Correa-Aragunde, N., Colman, S. L., Izquierdo-Álvarez, A., Fiol, D. F., et al. (2018). Regulation of SCFTIR1/AFBs E3 ligase assembly by s-nitrosylation of arabidopsis SKP1-like1 impacts on auxin signaling. *Redox Biol.* 18, 200–210. doi: 10.1016/j.redox.2018.07.003

Jacques, S., Ghesquière, B., De Bock, P.-J., Demol, H., Wahni, K., Willems, P., et al. (2015). Protein methionine sulfoxide dynamics in arabidopsis thaliana under oxidative stress. *Mol. Cell. Proteomics* 14, 1217–1229. doi: 10.1074/mcp.M114.043729

Jacques, S., Ghesquière, B., Van Breusegem, F., and Gevaert, K. (2013). Plant proteins under oxidative attack. *Proteomics* 13, 932–940. doi: 10.1002/pmic.201200237

Janků, M., Luhová, L., and Petřivalský, M. (2019). On the origin and fate of reactive oxygen species in plant cell compartments. *Antioxidants* 8, 105. doi: 10.3390/antiox8040105

Jia, H., Chen, S., Liu, D., Liesche, J., Shi, C., Wang, J., et al. (2018). Ethylene-induced hydrogen sulfide negatively regulates ethylene biosynthesis by persulfidation of ACO in tomato under osmotic stress. *Front. Plant Sci.* 9. doi: 10.3389/fpls.2018.01517

Jiang, G., Zeng, J., Li, Z., Song, Y., Yan, H., He, J., et al. (2020). Redox regulation of the NOR transcription factor is involved in the regulation of fruit ripening in tomato. *Plant Physiol.* 183, 671–685. doi: 10.1104/pp.20.00070

Jia, T., Zhang, K., Li, F., Huang, Y., Fan, M., and Huang, T. (2020). The AtMYB2 inhibits the formation of axillary meristem in arabidopsis by repressing RAX1 gene under environmental stresses. *Plant Cell Rep.* 39, 1755–1765. doi: 10.1007/s00299-020-02602-3

Kärkönen, A., and Kuchitsu, K. (2015). Reactive oxygen species in cell wall metabolism and development in plants. *Phytochemistry* 112, 22–32. doi: 10.1016/j.phytochem.2014.09.016

Katsuya-Gaviria, K., Caro, E., Carrillo-Barral, N., and Iglesias-Fernández, R. (2020). Reactive oxygen species (ROS) and nucleic acid modifications during seed dormancy. *Plants* 9, 679. doi: 10.3390/plants9060679

Kim, Y., Mun, B.-G., Khan, A. L., Waqas, M., Kim, H.-H., Shahzad, R., et al. (2018). Regulation of reactive oxygen and nitrogen species by salicylic acid in rice plants under salinity stress conditions. *PLos One* 13, e0192650. doi: 10.1371/journal.pone.0192650

Kolbert, Z., Feigl, G., Bordé, Á., Molnár, Á., and Erdei, L. (2017). Protein tyrosine nitration in plants: Present knowledge, computational prediction and future perspectives. *Plant Physiol. Biochem.* 113, 56–63. doi: 10.1016/j.plaphy.2017.01.028

Lambeck, I. C., Fischer-Schrader, K., Niks, D., Roeper, J., Chi, J.-C., Hille, R., et al. (2012). Molecular mechanism of 14-3-3 protein-mediated inhibition of plant nitrate reductase. *J. Biol. Chem.* 287, 4562–4571. doi: 10.1074/jbc.M111.323113

Levine, R. L., Mosoni, L., Berlett, B. S., and Stadtman, E. R. (1996). Methionine residues as endogenous antioxidants in proteins. *Proc. Natl. Acad. Sci. U.S.A.* 93, 15036–15040. doi: 10.1073/pnas.93.26.15036

Lindermayr, C., Saalbach, G., Bahnweg, G., and Durner, J. (2006). Differential inhibition of arabidopsis methionine adenosyltransferases by protein s-nitrosylation. *J. Biol. Chem.* 281, 4285–4291. doi: 10.1074/jbc.M511635200

Lindermayr, C., Sell, S., Müller, B., Leister, D., and Durner, J. (2010). Redox regulation of the NPR1-TGA1 system of arabidopsis thaliana by nitric oxide. *Plant Cell* 22, 2894–2907. doi: 10.1105/tpc.109.066464

Liu, J.-Z., Duan, J., Ni, M., Liu, Z., Qiu, W.-L., Whitham, S. A., et al. (2017). S-nitrosylation inhibits the kinase activity of tomato phosphoinositide-dependent kinase 1 (PDK1). *J. Biol. Chem.* 292, 19743–19751. doi: 10.1074/jbc.M117.803882

Liu, M., Gong, X., Alluri, R. K., Wu, J., Sablo, T., and Li, Z. (2012a). Characterization of RNA damage under oxidative stress in escherichia coli. *Biol. Chem.* 393, 123–132. doi: 10.1515/hsz-2011-0247

Liu, X.-L., Yu, H.-D., Guan, Y., Li, J.-K., and Guo, F.-Q. (2012b). Carbonylation and loss-of-function analyses of SBPase reveal its metabolic interface role in oxidative stress, carbon assimilation, and multiple aspects of growth and development in arabidopsis. *Mol. Plant* 5, 1082–1099. doi: 10.1093/mp/sss012

Lounifi, I., Arc, E., Molassiotis, A., Job, D., Rajjou, L., and Tanou, G. (2013). Interplay between protein carbonylation and nitrosylation in plants. *Proteomics* 13, 568–578. doi: 10.1002/pmic.201200304

Møller, I. M., Jensen, P. E., and Hansson, A. (2007). Oxidative modifications to cellular components in plants. *Annu. Rev. Plant Biol.* 58, 459–481. doi: 10.1146/annurev.arplant.58.032806.103946

Møller, I. M., and Kristensen, B. K. (2006). Protein oxidation in plant mitochondria detected as oxidized tryptophan. *Free Radic. Biol. Med.* 40, 430–435. doi: 10.1016/j.freeradbiomed.2005.08.036

Møller, I. M., Rogowska-Wrzesinska, A., and Rao, R. S. P. (2011). Protein carbonylation and metal-catalyzed protein oxidation in a cellular perspective. *J. Proteomics* 74, 2228–2242. doi: 10.1016/j.jprot.2011.05.004

Mabuchi, K., Maki, H., Itaya, T., Suzuki, T., Nomoto, M., Sakaoka, S., et al. (2018). MYB30 links ROS signaling, root cell elongation, and plant immune responses. *Proc. Natl. Acad. Sci.* 115, E4710–E4719. doi: 10.1073/pnas.1804233115

MacKintosh, C., and Meek, S. E. (2001). Regulation of plant NR activity by reversible phosphorylation, 14-3-3 proteins and proteolysis. *Cell Mol. Life Sci.* 58, 205–214. doi: 10.1007/PL00000848

Ma, Y., Dias, M. C., and Freitas, H. (2020). Drought and salinity stress responses and microbe-induced tolerance in plants. *Front. Plant Sci.* 11. doi: 10.3389/fpls.2020.591911

Mano, J., Miyatake, F., Hiraoka, E., and Tamoi, M. (2009). Evaluation of the toxicity of stress-related aldehydes to photosynthesis in chloroplasts. *Planta* 230, 639–648. doi: 10.1007/s00425-009-0964-9

Mano, J., Nagata, M., Okamura, S., Shiraya, T., and Mitsui, T. (2014). Identification of oxidatively modified proteins in salt-stressed arabidopsis: a carbonyl-targeted proteomics approach. *Plant Cell Physiol.* 55, 1233–1244. doi: 10.1093/pcp/pcu072

Mao, J., and Li, J. (2020). Regulation of three key kinases of brassinosteroid signaling pathway. *Int. J. Mol. Sci.* 21, E4340. doi: 10.3390/ijms21124340

Marino, D., and Moran, J. F. (2019). Can ammonium stress be positive for plant performance? *Front. Plant Sci.* 10. doi: 10.3389/fpls.2019.01103

Martínez-Lorente, S. E., Pardo-Hernández, M., Martí-Guillén, J. M., López-Delacalle, M., and Rivero, R. M. (2022). Interaction between melatonin and NO: Action mechanisms, main targets, and putative roles of the emerging molecule NOmela. *Int. J. Mol. Sci.* 23, 6646. doi: 10.3390/ijms23126646

Martinez, V., Nieves-Cordones, M., Lopez-Delacalle, M., Rodenas, R., Mestre, T., Garcia-Sanchez, F., et al. (2018). Tolerance to stress combination in tomato plants: New insights in the protective role of melatonin. *Molecules* 23, 535. doi: 10.3390/molecules23030535

Matamoros, M. A., and Becana, M. (2021). Molecular responses of legumes to abiotic stress: post-translational modifications of proteins and redox signaling. *J. Exp. Bot.* 72, 5876–5892. doi: 10.1093/jxb/erab008

Mata-Pérez, C., Padilla, M. N., Sánchez-Calvo, B., Begara-Morales, J. C., Valderrama, R., Chaki, M., et al. (2020). Endogenous biosynthesis of s-nitrosoglutathione from nitro-fatty acids in plants. *Front. Plant Sci.* 11. doi: 10.3389/fpls.2020.00962

Melo, P. M., Silva, L. S., Ribeiro, I., Seabra, A. R., and Carvalho, H. G. (2011). Glutamine synthetase is a molecular target of nitric oxide in root nodules of medicago truncatula and is regulated by tyrosine nitration. *Plant Physiol.* 157, 1505–1517. doi: 10.1104/pp.111.186056

Méndez, A. A. E., Mangialavori, I. C., Cabrera, A. V., Benavides, M. P., Vázquez-Ramos, J. M., and Gallego, S. M. (2020). Tyr-nitration in maize CDKA;1 results in lower affinity for ATP binding. *Biochim. Biophys. Acta (BBA) - Proteins Proteomics* 1868, 140479. doi: 10.1016/j.bbapap.2020.140479

Meyer, Y., Buchanan, B. B., Vignols, F., and Reichheld, J.-P. (2009). Thioredoxins and glutaredoxins: unifying elements in redox biology. *Annu. Rev. Genet.* 43, 335–367. doi: 10.1146/annurev-genet-102108-134201

Mittler, R. (2002). Oxidative stress, antioxidants and stress tolerance. *Trends Plant Sci.* 7, 405–410. doi: 10.1016/s1360-1385(02)02312-9

Mittler, R., Vanderauwera, S., Suzuki, N., Miller, G., Tognetti, V. B., Vandepoele, K., et al. (2011). ROS signaling: the new wave? *Trends Plant Sci.* 16, 300–309. doi: 10.1016/j.tplants.2011.03.007

Mueller, M. J. (2004). Archetype signals in plants: the phytoprostanes. *Curr. Opin. Plant Biol.* 7, 441–448. doi: 10.1016/j.pbi.2004.04.001

Mustafa, A. K., Gadalla, M. M., Sen, N., Kim, S., Mu, W., Gazi, S. K., et al. (2009). H2S signals through protein s-sulfhydration. *Sci. Signal* 2, ra72. doi: 10.1126/scisignal.2000464

Nadarajah, K. K. (2020). ROS homeostasis in abiotic stress tolerance in plants. *Int. J. Mol. Sci.* 21, 5208. doi: 10.3390/ijms21155208

Nan, N., Wang, J., Shi, Y., Qian, Y., Jiang, L., Huang, S., et al. (2020). Rice plastidial NAD-dependent malate dehydrogenase 1 negatively regulates salt stress response by reducing the vitamin B6 content. *Plant Biotechnol. J.* 18, 172–184. doi: 10.1111/pbi.13184

Nicolas-Francès, V., Rossi, J., Rosnoblet, C., Pichereaux, C., Hichami, S., Astier, J., et al. (2022). S-nitrosation of arabidopsis thaliana protein tyrosine phosphatase 1 prevents its irreversible oxidation by hydrogen peroxide. *Front. Plant Sci.* 13. doi: 10.3389/fpls.2022.807249

Niu, L., Yu, J., Liao, W., Xie, J., Yu, J., Lv, J., et al. (2019). Proteomic investigation of s-nitrosylated proteins during NO-induced adventitious rooting of cucumber. *IJMS* 20, 5363. doi: 10.3390/ijms20215363

Noctor, G., and Foyer, C. H. (2016). Intracellular redox compartmentation and ROS-related communication in regulation and signaling. *Plant Physiol.* 171, 1581–1592. doi: 10.1104/pp.16.00346

Nyström, T. (2005). Role of oxidative carbonylation in protein quality control and senescence. *EMBO J.* 24, 1311–1317. doi: 10.1038/sj.emboj.7600599

Ortega-Galisteo, A. P., Rodríguez-Serrano, M., Pazmiño, D. M., Gupta, D. K., Sandalio, L. M., and Romero-Puertas, M. C. (2012). S-nitrosylated proteins in pea (Pisum sativum l.) leaf peroxisomes: changes under abiotic stress. *J. Exp. Bot.* 63, 2089–2103. doi: 10.1093/jxb/err414

Palma, J. M., Mateos, R. M., López-Jaramillo, J., Rodríguez-Ruiz, M., González-Gordo, S., Lechuga-Sancho, A. M., et al. (2020). Plant catalases as NO and H2S targets. *Redox Biol.* 34, 101525. doi: 10.1016/j.redox.2020.101525

Pande, A., Mun, B. G., Rahim, W., Khan, M., Lee, D. S., Lee, G. M., et al. (2022). Phytohormonal regulation through protein s-nitrosylation under stress. *Front. Plant Sci.* 13. doi: 10.3389/fpls.2022.865542

Pardo-Hernández, M., López-Delacalle, M., Martí-Guillen, J. M., Martínez-Lorente, S. E., and Rivero, R. M. (2021). ROS and NO phytomelatonin-induced signaling mechanisms under metal toxicity in plants: A review. *Antioxidants* 10, 775. doi: 10.3390/antiox10050775

Pardo-Hernández, M., López-Delacalle, M., and Rivero, R. M. (2020). ROS and NO regulation by melatonin under abiotic stress in plants. *Antioxidants (Basel)* 9, 1078. doi: 10.3390/antiox9111078

Pathak, M. R., Teixeira da Silva, J. A., and Wani, S. H. (2014). Polyamines in response to abiotic stress tolerance through transgenic approaches. *GM Crops Food* 5, 87–96. doi: 10.4161/gmcr.28774

Paul, S., and Roychoudhury, A. (2020). Regulation of physiological aspects in plants by hydrogen sulfide and nitric oxide under challenging environment. *Physiologia Plantarum* 168, 374–393. doi: 10.1111/ppl.13021

Paul, B. D., and Snyder, S. H. (2012). H_2S signalling through protein sulfhydration and beyond. *Nat. Rev. Mol. Cell Biol.* 13, 499–507. doi: 10.1038/nrm3391

Petřivalský, M., and Luhová, L. (2020). Nitrated nucleotides: New players in signaling pathways of reactive nitrogen and oxygen species in plants. *Front. Plant Sci.* 11. doi: 10.3389/fpls.2020.00598

Poetsch, A. R. (2020). The genomics of oxidative DNA damage, repair, and resulting mutagenesis. *Comput. Struct. Biotechnol. J.* 18, 207–219. doi: 10.1016/j.csbj.2019.12.013

Polge, C., Jaquinod, M., Holzer, F., Bourguignon, J., Walling, L., and Brouquisse, R. (2009). Evidence for the existence in arabidopsis thaliana of the proteasome proteolytic pathway. *J. Biol. Chem.* 284, 35412–35424. doi: 10.1074/jbc.M109.035394

Puyaubert, J., Fares, A., Rézé, N., Peltier, J.-B., and Baudouin, E. (2014). Identification of endogenously s-nitrosylated proteins in arabidopsis plantlets: Effect of cold stress on cysteine nitrosylation level. *Plant Sci.* 215–216, 150–156. doi: 10.1016/j.plantsci.2013.10.014

Rabbani, N., Al-Motawa, M., and Thornalley, P. J. (2020). Protein glycation in plants–an under-researched field with much still to discover. *Int. J. Mol. Sci.* 21, 3942. doi: 10.3390/ijms21113942

Rey, P., Bécuwe, N., Barrault, M.-B., Rumeau, D., Havaux, M., Biteau, B., et al. (2007). The arabidopsis thaliana sulfiredoxin is a plastidic cysteine-sulfinic acid reductase involved in the photooxidative stress response. *Plant J.* 49, 505–514. doi: 10.1111/j.1365-313X.2006.02969.x

Richter, A. S., Wang, P., and Grimm, B. (2016). Arabidopsis mg-protoporphyrin IX methyltransferase activity and redox regulation depend on conserved cysteines. *Plant Cell Physiol.* 57, 519–527. doi: 10.1093/pcp/pcw007

Rinalducci, S., Campostrini, N., Antonioli, P., Righetti, P. G., Roepstorff, P., and Zolla, L. (2005). Formation of truncated proteins and high-molecular-mass aggregates upon soft illumination of photosynthetic proteins. *J. Proteome Res.* 4, 2327–2337. doi: 10.1021/pr0502368

Rinalducci, S., Murgiano, L., and Zolla, L. (2008). Redox proteomics: basic principles and future perspectives for the detection of protein oxidation in plants. *J. Exp. Bot.* 59, 3781–3801. doi: 10.1093/jxb/ern252

Rivero, R. M., Mestre, T. C., Mittler, R., Rubio, F., Garcia-Sanchez, F., and Martinez, V. (2014). The combined effect of salinity and heat reveals a specific physiological, biochemical and molecular response in tomato plants. *Plant Cell Environ.* 37, 1059–1073. doi: 10.1111/pce.12199

Roach, T., and Krieger-Liszkay, A. (2014). Regulation of photosynthetic electron transport and photoinhibition. *Curr. Protein Pept. Sci.* 15, 351–362. doi: 10.2174/1389203715666140327105143

Romero-Puertas, M. C., Laxa, M., Mattè, A., Zaninotto, F., Finkemeier, I., Jones, A. M. E., et al. (2007). S-nitrosylation of peroxiredoxin II e promotes peroxynitrite-mediated tyrosine nitration. *Plant Cell* 19, 4120–4130. doi: 10.1105/tpc.107.055061

Rouhier, N., Vieira Dos Santos, C., Tarrago, L., and Rey, P. (2006). Plant methionine sulfoxide reductase a and b multigenic families. *Photosynth Res.* 89, 247–262. doi: 10.1007/s11120-006-9097-1

Ryšlavá, H., Doubnerová, V., Kavan, D., and Vaněk, O. (2013). Effect of posttranslational modifications on enzyme function and assembly. *J. Proteomics* 92, 80–109. doi: 10.1016/j.jprot.2013.03.025

Sainz, M., Calvo-Begueria, L., Pérez-Rontomé, C., Wienkoop, S., Abián, J., Staudinger, C., et al. (2015). Leghemoglobin is nitrated in functional legume nodules in a tyrosine residue within the heme cavity by a nitrite/peroxide-dependent mechanism. *Plant J.* 81, 723–735. doi: 10.1111/tpj.12762

Sano, N., Rajjou, L., and North, H. M. (2020). Lost in translation: Physiological roles of stored mRNAs in seed germination. *Plants (Basel)* 9, E347. doi: 10.3390/plants9030347

Sawa, T., Ihara, H., Ida, T., Fujii, S., Nishida, M., and Akaike, T. (2013). Formation, signaling functions, and metabolisms of nitrated cyclic nucleotide. *Nitric. Oxide* 34, 10–18. doi: 10.1016/j.niox.2013.04.004

Serpa, V., Vernal, J., Lamattina, L., Grotewold, E., Cassia, R., and Terenzi, H. (2007). Inhibition of AtMYB2 DNA-binding by nitric oxide involves cysteine s-nitrosylation. *Biochem. Biophys. Res. Commun.* 361, 1048–1053. doi: 10.1016/j.bbrc.2007.07.133

Sevilla, F., Camejo, D., Ortiz-Espín, A., Calderón, A., Lázaro, J. J., and Jiménez, A. (2015). The thioredoxin/peroxiredoxin/sulfiredoxin system: current overview on its redox function in plants and regulation by reactive oxygen and nitrogen species. *J. Exp. Bot.* 66, 2945–2955. doi: 10.1093/jxb/erv146

Shacter, E. (2000). QUANTIFICATION AND SIGNIFICANCE OF PROTEIN OXIDATION IN BIOLOGICAL SAMPLES*. *Drug Metab. Rev.* 32, 307–326. doi: 10.1081/DMR-100102336

Shen, B., Jensen, R. G., and Bohnert, H. J. (1997). Increased resistance to oxidative stress in transgenic plants by targeting mannitol biosynthesis to chloroplasts. *Plant Physiol.* 113, 1177–1183. doi: 10.1104/pp.113.4.1177

Simms, C. L., Hudson, B. H., Mosior, J. W., Rangwala, A. S., and Zaher, H. S. (2014). An active role for the ribosome in determining the fate of oxidized mRNA. *Cell Rep.* 9, 1256–1264. doi: 10.1016/j.celrep.2014.10.042

Skubacz, A., Daszkowska-Golec, A., and Szarejko, I. (2016). The role and regulation of ABI5 (ABA-insensitive 5) in plant development, abiotic stress responses and phytohormone crosstalk. *Front. Plant Sci.* 7. doi: 10.3389/fpls.2016.01884

Smakowska, E., Czarna, M., and Janska, H. (2014). Mitochondrial ATP-dependent proteases in protection against accumulation of carbonylated proteins. *Mitochondrion* 19 Pt B, 245–251. doi: 10.1016/j.mito.2014.03.005

Song, S., Wang, H., Sun, M., Tang, J., Zheng, B., Wang, X., et al. (2019). Reactive oxygen species-mediated BIN2 activity revealed by single-molecule analysis. *New Phytol.* 223, 692–704. doi: 10.1111/nph.15669

Suzuki, N., Miller, G., Morales, J., Shulaev, V., Torres, M. A., and Mittler, R. (2011). Respiratory burst oxidases: the engines of ROS signaling. *Curr. Opin. Plant Biol.* 14, 691–699. doi: 10.1016/j.pbi.2011.07.014

Tada, Y., Spoel, S. H., Pajerowska-Mukhtar, K., Mou, Z., Song, J., Wang, C., et al. (2008). Plant immunity requires conformational charges of NPR1 *via* s-nitrosylation and thioredoxins. *Science* 321, 952–956. doi: 10.1126/science.1156970

Tanou, G., Job, C., Rajjou, L., Arc, E., Belghazi, M., Diamantidis, G., et al. (2009). Proteomics reveals the overlapping roles of hydrogen peroxide and nitric oxide in the acclimation of citrus plants to salinity. *Plant J.* 60, 795–804. doi: 10.1111/j.1365-313X.2009.04000.x

Tarrago, L., Laugier, E., Zaffagnini, M., Marchand, C., Le Maréchal, P., Rouhier, N., et al. (2009). Regeneration mechanisms of arabidopsis thaliana methionine sulfoxide reductases b by glutaredoxins and thioredoxins. *J. Biol. Chem.* 284, 18963–18971. doi: 10.1074/jbc.M109.015487

Tavares, C. P., Vernal, J., Delena, R. A., Lamattina, L., Cassia, R., and Terenzi, H. (2014). S-nitrosylation influences the structure and DNA binding activity of AtMYB30 transcription factor from arabidopsis thaliana. *Biochim. Biophys. Acta* 1844, 810–817. doi: 10.1016/j.bbapap.2014.02.015

Terrile, M. C., París, R., Calderón-Villalobos, L. I. A., Iglesias, M. J., Lamattina, L., Estelle, M., et al. (2012). Nitric oxide influences auxin signaling through s-nitrosylation of the arabidopsis TRANSPORT INHIBITOR RESPONSE 1 auxin receptor. *Plant J.* 70, 492–500. doi: 10.1111/j.1365-313X.2011.04885.x

Triantaphylidès, C., and Havaux, M. (2009). Singlet oxygen in plants: production, detoxification and signaling. *Trends Plant Sci.* 14, 219–228. doi: 10.1016/j.tplants.2009.01.008

Vaahtera, L., Brosché, M., Wrzaczek, M., and Kangasjärvi, J. (2014). Specificity in ROS signaling and transcript signatures. *Antioxid Redox Signal* 21, 1422–1441. doi: 10.1089/ars.2013.5662

Vandelle, E., and Delledonne, M. (2011). Peroxynitrite formation and function in plants. *Plant Sci.* 181, 534–539. doi: 10.1016/j.plantsci.2011.05.002

Vogt, W. (1995). Oxidation of methionyl residues in proteins: tools, targets, and reversal. *Free Radic. Biol. Med.* 18, 93–105. doi: 10.1016/0891-5849(94)00158-g

Wang, P., Du, Y., Hou, Y.-J., Zhao, Y., Hsu, C.-C., Yuan, F., et al. (2015). Nitric oxide negatively regulates abscisic acid signaling in guard cells by s-nitrosylation of OST1. *Proc. Natl. Acad. Sci. U.S.A.* 112, 613–618. doi: 10.1073/pnas.1423481112

Wang, Y.-Q., Feechan, A., Yun, B.-W., Shafiei, R., Hofmann, A., Taylor, P., et al. (2009). S-nitrosylation of AtSABP3 antagonizes the expression of plant immunity. *J. Biol. Chem.* 284, 2131–2137. doi: 10.1074/jbc.M806782200

Wang, Y., Yun, B.-W., Kwon, E., Hong, J. K., Yoon, J., and Loake, G. J. (2006). S-nitrosylation: an emerging redox-based post-translational modification in plants. *J. Exp. Bot.* 57, 1777–1784. doi: 10.1093/jxb/erj211

Waszczak, C., Akter, S., Eeckhout, D., Persiau, G., Wahni, K., Bodra, N., et al. (2014). Sulfenome mining in *Arabidopsis thaliana*. *Proc. Natl. Acad. Sci. U.S.A.* 111, 11545–11550. doi: 10.1073/pnas.1411607111

Waszczak, C., Akter, S., Jacques, S., Huang, J., Messens, J., and Van Breusegem, F. (2015). Oxidative post-translational modifications of cysteine residues in plant signal transduction. *J. Exp. Bot.* 66, 2923–2934. doi: 10.1093/jxb/erv084

Wilson, I. D., Neill, S. J., and Hancock, J. T. (2008). Nitric oxide synthesis and signalling in plants. *Plant Cell Environ.* 31, 622–631. doi: 10.1111/j.1365-3040.2007.01761.x

Wu, F., Chi, Y., Jiang, Z., Xu, Y., Xie, L., Huang, F., et al. (2020). Hydrogen peroxide sensor HPCA1 is an LRR receptor kinase in arabidopsis. *Nature* 578, 577–581. doi: 10.1038/s41586-020-2032-3

Yang, H., Mu, J., Chen, L., Feng, J., Hu, J., Li, L., et al. (2015). S-nitrosylation positively regulates ascorbate peroxidase activity during plant stress responses. *Plant Physiol.* 167, 1604–1615. doi: 10.1104/pp.114.255216

Yun, B.-W., Feechan, A., Yin, M., Saidi, N. B. B., Le Bihan, T., Yu, M., et al. (2011). S-nitrosylation of NADPH oxidase regulates cell death in plant immunity. *Nature* 478, 264–268. doi: 10.1038/nature10427

Zaffagnini, M., Morisse, S., Bedhomme, M., Marchand, C. H., Festa, M., Rouhier, N., et al. (2013). Mechanisms of nitrosylation and denitrosylation of cytoplasmic glyceraldehyde-3-phosphate dehydrogenase from arabidopsis thaliana*. *J. Biol. Chem.* 288, 22777–22789. doi: 10.1074/jbc.M113.475467

Zechmann, B. (2020). Subcellular roles of glutathione in mediating plant defense during biotic stress. *Plants (Basel)* 9, 1067. doi: 10.3390/plants9091067

Zhao, J. (2007). Interplay among nitric oxide and reactive oxygen species. *Plant Signaling Behav.* 2, 544–547. doi: 10.4161/psb.2.6.4802

Zhou, X., Joshi, S., Patil, S., Khare, T., and Kumar, V. (2022). Reactive oxygen, nitrogen, carbonyl and sulfur species and their roles in plant abiotic stress responses and tolerance. *J. Plant Growth Regul.* 41, 119–142. doi: 10.1007/s00344-020-10294-y

Zhou, H., Zhang, J., Shen, J., Zhou, M., Yuan, X., and Xie, Y. (2020). Redox-based protein persulfidation in guard cell ABA signaling. *Plant Signaling Behav.* 15, 1741987. doi: 10.1080/15592324.2020.1741987

frontiers | Frontiers in Plant Science

TYPE Original Research
PUBLISHED 22 December 2022
DOI 10.3389/fpls.2022.1058831

Chloroplast-localized GUN1 contributes to the acquisition of basal thermotolerance in *Arabidopsis thaliana*

Cecilia Lasorella[1†], Stefania Fortunato[1†], Nunzio Dipierro[1], Nicolaj Jeran[2], Luca Tadini[2], Federico Vita[1], Paolo Pesaresi[2] and Maria Concetta de Pinto[1*]

[1]Department of Bioscience, Biotechnology and Environment University of Bari Aldo Moro, Bari, Italy, [2]Department of Biosciences, University of Milano, Milano, Italy

OPEN ACCESS

EDITED BY
Laura De Gara,
Campus Bio-Medico University, Italy

REVIEWED BY
Rosa M. Rivero,
Center for Edaphology and Applied Biology of Segura (CSIC), Spain
Karin Krupinska,
University of Kiel, Germany
Piotr Gawroński,
Warsaw University of Life Sciences-SGGW, Warsaw, Poland

*CORRESPONDENCE
Maria Concetta de Pinto
mariaconcetta.depinto@uniba.it

†These authors have contributed equally to this work

SPECIALTY SECTION
This article was submitted to Plant Abiotic Stress, a section of the journal Frontiers in Plant Science

RECEIVED 30 September 2022
ACCEPTED 05 December 2022
PUBLISHED 22 December 2022

CITATION
Lasorella C, Fortunato S, Dipierro N, Jeran N, Tadini L, Vita F, Pesaresi P and de Pinto MC (2022) Chloroplast-localized GUN1 contributes to the acquisition of basal thermotolerance in *Arabidopsis thaliana*. *Front. Plant Sci.* 13:1058831. doi: 10.3389/fpls.2022.1058831

Heat stress (HS) severely affects different cellular compartments operating in metabolic processes and represents a critical threat to plant growth and yield. Chloroplasts are crucial for heat stress response (HSR), signaling to the nucleus the environmental challenge and adjusting metabolic and biosynthetic functions accordingly. GENOMES UNCOUPLED 1 (GUN1), a chloroplast-localized protein, has been recognized as one of the main players of chloroplast retrograde signaling. Here, we investigate HSR in Arabidopsis wild-type and *gun1* plantlets subjected to 2 hours of HS at 45°C. In wild-type plants, Reactive Oxygen Species (ROS) accumulate promptly after HS, contributing to transiently oxidize the cellular environment and acting as signaling molecules. After 3 hours of physiological recovery at growth temperature (22°C), the induction of enzymatic and non-enzymatic antioxidants prevents oxidative damage. On the other hand, *gun1* mutants fail to induce the oxidative burst immediately after HS and accumulate ROS and oxidative damage after 3 hours of recovery at 22°C, thus resulting in enhanced sensitivity to HS. These data suggest that GUN1 is required to oxidize the cellular environment, participating in the acquisition of basal thermotolerance through the redox-dependent plastid-to-nucleus communication.

KEYWORDS

heat stress, GENOMES UNCOUPLED 1, reactive oxygen species, redox regulation, retrograde signaling, thermotolerance

Introduction

Plants are constantly exposed to abiotic stresses throughout their entire life cycle, which heavily impact growth and yield. The effects of climate change increase the frequency and intensity of extreme events such as heat waves, compromising plant development and crop productivity irreversibly (Bita and Gerats, 2013). Among abiotic stresses, heat stress (HS) is considered one of the most detrimental for plants, since extreme temperature fluctuations cause impairment in essential biochemical and physiological processes (Hasanuzzaman et al., 2013). As sessile organisms, plants sense and respond to adverse environmental conditions activating defense systems (Zhu, 2016). The study of the mechanisms involved in plant perception and response to heat has, therefore, a great relevance in the actual climatic scenario.

Considering that photosynthesis-related processes are sensitive to thermal fluctuations, chloroplasts have been proposed as sensors of HS (Sun and Guo, 2016). Among the chloroplast protein complexes, the photosystem II, its oxygen-evolving complex, the electron transport chain and the carbon fixation system are particularly prone to damage due to high temperatures (Allakhverdiev et al., 2008). Furthermore, heat stress reduces the content of photosynthesis-associated pigments and alters cell membrane stability by protein denaturation and lipid peroxidation (Wise et al., 2004; Wahid et al., 2007; Allakhverdiev et al., 2008). The HS-mediated damage to photosynthetic apparatus inhibits the excitation energy transfer and the electron transport in the chloroplast, leading to an overproduction of Reactive Oxygen Species (ROS) and to an imbalance of redox homeostasis (Wang et al., 2018). ROS are produced in plastids in the forms of singlet oxygen, superoxide anion (O_2-), hydroxyl radicals and hydrogen peroxide (H_2O_2) (Noctor et al., 2002). ROS accumulation is controlled by scavenging and antioxidant machinery, including enzymes such as superoxide dismutase (SOD), catalases (CAT), ascorbate peroxidases (APX), and low molecular weight metabolites, like ascorbate (ASC), glutathione (GSH), tocopherols and carotenoids (Foyer and Noctor, 2013; Das et al., 2015). Although ROS were initially recognized as toxic by-products, a large number of evidence has shown the important role that these molecules may have in many essential plant processes (Farnese et al., 2016; Mittler, 2017). The role of ROS as oxidants or components of redox signaling mostly depends on a fine balance between the production and scavenging of these molecules in different organelles (Mittler, 2017).

In response to stress conditions, ROS can leave their production sites and, acting as secondary messengers, activate several signaling events (Pogson et al., 2008; Suzuki et al., 2012; Sgobba et al., 2015). In response to high temperatures, for instance, ROS act as retrograde signals, transmitting to the nucleus the redox alterations occurring in plastids (Singh et al., 2015; Hu et al., 2020);. In particular, ROS have been observed to elicit and regulate antioxidant enzymes and Heat Shock Proteins (HSPs) (Nishizawa et al., 2006; Volkov et al., 2006; Dickinson et al., 2018). Moreover, the presence of heat shock elements (HSE) in the promoter region of the Arabidopsis *APX1* and *APX2*, together with the increased thermo-sensitivity of Arabidopsis mutants defective in the biosynthetic pathways of antioxidants, supports the idea that a tight connection between ROS homeostasis and acclimation to HS exists (Pnueli et al., 2003; Larkindale et al., 2005).

In the last decades, plastid-localized Genomes Uncoupled (GUN) proteins have been identified as crucial in several processes involved in retrograde signaling (Susek et al., 1993; Mochizuki et al., 2001; Larkin et al., 2003; Strand et al., 2003; Koussevitzky et al., 2007; Woodson et al., 2011). Through chemical alteration of chloroplast biogenesis and physiology by either lincomycin (Lin) or norflurazon (NF) treatments, respectively, six *gun* mutants were isolated (Susek et al., 1993). After exposure to NF, all *gun* mutants expressed photosynthesis-associated nuclear genes (PhANGs), which on the contrary were repressed in wild type seedlings. Thus, it has been assumed that mutations in *GUN* genes led to the uncoupling of nuclear gene expression (NGE) with respect to the functional state of the chloroplast (Nott et al., 2006). GUN1 is a nuclear-encoded pentatricopeptide repeat protein with a C-terminal Small MutS-Relate domain, described as key player of plastid-to-nucleus retrograde signaling, response and adaptation to environmental challenges and plastid development (Koussevitzky et al., 2007; Wu et al., 2018; Pesaresi and Kim, 2019). Based on its amino acid sequence, GUN1 was initially identified as a nucleic acid-binding protein involved in DNA metabolism, gene expression, and DNA repair in the plastids (Koussevitzky et al., 2007). Successively, it has been proposed that GUN1 interacts with proteins rather than with nucleic acids. Among GUN1-interacting proteins, enzymes of the tetrapyrrole biosynthesis pathway and several proteins that participate in plastid gene expression (PGE) and protein homeostasis, such as plastid chaperons, have been identified (Colombo et al., 2016; Tadini et al., 2016; Zhao et al., 2019; Tadini et al., 2020; Wu and Bock, 2021). The identification of GUN1 putative interactors highlighted the role of GUN1 as a hub of multiple retrograde signaling pathways.

Despite the great attention on GUN1 role in the communication between chloroplast and nucleus, little information exists about its involvement in the signaling defense activated in response to HS. Here, we studied the role and interplay of GUN1 and redox signaling in heat stress response (HSR). The results indicate that *gun1* mutants are more sensitive to HS than wild-type plants and suggest that GUN1 could be required for basal thermotolerance, participating in the ROS-dependent oxidization of cellular environment, which is the basis for communication of plastid impairment to the nucleus.

Materials and methods

Plant materials, growth conditions and heat stress treatment

The Arabidopsis (*Arabidopsis thaliana*, genetic background Col-0) *gun1-102* T-DNA insertion mutant was previously described in Tadini et al. (2016). Wild type (wt) and *gun1-102* (hereafter indicated as *gun1*) seeds were surface-sterilized and sown out on Murashige and Skoog medium (Duchefa, Haarlem, The Netherlands) supplemented with 2% (w/v) sucrose and 1.5% (w/v) Phyto-Agar (Duchefa). After 2 days of stratification at 4°C in the dark, plantlets were grown in a growth chamber for 15 days (22°C, 80 µmol m^{-2} sec^{-1} on 16 h/8 h light/dark cycles).

On day 15, Arabidopsis wild-type and *gun1* plants were exposed to heat stress (45°C for 2 hours) according to Ling et al. (2018). To allow short-term and long-term physiological recovery, plants were then incubated in growth conditions (22°C) for 3 hours or 2 days, respectively. Samples for analysis were collected before HS (C), immediately after HS treatment, and after 3 hours (R) and 2 days (2d-RHS) of physiological recovery. Control plants for the experiments of 2d-RHS were collected after 17 days of growth at 22°C. Each biological replicate consisted of 90 plantlets per condition. Five biological replicates per timepoint were used while each experiment was repeated at least three times.

To measure root length in control, HS and recovery conditions, agar plates were oriented vertically in comparable growth conditions described above. To determine pigment contents leaves were separated from the roots, frozen in liquid nitrogen and stored at -80°C until analysis.

Determination of pigment content and maximum quantum yield of PSII

For pigment quantification, leaf samples (50 mg) were ground in liquid nitrogen with 80% acetone (1:20 w/v) and the homogenates centrifuged at 20,000 g for 20 minutes at 4°C. The supernatant absorbances at 663.2, 646.8 and 470 nm were spectrophotometrically measured according to Zhang and Kirkham (1996). Content of chlorophyll a (Chl a) and chlorophyll b (Chl b), as well as total carotenoids (xanthophyll and β-carotene), expressed as µg g^{-1} fresh weight, were calculated according to Lichtenthaler (1987):

$$\text{Chlorophyll a} = 12.25A_{663.2} - 2.79A_{646.8}$$

$$\text{Chlorophyll b} = 21.50A_{646.8} - 5.10A_{663.2}$$

$$\text{Carotenoids} = (1000A_{470} - 1.82C_a - 85.02C_b)/198$$

The maximum quantum yield of PSII (*Fv/Fm*) was measured by using the Imaging PAM (Walz, Effeltrich, Germany) as described in Tadini et al. (2012).

Proteasome activity

Proteasome activity was determined spectrofluorometrically by using the fluorogenic substrate Suc-LLYY-NH-AMC (Calbiochem), according to Paradiso et al. (2020). Arabidopsis plantlets were ground in liquid nitrogen and homogenized in a 1:3 (w/v) ratio with extraction buffer (50 mM Hepes-KOH, pH 7.2, 2 mM DTT, 2 mM ATP, 250 mM sucrose). After centrifugation at 20,000xg for 15 min at 4°C, supernatants were collected. 660 µL of samples, with 1mg mL^{-1} protein concentration, were mixed with 40 µL of assay buffer (100 mM Hepes-KOH, pH 7.8, 5mM $MgCl_2$, 10 mM KCl, 2 mM ATP). After 15 min of incubation at 30°C in the dark, the reaction was started by the addition of the fluorogenic substrate. The release of amino-methyl-coumarin (360 nm ex/460 nm em) was monitored between 0 and 120 min by RF-6000 spectrofluorophotometer (Shimadzu Corporation, Japan). Protein concentration was measured using Protein Assay System (Bio-Rad, Hercules, CA, USA) according to Bradford (1976), with serum albumin as standard.

Determination of ROS and oxidative markers

In situ O_2- and H_2O_2 accumulation in leaves was detected with nitroblue tetrazolium (NBT) and 3,3-diaminobenzidine (DAB), respectively, as described in Fortunato et al. (2022). The staining intensity was digitally acquired and quantified by ImageJ software (https://imagej.nih.gov/ij/). The relative O_2- and H_2O_2 levels were calculated as the percentage of NBT- and DAB-stained area of leaves, respectively.

The level of lipid peroxidation was evaluated in terms of malondialdehyde (MDA) content determined by the TBA reaction, as described by Paradiso et al. (2008). The amount of MDA-TBA complex was calculated using an extinction coefficient of 155 mM^{-1} cm^{-1}.

Protein oxidation was spectrophotometrically determined by measuring the content of carbonyl-groups reacting with dinitrophenylhydrazine (DNPH), according to Romero-Puertas et al. (2002). Carbonyl content was calculated using an extinction coefficient of 22 mM^{-1} cm^{-1}.

Analysis of enzymatic and non-enzymatic antioxidants

For ascorbate (ASC) and glutathione (GSH) analysis, 0.3 g of samples were homogenized at 4°C with 1.8 mL 5% (v/v)

trichloroacetic acid. After centrifugation at 18,000 x g for 20 minutes, the supernatants were collected and ASC and GSH levels were determined through the colorimetric assay described in de Pinto et al. (1999).

For quantifying the enzymatic antioxidant activities, 100 mg of samples were ground to fine powder in liquid nitrogen and mixed with 0.4 mL extraction buffer containing 50mM Tris-HCl pH 7.5, 0.05% (w/v) cysteine, 0.1% bovine serum albumin, 1 mM phenylmethanesulfonylfluoride. To determine the ascorbate peroxidase activity, 1 mM ASC was added to the buffer. After centrifugation at 20,000 x g for 20 minutes at 4°C, the supernatants were used for the spectrophotometric analysis.

Superoxide dismutase (SOD, EC 1.15.1.1) and catalase (CAT, EC 1.11.1.6) activities were spectrophotometrically determined following the methods described in Paradiso et al. (2020). Ascorbate peroxidase (APX, EC 1.11.1.11) was assayed according to de Pinto et al. (2000).

For Western Blot analyses of SOD, CAT and APX, total proteins were extracted from plantlets as described by Fortunato et al. (2022) and successively separated by SDS PAGE. Then, proteins were electrophoretically transferred to polyvinylidene fluoride membranes and incubated with the following specific antibodies: L-ascorbate peroxidase primary polyclonal antibody (n. AS08 368, Agrisera Vännäs, Sweden), which recognizes thylakoidal, stromal and cytosolic isoforms; Catalase (peroxisomal marker) primary polyclonal antibody (n. AS09 501, Agrisera Vännäs, Sweden); Fe-SOD primary polyclonal antibody (n. AS06 125, Agrisera Vännäs, Sweden), and the FTSH5 kindly donated by Wataru Sakamoto (Okayama University). As secondary antibody, the horseradish peroxidase (HRP)- conjugate Anti-Rabbit IgG (Promega, Madison, WI, USA) was used. Chemiluminescent signals were detected and quantified by ChemiDoc MP Imaging System and Quantity One® software (Bio-Rad Laboratories, Hercules, CA, USA), respectively.

Quantitative real-time PCR

Total RNA extraction was achieved using the Nippon Genetics Kit according to manufacturer protocol, using 50 mg (fresh weight) of leaf material. RNA concentration was determined by measuring the absorbance at 260 nm with NanoDrop2000 (Thermo Fisher Scientific, USA). cDNA was synthesized from 2µg of total RNA, using the iScript™ cDNA Synthesis Kit purchased by Bio-Rad according to the manufacturer's instructions. Gene expression analysis (qPCR) was performed using the BIO-RAD CFX Connect system (Bio-Rad, Hercules, CA, USA) employing 37.5 ng of cDNA for each reaction and SsoAdvanced Universal SYBR Green Supermix (Bio-Rad), according to the manufacturer's instruction for the detection system (Bio-Rad). *Ubiquitin10* (At4g05320) and *Actin8* (At1g49240) were used as housekeeping genes and three technical replicates were performed for each biological replicate (n=3). In all experiments, no template controls were also used. Housekeeping data were normalized according to Riedel et al. (2014).

Primers for quantitative real-time PCR (qRT-PCR) were designed by using Primer3 software (http://primer3.ut.ee/) and then double-checked using net primer software (http://www.premierbiosoft.com/netprimer/), except for the housekeeper primers (Giuntoli et al., 2017). Primer sequences used for quantitative PCR (qPCR) analyses are reported in Table S1.

Separation of real-time PCR products on 2% (w/v) agarose gels revealed single bands of the expected molecular weight. Relative quantification was performed according to the comparative Ct (threshold cycle) method ($2^{-\Delta\Delta Ct}$); (Livak and Schmittgen, 2001).

Statistical analysis

The data were expressed as the means ± standard error (SE). One-way analysis of variance (ANOVA) followed by a *post-hoc* Tukey's comparison test was used to calculate the difference between genotypes and treatments. Differences were considered statistically significant at a p-value< 0.05. All statistical analyses were performed by Minitab software (Minitab Inc., State College, PA, USA).

Results

Heat stress sensitivity of wild type and *gun1* plantlets

To analyze heat stress sensitivity, growth rate parameters were measured in 17-day-old wild type (wt) and *gun1* mutant plantlets. Plants were grown for 15 days at 22°C and exposed for 2 hours at 45°C (Heat Stress, HS). Plantlets were then incubated transferred in growth conditions to their optimal growth conditions (22°C; see *Materials and methods*) for 2 days to allow physiological recovery (2d-RHS), which was assessed by monitoring the photosynthetic parameter Fv/Fm. As a control (C), wt and *gun1* plants were grown at 22°C for 17 days. The phenotypical analysis showed that, after 2 days of recovery from HS (2d-RHS), *gun1* plantlets were significantly smaller than wt (Figure 1A). The visible phenotype was confirmed by measuring whole plant fresh weight, which resulted significantly decreased in *gun1* plantlets subjected to HS but did not show significant differences in wt plantlets, when compared to the untreated controls (Figure 1B). Root length did not change in HS-treated wt while, on the contrary, *gun1* roots were shorter than wt, already under control conditions, and the exposure to HS further reduced root elongation (Figure 1C). The photosynthetic efficiency, measured as the maximum quantum yield of PSII

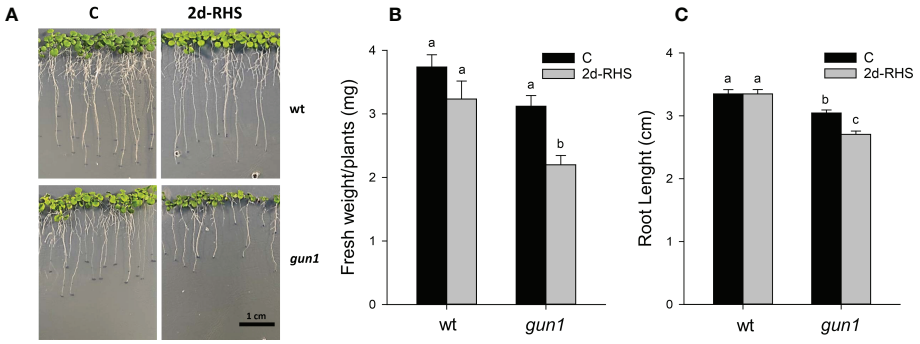

FIGURE 1
Growth parameters of 17-day-old wt and *gun1* plantlets, grown at control temperature (C) or subjected, after 15 days, to Heat Stress (HS; 2 hours at 45°C), followed by long-term recovery (2d-RHS; 2 days at 22°C). **(A)** Representative image of visible phenotypes, **(B)** Fresh Weight and **(C)** Root Length of plantlets measurements. The values are the means ± standard errors of five independent experiments. Different letters indicate significant differences obtained by one-way ANOVA test (P< 0.05).

(*Fv/Fm*), resulted decreased in a similar way in wt and *gun1* plantlets at 2d-RHS, when compared to control conditions (Figure 2A). Consistently, chlorophyll a and b content did not change significantly between wt and *gun1* (Figures 2B, C). On the other hand, a significant drop in carotenoid accumulation occurred in *gun1* mutant only (Figure 2D).

To dissect more in detail the molecular mechanisms underlying *gun1* sensitivity to heat, the transcript level of heat-dependent genes was assessed by quantitative Real-Time PCR (qRT-PCR) in 15 days-old plants before (C), right after the heat stress (HS, 2 hours at 45°C) and upon 3 hours of recovery at 22° C (R), when phenotypic differences were not detectable (Table S2). To this aim, the expression level of heat shock factor A2 (*HsfA2*), a key regulator of the heat stress response, and some heat shock proteins (*HSPs*), was studied. A significant and similar increase in the transcript levels of the nuclear *HsfA2*, the cytosolic *HSP101* and *HSP70* and the chloroplast *HSP26* occurred in response to HS in both wt and *gun1* genotypes. After 3h recovery (R), *HsfA2* and *HSP101* expression decreased in both genotypes, however, the reduction of both transcripts was more marked in *gun1* than in wt (Figures 3A, B). In addition, the expression of *HSP70* and *HSP26* did not change significantly after recovery (R) in wt, unlike in *gun1* (Figures 3C, D). To verify whether in *gun1* mutants heat stress could induce cytosolic folding stress, caused by the accumulation of plastid protein precursors and over-accumulation of cytosolic HSPs, as occurred when the mutants were grown in lincomycin conditions (Wu et al., 2019; Tadini et al., 2020), proteasomal activity and accumulation of FTSH5 plastid protease were analyzed. The proteasome activity in wt and *gun1* plantlets grown in control conditions, upon HS and after recovery did not display significant differences (Figure S1). Moreover, the accumulation of FTSH5 plastid protease pre-protein was not detectable upon HS treatment, while resulted to be accumulating in Lin-treated *gun1* seedlings, suggesting that Lin and HS trigger different non-overlapping signaling mechanisms (Figure S1).

ROS accumulation, oxidative markers, and hydrophilic antioxidants in wild type and *gun1* plantlets during HSR

ROS accumulation in response to HS was different between control and mutant genotypes (Figure 4). Under control conditions, the level of O_2-, visualized by NBT-staining, was significantly higher in *gun1* leaf tissue than in wt (Figure 4A). Nevertheless, in the *gun1* genetic background, the accumulation of O_2- decreased after HS, reaching bottom values after recovery (R). On the other hand, in wt, HS caused a prompt accumulation of O_2-, which successively decreased during the R phase (Figure 4A). Similarly, in wt, H_2O_2 levels, visualized by DAB-staining, increased after HS and returned to values comparable with control during the recovery (R) (Figure 4B). On the contrary, in *gun1*, H_2O_2 levels did not vary significantly after HS, but showed a high accumulation after recovery (Figure 4B). Furthermore, the level of lipid peroxidation was higher in *gun1* than in wt in control conditions (Figure 5A). This oxidative marker did not vary significantly in response to HS in wt plantlets, whereas it transiently increased in *gun1* mutants, to return to a baseline level after recovery. In wt, protein oxidation increased after HS and returned to values comparable with the control after recovery while, in *gun1* mutant background, the total level of protein carbonyl groups did not show significant changes after HS and R (Figure 5B). The total content of two major hydrophilic antioxidants, ascorbate (ASC) and glutathione (GSH), did not vary significantly between wt and *gun1*, under control conditions (Figures 5C, D). In *gun1*, the total content of the two antioxidants did not change either upon

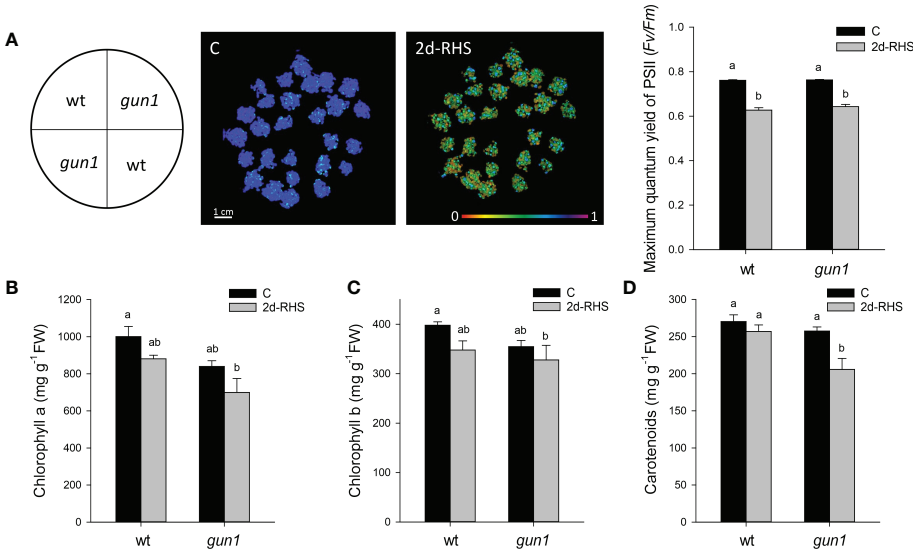

FIGURE 2
Photosynthetic parameters of 17 days-old wt and *gun1* plantlets, grown at control temperature (C) or subjected, after 15 days of growth, to Heat Stress (HS; 2 hours at 45°C), followed by long-term recovery (2d-RHS; 2 days at 22°C). **(A)** Photosynthetic performance of wt and *gun1*. The maximum quantum yield of PSII (*Fv/Fm*) was measured by using the IMAGING PAM (WALZ). **(B)** Chlorophyll a, **(C)** chlorophyll b and **(D)** carotenoids contents were as well determined. The values are the means ± standard errors of five independent experiments. Different letters indicate significant differences obtained by one-way ANOVA test (P< 0.05).

HS or after recovery (R). On the other hand, in wt total glutathione levels were lower after HS and both the antioxidants increased after recovery (Figures 5C, D). Moreover, only in wild type seedlings HS reduced the glutathione redox state, which returned to values comparable to control after recovery (Figure 5E).

Behaviour of ROS scavenging enzymes in wild type and *gun1* plantlets upon heat stress

To clarify the different accumulation of ROS in the two genotypes during the HSR, the behavior of the main ROS scavenging enzymes, namely superoxide dismutase (SOD), catalase (CAT) and ascorbate peroxidase (APX), was investigated.

Total SOD activity was similar in wt and *gun1* under control conditions and did not change significantly upon HS in both genotypes. After recovery (R), a rise in SOD activity occurred in wt control only (Figure 6A). The levels of FSD1 protein and transcript were analyzed by immunoblotting and qRT-PCR, respectively (Figures 6B, C). FSD1 protein accumulation was higher in wt than in *gun1* under control conditions. In both genotypes the protein level increased in response to HS, remaining at a higher level than control also after recovery (R) (Figure 6B). In wt plantlets, after HS a decrease in *FSD1* expression occurred, while during the recovery a clear and significant increase in the transcript level was observed (Figure 6C). The two thylakoidal Fe-SOD, *FSD2* and *FSD3* (Myouga et al., 2008), behaved differently when compared to *FSD1* (Figures 6D, E), which besides being present in the stroma of the chloroplast is also localized in the cytoplasm and nuclei (Dvořák et al., 2021). In both the genotypes, HS caused a strong decrease in *FSD2* expression, which remained low in *gun1* and increased in wt after recovery (Figure 6D). On the other hand, *FSD3* expression did not change in *gun1* in response to HS, while in wt decreased after HS and increased after recovery (Figure 6E). HS reduced the expression of cytosolic and chloroplastic copper/zinc superoxide dismutases (*CuZnSD1* and *CuZnSD2*, respectively) in both genotypes. However, after recovery (R), the transcript level of *CuZnSD1* and *CuZnSD2* was partially restored only in wt (Figures 6F, G).

In control conditions, total CAT activity, together with CAT2 protein and transcript levels were lower in *gun1* than in wt (Figure 7). HS caused, however, transient inhibition of CAT activity in wt only (Figure 7A). Despite the decrease in CAT activity observed in wt samples, CAT2 protein and transcript increased after HS, while did not significantly change in *gun1* (Figures 7B, C).

Moreover, after HS, total APX activity decreased in both genotypes, with a greater intensity in wt than in *gun1*. However, after recovery, APX activity was restored to control (C) level in wt while further decreased in *gun1* (Figure 8A). Western blotting analysis showed that in wt, the accumulation of cytosolic and

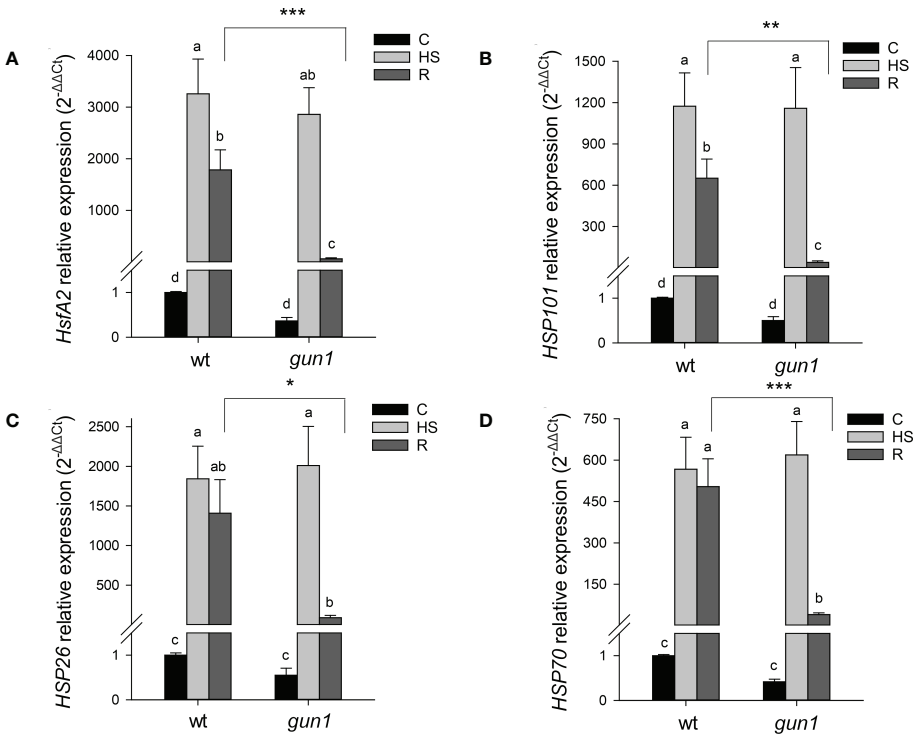

FIGURE 3
Relative expression of **(A)** *HsfA2*, **(B)** *HSP101*, **(C)** *HSP26* and **(D)** *HSP70* in 15 days-old wt and *gun1* plantlets, grown at control temperature (C) or subjected to Heat Stress (HS; 2 hours at 45°C), followed by short recovery (R; 3 hours at 22°C). The expression level of *HsfA2* and *HSPs* was normalized to that of *Ubiquitin10* (At4g05320) and *Actin8* (At1g49240) as internal references. For each sample, gene expression was related to the wt in control conditions **(C)**, set as 1. The values are the means ± SEs from three independent experiments, with three technical replicates for each experiment. Different letters indicate significant differences obtained by one-way ANOVA test ($p < 0.05$). T-test was applied to compare R samples among the genotypes. *$p \leq 0.05$; **$p \leq 0.01$; ***$p \leq 0.001$.

stromal APX was slightly increased upon HS, while the decrease of thylakoidal isoform was observed. On the other hand, in *gun1* samples, cytosolic and stromal APX isoenzymes showed a progressive decrease while tAPX accumulated in response to HS and decreased in R (Figure 8B).

In wt, the expression of cytosolic *APX1* was strongly reduced after HS and significantly increased after recovery, while in *gun1* not significant changes occurred (Figure 8C). The HS-inducible APX2 showed, however, highly increased expression after HS in both the genotypes. After recovery (R), *APX2* transcript remained high in wt and partially decreased in *gun1* (Figure 8C). At last, the expression of *tAPX* under control conditions was significantly lower in *gun1* than in wt. However, after HS a drop in *tAPX* transcript occurred in wt, while a progressive increase after HS and in R was observed in *gun1* mutants (Figure 8D).

Discussion

Retrograde signaling pathways allow the information flux from plastids to the nucleus. This intra-cellular communication becomes critical during chloroplast biogenesis (biogenic control) and upon alteration of plastid homeostasis in response to environmental stimuli (operational signaling) (Chan et al., 2016). GUN1-dependent signaling has been proposed as one of the main retrograde signaling pathways active during chloroplast biogenesis (Tadini et al., 2020; Shimizu and Masuda, 2021; Wu and Bock, 2021). Nevertheless, multiple evidence suggests that GUN1 also operates in adult plants, contributing to the operational control of chloroplasts (Cheng et al., 2011; Tadini et al., 2016; Guo et al., 2020). Indeed, GUN1 undergoes ta rapid turnover by the Clp protease, unless it becomes stable during the early stages of chloroplast biogenesis, and under stress conditions that trigger retrograde signaling pathways (Wu et al., 2018; Pesaresi and Kim, 2019).

GUN1 has been reported to be required for cold acclimation, as *gun1* seedlings fail to develop green functional chloroplasts when grown at 4°C (Marino et al., 2019). Moreover, the involvement of GUN1 in response to HS has been previously indicated by showing that *gun1* mutants have reduced basal thermotolerance but do not appear to be impaired in acquired thermotolerance (Miller et al., 2007). In accordance, our data

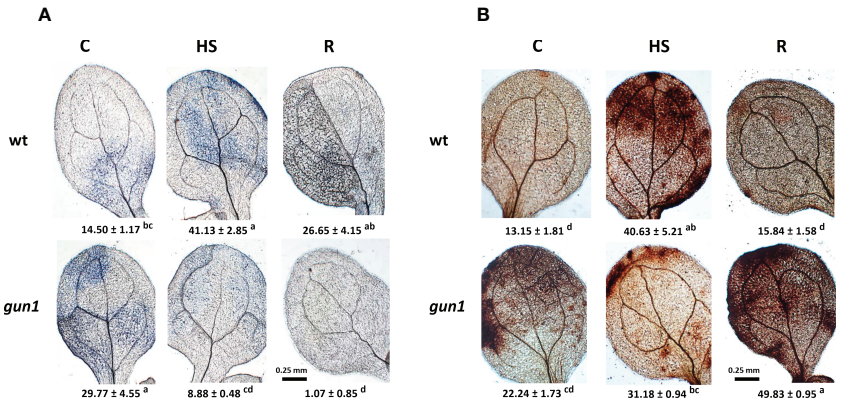

FIGURE 4
Accumulation of superoxide anion (O_2^-) and hydrogen peroxide (H_2O_2) in 15 days-old wt and *gun1* plantlets, grown at control temperature (C) or subjected to Heat Stress (HS; 2 hours at 45°C), followed by short recovery (R; 3 hours at 22°C). Representative images of **(A)** O_2^- accumulation, visualized by nitroblue tetrazolium (NBT)-staining and **(B)** H_2O_2 accumulation, visualized by diaminobenzidine (DAB)-staining. O_2^- and H_2O_2 analyses were repeated three times showing reproducible results. The percentage area (± SE) of 60 leaves (20 for each experiment) stained with NBT and DAB, respectively, are indicated. Letters indicate significant differences obtained by one-way ANOVA test (P< 0.05).

indicate the *gun1* mutants are more sensitive to HS than wt, as demonstrated by the reduced fresh weight and the inhibition of root elongation at 2 days of physiological recovery from HS (Figure 1). Furthermore, at 2d-RHS, despite *gun1* mutants show similar reduction in photosynthetic efficiency than wild type plants, have a reduced content of carotenoids (Figure 2). The decrease in carotenoids content may contribute to higher sensitivity to HS, since these molecules act not only as quenchers of triplet chlorophyll and singlet oxygen but might also stabilize and photo-protect the lipid phase of the thylakoid membranes (Havaux, 1998).

The lowered heat tolerance of *gun1* mutants is not due to cytosolic folding stress, which instead occurs in response lincomycin treatment (Figure S1; Wu et al., 2019; Tadini et al., 2020), suggesting the involvement of a different signaling mechanism. Moreover, the reduced basal thermotolerance of *gun1* mutants cannot be explained by the failure in the induction of *HSPs*, since in *gun1*, *HsfA2* and the cytosolic and chloroplastic *HSPs* analyzed were highly expressed after HS as in wild type plants. However, the higher decrease of *HSPs* after 3 hours of recovery from HS corroborates the idea of a lower thermotolerance of *gun1* mutants compared to wild type plants (Figure 3; Ahn et al., 2004; Charng et al., 2007).

It has been recently reported that during biogenic retrograde signaling, GUN1 mediates the formation of an H_2O_2- dependent oxidized environment, which might represent a redox-mediated communication pathway, aimed to signal the perturbation of chloroplast development (Fortunato et al., 2022).

A plethora of literature data indicate that environmental stresses, including high temperatures, lead to oxidative bursts of O_2- and/or H_2O_2 in plants (Foyer et al., 1997; Dat et al., 1998; Vallélian-Bindschedler et al., 1998). Accordingly, ROS produced in chloroplasts can work as plastid signals to activate the expression of genes coding for antioxidant enzymes and to fine-tune the stress-responsive apparatus for more effective adaptation to stresses (Sun and Guo, 2016). Chloroplasts have been shown to play an important role in heat-induced ROS accumulation and the subsequent expression of nuclear heat-responsive genes (Hu et al., 2020). The chloroplast-produced H_2O_2 working as signaling molecule for the heat-associated gene expression has been proposed as an interesting model for the generation of diurnal patterns of thermotolerance (Dickinson et al., 2018).

Our results show that in wt, immediately after HS, O_2- and H_2O_2 values increase, returning to values comparable to control conditions after 3 hours of physiological recovery, while a transient increase in protein oxidation was observed (Figures 4, 5B). This suggests that in this context ROS may contribute to oxidizing the cellular environment temporarily, triggering a signaling cascade. The transient oxidation of cellular environment has been confirmed by the changes in the glutathione redox state, which decreases after HS and returns to values comparable to control during the physiological recovery (Figure 5D). These results are in accordance with recent studies in which the redox-sensitive green fluorescent protein (roGFP2) was used to show that HS leads to increased oxidation in both cytosol and nucleus compartments. By analyzing transcript profiles of control and heat-stressed plantlets, the authors suggest that heat-induced changes in the nuclear redox state are essential for genetic and epigenetic regulation of HSR (Babbar et al., 2021).

In wt, the transient oxidative burst is also due to the lowered total activity of APX and CAT occurring immediately after HS (Figures 7A, B). Analyzing the protein levels of different APX

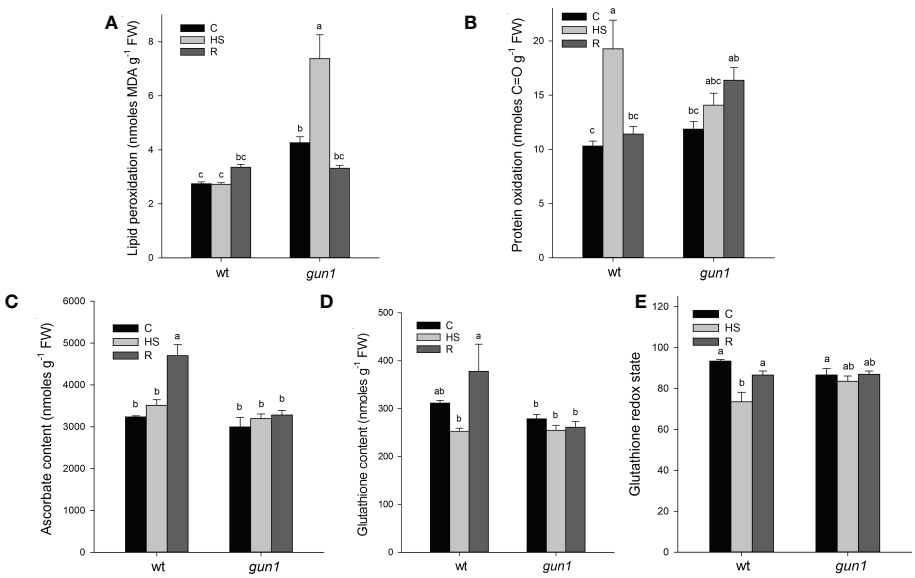

FIGURE 5
Oxidative markers and non-enzymatic antioxidants of Arabidopsis wild type (wt) and *gun1* plantlets, grown at control temperature (C) or subjected to Heat Stress (HS; 2 hours at 45°C), followed by short recovery (R; 3 hours at 22°C). **(A)** Lipid peroxidation, measured as malondialdehyde content and **(B)** protein oxidation measured as total protein carbonyl groups. **(C)** Total ascorbate and **(D)** glutathione contents. **(E)** Glutathione redox state calculated as percentage of the ratio between reduced and total glutathione. The values are the means ± standard errors of five independent experiments. Different letters indicate significant differences obtained by one-way ANOVA test (P< 0.05).

isoenzymes, it should be noted that, despite the significant decrease of the total activity, the levels of cytosolic and stromal APX proteins increased. At least for the cytosolic APX, two observations could explain this apparent inconsistency: 1) Immediately after HS, the expression level of *APX2* transcript significantly increased, as expected (Figure 8B; Panchuk et al., 2002; Suzuki et al., 2013; Balfagón et al., 2018); 2) It has been reported that after HS, APX1 protein forms high molecular weight complexes, loses the H_2O_2 removal activity, and behaves as chaperone protein. Interestingly, when plants are recovered under physiological conditions, the APX protein returns to dimeric or oligomeric form, recovering its H_2O_2- removal activity required to prevent oxidative damage (Kaur et al., 2021). On the other hand, protein and transcript levels of thylakoidal APX decreased immediately after HS. In this case, the loss or inactivation of tAPX may function as a part of plastid to nucleus retrograde signaling as occurs in light-induced photooxidative stress (Maruta et al., 2012).

Interestingly, also the decrease in CAT activity did not overlap with protein and transcript levels of CAT2, which accumulate immediately after HS. CAT is a peroxisomal enzyme with a pivotal role in redox regulation (Mhamdi et al., 2012). It has been shown that CAT can physically interact with cytosolic stress signaling proteins in plants (Foyer et al., 2020). Thus, it is likely that, upon HS, CAT becomes restrained to the cytosol and mediates redox signaling, as it occurs in mammalians (Walton et al., 2017).

In wt, 3 hours after physiological recovery from HS, both non-enzymatic and enzymatic antioxidants significantly increased, lowering ROS accumulation and preventing oxidative damage (Figures 4–8). In particular, the increase in SOD activity is due to an increase in the expression level of almost all the isoenzymes analyzed and the recovery in APX activity is due to the increased protein and expression level of all APX isoforms (Figure 8).

It is interesting to note that *gun1* mutants grown under physiological conditions show a higher O_2- accumulation and a greater level of lipid peroxidation than wt (Figure 4A), which suggests that *gun1* plastids are more inclined to suffer ROS-mediated damage (Ruckle et al., 2007; Fortunato et al., 2022). After HS, the decrease in O_2- implies the formation of more reactive hydroxyl radicals, which promptly react with lipids, causing a further increase in lipid peroxidation (Figure 5A; Farmer and Mueller, 2013). However, unlike wt, *gun1* mutants fail to induce an oxidative burst immediately after HS, since no O_2- neither H_2O_2 accumulate (Figure 4). Consistently, the content of antioxidants and the total activities of SOD and CAT did not show significant differences (Figures 5–7). The absence of a rise in H_2O_2 under HS may contribute to increased heat oxidative damage, as already suggested for *fsd2* and *fsd3* mutants (Bychkov et al., 2022).

In *gun1* mutants, after 3 hours of physiological recovery from HS non-enzymatic antioxidants, as well SOD and CAT activity do not significantly change, whereas a decline in total APX activity occurs, due to the failure in the rescue of the protein levels of

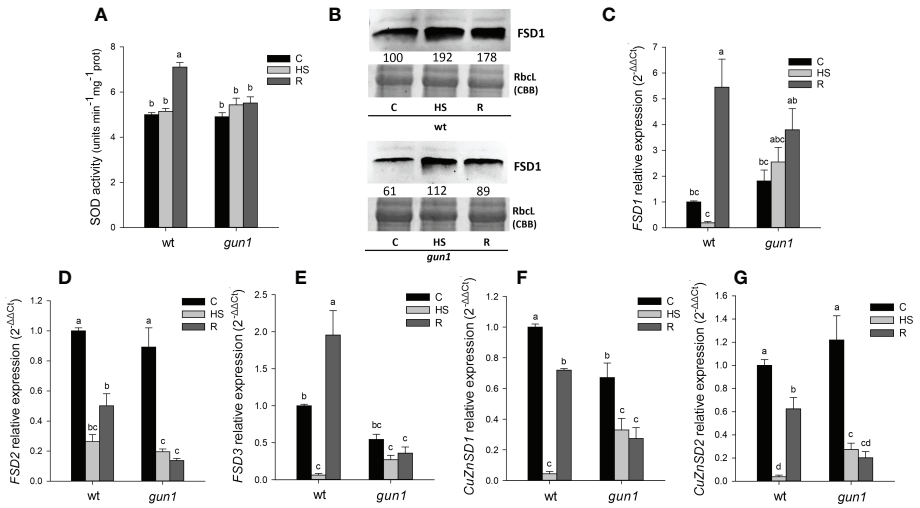

FIGURE 6
Superoxide dismutase (SOD) behavior in 15 days-old wt and *gun1* plantlets, grown at control temperature (C) or subjected to Heat Stress (HS; 2 hours at 45°C), followed by short recovery (R; 3 hours at 22°C). **(A)** Total SOD activity; values are the means ± standard errors (SE) of five independent experiments. Letters indicate significant differences obtained by one-way ANOVA test (P< 0.05). **(B)** Representative images from three independent experiments of FSD1 immuno-blotting; each well was loaded with 30 µg of proteins. Coomassie Brilliant Blue (CBB) staining of the gel served as a loading control. Quantification of signals (by Quantity One®) relative to the wt in control conditions (100%) is provided below the panel. Relative expression of **(C)** *FSD1*, **(D)** *FSD2*, **(E)** *FSD3*, **(F)** *CuZnSD1* **(G)** and *CuZnSD2*. The expression level of *SOD* genes was normalized to that of *Ubiquitin10* (At4g05320) and *Actin8* (At1g49240) as internal references. For each sample, gene expression was related to the wt in control conditions (C). Values are expressed as means ± SE from three independent experiments, with three technical replicates for each experiment. Different letters indicate significant differences obtained by one-way ANOVA test (p< 0.05).

chloroplastic and cytosolic APX. As a consequence, H_2O_2 accumulates, becoming responsible for oxidative damage. It has been reported that under photooxidative stress the absence of tAPX more than sAPX causes the accumulation of H_2O_2 and oxidized proteins (Maruta et al., 2010). Moreover, in the absence of the cytosolic APX1, the entire chloroplastic H_2O_2- scavenging system of Arabidopsis is impaired (Davletova et al., 2005), Thus, in *gun1* mutants the absence of the induction of APX1 expression

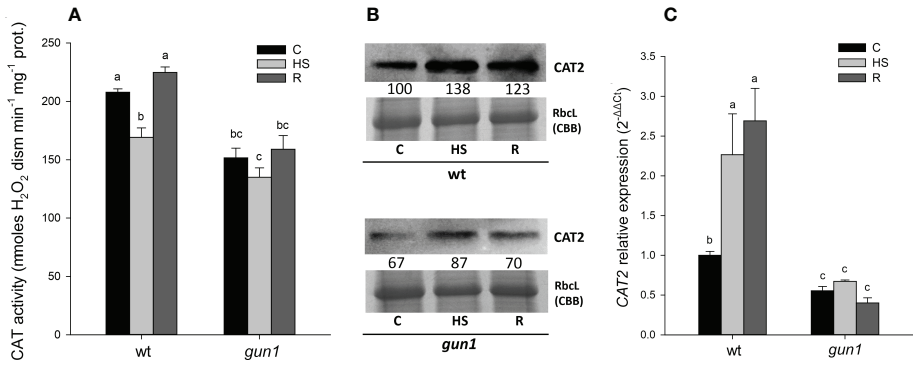

FIGURE 7
Catalase (CAT) behavior in 15 days-old wt and *gun1* plantlets, grown at control temperature (C) or subjected to Heat Stress (HS; 2 hours at 45° C), followed by short recovery (R; 3 hours at 22°C). **(A)** Total CAT activity. Values are the means ± standard errors (SE) of five independent experiments. Letters indicate significant differences obtained by one-way ANOVA test (P< 0.05). **(B)** Representative image from three independent experiments of CAT2 immunoblotting, each well was loaded with 30 µg of proteins. CBB staining of the gel is shown as equal loading control. Quantification of signals (by Quantity One®) relative to the wt in control conditions (100%) is provided below the panel. **(C)** Relative expression of *CAT2*. The expression level of *CAT2* was normalized to that of *Ubiquitin 10* (At4g05320) and *Actin8* (At1g49240) as internal references. For each sample, gene expression was related to the wt in control conditions (C). Values are the means ± SE from three independent experiments, with three technical replicates for each experiment. Letters indicate significant differences obtained by one-way ANOVA test (p< 0.05).

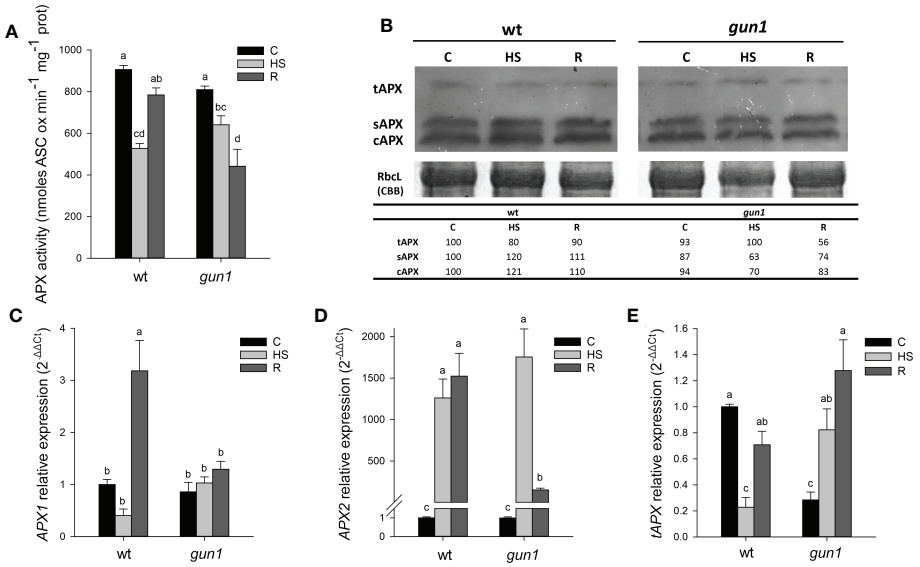

FIGURE 8
Ascorbate peroxidase (APX) behavior in 15 days-old wt and *gun1* plantlets, grown at control temperature (C) or subjected to Heat Stress (HS; 2 hours at 45°C), followed by short recovery (R; 3 hours at 22°C). **(A)** Total APX activity; values indicate means ± standard errors (SE) of five independent experiments. Letters indicate significant differences obtained by one-way ANOVA test (P< 0.05). **(B)** Representative image from three independent experiments of APX immuno-blotting; each well was loaded with 30 µg of proteins. CBB staining of the gel served as a loading control. Quantification of signals (by Quantity One®) relative to the wt in control conditions (100%) is provided below the panel tAPX, sAPX and cAPX are thylakoidal, stromal and cytosolic APX, respectively. Relative expression of **(C)** *APX1*, **(D)** *APX2* and **(E)** *tAPX*. The expression level of APX genes was normalized to that of *Ubiquitin10* (At4g05320) and *Actin8* (At1g49240) as internal references. For each sample, gene expression was related to wt in control conditions (C). Values indicate means ± SE from three independent experiments, with three technical replicates for each experiment. Different letters indicate significant differences obtained by one-way ANOVA test (p< 0.05).

(Figure 8C), could be in part responsible for the failure in thermotolerance acquisition.

However, in *gun1* mutants, the behavior of tAPX deserves more attention; indeed, it should be noted that the expression level of tAPX, which is lower than wt under physiological growth conditions, increased after HS and during the physiological recovery, despite the failure in the accumulation of the protein (Figures 8B, E). These results indicate that the expression of tAPX gene is under the control of the GUN1-mediated signaling pathway, albeit protein amount also appears to be subjected to post-transcriptional regulatory mechanisms that include cytosolic inhibition of protein translation and ubiquitin-mediated protein degradation (Wu et al., 2019; Tadini et al., 2020). This regulation has been described for several *PhANGs*-encoded proteins and, among those, tAPX itself (Wu et al., 2019).

Conclusions

Our data suggest that the transient oxidative burst occurring after HS is mandatory in basal thermotolerance acquisition. Indeed, in wt plants, ROS and oxidation of the cellular environment function as signals to activate the expression of genes adjusting stress-responsive systems for more successful adaptation to HS.

After HS, *gun1* mutants fail to induce ROS accumulation promptly, impairing the proper HSR. This leads to accumulating ROS and oxidative damage during physiological recovery at growth temperature, resulting in enhanced sensitivity to HS.

The results support the idea that GUN1 is required to oxidize the cellular environment, participating in the acquisition of basal thermotolerance through the redox-dependent plastid-to-nucleus communication.

Our results also indicate a pivotal role of tAPX in GUN1-dependent HSR; further investigation will be aimed at clarifying the mechanisms involved in this signaling pathway.

Data availability statement

The original contributions presented in the study are included in the article/Supplementary Material. Further inquiries can be directed to the corresponding author.

Author contributions

CL, SF, FV, and MCdP conceived and designed research. CL, SF, ND, NJ, LT, and FV performed the experiments. MCdP advised on the experiments. CL, SF, LT, FV, and MCdP drafted

the paper. MCdP and PP funded the project. All authors contributed to the discussion of the data and to the writing and agreed to the published version of the manuscript.

Funding

This project was supported by MUR—Ministero dell'Università e della Ricerca, grant number PRIN-2017, 2017FBS8YN.

Conflict of interest

The authors declare that the research was conducted in the absence of any commercial or financial relationships that could be construed as a potential conflict of interest.

Publisher's note

Supplementary material

The Supplementary Material for this article can be found online at: https://www.frontiersin.org/articles/10.3389/fpls.2022.1058831/full#supplementary-material

References

Ahn, Y. J., Claussen, K., and Zimmerman, J. L. (2004). Genotypic differences in the heat-shock response and thermotolerance in four potato cultivars. *Plant Sci.* 166, 901–911. doi: 10.1016/j.plantsci.2003.11.027

Allakhverdiev, S. I., Kreslavski, V. D., Klimov, V. V., Los, D. A., Carpentier, R., and Mohanty, P. (2008). Heat stress: An overview of molecular responses in photosynthesis. *Photosynth. Res.* 98, 541–550. doi: 10.1007/s11120-008-9331-0

Babbar, R., Karpinska, B., Grover, A., and Foyer, C. H. (2021). Heat-induced oxidation of the nuclei and cytosol. *Front. Plant Sci.* 11, 617779. doi: org/10.3389/fpls.2020.617779

Balfagón, D., Zandalinas, S. I., Baliño, P., Muriach, M., and Gómez-Cadenas, A. (2018). Involvement of ascorbate peroxidase and heat shock proteins on citrus tolerance to combined conditions of drought and high temperatures. *Plant Physiol. Biochem.* 127, 194–199. doi: 10.1016/j.plaphy.2018.03.029

Bita, C. E., and Gerats, T. (2013). Plant tolerance to high temperature in a changing environment: Scientific fundamentals and production of heat stress-tolerant crops. *Front. Plant Sci.* 4. doi: 10.3389/fpls.2013.00273

Bradford, M. (1976). A rapid and sensitive method for the quantitation of microgram quantities of protein utilizing the principle of protein-dye binding. *Anal. Biochem.* 72, 248–254. doi: 10.1006/abio.1976.9999

Bychkov, I. A., Andreeva, A. A., Kudryakova, N. V., Pojidaeva, E. S., and Kusnetsov, V. V. (2022). The role of PAP4/FSD3 and PAP9/FSD2 in heat stress responses of chloroplast genes. *Plant Sci.* 322, 111359. doi: 10.1016/J.PLANTSCI.2022.111359

Chan, K. X., Phua, S. Y., Crisp, P., McQuinn, R., and Pogson, B. J. (2016). Learning the languages of the chloroplast: Retrograde signaling and beyond. *Ann. Rev. Plant Biol.* 67, 25–53. doi: 10.1146/annurev-arplant-043015-111854

Charng, Y.-Y., Liu, H.-C., Liu, N.-Y., Chi, W.-T., Wang, C.-N., Chang, S.-H., et al. (2007). A heat-inducible transcription factor HsfA2 is required for extension of acquired thermotolerance in arabidopsis. *Plant Physiol.* 143, 251–262. doi: 10.1104/pp.106.091322

Cheng, J. A., He, C. X., Zhang, Z. W., Xu, F., Zhang, D. W., Wang, X., et al. (2011). Plastid signals confer arabidopsis tolerance to water stress. *Z. Naturforsch. C.* 66, 47–54. doi: 10.1016/j.pbi.2015.04.006

Colombo, M., Tadini, L., Peracchio, C., Ferrari, R., and Pesaresi, P. (2016). GUN1 a jack-of-all-trades in chloroplast protein homeostasis and signaling. *Front. Plant Sci.* 7, 1427. doi: 10.3389/fpls.2016.01427

Das, P., Nutan, K. K., Singla-Pareek, S. L., and Pareek, A. (2015). Oxidative environment and redox homeostasis in plants: Dissecting out significant contribution of major cellular organelles. *Front. Environ. Sci.* 2. doi: 10.3389/fenvs.2014.00070

Dat, J. F., Foyer, C. H., and Scott, I. M. (1998). Changes in salicylic acid and antioxidants during induced thermotolerance in mustard seedlings. *Plant Physiol.* 118, 1455–1461. doi: 10.1104/pp.118.4.1455

Davletova, S., Rizhsky, L., Liang, H. J., Zhong, S. Q., Oliver, D. J., Coutu, J., et al. (2005). Cytosolic ascorbate peroxidase 1 is a central component of the reactive oxygen gene network of arabidopsis. *Plant Cell* 17, 268–281. doi: 10.1105/tpc.104.026971

de Pinto, M. C., Francis, D., and De Gara, L. (1999). The redox state of the ascorbate-dehydroascorbate pair as a specific sensor of cell division in tobacco BY-2 cells. *Protoplasma* 209, 90–97. doi: 10.1007/BF01415704

de Pinto, M. C., Tommasi, F., and De Gara, L. (2000). Enzymes of the ascorbate biosynthesis and ascorbate-glutathione cycle in cultured cells of tobacco bright yellow 2. *Plant Physiol. Biochem.* 38, 541–550. doi: 10.1016/S0981-9428(00)00773-7

Dickinson, P. J., Kumar, M., Martinho, C., Yoo, S. J., Lan, H., Artavanis, G., et al. (2018). Chloroplast signaling gates thermotolerance in arabidopsis. *Cell Rep.* 22, 1657–1665. doi: 10.1016/j.celrep.2018.01.054

Dvořák, P., Krasylenko, Y., Ovecka, M., Basheer, J., Zapletalova, V., Samaj, J., et al. (2021). *In vivo* light-sheet microscopy resolves localisation patterns of FSD1 a superoxide dismutase with function in root development and osmoprotection. *Plant Cell Environ.* 44, 68–87. doi: 10.1111/pce.13894

Farmer, E. E., and Mueller, M. J. (2013). ROS-mediated lipid peroxidation and RES-activated signaling. *Annu. Rev. Plant Biol.* 64, 429–450. doi: 10.1146/annurev-arplant-050312-120132

Farnese, F. S., Menezes-Silva, P. E., Gusman, G. S., and Oliveira, J. A. (2016). When bad guys become good ones: The key role of reactive oxygen species and nitric oxide in the plant responses to abiotic stress. *Front. Plant Sci.* 7. doi: 10.3389/fpls.2016.00471

Fortunato, S., Lasorella, C., Tadini, L., Jeran, N., Vita, F., Pesaresi, P., et al. (2022). GUN1 involvement in the redox changes occurring during biogenic retrograde signaling. *Plant Sci.* 320, 111265. doi: 10.1016/j.plantsci.2022.111265

Foyer, C. H., Baker, A., Wright, M., Sparkes, I. A., Mhamdi, A., Schippers, J. H. M., et al. (2020). On the move: Redox-dependent protein relocation in plants. *J. Exp. Bot.* 71, 620–631. doi: 10.1093/jxb/erz330

Foyer, C. H., Lopez-Delgado, H., Dat, J. F., and Scott, I. M. (1997). Hydrogen peroxide-and glutathione-associated mechanisms of acclimatory stress tolerance and signalling. *Physiol. Plant* 100, 241–254. doi: 10.1111/j.1399-3054.1997.tb04780.x

Foyer, C. H., and Noctor, G. (2013). Redox signaling in plants. *Antioxidants. Redox Signal.* 18, 2087–2090. doi: 10.1089/ars.2013.5278

Giuntoli, B., Shukla, V., Maggiorelli, F., Giorgi, F. M., Lombardi, L., Perata, P., et al. (2017). Age-dependent regulation of ERF-VII transcription factor activity in arabidopsis thaliana. *Plant Cell Environ.* 40, 2333–2346. doi: 10.1111/pce.13037

Guo, J., Zhou, Y., Li, J., Sun, Y., Shangguan, Y., Zhu, Z., et al. (2020). COE 1 and GUN1 regulate the adaptation of plants to high light stress. *Biochem. Biophys. Res. Commun.* 521, 184–189. doi: 10.1016/J.BBRC.2019.10.101

Hasanuzzaman, M., Nahar, K., Alam, M. M., Roychowdhury, R., and Fujita, M. (2013). Physiological biochemical and molecular mechanisms of heat stress tolerance in plants. *Int. J. Mol. Sci.* 14, 9643–9684. doi: 10.3390/ijms14059643

Havaux, M. (1998). Carotenoids as membrane stabilizers in chloroplasts. *Trends Plant Sci.* 3, 147–151. doi: 10.1016/S1360-1385(98)01200-X

Hu, S., Ding, Y., and Zhu, C. (2020). Sensitivity and responses of chloroplasts to heat stress in plants. *Front. Plant Sci.* 11. doi: 10.3389/fpls.2020.00375

Kaur, S., Prakash, P., Bak, D.-H., Hong, S. H., Cho, C., Chung, M.-S., et al. (2021). Regulation of dual activity of ascorbate peroxidase 1 from arabidopsis thaliana by conformational changes and posttranslational modifications. *Front. Plant Sci.* 12. doi: 10.3389/fpls.2021.678111

Koussevitzky, S., Nott, A., Mockler, T. C., Hong, F., Sachetto-Martins, G., Surpin, M., et al. (2007). Signals from chloroplasts converge to regulate nuclear gene expression. *Correct: Science*. 316 (5825), 715–719. doi: 10.1126/science.1140516

Larkin, R. M., Alonso, J. M., Ecker, J. R., and Chory, J. (2003). GUN4 a regulator of chlorophyll synthesis and intracellular signaling. *Science* 299, 902–906. doi: 10.1126/science.1079978

Larkindale, J., Hall, J. D., Knight, M. R., and Vierling, E. (2005). Heat stress phenotypes of arabidopsis mutants implicate multiple signaling pathways in the acquisition of thermotolerance. *Plant Physiol.* 138, 882–897. doi: 10.1104/pp.105.062257

Lichtenthaler, H. K. (1987). Chlorophylls and carotenoids: Pigments of photosynthetic biomembranes. *Methods Enzymol.* 148, 350–382. doi: 10.1016/0076-6879(87)48036-1

Ling, Y., Serrano, N., Gao, G., Atia, M., Mokhtar, M., Woo, Y. H., et al. (2018). Thermopriming triggers splicing memory in arabidopsis. *J. Exp. Bot.* 69, 2659–2675. doi: 10.1093/jxb/ery062

Livak, K. J., and Schmittgen, T. D. (2001). Analysis of relative gene expression data using real-time quantitative PCR and the 2-ΔΔCT method. *Methods* 25, 402–408. doi: 10.1006/meth.2001.1262

Marino, G., Naranjo, B., Wang, J., Penzler, J. F., Kleine, T., and Leister, D. (2019). Relationship of GUN1 to FUG1 in chloroplast protein homeostasis. *Plant J.* 99, 521–535. doi: 10.1111/tpj.14342

Maruta, T., Noshi, M., Tanouchi, A., Tamoi, M., Yabuta, Y., Yoshimura, K., et al. (2012). H2O2-triggered retrograde signaling from chloroplasts to nucleus plays specific role in response to stress. *J. Biol. Chem.* 287, 11717–11729. doi: 10.1074/jbc.M111.292847

Maruta, T., Tanouchi, A., Tamoi, M., Yabuta, Y., Yoshimura, K., Ishikawa, T., et al. (2010). Arabidopsis chloroplastic ascorbate peroxidase isoenzymes play a dual role in photoprotection and gene regulation under photooxidative stress. *Plant Cell Physiol.* 51, 190–200. doi: 10.1093/pcp/pcp177

Mhamdi, A., Noctor, G., and Baker, A. (2012). Plant catalases: Peroxisomal redox guardians. *Arch. Biochem. Biophys.* 525, 181–194. doi: 10.1016/J.ABB.2012.04.015

Miller, G., Suzuki, N., Rizhsky, L., Hegie, A., Koussevitzky, S., and Mittler, R. (2007). Double mutants deficient in cytosolic and thylakoid ascorbate peroxidase reveal a complex mode of interaction between reactive oxygen species plant development and response to abiotic stresses. *Plant Physiol.* 144, 1777–1785. doi: 10.1104/pp.107.101436

Mittler, R. (2017). ROS are good. *Trends Plant Sci.* 22, 11–19. doi: 10.1016/j.tplants.2016.08.002

Mochizuki, N., Brusslan, J. A., Larkin, R., Nagatani, A., and Chory, J. (2001). Arabidopsis genomes uncoupled 5 (GUN5) mutant reveals the involvement of mg-chelatase h subunit in plastid-to-nucleus signal transduction. *PNAS* 98, 2053–2058. doi: 10.1073/pnas.98.4.2053

Myouga, F., Hosoda, C., Umezawa, T., Iizumi, H., Kuromori, T., Motohashi, R., et al. (2008). A heterocomplex of iron superoxide dismutases defends chloroplast nucleoids against oxidative stress and is essential for chloroplast development in arabidopsis. *Plant Cell* 20, 3148–3162. doi: 10.1105/tpc.108.061341

Nishizawa, A., Yabuta, Y., Yoshida, E., Maruta, T., Yoshimura, K., and Shigeoka, S. (2006). Arabidopsis heat shock transcription factor A2 as a key regulator in response to several types of environmental stress. *Plant J.* 48, 535–547. doi: 10.1111/j.1365-313X.2006.02889.x

Noctor, G., Veljovic-Jovanovic, S., Driscoll, S., Novitskaya, L., and Foyer, C. H. (2002). Drought and oxidative load in the leaves of C3 plants: A predominant role for photorespiration? *Ann. Bot.* 89, 841–850. doi: 10.1093/aob/mcf096

Nott, A., Jung, H. S., Koussevitzky, S., and Chory, J. (2006). Plastid-to-nucleus retrograde signaling. *Annu. Rev. Plant Biol.* 57, 739–759. doi: 10.1146/annurev.arplant.57.032905.105310

Panchuk, I. I., Volkov, R. A., and Schöffl, F. (2002). Heat stress- and heat shock transcription factor-dependent expression and activity of ascorbate peroxidase in arabidopsis. *Plant Physiol.* 129, 838–853. doi: 10.1104/pp.001362

Paradiso, A., Berardino, R., De Pinto, M. C., Sanità Di Toppi, L., Storelli, M. M., Tommasi, F., et al. (2008). Increase in ascorbate-glutathione metabolism as local and precocious systemic responses induced by cadmium in durum wheat plants. *Plant Cell Physiol.* 49, 362–374. doi: 10.1093/pcp/pcn013

Paradiso, A., Domingo, G., Blanco, E., Buscaglia, A., Fortunato, S., Marsoni, M., et al. (2020). Cyclic AMP mediates heat stress response by the control of redox homeostasis and ubiquitin-proteasome system. *Plant Cell Environ.* 43, 2727–2742. doi: 10.1111/pce.13878

Pesaresi, P., and Kim, C. (2019). Current understanding of GUN1: a key mediator involved in biogenic retrograde signaling. *Plant Cell Rep.* 38, 819–823. doi: 10.1007/s00299-019-02383-4

Pnueli, L., Liang, H., Rozenberg, M., and Mittler, R. (2003). Growth suppression altered stomatal responses and augmented induction of heat shock proteins in cytosolic ascorbate peroxidase (Apx1)-deficient arabidopsis plants. *Plant J.* 34, 187–203. doi: 10.1046/j.1365-313X.2003.01715.x

Pogson, B. J., Woo, N. S., Förster, B., and Small, I. D. (2008). Plastid signalling to the nucleus and beyond. *Trends Plant Sci.* 13, 602–609. doi: 10.1016/j.tplants.2008.08.008

Riedel, G., Rüdrich, U., Fekete-Drimusz, N., Manns, M. P., Vondran, F. W. R., and Bock, M. (2014). An extended ΔCT-method facilitating normalisation with multiple reference genes suited for quantitative RT-PCR analyses of human hepatocyte-like cells. *PloS One* 9, 2–6. doi: 10.1371/journal.pone.0093031

Romero-Puertas, M. C., Palma, J. M., Gómez, M., Del Río, L. A., and Sandalio, L. M. (2002). Cadmium causes the oxidative modification of proteins in pea plants. *Plant Cell Environ.* 25, 677–686. doi: 10.1046/j.1365-3040.2002.00850.x

Ruckle, M. E., DeMarco, S. M., and Larkin, R. M. (2007). Plastid signals remodel light signaling networks and are essential for efficient chloroplast biogenesis in arabidopsis. *Plant Cell* 19, 3944–3960. doi: 10.1105/tpc.107.054312

Sgobba, A., Paradiso, A., Dipierro, S., de Gara, L., and de Pinto, M. C. (2015). Changes in antioxidants are critical in determining cell responses to short- and long-term heat stress. *Physiol. Plant* 153, 68–78. doi: 10.1111/ppl.12220

Shimizu, T., and Masuda, T. (2021). The role of tetrapyrrole-and GUN1-dependent signaling on chloroplast biogenesis. *Plants* 10, 196. doi: 10.3390/plants10020196

Singh, R., Singh, S., Parihar, P., Singh, V. P., and Prasad, S. M. (2015). Retrograde signaling between plastid and nucleus: A review. *J. Plant Physiol.* 181, 55–66. doi: 10.1016/j.jplph.2015.04.001

Strand, A., Asami, T., Alonso, J., Ecker, J. R., and Chory, J. (2003). Chloroplast to nucleus communication triggered by accumulation of mg-protoporphyrinIX. *Nature* 421, 79–83. doi: 10.1038/nature01204

Sun, A. Z., and Guo, F. Q. (2016). Chloroplast retrograde regulation of heat stress responses in plants. *Front. Plant Sci.* 7. doi: 10.3389/fpls.2016.00398

Susek, R. E., Ausubel, F. M., and Chory, J. (1993). Signal transduction mutants of arabidopsis uncouple nuclear CAB and RBCS gene expression from chloroplast development. *Cell* 74, 787–799. doi: 10.1016/0092-8674(93)90459-4

Suzuki, N., Koussevitzky, S., Mittler, R., and Miller, G. (2012). ROS and redox signalling in the response of plants to abiotic stress. *Plant Cell Environ.* 35, 259–270. doi: 10.1111/j.1365-3040.2011.02336.x

Suzuki, N., Miller, G., Sejima, H., Harper, J., and Mittler, R. (2013). Enhanced seed production under prolonged heat stress conditions in arabidopsis thaliana plants deficient in cytosolic ascorbate peroxidase 2. *J. Exp. Bot.* 64, 253–263. doi: 10.1093/jxb/ers335

Tadini, L., Peracchio, C., Trotta, A., Colombo, M., Mancini, I., Jeran, N., et al. (2020). GUN1 influences the accumulation of NEP-dependent transcripts and chloroplast protein import in arabidopsis cotyledons upon perturbation of chloroplast protein homeostasis. *Plant J.* 101, 1198–1220. doi: 10.1111/tpj.14585

Tadini, L., Pesaresi, P., Kleine, T., Rossi, F., Guljamow, A., Sommer, F., et al. (2016). Gun1 controls accumulation of the plastid ribosomal protein S1 at the protein level and interacts with proteins involved in plastid protein homeostasis. *Plant Physiol.* 170, 1817–1830. doi: 10.1104/pp.15.02033

Tadini, L., Romani, I., Pribil, M., Jahns, P., Leister, D., and Pesaresi, P. (2012). Thylakoid redox signals are integrated into organellar-gene-expression-dependent retrograde signaling in the prors1-1 mutant. *Front. Plant Sci.* 3. doi: 10.3389/Fpls.2012.00282

Vallélian-Bindschedler, L., Schweizer, P., Mösinger, E., and Métraux, J. P. (1998). Heat-induced resistance in barley to powdery mildew (Blumeria graminis f.sp.hordei) is associated with a burst of active oxygen species. *Physiol. Mol. Plant Pathol.* 52, 185–199. doi: 10.1006/PMPP.1998.0140

Volkov, R. A., Panchuk, I. I., Mullineaux, P. M., and Schöffl, F. (2006). Heat stress-induced H2O2 is required for effective expression of heat shock genes in arabidopsis. *Plant Mol. Biol.* 61, 733–746. doi: 10.1007/s11103-006-0045-4

Wahid, A., Gelani, S., Ashraf, M., and Foolad, M. R. (2007). Heat tolerance in plants: An overview. *Environ. Exp. Bot.* 61, 199–223. doi: 10.1016/j.envexpbot.2007.05.011

Walton, P. A., Brees, C., Lismont, C., Apanasets, O., and Fransen, M. (2017). The peroxisomal import receptor PEX5 functions as a stress sensor retaining catalase in the cytosol in times of oxidative stress. *Biochim. Biophys. Acta - Mol. Cell Res.* 1864, 1833–1843. doi: 10.1016/J.BBAMCR.2017.07.013

Wang, Q. L., Chen, J. H., He, N. Y., and Guo, F. Q. (2018). Metabolic reprogramming in chloroplasts under heat stress in plants. *Int. J. Mol. Sci.* 19, 849. doi: 10.3390/ijms19030849

Wise, R. R., Olson, A. J., Schrader, S. M., and Sharkey, T. D. (2004). Electron transport is the functional limitation of photosynthesis in field-grown pima cotton plants at high temperature. *Plant Cell Environ.* 27, 717–724. doi: 10.1111/j.1365-3040.2004.01171.x

Woodson, J. D., Perez-Ruiz, J. M., and Chory, J. (2011). Heme synthesis by plastid ferrochelatase i regulates nuclear gene expression in plants. *Curr. Biol.* 21, 897–903. doi: 10.1016/j.cub.2011.04.004

Wu, G. Z., and Bock, R. (2021). GUN control in retrograde signaling: How GENOMES UNCOUPLED proteins adjust nuclear gene expression to plastid biogenesis. *Plant Cell* 33, 457–474. doi: 10.1093/plcell/koaa048

Wu, G. Z., Chalvin, C., Hoelscher, M., Meyer, E. H., Wu, X. N., and Bock, R. (2018). Control of retrograde signaling by rapid turnover of GENOMES UNCOUPLED1. *Plant Physiol.* 176, 2472–2495. doi: 10.1104/pp.18.00009

Wu, G.-Z., Meyer, E. H., Wu, S., and Bock, R. (2019). Extensive posttranscriptional regulation of nuclear gene expression by plastid retrograde signals. *Plant Physiol.* 180, 2034–2048. doi: 10.1104/pp.19.00421

Zhang, J., and Kirkham, M. B. (1996). Antioxidant responses to drought in sunflower and sorghum seedlings. *New Phytol.* 132, 361–373. doi: 10.1111/j.1469-8137.1996.tb01856.x

Zhao, X., Huang, J., and Chory, J. (2019). GUN1 interacts with MORF2 to regulate plastid RNA editing during retrograde signaling. *Proc. Natl. Acad. Sci.* 116, 10162–10167. doi: 10.1073/pnas.1820426116

Zhu, J. K. (2016). Abiotic stress signaling and responses in plants. *Cell* 167, 313–324. doi: 10.1016/j.cell.2016.08.029

frontiers | Frontiers in Plant Science

TYPE Original Research
PUBLISHED 06 January 2023
DOI 10.3389/fpls.2022.1040456

OPEN ACCESS

EDITED BY
Keshav Dahal,
Agriculture and Agri-Food Canada (AAFC), Canada

REVIEWED BY
María José García,
University of Cordoba, Spain
Franck E. Dayan,
Colorado State University, United States

*CORRESPONDENCE
Mercedes Royuela
royuela@unavarra.es

SPECIALTY SECTION
This article was submitted to Plant Abiotic Stress, a section of the journal Frontiers in Plant Science

RECEIVED 09 September 2022
ACCEPTED 15 December 2022
PUBLISHED 06 January 2023

CITATION
Eceiza MV, Barco-Antoñanzas M, Gil-Monreal M, Huybrechts M, Zabalza A, Cuypers A and Royuela M (2023) Role of oxidative stress in the physiology of sensitive and resistant *Amaranthus palmeri* populations treated with herbicides inhibiting acetolactate synthase. *Front. Plant Sci.* 13:1040456. doi: 10.3389/fpls.2022.1040456

Role of oxidative stress in the physiology of sensitive and resistant *Amaranthus palmeri* populations treated with herbicides inhibiting acetolactate synthase

Mikel Vicente Eceiza[1], María Barco-Antoñanzas[1], Miriam Gil-Monreal[1], Michiel Huybrechts[2], Ana Zabalza[1], Ann Cuypers[2] and Mercedes Royuela[1]*

[1]Institute for Multidisciplinary Research in Applied Biology (IMAB), Public University of Navarre, Pamplona, Spain, [2]Environmental Biology, Centre for Environmental Sciences, Hasselt University, Diepenbeek, Belgium

The aim of the present study was to elucidate the role of oxidative stress in the mode of action of acetolactate synthase (ALS) inhibiting herbicides. Two populations of *Amaranthus palmeri* S. Watson from Spain (sensitive and resistant to nicosulfuron, due to mutated ALS) were grown hydroponically and treated with different rates of the ALS inhibitor nicosulfuron (one time and three times the field recommended rate). Seven days later, various oxidative stress markers were measured in the leaves: H_2O_2, MDA, ascorbate and glutathione contents, antioxidant enzyme activities and gene expression levels. Under control conditions, most of the analysed parameters were very similar between sensitive and resistant plants, meaning that resistance is not accompanied by a different basal oxidative metabolism. Nicosulfuron-treated sensitive plants died after a few weeks, while the resistant ones survived, independently of the rate. Seven days after herbicide application, the sensitive plants that had received the highest nicosulfuron rate showed an increase in H_2O_2 content, lipid peroxidation and antioxidant enzymatic activities, while resistant plants did not show these responses, meaning that oxidative stress is linked to ALS inhibition. A supralethal nicosulfuron rate was needed to induce a significant oxidative stress response in the sensitive population, providing evidence that the lethality elicited by ALS inhibitors is not entirely dependent on oxidative stress.

KEYWORDS

oxidative stress, nicosulfuron, herbicide mode of action, acetolactate synthase, *Amaranthus palmeri*

1 Introduction

Weed control is and has always been a major challenge for agriculture worldwide. Among all the implemented methods to minimise or avoid the many problems derived from weeds, herbicides continue being the most widely used tools for weed control (Edwards and Hannah, 2014). Herbicides inhibit specific molecular target sites within plant biological pathways and processes, and are classified into groups according to their target. Acetolactate synthase (ALS) inhibiting herbicides are some of the most popular postemergence herbicides worldwide owing to their efficacy and relatively low environmental impact (Mazur and Falco, 1989). ALS inhibitors form a diverse herbicide group with several families, where sulfonylureas are included. The inhibition of the key enzyme ALS in the pathway of biosynthesis of the branched-chain amino acids, isoleucine, leucine, and valine, is the common mechanism of action of all these herbicides (Zhou et al., 2007). Despite the extended usage of ALS inhibitors, and the fact that this mechanism of action was discovered decades ago, their mode of action has not been completely elucidated, even though some physiological effects are known. Among other effects, ALS inhibition leads to growth arrest, impairment of carbohydrate utilisation by roots and carbohydrate accumulation in leaves (Zabalza et al., 2008; Orcaray et al., 2011), alterations in phosphorus metabolism (Dragicević et al., 2011), and decrease of protein levels in favour of free amino acid pool (Shaner and Reider, 1986; Scarponi et al., 1995; Scarponi et al., 1997; Sidari et al., 1998; Zulet et al., 2013). Another reported effect, albeit less studied, is oxidative stress.

Oxidative stress develops as a result of an imbalance between reactive oxygen species (ROS) and antioxidant mechanisms in favour of the former, which manifests in oxidative damage in biomolecules and/or a stimulation of antioxidant systems (Demidchik, 2015). This imbalance is developed in response to almost all biotic and abiotic stresses. Under adequate conditions, ROS production and antioxidant activity are balanced, but stressful conditions usually lead to oxidative stress. As happens with other herbicides that inhibit amino acid biosynthesis, such as glyphosate (Ahsan et al., 2008; Gomes and Juneau, 2016; Ostera et al., 2016; de Freitas-Silva et al., 2017; Eceiza et al., 2022) or glufosinate (Takano et al., 2019), ALS inhibitors are thought to cause moderate oxidative stress secondarily, not being the main cause of plant death (Zabalza et al., 2007; Caverzan et al., 2019).

Over-reliance on herbicides can lead to the selection for resistant weeds (Yu and Powles, 2014) and, as a consequence of the massive usage of ALS inhibitors, 170 species have evolved populations with resistance to ALS-inhibiting herbicides (Heap, 2022), which makes them the group of herbicides with the highest number of weed species containing at least one resistant population (Heap, 2022). One of those species is *Amaranthus palmeri* S. Watson, a C4 weed whose fast growth, seed dispersal and extremely high genetic variability, makes it prone to the development of resistance to herbicides, make its control really difficult. Resistance mechanisms can be classified in target-site resistances (TSR) and non-target-site resistances (NTSR), depending on whether resistance is based in the target molecule or is a generalist mechanism developed independently of the target. In *A. palmeri*, although NTSR to ALS inhibitors mechanisms have been reported (Nakka et al., 2017), resistance to ALS inhibitors is more commonly TSR; specifically, substitution mutations in the *ALS* gene that make the enzyme insensitive to the action of ALS inhibitors. This is also the main mechanism detected in populations of other species like *Digitaria sanguinalis* (Murphy and Tranel, 2019) or *Papaver rhoeas* (Rey-Caballero et al., 2017).

Amaranthus palmeri is native to America, where the majority of resistant populations have been found: Kansas (USA) (Sprague et al., 1997; Chaudhari et al., 2020), Argentina (Larran et al., 2017), Brazil (Küpper et al., 2017), etc. This species has been introduced in other continents and, since 2007, it is present in Spain (Torra et al., 2020). Moreover, resistant biotypes to ALS inhibitors have been recently found in Catalonia, Spain, due to several amino acid substitutions in the *ALS* gene in positions Pro-197, Trp-574, and Ser-653 (Torra et al., 2020). This resistance mechanism is well characterised, but the possible physiological implications of this mutation and the physiological effects triggered by the exposure to an ALS inhibiting herbicide in these resistant weeds is not known. The genetic similarity of these *A. palmeri* populations with TSR and the sensitive population of reference (only ALS point mutations), gives the opportunity to study the physiological responses of resistant biotypes to ALS inhibitors, and specifically the role of oxidative stress in the mode of action of ALS inhibitors, and in the resistance to these herbicides.

As stated before, ALS inhibitors have been previously linked to oxidative stress. However, three key aspects of this connection remain to be elucidated. The first one is the importance of oxidative stress in the toxicity of these herbicides and the role that this stress may play in their mode of action. The second one refers to the origin of the oxidative stress triggered by herbicide application. How oxidative stress is generated, and whether it is caused in some way by ALS inhibition or if it is an independent secondary effect of the herbicide target, is not well known. Finally, the third refers to the resistant weed populations. Basal oxidative status of resistant individuals may be different from that of sensitive individuals. Whether or not it is different, sensitive and resistant plants may also respond differently to herbicide treatment in terms of oxidative stress. In this sense, comparing the oxidative stress produced by an ALS inhibitor in a sensitive population and in a resistant population by a TSR mechanism, where the target enzyme is insensitive to the herbicide, would allow evaluating if ALS inhibition is somehow the cause of oxidative stress. In addition, the oxidative status of these populations can also be analysed and contrasted with the response to the herbicide.

In this study, the main objective was to evaluate the impact of *ALS* gene mutations and of ALS inhibitor treatment on

oxidative stress. To this aim, the basal pattern and the response of a sensitive and a resistant population of *A. palmeri* to different rates of the ALS inhibitor nicosulfuron, a sulfonylurea, were evaluated, in terms of oxidative stress and antioxidant responses. This study will help to establish the possible physiological alterations of the oxidative status in sensitive and resistant plants, the physiological importance of this oxidative stress and whether ALS inhibition is causing the oxidative stress.

2 Materials and methods

2.1 Plant material and treatment application

The seeds of the *A. palmeri* populations nicosulfuron-sensitive (S) and resistant (R) were kindly provided by Dr. Joel Torra (University of Lleida, Catalonia, Spain) and were originally collected from Lleida (Spain). In R plants, resistance is supposed to be conferred by a mutation in Ser-653 and/or Trp-574 (Torra et al., 2020).

Plants were cultivated and grown hydroponically. Briefly, seeds were surface sterilized prior to germination (Labhilili et al., 1995). For germination, seeds were incubated for 4 days at 4 °C in darkness. Then, they were maintained for 60 h in a light/darkness cycle of 16 h/8 h at a temperature of 30 °C/18 °C. After germination, plants were transferred to aerated 2.7 L hydroponic tanks in a phytotron (day/night, 16 h/8 h; light intensity, 0.5 mmol s^{-1} m^{-2} PAR; temperature, 22/18 °C; relative humidity, 60/70%). The plants remained in the vegetative phenological stage throughout the entire course of the experiment. The full-strength Hoagland solution with 15 mM KNO_3 (Hoagland and Arnon, 1950) was used as nutrient solution. All the analytical determinations were made on plants in the vegetative phenological stage.

Plants were treated after reaching the growth stage defined as BBCH 14.35 (19-22 days old). Nicosulfuron (commercial product: Samson®, Key, Tárrega, CAT, Spain) was applied at two different rates: recommended field rate (FR) or 3 times FR (3FR), being FR 0.06 kg ha^{-1} (Huang et al., 2019). The herbicide was sprayed using an aerograph (model Definik, Sagola, Vitoria-Gasteiz, EUS, Spain) connected to a compressor (model Werther one, Breverrato, Italy; 60 W, 10 L m^{-1}, 2.5 bar). On each population, untreated plants (rate 0, control) were sprayed with water using the same aerograph and compressor.

2.2 Analytical determinations

One week after herbicide treatment, leaves were sampled, frozen in liquid N_2 and stored at -80 °C. Leaf samples were powdered with a Retsch mixer mill (MM200, Retsch, Haan, Germany) and the amount of tissue needed for each analytical determination was separated. Several treated and untreated plants were left in the phytotron to check the lethality of the applied nicosulfuron rates.

2.2.1 DNA analysis: Derived Cleaved Amplified Polymorphic Sequences (dCAPS) assay for the resistant mutation

Genomic DNA was extracted from previously ground *A. palmeri* leaves (0.1 g), as described before (Fernández-Escalada et al., 2016). DNA was quantified and analysed using a Synergy™ HT Multi-Detection Microplate Reader (BioTek Instruments Inc., Winooski, VT, USA) and its quality was checked using 1% agarose gel electrophoresis. Extracted gDNA was used to perform the Derived Cleaved Amplified Polymorphic Sequences (dCAPS) assay for resistant mutations in two *ALS* positions: Trp-574 and Ser-653, to confirm which mutation(s) occurred.

The dCAPS analyses were conducted to determine the possible mutant ALS alleles, as described before (Barco-Antoñanzas et al., 2022).

2.2.2 H_2O_2 detection

Hydrogen peroxide (H_2O_2) concentration was determined using the Amplex™ Red Hydrogen Peroxide/Peroxidase Assay Kit (Invitrogen, Thermo Fisher Scientific, Carlsbad, CA, USA) according to Deckers et al. (2020) in a FLUOstar Omega microplate reader (BMG Labtech, Ortenberg, Germany). Results for each herbicide treatment were expressed in % of the respective untreated plants of the same population to remove daily variability.

2.2.3 Lipid peroxidation

Lipid peroxidation was determined by spectrophotometric detection of malondialdehyde (Hodges et al., 1999). Samples (0.05 g) were homogenised and MDA-TBA complex was extracted as described in Eceiza et al. (2022). Malondialdehyde-TBA complex content was measured at 532 nm and correction for unspecific turbidity and sugar-TBA complexes was done by subtracting the absorbance of the same sample at 600 and 400 nm respectively (Hodges et al., 1999; Verma and Dubey, 2003).

2.2.4 Glutathione and related compounds

Glutathione was extracted from samples (0.1 g) in 1 mL 1 M HCl, derivatised with 5-iodoacetamide fluorescein (Eceiza et al., 2022) and reduced with tributylphosphine (Zinellu et al., 2005). Glutathione content was measured by capillary electrophoresis (CE) equipped with a laser-induced fluorescence detector (Zulet et al., 2015).

Reduced glutathione (GSH) was determined directly by injection of an aliquot in the CE. Oxidised glutathione (GSSG) was reduced with 10% tributylphosphine and then total GSH, cysteine (Cys) and γ-glutamyl-cysteine (GGC) were analysed by

CE. GSSG was determined as the difference between both total and reduced GSH values (Eceiza et al., 2022).

2.2.5 Ascorbate

Ascorbate was extracted from samples (0.05 g) in 0.3 mL ice cold 2% meta-phosphoric acid containing 1 mM EDTA (Schützendübel et al., 2002). The homogenate was filtered (0.22 µm, Millex GV),. Ascorbate was analysed by high-performance CE in a Beckman Coulter P/ACE MDQ (Fullerton, CA, USA) associated with a diode array detector (Herrero-Martínez et al., 2000) and equipped with the P/ACE station software for instrument control and data handling (Eceiza et al., 2022).

Reduced ascorbate was determined directly by injecting an aliquot in the CE. Dehydroascorbic acid was reduced with 200 mM dithiothreitol and then total ascorbate was analysed by CE. Dehydroascorbic acid was determined as the difference between both ascorbate values (Eceiza et al., 2022).

2.2.6 Enzymatic activities

For the enzymatic activities, proteins were extracted from samples (0.1 g) as described in Eceiza et al. (2022). Activities of four antioxidant enzymes were measured according to Eceiza et al. (2022): superoxide dismutase (SOD), catalase (CAT) peroxidase (POX) and glutathione reductase (GR). SOD activity was measured as the disappearance of superoxide formed by the reaction between xanthine and xanthine oxidase. Increase in absorbance due to the disappearance of superoxide was measured at 550 nm. CAT activity was measured as the disappearance of H_2O_2. Decrease in absorbance owing to the disappearance of H_2O_2 was measured at 280 nm. Activity of peroxidases was measured with guaiacol as the substrate. Increase in the absorbance due to oxidation of guaiacol was measured at 470 nm. GR activity was measured with NADPH as the substrate. Decrease in absorbance due to the oxidation of NADPH was measured at 340 nm. Results of the four enzymatic activities were related to total soluble protein, measured in the same extracts (Bradford, 1976). A synergy™ HT Multi-Detection Microplate Reader (BioTek Instruments Inc., Winooski, VT, USA) was used for absorbance measurements.

2.2.7 Gene expression analysis

Relative transcript level was calculated for three genes encoding antioxidant enzymes, corresponding to two isozymes of SOD (*CuZnSOD* and *MnSOD*) and CAT (*CAT*).

RNA extraction and the subsequent cDNA synthesis were performed according to Fernández-Escalada et al. (2017). The cDNA was diluted tenfold and stored at -20 °C until analysis as described in Hendrix et al. (2020). Primers (Supplementary Table 1) were designed using the coding sequence of *A. palmeri* and crossed with *Amaranthus hypochondriacus* in the case of both SOD isozymes and *Spinacia oleracea* in the case of *CAT*, using Primer 3 software. Their specificity was verified in silico using NCBI BLAST.

Quantitative real-time PCR (qPCR) was performed using the Quantinova™ SYBR® Green PCR Kit (Qiagen, Hilden, Germany) and according to Hendrix et al. (2020). The amplification conditions were the following: 2 min at 95 °C, 60 cycles of 5 s at 95 °C and 25 s at the annealing temperature (Supplementary Table 1). In order to confirm product specificity, a melt curve was generated. Relative gene expression levels were calculated using the $2^{-\Delta Cq}$ method. Data were normalised against the expression of a set of stable reference genes selected *via* the GrayNorm algorithm (Remans et al., 2014) listed in Supplementary Table 1; and whose primers were designed using the sequence of *A. palmeri* and crossed with *A. hypochondriacus*. Primer efficiencies were obtained using a standard curve of a two-fold dilution series generated from a pooled sample. The optimal annealing temperature (58-60 °C) for each primer was determined by gradient PCR, and only primers with an efficiency between 80 and 120% were used for qPCR analysis.

2.3 Statistical analysis

Separately maintained individual plants were considered as biological replicates. For statistical analyses, plants were separated according to their resistance level: sensitive (no mutations in *ALS*) and resistant (mutations in Trp-574 or Trp-574+Ser-653). Each mean value was calculated using samples from 4 different individual plants with the same genotype (sensitive or resistant) that received the same herbicide treatment. Possible difference between untreated (control) plants of each population was evaluated using Student's t-test and considered significant when p-value ≤ 0.05. In each population, the differences between plants that had received a herbicide treatment (FR of nicosulfuron or 3FR of nicosulfuron) and the untreated plants of the same population were evaluated using Student's t-test and considered significant when p-value ≤ 0.05. Significant differences between untreated plants of both populations are highlighted in the figures with pound symbols. Significant differences between untreated and treated plants within each population are highlighted in the figures with asterisks.

All statistical analyses were carried out using SPSS 27 software. Graphs were constructed using Sigma Plot 12 software.

3 Results

Untreated S and R plants grew equally. Treated S plants were alive one week after treatment (when leaves were sampled), but died in the following few weeks, as a result of a slow herbicidal

response. Resistant plants did not die in response to herbicide treatment.

3.1 Genotyping of R plants (dCAPS)

The resistance genotyping of the resistant individuals is shown in Table 1. All R plants contained the Trp-574 mutation and were heterozygous for this trait, so it can be established as the main mutation conferring resistance in this population. An example of a representative agarose gel showing the detection of heterozygosity by dCAPS is shown (Supplementary Figure 1).

Most plants showed the Trp-574 mutation as a single mutation, but some plants also contained the Ser-653 mutation, being then resistant due to a double mutation. While the genotyping of the resistant population was based on almost 100 individuals, the individuals used for the physiological study were selected to have only the Trp-574 mutation, ensuring the genetic similarity of the population.

3.2 H_2O_2 and MDA content

There was a similar H_2O_2 concentration in untreated S and R plants (Supplementary Table 2). Nicosulfuron treatment induced H_2O_2 accumulation, especially in S plants treated with 3FR (Figure 1A). For its part, MDA basal levels (of untreated plants) were similar in S and R plants (Figure 1B). MDA content increased proportionally to nicosulfuron rate in S plants, with a significant MDA accumulation in plants treated with 3FR (Figure 1B). In R plants, however, no significant changes were detected.

3.3 Non-enzymatic antioxidants

Untreated S plants showed a higher total GSH content than R plants, more due to the GSH content than to the GSSG content (Figures 2A, B, E). Both GSH and especially GSSG contents dropped with FR in S plants, a tendency that may also be seen in Cys content in R plants (Figure 2C), although in both cases no significant differences were found. GGC content and GSH to GSSG ratio did not show any significant variations between untreated and treated plants (Figures 2D, F) and none of these parameters changed in response to nicosulfuron in R plants.

Nicosulfuron treatment did not induce remarkable changes in ascorbic acid and dehydroascorbic acid content (Figure 3). Ascorbic acid content showed a decreasing tendency in S plants with FR, but with 3FR it was very similar to that of the control (Figure 3A). The pattern was the same for dehydroascorbic acid (Figure 3B) the sum of ascorbic acid and dehydroascorbic acid (Figure 3C) and ascorbic acid to dehydroascorbic acid ratio (Figure 3D). None of the analysed parameters showed any variation in R plants.

3.4 Antioxidant enzymatic activities and gene expressions

Activities of four antioxidant enzymes were measured: SOD, CAT, GR, and POX. SOD and CAT are important antioxidant enzymes that scavenge superoxide and H_2O_2, respectively. GR is a key enzyme in the glutathione-ascorbate cycle that catalyses GSH turnover *via* GSSG reduction (Carlberg and Mannervik, 1985), while peroxidases conform a vast group of enzymes with many different functions, including antioxidant activity (Radwan and Fayez, 2016). Basal enzymatic activities of S and R plants were statistically similar (Figure 4). SOD (Figure 4A) and GR (Figure 4C) activities increased in S plants with herbicide treatment, being the increases significant with 3FR; in R plants no significant changes were observed. CAT showed a similar increasing tendency in S plants, and a decreasing tendency in R plants, but in none of these cases was it significant (Figure 4B). POX tended to increase proportionally to nicosulfuron rate in both populations, yet it was not significant (Figure 4D).

Regarding gene expressions, relative transcript levels were calculated for three genes encoding two isozymes of superoxide dismutase (*CuZnSOD* and *MnSOD*) and catalase (*CAT*). Both SOD and CAT are important antioxidant enzymes that act as superoxide

TABLE 1 Genotyping of resistant (R) *Amaranthus palmeri* plants original from Lleida (Catalonia, Spain).

Mutation type	Mutation	% of total R (mutated) individuals	Heterozygous individuals (Trp-574) (%)	Homozygous individuals (Trp-574) (%)	Heterozygous individuals (Ser-653) (%)	Homozygous individuals (Ser-653) (%)
Simple	Trp-574	95.24	95	5	–	–
Simple	Ser-653	0	–	–	–	–
Double	Trp-574 + Ser-653	4.76	100	0	50	50

Percentages of plants with each mutation(s) with respect to total resistant plants; and of heterozygous individuals for each mutation with respect to all plants containing that mutation are shown.

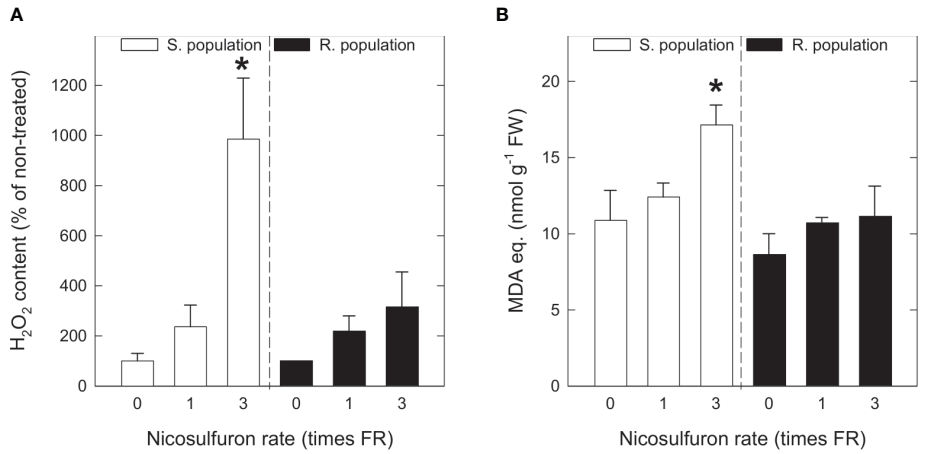

FIGURE 1
H_2O_2 content **(A)** and malondialdehyde (MDA) equivalents **(B)** in *Amaranthus palmeri* sensitive (S, white) and resistant (R, black) populations treated with different nicosulfuron rates (X axis, times recommended field rate or FR, FR = 0.06 kg ha^{-1}). Mean ± SE (n = 4). For each population, significant differences between treatments and their respective untreated are highlighted with asterisks (Student's t-test, p value ≤ 0.05).

and H_2O_2 (two of the main ROS) scavengers, respectively. Superoxide dismutase isozymes differ in the location: CuZnSOD is found in cytosol, chloroplasts and peroxisomes and MnSOD is found in mitochondria and peroxisomes (Houmani et al., 2016). Firstly, untreated plants of both populations were compared and then, for treated plants in each population, the relative copy number (fold change) with respect to the respective untreated samples was calculated. None of the three analysed genes (*CuZnSOD*, *MnSOD*, and *CAT*) presented remarkable differences between untreated S and R plants (Supplementary Table 2). Gene expressions of the three of them were similar in the S population independently of nicosulfuron rate, and they tended to decrease with nicosulfuron rate in the R population, but no significant differences were observed (Figure 5).

4 Discussion

4.1 Resistance confirmation: Trp-574, the main mutation

According to Torra et al. (2020), resistance of resistant plants was conferred by Ser-653 and Trp-574 mutations. In this study, the Trp-574 mutation was found in all resistant plants and, in most of them, it was present as a heterozygous single mutation. In addition, in the 5% of the resistant individuals, Trp-574 mutation was complemented with the Ser-653 mutation. In order to minimise the genetic variability of the resistant plants, the physiological study was performed with plants only containing the Trp-574 mutation.

Trp-574 substitution is the most common point mutation that confers resistance to ALS inhibitors (Molin et al., 2016; Singh et al., 2019; Torra et al., 2020) and it has been found in populations of many other weeds including grasses (Yu et al., 2010; Hamouzová et al., 2014; Hernández et al., 2015; Deng et al., 2017; Mei et al., 2017; Wang et al., 2019). It is known to confer a broad cross-resistance to several chemical families of ALS inhibitors apart from sulfonlyureas, such as imidazolinones and triazolpirimidines (Yu et al., 2012; Küpper et al., 2017).

The mutant allele is dominant, and is not supposed to alter ALS functionality significantly (Yu et al., 2010). Moreover, according to previous studies, Trp-574 mutation does not endow the plants with additional physiological traits, as mutated and unmutated plants show similar growth and total amino acid, soluble sugar, and starch contents (Barco-Antoñanzas et al., 2022). This means that the mutation confers an important cross-resistance to ALS inhibitors with apparently negligible fitness costs (Tranel and Wright, 2002). Thus, as long as selection pressure made by ALS-inhibiting herbicides in fields continues, the prevalence of the Trp-574 mutation and hence the proportion of ALS inhibitor-resistant individuals is expected to rise, making resistance to ALS inhibitors an increasingly serious issue.

The present study showed that Trp-574 mutation does not have implications in the basal oxidative state either, as untreated S and R plants showed similar values for almost all the analysed parameters. Similar basal MDA and antioxidant levels in S and R plants mean that herbicide resistance is not accompanied by a different oxidative profile or an intrinsically enhanced antioxidant system, and there are no changes associated to the oxidative status in the R plants with respect to the S ones. The resistance is restricted to just the herbicide target (ALS enzyme), so any side effect of nicosulfuron that is not linked to ALS inhibition should occur in both sensitive and resistant plants.

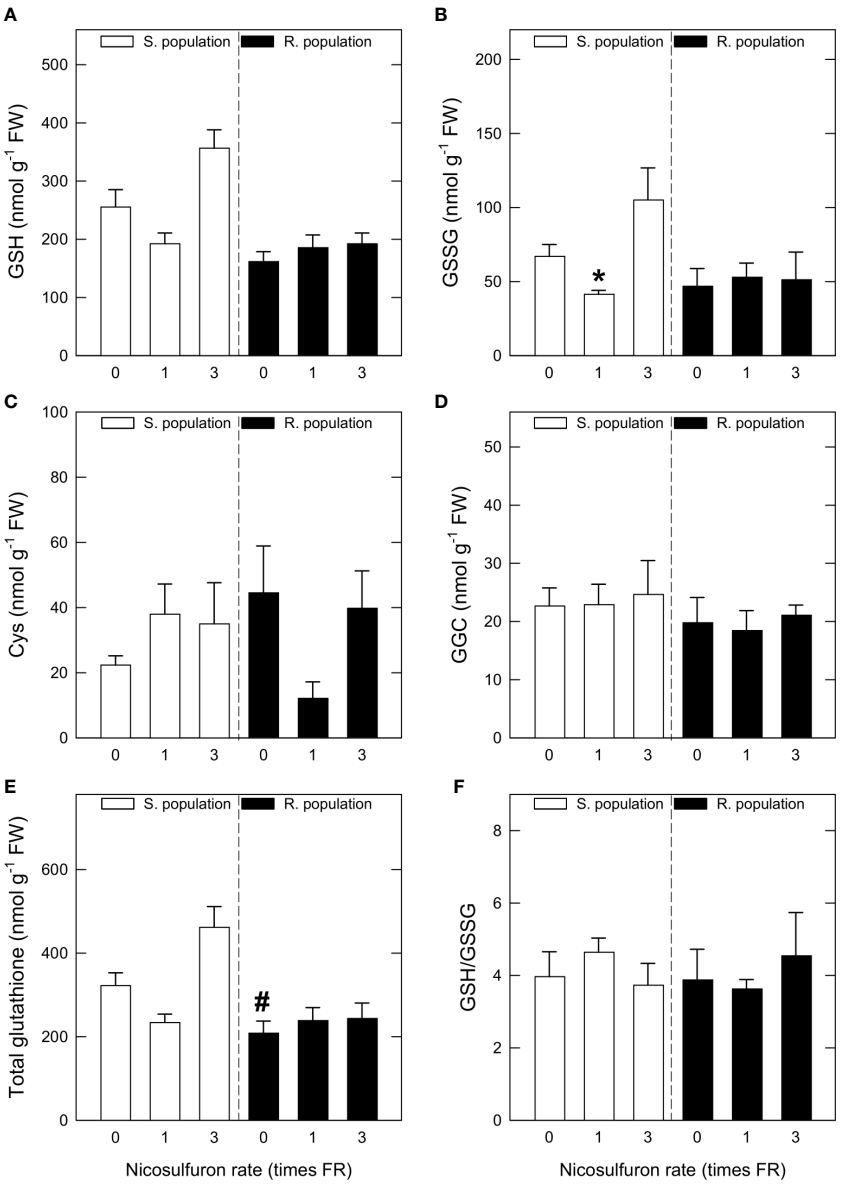

FIGURE 2
Reduced glutathione (GSH) content **(A)**, oxidised glutathione (GSSG) content **(B)**, γ-glutamyl-cysteine (GGC) content **(C)**, Cys content **(D)**, sum of GSH and GSSG (total glutathione) contents **(E)** and GSH to GSSG ratio **(F)** in *Amaranthus palmeri* sensitive (S, white) and resistant (R, black) populations treated with different nicosulfuron rates (X axis, times recommended field rate or FR, FR = 0.06 kg ha^{-1}). Mean ± SE (n = 4). Significant differences between untreated S and R plants are highlighted with pound symbols (Student's t-test, p value ≤ 0.05). For each population, significant differences between treatments and their respective untreated are highlighted with asterisks; (Student's t-test, p value ≤ 0.05). "#" indicates pound.

4.2 ALS inhibition causes oxidative damage in sensitive plants treated with high herbicide rates

That nicosulfuron has the potential of causing oxidative stress is made clear by the H_2O_2 accumulation induced by the herbicide treatment, which is especially remarkable in the S plants treated with 3FR. Hydrogen peroxide is an ubiquitous ROS synthesised in many physiological processes with plenty of biological functions, however, its formation usually increases under stress conditions and induces oxidative damage, mainly through hydroxyl (•OH) formation (Demidchik, 2015). This H_2O_2 accumulation following nicosulfuron treatment has been observed before in other species, especially in maize (Wang et al., 2018a; Wang et al., 2018c; Liu et al., 2019; Yang et al., 2021). In *A. palmeri*, a significant accumulation only occurred in S plants.

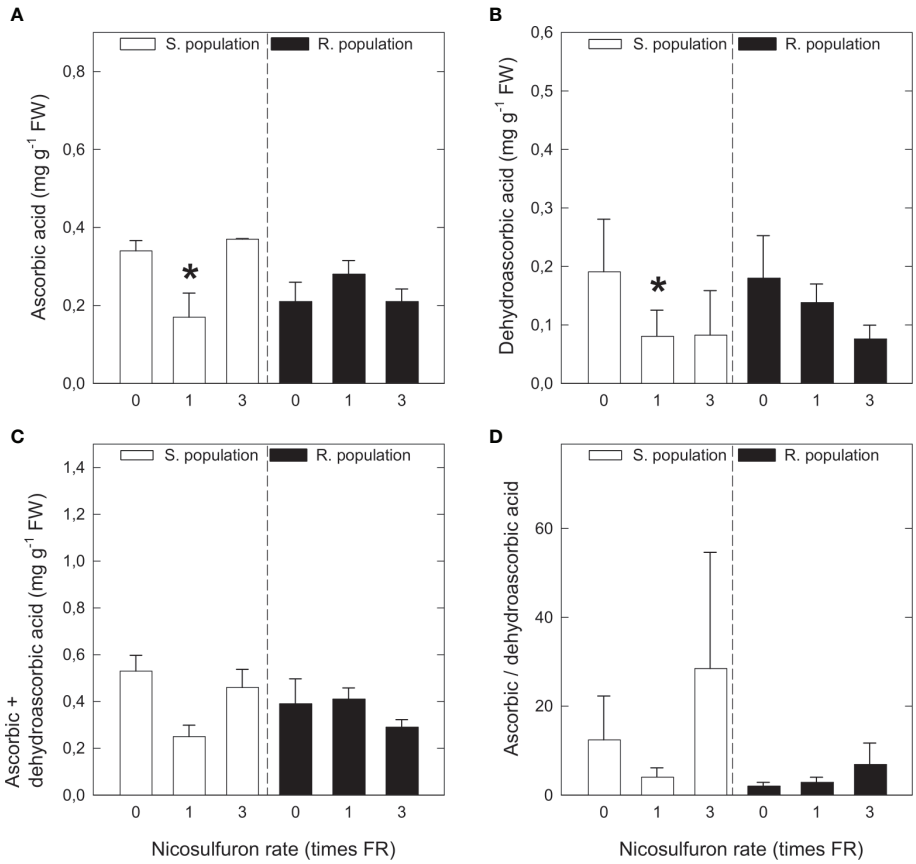

FIGURE 3
Ascorbic acid content **(A)**, dehydroascorbic acid content **(B)**, sum of ascorbic acid and dehydroascorbic acid **(C)** and ascorbic acid to dehydroascorbic acid ratio **(D)** in *Amaranthus palmeri* sensitive (S, white) and resistant (R, black) populations treated with different nicosulfuron rates (X axis, times recommended field rate or FR, FR = 0.06 kg ha^{-1}). Mean ± SE (n = 4). For each population, significant differences between treatments and their respective untreated are highlighted with asterisks (Student's t test, p value ≤ 0.05).

The fact that resistance is strictly based on the ALS enzyme and is not accompanied by a different oxidative metabolism, evidences that H_2O_2 formation is mainly due to ALS inhibition.

Physiological effects elicited by ALS inhibition have been related to oxidative stress beforehand, but the exact mechanisms induced by ALS inhibition that end ROS production are still unknown. One hypothesis is the activation of hypoxic metabolism (fermentation) in response to herbicide treatment, owing to a lower carbohydrate usage in roots (Gaston et al., 2002; Zabalza et al., 2005). In hypoxic tissues, H_2O_2 formation occurs because of over-reduction of redox chains (Blokhina et al., 2003). Another possible explanation for ROS formation after ALS inhibition would be residual respiration. Plants treated with ALS inhibitors are supposed to display higher residual respiration, increasing oxygen consumption and giving rise to a greater proportion of oxygen available to be used in the formation of ROS (Zabalza et al., 2007).

MDA is the main indicator of lipid peroxidation, and its accumulation is an almost unequivocal sign of oxidative damage. MDA accumulation in response to nicosulfuron treatment has been reported before in various species (Wang et al., 2018a; Liu et al., 2019; Silva et al., 2020; Concato et al., 2022); and it has been reported in pea leaves treated with imazethapyr, another ALS-inhibiting herbicide (Zabalza et al., 2007). In the present study, MDA increased proportionally to nicosulfuron rate in S plants, with a significant accumulation in plants treated with 3FR, and no major changes in R plants. These results are very consistent with the observed H_2O_2 accumulation and confirm a moderate oxidative damage in sensitive plants treated with 3FR.

4.3 Disparate activation of antioxidant systems in response to herbicide treatment

Moving into antioxidant systems, there was not a clear pattern in GSH contents and precursors, and in neither of the two populations is glutathione synthesis significantly enhanced

10.3389/fpls.2022.1040456

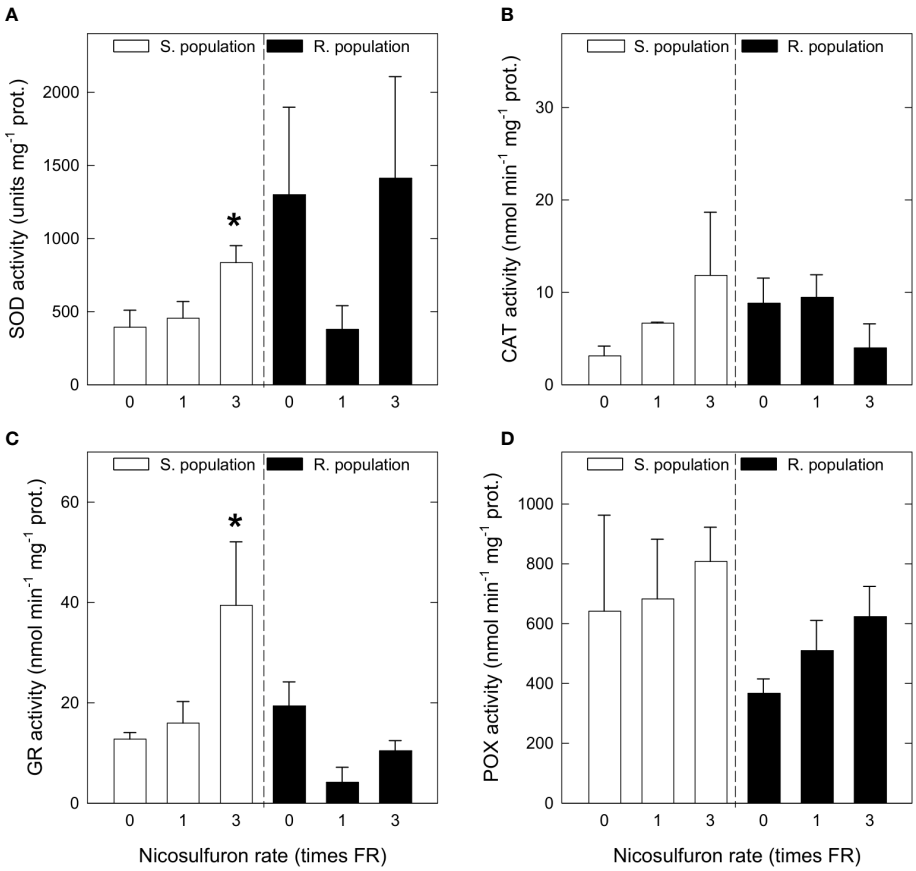

FIGURE 4
Superoxide dismutase (SOD) activity **(A)**, catalase (CAT) activity **(B)**, glutathione reductase (GR) activity **(C)** and peroxidases (POX) activity **(D)** in *Amaranthus palmeri* sensitive (S, white) and resistant (R, black) populations treated with different nicosulfuron rates (X axis, times recommended field rate or FR, FR = 0.06 kg ha^{-1}). Mean ± SE (n = 4). For each population, significant differences between treatments and their respective untreated are highlighted with asterisks (Student's t-test, p value ≤ 0.05).

by herbicide treatment, although there is an increasing tendency in S plants treated with 3FR. Nevertheless, there is some evidence that glutathione is acting as an endogenous antioxidant in treated S plants since GR activity strongly increases in S plants treated with 3FR. Glutathione's antioxidant activity is based on the reduction of H_2O_2 and peroxidised lipids, both of which are highly accumulated in S plants treated with 3FR. In return, GSH is oxidised to GSSG. Glutathione reductase, which follows the same pattern as the oxidative damage markers (H_2O_2 and MDA accumulation), catalyses GSSG to GSH reduction (Prego, 1995; Couto et al., 2016). Thus, it is likely that, in S plants treated with 3FR, glutathione's antioxidant activity is much higher, but no decrease in GSH content in favour of GSSG is observed due to a hugely increased GR activity.

Although ascorbic acid content decreased in S plants with FR, dehydroascorbic acid also decreased with the same rate, so the oxidative status of the plant is not altered in this sense. Furthermore, in plants treated with 3FR, the only rate with which a clear oxidative stress is induced, values for both compounds are similar to the ones in untreated plants. In R plants, no significant changes in antioxidant systems were detected, showing that R plants do not suffer oxidative stress after nicosulfuron application, and hence reinforcing the hypothesis that oxidative stress induced in S plants is related to ALS inhibition.

Activity of peroxidases could have been expected to increase, as a peroxidase (exactly glutathione peroxidase) is the enzyme that catalyses GSH oxidation (Prego, 1995). Nevertheless, only a slight, non-significant increase occurred, possibly because peroxidases are a very diverse group of enzymes involved in many physiological processes apart from the antioxidant system, such as germination, cell elongation, and lignification (Shigeto and Tsutsumi, 2016).

About the other two enzymes, SOD and CAT, what was observed with enzymatic activities was different to the observed in gene expression. Enzymatic activities of both enzymes tended

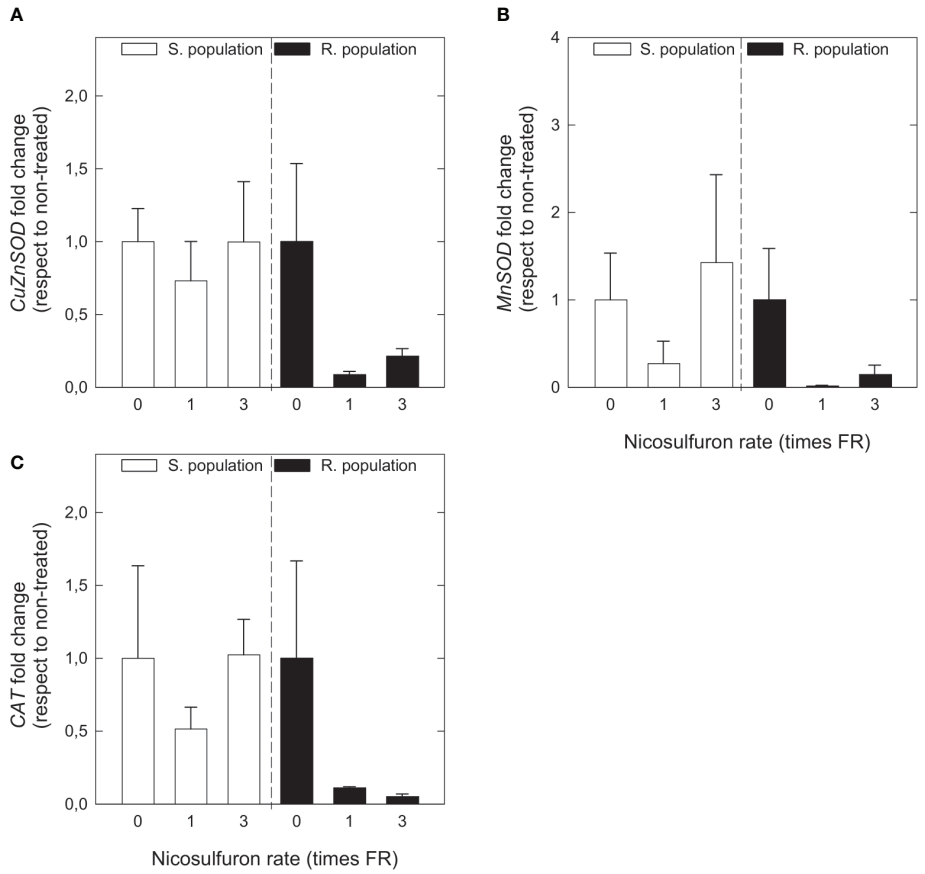

FIGURE 5
CuZn superoxide dismutase (*CuZnSOD*) gene expression **(A)**, Mn superoxide dismutase (*MnSOD*) gene expression **(B)** and catalase (*CAT*) gene expression **(C)** in *Amaranthus palmeri* sensitive (S, white) and resistant (R, black) populations), in relative fold change with respect to untreated plants of each population, treated with different nicosulfuron rates (X axis, times recommended field rate or FR, FR = 0.06 kg ha^{-1}). Mean ± SE (n = 4). For each population, no significant differences between treatments and their respective untreated were observed (Student's t test, p value ≤ 0.05).

to increase with nicosulfuron rate in S plants, although the increase was only significant in the case of SOD. This enzyme is a major superoxide scavenger. Superoxide is a more reactive and much less stable ROS than H_2O_2, but both ROS are strongly related (Demidchik, 2015). In view of the accumulation of H_2O_2 and the increase of SOD activity in S plants treated with 3FR, it is likely that superoxide formation is also increased in these plants. For its part, the increase of CAT activity with nicosulfuron rate in S plants was less clear, and in R plants it even showed a decreasing tendency. The cause of non-significance in S plants and the decreasing tendency in R plants could be a slight enzymatic inhibition caused by herbicidal activity. Concato et al. (2022) investigated the effects of various ALS inhibitors, including nicosulfuron, on the antioxidant system of *Brassica napus* and found that CAT was inhibited by all of them, similar to the study by Qian et al. (2011) in *Arabidopsis thaliana*. The difference in behaviour between the two populations is probably due to the huge H_2O_2 accumulation in S plants. Regarding gene expressions of *CuZnSOD*, *MnSOD* and *CAT*, both SOD isozymes and CAT behaved similarly, not following a clear pattern in S plants and with a tendency to decrease with nicosulfuron rate in R plants. This evidences that, in response to oxidative stress caused by nicosulfuron, SOD and CAT are induced posttranscriptionally.

These results do not entirely match with results from other species, especially *Zea mays*, where several studies have observed a clear activation of the antioxidant systems in response to nicosulfuron treatment (Wang et al., 2018a; Wang et al., 2018c; Liu et al., 2019; Yang et al., 2021). Biochemical and physiological differences between *Z. mays* and *A. palmeri* might explain the differences in the antioxidative response. Maize has a variable tolerance to sulfonylurea herbicides, which is not based on ALS but on a rapid metabolic inactivation by hydroxylation on the pyrimidine ring followed by glucose conjugation, with an important involvement of cytochrome P450 (Wittenbach et al., 1994; Dragičević et al., 2012). This sulfonylurea-resistance

mechanism has been associated with oxidative metabolism, probably involving an important antioxidant induction (Wang et al., 2018b).

4.4 Toxicity of ALS inhibitors is independent of oxidative stress

Finally, the most remarkable effect of nicosulfuron was oxidative damage in S plants, caused by ROS overproduction. Given that ROS formation was related to ALS inhibition, it can be taken as a general effect of ALS-inhibiting herbicides. The physiological mechanisms that link ALS inhibition with ROS formation are yet to be demonstrated and make up a potential object of study.

However, oxidative damage was only significant in S plants treated with 3FR (at least one week after treatment), when FR was already lethal for these plants after a couple weeks. This evidences that, as proposed before (Zabalza et al., 2007), oxidative damage is not one of the main causes of plant death. ALS-inhibiting herbicides trigger a moderate oxidative stress through ALS inhibition, but this oxidative stress is independent of herbicide toxicity.

5 Conclusion

To sum up, the resistance mechanism to ALS-inhibiting herbicides in the studied *A. palmeri* population is restricted to the target and is not accompanied by a different oxidative status. In response to high (supralethal) rates of nicosulfuron, sensitive plants suffer oxidative damage related to ALS inhibition. This oxidative damage is palliated, somewhat owing to the antioxidant role of glutathione and the antioxidant enzymes, and is not one of the main causes of plant death. Resistant plants do not suffer oxidative damage nor increase their antioxidant activity. Having concluded that triggered oxidative stress is due to ALS inhibition, the presented results are surely extensible to other ALS-inhibiting herbicides to which plants with Trp-574 mutation are resistant. However, other plants species or plants with different resistance mechanisms may respond differently.

Data availability statement

The raw data supporting the conclusions of this article will be made available by the authors, without undue reservation.

Author contributions

MR and AZ conceived the study. AZ, AC, and MR designed the experiments. MB-A, ME, and MH performed the experiments and analysed the data. ME wrote the draft of the manuscript. MG-M, MH, AZ, AC, and MR revised the manuscript. ME wrote the final version of the manuscript. All authors read and approved the final manuscript.

Funding

This work was financed by the Public University of Navarre (Project UPNA20-6138) and the Spanish Ministry of Science and Innovation (2020 117723-RB-100). ME is the holder of a predoctoral fellowship of the Basque Government and he also received a mobility grant from the same Government.

Acknowledgments

The authors would like to acknowledge G. Garijo, J. Encinas and C. Jiménez for technical assistance, and J. Torra (University of Lleida, CAT, Spain) for providing seeds.

Conflict of interest

The authors declare that the research was conducted in the absence of any commercial or financial relationships that could be construed as a potential conflict of interest.

Publisher's note

Supplementary material

The Supplementary Material for this article can be found online at: https://www.frontiersin.org/articles/10.3389/fpls.2022.1040456/full#supplementary-material

References

Ahsan, N., Lee, D. G., Lee, K. W., Alam, I., Lee, S. H., Bahk, J. D., et al. (2008). Glyphosate-induced oxidative stress in rice leaves revealed by proteomic approach. *Plant Physiol. Biochem.* 46, 1062–1070. doi: 10.1016/j.plaphy.2008.07.002

Barco-Antoñanzas, M., Gil-Monreal, M., Eceiza, M. V., Royuela, M., and Zabalza, A. (2022). Primary metabolism in an *Amaranthus palmeri* population with multiple resistance to glyphosate and pyrithiobac herbicides. *Plant Sci.* 318, 111212. doi: 10.1016/j.plantsci.2022.111212

Blokhina, O., Virolainen, E., and Fagerstedt, K. V. (2003). Antioxidants, oxidative damage and oxygen deprivation stress: A review. *Ann. Bot.* 91, 179–194. doi: 10.1093/aob/mcf118

Bradford, M. (1976). A rapid and sensitive method for the quantitation of microgram quantities of protein utilizing the principle of protein-dye binding. *Anal. Biochem.* 72, 248–254. doi: 10.1006/abio.1976.9999

Carlberg, I., and Mannervik, B. (1985). "Glutathione reductase," in. *Methods Enzymology* 113, 484–490. doi: 10.1016/S0076-6879(85)13062-4

Caverzan, A., Piasecki, C., Chavarria, G., Stewart, C., and Vargas, L. (2019). Defenses against ROS in crops and weeds: The effects of interference and herbicides. *Int. J. Mol. Sci.* 20, 1086. doi: 10.3390/ijms20051086

Chaudhari, S., Varanasi, V. K., Nakka, S., Bhowmik, P. C., Thompson, C. R., Peterson, D. E., et al. (2020). Evolution of target and non-target based multiple herbicide resistance in a single palmer amaranth (*Amaranthus palmeri*) population from Kansas. *Weed Technol.* 34, 447–453. doi: 10.1017/wet.2020.32

Concato, A. C., Galon, L., Sutorillo, N. T., Tamagno, W. A., de Paula, M. O., Vanin, A. P., et al. (2022). Does the application of herbicides with distinct mechanisms of action change enzymatic activity and grain yield of clearfield® canola? *Aust. J. Crop Sci.* 16, 93–102. doi: 10.21475/ajcs.22.16.01.p3282

Couto, N., Wood, J., and Barber, J. (2016). The role of glutathione reductase and related enzymes on cellular redox homoeostasis network. *Free Radic. Biol. Med.* 95, 27–42. doi: 10.1016/j.freeradbiomed.2016.02.028

Deckers, J., Hendrix, S., Prinsen, E., Vangronsveld, J., and Cuypers, A. (2020). Identifying the pressure points of acute cadmium stress prior to acclimation in *Arabidopsis thaliana*. *Int. J. Mol. Sci.* 21, 1–22. doi: 10.3390/ijms21176232

de Freitas-Silva, L., Rodríguez-Ruiz, M., Houmani, H., da Silva, L. C., Palma, J. M., and Corpas, F. J. (2017). Glyphosate-induced oxidative stress in *Arabidopsis thaliana* affecting peroxisomal metabolism and triggers activity in the oxidative phase of the pentose phosphate pathway (OxPPP) involved in NADPH generation. *J. Plant Physiol.* 218, 196–205. doi: 10.1016/j.jplph.2017.08.007

Demidchik, V. (2015). Mechanisms of oxidative stress in plants: From classical chemistry to cell biology. *Environ. Exp. Bot.* 109, 212–228. doi: 10.1016/j.envexpbot.2014.06.021

Deng, W., Yang, Q., Zhang, Y., Jiao, H., Mei, Y., Li, X., et al. (2017). Cross-resistance patterns to acetolactate synthase (ALS)-inhibiting herbicides of flixweed (*Descurainia sophia* l.) conferred by different combinations of ALS isozymes with a pro-197-Thr mutation or a novel trp-574-Leu mutation. *Pestic. Biochem. Physiol.* 136, 41–45. doi: 10.1016/j.pestbp.2016.08.006

Dragicević, V., Simić, M., Brankov, M., Spasojević, I., and Kresović, B. (2011). Alterations of phosphorus metabolism in maize inbred lines influenced by herbicides. *Herbologia* 12, 93–101.

Dragičević, V., Simić, M., Sečanski, M., Cvijanović, G., and Nišavić, A. (2012). Study of the susceptibility of maize lines to some sulfonylurea herbicides. *Genetika* 44, 355–366. doi: 10.2298/GENSR1202355D

Eceiza, M. V., Gil-Monreal, M., Barco-Antoñanzas, M., Zabalza, A., and Royuela, M. (2022). The moderate oxidative stress induced by glyphosate is not detected in *Amaranthus palmeri* plants overexpressing EPSPS. *J. Plant Physiol.* 274, 153720. doi: 10.1016/j.jplph.2022.153720

Edwards, R., and Hannah, M. (2014). Focus on weed control. *Plant Physiol.* 166, 1087–1089. doi: 10.1104/pp.114.900496

Fernández-Escalada, M., Gil-Monreal, M., Zabalza, A., and Royuela, M. (2016). Characterization of the *Amaranthus palmeri* physiological response to glyphosate in susceptible and resistant populations. *J. Agric. Food Chem.* 64, 95–106. doi: 10.1021/acs.jafc.5b04916

Fernández-Escalada, M., Zulet-González, A., Gil-Monreal, M., Zabalza, A., Ravet, K., Gaines, T., et al. (2017). Effects of EPSPS copy number variation (CNV) and glyphosate application on the aromatic and branched chain amino acid synthesis pathways in amaranthus palmeri. *Front. Plant Sci.* 8. doi: 10.3389/fpls.2017.01970

Gaston, S., Zabalza, A., Gonzalez, E. M., Arrese-Igor, C., Aparicio-Tejo, P. M., and Royuela, M. (2002). Imazethapyr, an inhibitor of the branched-chain amino acid biosynthesis, induces aerobic fermentation in pea plants. *Physiol. Plant* 114, 524–532. doi: 10.1034/j.1399-3054.2002.1140404.x

Gomes, M. P., and Juneau, P. (2016). Oxidative stress in duckweed (*Lemna minor* l.) induced by glyphosate: Is the mitochondrial electron transport chain a target of this herbicide? *Environ. Pollut.* 218, 402–409. doi: 10.1016/j.envpol.2016.07.019

Hamouzová, K., Košnarová, P., Salava, J., Soukup, J., and Hamouz, P. (2014). Mechanisms of resistance to acetolactate synthase-inhibiting herbicides in populations of *Apera spica-venti* from the Czech republic. *Pest Manage. Sci.* 70, 541–548. doi: 10.1002/ps.3563

Heap, I. (2022) *The international survey of herbicide resistant weeds*. Available at: http://www.weedscience.com/Home.aspx (Accessed July 8, 2021).

Hendrix, S., Jozefczak, M., Wójcik, M., Deckers, J., Vangronsveld, J., and Cuypers, A. (2020). Glutathione: A key player in metal chelation, nutrient homeostasis, cell cycle regulation and the DNA damage response in cadmium-exposed *Arabidopsis thaliana*. *Plant Physiol. Biochem.* 154, 498–507. doi: 10.1016/j.plaphy.2020.06.006

Hernández, M. J., León, R., Fischer, A. J., Gebauer, M., Galdames, R., and Figueroa, R. (2015). Target-site resistance to nicosulfuron in johnsongrass (*Sorghum halepense*) from Chilean corn fields. *Weed Sci.* 63, 631–640. doi: 10.1614/ws-d-14-00167.1

Herrero-Martínez, J. M., Simó-Alfonso, E. F., Ramis-Ramos, G., Deltoro, V. I., Calatayud, A., and Barreno, E. (2000). Simultaneous determination of l-ascorbic acid, glutathione, and their oxidized forms in ozone-exposed vascular plants by capillary zone electrophoresis. *Environ. Sci. Technol.* 34, 1331–1336. doi: 10.1021/es991068l

Hoagland, D. R., and Arnon, D. I. (1950). The water-culture method for growing plants without soil. *Calif. Agric. Exp. Stn. Circ.* 347, 1–32.

Hodges, D. M., DeLong, J. M., Forney, C. F., and Prange, R. K. (1999). Improving the thiobarbituric acid-reactive-substances assay for estimating lipid peroxidation in plant tissues containing anthocyanin and other interfering compounds. *Planta* 207, 604–611. doi: 10.1007/s004250050524

Houmani, H., Rodríguez-ruiz, M., Palma, J. M., Abdelly, C., and Corpas, F. J. (2016). Modulation of superoxide dismutase (SOD) isozymes by organ development and high long-term salinity in the halophyte *Cakile maritima*. *Protoplasma* 253, 885–894. doi: 10.1007/s00709-015-0850-1

Huang, Z., Huang, H., Chen, J., Chen, J., Wei, S., and Zhang, C. (2019). Nicosulfuron-resistant *Amaranthus retroflexus* L. in Northeast China. *Crop Protection* 122, 79–83. doi: 10.1016/j.cropro.2019.04.024

Küpper, A., Borgato, E. A., Patterson, E. L., Netto, A. G., Nicolai, M., De Carvalho, S. J. P., et al. (2017). Multiple resistance to glyphosate and acetolactate synthase inhibitors in palmer amaranth (*Amaranthus palmeri*) identified in Brazil. *Weed Sci.* 65, 317–326. doi: 10.1017/wsc.2017.1

Labhilili, M., Joudrier, P., and Gautier, M. F. (1995). Characterization of cDNAs encoding triticum durum dehydrins and their expression patterns in cultivars that differ in drought tolerance. *Plant Sci.* 112, 219–230. doi: 10.1016/0168-9452(95)04267-9

Larran, A. S., Palmieri, V. E., Perotti, V. E., Lieber, L., Tuesca, D., and Permingeat, H. R. (2017). Target-site resistance to acetolactate synthase (ALS)-inhibiting herbicides in *Amaranthus palmeri* from Argentina. *Pest Manage. Sci.* 73, 2578–2584. doi: 10.1002/ps.4662

Liu, S., He, Y., Tian, H., Yu, C., Tan, W., Li, Z., et al. (2019). Application of brassinosteroid mimetics improves growth and tolerance of maize to nicosulfuron toxicity. *J. Plant Growth Regul.* 38, 701–712. doi: 10.1007/s00344-018-9883-y

Mazur, B. J., and Falco, S. C. (1989). The development of herbicide resistant crops. *Annu. Rev. Plant Physiol. Plant Mol. Biol.* 40, 441–470. doi: 10.1146/annurev.pp.40.060189.002301

Mei, Y., Si, C., Liu, M., Qiu, L., and Zheng, M. (2017). Investigation of resistance levels and mechanisms to nicosulfuron conferred by non-target-site mechanisms in large crabgrass (*Digitaria sanguinalis* l.) from China. *Pestic. Biochem. Physiol.* 141, 84–89. doi: 10.1016/j.pestbp.2016.12.002

Molin, W. T., Nandula, V. K., Wright, A. A., and Bond, J. A. (2016). Transfer and expression of ALS inhibitor resistance from palmer amaranth (*Amaranthus palmeri*) to an *A. spinosus* × *a. palmeri* hybrid. *Weed Sci.* 64, 240–247. doi: 10.1614/WS-D-15-00172.1

Murphy, B., and Tranel, P. (2019). Target-site mutations conferring herbicide resistance. *Plants* 8, 382. doi: 10.3390/plants8100382

Nakka, S., Thompson, C. R., Peterson, D. E., and Jugulam, M. (2017). Target site–based and non–target site based resistance to ALS inhibitors in palmer amaranth (*Amaranthus palmeri*). *Weed Sci.* 65, 681–689. doi: 10.1017/wsc.2017.43

Orcaray, L., Igal, M., Zabalza, A., and Royuela, M. (2011). Role of exogenously supplied ferulic and p-coumaric acids in mimicking the mode of action of

acetolactate synthase inhibiting herbicides. *J. Agric. Food Chem.* 59, 10162–10168. doi: 10.1021/jf2025538

Ostera, J. M., Malanga, G., and Puntarulo, S. (2016). Actualización sobre aspectos oxidativos del efecto del glifosato en sistemas biológicos. *Biotecnia* XVIII, 3–10. doi: 10.18633/bt.v18i2.279

Prego, E. C. (1995). La glutation reductasa y su importancia biomédica. *Rev. Cuba. Investig. Biomédicas* 14, 13–16.

Qian, H., Wang, R., Hu, H., Lu, T., Chen, X., Ye, H., et al. (2011). Enantioselective phytotoxicity of the herbicide imazethapyr and its effect on rice physiology and gene transcription. *Environ. Sci. Technol.* 45, 7036–7043. doi: 10.1021/es200703v

Radwan, D. E. M., and Fayez, K. A. (2016). Photosynthesis, antioxidant status and gas-exchange are altered by glyphosate application in peanut leaves. *Photosynthetica* 54, 307–316. doi: 10.1007/s11099-016-0075-3

Remans, T., Keunen, E., Bex, G. J., Smeets, K., Vangronsveld, J., and Cuypers, A. (2014). Reliable gene expression analysis by reverse transcription-quantitative PCR: Reporting and minimizing the uncertainty in data accuracy. *Plant Cell* 26, 3829–3837. doi: 10.1105/tpc.114.130641

Rey-Caballero, J., Menéndez, J., Osuna, M. D., and Torra, J. (2017). Target-site and non-target-site resistance mechanisms to ALS inhibiting herbicides in *Papaver rhoeas*. *Pestic. Biochem. Physiol.* 138, 57–65. doi: 10.1016/j.pestbp.2017.03.001

Scarponi, L., Alla, M. M. N., and Martinetti, L. (1995). Consequences on nitrogen-metabolism in soybean (*Glycine-max* l) as a result of imazethapyr action on acetohydroxy acid synthase. *J. Agric. Food Chem.* 43, 809–814. doi: 10.1021/jf00051a047

Scarponi, L., Younis, M. E., Standardi, A., Hassan, N. M., and Martinetti, L. (1997). Effects of chlorimuron-ethyl, imazethapyr, and propachlor on free amino acids and protein formation in *Vicia faba* l. *J. Agric. Food Chem.* 45, 3652–3658. doi: 10.1021/jf960771f

Schützendübel, A., Nikolova, P., Rudolf, C., and Polle, A. (2002). Cadmium and H_2O_2-induced oxidative stress in *Populus* × *canescens* roots. *Plant Physiol. Biochem.* 40, 577–584. doi: 10.1016/S0981-9428(02)01411-0

Shaner, D. L., and Reider, M. L. (1986). Physiological responses of corn (*Zea mays*) to AC 243,997 in combination with valine, leucine, and isoleucine. *Pestic. Biochem. Physiol.* 25, 248–257. doi: 10.1016/0048-3575(86)90051-9

Shigeto, J., and Tsutsumi, Y. (2016). Diverse functions and reactions of class III peroxidases. *New Phytol.* 209, 1395–1402. doi: 10.1111/nph.13738

Sidari, M., Pusino, A., Gessa, C., and Cacco, G. (1998). Effect of imazamethabenz-methyl on nitrate uptake in wheat (*Triticum durum* l.). *J. Agric. Food Chem.* 46, 2800–2803. doi: 10.1021/jf970958m

Silva, F. B., Costa, A. C., Müller, C., Nascimento, K. T., Batista, P. F., Vital, R. G., et al. (2020). *Dipteryx alata*, a tree native to the Brazilian cerrado, is sensitive to the herbicide nicosulfuron. *Ecotoxicology* 29, 217–225. doi: 10.1007/s10646-019-02154-7

Singh, S., Singh, V., Salas-Perez, R. A., Bagavathiannan, M. V., Lawton-Rauh, A., and Roma-Burgos, N. (2019). Target-site mutation accumulation among ALS inhibitor-resistant palmer amaranth. *Pest Manage. Sci.* 75, 1131–1139. doi: 10.1002/ps.5232

Sprague, C. L., Stoller, E. W., Wax, L. M., and Horak, M. J. (1997). Palmer amaranth (*Amaranthus palmeri*) and common waterhemp (*Amaranthus rudis*) resistance to selected ALS-inhibiting herbicides. *Weed Sci.* 45, 192–197. doi: 10.1017/s0043174500092705

Takano, H. K., Beffa, R., Preston, C., Westra, P., and Dayan, F. E. (2019). Reactive oxygen species trigger the fast action of glufosinate. *Planta* 249, 1837–1849. doi: 10.1007/s00425-019-03124-3

Torra, J., Royo-Esnal, A., Romano, Y., Osuna, M. D., León, R. G., and Recasens, J. (2020). *Amaranthus palmeri* a new invasive weed in Spain with herbicide resistant biotypes. *Agronomy* 10, 1–13. doi: 10.3390/agronomy10070993

Tranel, P. J., and Wright, T. R. (2002). Resistance of weeds to ALS inhibiting herbicides: what have we learned? *Weed Sci.* 50, 700–712. doi: 10.1614/0043-1745(2002)050[0700:RROWTA]2.0.CO;2

Verma, S., and Dubey, R. S. (2003). Lead toxicity induces lipid peroxidation and alters the activities of antioxidant enzymes in growing rice plants. *Plant Sci.* 164, 645–655. doi: 10.1016/S0168-9452(03)00022-0

Wang, Q., Ge, L., Zhao, N., Zhang, L., You, L., Wang, D., et al. (2019). A trp-574-Leu mutation in the acetolactate synthase (ALS) gene of *Lithospermum arvense* l. confers broad-spectrum resistance to ALS inhibitors. *Pestic. Biochem. Physiol.* 158, 12–17. doi: 10.1016/j.pestbp.2019.04.001

Wang, J., Zhong, X., Li, F., and Shi, Z. (2018a). Effects of nicosulfuron on growth, oxidative damage, and the ascorbate-glutathione pathway in paired nearly isogenic lines of waxy maize (*Zea mays* l.). *Pestic. Biochem. Physiol.* 145, 108–117. doi: 10.1016/j.pestbp.2018.01.015

Wang, J., Zhong, X. M., Lv, X. L., Shi, Z. S., and Li, F. H. (2018b). Photosynthesis and physiology responses of paired near-isogenic lines in waxy maize (*Zea mays* l.) to nicosulfuron. *Photosynthetica* 56, 1059–1068. doi: 10.1007/s11099-018-0816-6

Wang, J., Zhong, X., Zhu, K., Lv, J., Lv, X., Li, F., et al. (2018c). Reactive oxygen species, antioxidant enzyme activity, and gene expression patterns in a pair of nearly isogenic lines of nicosulfuron-exposed waxy maize (*Zea mays* l.). *Environ. Sci. pollut. Res.* 25, 19012–19027. doi: 10.1007/s11356-018-2105-0

Wittenbach, V. A., Koeppe, M. K., Lichtner, F. T., Zimmerman, W. T., and Reiser, R. W. (1994). Basis of selectivity of triflusulfuron methyl in sugar beets (*Beta vulgaris*). *Pestic. Biochem. Physiol.* 49, 72–81. doi: 10.1006/pest.1994.1035

Yang, M., Li, X., Jinling, H., Qing, Y., and Wang, J. (2021). Nicosulfuron stress on active oxygen accumulation, antioxidant system and related gene expression in sweet maize seedlings. *J. Nucl. Agric. Sci.* 35, 2182–2193. doi: 10.11869/J.ISSN.100-8551.2021.09.2182

Yu, Q., Han, H., Li, M., Purba, E., Walsh, M. J., and Powles, S. B. (2012). Resistance evaluation for herbicide resistance-endowing acetolactate synthase (ALS) gene mutations using *Raphanus raphanistrum* populations homozygous for specific ALS mutations. *Weed Res.* 52, 178–186. doi: 10.1111/j.1365-3180.2012.00902.x

Yu, Q., Han, H., Vila-Aiub, M. M., and Powles, S. B. (2010). AHAS herbicide resistance endowing mutations: Effect on AHAS functionality and plant growth. *J. Exp. Bot.* 61, 3925–3934. doi: 10.1093/jxb/erq205

Yu, Q., and Powles, S. B. (2014). Resistance to AHAS inhibitor herbicides: Current understanding. *Pest Manage. Sci.* 70, 1340–1350. doi: 10.1002/ps.3710

Zabalza, A., Gálvez, L., Marino, D., Royuela, M., Arrese-Igor, C., and González, E. M. (2008). The application of ascorbate or its immediate precursor, galactono-1,4-lactone, does not affect the response of nitrogen-fixing pea nodules to water stress. *J. Plant Physiol.* 165, 805–812. doi: 10.1016/j.jplph.2007.08.005

Zabalza, A., Gaston, S., Sandalio, L. M., del Río, L. A., and Royuela, M. (2007). Oxidative stress is not related to the mode of action of herbicides that inhibit acetolactate synthase. *Environ. Exp. Bot.* 59, 150–159. doi: 10.1016/j.envexpbot.2005.11.003

Zabalza, A., González, E. M., Arrese-Igor, C., and Royuela, M. (2005). Fermentative metabolism is induced by inhibiting different enzymes of the branched-chain amino acid biosynthesis pathway in pea plants. *J. Agric. Food Chem.* 53, 7486–7493. doi: 10.1021/jf050654x

Zhou, Q., Liu, W., Zhang, Y., and Liu, K. K. (2007). Action mechanisms of acetolactate synthase-inhibiting herbicides. *Pestic. Biochem. Physiol.* 89, 89–96. doi: 10.1016/j.pestbp.2007.04.004

Zinellu, A., Sotgia, S., Posadino, A. M., Pasciu, V., Perino, M. G., Tadolini, B., et al. (2005). Highly sensitive simultaneous detection of cultured cellular thiols by laser induced fluorescence-capillary electrophoresis. *Electrophoresis* 26, 1063–1070. doi: 10.1002/elps.200406191

Zulet, A., Gil-Monreal, M., Villamor, J. G., Zabalza, A., van der Hoorn, R. A. L., and Royuela, M. (2013). Proteolytic pathways induced by herbicides that inhibit amino acid biosynthesis. *PloS One* 8, e73847. doi: 10.1371/journal.pone.0073847

Zulet, A., Gil-Monreal, M., Zabalza, A., van Dongen, J. T., and Royuela, M. (2015). Fermentation and alternative oxidase contribute to the action of amino acid biosynthesis-inhibiting herbicides. *J. Plant Physiol.* 175, 102–112. doi: 10.1016/j.jplph.2014.12.004

frontiers | Frontiers in Plant Science

TYPE Original Research
PUBLISHED 10 January 2023
DOI 10.3389/fpls.2022.1040117

OPEN ACCESS

EDITED BY
Sabine Lüthje,
University of Hamburg, Germany

REVIEWED BY
Won-Gyu Choi,
University of Nevada, Reno, United States
Hartwig Luethen,
University of Hamburg, Germany

*CORRESPONDENCE
Claudia-Nicole Meisrimler
claudia.meisrimler@canterbury.ac.nz

SPECIALTY SECTION
This article was submitted to Plant Abiotic Stress, a section of the journal Frontiers in Plant Science

RECEIVED 08 September 2022
ACCEPTED 13 December 2022
PUBLISHED 10 January 2023

CITATION
Allan C, Tayagui A, Hornung R, Nock V and Meisrimler C-N (2023) A dual-flow RootChip enables quantification of bi-directional calcium signaling in primary roots.
Front. Plant Sci. 13:1040117.
doi: 10.3389/fpls.2022.1040117

A dual-flow RootChip enables quantification of bi-directional calcium signaling in primary roots

Claudia Allan [1], Ayelen Tayagui [1,2,3], Rainer Hornung [4], Volker Nock [2,3] and Claudia-Nicole Meisrimler [1*]

[1]School of Biological Sciences, University of Canterbury, Christchurch, New Zealand, [2]Department of Electrical and Computer Engineering, University of Canterbury, Christchurch, New Zealand, [3]MacDiarmid Institute for Advanced Materials and Nanotechnology, Wellington, New Zealand, [4]imec Netherlands, Holst Centre, Eindhoven, Netherlands

One sentence summary: Bi-directional-dual-flow-RootChip to track calcium signatures in *Arabidopsis* primary roots responding to osmotic stress.

Plant growth and survival is fundamentally linked with the ability to detect and respond to abiotic and biotic factors. Cytosolic free calcium (Ca^{2+}) is a key messenger in signal transduction pathways associated with a variety of stresses, including mechanical, osmotic stress and the plants' innate immune system. These stresses trigger an increase in cytosolic Ca^{2+} and thus initiate a signal transduction cascade, contributing to plant stress adaptation. Here we combine fluorescent G-CaMP3 *Arabidopsis thaliana* sensor lines to visualise Ca^{2+} signals in the primary root of 9-day old plants with an optimised dual-flow RootChip (dfRC). The enhanced polydimethylsiloxane (PDMS) bi-directional-dual-flow-RootChip (bi-dfRC) reported here adds two adjacent inlet channels at the base of the observation chamber, allowing independent or asymmetric chemical stimulation at either the root differentiation zone or tip. Observations confirm distinct early spatio-temporal patterns of salinity (sodium chloride, NaCl) and drought (polyethylene glycol, PEG)-induced Ca^{2+} signals throughout different cell types dependent on the first contact site. Furthermore, we show that the primary signal always dissociates away from initially stimulated cells. The observed early signaling events induced by NaCl and PEG are surprisingly complex and differ from long-term changes in cytosolic Ca^{2+} reported in roots. Bi-dfRC microfluidic devices will provide a novel approach to challenge plant roots with different conditions simultaneously, while observing bi-directionality of signals. Future applications include combining the bi-dfRC with H_2O_2 and redox sensor lines to test root systemic signaling responses to biotic and abiotic factors.

KEYWORDS

abiotic stress, calcium, signalling, *Arabidopsis*, microfluidics, root, osmotic stress

1 Introduction

Physiological processes in eukaryotic organisms rely on a functional signal transduction system to coordinate external and internal signals resulting in appropriated response. External signals, including abiotic and biotic stress, depend on initial perception by cell-surface receptors, cellular transmission and translation that allow plants to balance external fluctuations in an ever-changing environment. Calcium (Ca^{2+}) is an essential macronutrient in plants, where it is a component of cell walls, membranes, proteins and finally, yet importantly, a key messenger involved in signal transduction (Bergey et al., 2014). Changes in cytosolic free Ca ion ([Ca^{2+}]cyt) concentrations serve as a signal, which translates into downstream responses (McAinsh and Pittman, 2009; Dodd et al., 2010; Thor and Peiter, 2014). These signals are known to be associated with different patterns of transient, sustained, or oscillatory rises in [Ca^{2+}]cyt – comparable to a Morse code (De Koninck and Schulman, 1998; McAinsh & Pittman, 2009). Commonly, a message is converted into a Ca^{2+} signal (transmissible form), followed by diverse transmission and transduction of the signal, which associates with a decoding machinery allowing the cell to interpret Ca^{2+} signatures generated under different environmental stresses (Allan et al., 2022a). The coding function relies on maintaining constantly low levels of [Ca^{2+}]cyt around 0.1 µM. Buffers, H^+/Ca^{2+} antiporters and Ca^{2+}-ATPases, actively remove Ca^{2+} from the cytosol into the apoplast or intracellular stores (Connorton et al., 2012; Bonza et al., 2016). In tandem, Ca^{2+} can move down the concentration gradient into the cytosol through channel proteins, subsequently generating a signal. In order to code for downstream pathways, like gene (de-) activation, the signal must be interpreted and communicated into a cellular response *via* calcium binding proteins (CBPs), e.g. Ca^{2+}-Dependent Protein Kinases (CPKs) and Calcineurin-B Like proteins (CBLs) (Bergey et al., 2014; Wagner et al., 2015; Thoday-Kennedy et al., 2015; Zhang et al., 2016; Zhu et al., 2016).

So far, the majority of [Ca^{2+}]cyt measurements and experiments have been accomplished in *Arabidopsis thaliana (Arabidopsis)*. In recent years a variety of approaches have been used for this, including the luminescent Ca^{2+}-interacting aequorin protein, (Knight et al., 1991), G-CaMP3 (Toyota et al., 2018), as well as ratiometric biosensors like the MatryoshCaMP6s calcium sensors (Ast et al., 2017). The visualisation of cytosolic calcium transients using luminescent or fluorescent sensors has revealed stimulus-specific calcium signatures and long-distance communication in roots (Knight et al., 1997; Kiegle et al., 2000; Krebs et al., 2012; Choi et al., 2014; Xiong et al., 2014; Behera et al., 2015; Keinath et al., 2015). However, mimicking complex soil environments that roots are exposed to, whilst being able to control these conditions and quantify the effects, has been technically challenging. To overcome these challenges, microfluidic approaches have been combined with advanced microscopy in recent years. The use of microfluidics has been shown to allow for dynamic experiments that mimic environmental complexity found in the soil in a high spatio-temporal resolution on organismal and cellular level for force sensing and flow stream shaping of tip growing organisms (Bhatia & Ingber, 2014; Nezhad, 2014; Zheng et al., 2016; Tayagui et al., 2017; Sun et al., 2020). Particularly significant breakthroughs have been made by the introduction of 'soil-on-a-chip' microfluidic technologies to investigate root-microbe interactions and the dual-flow-RootChip (dfRC) platform, the latter which allows for the cultivation of *Arabidopsis* roots in asymmetric microenvironments (Stanley and van der Heijden, 2017; Stanley et al., 2018). Building on this platform, we have previously reported the basic chip design (Allan et al., 2022b) and operation of a bi-directional-dual-flow-RootChip (bi-dfRC). In the following we expand on the platform and demonstrate the use of the bi-dfRC to study the directionality and role of Ca^{2+} signaling in plant roots in response to stress factors. The bi-dfRC expands on conventional dfRCs (Stanley et al., 2018) by adding bi-directional flow capabilities for guided root growth and controlled exposure of the root to independent or asymmetric solute gradients. To probe for Ca^{2+} directional localisation in *Arabidopsis* root systems, a G-CaMP3 line (Toyota et al., 2018) was combined with the polydimethylsiloxane (PDMS) root chip technology. We demonstrate that a bi-directional flow system allows for studying directionality of Ca^{2+} signals upon selective application of stresses from adjacent directions. These findings are discussed in context with existing literature on varying Ca^{2+} sensing machinery in plant roots that may allow to distinguish local stress application and elicit downstream long-distance systemic signaling as a response, thus fine-tuning adaptation processes.

2 Methods

2.1 Bi-directional-dual-flow-RootChip fabrication

Microfluidic chips were fabricated using photolithography and replica molding (Orcheston-Findlay et al., 2018). In brief, designs were created using software (Mentor Graphics, v2020.1), and transferred to photo-masks (Nanofilm) using a laser mask writer (Heidelberg µPG101) and wet-etching. Single-side polished silicon wafers (4", Prime grade, WaferPro) were dehydrated in an oven (Hearatherm) at 180°C for 24 hours and cleaned in a O_2-plasma cleaner (PIE Scientific Tergeo) at 100 W for 10 min. After cleaning, dry-film, negative-tone photoresist (SUEX 100, DJMicrolaminates) was laminated (Sky-335R6) onto the wafer. The chip design was then transferred into the photoresist by exposure of the prepared photomask in a mask aligner (MA-6, SUSS MicroTec). After

exposure to UV light, the wafer was baked on a hot plate (HS40, Torrey Pines Scientific) for 5 min at 65°C and 20 min at 95°C. Transferred chip structures were developed in propylene glycol methyl ether acetate (PGMEA) developer for 30 min and rinsed with isopropanol for 5 min. Lastly, the wafer was hard-baked on the hot plate for 1 hour at 125°C, yielding a mold ready for replica-molding (Xia and Whitesides, 1998).

Prior to molding, the silicon wafer was pre-treated with an anti-adhesion agent (Trichloro (1H,1H,2H,2H-perfluorooctyl) silane, Sigma-Aldrich) to prevent sticking of the elastomer cast during the subsequent replica-molding. This step was repeated after 10 subsequent uses of the wafer as mold master. For replica-molding, PDMS (Sylgard 184, Electropar) pre-polymer silicone elastomer base was mixed thoroughly with silicone elastomer curing agent at a 10:1 (w/w) ratio and degassed to remove air bubbles. Once cast onto the wafer mold, the PDMS was degassed again and placed on a hot plate at 80°C for 2 hours to cure. Subsequently, the PDMS was carefully peeled off from the wafer and cured on the hot plate for a further 2 hours at 80°C. Following the second curing bake, inlet and outlet holes were core-punched (Ø1 mm & 3 mm, ProSciTech) and the PDMS was cut into individual bi-dfRC chips using a guillotine or scalpel. Chips were then O_2-plasma activated (PIE Scientific Tergeo) at 15 W power for 1 minute and bonded to pre-cleaned microscope slides (26×60 mm, Lab Supply) by lightly pressing the exposed surfaces of the PDMS and glass together. Bonded chips were then baked for 2 hours on a hot plate at 80°C to strengthen the bond.

To permanently retain the hydrophilicity of microfluidic channels (Hemmilä et al., 2012; Hashemi et al., 2017) and reduce diffusion of small molecules into PDMS, assembled chips were placed in the plasma cleaner (PIE Scientific Tergeo) and exposed to 30 W power for 3 min. Following activation, 22% w/v polyvinylpyrrolidone (PVP, Sigma-Aldrich) in DI water was pipetted into the microchannels for 1 minute to permanently alter the hydrophilic retention of PDMS. Microchannels were then washed with DI water and dried using a pressurised nitrogen gun. For storage, chips were placed in a vacuum desiccator for 3 hours, then sealed shut using vacuum-sealable food storage bags (Sunbeam). In order to obtain high-quality images of the microfluidic device microchannels an epoxy dye protocol was used (Soffe et al., 2020). For this, Sudan dye (Sigma-Aldrich) was added to 1 mL of toluene (Sigma-Aldrich) and Norland Optical Adhesive (NOA72, Norland Products). After toluene evaporated, 60 µL of the dye was added to the inlet and outlet channels of the bi-dfRC using a pipette. The dye entered the inlet channels *via* passive pumping (Hosokawa et al., 2004) and was cured using a spot UV curing system (OmniCure® S2000).

2.2 Asymmetric co-flowing solutions

A dual-pressure syringe pump system (NE-1010, New Era Pump Systems Inc) was used to deliver singular or dual treatment into the bi-dfRC observation chamber (OC). The pump system holds syringes (BD, MediRay) connected to the chip via 1/16" OD ethylene tetrafluoroethylene (ETFE) tubing (Kinesis), primed with a silicone tubing sleeve (Darwin Microfluidics) and short 1.5 mm OD metal tubes. Flow rate was set to 20 µL per minute.

2.3 Seed vernalisation and germination on the bi-directional-dual-flow-RootChip

In this study, Col-0 and G-CaMP3 *Arabidopsis* lines (originating from Toyota et al., 2018) were treated similarly throughout all experiments. Seeds were sterilised in 0.1% Triton X-100 for 3 min, followed by 70% ethanol (EtOH) for 2 min, subsequently washed 4 times with sterile Milli-Q® water (Merck). Pre-sterilised seeds were vernalised in water at 4°C for approximately 12 hours. Seeds were cultured onto half-strength Murashige and Skoog (½ MS) medium (Duchefa), 0.31 mM MES (Sigma-Aldrich) and 8% agarose. Plants on plates were grown for 4-days at a short-day cycle (8 h light, 16 h dark) with 65% humidity and 150 µmol m^{-2} s^{-1} per µA light intensity. On chip sub-culturing was achieved by transferring 4-day old *Arabidopsis* plants directly onto the pre-sterilised bi-dfRCs. Prior to sub-culturing, microchannels and inlets were pre-sterilised with 70% ethanol, and then washed with ½ MS/0.31 mM MES liquid medium. Agarose squares (4×4 mm) were oriented above the root inlet channel. Plants were aligned with the agarose squares and primary roots were carefully situated into the root inlet channel. Chips were stored in plastic incubation chambers (Nunc OmniTray single-well plates; Thermo Fisher Scientific), surrounded by sterile Milli-Q water, for humidity. The set-up was incubated for 5-days under the pre-alluded short-day cycle (8 h light; 16 h dark). The set up was tilted at a 45-degree angle to promote root growth into the bi-dfRC microchannel.

2.4 Fluorescence microscopy, image editing and quantification analysis

For epifluorescence microscopy, all images and videos were obtained with a Zeiss (AX10) 5x lens (EC Plan-Neofluar 5x/0.15 M27) (Supplemental Figure 1A). Ca^{2+} fluorescence was observed with an eGFP filter (38 HE Green Fluorescent Prot BP 450-590) and bright field (BF) was set to 2.7 ms exposure, TL lamp 30%. Images and videos were analysed either in in Fiji-ImageJ (Schindelin et al., 2012) or ZEN Blue software (Zeiss). *Arabidopsis* root tip quantification was accomplished utilising the freehand selection tool. Treatments were applied as either a control solution (½ Murashige and Skoog (MS) medium, plus 0.31 mM 2-(N-morpholino) ethanesulfonic acid (MES)

dissolved in Milli-Q® water) or stress solution (100 mM sodium chloride (NaCl) or 20% polyethylene glycol dissolved in ½ MS/0.31mM MES media). For raw data collection fluorescence intensity was measured in the original raw video frames. Linear section 1 was sampled at the root tip columella cells, while linear sections 2 and 3 represent meristematic and elongation zone 1 and 2(ME1 and ME2) of the root, respectively, and linear sections 4 and 5 represent elongation and differentiation zone 1 and 2 (ED1 and ED2) of the root, respectively (Supplemental Figure 1B). Linear quantification was carried out with the straight-segmented tool. Five linear sections were aligned adjacently per sample, with an intersection space of 290 µm between sites 1 to 4, and 580 µm between site 4 and 5 (Supplemental Figure 1B). An analogue-to-digital conversion in ImageJ (Fiji) was used to convert evenly spaced values into a signal. Additionally, the ROI Manager, Multi Measure tool was used for a rapid semi-automatic measurement of all frames in the video. Fluorescent plot profiles at each linear section and time interval were analysed into raw data files in Excel (16.61.1 (22052000), Microsoft). Statistical analysis and graphs were conducted in Prism (V8.4.3, GraphPad). Original videos have been compressed to reduce size below 30 MB/video. Videos were exported as AVI M-JPEG compression with 100% quality and set to 30 fps, in Zen blue. Original videos are 568 images taken over 3 minutes and 3.3 fps.

2.5 Kymograph generation

Kymographs were used to show spatial intensity over time for exemplified roots. For this, original.czi files were converted into.avg video formats using Zen blue software, without compression. Every picture frame was defined as a time-point. The fluorescence intensity (corresponds to cytosolic Ca^{2+}) of transverse pixel sections was summed up for each spatio-temporal position.

An in-house python script was developed with PyCharm (www.jetbrains.com) in Python ver. 3.6 (https://www.python.org/downloads/release/python-360/) to generate kymographs. The main functionalities were provided by the open-source computer vision library OpenCV (https://pypi.org/project/opencv-python/). The script reads out every picture within the video and applies a summation longitudinal or across the root in a manually predefining region of interest (ROI). Operation of the script is controlled *via* command line interface using the standard library argparse (https://docs.python.org/3/library/argparse.html).

3 Results and discussion

Site-specific exposure of environmental stress to plant roots has the potential to yield new insight into how plants detect and respond to abiotic and biotic factors. To study the role of Ca^{2+} signals, existing dfRC technology was adapted and extended in this research to enable bi-directional stimulation. The enhanced bi-dfRC allows for the cultivation of *Arabidopsis* roots to capture root elongation, cellular localisation and dispersion patterns of fluorescent signals of any kind. We used G-CaMP3 expressing *Arabidopsis* plants to observe NaCl and PEG-induced Ca^{2+} signals in the primary root. The need to modify a bi-dfRC design became apparent during initial experiments related to Ca^{2+} quantification with the conventional dfRC based on the design by Stanley et al., 2018 (data not shown). During these early NaCl treatment experiments, it became evident that a chip, which also enables probing from the root tip, would be of significant advantage. Such a device would allow users to quantify the signal in a spatio-temporal manner, in dependence on the first contact site, as well as with different solutions on each side of a root. This is of importance when elucidating difference in signal dispersion within the system, which can then be used as the basis for modelling approaches. By utilising G-CaMP3 lines for this, results can be compared to prior observations found with varying intensiometric calcium indicators, including R-GECO1 lines (Stanley et al., 2018). In particular, two different osmolytes, NaCl and PEG, were used in comparison to control treatment to explore Ca^{2+} responses in roots within 180 s post-treatment application.

3.1 Bi-directional-dual-flow-RootChip design

Identical in dimension to the conventional dfRC design (Stanley et al., 2018), the bi-dfRC adds a second adjacent set of externally accessible microchannels (Allan et al., 2022b), which are connected to the base of the root observation chamber (OC) for flow reversal (Figure 1A). As shown in Figure 1A, the root OC itself contains 34 pairs of triangular elastomeric micropillars for root guidance and force sensing. Connected to each OC are a singular media port and plant seeding area for root growth (Figure 1B), as well as the four media inlets/outlets (A & B top, C & D bottom) for chemical treatment application. As indicated in Figure 1C, using these extra inlets/outlets, chemical treatment can either be applied through inlets A and B for application of solutions from the differentiation (shoot) site or through inlets C and D for application of solution from the root tip (root) site. In either case, the other inlets then become the outlets, thus adding bi-directional treatment capabilities for targeted application of stress conditions in varying local root tissues. Independent bi-dfRCs were combined into one PDMS device to yield one to five parallel OCs on a single glass substrate (Figure 1B). Following sub-culture of 4-day old *Arabidopsis* roots from plant culture into the bi-dfRC, the roots grow into the OCs over another 5-

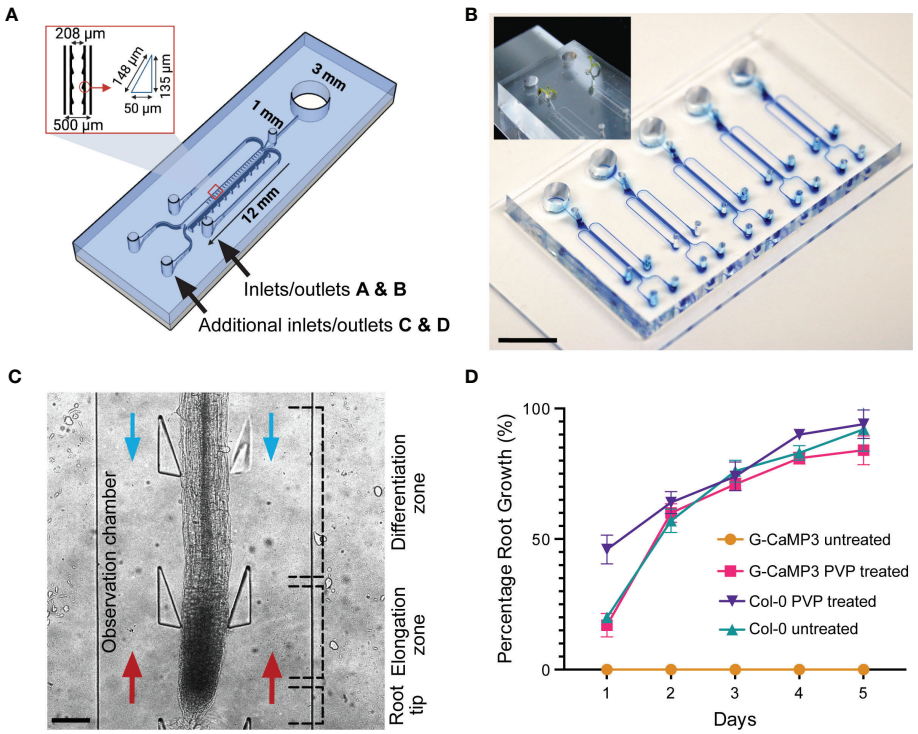

FIGURE 1
Bi-directional dual-flow-RootChip (Bi-dfRC) for laminar flow perfusion of stress treatments at the tip and differentiation zone of *Arabidopsis* roots. **(A)** Schematic diagram of the bi-dfRC including pillar array dimensions (identical to the conventional dfRC) in addition to a second set of inlets/outlets C & D for bi-directional stress application at the tip or differentiation zone. **(B)** Image of epoxy dye (blue) filled microchannels for visualisation of root observation chamber joining 4 inlet/outlets. 9-day old *Arabidopsis* G-CaMP3 plants cultured into the root inlet of the bi-dfRC depicted top left (scale bar 10 mm). **(C)** *Arabidopsis* G-CaMP3 root situated in the bi-dfRC observation chamber highlighting key zones (tip, elongation, and differentiation zone) and treatment orientation (blue arrows from top inlets A & B, red arrows from bottom inlets C & D, scale bar 200 µm). **(D)** Average percentage of *Arabidopsis* G-CaMP3 and Col-0 root growth into PVP-treated and untreated microchannels over 5-days (n= 100).

days (Figure 1B), upon which stress treatments can be applied at the differentiation zone or tip (Figure 1C).

3.2 Hydrophilic retention of microchannels

Many PDMS microfluidic systems require hydrophilic retention or water retention to promote protrusion of tip growing organisms into fluidic microchannels (Halldorsson et al., 2015). PDMS chips however, naturally exhibit hydrophobic or water repelling surface properties in their native form (Hemmilä et al., 2012). This is in contrast to the glass base of the bi-dfRC, which typically has hydrophilic surface properties. By combining the two materials during chip fabrication, the resulting devices and OCs present a partially hydrophobic environment without further treatment (Guckenberger et al., 2014). We observed that devices with exposed hydrophobic PDMS surfaces directly hindered the root growth of the G-CaMP3 sensor line into bi-dfRC devices. Interestingly, the same surface properties had no impact on the growth of wild type Col-0 roots in our work (Figure 1D) and no growth inhibition for the R-GECO1-expressing *Arabidopsis* roots has been reported (Stanley et al., 2018). This difference in behavior may relate to sensing mechanisms of hydrophobic, hydrophilic, ionic and non-ionic surfaces by roots. The fully impaired protrusion of roots from G-CaMP3 lines into partially hydrophobic and hydrophilic surfaces points to a disturbance of surface sensing and charge in these lines, and the involvement of Ca^{2+} in this process. A known property of G-CaMP3 sensor lines is enhanced kinetics for high-speed Ca^{2+} imaging (Russell, 2011). Hence, G-CaMP3 may quench free cytosolic Ca^{2+} away from other essential physiological processes including stomatal closure, water-sensing mechanisms and sensing of varying surfaces (Cho et al., 2017). It has been reported that hydrophobic soil increases with lower pH, whereas hydrophilic soils are retained at a pH of approximately 6.5 and higher (Vogelmann et al., 2013). While, together with our observation of growth inhibition, this suggests that a fully hydrophilic microchannel should re-initiate G-CaMP3 root growth, further insight is needed to understand the details of

how roots sense surface charge, hydrophobicity and other properties, as well as the role of Ca^{2+} in these important processes.

To test whether modified surface properties would facilitate G-CaMP3 root growth, partially hydrophobic microchannels were initially made temporarily hydrophilic *via* plasma activation, a method which exposes given surfaces to oxygen plasma (Jokinen et al., 2012). However, PDMS only retains this plasma-activated surface modification for minutes to hours, which severely limits its use for long-term culture (Plegue et al., 2018). To permanently preserve the hydrophilic surface, PVP - a polymer that reduces the hydrophobicity of surface particles (Kao et al., 2003), was reacted with the plasma-activated PDMS (Hashemi et al., 2017). This rendered the PDMS, and thus the bi-dfRC device OCs, permanently hydrophilic. As is demonstrated by Figure 1D, plasma-activated but PVP untreated G-CaMP3 root growth did not grow into the bi-dfRC OCs. In contrast, devices treated with PVP did not exhibit any growth limitations on G-CaMP3 roots.

3.3 Mechanics underpinning fluid flow control

While increasing functionality, adding additional inlets/outlets to a microfluidic device has the potential to increase the complexity for flow control (Figure 2A). This may lead to air bubble formation in the bi-dfRC microchannel during pressurised, controlled and active syringe pumping (Figure 2B). Backflow and leakage are a common cause of air bubble formation in microfluidic devices, a consequence of fluid flow resistance and limited flow rate control (Nakayama et al., 2006). This phenomenon is commonly caused by PDMS tearing at the inlet/outlet channels, varying circuit components or the defined size and length of circuit tubing (Xue et al., 2012). Air bubble formation in the bi-dfRC also has the potential to disrupt asymmetric profusion of two test solutions at the same time, thus leading to the mixing of these (Olanrewaju et al., 2018).

To prevent the aforementioned issues, and achieve optimal fluid-flow rate control, air bubble generation was actively minimised using the following optimisations. To prevent cracking of PDMS inlets and subsequent open-loop circulation/backflow and leakage, 'flexible ends' for the low compliance ETFE tubing networks were constructed. Short sections of flexible tubing (Masterflex Tygon, DO-06409-16; L= 1 cm) were used to connect the stiffer tubing to pre-made 1 mm × 1 cm metal tubes with a 90-degree bend (Dispensing Tips, Nordson), as shown in Figure 2C. To expel air bubbles and dry out microchannels during fabrication, each chip was

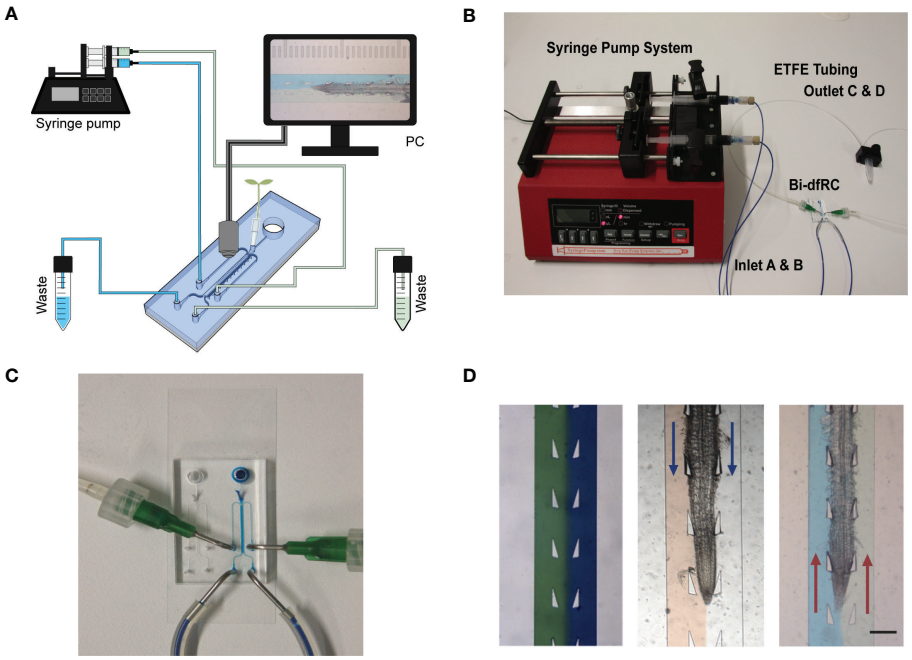

FIGURE 2
Bi-directional dual-flow-RootChip (Bi-dfRC) imaging set up. **(A)** Schematic diagram of the bi-dfRC set up with syringe pump system and tubing array for imaging. **(B)** Photograph of the syringe pump system, tubing and chip adapter used for the delivery of asymmetric test solutions into the bi-dfRC microchannels. **(C)** Close-up depicting the fluid flow into the observation chamber delivered by tubing network into the bi-dfRC in the absence of a root using blue dye (scale bar 5 mm). **(D)** *Arabidopsis* 9-day old G-CaMP3 root under asymmetric fluidic flow visualised using coloured dye in the absence and presence (flow direction indicated with blue arrows for differentiation zone and red arrows for tip) of a root (scale bar 350 μm).

degassed for two hours (Karlsson et al., 2013; Asghar et al., 2016). Prior to on-chip root sub-culture, microchannels were pre-wetted with control media *via* passive pumping. To expel any air bubbles retained in the microchannels after this, negative pressure was generated *via* active syringe pump back pumping into the syringes, thus further reducing the size of any air bubble (Liu & Li, 2015). Lastly, to avoid air bubble introduction upon media injection *via* the tubing array, microchannels harboring roots were pre-flushed with control media and inlets were primed with media droplets. In tandem, the tubing was primed with desired treatment by pre-pumping the media through the tubing array. Both droplets were touched together, creating a wet seal, avoiding bubble introduction.

Fine tuning flow rate control, air bubble formation and system set up presented a dual process to optimise steady laminar flow perfusion of test solutions. In order to observe successful asymmetric flow of simultaneous test solutions in the bi-dfRC OCs, coloured dyes were first pumped into the microchannel (Figure 2D). Flow rate control and tubing array maintain the delivery of asymmetric flow at the same constant speed of 20 µl/min for both sites. As observed in Figure 2D, solution(s) injected on each side of the root remain on the initial side without observed diffusion. Hence, two different stimulation solutions do not cross-mix when applied on different sides of the root. This highlighted the retention of co-flow in the bi-dfRC microchannels in the presence of an *Arabidopsis* root (Figure 2D).

3.4 NaCl and PEG induce an early calcium burst in the primary root

Calcium signals have been shown to be involved in early plant defence sensing, and response to salt and drought stress (Knight et al., 1997; Kiegle et al., 2000; Li et al., 2022). Prior studies tracked Ca^{2+} signals utilising various green fluorescent sensors including R-GECO1 (Stanley et al., 2018), YCNano-65 (Choi et al., 2014) and MatryoshCaMP6s (Ast et al., 2017). Based on refined spatio-temporal resolution and sensitivity, G-CaMP3 expressing *Arabidopsis* lines (Bi et al., 2021), with fast responsiveness towards Ca^{2+} oscillations were chosen to study the early Ca^{2+} response upon NaCl-induced salinity stress and PEG-induced drought stress. It should be noted that limitations exist with Ca^{2+} sensor technology, including Ca^{2+} quenching (Ca^{2+} sensor binding to Ca^{2+}) and buffering the Ca^{2+} response (Granqvist et al., 2012). Additionally, it has been reported that some Ca^{2+} sensors are more sensitive towards physiological response mechanisms, such as G-CaMP6 reporting Ca^{2+} bursts from single action potentials (Cho et al., 2017). Moreover, variations of such factors may have an underlying effect on the observable physiological response of the root towards various stressors, limiting spatiotemporal resolution of the Ca^{2+} signal. As such, comparison of experimental observations using different sensors can be difficult at times due to the varying kinetics. Consequently, differences in observed Ca^{2+} spatio-temporal transmission within the literature is expected and will be further discussed in the sections below.

3.4.1 The initial contact site with NaCl and PEG affect Ca^{2+} signal direction

Ca^{2+} signals primarily initiated in root tissue directly exposed to NaCl or PEG, then dispersed shoot or root ward depending on the first contact site of the stressor. The solution moves through the channel with a constant flow rate of 20 µL/min, due to the known dimensions of the channel and the root we can calculate that the solution needs ~1.76 sec to fill the 12 mm channel, when the root has grown 6 mm (50%) into the channel. Hence, the solution moves through the bi-dfRC with a speed of ~$6.84*10^3$ µm/s. In contrast, the observed Ca^{2+} signal in the root induced by NaCl or PEG move at a speed of 4-14 µm/s, which is far slower than the solution. Therefore, it can be excluded that the flow of the solution in the channel of the chip is responsible for the movement of the Ca^{2+} signal within the root. NaCl-induced salinity stress and PEG-induced drought stress both reduce water absorption and obstruct water movement, inducing downstream osmotic and oxidative stress pathways (Ma et al., 2020). Here, we show differences in signal heterogeneity during local cellular and systemic Ca^{2+} signaling in roots responding to alternative types of osmotic stress inducing compounds.

The spatio-temporal Ca^{2+} signals responding to environmental stress are shared between many organisms, including animals and plants (Clapham, 2007; Manishankar et al., 2018). In plant leaves and root tissues, increase of cytosolic Ca^{2+} has previously shown local osmotic stress applications (Liu et al., 2010; Choi et al., 2014; Ast et al., 2017; Huang et al., 2017; Stanley et al., 2018; Zhang et al., 2020). The signal has been documented as a 'wave' that initiated from site-specific NaCl stress at the lateral root (Choi et al., 2014). Specifically, the signal observed in Choi et al., 2014 initiated at the tip, emanated through cortical and endodermal cells of the lateral root, yet was not observed in epidermal cells. The Ca^{2+} wave then traversed through the primary root, splitting bi-directionally shoot and tip-ward, at a speed of 400 µm/s. The signal also systemically transmitted to above regions of the plant, moving through the hypocotyl (Choi et al., 2014) and leaves (Xiong et al., 2014). We show Ca^{2+} signal localisation and orientation in primary roots responding to a full or one-sided NaCl and PEG solution at the tip or differentiation zone. Based on former literature that observed Ca^{2+} signaling in response to NaCl treatment, 100 mM NaCl was chosen for the presented experiments (Choi et al., 2014; Stanley et al., 2018). Effects of 100 mM NaCl treatment on *Arabidopsis* has been well studied in the past, which allows integration of our insights into the existing knowledge (Yang et al., 2019; Cackett et al., 2022). PEG-6000 is known to induce drought stress *via* lowering plants

water potential as a result of osmotic stress (Sevindik et al., 2022). Prior observations revealed a strong physiological drought inducing response at a concentration of 20% (Hellal et al., 2018; Huang et al., 2021). In complement, preliminary data detailed in Allan, 2021 showed 20% PEG induced the strongest Ca^{2+} response compared to lower fluorescence intensities observed at 0%, 5%, 10% and 40% concentrations. All G-CaMP3 and Col-0 control figures and videos are provided in the supplemental material (Supplemental Figure 2; Supplemental Videos 9, 10). Ca^{2+} increased at epidermal cells of the differentiation zone upon first contact with the NaCl stressor applied at the shoot site. The propagating Ca^{2+} signal increased in intensity 1.5-fold and transmitted from the initial site, moving through the cortical and endodermal cells on both sides of the root, to the stele tissue. The signal also dispersed tip-ward through the epidermal, cortical and stele tissue, followed by a systemic increase of Ca^{2+} at the tip (P-value ≤ 0.02). The signal transferred longitudinally through the cortical and stele tissues, at a speed of 6.8 µm/s (SD = 0.9, n = 10) (Figures 3A, B, 4A; Supplemental Figures 3A, B, 5; Supplemental Video 1). The same Ca^{2+} signal was observed following PEG treatment at the differentiation zone, increasing in intensity 1.5-fold. Opposingly to the signal observed under salt, Ca^{2+} propagated from the endodermis/cortex into adjacent tissues, then traveled tip-ward at a faster speed of 11.6 µm/s (SD =1.6, n = 5) (Figures 5A, B, 6A; Supplemental Figures 4A, B, 5; Supplemental Video 2).

Conversely, following full NaCl treatment at the tip, Ca^{2+} upregulated at the columella cells, then increased in intensity 2.5-fold (P-value ≤ 0.05). This was followed by a Ca^{2+} wave that traveled shoot-ward throughout the stele tissue of the elongation zone to the differentiation zone at a speed of 5.9 µm/s (SD = 0.4, n = 10) (Figures 3C, D, 4B; Supplemental Figures 3C, D, 5; Supplemental Video 3). The same signal was observed following PEG treatment at the tip, whereby the signal increased 4-fold at the columella cells (p-value ≤ 0.0017). This signal was stronger in the endodermis and cortex, yet traveled shoot-ward at an increased speed of 10.5 µm/s (SD =1.6, n = 5) (Figures 5C, D, 6B; Supplemental Figures 4C, D, 5; Supplemental Video 4). Summarising, different root tissues are involved in local and systemic transmission of early Ca^{2+} signals in response to two different types of osmolyte. The resulting temporal signal patterns depended on the first contact site (differentiation zone or tip) and the inducing stressor. Early studies showed Ca^{2+} release, and corresponding increase in G-CaMP3 fluorescence, initiated in the root system upon immersion of entire 6 to 7-day old plantlets in NaCl (Knight et al., 1997; Kiegle et al., 2000). Patch clamp studies utilising protoplasts from maize root tips also showed cytosolic Ca^{2+} increased following PEG treatment (Liu et al., 2010). Later studies on the spatio-temporal NaCl induced-Ca^{2+} burst in lateral roots showed signal heterogenicity in the tissue and cell specificity (Choi et al., 2014; Ast et al., 2017). In roots expressing the ratiometric MatryoshCaMP6s transgenic detector, Ca^{2+} initially upregulated within defined cells of the root cap 4 s following NaCl application at the tip, then increased in intensity, while travelling through lateral root cap, epidermis and cortex within 39 s (Ast et al., 2017). Prior observations also showed a Ca^{2+} burst in different cells of *P. edulis* root tips, induced by submerging the planets in PEG for 10 minutes (Jing et al., 2019). Site specifically applying NaCl at the region where the lateral root protruded from the primary root revealed Ca^{2+} signaling originated at the localised cells of the cortical and endodermal cell layers (Choi et al., 2014). As discussed, this was followed by fast systemic signal propagation throughout the root expressing FRET based YCNano-65 sensor, depending on the conductance of Ca^{2+} through the ion channel protein Two Pore Channel 1 (TPC1) (Choi et al., 2014). A much slower Ca^{2+} signal was observed compared to Choi et al., 2014. This discrepancy may be due to the use of a bi-dfRC system combined with the G-CaMP3 sensor, compared to an agarose gel-based system incorporated with the FRET based YCNano-65 sensor (Choi et al., 2014). Moreover, YCNano-65 has been shown to have a dissociation constant (K_d) of 64.8 nM (Horikawa et al., 2010), compared to 660 nM in G-CaMP3 (Tian et al., 2009), which may lead to a faster documented signal, but also different physiological effects on the sensor line overall.

Interestingly, the initial Ca^{2+} release, and corresponding increase in G-CaMP3 fluorescence, and longitudinal dispersion of Ca^{2+} following primary root tip exposure to NaCl and PEG in G-CaMP3 transgenic roots reported here was slower, yet comparable to observations in Ast et al., 2017, utilising ratiometric MatryoshCaMP6s expressing roots. Additionally, the systemic transmission of Ca^{2+} through varying tissues following initial Ca^{2+} release, and corresponding increase in G-CaMP3 fluorescence, at both the differentiation zone or tip treatment sites showed a similar tissue-specific dispersion pattern.

3.4.2 Different transverse and longitudinal tissue specific Ca^{2+} signals arise following one-sided NaCl and PEG treatment

The NaCl and PEG-induced Ca^{2+} signals initiated on the treated side of the root. Observations showed varying cell types and tissues were involved in the spatio-temporal dispersion of Ca^{2+}, in dependence on the initial stress site. A one-sided NaCl or PEG treatment at the differentiation zone always led to a transversely moving signal, from the contact to the non-contact side. The signal then moved longitudinally to the tip. Upon NaCl treatment at the differentiation zone, the Ca^{2+} burst emanated from epidermal cells spanning the elongation and differentiation zone on the treatment side of the root, in addition to the root tip. The signal increased 1.5-fold in intensity and transversely moved from the treated to untreated side of the root at a speed of 9.4 µm/s. A secondary Ca^{2+} wave was observed, which moved

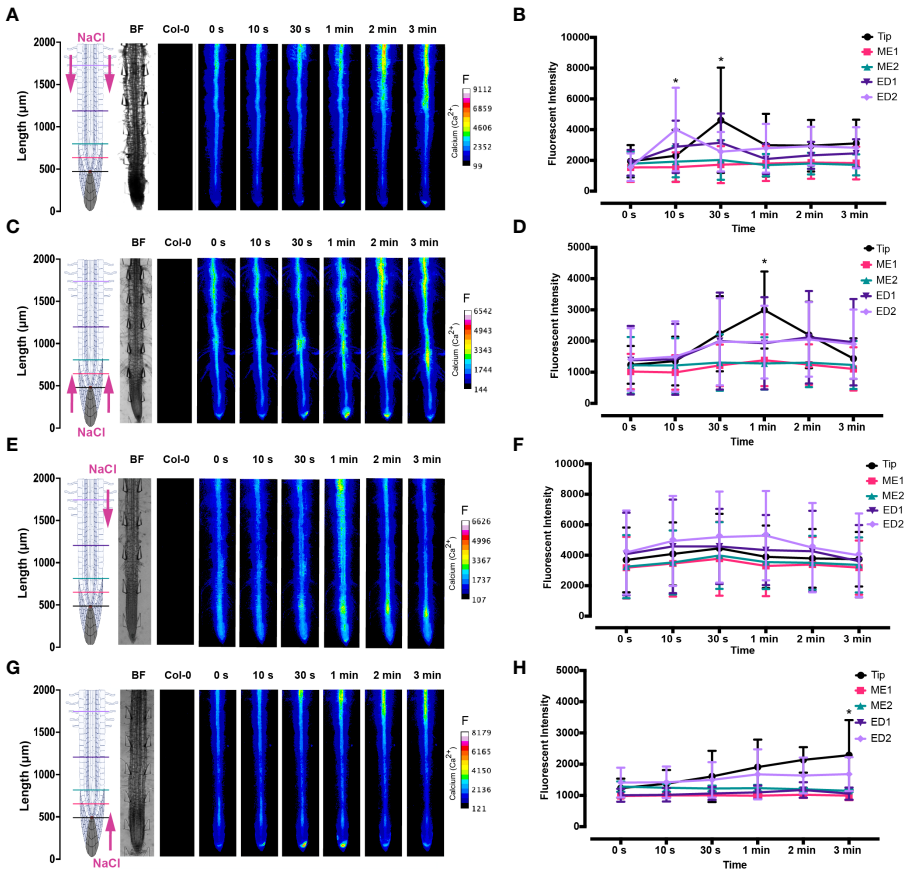

FIGURE 3
Fluorescence intensity of Ca^{2+} in *Arabidopsis* G-CaMP3 roots exposed to NaCl (100 mM). Fluorescence was observed for 180 s post NaCl treatment. **(A)** Heat map depicting Ca^{2+} release, corresponding to increase in G-CaMP3 fluorescence. Five linear sections used for fluorescence quantification upon targeted application of NaCl treatment through inlets A (left) & B (right) at the differentiation zone (DZ) are shown (n= 10). Colour change indicates an increase in Ca^{2+} fluorescence. Root schematic depicting treatment application, orientation (salt; NaCl and control; MS media) and linear sections (refer to key), bright field (BF) and control (wild type Col-0) roots displayed on the left. Scale; F= fluorescence intensity. **(B)** Line graph with two-way ANOVA multiple comparisons Tukey's honestly significant difference (HSD) mean comparison test (P-value ≤ 0.05) depicting average fluorescence intensity (ADU; analogue digital units) of Ca^{2+} across five linear sections (Tip, ME1, ME2, ED1 & ED2) upon targeted exposure of salt treatment through inlets A & B at the DZ (n = 10). Asterisks (*) indicate statistical significance. **(C)** Heat map depicting Ca^{2+} release, and corresponding increase in G-CaMP3 fluorescence, upon salt treatment through inlets C (left) & D (right) at the tip (n= 10). **(D)** Line graph depicting average fluorescence intensity of Ca^{2+} across five linear sections following salt treatment through inlets C & D at the tip (n= 10). **(E)** Heat map depicting Ca^{2+} release, and corresponding increase in G-CaMP3 fluorescence, upon salt treatment through inlet B and control media through inlet A at the DZ (n= 10). **(F)** Line graph depicting average fluorescence intensity of Ca^{2+} across five linear sections following salt treatment through inlet B and control treatment through inlet A at the DZ (n= 10). **(G)** Heat map depicting Ca^{2+} release, and corresponding increase in G-CaMP3 fluorescence, upon salt treatment through inlet D and control treatment through inlet C at the tip (n= 5). **(H)** Line graph depicting average fluorescence intensity of Ca^{2+} across five linear sections upon salt treatment through inlet D and control through inlet C at the tip (n= 5).

longitudinally to the root tip through stele tissue at a speed of 5.2 µm/s (SD = 0.57, n= 10) (Figures 3E, F, 4C; Supplemental Figures 3E, F, 5; Supplemental Video 5). PEG induced the same transverse signal response yet this was faster, less intense and did not transmit to the untreated side of the root. Additionally, the secondary longitudinal Ca^{2+} signal transmitted not only tip-ward, but bi-directionally, root and shoot ward at a speed of 11 µm/s (SD = 1.4, n= 5) through cortical and stele tissue. (Figures 5E, F, 6C; Supplemental Figures 4E, F, 5; Supplemental Video 6). Prior observations show the NaCl-induced Ca^{2+} signal traveled transversely at a comparable rate 14.1 µm/s (Stanley et al., 2018). This traversing Ca^{2+} wave is only observed following one-side osmolyte treatment at the differentiation zone and not the tip. This suggests that the traversing Ca^{2+} signal observed is due to the Ca^{2+} signal itself, rather than the diffusion of NaCl or PEG into the root.

Excitingly, for the first time we show a one-side NaCl and PEG treatment from the tip. The Ca^{2+} burst localised on the right side of the columella cells, which then increased in intensity on the right side of the tip by 2.5-fold. Next, the Ca^{2+} signal

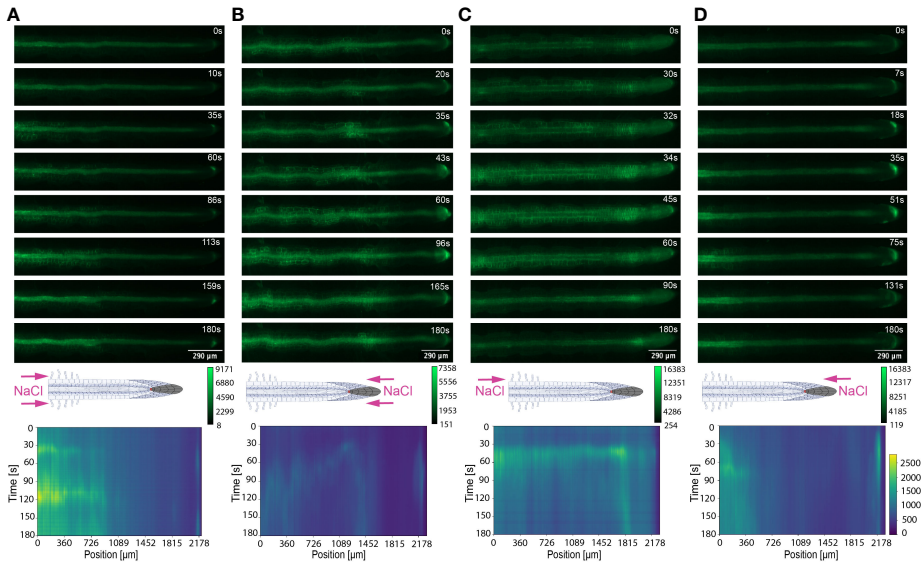

FIGURE 4
Key Ca^{2+} signal localisation in *Arabidopsis* roots exposed to 100 mM NaCl. Schematic diagrams depict treatment localisation and orientation at the root within the bi-dfRC with fluorescent intensity calibration bars. Kymographs depict the spatial fluorescense of GFP corresponding to Ca^{2+} in the root over time, in dependence of treatment orientation and localisation. GFP fluorescence in kymographs is color coded, ranging from dark blue to yellow (normalized for all samples). **(A)** Key Ca^{2+} localisation pattern upon NaCl treatment through inlets A & B of the bi-dfRC at the differentiation zone. **(B)** Key Ca^{2+} localisation pattern upon NaCl treatment through inlets C & D of the bi-dfRC at the tip. **(C)** Key Ca^{2+} localisation pattern upon NaCl treatment through inlet B (top) and control treatment through inlet A (base) of the bi-dfRC at the differentiation zone. **(D)** Key Ca^{2+} localisation pattern upon NaCl treatment through inlet D (top) and control treatment through inlet C (base) of the bi-dfRC at the tip.

dispersed shoot-ward through stele tissue and cortical tissue of the differentiation zone, at a speed of 4.2 µm/s (SD = 0.51, n= 5) (Figures 3G, H, 4D; Supplemental Figures 3G, H, 5; Supplemental Video 7). PEG induced a similar signal response (P-value ≤ 0.0441), however traveled faster at a speed of 14.2 µm/s (SD = 1.9, n= 5), and reaching a 0.5-fold higher intensity (Figures 5G, H, 6D; Supplemental Figures 3G, H, 5; Supplemental Video 8).

The associated kymographs show that Ca^{2+} signals can orient in different directions based on the initial NaCl or PEG treatment site. Moreover, both PEG and NaCl induced a strong Ca^{2+} burst at the tip if the stress is applied locally. However, PEG induced a stronger signal throughout the differentiation zone in all treatments (Figures 4A, B). Plant root responses to environmental stress are highly sensitive and differ at the cellular, tissue, and organ level (Duan et al., 2015). Moreover, site specific localisation of osmotic stress to varying tissues at the primary root suggests plants are well adapted to sense environmental stress directly in affected tissues. Building on early observations, we show the initial Ca^{2+} signal in the primary root is not only site-specific to cells exposed to locally applied osmotic stressors, but also systemically transmits away from initially stimulated cells, at the tip and differentiation zone. Additionally, the Ca^{2+} wave passed through different root tissues and cells depending on the initial site of Ca^{2+} release, and corresponding increase in G-CaMP3 fluorescence. Osmotic stress inhibits plant root growth and development *via* redistribution of the stress hormone auxin from the quiescent center (QC) and root cap to the epidermal and cortical cells of the elongation zone, causing the root to bend away from high salt concentrations (Smolko et al., 2021). Additionally, when cells are exposed to auxin, membrane-bound proton pumps export H^+, decreasing apoplastic pH and ultimately leading to cell wall loosening – known as the acid growth hypothesis (Arsuffi & Braybrook, 2018). Prior studies showed that Ca^{2+} signaling participated in root growth and stress sensing *via* modulating auxin responses to abiotic stress (Shih et al., 2015; Dindas et al., 2018; Leitão et al., 2019).

The different Ca^{2+} signal patterns responding to NaCl and PEG in varying orientations and localisations observed here may be intrinsically linked to auxin movement and root growth under osmotic stress. Further studies will be needed to clearly link the exact signaling mechanisms.

We also observed varying rates of longitudinal Ca^{2+} transmission depending on the localisation and orientation of NaCl or PEG treatment. Prior observations showed that signal

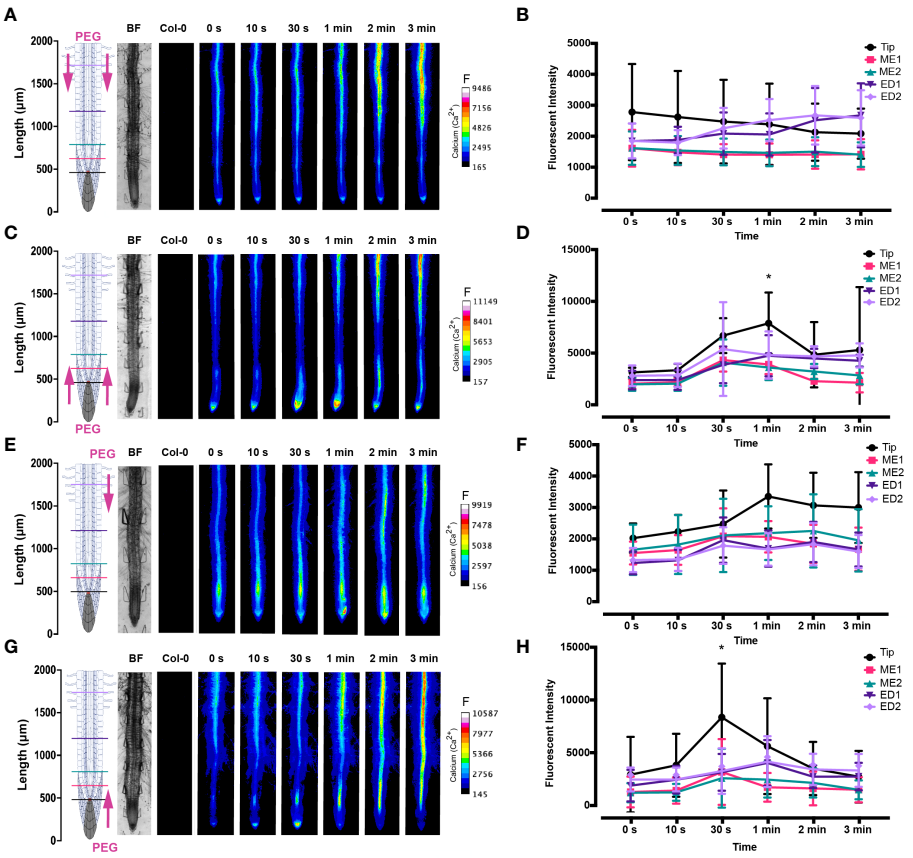

FIGURE 5
Fluorescence intensity of Ca^{2+} in *Arabidopsis* G-CaMP3 roots exposed to PEG (20%). Fluorescence was observed for 180 s post PEG treatment. **(A)** Heat map view depicting Ca^{2+} release, corresponding to increase in G-CaMP3 fluorescence. Five linear sections used for fluorescence quantification upon targeted application of PEG treatment through inlets A (left) & B (right) at the differentiation zone (DZ) are shown (n= 5). Colour change indicates an increase in Ca^{2+} fluorescence. Root schematic depicting treatment application, orientation (Polyethylene glycol; PEG and control; MS media) and linear sections (refer to colour key), bright field (BF) and control (wild type Col-0) roots displayed on the left. Scale; F= fluorescence intensity. **(B)** Line graph with two-way ANOVA multiple comparisons Tukey's honestly significant difference (HSD) mean comparison test (P-value ≤ 0.05) depicting average fluorescence intensity (ADU; analogue digital units) of Ca^{2+} across 5 linear sections (Tip, ME1, ME2, ED1 & ED2) upon targeted exposure of PEG treatment through inlets A & B at the DZ (n = 5). Asterisks (*) indicate statistical significance. **(C)** Heat map depicting Ca^{2+} release, and corresponding increase in G-CaMP3 fluorescence, upon PEG treatment through inlets C (left) & D (right) at the tip (n= 5). **(D)** Line graph depicting average fluorescence intensity of Ca^{2+} across 5 linear sections following PEG treatment through inlets C & D at the tip (n= 5). **(E)** Heat map depicting Ca^{2+} release, and corresponding increase in G-CaMP3 fluorescence, upon PEG treatment through inlet B and control media through inlet A at the DZ (n= 5). **(F)** Line graph depicting average fluorescence intensity of Ca^{2+} across 5 linear sections following PEG treatment through inlet B and control treatment through inlet A at the DZ (n= 5). **(G)** Heat map depicting Ca^{2+} release, and corresponding increase in G-CaMP3 fluorescence, upon PEG treatment through inlet D and control treatment through inlet C at the tip (n= 5). **(H)** Line graph depicting average fluorescence intensity of Ca^{2+} across 5 linear sections upon PEG treatment through inlet D and control through inlet C at the tip (n= 5).

cross-talk exists between extracellular reactive oxygen species (ROS) hydrogen peroxide (H_2O_2), and intracellular Ca^{2+} for systemic propagation of the signal between varying cells and tissue (Gilroy et al., 2014; Stanley et al., 2018). Longitudinal signal transmission rates can vary based on the number of cell boundaries present within varying root tissues (Gilroy et al., 2014). Moreover, the different longitudinal tissue specific signals observed between full and one-sided NaCl or PEG treatment may generate varying signal speeds. Such findings suggest that differences in cell types and tissues may regulate how the Ca^{2+} signals are sensed, transmitted over space and time and decoded into a response. This includes the existence of 1085 distinct proteins associated with Ca^{2+} binding and/or calcium ion sensor activity (Allan et al., 2022a). Employment of such cell or stimulus specific decoders and responders in roots may impact the transmission pattern of Ca^{2+} transient signatures across

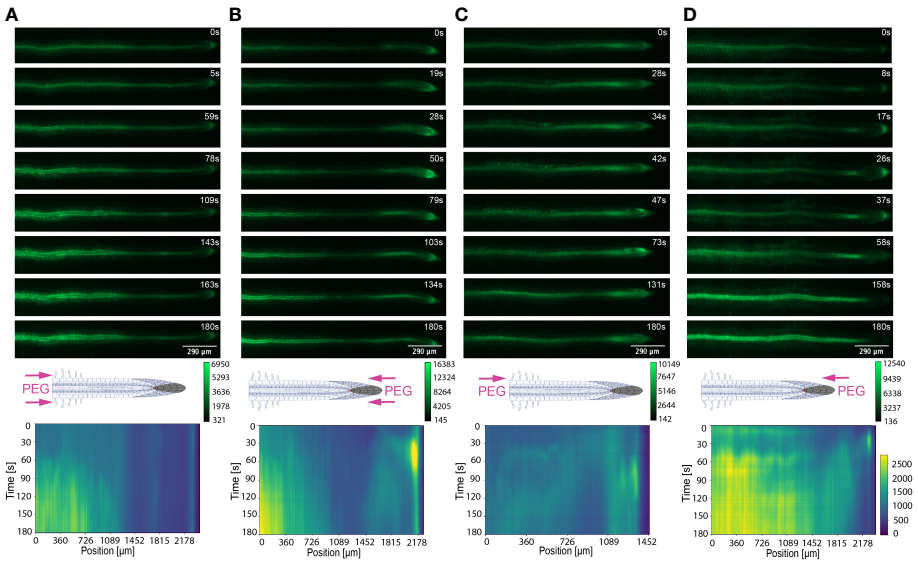

FIGURE 6
Key Ca^{2+} signal localisation in *Arabidopsis* roots exposed to 20% PEG. Schematic diagrams depict treatment localisation and orientation at the root within the bi-dfRC with fluorescent intensity calibration bars. Kymographs depict the spatial fluorescense of GFP corresponding to Ca^{2+} in the root over time, in dependence of treatment orientation and localisation. GFP fluorescence in kymographs is color coded, ranging from dark blue to yellow (normalized for all samples). **(A)** Key Ca^{2+} localisation pattern upon PEG treatment through inlets A & B of the bi-dfRC at the differentiation zone. **(B)** Key Ca^{2+} localisation pattern upon PEG treatment through inlets C & D of the bi-dfRC at the tip. **(C)** Key Ca^{2+} localisation pattern upon PEG treatment through inlet B (top) and control treatment through inlet A (base) of the bi-dfRC at the differentiation zone. **(D)** Key Ca^{2+} localisation pattern upon PEG treatment through inlet D (top) and control treatment through inlet C (base) of the bi-dfRC at the tip.

varying tissues for long distance signaling, in dependence of the exact localisation of an external stress in the soil. Overall, the presented research focused on optimising a bi-dfRC microfluidic device that allowed precise tracking of root Ca^{2+} signal directionality in response to stress solution in varying orientations and localisations. Summarising, we reported novel insights into the traverse and longitudinal directionality of osmolyte induced-Ca^{2+} signals. These signals were transmitted root or shoot-ward in depends of on the first contact site with the stress solution. Results presented here suggest that plants may use different sensing machinery in response to abiotic stress conditions. However, more research is required to confirm that the varying signal responses may fine tune adaptation processes.

4 Conclusion

Advances in bi-dfRC technology have revealed fascinating Ca^{2+} signal patterns in response to osmotic stress in varying localisations and orientations in the primary root. We show both NaCl and PEG treatments induced a Ca^{2+} signal that initially upregulated at the cells in first contact with the stressor. Following osmolyte treatment at the root tip, the Ca^{2+} signal initiated at the columella cells. Whereas, osmolyte treatment at the shoot site resulted primarily in cytosolic Ca^{2+} increase in the epidermal and cortical tissues of the differentiation zone. The following systemic transmission of Ca^{2+} is always oriented away from the initial contact site, and propagated faster in PEG than NaCl treated roots. Interestingly the signal moved longitudinally through different cell types depending on the localisation and orientation of the stress. Additionally, a one-sided NaCl or PEG treatment at the shoot site induced a Ca^{2+} signal that primarily traveled transversely through the root. The signal patterns observed here are complex, given that the root is a cylindrical 3D object compared to leaves, which can be simplified as a cuboid object. Hence, present results are limited by our 2D observations, due to the given speed limit of imaging processes to date.

Many Ca^{2+} sensors are now implemented in research, so it is important to note that their kinetics widely vary (Mertes et al., 2022). The G-CaMP3 sensor uitilised here harbours increased sensitivity and binding affinity compared to prior G-CaMP family sensors (Tian et al., 2009). However, more recently engineered Ca^{2+} sensors, including FRET-based MatryoshCaMP6s, exhibit superior fluorescence, dynamic range and sensitivity (Ast et al., 2017). Consequently, limitations of spatiotemporal resolution still exist

using the G-CaMP3 sensor, as the signal speed and intensity observed may vary in prior and future studies, depending on the system and fluorescence indicator chosen. Moving forward, there is a need to be thoughtful about the side effects fluorescent sensors may have on plant physiological stress responses towards varying environmental stressors. The presented bi-dfRC application is not restricted to NaCl and PEG-induced Ca^{2+} stress signaling. We propose the asymmetric laminar flow capabilities of the bi-dfRC will present a broad application basis to investigate defence signaling in response to abiotic osmolytes and biotic peptides, and the combinatory effects of both. Future applications will also provide insight into possible paralleled signaling between Ca^{2+} and the ROS H_2O_2, in addition to downstream signaling including nitric oxide (NO) and lipids, while observing and tracking RNA and protein movement within root cells. We believe that this technology will position us better for future studies that will potentially lead to novel insights into mechanisms of molecular adaptations that underlie improved tolerance and survival of crop plants to challenges imposed by climate and pathogens.

Data availability statement

The raw data supporting the conclusions of this article will be made available by the authors, without undue reservation.

Author contributions

C-NM and VN supervised the experiments. CA performed and designed the experiments and analysed the data. R.H. wrote the script for Ca^{2+} quantification and Kymogram analysis. VN designed and prepared the wafer for the chips. AT provided technical assistance to CA. C-NM and VN conceived the project. CA wrote the article with contributions of all the authors. C-NM and VN supervised and completed the writing. C-NM agrees to serve as the author responsible for contact and ensures communication. All authors contributed to the article and approved the submitted version.

Funding

PhD student C. Allan receives a scholarship from the Biomolecular Interaction Centre, Christchurch. Furthermore, research was supported by funding to Meisrimler by the Faculty of Science, University of Canterbury and Royal Society Te Apārangi Catalyst funding CSG-UOC1902 and to V. Nock by the Rutherford Discovery Fellowship RDF-19-UOC-019 and Biomolecular Interaction Centre funding.

Acknowledgment

The authors thank R. Morris and S. Eccersall for proof reading the manuscript and critical feedback. We are grateful to M. Toyota for sharing G-CaMP3 lines used in this study.

Conflict of interest

The authors declare that the research was conducted in the absence of any commercial or financial relationships that could be construed as a potential conflict of interest.

Publisher's note

Supplementary material

The Supplementary Material for this article can be found online at: https://www.frontiersin.org/articles/10.3389/fpls.2022.1040117/full#supplementary-material

SUPPLEMENTARY VIDEO 1
An *Arabidopsis* G-CaMP3 root exposed to 100 mM NaCl at the differentiation zone via inlets A & B of the bi-dfRC. At time interval 20 s, mature cells are primarily stimulated (GFP). The playback rate is 30 fps. Scale bar, 290 µm.

SUPPLEMENTARY VIDEO 2
An *Arabidopsis* G-CaMP3 root exposed to 20% PEG at the differentiation zone via inlets A & B of the bi-dfRC. At time interval 30 s, mature cells are primarily stimulated (GFP). The playback rate is 30 fps. Scale bar, 290 µm.

SUPPLEMENTARY VIDEO 3
An *Arabidopsis* G-CaMP3 root exposed to 100 mM NaCl at the tip via inlets C & D of the bi-dfRC. At time interval 10 s, tip cells are primarily stimulated (GFP). The playback rate is 30 fps. Scale bar, 290 µm.

SUPPLEMENTARY VIDEO 4
An *Arabidopsis* G-CaMP3 root exposed to 20% PEG at the tip *via* inlets C & D of the bi-dfRC. At time interval 10 s, tip cells are primarily stimulated (GFP). The playback rate is 30 fps. Scale bar, 290 µm.

SUPPLEMENTARY VIDEO 5
An *Arabidopsis* G-CaMP3 root exposed to 100 mM NaCl through inlet B (top) and control through inlet A (base) of the bi-dfRC at the differentiation zone. At time interval 25 s, mature cells are primarily stimulated (GFP). The playback rate is 30 fps. Scale bar, 290 µm.

SUPPLEMENTARY VIDEO 6
An *Arabidopsis* G-CaMP3 root exposed to 20% PEG through inlet A (base) and control through inlet B (top) of the bi-dfRC at the differentiation zone.

At time interval 30 s, mature cells are primarily stimulated (GFP). The playback rate is 30 fps. Scale bar, 290 μm.

SUPPLEMENTARY VIDEO 7

An *Arabidopsis* G-CaMP3 root exposed to 100 mM NaCl through inlet D (top) and control through inlet C (base) of the bi-dfRC at the tip. At time interval 10 s, tip cells are primarily stimulated (GFP). The playback rate is 30 fps. Scale bar, 290 μm.

SUPPLEMENTARY VIDEO 8

An *Arabidopsis* G-CaMP3 root exposed to 20% PEG through inlet D (top) and control through inlet C (base) of the bi-dfRC at the tip. At time interval 10 s, tip cells are primarily stimulated (GFP). The playback rate is 30 fps. Scale bar, 290 μm.

SUPPLEMENTARY VIDEO 9

An *Arabidopsis* G-CaMP3 root exposed to control ½ MS/0.31 mM MES media through inlet A & B of the bi-dfRC at the differentiation zone. No Ca^{2+} burst is observed. The playback rate is 30 fps. Scale bar, 290 μm.

SUPPLEMENTARY VIDEO 10

An *Arabidopsis* G-CaMP3 root exposed to control ½ MS/0.31 mM MES media through inlet C & D of the bi-dfRC at the differentiation zone. No Ca^{2+} burst is observed. The playback rate is 30 fps. Scale bar, 290 μm.

References

Allan, C. (2021). Implementation of a novel bi-directional dual-flow-RootChip to investigate the effects of osmotic stress on calcium signalling in *Arabidopsis thaliana* roots. (University of Canterbury MSc thesis). doi: 10.26021/11069

Allan, C., Morris, R. J., and Meisrimler, C. N. (2022a). Encoding, transmission, decoding, and specificity of calcium signals in plants. *J. Exp. Bot.* 73 (11), 3372–3385. doi: 10.1093/jxb/erac105

Allan, C., Tayagui, A., Nock, V., and Meisrimler, C. N. (2022b). "Novel bi-directional dual-flow-RootChip to study effects of osmotic stress on calcium signalling in *Arabidopsis* roots," in *2022 IEEE 35th International Conference on Micro Electro Mechanical Systems Conference (MEMS)*, 2022, 896–899. doi: 10.1109/MEMS51670.2022.9699700

Arsuffi, G., and Braybrook, S. A. (2018). Acid growth: an ongoing trip. *J. Exp. Bot.* 69 (2), 137–146. doi: 10.1093/jxb/erx390

Asghar, W., Yuksekkaya, M., Shafiee, H., Zhang, M., Ozen, M. O., Inci, F., et al. (2016). Engineering long shelf life multi-layer biologically active surfaces on microfluidic devices for point of care applications. *Sci. Rep.* 6 (1), 1–10. doi: 10.1038/srep21163

Ast, C., Foret, J., Oltrogge, L. M., De Michele, R., Kleist, T. J., Ho, C. H., et al. (2017). Ratiometric matryoshka biosensors from a nested cassette of green-and orange-emitting fluorescent proteins. *Nat. Commun.* 8 (1), 431. doi: 10.1038/s41467-017-00400-2

Behera, S., Wang, N., Zhang, C., Schmitz-Thom, I., Strohkamp, S., Schültke, S., et al. (2015). Analyses of Ca_{2+} dynamics using a ubiquitin-10 promoter-driven yellow cameleon 3.6 indicator reveal reliable transgene expression and differences in cytoplasmic Ca_{2+} responses in *Arabidopsis* and rice (Oryza sativa) roots. *New Phytol.* 206 (2), 751–760. doi: 10.1111/nph.13250

Bergey, D. R., Kandel, R., Tyree, B. K., Dutt, M., and Dhekney, S. A. (2014). The role of calmodulin and related proteins in plant cell function: an ever-thickening plot. *Springer Sci. Rev.* 2 (1), 145–159. doi: 10.1007/s40362-014-0025-z

Bhatia, S. N., and Ingber, D. E. (2014). Microfluidic organs-on-chips. *Nat. Biotechnol.* 32 (8), 760–772. doi: 10.1038/nbt.2989

Bi, X., Beck, C., and Gong, Y. (2021). Genetically encoded fluorescent indicators for imaging brain chemistry. *Biosensors* 11 (4), 116. doi: 10.3390/bios11040116

Bonza, M. C., Luoni, L., Olivari, C., and De Michelis, M. I. (2016). "Plant type 2B Ca_{2+}-ATPases: the diversity of isoforms of the model plant *Arabidopsis thaliana*," in Regulation of Ca_{2+}-ATPases, V-ATPases and f-ATPases. *Advances in Biochemistry in Health and Disease*. Springer, Cham. vol 14, 227–241. doi: 10.1007/978-3-319-24780-9_13

Cackett, L., Cannistraci, C. V., Meier, S., Ferrandi, P., Pěnčík, A., Gehring, C., et al. (2022). Salt-specific gene expression reveals elevated auxin levels in *Arabidopsis thaliana* plants grown under saline conditions. *Front. Plant Sci.* 13, 804716. doi: 10.3389/fpls.2022.804716

Choi, W. G., Toyota, M., Kim, S. H., Hilleary, R., and Gilroy, S. (2014). Salt stress-induced Ca_{2+} waves are associated with rapid, long-distance root-to-shoot signaling in plants. *Proc. Natl. Acad. Sci.* 111 (17), 6497–6502. doi: 10.1073/pnas.1319955111

Cho, J. H., Swanson, C. J., Chen, J., Li, A., Lippert, L. G., Boye, S. E., et al. (2017). The gcamp-r family of genetically encoded ratiometric calcium indicators. *ACS Chem. Biol.* 12 (4), 1066–1074. doi: 10.1021/acschembio.6b00883

Clapham, D. E. (2007). Calcium signaling. *Cell* 131 (6), 1047–1058. doi: 10.1016/j.cell.2007.11.028

Connorton, J. M., Webster, R. E., Cheng, N., and Pittman, J. K. (2012). Knockout of multiple *Arabidopsis* cation/H_{+} exchangers suggests isoform-specific roles in metal stress response, germination and seed mineral nutrition. *PloS One* 7(10), e47455. doi: 10.1371/journal.pone.0047455

De Koninck, P., and Schulman, H. (1998). Sensitivity of CaM kinase II to the frequency of Ca_{2+} oscillations. *Science* 279 (5348), 227–230. doi: 10.1126/science.279.5348.22

Dindas, J., Scherzer, S., Roelfsema, M. R. G., von Meyer, K., Müller, H. M., Al-Rasheid, K. A. S., et al. (2018). AUX1-mediated root hair auxin influx governs SCFTIR1/AFB-type Ca_{2+} signaling. *Nat. Commun.* 9 (1), 1–10. doi: 10.1038/s41467-018-03582-5

Dodd, A. N., Kudla, J., and Sanders, D. (2010). The language of calcium signaling. *Annu. Rev. Plant Biol.* 61, 593–620. doi: 10.1146/annurev-arplant-070109-104628

Duan, L., Sebastian, J., and Dinneny, J. R. (2015). Salt-stress regulation of root system growth and architecture in *Arabidopsis* seedlings. *Plant Cell Expans. Methods in Molecular Biology*. Humana Press, New York, NY. vol 1242, 105–122. doi: 10.1007/978-1-4939-1902-4_10

Gilroy, S., Suzuki, N., Miller, G., Choi, W.-G., Toyota, M., Devireddy, A. R., et al. (2014). A tidal wave of signals: calcium and ROS at the forefront of rapid systemic signaling. *Trends Plant Sci.* 19, 623–630. doi: 10.1016/j.tplants.2014.06.013

Granqvist, E., Wysham, D., Hazledine, S., Kozlowski, W., Sun, J., Charpentier, M., et al. (2012). Buffering capacity explains signal variation in symbiotic calcium oscillations. *Plant Physiol.* 160, 2300–2310. doi: 10.1104/pp.112.205682

Guckenberger, D. J., Berthier, E., Young, E. W., and Beebe, D. J. (2014). Fluorescence-based assessment of plasma-induced hydrophilicity in microfluidic devices via Nile red adsorption and depletion. *Analytical Chem.* 86 (15), 7258–7263. doi: 10.1021/ac501259n

Halldorsson, S., Lucumi, E., Gómez-Sjöberg, R., and Fleming, R. M. (2015). Advantages and challenges of microfluidic cell culture in polydimethylsiloxane devices. *Biosensors Bioelectronics* 63, 218–231. doi: 10.1016/j.bios.2014.07.029

Hashemi, A., de Decker, F., Orcheston-Findlay, L., Ali, M. A., Alkaisi, M. M., and Nock, V. (2017). Enhanced pattern resolution, swelling-behaviour and biocompatibility of bioimprinted casein microdevices. *AIP Adv.* 7 (11), 115019. doi: 10.1063/1.4991783

Hellal, F. A., El-Shabrawi, H. M., Abd El-Hady, M., Khatab, I. A., El-Sayed, S. A. A., and Abdelly, C. (2018). Influence of PEG induced drought stress on molecular and biochemical constituents and seedling growth of Egyptian barley cultivars. *J. Genet. Eng. Biotechnol.* 16 (1), 203–212. doi: 10.1016/j.jgeb.2017.10.009

Hemmilä, S., Cauich-Rodríguez, J. V., Kreutzer, J., and Kallio, P. (2012). Rapid, simple, and cost- effective treatments to achieve long-term hydrophilic PDMS surfaces. *Appl. Surface Sci.* 258 (24), 9864–9875. doi: 10.1016/j.apsusc.2012.06.044

Horikawa, K., Yamada, Y., Matsuda, T., Kobayashi, K., Hashimoto, M., Matsu-ura, T., et al. (2010). Spontaneous network activity visualized by ultrasensitive Ca_{2+} indicators, yellow cameleon-nano. *Nat. Methods* 7 (9), 729–732. doi: 10.1038/nmeth.1488

Hosokawa, K., Sato, K., Ichikawa, N., and Maeda, M. (2004). Power-free poly (dimethylsiloxane) microfluidic devices for gold nanoparticle-based DNA analysis. *Lab. Chip* 4 (3), 181–185. doi: 10.1039/b403930k

Huang, J., Chen, Q., Rong, Y., Tang, B., Zhu, L., Ren, R., et al. (2021). Transcriptome analysis revealed gene regulatory network involved in PEG-induced drought stress in tartary buckwheat (*Fagopyrum tararicum*). *PeerJ* 9, e11136. doi: 10.7717/peerj.11136

Huang, F., Luo, J., Ning, T., Cao, W., Jin, X., Zhao, H., et al. (2017). Cytosolic and nucleosolic calcium signaling in response to osmotic and salt stresses are

independent of each other in roots of *Arabidopsis* seedlings. *Front. Plant Sci.* 8, 1648. doi: 10.3389/fpls.2017.01648

Jing, X., Cai, C., Fan, S., Wang, L., and Zeng, X. (2019). Spatial and temporal calcium signaling and its physiological effects in moso bamboo under drought stress. *Forests* 10 (3), 224. doi: 10.3390/f10030224

Jokinen, V., Suvanto, P., and Franssila, S. (2012). Oxygen and nitrogen plasma hydrophilization and hydrophobic recovery of polymers. *Biomicrofluidics* 6 (1), 016501. doi: 10.1063/1.3673251

Kao, C. Y., Lo, T. C., and Lee, W. C. (2003). Influence of polyvinylpyrrolidone on the hydrophobic properties of partially porous poly (styrene–divinylbenzene) particles for biological applications. *J. Appl. Polymer Sci.* 87 (11), 1818–1824. doi: 10.1002/app.11653

Karlsson, J. M., Gazin, M., Laakso, S., Haraldsson, T., Malhotra-Kumar, S., Mäki, M., et al. (2013). Active liquid degassing in microfluidic systems. *Lab. Chip* 13 (22), 4366–4373. doi: 10.1039/c3lc50778e

Keinath, N. F., Waadt, R., Brugman, R., Schroeder, J. I., Grossmann, G., Schumacher, K., et al. (2015). Live cell imaging with r-GECO1 sheds light on flg22-and chitin-induced transient [Ca_{2+}] cyt patterns in *Arabidopsis*. *Mol. Plant* 8 (8), 1188–1200. doi: 10.1016/j.molp.2015.05.006

Kiegle, E., Moore, C. A., Haseloff, J., Tester, M. A., and Knight, M. R. (2000). Cell-type-specific calcium responses to drought, salt and cold in the *Arabidopsis* root. *Plant J.* 23 (2), 267–278. doi: 10.1046/j.1365-313x.2000.00786.x

Knight, M. R., Campbell, A. K., Smith, S. M., and Trewavas, A. J. (1991). Transgenic plant aequorin reports the effects of touch and cold-shock and elicitors on cytoplasmic calcium. *Nature* 352, 524–526. doi: 10.1038/352524a0

Knight, H., Trewavas, A. J., and Knight, M. R. (1997). Calcium signalling in *Arabidopsis thaliana* responding to drought and salinity. *Plant J.* 12 (5), 1067–1078. doi: 10.1046/j.1365-313X.1997.12051067.x

Krebs, M., Held, K., Binder, A., Hashimoto, K., Den Herder, G., Parniske, M., et al. (2012). FRET-based genetically encoded sensors allow high-resolution live cell imaging of Ca_{2+} dynamics. *Plant J.* 69 (1), 181–192. doi: 10.1111/j.1365-313X.2011.04780.x

Leitão, N., Dangeville, P., Carter, R., and Charpentier, M. (2019). Nuclear calcium signatures are associated with root development. *Nat. Commun.* 10 (1), 1–9. doi: 10.1038/s41467-019-12845-8

Li, Y., Liu, Y., Jin, L., and Peng, R. (2022). Crosstalk between Ca_{2+} and other regulators assists plants in responding to abiotic stress. *Plants* 11 (10), 1351. doi: 10.3390/plants11101351

Liu, J., and Li, S. (2015). "Numerical analysis of air bubble formation in PDMS micro-channels in negative pressure-driven flow," in *2015 International Conference on Fluid Power and Mechatronics (FPM)*, 2015, pp. 686–690. doi: 10.1109/FPM.2015.7337202

Liu, Z., Ma, Z., Guo, X., Shao, H., Cui, Q., and Song, W. (2010). Changes of cytosolic Ca_{2+} fluorescence intensity and plasma membrane calcium channels of maize root tip cells under osmotic stress. *Plant Physiol. Biochem.* 48 (10-11), 860–865. doi: 10.1016/j.plaphy.2010.08.008

Ma, Y., Dias, M. C., and Freitas, H. (2020). Drought and salinity stress responses and microbe-induced tolerance in plants. *Front. Plant Sci.* 11, 591911. doi: 10.3389/fpls.2020.591911

Manishankar, P., Wang, N., Köster, P., Alatar, A. A., and Kudla, J. (2018). Calcium signaling during salt stress and in the regulation of ion homeostasis. *J. Exp. Bot.* 69 (17), 4215–4226. doi: 10.1093/jxb/ery201

McAinsh, M. R., and Pittman, J. K. (2009). Shaping the calcium signature. *New Phytol.* 181 (2), 275–294. doi: 10.1111/j.1469-8137.2008.02682.x

Mertes, N., Busch, M., Huppertz, M. C., Hacker, C. N., Wilhelm, J., Gürth, C. M., et al. (2022). Fluorescent and bioluminescent calcium indicators with tuneable colors and affinities. *J. Am. Chem. Soc.* 144 (15), 6928–6935. doi: 10.1021/jacs.2c01465

Nakayama, T., Kurosawa, Y., Furui, S., Kerman, K., Kobayashi, M., Rao, S. R., et al. (2006). Circumventing air bubbles in microfluidic systems and quantitative continuous- flow PCR applications. *Analytical Bioanalytical Chem.* 386 (5), 1327–1333. doi: 10.1007/s00216-006-0688-7

Nezhad, A. S. (2014). Microfluidic platforms for plant cells studies. *Lab. Chip* 14 (17), 3262–3274. doi: 10.1039/C4LC00495G

Olanrewaju, A., Beaugrand, M., Yafia, M., and Juncker, D. (2018). Capillary microfluidics in microchannels: from microfluidic networks to capillaric circuits. *Lab. Chip* 18 (16), 2323–2347. doi: 10.1039/C8LC00458G

Orcheston-Findlay, L., Hashemi, A., Garrill, A., and Nock, V. (2018). A microfluidic gradient generator to simulate the oxygen microenvironment in cancer cell culture. *Microelectronic Eng.* 195, 107–113. doi: 10.1016/j.mee.2018.04.011

Plegue, T. J., Kovach, K. M., Thompson, A. J., and Potkay, J. A. (2018). Stability of polyethylene glycol and zwitterionic surface modifications in PDMS microfluidic flow chambers. *Langmuir* 34 (1), 492–502. doi: 10.1021/acs.langmuir.7b03095

Russell, J. T. (2011). Imaging calcium signals *in vivo*: a powerful tool in physiology and pharmacology. *Br. J. Pharmacol.* 163 (8), 1605–1625. doi: 10.1111/j.1476-5381.2010.00988.x

Schindelin, J., Arganda-Carreras, I., Frise, E., Kaynig, V., Longair, M., Pietzsch, T., et al. (2012). Fiji: an open-source platform for biological-image analysis. *Nat. Methods* 9 (7), 676–682. doi: 10.1038/nmeth.2019

Sevindik, B., Sevindik, O., and Selli, S. (2022). Effect of drought stress induced by PEG 6000 on *Ocimum basilicum* L. aroma profile. *J. Food Process. Preservation* 46 (6), e15948. doi: 10.1111/jfpp.15948

Shih, H.-W., DePew, C. L., Miller, N. D., and Monshausen, G. B. (2015). The cyclic nucleotide-gated channel CNGC14 regulates root gravitropism in *Arabidopsis thaliana*. *Curr. Biol.* 25, 3119–3125. doi: 10.1016/j.cub.2015.10.025

Smolko, A., Bauer, N., Pavlović, I., Pěnčík, A., Novák, O., and Salopek-Sondi, B. (2021). Altered root growth, auxin metabolism and distribution in *Arabidopsis thaliana* exposed to salt and osmotic stress. *Int. J. Mol. Sci.* 22 (15), 7993. doi: 10.3390/ijms22157993

Soffe, R., Mach, A. J., Onal, S., Nock, V., Lee, L. P., and Nevill, J. T. (2020). Art-on-a-Chip: Preserving microfluidic chips for visualization and permanent display. *Small* 16 (34), 2002035. doi: 10.1002/smll.202002035

Stanley, C. E., Shrivastava, J., Brugman, R., Heinzelmann, E., van Swaay, D., and Grossmann, G. (2018). Dual-flow-RootChip reveals local adaptations of roots towards environmental asymmetry at the physiological and genetic levels. *New Phytol.* 217 (3), 1357–1369. doi: 10.1111/nph.14887

Stanley, C. E., and van der Heijden, M. G. (2017). Microbiome-on-a-chip: new frontiers in plant–microbiota research. *Trends Microbiol.* 25 (8), 610–613. doi: 10.1016/j.tim.2017.05.001

Sun, Y., Tayagui, A., Garrill, A., and Nock, V. (2020). Microfluidic platform for integrated compartmentalization of single zoospores, germination and measurement of protrusive force generated by germ tubes. *Lab. Chip* 20 (22), 4141–4151. doi: 10.1039/D0LC00752H

Tayagui, A., Sun, Y., Collings, D. A., Garrill, A., and Nock, V. (2017). An elastomeric micropillar platform for the study of protrusive forces in hyphal invasion. *Lab. Chip* 17 (21), 3643–3653. doi: 10.1039/C7LC00725F

Thoday-Kennedy, E. L., Jacobs, A. K., and Roy, S. J. (2015). The role of the CBL–CIPK calcium signalling network in regulating ion transport in response to abiotic stress. *Plant Growth Regul.* 76 (1), 3–12. doi: 10.1007/s10725-015-0034-1

Thor, K., and Peiter, E. (2014). Cytosolic calcium signals elicited by the pathogen-associated molecular pattern flg22 in stomatal guard cells are of an oscillatory nature. *New Phytol.* 204 (4), 873–881. doi: 10.1111/nph.13064

Tian, L., Hires, S. A., Mao, T., Huber, D., Chiappe, M. E., Chalasani, S. H., et al. (2009). Imaging neural activity in worms, flies and mice with improved GCaMP calcium indicators. *Nat. Methods* 6 (12), 875–881. doi: 10.1038/nmeth.1398

Toyota, M., Spencer, D., Sawai-Toyota, S., Jiaqi, W., Zhang, T., Koo, A. J., et al. (2018). Glutamate triggers long-distance, calcium-based plant defense signaling. *Science* 361 (6407), 1112–1115. doi: 10.1126/science.aat7744

Vogelmann, E. S., Reichert, J. M., Prevedello, J., and Awe, G. O. (2013). Hydro-physical processes and soil properties correlated with origin of soil hydrophobicity. *Ciec. Rural* 43 (9), 1582–1589. doi: 10.1590/S0103-84782013005000107

Wagner, S., Behera, S., De Bortoli, S., Logan, D. C., Fuchs, P., Carraretto, L., et al. (2015). The EF-hand Ca_{2+} binding protein MICU choreographs mitochondrial Ca_{2+} dynamics in *Arabidopsis*. *Plant Cell* 27 (11), 3190–3212. doi: 10.1105/tpc.15.00509

Xia, Y., and Whitesides, G. M. (1998). Soft lithography. *Annu. Rev. Materials Sci.* 28 (1), 153–184. doi: 10.1146/annurev.matsci.28.1.153

Xiong, T. C., Ronzier, E., Sanchez, F., Corratgé-Faillie, C., Mazars, C., and Thibaud, J. B. (2014). Imaging long distance propagating calcium signals in intact plant leaves with the BRET-based GFP-aequorin reporter. *Front. Plant Sci.* 5, 43. doi: 10.3389/fpls.2014.00043

Xue, X., Patel, M. K., Kersaudy-Kerhoas, M., Desmulliez, M. P., Bailey, C., and Topham, D. (2012). Analysis of fluid separation in microfluidic T-channels. *Appl. Math. Model.* 36 (2), 743–755. doi: 10.1016/j.apm.2011.07.009

Yang, Y., Zhang, C., Tang, R. J., Xu, H. X., Lan, W. Z., Zhao, F., et al. (2019). Calcineurin b-like proteins CBL4 and CBL10 mediate two independent salt tolerance pathways in *Arabidopsis*. *Int. J. Mol. Sci.* 20 (10), 2421. doi: 10.3390/ijms20102421

Zhang, S., Wu, Q. R., Liu, L. L., Zhang, H. M., Gao, J. W., and Pei, Z. M. (2020). Osmotic stress alters circadian cytosolic Ca_{2+} oscillations and OSCA1 is required in circadian gated stress adaptation. *Plant Signaling Behav.* 15 (12), 1836883. doi: 10.1080/15592324.2020.1836883

Zhang, K., Yue, D., Wei, W., Hu, Y., Feng, J., and Zou, Z. (2016). Characterization and functional analysis of calmodulin and calmodulin-like genes in *Fragaria vesca*. *Front. Plant Sci.* 7, 1820. doi: 10.3389/fpls.2016.01820

Zheng, W., Huang, R., Jiang, B., Zhao, Y., Zhang, W., and Jiang, X. (2016). An early-stage atherosclerosis research model based on microfluidics. *Small* 12 (15), 2022–2034. doi: 10.1002/smll.201503241

Zhu, Y., Yan, J., Liu, W., Liu, L., Sheng, Y., Sun, Y., et al. (2016). Phosphorylation of a NAC transcription factor by a calcium/calmodulin-dependent protein kinase regulates abscisic acid-induced antioxidant defense in maize. *Plant Physiol.* 171 (3), 1651–1664. doi: 10.1104/pp.16.00168

frontiers | Frontiers in Plant Science

TYPE Review
PUBLISHED 30 March 2023
DOI 10.3389/fpls.2023.1158184

OPEN ACCESS

EDITED BY
María C. Romero-Puertas,
Experimental Station of Zaidín (CSIC), Spain

REVIEWED BY
Noelia Foresi,
CONICET Mar del Plata, Argentina
Ana Jiménez,
Center for Edaphology and Applied Biology of Segura (CSIC), Spain

*CORRESPONDENCE
Capilla Mata-Pérez
capilla.mata@usal.es
Inmaculada Sánchez-Vicente
elfik@usal.es

†These authors have contributed equally to this work

SPECIALTY SECTION
This article was submitted to Plant Abiotic Stress, a section of the journal Frontiers in Plant Science

RECEIVED 03 February 2023
ACCEPTED 14 March 2023
PUBLISHED 30 March 2023

CITATION
Mata-Pérez C, Sánchez-Vicente I, Arteaga N, Gómez-Jiménez S, Fuentes-Terrón A, Oulebsir CS, Calvo-Polanco M, Oliver C and Lorenzo Ó (2023) Functions of nitric oxide-mediated post-translational modifications under abiotic stress.
Front. Plant Sci. 14:1158184.
doi: 10.3389/fpls.2023.1158184

Functions of nitric oxide-mediated post-translational modifications under abiotic stress

Capilla Mata-Pérez*†, Inmaculada Sánchez-Vicente*†, Noelia Arteaga, Sara Gómez-Jiménez, Andrea Fuentes-Terrón, Cylia Salima Oulebsir, Mónica Calvo-Polanco, Cecilia Oliver and Óscar Lorenzo

Institute for Agrobiotechnology Research (CIALE), Faculty of Biology, University of Salamanca, Salamanca, Spain

Environmental conditions greatly impact plant growth and development. In the current context of both global climate change and land degradation, abiotic stresses usually lead to growth restriction limiting crop production. Plants have evolved to sense and respond to maximize adaptation and survival; therefore, understanding the mechanisms involved in the different converging signaling networks becomes critical for improving plant tolerance. In the last few years, several studies have shown the plant responses against drought and salinity, high and low temperatures, mechanical wounding, heavy metals, hypoxia, UV radiation, or ozone stresses. These threats lead the plant to coordinate a crosstalk among different pathways, highlighting the role of phytohormones and reactive oxygen and nitrogen species (RONS). In particular, plants sense these reactive species through post-translational modification (PTM) of macromolecules such as nucleic acids, proteins, and fatty acids, hence triggering antioxidant responses with molecular implications in the plant welfare. Here, this review compiles the state of the art about how plant systems sense and transduce this crosstalk through PTMs of biological molecules, highlighting the *S*-nitrosylation of protein targets. These molecular mechanisms finally impact at a physiological level facing the abiotic stressful traits that could lead to establishing molecular patterns underlying stress responses and adaptation strategies.

KEYWORDS

abiotic stress, gasotransmitter, nitroalkylation, nitrosative stress, oxidative stress, reactive oxygen species, reactive nitrogen species, *S*-nitrosylation

Background

Plants, as sessile organisms, are regularly challenged by several abiotic stresses involving water availability, temperature fluctuations, UV radiation, or the presence of heavy metals in land. Under normal conditions, aerobic metabolism results in the production of reactive oxygen species (ROS) highlighting superoxide anion ($O_2^{\cdot -}$), hydrogen peroxide (H_2O_2), or hydroxyl radical ($^{\cdot}OH$). Likewise, reactive nitrogen species (RNS) are another group of molecules derived from nitric oxide ($^{\cdot}NO$) including free radicals like $^{\cdot}NO$ or nitrogen dioxide ($^{\cdot}NO_2$) and non-radicals such as *S*-nitrosothiols (SNO) or peroxynitrite ($ONOO^-$) (Halliwell, 2006; del Río, 2015). A NO gasotransmitter has been described to play key regulatory roles in almost all aspects of the plant life cycle as well as responses to (a)biotic stresses with miscellaneous mechanisms that have not been fully understood yet (Freschi, 2013; Yu et al., 2014; Puyaubert and Baudouin, 2014a; Domingos et al., 2015; Trapet et al., 2015; Fancy et al., 2017; Begara-Morales et al., 2018).

The exposure to environmental perturbations leads to the accumulation of reactive oxygen and nitrogen species (RONS) in cells. Such increase prompts a reprogramming of their metabolism, especially aimed to neutralize such oxidative or nitrosative stresses (Apel and Hirt, 2004; Radi, 2012). Moreover, abnormal amounts of RONS cause the oxidation of cellular components hampering enzymatic activities or affecting organelle integrity. On the other hand, to counteract the action of these reactive species, enzymatic and molecular antioxidants are produced at the cellular level. These RONS impact plant function through post-translational modifications (PTMs) of macromolecules such as proteins, nucleic acids, or lipids (Figure 1). Cysteine (Cys) and methionine (Met) are the most oxidation-susceptible residues within amino acids. The free thiol group (-SH) of Cys can be gradually oxidized to *S*-nitrosothiol (-SNO), sulfenic acid (-SOH), disulfide bridge (-SS-), a covalent attachment of glutathione (*S*-glutathionylation, -SSG), sulfinic acid ($-SO_2H$), or sulfonic acid ($-SO_3H$) (Spoel and Van Ooijen, 2014). Most of these modifications are readily reversible, with the latter two often described as irreversible. In fact, the reversibility of modifications happening in this intrinsically nucleophilic amino acid provides many different cellular signaling opportunities to regulate plant function.

Furthermore, $^{\cdot}NO$ can interact with ROS, especially with $O_2^{\cdot -}$ to generate $ONOO^-$, which mediates the irreversible nitration of tyrosine residues (NO_2-Tyr) within proteins, a PTM that alters the protein conformation and mostly provokes loss of function or activity (Radi, 2004). More attention has been given to *S*-nitrosylation, a PTM resulting from the reversible and covalent *S*-linked NO group to the reactive -SH of a Cys residue (Figure 1). *S*-nitrosylation is considered

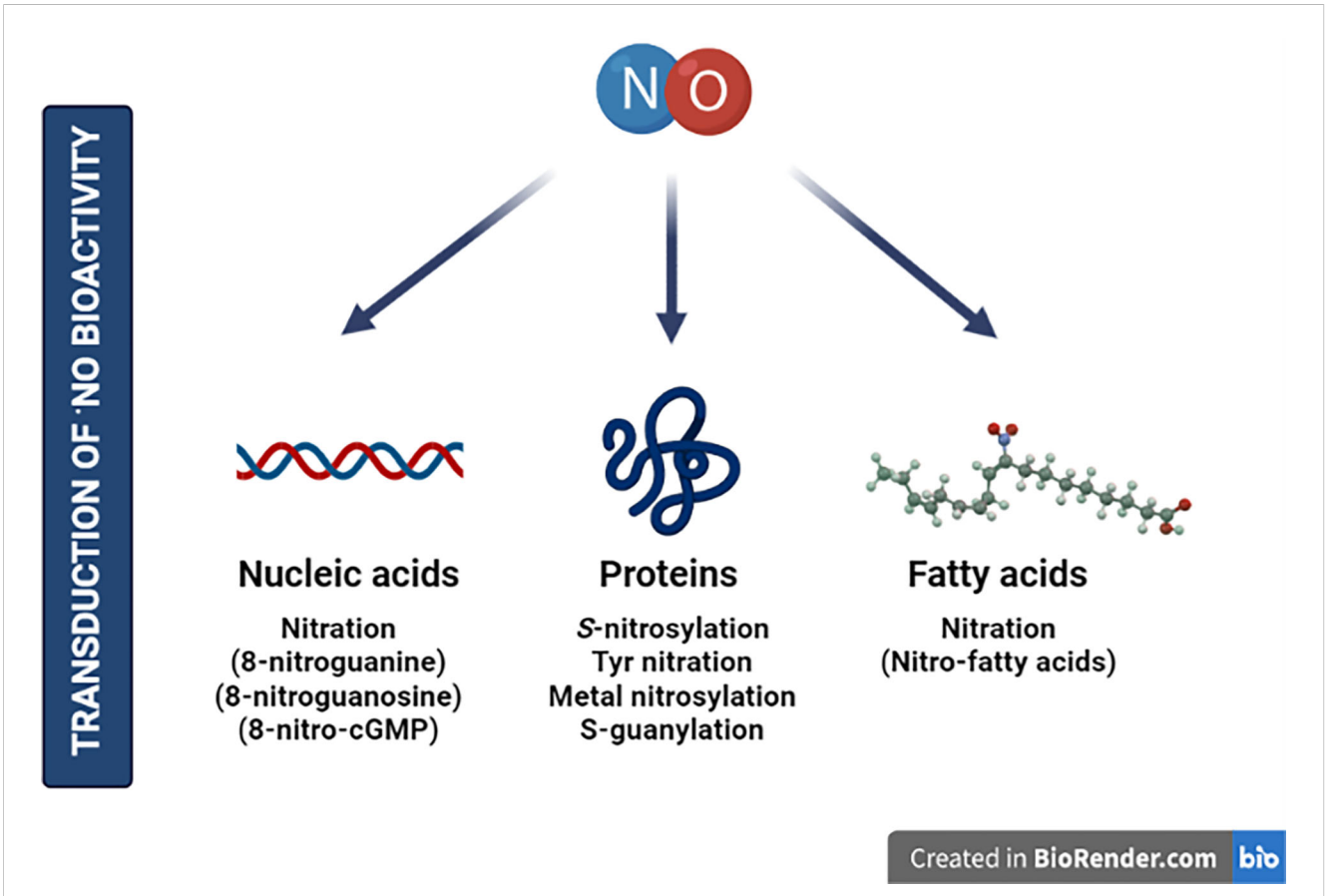

FIGURE 1
Nitric oxide is considered an essential gasotransmitter for the transduction of bioactivity in plants. Although the main effects described correspond to protein targets, other molecules are susceptible to be modified by NO—including nucleic acids or fatty acids—highlighting molecular points to be explored in future research. Created by BioRender.com.

one of the key mechanisms for the transduction of ˙NO bioactivity in plants. This modification modulates protein activities through several mechanisms, including stability, conformation, subcellular localization, biochemical activity, or even protein–protein interactions (Hess et al., 2005; Astier et al., 2011; Astier et al., 2012; Lamotte et al., 2014).

On the other hand, nitration of nucleic acids by RNS also represents one of the key mechanisms mediating the biological activity of NO in all types of organisms (Figure 1). Nitration of nucleotides was first described in the early 1990s with the identification of 8-nitroguanine (Yermilov et al., 1995a; Yermilov et al., 1995b; Pinlaor et al., 2003; Ma et al., 2004), 8-nitroguanosine (Niles et al., 2001; Akaike et al., 2003), and 8-nitroguanosine 3'5'-cyclic monophosphate (8-nitro-cGMP) (Sawa et al., 2007) in animal systems. It is noteworthy that 8-nitro-cGMP, being a unique dual signaling molecule, was described to hold powerful redox and electrophilic activities among the identified nitrated guanine derivatives (Sawa et al., 2007). The electrophilic properties of 8-nitro-cGMP can irreversibly modify protein thiols through a novel PTM known as *S*-guanylation (Sawa et al., 2007). It was firstly considered as a marker of nitrosative stress in degenerative diseases, cancer, or other inflammatory conditions (Ohshima et al., 2006); however, recent studies have evidenced biological activities and signaling functions of 8-nitro-cGMP through *S*-guanylation in animal systems (Ihara et al., 2011; Nishida et al., 2016). In plants, there is still insufficient information about the role of nitrated nucleotides on physiology and signaling. However, recent observations have shown the implication of cGMP and 8-nitro-cGMP in *Arabidopsis thaliana* stomatal guard cells opening (Joudoi et al., 2013; Honda et al., 2015).

Finally, fatty acids, especially polyunsaturated fatty acids (PUFAs), are also targeted by RONS. PUFAs are major components of plant membranes and react with ROS through so-called lipid oxidation events, highlighting the peroxidation reactions resulting in the formation of a lipid radical (Vistoli et al., 2013, Alché, 2019). These events occur in plants as a signaling mechanism and after a plethora of stress conditions including high light intensity (Yin et al., 2010). Furthermore, PUFAs, through the activity of lipoxygenase enzymes, are precursors of different signaling molecules, including oxylipins or other oxidized fatty acids, deriving in the production of key phytohormones such as jasmonates (JAs) (Wasternack and Song, 2017). However, a growing body of plant studies is drawing attention to the modification of unsaturated fatty acids by NO and nitrite (NO_2^-)-derived RNS leading to nitro-fatty acid (NO_2-FA) formation. NO_2-FAs are endogenously present in plant systems mainly in the form of nitro-linolenic (NO_2-Ln) and nitro-oleic (NO_2-OA) acids with relevant physiological roles as signaling molecules in (a)biotic stresses, growth, and development (Mata-Pérez et al., 2016c; Arruebarrena Di Palma et al., 2020; Di Fino et al., 2020; Vollár et al., 2020). The mechanisms of action described for NO_2-FAs involve the ability to act as NO donors, hence modifying proteins through *S*-nitrosylation (Lima et al., 2005; Gorczynski et al., 2007; Faine et al., 2010; Mata-Pérez et al., 2016b) or nitroalkylation (Figure 1). The latter is a reversible process based on the strong electrophilicity of the β-carbon adjacent to the nitro group (-NO_2) and its appetence for soft nucleophiles like Cys or histidine (His) residues (Baker et al., 2007; Geisler and Rudolph, 2012). Thus, nitroalkylation has the capacity to regulate physiological processes in eukaryotes by modulating the activity of transcription factors (TFs) and enzymatic reactions (reviewed in Schopfer et al., 2011; Aranda-Caño et al., 2019). Recently, it has been demonstrated that RONS may be responsible for compromising the stability of this PTM, at least *in vitro*. The oxidation of NO_2-FA-protein adducts through RONS such as H_2O_2 or $ONOO^-$ leads to the release of free NO_2-FAs. Therefore, this oxidation-mediated rupture might act as a mechanism to keep the protein targets sequestered and subsequently released after nitro-oxidative stress (Padilla et al., 2017).

Considering the accumulation of ROS and RNS is a key feature underlying abiotic stressful traits; here, we compile the state of the art about how plants sense, transduce, and integrate the crosstalk between RONS and their impact on plant function and metabolism that could lead us to establish molecular patterns underlying abiotic stress responses and subsequent adaptation strategies in a constantly changing environment.

Drought and salt stress

Plants show a dramatic increase in RONS levels (Bolwell and Wojtaszek, 1997; Navrot et al., 2007; Moreau et al., 2010) that should be controlled to avoid toxic concentrations and to maintain the redox balance during stress. In fact, the alleviation of salt or drought stress through NO is also observed when rat nitric oxide synthase (NOS) is overexpressed in Arabidopsis and rice (Shi et al., 2012; Cai et al., 2015). However, RONS can mainly transmit their activity through PTMs and, among those mediated by RNS, highlight cysteine *S*-nitrosylation or tyrosine nitration of proteins (Figure 2).

In Arabidopsis, NO-mediated *S*-nitrosylation has been reported for several TFs involved in abiotic stress responses such as MYB2 or ABI5 (Serpa et al., 2007; Albertos et al., 2015). These TFs participate in abscisic acid (ABA)-mediated regulation under drought stress. MYB2, a member of the MYB TF family, was described to undergo *S*-nitrosylation at Cys53, affecting its DNA binding activity, and indicated to be involved in ABA signaling (Serpa et al., 2007). ABI5 is involved in the repression of germination and seedling establishment (Lopez-Molina and Chua, 2000; Finkelstein et al., 2002). This TF works in the core of ABA signaling together with PYR/PYL/RCAR receptors, PP2C phosphatases, and SnRK2 kinases (Skubacz et al., 2016). ABI5, being a pivotal NO sensor in seeds, is influenced by NO at transcriptional and post-translational levels. Albertos et al. (2015) showed that *S*-nitrosylation of ABI5 at Cys153 facilitates its degradation through the proteasome, therefore leading to both seed germination and seedling growth under favorable conditions, demonstrating an antagonism role between NO and ABA during this process. Moreover, NO also impacts ABA perception through the tyrosine nitration and *S*-nitrosylation of PYR/PYL/RCAR receptors (Castillo et al., 2015). ABA is considered a stress-related hormone; in fact, ABA levels increase during water deficiency (reviewed in Swamy and Smith, 1999). In addition,

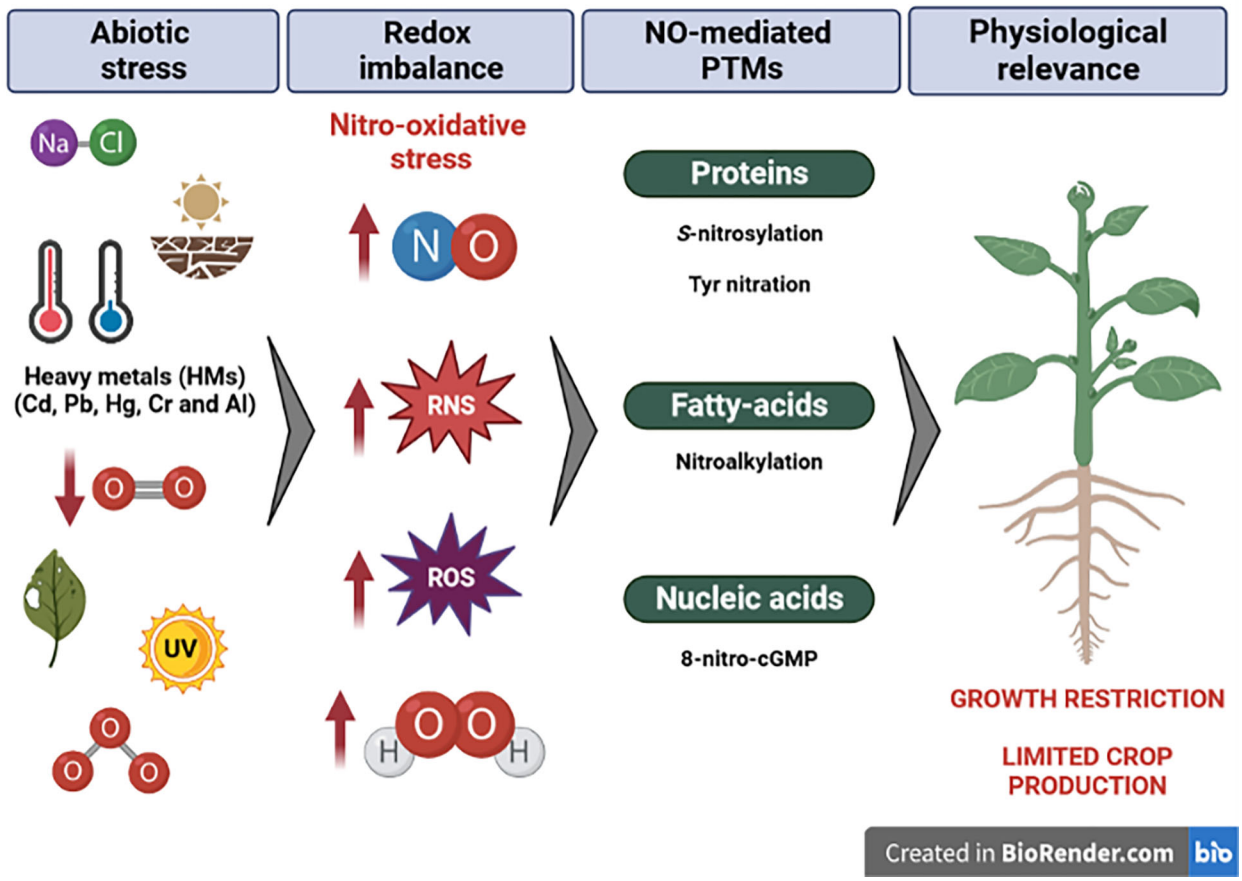

FIGURE 2
Different abiotic situations promote a redox imbalance linked to nitro-oxidative stress. Plant adaptation implies molecular strategies triggered by NO modifications to alleviate negative effects to readjust their growth and development. Created by BioRender.com.

abiotic stress conditions are known to be accompanied by an increase in RONS, and ABA increase also leads to the accumulation of NO and ROS. This scenario prompts a rise of peroxynitrite ($ONOO^-$) content that mediates the nitration of ABA receptors rendering the proteins inactive, targeting them for proteasome degradation and possibly acting as a rapid mechanism to reduce ABA effects. By contrast, *S*-nitrosylation of ABA receptors does not alter their function *in vitro*, suggesting that different NO-related PTMs may act throughout the ABA signaling cascade to attenuate ABA-triggered responses (Castillo et al., 2015). Furthermore, NO regulates the OPEN STOMATA 1 (OST1)/SUCROSE NONFERMENTING 1 (SNF1)-related protein kinase 2.6 (SnRK2.6) by *S*-nitrosylation at Cys137 in cell guards, showing a negative regulation of ABA signaling (Wang et al., 2015). This PTM induces a negative effect on stomata closure during drought stress, observed in cell guards from NO over-accumulating mutants of Arabidopsis (*atgsnor1-2*). Consequently, the *S*-nitrosylation of SnRK2.6 disrupts the ABA-dependent stomata closure (Wang et al., 2015). In the same species, a differential Tyr-nitrated protein profile was observed between wild-type plants and *kea1kea2* (K^+/H^+ antiporters) knockout mutants. The latter has closed stomata and shows a higher capacity to resist drought stress compared to the wild-type accession; both results suggest that impaired chloroplast K^+ could affect the expression of nitrated proteins (Sánchez-McSweeney et al., 2021). Also related to stomatal opening, it has been shown that 8-nitro-cGMP induced stomatal closure in the light, while cGMP did not (Joudoi et al., 2013). The signaling action of 8-nitro-cGMP is mediated by the modulation of Ca^{2+} channels, leading to the activation of SLAC1 (SLOW ANION CHANNEL 1), hence promoting stomatal closure. Furthermore, a metabolite derived from 8-nitro-cGMP, the 8-SH-cGMP, is also involved in the closure of stomata pores (Honda et al., 2015); however, the involvement of *S*-guanylation has yet not been evidenced.

A common and widely described feature underlying salt stress is the increase of the NO and the SNO content (Valderrama et al., 2007; Begara-Morales et al., 2014; Jain et al., 2018). First studies about the involvement of NO-PTMs under salinity were carried out in olive plants where an increase of NO and SNO levels together with a rise of the protein tyrosine nitration profile were described (Valderrama et al., 2007). Sunflower seedlings exposed to NaCl exhibited enhanced tyrosine nitration of cytosolic and oil bodies' proteins with an enhanced gradient of nitrated proteins from the root tip to the differentiation zone and from the outer layers to the deep-seated cells (David et al., 2015). These results led the authors to think that this is a mechanism to keep oil bodies so that plants can survive longer under salt stress. Jain and Bhatla (2018) demonstrated that the tyrosine nitration of cytosolic peroxidase

leads to an increase in its activity after NO exogenous treatment in sunflower seedling cotyledons. However, there is a discrepancy in this regard because the nitration of another peroxidase from the ascorbate–glutathione cycle, the ASCORBATE PEROXIDASE (APX) from *Pisum sativum*, leads to a reduction of its H_2O_2 detoxification activity (Begara-Morales et al., 2014). This discrepancy might be explained by the different tissues or plant species explored. Curiously, APX enzyme shows a dual regulation by NO due to the fact that GSNO prompts the enhancement of the activity through *S*-nitrosylation. In fact, under salinity conditions, pea plants show that APX is *S*-nitrosylated; this PTM leads to an increase in its activity (Begara-Morales et al., 2014). Despite the fact that PTM has not been demonstrated, several studies have shown the effect of NO in APX activity under salinity and non-stress conditions. On one hand, several works reveal that APX activity is inhibited after pharmacological treatments with NO donors in different plant species including tobacco and sweet pepper fruits (Clark et al., 2000; González-Gordo et al., 2022). Conversely, an increased APX activity has been demonstrated in sweet potato or soybean plants exposed to NO donors (Keyster et al., 2011; Lin et al., 2011); these results highlight that depending on the plant species and the source of NO applied, the impact on APX bioactivity might vary. On the other hand, the protective effect of NO on different plant species (i.e., barley, soybean, or mustard) exposed to salt stress through the increase of APX activity (Egbichi et al., 2014; Fatma et al., 2016; Yin et al., 2021) and under drought stress in watermelon plants (Hamurcu et al., 2020) has been revealed. Recently, Arabidopsis APX recombinant protein has been shown to be modulated by nitroalkylation, specifically by NO_2-Ln (Aranda-Caño et al., 2019). This modification leads to a decrease in its enzymatic activity under normal conditions, therefore showing how different NO-related molecules can differentially modulate protein bioactivity. Although this result has been observed under non-stress conditions, nitroalkylation of the peroxiredoxin Tsa1—involved in ROS alleviation—from *Saccharomyces cerevisiae* by NO_2-OA is abolished under heat stress (Aranda-Caño et al., 2022). The authors considered that nitroalkylation of Tsa1, in the absence of stress, is a way to keep the enzyme sequestered and inactive, while, upon stress, where a rise of RONS takes place, the enzyme can be released and trigger its antioxidant properties. We cannot rule out that something similar might be happening to APX where, upon drought or salinity stress, nitroalkylation can release APX, leading to H_2O_2 detoxification.

Similarly in pea plants, Camejo et al. (2013) demonstrated that salinity stress induces the *S*-nitrosylation of PEROXIREDOXIN IIF (PrxIIF) in the mitochondria, which reduces its peroxidase activity, due to a conformational change in the protein structure, acquiring a transnitrosylase activity and subsequently broadening the effects of protein *S*-nitrosylation (Camejo et al., 2013; Camejo et al., 2015).

Finally, there are other pieces of evidence about NO implication during salt stress alleviation that are described below. Polyamine (PA) biosynthesis is activated and induces the accumulation of H_2O_2 and several antioxidant activities during salinity (Tanou et al., 2014). In citrus plants, putrescine or spermidine led to the suppression of protein carbonylation and tyrosine nitration whereas protein *S*-nitrosylation was elicited by these molecules. Furthermore, a proteomic approach on citrus plants concomitantly exposed to PAs and NaCl showed the *S*-nitrosylation of catalase enzyme, which was accompanied by an induction of its enzymatic activity, suggesting an interplay between protein *S*-nitrosylation and protein carbonylation (Tanou et al., 2014). The positive role of NO in salt stress alleviation is also evident in tomato seedlings, showing an increase in *S*-nitrosylated proteins under NaCl treatment (Wang et al., 2022; Wei et al., 2022). Some of them are involved in MAPK signaling showing a downregulation in S-adenosyl-L-methionine (SAM) proteins like SAM1 and SAM3 (precursor of ethylene biosynthesis), SnRK, and PP2C, and upregulation of *MAPK*, *MAPKK*, and *MAPKK5* at the transcriptional level when plants grew under salt stress plus GSNO, protecting tomato seedlings from this stress (Wei et al., 2022). Another evidence about the role of NO during salt stress alleviation is the increase of the tomato MONODEHYDROASCORBATE REDUCTASE (MDHAR) activity through *S*-nitrosylation after exposure to salt stress, due to the important role of this enzyme during the ascorbic acid regeneration during ROS detoxification (Qi et al., 2020).

High and low-temperature stress

Heat and cold stresses promote changes that affect plants at the molecular level leading to plant dysfunction (Sánchez-Vicente and Lorenzo, 2021). The tolerance of plants to non-optimal temperatures seems to be linked to the redox regulatory system, which integrates information from metabolism through thiol-containing proteins to modulate cell status and minimize cellular damage (Dietz, 2008).

Heat stress (HS) deeply impacts plant development, including seed yield losses and crop quality (Sehgal et al., 2018), seed germination in Arabidopsis (Toh et al., 2008), leaf senescence in bent grass (Rossi et al., 2017), and photosynthetic damage (Wang et al., 2018). HS causes an increment in the oxidation level in both the nucleus and cytosol, which could be related to both genetic and epigenetic adaptive reprogramming (Babbar et al., 2021). The role of NO has been widely described under high temperatures (Lee et al., 2008), having shown that mutants impaired in NO homeostasis display abnormal growth and development, and the seed production is compromised under different temperatures (Sánchez-Vicente and Lorenzo, 2021). In addition, both deficient and SNO/NO over-accumulators are affected in the response to HS and thermotolerance capacities (Lee et al., 2008; Xuan et al., 2010). NO mechanisms during plant acclimation to HS include activation of cellular responses through the *S*-nitrosylation of the trihelix TF GT-1, which promotes its binding to *HEAT SHOCK TRANSCRIPTION FACTOR A2* (*HsfA2*) promoter (He et al., 2022). During germination, Cys *S*-nitrosylation has been described as an important PTM, where high temperature and the photoreceptor phytochrome B (phyB) modulate antagonistically LONG HYPOCOTYL IN FAR-RED (HFR1)-SNO to coordinate seed thermotolerance (Ying et al., 2022).

Tyr nitration is also a PTM closely related to HS response. Large-scale analyses have shown great changes in the nitroproteome of *Helianthus annuus* seedlings exposed to HS, with the FERREDOXIN–NADP REDUCTASE (FNR) (Chaki et al., 2011)

and CARBONIC ANHYDRASE (CA) being two of these proteins modulated by Tyr nitration (Chaki et al., 2013). These modifications inhibit its activity, finally impacting the photosynthesis process. Also related to nitration but of fatty acids (NO_2-FAs), it has been shown that exogenous treatments with NO_2-Ln induce the expression of genes involved in the HS response and the acquisition of thermotolerance, highlighting heat shock proteins (HSPs) and heat shock TFs (HSFs) (Mata-Pérez et al., 2016a).

Like HS, cold stress constitutes a harmful situation as an important yield-limiting factor. Under low temperatures, plants suffer changes at the biochemical and physiological levels, leading to transcriptional modifications, cellular dysfunction, changes in the membrane composition and fluidity, metabolic imbalance, and changes in enzyme activity (Manasa et al., 2022). Plant acclimation and adaptation to cold conditions implies a profound reorganization of transcriptome, metabolome, and proteome. In *Brassica juncea*, low-temperature stress led to important differences in the nitrosoproteome, which can be related to cold stress-induced photosynthetic inhibition (Abat and Deswal, 2009). In this context, previous research showed modulation of cold-responsive proteins by *S*-nitrosylation as an important cue to attenuate stress, focusing on the regulation of nuclear trafficking to control cellular metabolism and redox status (Sehrawat et al., 2019). Furthermore, it has been recently described a rise in the *S*-nitrosylation level by brassinosteroids under low-temperature conditions in mini-Chinese cabbage seedlings to ameliorate plant damage (Gao et al., 2022). Furthermore, NO acts downstream of H_2O_2 and cooperates with JAs in freeze tolerance (Liu et al., 2019). In *Pisum sativum*, an increase in both *S*-nitrosylation and Tyr nitration has been detected during cold stress situations (Corpas et al., 2008; Airaki et al., 2012), highlighting the central role of PTMs during its perception and response. Both *S*-nitrosylation and Tyr nitration play a role during cold stress responses, controlling photosynthetic, metabolic, defense, and signaling-related proteins that lead to adaptive responses, highlighting HSPs, GST, DHAR, RuBisCO, GAPDH, and SAHH1/HOG1 (Sehrawat et al., 2013; Puyaubert et al., 2014b). These results point to a possible crosstalk between different redox PTMs during stress adaptation, involving genetic and metabolic reprogramming. Overall, results derived from these studies show how PTMs, and especially those triggered by RONS, are crucial for the perception and response to stressful situations related to drastic temperature alterations.

Mechanical wounding

From all the stress a plant faces, injury is one of the most common; it can be caused by (a)biotic factors such as rain, wind, herbivores, and insects. It offers an easy way of entry for opportunistic pathogens through the open wounds. The defenses activated by mechanical injury (wounding) are like the ones activated by herbivores and insects (Reymond et al., 2000; Arimura et al., 2005; Rehrig et al., 2014); thus, they can mimic a biotic stress-like trait.

In response to pathogens and wounding, the emerging signaling molecules in plant immunity activation are ROS (Mittler et al., 2011; Suzuki and Mittler, 2012). When an injury occurs, the immediate region is the first to react. Among the changes that take place in the plant are alterations in the Ca^{2+} concentration in the plasma, the synthesis of secondary messengers, RONS, and a sharp increase in the levels of fight hormones such as JA and ABA (Mostafa et al., 2022). A cell-to-cell process allows Ca^{2+} and ROS to go through the xylem, parenchyma, and phloem tissues to reach the undamaged areas of the plant (Farmer and Ryan, 1992). A feedback loop between NO and ROS has been shown to exist, and ROS/NO balance is a crucial factor in determining how cells respond to abiotic stress caused by antioxidant defenses and ROS generation. Direct NO-dependent protein regulation is the subject of another area of study, particularly through the main NO-PTMs such as *S*-nitrosylation and protein nitration (Figure 2) (Neill et al., 2003; Neill et al., 2007; Astier et al., 2012). The NO_2-Tyr levels in sunflower hypocotyl cells have been shown to rise following mechanical damage (Chaki et al., 2010). The authors suggested that the damage resulted in a buildup of GSNO under oxidative stress. The process of tyrosine nitration brought on by $ONOO^-$ production may be mediated by *S*-nitrosothiols (SNOs). This is most likely caused by the fact that in the presence of oxygen (O_2), GSNO degrades to the subsequent radicals, glutathione (GS) and $ONOO^-$, which are responsible for the observed rise in protein tyrosine nitration levels. In conclusion, sunflower seedlings are subjected to nitrosative stress, and SNO may act as a unique injury signal in plants (Chaki et al., 2010).

Extrafascicular phloem (EFP) is a defensive structure against herbivorous animals developed by cucurbits. Mechanical leaf wounding induces a systemic wound response through the tight regulation of RONS signaling. Quickly after the injury, the activities of key antioxidant enzymes like dehydroascorbate reductase (DHAR), glutathione reductase (GR), and ascorbate peroxidase (APX) decreased together with ascorbate and glutathione content. Opposite behavior on NO-PTMs was observed with a decrease in protein *S*-nitrosylation and an increase in protein tyrosine nitration over time. Collectively, the accumulation of ROS within the EFP leads to a change in RONS composition from NO to its more nitrating species including $ONOO^-$ and NO_2 curving the stress dynamics and the redox status after mechanical wounding (Gaupels et al., 2016). Another study performed in sea rockets (*Cakile maritima* L.) pinched with striped-tip forceps showed a differential modulation in the damaged hypocotyls and unwounded organs. Wounded hypocotyls exhibited an active RONS metabolism with increased protein nitration in green cotyledons causing long-distance signals that could elicit responses in unwounded tissues. These data, therefore, confirm the existence of local and long-distance responses that counteract negative effects and provide appropriate responses, enabling the wounded seedlings to survive (Houmani et al., 2018).

Other studies in tomato plants have shown that NO may have a role in downregulating the expression of wound-inducible genes during pathogenesis (Orozco-Cárdenas and Ryan, 2002). To activate wound signaling, tomato plants respond to injury and elicitors by accumulating high amounts of H_2O_2, and it has been suggested that NO may function as an antioxidant, preventing ROS

damage to plant cells and tissues (Lin et al., 2011). Closely related, mechanical wounding enhances freezing tolerance in untreated systemic leaves of wheat plants through the accumulation of NO and H_2O_2 and further modifications in the photosystem and antioxidant system (Si et al., 2017). Also, after injuring potato leaflets, a NO burst takes place, which is required to start the healing process (París et al., 2007). Overall, RONS are key molecules in mediating the response of the plant to mechanical injuries.

Heavy metals

The definition of heavy metals (HMs) was established by Hawkers in 1997 as the group of metals and metalloids with an atomic density greater than 4 g/cm^3, or five times or more than that of water (Hawkes, 1997). However, their chemical properties make HMs both indispensable and toxic, even at low concentrations, for plants (Duruibe et al., 2007; Zitka et al., 2013). HMs are classified as essentials and nonessentials. Essential HMs, like Cu, Fe, Mn, Co, Zn, or Ni, are required for fundamental biological processes as they serve, for instance, as enzyme cofactors, whereas nonessential HMs, such as Cd, Pb, Hg, Cr, and Al, are not required by plants for their metabolic processes (Zitka et al., 2013; Raychaudhuri et al., 2021).

HMs have been considered major environmental pollutants altering plant metabolism, growth, and biomass production (Nagajyoti et al., 2010) and essential HMs are even toxic at excessive concentrations (Rascio and Navari-Izzo, 2011; Hossain et al., 2012). Those elements negatively affect plant molecular physiology and biochemistry by generating several stresses including oxidative and nitrosative ones (Hoque et al., 2021). The major risk of HM poisoning is the enhanced production of ROS (Figure 2), as they usually interfere with natural ROS metabolism and homeostasis, exposing cells to oxidative stress (Nagajyoti et al., 2010; Zitka et al., 2013; Zandi and Schnug, 2022). With this aim, numerous studies have demonstrated a relationship between ROS-scavenging systems and HMs in different plant species such as *Colobanthus quitensis* (Contreras et al., 2018), *Vaccinium myrtillus* L. (Kandziora-Ciupa et al., 2013), and *Pteris vittate*, which is considered an HM-resistant plant (Srivastava et al., 2005). Furthermore, RNS metabolism has also been defined as a mechanism of response against HMs, where NO has shown a protective effect under HMs throughout protein *S*-nitrosylation (Figure 2), as previously reviewed (Gill et al., 2013; Romero-Puertas et al., 2013; Saxena and Shekhawat, 2013). There is also an overproduction of $ONOO^-$ in Arabidopsis root peroxisomes (Corpas and Barroso, 2014) and an alteration of the protein tyrosine nitration profile under HMs (Feigl et al., 2016; Kolbert et al., 2018) or its derivatives such as arsenate (Leterrier et al., 2012) or indium (Zhao et al., 2022). The response to HMs is usually linked to RONS production and antioxidant system modulation. For example, the presence of Cd in wheat has shown that NO can significantly increase plant resistance by reducing ROS accumulation as well as increasing the antioxidant defense system and nutrient assimilation (Kaya et al., 2020), therefore reinforcing the role of NO in alleviating abiotic stress. In the case of Zn, an interplay between H_2O_2 and *S*-nitrosothiol signaling has been described in Arabidopsis plants, throughout the inactivation of GSNO reductase by Zn-induced H_2O_2 (Kolbert et al., 2019).

Furthermore, the protective role of NO in Cd toxicity has been related to the reduction of lipid peroxidation and the inhibition of H_2O_2 accumulation at a molecular level in barley, where SNP application significantly reduced Cd growth inhibitory effects by the improvement in chlorophyll content, regulating the activity of antioxidant enzymes and causing a decrease in lipid peroxidation and MDA content (Alp et al., 2022). In addition, as NO is tightly associated with phytohormone signaling, some studies have been aimed to understand how the interaction between NO and phytohormones is altered during HM stress and tolerance (Asgher et al., 2017; Demecsová and Tamás, 2019; Pande et al., 2022). In this context, NO has been shown to reduce Al accumulation in the root apices of wheat regulating the hormonal equilibrium of gibberellins and auxin, enhancing plant tolerance to Al stress (He et al., 2012). There is a complex NO-auxin crosstalk involved in HM stress, where long-term Cu^{2+} exposure causes an increase in NO production and a repression of auxin by inhibiting PIN1-mediated auxin transport-dependent gene expression in Arabidopsis root tips (Kolbert et al., 2012). In the case of *Medicago truncatula*, NO supplementation improves Cd stress tolerance by reducing the activity of IAA oxidase to maintain auxin equilibrium (Xu et al., 2010). Something similar happens in tomato roots during Cd stress, where the addition of IAA with Cd upregulates components of the AsA-GSH cycle for balancing ROS (Khan et al., 2019).

Thus, a clear relationship between RONS metabolism as a defense mechanism against HMs toxicity has been reported. Several studies carried out in plants have demonstrated the impact of potentially toxic HMs on the homeostasis of ROS-scavenging systems and the protective effects of NO under HM stress.

Hypoxia

Plants, as aerobic organisms, rely on oxygen for their respiration and mitochondrial energy generation. However, different developmental and environmental conditions can lead to decreased O_2 levels (Weits et al., 2021) such as soil waterlogging and submergence (caused by excessive rain) or pathogen infection. As a result, plants face hypoxia stress when partial O_2 deficiency (usually between 1% and 5% O_2) limits aerobic respiration, while anoxia takes place in total O_2 depletion (Sasidharan et al., 2017). This situation leads to stress-related effects such as lack of energy, saturated electron transfer chain, or high levels of reducing equivalents, thus constraining growth and crop productivity (reviewed in Jethva et al., 2022).

To survive during environmentally low O_2 conditions, plants have developed several morphological and physiological mechanisms of adaptation (Kende et al., 1998; Drew et al., 2000). O_2 deficiency significantly decreases ATP content due to restrictions on aerobic metabolism (Bailey-Serres and Voesenek, 2008). As a result, plants need to re-route their energy metabolism to guarantee survival, leading to cell acidification and the

accumulation of RONS like NO, which potentially lead to cell damage when their production exceeds threshold levels (Hebelstrup and Møller, 2015; Turkan, 2018). However, under moderate concentrations, these factors act as key signaling molecules involved in stress adaptation responses through transcriptional regulation, enzyme activity, and secondary messengers that help maintain cellular homeostasis (Gaupels et al., 2011; Mengel et al., 2013; Lamotte et al., 2015).

Although RONS are involved in many processes aimed to get a fine-tuned response to hypoxia, we have focused on key PTMs triggered by NO (Manrique-Gil et al., 2021) (Figure 2). *S*-nitrosylated proteins potentially implicated in flooding signaling and adaptation include ACONITASE (Gupta et al., 2012), CYTOCHROME C OXIDASE (COX) (Millar and Day, 1996), PHYTOGLOBIN 1 (PGB1) (Perazzolli et al., 2004), membrane-bound NADPH oxidases (RBOHs) (Yun et al., 2011), and GSNO REDUCTASE 1 (GSNOR1) (Zhan et al., 2018).

Under hypoxia, inhibition of ACONITASE by *S*-nitrosylation leads to the accumulation of several metabolic intermediates such as citrate, which induces *ALTERNATIVE OXIDASE 1A* (*AOX1A*) expression and increases its activity in Arabidopsis (Gupta et al., 2012). NO is an inducer for AOX (Royo et al., 2015), but a NO burst may inhibit COX activity (Millar and Day, 1996; Brown, 2001). This altered bioactivity of AOX and COX suggests that NO plays a role in plant mitochondrial respiration under hypoxic conditions (reviewed in Sasidharan et al., 2018). In this context, *AOX* induction can promote anaerobic ATP synthesis, which increases energy efficiency as an adaptive response to hypoxia (Millar and Day, 1996; Vishwakarma et al., 2018). This suggests that AOX overexpression in crops could be a target in breeding programs aimed at flooding and waterlogging tolerance. In addition, redox mechanisms are also involved in the post-translational regulation of AOX activity by the formation of a thiohemiacetal at CysI with 2-oxo acids (Gupta et al., 2009; Selinski et al., 2017; Selinski et al., 2018). Under normoxia, AOX limits uncontrolled ROS production by preventing over-reduction of the electron transport chain (reviewed in Selinski et al., 2018). However, under hypoxic conditions, AOX limits superoxide generation and increases NO production, thus preventing nitro-oxidative stress during re-oxygenation (Vishwakarma et al., 2018; Jayawardhane et al., 2020). In 2018, Vishwakarma and colleagues concluded that *AOX* has a distinct role depending on the O_2 availability since AOX can produce NO under hypoxia whereas it scavenges NO in normoxic conditions.

Another crucial strategy of adaptation under hypoxia relies on the phytoglobin/NO cycle, in which phytoglobins (PGBs) modulate $NAD(P)^+$ and nitrate regeneration under hypoxia, which, in turn, fuels glycolysis and ATP production (Perazzolli et al., 2004; Igamberdiev et al., 2005; Gupta and Igamberdiev, 2016). This cycle helps to retain the energy status of the plant through NO scavenging by PGB1 *via* *S*-nitrosylation (Perazzolli et al., 2004; Rubio et al., 2019), metal nitrosylation (Perazzolli et al., 2004), and Tyr nitration (Sainz et al., 2015).

RBOHs are key proteins involved in plant responses to hypoxia by modulating ROS signaling (Rajhi et al., 2011; Pucciariello et al., 2012; Yeung et al., 2018). In several species, RBOH-mediated ROS accumulation in the root cortical cells leads to programmed cell death and thus to the generation of flooding-induced aerenchyma tissue (Rajhi et al., 2011; Yamauchi et al., 2014; Yamauchi et al., 2017). The impact of RBOH in ROS production is tightly regulated *via* several PTMs, including NO-mediated *S*-nitrosylation (Yun et al., 2011). Yun et al. studied the NO and reactive oxygen intermediaries' (ROIs') involvement in hypersensitive response (HR) during microbial infection. Their results show that *S*-nitrosylation of AtRBOHD at Cys 890 reduces its activity, limiting the cell death caused by stress-induced oxidative bursts.

NO signaling is also linked to autophagy in the hypoxic response in Arabidopsis since *S*-nitrosylation of GSNOR1 at Cys 10 induces conformational changes that lead to its selective degradation in the autophagosome (Zhan et al., 2018). NO can also react with O_2^-, producing $ONOO^-$ and reducing H_2O_2 generation, which might avoid cell death (Chen et al., 2009).

NO-related PTMs are thought to be involved in hyponastic leaf movement (Hebelstrup et al., 2012) and aerenchyma generation (Wany et al., 2017), both ethylene-mediated flood-adaptive traits (reviewed in Sasidharan et al., 2021). Regarding aerenchyma formation, Wany, Kumari, and Gupta demonstrated that not only ethylene, but also hypoxia-induced NO plays an important role in root cortical cell death. It has been reported that NO modulates ROS production, lipid peroxidation, and tyrosine nitration, but its mechanistic role in aerenchyma generation is still unknown. However, the observation of a nitrosylated 63-kDa protein suggests that $ONOO^-$ and changes in protein activity may be involved. NO is also important for these ethylene-mediated adaptive responses since it can activate ethylene biosynthesis, potentially by *S*-nitrosylation of key enzymes such as ACC synthase and oxidase (Li et al., 2016).

UV radiation

Plants and algae produce organic matter from CO_2 and water using light energy in a process called photosynthesis, which takes place in the chloroplasts. However, light is one of the major stress factors resulting in ROS generation in chloroplasts that produces photo-oxidative damage, the inhibition of photosynthesis, and cell death (Li et al., 2009; Shi et al., 2022). Light information is perceived by both chloroplasts, where photosynthesis takes place, and photoreceptors, which act in response to light initiating a signaling process (Li et al., 2009).

UV-B (280-315 nm) is a minor component of sunlight that is receiving special interest from researchers as it is increasing because of stratospheric ozone reduction (Caldwell et al., 2003). As happens in several stress responses, hormones act downstream of the UV-B signaling pathway (Vanhaelewyn et al., 2016). In response to UV-B, the production of ROS increases, with multiple sources responsible for this production (Mackerness et al., 2001). This increase in ROS levels leads to the production of hormones such as salicylic acid, ethylene, and JA, which play a role in response to multiple stress conditions (Reymond and Farmer, 1998). UV resistance locus8 (*UVR8*) is a photoreceptor (Kliebenstein et al., 2002) that localizes as a dimer in the cytoplasm and, in the presence of UV-B,

accumulates as monomers in the nucleus where it interacts with the multifunctional E3 ubiquitin ligase CONSTITUTIVELY PHOTOMORPHOGENIC (COP1), abolishing its function and, as a consequence, causing the accumulation of its targets such as *ELONGATED HYPOCOTYL5* [*HY5*, a basic leucine zipper (bZIP) TF] and *HY5 HOMOLOG* (*HYH*) (Kaiserli and Jenkins, 2007; Brown and Jenkins, 2008; Favory et al., 2009). Both HY5 and HYH play an antagonistic role to PHYTOCHROME INTERACTING FACTOR1 (PIF1) and PIF3 in regulating cell death and photooxidative response (Chen et al., 2013; Vanhaelewyn et al., 2016). In parallel, NO levels increase in response to UV-B in plants (Mackerness et al., 2001; Zhang et al., 2003) and it acts as an important factor in protecting plants against UV-B effects. It has been reported that when plants with a decrease of endogenous NO are exposed to UV-B radiation, damaged symptoms are enhanced (Cassia et al., 2019). The perception of UV-B by UVR8 leads to an increase in these NO levels regulating the stomatal closure, protecting the microtubules organization, scavenging ROS, and upregulating *HY5* (Krasylenko et al., 2012; Tossi et al., 2014; Li et al., 2022). Moreover, UV-B light response includes a crosstalk among H_2O_2 (produced by AtRBOHD and AtRBOHF), NO, and UVR8 (He et al., 2013; Wu et al., 2016). However, the precise role of NO in this relationship among them has not been studied yet, opening the possibility of a post-translational regulation of some of the key proteins in UV-B response by NO.

Ozone

Tropospheric ozone (O_3) is considered a major phytotoxic air pollutant that causes detrimental effects in ecosystems and agricultural systems worldwide (Ainsworth et al., 2012; Tai et al., 2021; Wu et al., 2022), and it is formed through the action of light-driven chemical reactions involving nitrogen oxides (NOx) and volatile organic compounds. Ozone is a powerful oxidizing agent that accesses plants *via* stomata and breaks into ROS in the apoplast (Ainsworth, 2017; Waszczak et al., 2018). High levels of O_3 in plants induce decreases in photosynthesis and stomatal conductance rates, photosynthetic proteins, and pigments (Brosché et al., 2010; Kontunen-Soppela et al., 2010; Ainsworth, 2017; Nanni et al., 2022), chloroplast development (Nagatoshi et al., 2016), and cell death (Overmyer et al., 2005; Horak et al., 2016; Sierla et al., 2018). Transcriptional reprogramming in O_3-affected plants has been identified in several species (revised in Morales et al., 2021), and the TF families studied include the *Ethylene Response Factors* (*ERF*), *TGA*, *WRKY* (Xu et al., 2015; Hoang et al., 2017; Morales et al., 2021), and *cysteine-rich receptor-like kinases* (*CRKs*) encoding regulators of hormone signaling (Wrzaczek et al., 2010). Furthermore, the mechanisms of plant responses to O_3 have been linked to the function of the mitogen-activated protein kinase 12 (MAPK12) and the transcription reprogramming of the plants. Among them, the TF GOLDEN2-LIKE (GLK1 and GLK2) was related to the O_3 tolerance of plants through the regulation of stomatal movement (Fiscus et al., 2005; Puckette et al., 2008; Brosché et al., 2010; Nagatoshi et al., 2016; Mills et al., 2018) and the WKRY and MYB families of TFs with the control of anthocyanin and proanthocyanidin biosynthesis (Duan et al., 2018; Zhang et al., 2022). Moreover, it has been shown that O_3 stimulates the production of NO (Ederli et al., 2006; Ahlfors et al., 2009; Kabange et al., 2022), probably by the action of the nitrate reductase (NR) (Xu et al., 2012). NO induced by ozone will contribute to the generation of ROS and different signaling pathways in plants (Hasan et al., 2021; Mukherjee, 2022), possibly altering NO-ROS balancing or the plant hormonal homeostasis (Ahlfors et al., 2009). The mechanisms of NO regulation induced by O_3 were studied through the proteome analysis in poplar leaves. High levels of O_3 induced changes in total nitrite and *S*-nitrosothiol contents and affected the *S*-nitrosylated status of proteins (Figure 2) (Vanzo et al., 2014). Hence, key proteins related to the phenylpropanoid pathway (PAL2), photosynthetic activity (Chlorophyll a/b binding proteins), and cell wall composition (alpha-N-arabinofuranosidase) were significantly de-nitrosylated after ozone exposure, while others were putative targets of *S*-nitrosylation, such as the Ribulose-phosphate 3-epimerase, the Peroxiredoxin 5, and the Tubulin alpha-chain (revised in Vanzo et al., 2014).

In conclusion, the mechanisms of plant responses to high O_3 are complex and far from being completely understood. The exposure of plants to O_3 will promote different molecular and physiological responses related to ROS and NO that will vary according to the plant sensitivity to this pollutant, with broad implications on plant defense mechanisms that will be critical for their adaptation to a constantly changing environment.

Conclusions and future perspectives

Plant welfare and crop yield are continuously influenced by environmental factors, pests, or nutrient availability in the soil. Abiotic stresses hamper plant fitness by impacting the morphology, biochemistry, and physiology, which are tightly connected to the growth and yield of the plant. Nitro-oxidative stress is a common feature underlying abiotic stresses. The ROS and RNS produced can transduce their bioactivity through the post-translational modification of biomolecules, therefore modulating the molecular mechanisms involved in the redox control of plant processes. Although many nitrated and *S*-nitrosylated proteins have been identified, new protein modifications mediated by nitro-fatty acids or nucleic acids—including nitroalkylation or *S*-guanylation—have been scarcely explored during abiotic stress. In this context, more research is needed to better comprehend the biological implications of these NO-modified biomolecules into the redox regulation of abiotic stresses. The data provided here expand our understanding of how NO and NO-related molecules, through the post-translational modification of biomolecules, can modulate the redox fitness, therefore providing the biological framework for future research to improve plant tolerance to abiotic stress.

Author contributions

All authors contributed equally to the conceptualization, writing of the original draft, review and editing. OL is responsible for supervision and funding acquisition.

Funding

This work was financed by grants PID2020-119731RB-I00 from the Ministerio de Ciencia e Innovación (MCIN/AEI), SA137P20 from Junta de Castilla y León and Escalera de Excelencia CLU-2018-04 co-funded by the P.O. FEDER of Castilla y León 2014–2020 Spain (to OL). SG-J is supported by FPU grant. CO is supported by the USAL4EXCELLENCE program from Universidad de Salamanca and CSO is supported by a PhD program in foreign countries from the Argelian government.

Acknowledgments

We thank the BIO2015-68957-REDT and RED2018-102397-T Spanish network for stimulating discussions.

Conflict of interest

The authors declare that the research was conducted in the absence of any commercial or financial relationships that could be construed as a potential conflict of interest.

Publisher's note

References

Abat, J. K., and Deswal, R. (2009). Differential modulation of s-nitrosoproteome of brassica juncea by low temperature: change in s-nitrosylation of rubisco is responsible for the inactivation of its carboxylase activity. *Proteomics* 9, 4368–4380. doi: 10.1002/pmic.200800985

Ahlfors, R., Brosché, M., Kollist, H., and Kangasjärvi, J. (2009). Nitric oxide modulates ozone-induced cell death, hormone biosynthesis and gene expression in arabidopsis thaliana. *Plant J.* 58, 1–12. doi: 10.1111/j.1365-313X.2008.03756.x

Ainsworth, E. A. (2017). Understanding and improving global crop response to ozone pollution. *Plant J.* 90, 886–897. doi: 10.1111/tpj.13298

Ainsworth, E. A., Yendrek, C. R., Sitch, S., Collins, W. J., and Emberson, L. D. (2012). The effects of tropospheric ozone on net primary productivity and implications for climate change. *Annu. Rev. Plant Biol.* 63, 637–661. doi: 10.1146/annurev-arplant-042110-103829

Airaki, M., Leterrier, M., Mateos, R. M., Valderrama, R., Chaki, M., Barroso, J. B., et al. (2012). Metabolism of reactive oxygen species and reactive nitrogen species in pepper (Capsicum annuum l.) plants under low temperature stress. *Plant Cell Environ.* 35, 281–295. doi: 10.1111/j.1365-3040.2011.02310.x

Akaike, T., Okamoto, S., Sawa, T., Yoshitake, J., Tamura, F., Ichimori, K., et al. (2003). 8-nitroguanosine formation in viral pneumonia and its implication for pathogenesis. *Proc. Natl. Acad. Sci. U. S. A.* 100, 685–690. doi: 10.1073/pnas.0235623100

Albertos, P., Romero-Puertas, M. C., Tatematsu, K., Mateos, I., Sánchez-Vicente, I., Nambara, E., et al. (2015). S-nitrosylation triggers ABI5 degradation to promote seed germination and seedling growth. *Nat. Commun.* 6, 1–10. doi: 10.1038/ncomms9669

Alché, J. D. D. (2019). A concise appraisal of lipid oxidation and lipoxidation in higher plants. *Redox Biol.* 23, 101136. doi: 10.1016/j.redox.2019.101136

Alp, K., Terzi, H., and Yildiz, M. (2022). Proteomic and physiological analyses to elucidate nitric oxide-mediated adaptive responses of barley under cadmium stress. *Physiol. Mol. Biol. Plants* 28, 1467–1476. doi: 10.1007/s12298-022-01214-3

Apel, K., and Hirt, H. (2004). Reactive oxygen species: metabolism, oxidative stress and signal transduction. *Annu. Rev. Plant Biol.* 55, 373–399. doi: 10.1146/annurev.arplant.55.031903.141701

Aranda-Caño, L., Sánchez-Calvo, B., Begara-Morales, J. C., Chaki, M., Mata-Pérez, C., Padilla, M. N., et al. (2019). Post-translational modification of proteins mediated by nitro-fatty acids in plants: nitroalkylation. *Plants (basel)* 8 (4), 82. doi: 10.3390/plants8040082

Aranda-Caño, L., Valderrama, R., Pedrajas, J. R., Begara-Morales, J. C., Chaki, M., Padilla, M. N., et al. (2022). Nitro-oleic acid-mediated nitroalkylation modulates the antioxidant function of cytosolic peroxiredoxin Tsa1 during heat stress in saccharomyces cerevisiae. *Antioxidants* 11, 972. doi: 10.3390/antiox11050972

Arimura, G. I., Kost, C., and Boland, W. (2005). Herbivore-induced, indirect plant defences. *Biochim. Et Biophys. Acta (BBA) - Mol. Cell Biol. Lipids* 1734 (2), 91–111. doi: 10.1016/j.bbalip.2005.03.001

Arruebarrena Di Palma, A., Di Fino, L. M., Salvatore, S. R., D'Ambrosio, J. M., Garćia-Mata, C., Schopfer, F. J., et al. (2020). Nitro-oleic acid triggers ROS production *via* NADPH oxidase activation in plants: A pharmacological approach. *J. Plant Physiol.* 246-247, 153128. doi: 10.1016/j.jplph.2020.153128

Asgher, M., Per, T. S., Masood, A., Fatma, M., Freschi, L., Corpas, F. J., et al. (2017). Nitric oxide signaling and its crosstalk with other plant growth regulators in plant responses to abiotic stress. *Environ. Sci. pollut. Res.* 24, 2273–2285. doi: 10.1007/s11356-016-7947-8

Astier, J., Kulik, A., Koen, E., Besson-Bard, A., Bourque, S., Jeandroz, S., et al. (2012). Protein s-nitrosylation: What's going on in plants? *Free Radic. Biol. Med.* 53, 1101–1110. doi: 10.1016/j.freeradbiomed.2012.06.032

Astier, J., Rasul, S., Koen, E., Manzoor, H., Besson-Bard, A., Lamotte, O., et al. (2011). S-nitrosylation: An emerging post-translational protein modification in plants. *Plant Sci.* 181, 527–533. doi: 10.1016/j.plantsci.2011.02.011

Babbar, R., Karpinska, B., Grover, A., and Foyer, C. H. (2021). Heat-induced oxidation of the nuclei and cytosol. *Front. Plant Sci.* 11. doi: 10.3389/fpls.2020.617779

Bailey-Serres, J., and Voesenek, L. A. C. J. (2008). Flooding stress: Acclimations and genetic diversity. *Annu. Rev. Plant Biol.* 59, 313–339. doi: 10.1146/annurev.arplant.59.032607.092752

Baker, L. M., Baker, P. R., Golin-Bisello, F., Schopfer, F. J., Fink, M., Woodcock, S. R., et al. (2007). Nitro-fatty acid reaction with glutathione and cysteine. kinetic analysis of thiol alkylation by a Michael addition reaction. *J. Biol. Chem.* 282, 31085–31093. doi: 10.1074/jbc.M704085200

Begara-Morales, J. C., Chaki, M., Valderrama, R., Sanchez-Calvo, B., Mata-Perez, C., Padilla, M. N., et al. (2018). Nitric oxide buffering and conditional nitric oxide release in stress response. *J. Exp. Bot.* 69, 3425–3438. doi: 10.1093/jxb/ery072

Begara-Morales, J. C., Sánchez-Calvo, B., Chaki, M., Valderrama, R., Mata-Pérez, C., López-Jaramillo, J., et al. (2014). Dual regulation of cytosolic ascorbate peroxidase (APX) by tyrosine nitration and s-nitrosylation. *J. Exp. Bot.* 65:2, 527–538. doi: 10.1093/jxb/ert396

Bolwell, G. P., and Wojtaszek, P. (1997). Mechanisms for the generation of reactive oxygen species in plant defence–a broad perspective. *Physiol. Mol. Plant Pathol.* 51, 347–366. doi: 10.1006/pmpp.1997.0129

Brosché, M., Merilo, E., Mayer, F., Pechter, P., Puz~orjova, I., Brader, G., et al. (2010). Natural variation in ozone sensitivity among arabidopsis thaliana accessions and its relation to stomatal conductance. *Plant Cell Environ.* 33, 914–925. doi: 10.1111/j.1365-3040.2010.02116.x

Brown, G. C. (2001). Regulation of mitochondrial respiration by nitric oxide inhibition of cytochrome c oxidase. *Biochim. Biophys. Acta BBA - Bioenerg.* 1504, 46–57. doi: 10.1016/S0005-2728(00)00238-3

Brown, B. A., and Jenkins, G. I. (2008). UV-B signaling pathways with different fluence-rate response profiles are distinguished in mature arabidopsis leaf tissue by requirement for UVR8, HY5 and HYH. *Plant Physiol.* 146:2, 576–588. doi: 10.1104/pp.107.108456

Cai, W., Liu, W., Wang, W. S., Fu, Z. W., Han, T. T., and Lu, Y. T. (2015). Overexpression of rat neurons nitric oxide synthase in rice enhances drought and salt tolerance. *PloS One* 10 (6), e0131599. doi: 10.1371/journal.pone.0131599

Caldwell, M. M., Ballaré, C. L., Bornman, J. F., Flint, S. D., Björn, L. O., Teramura, A. H., et al. (2003). Terrestrial ecosystems, increased solar ultraviolet radiation and interactions with other climatic change factors. *Photochem. Photobiol. Sci.* 2:1, 29–38. doi: 10.1039/b211159b

Camejo, D., del Carmen Romero-Puertas, M., Rodríguez-Serrano, M., Sandalio, L. M., Lázaro, J. J., Jiménez, A., et al. (2013). Salinity-induced changes in s-nitrosylation of pea mitochondrial proteins. *J. Proteomics* 79, 87–99. doi: 10.1016/j.jprot.2012.12.003

Camejo, D., Ortiz-Espín, A., Lázaro, J. J., Romero-Puertas, M. C., Lázaro-Payo, A., Sevilla, F., et al. (2015). Functional and structural changes in plant mitochondrial PrxII f caused by NO. *J. Proteomics* 119, 112–125. doi: 10.1016/j.jprot.2015.01.022

Cassia, R., Amenta, M., Fernández, M. B., Nocioni, M., and Dávila, V. (2019). "The role of nitric oxide in the antioxidant defense of plants exposed to UV-b radiation," in *Reactive oxygen, nitrogen and sulfur species in plants: production, metabolism, signaling and defense mechanisms*, 555–572. doi: 10.1002/9781119468677.ch22

Castillo, M., Lozano-Juste, J., González-Guzmán, M., Rodriguez, L., Rodriguez, P. L., and León, J. (2015). Inactivation of PYR/PYL/RCAR ABA receptors by tyrosine nitration may enable rapid inhibition of ABA signaling by nitric oxide in plants. *Sci. Signaling* 8, ra89. doi: 10.1126/scisignal.aaa7981

Chaki, M., Carreras, A., López-Jaramillo, J., Begara-Morales, J. C., Sánchez-Calvo, B., Valderrama, R., et al. (2013). Tyrosine nitration provokes inhibition of sunflower carbonic anhydrase (β-CA) activity under high temperature stress. *Nitric. Oxide* 29, 30–33. doi: 10.1016/j.niox.2012.12.003

Chaki, M., Valderrama, R., Fernández-Ocaña, A. M., Carreras, A., Gómez-Rodríguez, M. V., López-Jaramillo, J., et al. (2011). High temperature triggers the metabolism of s-nitrosothiols in sunflower mediating a process of nitrosative stress which provokes the inhibition of ferredoxin-NADP reductase by tyrosine nitration. *Plant Cell Environ.* 34, 1803–1818. doi: 10.1111/j.1365-3040.2011.02376.x

Chaki, M., Valderrama, R., Fernández-Ocaña, A. M., Carreras, A., Gómez-Rodríguez, M. V., Pedrajas, J. R., et al. (2010). Mechanical wounding induces a nitrosative stress by down-regulation of GSNO reductase and an increase in s-nitrosothiols in sunflower (Helianthus annuus) seedlings. *J. Exp. Bot.* 62:6, 1803–1813. doi: 10.1093/jxb/erq358

Chen, K., Chen, L., Fan, J., and Fu, J. (2013). Alleviation of heat damage to photosystem II by nitric oxide in tall fescue. *Photosynth. Res.* 116, 21–31. doi: 10.1007/s11120-013-9883-5

Chen, R., Sun, S., Wang, C., Li, Y., Liang, Y., An, F., et al. (2009). The arabidopsis PARAQUAT RESISTANT2 gene encodes an s-nitrosoglutathione reductase that is a key regulator of cell death. *Cell Res.* 19, 1377–1387. doi: 10.1038/cr.2009.117

Clark, D., Durner, J., Navarre, D. A., and Klessig, D. F. (2000). Nitric oxide inhibition of tobacco catalase and ascorbate peroxidase. *Mol. Plant Microbe Interact.* 13 (12), 1380–1384. doi: 10.1094/MPMI.2000.13.12.1380

Contreras, R. A., Pizarro, M., Köhler, H., Sáez, C. A., and Zúñiga, G. E. (2018). Copper stress induces antioxidant responses and accumulation of sugars and phytochelatins in Antarctic colobanthus quitensis (Kunth) bartl. *Biol. Res.* 51, 48. doi: 10.1186/S40659-018-0197-0

Corpas, F. J., and Barroso, J. B. (2014). Peroxynitrite (ONOO–) is endogenously produced in arabidopsis peroxisomes and is overproduced under cadmium stress. *Ann. Bot.* 113, 87–96. doi: 10.1093/AOB/MCT260

Corpas, F. J., Chaki, M., Fernández-Ocaña, A., Valderrama, R., Palma, J. M., Carreras, A., et al. (2008). Metabolism of reactive nitrogen species in pea plants under abiotic stress conditions. *Plant Cell Physiol.* 49, 1711–1722. doi: 10.1093/pcp/pcn144

David, A., Yadav, S., Baluška, F., and Bhatla, S. C. (2015). Nitric oxide accumulation and protein tyrosine nitration as a rapid and long distance signalling response to salt stress in sunflower seedlings. *Nitric. Oxide* 50, 28–37. doi: 10.1016/j.niox.2015.08.003

del Río, L. A. (2015).). ROS and RNS in plant physiology: an overview. *J. Exp. Bot.* 66, 2827–2837. doi: 10.1093/jxb/erv099

Demecsová, L. , and Tamás, L. (2019). Reactive oxygen species, auxin and nitric oxide in metal-stressed roots: toxicity or defence. *BioMetals* 32(5): 717–744. doi: 10.1007/S10534-019-00214-3

Dietz, K. J. (2008). Redox signal integration: from stimulus to networks and genes. *Physiol. Plant* 133, 459–468. doi: 10.1111/j.1399-3054.2008.01120.x

Di Fino, L. M., Cerrudo, I., Salvatore, S. R., Schopfer, F. J., García-Mata, C., and Laxalt, A. M. (2020). Exogenous nitro-oleic acid treatment inhibits primary root growth by reducing the mitosis in the meristem in arabidopsis thaliana. *Front. Plant Sci.* 11. doi: 10.3389/fpls.2020.01059

Domingos, P., Prado, A. M., Wong, A., Gehring, C., and Feijo, J. A. (2015). Nitric oxide: A multitasked signaling gas in plants. *Mol. Plant* 8, 506–520. doi: 10.1016/j.molp.2014.12.010

Drew, M. C., He, C.-J., and Morgan, P. W. (2000). Programmed cell death and aerenchyma formation in roots. *Trends Plant Sci.* 5, 123–127. doi: 10.1016/S1360-1385(00)01570-3

Duan, S. W., Wang, J. J., Gao, C. H., Jin, C. Y., Li, D., Peng, D. S., et al. (2018). Functional characterization of a heterologously expressed brassica napus WRKY41-1 transcription factor in regulating anthocyanin biosynthesis in arabidopsis thaliana. *Plant Sci.* 268, 47–53. doi: 10.1016/j.plantsci.2017.12.010

Duruibe, J., Ogwuegbu, M., and Egwurugwu, J. (2007). Heavy metal pollution and human biotoxic effects. *Int. J. Phys. Sci.* 2, 112–118. doi: 10.5897/IJPS.9000289

Ederli, L., Morettini, R., Borgogni, A., Wasternack, C., Miersch, O., Reale, L., et al. (2006). Interaction between nitric oxide and ethylene in the induction of alternative oxidase in ozone-treated tobacco plants. *Plant Physiol.* 142, 595–608. doi: 10.1104/pp.106.085472

Egbichi, M., Keyster, N., and Ludidi., (2014). Effect of exogenous application of nitric oxide on salt stress responses of soybean. *South Afr. J. Bot.* 90, 131–136. doi: 10.1016/j.sajb.2013.11.002

Faine, L. A., Cavalcanti, D. M., Rudnicki, M., Ferderbar, S., Macedo, S. M., Souza, H. P., et al. (2010). Bioactivity of nitrolinoleate: effects on adhesion molecules and CD40eCD40L system. *J. Nutr. Biochem.* 21 (2), 125–132. doi: 10.1016/j.jnutbio.2008.12.004

Fancy, N. N., Bahlmann, A. K., and Loake, G. J. (2017). Nitric oxide function in plant abiotic stress. *Plant Cell Environ.* 40, 462–472. doi: 10.1111/pce.12707

Farmer, E. E., and Ryan, C. A. (1992). Octadecanoid precursors of jasmonic acid activate the synthesis of wound-inducible proteinase inhibitors. *Plant Cell* 4 (2), 129–134. doi: 10.1105/tpc.4.2.129

Fatma, M., Masood, A., Per, T. S., and Khan, N. A. (2016). Nitric oxide alleviates salt stress inhibited photosynthetic performance by interacting with sulfur assimilation in mustard. *Front. Plant Sci.* 7. doi: 10.3389/fpls.2016.00521

Favory, J. J., Stec, A., Gruber, H., Rizzini, L., Oravecz, A., Funk, M., et al. (2009). Interaction of COP1 and UVR8 regulates UV-b induced photomorfogenesys and stress acclimatation in arabidopsis. *EMBO J.* 28:5, 591–601. doi: 10.1038/emboj.2009.4

Feigl, G., Kolbert, Z., Lehotai, N., Molnár, Á., Ördög, A., Bordé, Á., et al. (2016). Different zinc sensitivity of brassica organs is accompanied by distinct responses in protein nitration level and pattern. *Ecotoxicol. Environ. Saf.* 125, 141–152. doi: 10.1016/J.ECOENV.2015.12.006

Finkelstein, R. R., Gampala, S. S., and Rock, C. D. (2002). Abscisic acid signaling in seeds and seedlings. *Plant Cell.* 14 Suppl (Suppl), S15–S45. doi: 10.1105/tpc.010441

Fiscus, E. L., Booker, F. L., and Burkey, K. O. (2005). Crop responses to ozone: uptake, modes of action, carbon assimilation and partitioning. *Plant Cell Environ.* 28, 997–1011. doi: 10.1111/j.1365-3040.2005.01349.x

Freschi, L. (2013). Nitric oxide and phytohormone interactions: Current status and perspectives. *Front. Plant Sci.* 4. doi: 10.3389/fpls.2013.00398

Gao, X., Ma, J., Tie, J., Li, Y., Hu, L., and Yu, J. (2022). BR-Mediated protein s-nitrosylation alleviated low-temperature stress in mini Chinese cabbage (Brassica rapa ssp. *pekinensis) Int. J. Mol. Sci.* 23, 10964. doi: 10.3390/ijms231810964

Gaupels, F., Furch, A. C. U., Zimmermann, M. R., Chen, F., Kaever, V., Buhtz, A., et al. (2016). Systemic induction of NO-, redox-, and cGMP signaling in the pumpkin extrafascicular phloem upon local leaf wounding. *Front. Plant Sci.* 7. doi: 10.3389/fpls.2016.00154

Gaupels, F., Kuruthukulangarakoola, G. T., and Durner, J. (2011). Upstream and downstream signals of nitric oxide in pathogen defence. *Curr. Opin. Plant Biol.* 14, 707–714. doi: 10.1016/j.pbi.2011.07.005

Geisler, A. C., and Rudolph, T. K. (2012). Nitroalkylation a redox sensitive signaling pathway. *Biochem. Biophys. Acta* 1820 (6), 777–784. doi: 10.1016/j.bbagen.2011.06.014

Gill, S. S., Hasanuzzaman, M., Nahar, K., Macovei, A., and Tuteja, N. (2013). Importance of nitric oxide in cadmium stress tolerance in crop plants. *Plant Physiol. Biochem.* 63, 254–261. doi: 10.1016/J.PLAPHY.2012.12.001

González-Gordo, S., Rodríguez-Ruiz, M., López-Jaramillo, J., Muñoz-Vargas, M. A., Palma, J. M., and Corpas, F. J. (2022). Nitric oxide (NO) differentially modulates the ascorbate peroxidase (APX) isozymes of sweet pepper (Capsicum annuum l.) fruits. *Antioxidants* 11, 765. doi: 10.3390/antiox11040765

Gorczynski, M. J., Huang, J., Lee, H., and King, S. B. (2007). Evaluation of nitroalkenes as nitric oxide donors. *Bioorg. med. Chem. Lett.* 17, 2013–2017. doi: 10.1016/j.bmcl.2007.01.016

Gupta, K. J., and Igamberdiev, A. U. (2016). Reactive nitrogen species in mitochondria and their implications in plant energy status and hypoxic stress tolerance. *Front. Plant Sci.* 7. doi: 10.3389/fpls.2016.00369

Gupta, K. J., Shah, J. K., Brotman, Y., Jahnke, K., Willmitzer, L., Kaiser, W. M., et al. (2012). Inhibition of aconitase by nitric oxide leads to induction of the alternative oxidase and to a shift of metabolism towards biosynthesis of amino acids. *J. Exp. Bot.* 63, 1773–1784. doi: 10.1093/jxb/ers053

Gupta, K. J., Zabalza, A., and Van Dongen, J. T. (2009). Regulation of respiration when the oxygen availability changes. *Physiol. Plant* 137, 383–391. doi: 10.1111/j.1399-3054.2009.01253.x

Halliwell, B. (2006). Reactive species and antioxidants. redox biology is a fundamental theme of aerobic life. *Plant Physiol.* 141, 312–322. doi: 10.1104/pp.106.077073

Hamurcu, M., Khan, M. K., Pandey, A., Ozdemir, C., Avsaroglu, Z. Z., Elbasan, F., et al. (2020). Nitric oxide regulates watermelon (Citrullus lanatus) responses to drought stress. *3 Biotech.* 10 (11), 494. doi: 10.1007/s13205-020-02479-9

Hasan, M., Rahman, M., Skalicky, M., Alabdallah, N. M., Waseem, M., Jahan, M. S., et al. (2021). Ozone induced stomatal regulations, MAPK and phytohormone signaling in plants. *Intl J. Mol. Sci.* 22 (12), 6304. doi: 10.3390/ijms22126304

Hawkes, S. J. (1997). What is a "Heavy metal"? *J. Chem. Educ.* 74, 1374. doi: 10.1021/ed074p1374

He, N. Y., Chen, L. S., Sun, A. Z., Zhao, Y., Yin, S. N., and Guo, F. Q. (2022). A nitric oxide burst at the shoot apex triggers a heat-responsive pathway in arabidopsis. *Nat. Plants* 8, 434–450. doi: 10.1038/s41477-022-01135-9

He, H. Y., He, L. F., Gu, M. H., and Li, X. F. (2012). Nitric oxide improves aluminum tolerance by regulating hormonal equilibrium in the root apices of rye and wheat. *Plant Sci.* 183, 123–130. doi: 10.1016/J.PLANTSCI.2011.07.012

He, J. M., Ma, X. G., Zhang, Y., Sun, T. F., Xu, F. F., Chen, Y. P., et al. (2013). Role and interrelationship of gα protein, hydrogen peroxide, and nitric oxide in ultraviolet b-induced stomatal closure in arabidopsis leaves. *Plant Physiol.* 161 (3), 1570–1583. doi: 10.1104/pp.112.211623

Hebelstrup, K. H., and Møller, I. M. (2015). "Mitochondrial signaling in plants under hypoxia: Use of reactive oxygen species (ROS) and reactive nitrogen species (RNS)," in *Reactive oxygen and nitrogen species signaling and communication in plants signaling and communication in plants*. Eds. K. J. Gupta and A. U. Igamberdiev (Cham: Springer International Publishing), 63–77. doi: 10.1007/978-3-319-10079-1_4

Hebelstrup, K. H., van Zanten, M., Mandon, J., Voesenek, L. A. C. J., Harren, F. J. M., Cristescu, S. M., et al. (2012). Haemoglobin modulates NO emission and hyponasty under hypoxia-related stress in arabidopsis thaliana. *J. Exp. Bot.* 63, 5581–5591. doi: 10.1093/jxb/ers210

Hess, D. T., Matsumoto, A., Kim, S. O., Marshall, H. E., and Stamler, J. S. (2005). Protein s-nitrosylation: Purview and parameters. *Nat. Rev. Mol. Cell Biol.* 6, 150–166. doi: 10.1038/nrm1569

Hoang, X. L. T., Nhi, D. N. H., Thu, N. B. A., Thao, N. P., and Tran, L. P. (2017). Transcription factors and their roles in signal transduction in plants under abiotic stresses. *Curr. Genomics* 18, 483–497. doi: 10.2174/1389202918666170227150057

Honda, K., Yamada, N., Yoshida, R., Ihara, H., Sawa, T., Akaike, T., et al. (2015). 8-mercapto-cyclic GMP mediates hydrogen sulfide-induced stomatal closure in arabidopsis. *Plant Cell Physiol.* 56, 1481–1489. doi: 10.1093/pcp/pcv069

Hoque, M. N., Tahjib-Ul-arif, M., Hannan, A., Sultana, N., Akhter, S., Hasanuzzaman, M., et al. (2021). Melatonin modulates plant tolerance to heavy metal stress: Morphological responses to molecular mechanisms. *Int. J. Mol. Sci.* 22 (21), 11445. doi: 10.3390/IJMS222111445

Horak, H., Sierla, M., Wang, C., Wang, Y. S., Nuhkat, M., Valk, E., et al. (2016). A dominant mutation in the ht1 kinase uncovers roles of MAP kinases and GHR1 in CO2-induced stomatal closure. *Plant Cell* 28, 2493–2509. doi: 10.1105/tpc.16.00131

Hossain, M. A., Piyatida, P., Teixeira Da Silva, J. A., and Fujita, M. (2012). Molecular mechanism of heavy metal toxicity and tolerance in plants: central role of glutathione in detoxification of reactive oxygen species and methylglyoxal. *J. od Bot.* 2012, 1–37. doi: 10.1155/2012/872875

Houmani, H., Rodríguez-Ruiz, M., Palma, J. M., and Corpas, F. J. (2018). Mechanical wounding promotes local and long distance response in the halophyte cakile maritima through the involvement of the ROS and RNS metabolism. *Nitric. Oxide* 74, 93–101. doi: 10.1016/j.niox.2017.06.008

Igamberdiev, A. U., Baron, K., Manac'h-Little, N., Stoimenova, M., and Hill, R. D. (2005). The Haemoglobin/Nitric oxide cycle: Involvement in flooding stress and effects on hormone signalling. *Ann. Bot.* 96, 557–564. doi: 10.1093/aob/mci210

Ihara, H., Sawa, T., Nakabeppu, Y., and Akaike, T. (2011). Nucleotides function as endogenous chemical sensors for oxidative stress signaling. *J. Clin. Biochem. Nutr.* 48, 33–39. doi: 10.3164/jcbn.11-003FR

Jain, P., and Bhatla, S. C. (2018). Tyrosine nitration of cytosolic peroxidase is probably triggered as a long distance signaling response in sunflower seedling cotyledons subjected to salt stress. *PloS One* 13, e0197132. doi: 10.1371/journal.pone.0197132

Jain, P., von Toerne, C., Lindermayr, C., and Bhatla, S. C. (2018). S-nitrosylation/denitrosylation as a regulatory mechanism of salt stress sensing in sunflower seedlings. *Physiol. Plant.* 162, 49–72. doi: 10.1111/ppl.12641

Jayawardhane, J., Cochrane, D. W., Vyas, P., Bykova, N. V., Vanlerberghe, G. C., and Igamberdiev, A. U. (2020). Roles for plant mitochondrial alternative oxidase under normoxia, hypoxia, and reoxygenation conditions. *Front. Plant Sci.* 11. doi: 10.3389/fpls.2020.00566

Jethva, J., Schmidt, R. R., Sauter, M., and Selinski, J. (2022). Try or die: Dynamics of plant respiration and how to survive low oxygen conditions. *Plants* 11, 205. doi: 10.3390/plants11020205

Joudoi, T., Shichiri, Y., Kamizono, N., Akaike, T., Sawa, T., Yoshitake, J., et al. (2013). Nitrated cyclic GMP modulates guard cell signaling in arabidopsis. *Plant Cell* 25, 558–571. doi: 10.1105/tpc.112.105049

Kabange, N. R., Mun, B. G., Lee, S. M., Kwon, Y., Lee, D., Lee, G. M., et al. (2022). Nitric oxide: A core signaling molecule under elevated GHGs (CO2, CH4, N2O, O3)-mediated abiotic stress in plants. *Front. Plant Sci.* 13. doi: 10.3389/fpls.2022.994149

Kaiserli, E, and Jenkins, GI (2007). UV-B promotes rapid nuclear translocation of the UV-B-specific signaling component UVR8 and activates its function in the nucleus. *Plant Cell* 19 (8), 2662–73.

Kandziora-Ciupa, M., Ciepał, R., Nadgórska-Socha, A., and Barczyk, G. (2013). A comparative study of heavy metal accumulation and antioxidant responses in vaccinium myrtillus l. leaves in polluted and non-polluted areas. *Environ. Sci. pollut. Res.* 20, 4920–4932. doi: 10.1007/S11356-012-1461-4

Kaya, C., Ashraf, M., Alyemeni, M. N., and Ahmad, P. (2020). Responses of nitric oxide and hydrogen sulfide in regulating oxidative defence system in wheat plants grown under cadmium stress. *Physiol. Plant* 168, 345–360. doi: 10.1111/PPL.13012

Kende, H., van der Knaap, E., and Cho, H.-T. (1998). Deepwater rice: A model plant to study stem Elongation1. *Plant Physiol.* 118, 1105–1110. doi: 10.1104/pp.118.4.1105

Keyster, M., Klein, A., Egbichi, I., Jacobs, A., and Ludidi, N. (2011). Nitric oxide increases the enzymatic activity of three ascorbate peroxidase isoforms in soybean root nodules. *Plant Signaling Behav.* 6, 956–961. doi: 10.4161/psb.6.7.14879

Khan, M. Y., Prakash, V., Yadav, V., Chauhan, D. K., Prasad, S. M., Ramawat, N., et al. (2019). Regulation of cadmium toxicity in roots of tomato by indole acetic acid with special emphasis on reactive oxygen species production and their scavenging. *Plant Physiol. Biochem.* 142, 193–201. doi: 10.1016/J.PLAPHY.2019.05.006

Kliebenstein, D. J., Lim, J. E., Landry, L. G., and Last, R. L. (2002). Arabidopsis UVR8 regulates ultraviolet-b signal transduction and tolerance and contains sequence similarity to human regulator of chromatin condensation 1. *Plant Physiol.* 30 (1), 234–243. doi: 10.1104/pp.005041

Kolbert, Z., Molnár, Á., Szollosi, R., Feigl, G., Erdei, L., and Ördög, A. (2018). Nitro-oxidative stress correlates with Se tolerance of astragalus species. *Plant Cell Physiol.* 59, 1827–1843. doi: 10.1093/PCP/PCY099

Kolbert, Z., Molnï, Ï., Olï, D., Feigl, G., HorvÏ, E., Erdei, L., et al. (2019). S-nitrosothiol signaling is involved in regulating hydrogen peroxide metabolism of zinc-stressed arabidopsis. *Plant Cell Physiol.* 60 (11), 2449–2463. doi: 10.1093/pcp/pcz138

Kolbert, Z., Petõ, A., Lehotai, N., Feigl, G., and Erdei, L. (2012). Long-term copper (Cu 2+) exposure impacts on auxin, nitric oxide (NO) metabolism and morphology of arabidopsis thaliana l. *Plant Growth Regul.* 68, 151–159. doi: 10.1007/s10725-012-9701-7

Kontunen-Soppela, S., Parviainen, J., Ruhanen, H., Brosché, M., Keinänen, M., Thakur, R. C., et al. (2010). Gene expression responses of paper birch (Betula papyrifera) to elevated CO2 and O3 during leaf maturation and senescence. *Environ. pollut.* 158, 959–968. doi: 10.1016/j.envpol.2009.10.008

Krasylenko, Y. A., Yemets, A. I., Sheremet, Y. A., and Blume, Y. B. (2012). Nitric oxide as a critical factor for perception of UV-b irradiation by microtubules in arabidopsis. *Physiol. Plant* 145 (4), 505–515. doi: 10.1111/j.1399-3054.2011.01530.x

Lamotte, O., Bertoldo, J. B., Besson-Bard, A., Rosnoblet, C., Aime, S., Hichami, S., et al. (2014). Protein s-nitrosylation: Specificity and identification strategies in plants. *Front. Chem.* 2. doi: 10.3389/fchem.2014.00114

Lamotte, O., Bertoldo, J. B., Besson-Bard, A., Rosnoblet, C., Aimé, S., Hichami, S., et al. (2015). Protein s-nitrosylation: specificity and identification strategies in plants. *Front. Chem.* 2. doi: 10.3389/fchem.2014.00114

Lee, U., Wie, C., Fernandez, B. O., Feelisch, M., and Vierling, E. (2008). Modulation of nitrosative stress by s-nitrosoglutathione reductase is critical for thermotolerance and plant growth in arabidopsis. *Plant Cell* 20, 786–802. doi: 10.1105/tpc.107.052647

Leterrier, M., Airaki, M., Palma, J. M., Chaki, M., Barroso, J. B., and Corpas, F. J. (2012). Arsenic triggers the nitric oxide (NO) and s-nitrosoglutathione (GSNO) metabolism in arabidopsis. *Environ. pollut.* 166, 136–143. doi: 10.1016/J.ENVPOL.2012.03.012

Li, X., Liu, Z., Ren, H., Kundu, M., Zhong, F. W., Wang, L., et al. (2022). Dynamics and mechanism of dimer dissociation of photoreceptor UVR8. *Nat. Commun.* 13 (1), 93. doi: 10.1038/s41467-021-27756-w

Li, X., Pan, Y., Chang, B., Wang, Y., and Tang, Z. (2016). NO promotes seed germination and seedling growth under high salt may depend on EIN3 protein in arabidopsis. *Front. Plant Sci.* 6. doi: 10.3389/fpls.2015.01203

Li, Z., Wakao, S., Fischer, B. B., and Niyogi, K. K. (2009). Sensing and responding to excess light. *Annu. Rev. Plant Biol.* 60, 239–260. doi: 10.1146/annurev.arplant.58.032806.103844

Lima, E. S., Bonini, M. G., Augusto, O., Barbeiro, H. V., Souza, H. P., and Abdalla, D. S. (2005). Nitrated lipids decompose to nitric oxide and lipid radicals and cause vasorelaxation. *Free Radic. Biol. Med.* 39 (4), 532–539. doi: 10.1016/j.freeradbiomed.2005.04.005

Lin, C. C., Jih, P. J., Lin, H. H., Lin, J. S., Chang, L. L., Shen, Y. H., et al. (2011). Nitric oxide activates superoxide dismutase and ascorbate peroxidase to repress the cell death induced by wounding. *Plant Mol. Biol.* 77, 235–249. doi: 10.1007/s11103-011-9805-x

Liu, T., Xu, J., Li, J., and Hu, X. (2019). NO is involved in JA- and H2O2-mediated ALA-induced oxidative stress tolerance at low temperatures in tomato. *Environ. Exp. Bot.* 161, 334–343. doi: 10.1016/j.envexpbot.2018.10.020

Lopez-Molina, L., and Chua, N. H. (2000). A null mutation in a bZIP factor confers ABA-insensitivity in arabidopsis thaliana. *Plant Cell Physiol.* 41 (5), 541–547. doi: 10.1093/pcp/41.5.541

Ma, N., Adachi, Y., Hiraku, Y., Horiki, N., Horiike, S., Imoto, I., et al. (2004). Accumulation of 8-nitroguanine in human gastric epithelium induced by helicobacter pylori infection. *Biochem. Biophys. Res. Commun.* 319, 506–510. doi: 10.1016/j.bbrc.2004.04.193

Mackerness, S. A. H., John, C. F., Jordan, B., and Thomas, B. (2001). Early signaling componenets in ultraviolet-b responses: distinct roles for different reactive oxygen species and nitric oxide. *FEBS Lett.* 489 (2-3), 237–242. doi: 10.1016/s0014-5793(01)02103-2

Manasa, S. L., Panigrahy, M., Panigrahi, K. C. S., and Rout, G. R. (2022). Overview of cold stress regulation in plants. *Bot. Rev.* 88, 359–387. doi: 10.1007/s12229-021-09267-x

Manrique-Gil, I., Sánchez-Vicente, I., Torres-Quezada, I., and Lorenzo, O. (2021). Nitric oxide function during oxygen deprivation in physiological and stress processes. *J. Exp. Bot.* 72, 904–916. doi: 10.1093/jxb/eraa442

Mata-Pérez, C., Begara-Morales, J. C., Chaki, M., Sánchez-Calvo, B., Valderrama, R., Padilla, M. N., et al. (2016c). Protein tyrosine nitration during development and abiotic stress response in plants. *Front. Plant Sci.* 7. doi: 10.3389/fpls.2016.01699

Mata-Pérez, C., Sánchez-Calvo, B., Begara-Morales, J. C., Carreras, A., Padilla, M. N., Melguizo, M., et al. (2016b). Nitro-linolenic acid is a nitric oxide donor. *Nitric. Oxide* 57, 57–63. doi: 10.1016/j.niox.2016b.05.003

Mata-Pérez, C., Sánchez-Calvo, B., Padilla, M. N., Begara-Morales, J. C., Luque, F., Melguizo, M., et al. (2016a). Nitro-fatty acids in plant signaling: Nitro-linolenic acid induces the molecular chaperone network in arabidopsis. *Plant Physiol.* 170, 686–701. doi: 10.1104/pp.15.01671

Mengel, A., Chaki, M., Shekariesfahlan, A., and Lindermayr, C. (2013). Effect of nitric oxide on gene transcription – s-nitrosylation of nuclear proteins. *Front. Plant Sci.* 4. doi: 10.3389/fpls.2013.00293

Millar, A. H., and Day, D. A. (1996). Nitric oxide inhibits the cytochrome oxidase but not the alternative oxidase of plant mitochondria. *FEBS Lett.* 398, 155–158. doi: 10.1016/S0014-5793(96)01230-6

Mills, G., Sharps, K., Simpson, D., Pleijel, H., Broberg, M., Uddling, J., et al. (2018). Ozone pollution will compromise efforts to increase global wheat production. *Global Change Biol.* 24, 3560–3574. doi: 10.1111/gcb.14157

Mittler, R., Vanderauwera, S., Suzuki, N., Miller, G., Tognetti, V. B., Vandepoele, K., et al. (2011). ROS signaling: the new wave? *Trends Plant Sci.* 16 (6), 300–309. doi: 10.1016/j.tplants.2011.03.007

Morales, L. O., Shapiguzov, A., Safronov, O., Lepälä, J., Vaahtera, L., Yarmolinsky, D., et al. (2021). Ozone responses in arabidopsis: beyond stomatal conductance. *Plant Physiol.* 186, 180–192. doi: 10.1093/plphys/kiab097

Moreau, M., Lindermayr, C., Durner, J., and Klessig, D. F. (2010). NO synthesis and signaling in plants–where do we stand? *Physiol. Plant.* 138, 372–383. doi: 10.1111/j.1399-3054.2009.01308.x

Mostafa, S., Wang, Y., Zeng, W., and Jin, B. (2022). Plant responses to herbivory, wounding, and infection. *Int. J. Mol. Sci.* 23 (13), 7031. doi: 10.3390/ijms23137031

Mukherjee, S. (2022). "Atmospheric nitric oxide (NO) regulates ozone (O3)-induced stress signaling in plants: Ally or foe?," in *Plant stress: Challenges and management in the new decade* (Cham, Switzerland: Springer), 89–96. doi: 10.1007/978-3-030-95365-2_5

Nagajyoti, P. C., Lee, K. D., and Sreekanth, T. V. M. (2010). Heavy metals, occurrence and toxicity for plants: a review. *Environ. Chem. Letters.* 8 (3), 199–216. doi: 10.1007/S10311-010-0297-8

Nagatoshi, Y., Mitsuda, N., Hayashi, M., Inoue, S., Okuma, E., Kubo, A., et al. (2016). GOLDEN 2-LIKE transcription factors for chloroplast development affect ozone tolerance through the regulation of stomatal movement. *Proc. Natl. Acad. Sci. U S A.* 113 (15), 4218–4223. doi: 10.1073/pnas.1513093113

Nanni, A. V., Morse, A. M., Newman, J. R. B., Choquette, N. E., Wedow, J. M., Liu, Z., et al. (2022). Variation in leaf transcriptome responses to elevated ozone corresponds with physiological sensitivity to ozone across maize inbred lines. *Genetics* 221, iyac080. doi: 10.1093/genetics/iyac080

Navrot, N., Rouhier, N., Gelhaye, E., and Jacquot, J. (2007). Reactive oxygen species generation and antioxidant systems in plant mitochondria. *Physiol. Plant.* 129, 185–195. doi: 10.1111/j.1399-3054.2006.00777.x

Neill, S., Bright, J., Desikan, R., Hancock, J., Harrison, J., and Wilson, I. (2007). Nitric oxide evolution and perception. *J. Exp. Bot.* 59 (1), 25–35. doi: 10.1093/jxb/erm218

Neill, S. J., Desikan, R., and Hancock, J. T. (2003). Nitric oxide signalling in plants. *New Phytol.* 159 (1), 11–35. doi: 10.1046/j.1469-8137.2003.00804.x

Niles, J. C., Wishnok, J. S., and Tannenbaum, S. R. (2001). A novel nitroimidazole compound formed during the reaction of peroxynitrite with 2',3',5'-tri-O-acetyl-guanosine. *J. Am. Chem. Soc* 123, 12147–12151. doi: 10.1021/ja004296k

Nishida, M., Kumagai, Y., Ihara, H., Fujii, S., Motohashi, H., and Akaike, T. (2016). Redox signaling regulated by electrophiles and reactive sulfur species. *J. Clin. Biochem. Nutr.* 58, 91–98. doi: 10.3164/jcbn.15-111

Ohshima, H., Sawa, T., and Akaike, T. (2006). 8-nitroguanine, a product of nitrative DNA damage caused by reactive nitrogen species: formation, occurrence, and implications in inflammation and carcinogenesis. *Antioxid. Redox Signal.* 8, 1033–1045. doi: 10.1089/ars.2006.8.1033

Orozco-Cárdenas, M. L., and Ryan, C. A. (2002). Nitric oxide negatively modulates wound signaling in tomato plants. *Plant Physiol.* 130 (1), 487–493. doi: 10.1104/pp.008375

Overmyer, K., Brosché, M., Pellinen, R., Kuittinen, T., Tuominen, H., Ahlfors, R., et al. (2005). Ozone-induced programmed cell death in the arabidopsis radical-induced cell death1 mutant. *Plant Physiol.* 137, 1092–1104. doi: 10.1104/pp.104.055681

Padilla, M. N., Mata-Pérez, C., Melguizo, M., and Barroso, J. B. (2017). *In vitro* nitro-fatty acid release from cys-NO_2-fatty acid adducts under nitro-oxidative conditions. *Nitric. Oxide* 68, 14–22. doi: 10.1016/j.niox.2016.12.009

Pande, A., Mun, B. G., Rahim, W., Khan, M., Lee, D. S., Lee, G. M., et al. (2022). Phytohormonal regulation through protein s-nitrosylation under stress. *Front. Plant Sci.* 13. doi: 10.3389/FPLS.2022.865542

París, R., Lamattina, L., and Casalongué, C. A. (2007). Nitric oxide promotes the wound-healing response of potato leaflets. *Plant Physiol. Biochem.* 45 (1), 80–86. doi: 10.1016/j.plaphy.2006.12.001

Perazzolli, M., Dominici, P., Romero-Puertas, M. C., Zago, E., Zeier, J., Sonoda, M., et al. (2004). Arabidopsis nonsymbiotic hemoglobin AHb1 modulates nitric oxide bioactivity. *Plant Cell.* 16, 2785–2794. doi: 10.1105/tpc.104.025379

Pinlaor, S., Yongvanit, P., Hiraku, Y., Ma, N., Semba, R., Oikawa, S., et al. (2003). 8-nitroguanine formation in the liver of hamsters infected with opisthorchis viverrini. *Biochem. Biophys. Res. Commun.* 309, 567–571. doi: 10.1016/j.bbrc.2003.08.039

Pucciariello, C., Parlanti, S., Banti, V., Novi, G., and Perata, P. (2012). Reactive oxygen species-driven transcription in arabidopsis under oxygen Deprivation1[W]. *Plant Physiol.* 159, 184–196. doi: 10.1104/pp.111.191122

Puckette, M. C., Tang, Y., and Mahalingam, R. (2008). Transcriptomic changes induced by acute ozone in resistant and sensitive medicago truncatula accessions. *BMC Plant Biol.* 8, 46. doi: 10.1186/1471-2229-8-46

Puyaubert, J., and Baudouin, E. (2014a). New clues for a cold case: nitric oxide response to low temperature. *Plant Cell Environ.* 37 (12), 2623–2630. doi: 10.1111/pce.12329

Puyaubert, J., Fares, A., Rézé, N., Peltier, J.-B., and Baudouin, E. (2014b). Identification of endogenously s-nitrosylated proteins in arabidopsis plantlets: effect of cold stress on cysteine nitrosylation level. *Plant Sci.* 215-216, 150–156. doi: 10.1016/j.plantsci.2013.10.014

Qi, Q., Yanyan, D., Yuanlin, L., Kunzhi, L., Huini, X., and Xudong, S. (2020). Overexpression of SlMDHAR in transgenic tobacco increased salt stress tolerance involving s-nitrosylation regulation. *Plant Sci.* 299, 110609. doi: 10.1016/j.plantsci.2020.110609

Radi, R. (2004). Nitric oxide, oxidants and protein tyrosine nitration. *Proc. Natl. Acad. Sci. U.S.A.* 101, 4003–4008. doi: 10.1073/pnas.0307446101

Radi, R. (2012). Protein tyrosine nitration: biochemical mechanisms and structural basis of functional effects. *Acc. Chem. Res.* 46, 550–559. doi: 10.1021/ar300234c

Rajhi, I., Yamauchi, T., Takahashi, H., Nishiuchi, S., Shiono, K., Watanabe, R., et al. (2011). Identification of genes expressed in maize root cortical cells during lysigenous aerenchyma formation using laser microdissection and microarray analyses. *New Phytol.* 190, 351–368. doi: 10.1111/j.1469-8137.2010.03535.x

Rascio, N., and Navari-Izzo, F. (2011). Heavy metal hyperaccumulating plants: How and why do they do it? and what makes them so interesting? *Plant Sci.* 180, 169–181. doi: 10.1016/J.PLANTSCI.2010.08.016

Raychaudhuri, S., Pramanick, P., Talukder, P., and Basak, A. (2021). "Polyamines, metallothioneins, and phytochelatins–natural defense of plants to mitigate heavy metals," in *Studies in natural products chemistry* (Elsevier), 227–261. doi: 10.1016/B978-0-12-819487-4.00006-9

Rehrig, E. M., Appel, H. M., Jones, A. D., and Schultz, J. C. (2014). Roles for jasmonate- and ethylene-induced transcription factors in the ability of arabidopsis to respond differentially to damage caused by two insect herbivores. *Front. Plant Sci.* 5. doi: 10.3389/fpls.2014.00407

Reymond, P., and Farmer, E. E. (1998). Jasmonate and salicylate as global signals for defense gene expression. *Curr. Opin. Plant Biol.* 1 (5), 404–411. doi: 10.1016/s1369-5266(98)80264-1

Reymond, P., Weber, H., Damond, M., and Farmer, E. E. (2000). Differential gene expression in response to mechanical wounding and insect feeding in arabidopsis. *Plant Cell* 12 (5), 707–719. doi: 10.1105/tpc.12.5.707

Romero-Puertas, M. C., Rodríguez-Serrano, M., and Sandalio, L. M. (2013). Protein s-nitrosylation in plants under abiotic stress: an overview. *Front. Plant Sci.* 4. doi: 10.3389/FPLS.2013.00373

Rossi, S., Burgess, P., Jespersen, D., and Huang, B. (2017). Heat-induced leaf senescence associated with chlorophyll metabolism in bentgrass lines differing in heat tolerance. *Crop Sci.* 57, 169–178. doi: 10.2135/cropsci2016.06.0542

Royo, B., Moran, J. F., Ratcliffe, R. G., and Gupta, K. J. (2015). Nitric oxide induces the alternative oxidase pathway in arabidopsis seedlings deprived of inorganic phosphate. *J. Exp. Bot.* 66, 6273–6280. doi: 10.1093/jxb/erv338

Rubio, M. C., Calvo-Begueria, L., Díaz-Mendoza, M., Elhiti, M., Moore, M., Matamoros, M. A., et al. (2019). Phytoglobins in the nuclei, cytoplasm and chloroplasts modulate nitric oxide signaling and interact with abscisic acid. *Plant J.* 100, 38–54. doi: 10.1111/tpj.14422

Sainz, M., Calvo-Begueria, L., Pérez-Rontomé, C., Wienkoop, S., Abián, J., Staudinger, C., et al. (2015). Leghemoglobin is nitrated in functional legume nodules in a tyrosine residue within the heme cavity by a nitrite/peroxide-dependent mechanism. *Plant J.* 81, 723–735. doi: 10.1111/tpj.12762

Sánchez-McSweeney, A., González-Gordo, S., Aranda-Sicilia, M. N., Rodríguez-Rosales, M. P., Venema, K., Palma, J. M., et al. (2021). Loss of function of the chloroplast membrane K /H antiporters AtKEA1 and AtKEA2 alters the ROS and NO metabolism but promotes drought stress resilience. *Plant Physiol. Biochem.* 160, 106–119. doi: 10.1016/j.plaphy.2021.01.010

Sánchez-Vicente, I., and Lorenzo, O. (2021). Nitric oxide regulation of temperature acclimation: a molecular genetic perspective. *J. Exp. Bot.* 72 (16), 5789–5794. doi: 10.1093/jxb/erab049

Sasidharan, R., Bailey-Serres, J., Ashikari, M., Atwell, B. J., Colmer, T. D., Fagerstedt, K., et al. (2017). Community recommendations on terminology and procedures used in flooding and low oxygen stress research. *New Phytol.* 214, 1403–1407. doi: 10.1111/nph.14519

Sasidharan, R., Hartman, S., Liu, Z., Martopawiro, S., Sajeev, N., van Veen, H., et al. (2018). Signal dynamics and interactions during flooding Stress1[OPEN]. *Plant Physiol.* 176, 1106–1117. doi: 10.1104/pp.17.01232

Sasidharan, R., Schippers, J. H. M., and Schmidt, R. R. (2021). Redox and low-oxygen stress: signal integration and interplay. *Plant Physiol.* 186, 66–78. doi: 10.1093/plphys/kiaa081

Sawa, T., Zaki, M. H., Okamoto, T., Akuta, T., Tokutomi, Y., Kim-Mitsuyama, S., et al. (2007). Protein s-guanylation by the biological signal 8-nitroguanosine 3′,5′-cyclic monophosphate. *Nat. Chem. Biol.* 3, 727–735. doi: 10.1038/nchembio.2007.33

Saxena, I., and Shekhawat, G. S. (2013). Nitric oxide (NO) in alleviation of heavy metal induced phytotoxicity and its role in protein nitration. *Nitric. Oxide* 32, 13–20. doi: 10.1016/J.NIOX.2013.03.004

Schopfer, F. J., Cipollina, C., and Freeman, B. A. (2011). Formation and signaling actions of electrophilic lipids. *Chem. Rev.* 111 (10), 5997–6021. doi: 10.1021/cr200131e

Sehgal, A., Sita, K., Siddique, K. H. M., Kumar, R., Bhogireddy, S., Varshney, R. K., et al. (2018). Drought or/and heat-stress effects on seed filling in food crops: Impacts on functional biochemistry, seed yields, and nutritional quality. *Front. Plant Sci.* 9. doi: 10.3389/fpls.2018.01705

Sehrawat, A., Gupta, R., and Deswal, R. (2013). Nitric oxide-cold stress signalling cross-talk, evolution of a novel regulatory mechanism. *Proteomics* 13, 1816–1835. doi: 10.1002/pmic.201200445

Sehrawat, A., Sougrakpam, Y., and Deswal, R. (2019). Cold modulated nuclear s-nitrosoproteome analysis indicates redox modulation of novel brassicaceae specific, myrosinase and napin in brassica juncea. *Environ. Exp. Bot.* 161, 312–333. doi: 10.1016/j.envexpbot.2018.10.010

Selinski, J., Hartmann, A., Kordes, A., Deckers-Hebestreit, G., Whelan, J., and Scheibe, R. (2017). Analysis of posttranslational activation of alternative oxidase isoforms. *Plant Physiol.* 174, 2113–2127. doi: 10.1104/pp.17.00681

Selinski, J., Scheibe, R., Day, D. A., and Whelan, J. (2018). Alternative oxidase is positive for plant performance. *Trends Plant Sci.* 23 (7), 588–597. doi: 10.1016/j.tplants.2018.03.012

Serpa, V., Vernal, J., Lamattina, L., Grotewold, E., Cassia, R., and Terenzi, H. (2007). Inhibition of AtMYB2 DNA-binding by nitric oxide involves cysteine s-nitrosylation. *Biochem. Biophys. Res. Commun.* 361, 1048–1053. doi: 10.1016/j.bbrc.2007.07.133

Shi, Y., Ke, X., Yang, X., Liu, Y., and Hou, X. (2022). Plants response to light stress. *J. Genet. Genomics* 49 (8), 735–747. doi: 10.1016/j.jgg.2022.04.017

Shi, H. T., Li, R. J., Cai, W., Liu, W., Wang, C. L., and Lu, Y. T. (2012). Increasing nitric oxide content in arabidopsis thaliana by expressing rat neuronal nitric oxide synthase resulted in enhanced stress tolerance. *Plant Cell Physiol.* 53 (2), 344–357. doi: 10.1093/pcp/pcr181

Si, T., Wang, X., Wu, L., Zhao, C., Zhang, L., Huang, M., et al. (2017). Nitric oxide and hydrogen peroxide mediate wounding-induced freezing tolerance through modifications in photosystem and antioxidant system in wheat. *Front. Plant Sci.* 8. doi: 10.3389/fpls.2017.01284

Sierla, M., Hõrak, H., Overmyer, K., Waszczak, C., Yarmolinsky, D., Maierhofer, T., et al. (2018). The receptor-like pseudokinase GHR1 is required for stomatal closure. *Plant Cell* 30, 2813–2837. doi: 10.1105/tpc.18.00441

Skubacz, A., Daszkowska-Golec, A., and Szarejko, I. (2016). The role and regulation of ABI5 (ABA-insensitive 5) in plant development, abiotic stress responses and phytohormone crosstalk. *Front. Plant Sci.* 7. doi: 10.3389/fpls.2016.01884

Spoel, S. H., and Van Ooijen, G. (2014). Circadian redox signaling in plant immunity and abiotic stress. *Antioxid. Redox Signal* 20 (18), 3024–3039. doi: 10.1089/ars.2013.5530

Srivastava, M., Ma, L. Q., Singh, N., and Singh, S. (2005). Antioxidant responses of hyper-accumulator and sensitive fern species to arsenic. *J. Exp. Bot.* 56, 1335–1342. doi: 10.1093/JXB/ERI134

Suzuki, N., and Mittler, R. (2012). Reactive oxygen species-dependent wound responses in animals and plants. *Free Radical Biol. Med.* 53 (12), 2269–2276. doi: 10.1016/j.freeradbiomed.2012.10.538

Swamy, P. M., and Smith, B. N. (1999). Role of abscisic acid in plant stress tolerance. *Curr. Sci.* 76, 1220–1227.

Tai, A. P. K., Sadiq, M., Pang, J. Y. S., Yung David, H. Y., and Feng, Z. (2021). Impacts of surface ozone pollution on global crop yields: comparing different ozone exposure metrics and incorporating co-effects of CO2. *Front. Sustain. Food Syst.* 29. doi: 10.3389/fsufs.2021.534616

Tanou, G., Ziogas, V., Belghazi, M., Christou, A., Filippou, P., Job, D., et al. (2014). Polyamines reprogram oxidative and nitrosative status and the proteome of citrus plants exposed to salinity stress. *Plant Cell Environ.* 37, 864–885. doi: 10.1111/pce.12204

Toh, S., Imamura, A., Watanabe, A., Nakabayashi, K., Okamoto, M., Jikumaru, Y., et al. (2008). High temperature-induced abscisic acid biosynthesis and its role in the inhibition of gibberellin action in arabidopsis seeds. *Plant Physiol.* 146, 1368–1385. doi: 10.1104/pp.107.113738

Tossi, V., Lamattina, L., Jenkins, G. I., and Cassia, R. O. (2014).). ultraviolet-b-induced stomatal closure in arabidopsis is regulated by the UV RESISTANCE LOCUS8 photoreceptor in a nitric oxide-dependent mechanism. *Plant Physiol.* 164 (4), 2220–2230. doi: 10.1104/pp.113.231753

Trapet, P., Kulik, A., Lamotte, O., Jeandroz, S., Bourque, S., Nicolas-Frances, V., et al. (2015). NO signaling in plant immunity: A tale of messengers. *Phytochemistry* 112, 72–79. doi: 10.1016/j.phytochem.2014.03.015

Turkan, I. (2018). ROS and RNS: key signalling molecules in plants. *J. Exp. Bot.* 69, 3313–3315. doi: 10.1093/jxb/ery198

Valderrama, R., Corpas, F. J., Carreras, A., Fernández-Ocaña, A., Chaki, M., Luque, F., et al. (2007). Nitrosative stress in plants. *FEBS Lett.* 581, 453–461. doi: 10.1016/j.febslet.2007.01.006

Vanhaelewyn, L., Prinsen, E., van der Straeten, D., and Vandenbussche, F. (2016). Hormone-controlled UV-b responses in plants. *J. Exp. Bot.* 67 (15), 4469–4482. doi: 10.1093/jxb/erw261

Vanzo, E., Ghirardo, A., Merl-Pham, J., Lindemayr, C., Heller, W., Hauck, S. M., et al. (2014). S-nitroso-proteome in poplar leaves in response to acute ozone stress. *PloS One* 9 (9), e106886. doi: 10.1371/journal.pone.0106886

Vishwakarma, A., Kumari, A., Mur, L. A. J., and Gupta, K. J. (2018). A discrete role for alternative oxidase under hypoxia to increase nitric oxide and drive energy production. *Free Radic. Biol. Med.* 122, 40–51. doi: 10.1016/j.freeradbiomed.2018.03.045

Vistoli, G., De Maddis, D., Cipak, A., Zarkovic, N., Carini, M., and Aldini, G. (2013). Advanced glycoxidation and lipoxidation end products (AGEs and ALEs): an overview of their mechanisms of formation. *Free Radic. Res.* 47 (Suppl 1), 3–27. doi: 10.3109/10715762.2013.815348

Vollár, M., Feigl, G., Oláh, D., Horváth, A., Molnár, Á., Kúsz, N., et al. (2020). Nitro-oleic acid in seeds and differently developed seedlings of brassica napus l. *Plants (basel Switzerland)* 9 (3), 406. doi: 10.3390/plants9030406

Wang, Q. L., Chen, J. H., He, N. Y., and Guo, F. Q. (2018). Metabolic reprogramming in chloroplasts under heat stress in plants. *Int. J. Mol. Sci.* 19, 849. doi: 10.3390/ijms19030849

Wang, P., Du, Y., Hou, Y., Zhao, Y., Hsu, C., Yuan, F., et al. (2015). Nitric oxide negatively regulates abscisic acid signaling in guard cells by s-nitrosylation of OST1. *Proc. Natl. Acad. Sci.* 112, 613–618. doi: 10.1073/pnas.1423481112

Wang, C., Wei, L., Zhang, J., Hu, D., Gao, R., Liu, Y., et al. (2022). Nitric oxide enhances salt tolerance in tomato seedlings by regulating endogenous s-nitrosylation levels. *J. Plant Growth Regul.* 42, 275–293. doi: 10.1007/s00344-021-10546-5

Wany, A., Kumari, A., and Gupta, K. J. (2017). Nitric oxide is essential for the development of aerenchyma in wheat roots under hypoxic stress. *Plant Cell Environ.* 40 (12), 3002–3017. doi: 10.1111/pce.13061

Wasternack, C., and Song, S. (2017). Jasmonates: biosynthesis, metabolism, and signaling by proteins activating and repressing transcription. *J. Exp. Bot.* 68 (6), 1303–1321. doi: 10.1093/jxb/erw443

Waszczak, C., Carmody, M., and Kangasja¨rvi, J. (2018). Reactive oxygen species in plant signaling. *Annu. Rev. Plant Biol.* 69, 209–236. doi: 10.1146/annurev-arplant-042817-040322

Wei, L., Zhang, J., Wei, S., Hu, D., Liu, Y., Feng, L., et al. (2022). Nitric oxide enhanced salt stress tolerance in tomato seedlings, involving phytohormone equilibrium and photosynthesis. *Int. J. Mol. Sci.* 23, 4539. doi: 10.3390/ijms23094539

Weits, D. A., van Dongen, J. T., and Licausi, F. (2021). Molecular oxygen as a signaling component in plant development. *New Phytol.* 229, 24–35. doi: 10.1111/nph.16424

Wrzaczek, M., Brosché, M., Salojärvi, J., Kangasjärvi, S., Idänheimo, N., Mersmann, S., et al. (2010). Transcriptional regulation of the CRK/DUF26 group of receptor-like protein kinases by ozone and plant hormones in arabidopsis. *BMC Plant Biol.* 10, 95. doi: 10.1186/1471-2229-10-95

Wu, R., Agathokleous, E., Yung, D. H. Y., Tai, A. P. K., Shang, B., and Feng, Z. (2022). Joint impacts of ozone pollution and climate change on yields of Chinese winter wheat. *Atmospheric pollut. Research* 13, 101509. doi: 10.1016/j.apr.2022.101509

Wu, Q., Su, N., Zhang, X., Liu, Y., Cui, J., and Liang, Y. (2016). Hydrogen peroxide, nitric oxide and UV RESISTANCE LOCUS8 interact to mediate UV-b-induced anthocyanin biosynthesis in radish sprouts. *Sci. Rep.* 6, 29164. doi: 10.1038/srep29164

Xu, E., Vaahtera, L., H~orak, H., Hincha, D. K., Heyer, A. G., and Brosché, M. (2015). Quantitative trait loci mapping and transcriptome análisis reveal candidate genes regulating the response to ozone in arabidopsis thaliana. *Plant Cell Environ.* 38, 1418–1433. doi: 10.1111/pce.12499

Xu, J., Wang, W., Yin, H., Liu, X., Sun, H., and Mi, Q. (2010). Exogenous nitric oxide improves antioxidative capacity and reduces auxin degradation in roots of medicago truncatula seedlings under cadmium stress. *Plant Soil* 326, 321–330. doi: 10.1007/s11104-009-0011-4

Xu, M., Zhu, Y., Dong, J., Jin, H., Sun, L., Wang, Z., et al. (2012). Ozone induces flavonol production of ginkgo biloba cells dependently on nitrate reductase mediated nitric oxide signaling. *Envir. Exp. Bot.* 75, 114–119. doi: 10.1016/j.envexpbot.2011.09.005

Xuan, Y., Zhou, S., Wang, L., Cheng, Y., and Zhao, L. (2010). Nitric oxide functions as a signal and acts upstream of AtCaM3 in thermotolerance in arabidopsis seedlings. *Plant Physiol.* 153, 1895–1906. doi: 10.1104/pp.110.160424

Yamauchi, T., Watanabe, K., Fukazawa, A., Mori, H., Abe, F., Kawaguchi, K., et al. (2014). Ethylene and reactive oxygen species are involved in root aerenchyma formation and adaptation of wheat seedlings to oxygen-deficient conditions. *J. Exp. Bot.* 65, 261–273. doi: 10.1093/jxb/ert371

Yamauchi, T., Yoshioka, M., Fukazawa, A., Mori, H., Nishizawa, N. K., Tsutsumi, N., et al. (2017). An NADPH oxidase RBOH functions in rice roots during lysigenous

aerenchyma formation under oxygen-deficient conditions. *Plant Cell* 29, 775–790. doi: 10.1105/tpc.16.00976

Yermilov, V., Rubio, J., Becchi, M., Friesen, M. D., Pignatelli, B., and Ohshima, H. (1995a). Formation of 8-nitroguanine by the reaction of guanine with peroxynitrite *in vitro*. *Carcinogenesis* 16, 2045–2050. doi: 10.1093/carcin/16.9.2045

Yermilov, V., Rubio, J., and Ohshima, H. (1995b). Formation of 8-nitroguanine in DNA treated with peroxynitrite *in vitro* and its rapid removal from DNA by depurination. *FEBS Lett.* 376, 207–210. doi: 10.1016/0014-5793(95)01281-6

Yeung, E., van Veen, H., Vashisht, D., Sobral Paiva, A. L., Hummel, M., Rankenberg, T., et al. (2018). A stress recovery signaling network for enhanced flooding tolerance in arabidopsis thaliana. *Proc. Natl. Acad. Sci. U. S. A.* 115, E6085–E6094. doi: 10.1073/pnas.1803841115

Yin, X., Hu, Y., Meng, L., Zhang, X., Liu, H., Wang, L., et al. (2021). Effects of exogenous nitric oxide on wild barley (Hordeum brevisubulatum) under salt stress. *Biotechnol. Biotechnol. Equip.* 1, 2005–2016. doi: 10.1080/13102818.2022.2041096

Yin, L., Mano, J., Wang, S., Tsuji, W., and Tanaka, K. (2010). The involvement of lipid peroxide-derived aldehydes in aluminum toxicity of tobacco roots plant physiol. *Plant. Physiol.* 152, 1406–1417. doi: 10.1104/pp.109.151449

Ying, S., Yang, W., Li, P., Hu, Y., Lu, S., Zhou, Y., et al. (2022). Phytochrome b enhances seed germination tolerance to high temperature by reducing s-nitrosylation of HFR1. *EMBO Rep.* 23, e54371. doi: 10.15252/embr.202154371

Yu, M., Lamattina, L., Spoel, S. H., and Loake, G. J. (2014). Nitric oxide function in plant biology: A redox cue in deconvolution. *New Phytol.* 202, 1142–1156. doi: 10.1111/nph.12739

Yun, B.-W., Feechan, A., Yin, M., Saidi, N. B. B., Le Bihan, T., Yu, M., et al. (2011). S-nitrosylation of NADPH oxidase regulates cell death in plant immunity. *Nature* 478, 264–268. doi: 10.1038/nature10427

Zandi, P., and Schnug, E. (2022). Reactive oxygen species, antioxidant responses and implications from a microbial modulation perspective. *Biol. (Basel)* 11, 155–185. doi: 10.3390/BIOLOGY11020155

Zhan, N., Wang, C., Chen, L., Yang, H., Feng, J., Gong, X., et al. (2018). S-nitrosylation targets GSNO reductase for selective autophagy during hypoxia responses in plants. *Mol. Cell* 71, 142–154. doi: 10.1016/j.molcel.2018.05.024

Zhang, M., An, L., Feng, H., Chen, T., Chen, K., Liu, Y., et al. (2003). The cascade mechanisms of nitric oxide as a second messenger of ultraviolet b in inhibiting mesocotyl elongations. *Photochem. Photobiol.* 77 (2), 219–225. doi: 10.1562/0031-8655(2003)077<0219:tcmono>2.0.co;2

Zhang, J., Wang, Y., Mao, Z., Liu, W., Ding, L., Zhang, X., et al. (2022). Transcription factor McWRKY71 induced by ozone stress regulates anthocyanin and proanthocyanidin biosynthesis in malus crabapple. *Ecotoxicol. Environ. Saf.* 232, 113274. doi: 10.1016/j.ecoenv.2022.113274

Zhao, H., Qian, R., Liang, X., Ou, Y., Sun, C., and Lin, X. (2022). Indium induces nitro-oxidative stress in roots of wheat (Triticum aestivum). *J. Hazard. Mater.* 428, 128260. doi: 10.1016/J.JHAZMAT.2022.128260

Zitka, O., Krystofova, O., Hynek, D., Sobrova, P., Kaiser, J., Sochor, J., et al. (2013). *Metal transporters in plants* (Berlin Heidelberg: Springer-Verlag), 19–41. doi: 10.1007/978-3-642-38469-1_2

Frontiers in Plant Science

Cultivates the science of plant biology and its applications

The most cited plant science journal, which advances our understanding of plant biology for sustainable food security, functional ecosystems and human health.

Discover the latest Research Topics

See more →

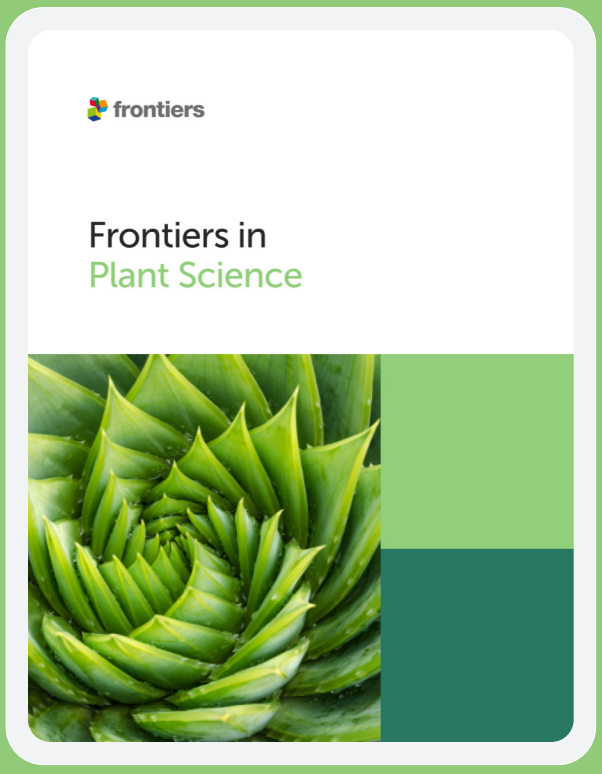

Frontiers

Avenue du Tribunal-Fédéral 34
1005 Lausanne, Switzerland
frontiersin.org

Contact us

+41 (0)21 510 17 00
frontiersin.org/about/contact